

9/83

10-03-820

FIFTH SEMIANNUAL STATUS REPORT
1 April 1980 - 30 September 1980

ENERGY EFFICIENT ENGINE
COMPONENT DEVELOPMENT AND INTEGRATION PROGRAM

19 December 1980

Contract NAS3-20646



Prepared for

NATIONAL AERONAUTICS AND SPACE ADMINISTRATION
Lewis Research Center
Cleveland, Ohio

(NACA-CR-173884) ENERGY EFFICIENT ENGINE
COMPONENT DEVELOPMENT AND INTEGRATION
PROGRAM Semiannual Status Report, 1 Apr. -
30 Sep. 1980 (Pratt and Whitney Aircraft
Group) 392 p HC A17/AF A01

884-32389

Unclass

CSCI 21E G3/07 21952



PWA-5594-142

PRATT & WHITNEY AIRCRAFT GROUP
Commercial Products Division



EAST HARTFORD, CONNECTICUT

FIFTH SEMIANNUAL STATUS REPORT
1 April 1980 - 30 September 1980

ENERGY EFFICIENT ENGINE
COMPONENT DEVELOPMENT AND INTEGRATION PROGRAM

19 December 1980

Contract NAS3-20646



Prepared for
NATIONAL AERONAUTICS AND SPACE ADMINISTRATION
Lewis Research Center
Cleveland, Ohio

PWA-5594-142

PRATT & WHITNEY AIRCRAFT GROUP

Commercial Products Division



EAST HARTFORD, CONNECTICUT

FOREWORD

This contract effort is being conducted as part of NASA's Energy Efficient Engine Project. It is managed by the NASA-Lewis Research Center, with N.T. Saunders serving as the NASA Project Manager and J.W. Schaefer serving as NASA's Assistant Project Manager responsible for this contract.

This semiannual report covers the work performed under Contract NAS3-20646 for the period of 1 April 1979 through 30 September 1979. It is published for technical information only and does not necessarily represent recommendations, conclusions, or the approval of NASA. The data generated under this contract are being disseminated within the United States in advance of general publication to accelerate domestic technology transfer. Since all data reported herein are preliminary information, they should not be published by the recipients prior to general publication by either the contractor or NASA.

PRECEDING PAGE BLANK NOT FILMED

TABLE OF CONTENTS

<u>Section</u>	<u>Page</u>
Foreword	
Table of Contents	
List of Illustrations	
1.0 INTRODUCTION	1
2.0 HIGHLIGHTS OF WORK ACCOMPLISHED	9
3.0 TECHNICAL DISCUSSION	11
3.1 Task 1 - Flight Propulsion System Design	11
3.1.1 Overall Objective	11
3.1.2 Task Overview	11
3.1.3 Propulsion System Analysis and Design Update	14
3.1.4 Program Risk Assessment	45
3.2 Task 2 - Component Technology	46
3.2.1 Overall Objective	46
3.2.2 Task Objective	46
3.2.3 Fan	50
3.2.4 Low-Pressure Compressor	106
3.2.5 High-Pressure Compressor	121
3.2.6 Combustor	145
3.2.7 High-Pressure Turbine	191
3.2.8 Low-Pressure Turbine	273
3.2.9 Exhaust/Mixer System	349
3.3 Task 3 - Core	357
3.4 Task 4 - Integrated Core/Low Spool	357

LIST OF ILLUSTRATIONS

<u>Number</u>	<u>Title</u>	<u>Page</u>
1	Overall Program Logic Diagram	3
2	Energy Efficient Engine Flight Propulsion System Cross-Section	7
3	Task 1 Logic Diagram	12
4	Task 1 Work Plan Schedule	13
5	Energy Efficient Engine Current Active Clearance Control System	20
6	Energy Efficient Engine Secondary Flow Map	21
7	Updated Fan Impact on Flight Propulsion System Cruise Thrust Specific Fuel Consumption - Lower peak fan efficiency has caused a 0.1-percent penalty at part power cruise.	30
8	Flight Propulsion System	36
9	Effect of Exhaust Nozzle Area Variation on Integrated Core/Low Spool Performance (Base area is design table value)	39
10	Separate Flow Exhaust Nozzle	44
11	Task 2 Logic Diagram	48
12	Task 2 Work Plan Schedule	49
13	Fan Program Logic Diagram	51
14	Fan Program Work Plan Schedule	52
15	Fan Component	56
16	General Blade Description	57
17	Blade Frequency Characteristics	60
18	Blade Flutter Characteristics	61
19	Blade Internal Surface Stresses at Solid-to-Hollow Transition Region	62

PRECEDING PAGE BLANK NOT FILMED

LIST OF ILLUSTRATIONS (Continued)

<u>Number</u>	<u>Title</u>	<u>Page</u>
20	Fan Blade Leading Edge Bird Ingestion Parameter	63
21	Shrouded Fan Component	65
22	Fan Flowpath	69
23	Aerodynamic Design Parameters: Fan Pressure Ratio and Recovery	70
24	Aerodynamic Design Parameters: Fan Exit Guide Vane Inlet Air Angles	70
25	Aerodynamic Design Parameters: Stator 1 Inlet Air Angles	71
26	Aerodynamic Design Parameters: Fan Design Loading	71
27	Aerodynamic Design Parameters: Sea Level Takeoff Loadings	72
28	Aerodynamic Design Parameters: Surge D-Factors	72
29	Aerodynamic Design Parameters: Rotor Recovery Versus Tip Mach Number	73
30	Blade Design Details: A Prime Incidence Versus Span	73
31	Blade Design Details: Suction Surface Incidence Versus Span	74
32	Blade Design Details: Choke Margin Versus Span	74
33	Blade Design Details: Actual Deviation Versus Span	75
34	Blade Design Details Metal Angle Versus Span	75
35	Blade Design Details Geometry Comparisons	76
36	Blade/Disk Attachment Stress Summary	80
37	Energy Efficient Engine Shrouded Fan Blade Resonance Diagram	80
38	Fan Containment Case	82

LIST OF ILLUSTRATIONS (Continued)

<u>Number</u>	<u>Title</u>	<u>Page</u>
39	Fan Stubshaft	84
40	Fan Hub	85
41	Nose Cone Assembly	86
42	Shrouded Fan Rotor Assembly Materials	87
43	Hollow Blade Technology Program Work Plan Schedule	89
44	Hollow Blade Production Sequence	91
45	General Description TRW Specimen	92
46	Schematic Illustration of Camber Tooling	97
47	Chain Micro-voids Along Bond Line at 500x Magnification	100
48	Fracture Surface of Brittle Bond Plane Tensile Specimen Failure	100
49	Scanning Electron Microscope Micrograph of Bond Plane Tensile Failure at 2000x Magnification Showing 4 Apparent Voids on Fracture Surface	101
50	Stereo Pair Micrograph (500x) of an Apparent Void on Bond Plane Tensile Failure Fracture Surface	102
51	Scanning Electron Microscope Micrograph (2000x) 0.010-inch Sheet Laminate	104
52	Chain Micro-voids Along Bond Line at 1000x Magnification	104
53	Linear Beta Fleck Located at Bond Line	105
54	Beta Fleck (200x) Centered on Bond Line	106
55	Low-Pressure Compressor Program Logic Diagram	107
56	Low-Pressure Compressor Program Component Effort Work Plan Schedule	108

LIST OF ILLUSTRATIONS (Continued)

<u>Number</u>	<u>Title</u>	<u>Page</u>
57	Low-Pressure Compressor Component	110
58	Low-Pressure Compressor Pressure and Temperature Analysis Results	116
59	Low Cost Integrated Core/Low Spool Low-Pressure Compressor Component	118
60	Number 1 and 2 Bearing Compartment	119
61	Number 1 and 2 Bearing Support Flange	120
62	High-Pressure Compressor Program Logic Diagram	122
63	High-Pressure Compressor Component Effort Work Plan Schedule	123
64	High-Pressure Compressor Component	126
65	High-Pressure Compressor Rig	127
66	Compressor Intermediate Case Integrated with the High-Pressure Compressor Component	131
67	High-Pressure Compressor Drum Rotor Assembly	134
68	High-Pressure Compressor Drum Rotor Assembly	135
69	High-Pressure Compressor 14th and 15th Stage Disk	136
70	High-Pressure Compressor Rig Split Front Vane Case	137
71	High-Pressure Compressor Rig Split Rear Case During Set-up Before Final Inner and Outer Surface Machining	139
72	High-Pressure Compressor Rig Intermediate Case Inner Case Detail During Rear Flange Machining Operation	141
73	High-Pressure Compressor Rig Intermediate Case Outer Case Detail After Hole Drilling Operation Before Strut Weldment	142

LIST OF ILLUSTRATIONS (Continued)

<u>Number</u>	<u>Title</u>	<u>Page</u>
74	High-Pressure Compressor Intermediate Case Strut	143
75	Number 4 Bearing Support Case	144
76	Combustor Program Logic Diagram	147
77	Combustor Component Effort Work Plan Schedule	148
78	Combustor Component	150
79	Combustor Component Rig	151
80	High-Pressure Compressor Exit Guide Vane Assembly	153
81	Combustor Carburetor Tube Configuration	155
82	Fuel Nozzle Support Assembly Stress Summary	157
83	Fuel Nozzle Candidate Designs	159
84	Existing Ignitor Modified for Use in Combustor	161
85	Combustor Rig/Facility Mounting Scheme	162
86	Full Annular Rig Instrumentation	164
87	Instrumentation Probes	165
88	Fuel Supply Manifolds and Shroud	167
89	Diffuser Case Wax Pattern	168
90	Comparison of the Baseline Strut and the Revised Strut	169
91	Inner Shroud Wake Rake Traverse Results	170
92	Combustor Sector Rig Test Program Work Plan Schedule	172
93	Combustor Sector Rig Cross-Section	173
94	Revised Combustor Assembly with Segmented Liners	175
95	Main Zone Fuel Injector Configurations	175
96	Liner Segment Details	

LIST OF ILLUSTRATIONS (Continued)

<u>Number</u>	<u>Title</u>	<u>Page</u>
97	Segment Combustor Rig Assembly	179
98	Carburetor Tube Modifications for Reduced NOx	181
99	High Power NOx Emissions Characteristics	182
100	Comparison of Idle Emissions for Various Pilot Inner/Outer Swirler Blockage	184
101	Comparison of Idle Emissions for the Redesigned Pilot Nozzle	185
102	Variations of Carbon Monoxide Emissions With Performance F/A at Approach Condition	186
103	Combustor Air Flow Distribution (Based on sector rig test results)	188
104	Altitude Relight Test Results	189
105	Sea Level Start Program	190
106	High-Pressure Turbine Program Logic Diagram	192
107	High-Pressure Turbine Component Effort Work Plan Schedule	193
108	High-Pressure Turbine Component	196
109	High-Pressure Turbine "Warm" Test Rig	197
110	High-Pressure Turbine Transition Duct	200
111	High-Pressure Turbine Component Flowpath	202
112	Final Vane Mean Section Airfoil Contour and Loading Diagrams	204
113	High-Pressure Turbine Vane - Stacked view	205
114	Final Design Blade Mean Section Contour and Loading Diagram	206
115	High-Pressure Turbine Blade - Stacked view	207
116	Vane Final Cooling Design	210
117	Combustor Exit Temperature Profile Used in Vane Design	212
118	Vane Metal Temperature Distribution	213

LIST OF ILLUSTRATIONS (Continued)

<u>Number</u>	<u>Title</u>	<u>Page</u>
119	Vane Inner and Outer Diameter Platform Cooling Hole Arrangement	214
120	Vane Inner and Outer Diameter Platform Cooling Hole Arrangement	215
121	Vane Strain Ranges	216
122	High-Pressure Turbine Blade Cooling Design	218
123	Blade Temperature Profile	219
124	Blade Mid-Span Section Isotherm	220
125	Blade Strain Ranges	222
126	High-Pressure Turbine Secondary Flow Map	223
127	Rotor Secondary Flow Features	224
128	Nozzle Configuration for the Tangential On-Board Injection System	225
129	Front Rim Cavity "Mini" Tangential On-Board Injection System	226
130	Blade Coolant Supply System	227
131	Vane Cooling Air Sealing Arrangement	230
132	High-Pressure Compressor Discharge Seal	231
133	Disk, Blade, Sideplate, and Vortex Plate Final Design	232
134	High-Pressure Turbine Rotor	233
135	Rim Area and Cooling Hole Cyclic Lives	234
136	Blade Attachment Stress Study Results	235
137	High-Pressure Turbine Required Secondary Axis Crystal Orientation	236
138	High-Pressure Turbine Blade Resonance Diagram	237

LIST OF ILLUSTRATIONS (Continued)

<u>Number</u>	<u>Title</u>	<u>Page</u>
139	High-Pressure Turbine Active Clearance Control Blade Outer Airseal Features	239
140	Ceramic Outer Air Seal Shoe	241
141	High-Pressure Turbine Blade Tip Clearances	243
142	Final Definition of the Hot Strut Case	245
143	NASTRAN Model of the Hot Strut Case	247
144	Hot Strut Case Radial and Circumferential Deflection Summary	248
145	Hot Strut Case Radial and Axial Deflection Summary	249
146	Hot Strut Fairing Clearance Summary	250
147	Flight Propulsion System Hot Strut Low Cycle Fatigue Lives	252
148	Integtated Core/Low Spool Hot Strut Low Cycle Fatigue Lives	253
149	High-Pressure Turbine Rig Secondary Flows	256
150	Active Clearance Control Growth Summary	257
151	High-Pressure Turbine "Warm" Rig Critical Speeds and Mode Shapes	259
152	Cooling Model Test Program Work Plan Schedule	266
153	Root and Tip Turn Flow Visualization Models	267
154	Modified Two-Dimensional Cooling Model	269
155	High-Pressure Turbine 5x Blade Plastic Cooling Model	270
156	High-Pressure Turbine Three-Dimensional Cooling Model	271
157	Low-Pressure Turbine Program Logic Diagram	274
158	Low-Pressure Turbine Component Effort Work Plan Schedule	275

LIST OF ILLUSTRATIONS (Continued)

<u>Number</u>	<u>Title</u>	<u>Page</u>
159	Low-Pressure Turbine Component	277
160	Low-Pressure Turbine Flowpath Comparison	281
161	Low-Pressure Turbine Second Vane Mean Section Geometry	283
162	Low-Pressure Turbine Second Blade Mean Section Geometry	284
163	Low-Pressure Turbine Third Vane Mean Section Geometry	285
164	Low-Pressure Turbine Third Blade Mean Section Geometry	286
165	Low-Pressure Turbine Fourth Vane Mean Section Geometry	287
166	Low-Pressure Turbine Fourth Blade Mean Section Geometry	288
167	Low-Pressure Turbine Fifth Vane Mean Section Geometry	289
168	Low-Pressure Turbine Fifth Blade Mean Section Geometry	290
169	Low-Pressure Turbine Exit Guide Vane Mean Section Geometry	291
170	Low-Pressure Turbine Exit Guide Vane Mean Section Compressible Mach Number Distribution	292
171	Second Stage Vane Durability Design Conditions and Calculated Stress (Vane material: PWA 1480 Coating: PWA 73)	294
172	Second Stage Blade Durability Design Conditions and Calculated Stress (Blade material: PWA 1447; Coating: PWA 73)	295
173	Third Stage Vane Durability Design Conditions and Calculated Stress (Vane material: PWA 1455; No coating)	296

LIST OF ILLUSTRATIONS (Continued)

<u>Number</u>	<u>Title</u>	<u>Page</u>
174	Third Stage Blade Durability Design Conditions and Calculated Stress (Blade material: PWA 655; No coating)	297
175	Fourth Stage Vane Durability Design Conditions and Calculated Stress (Vane material: PWA 655; No coating)	298
176	Fourth Stage Blade Durability Design Conditions and Calculated Stress (Blade material: PWA 655; No coating)	299
177	Fifth Stage Vane Durability Design Conditions and Calculated Stress (Vane material: PWA 655; No coating)	300
178	Fifth Stage Blade Durability Design Conditions and Calculated Stress (Blade material: PWA 655; No coating)	301
179	Low-Pressure Turbine Second Stage Rotor Resonance Diagram	302
180	Low-Pressure Turbine Third Stage Rotor Resonance Diagram	303
181	Low-Pressure Turbine Fourth Stage Rotor Resonance Diagram	304
182	Low-Pressure Turbine Fifth Stage Rotor Resonance Diagram	305
183	Shrouded Turbine Blade Flutter Analysis	306
184	Low-Pressure Turbine Damped Number 5 Bearing Compartment	308
185	Low-Pressure Turbine Rotor Construction	310
186	Low-Pressure Turbine Component Major Features (Preliminary Design Review Configuration)	311
187	Low-Pressure Turbine Inner Air Seal Design Schemes	313
188	Low-Pressure Turbine Active Clearance Control System (Preliminary Design Review Configuration)	314

LIST OF ILLUSTRATIONS (Continued)

<u>Number</u>	<u>Title</u>	<u>Page</u>
189	Modified Low-Pressure Turbine Active Clearance Control System	315
190	Low-Pressure Turbine Cooling Passages	317
191	Boundary Layer Test Program Work Plan Schedule	319
192	Turbulent Boundary Layer Velocity Profiles Using Dimensionless Parameters	322
193	Comparison of Measured Integral Parameters for the "Squared-off" Test Section with Theoretical Predictions	323
194	Comparison of the Measured Mean Velocity Profile Data (Squared-off) with Theoretical Predictions	324
196	Comparison of the Measured Mean Velocity Profile Data (Aft-loaded) with Theoretical Predictions	325
195	Comparison of Measured Integral Parameters for the Aft-loaded Test with Theoretical Predictions	326
197	Distribution of Boundary Layer Momentum Loss Thickness Reynolds number, Shape Factor, and Skin Friction	327
196	Comparison of Measured Total Turbulence Intensity Profiles with Flat Plate Data	329
199	Distribution of Normalized Turbulence Intensity Components in the Fully Turbulent Region of the Squared-off Test Configuration	330
200	Distribution of Normalized Turbulence Intensity Components in the Transitional Region of the Squared-off Test Configuration	331
201	Growth of Turbulence Intensity in the Laminar Region of Each Boundary Layer	333
202	Subsonic Cascade Test Program Work Plan Schedule	335
203	Subsonic Cascade Losses Compared to Incidence	337

LIST OF ILLUSTRATIONS (Continued)

<u>Number</u>	<u>Title</u>	<u>Page</u>
204	Subsonic Cascade Losses Compared to Incidence	339
205	Subsonic Cascade Losses Compared to Mach Number	340
206	Subsonic Cascade Losses Compared to Incidence	342
207	Subsonic Cascade Losses Compared to Mach Number	343
208	Transition Duct Work Plan Schedule	345
209	Low-Pressure Turbine Build 2 Transition Duct	347
210	Low-Pressure Turbine Transition Duct Rig Showing Modifications for Build 2	348
211	Mixer Component Logic Diagram	350
212	Mixer Component Work Plan Schedule	351
213	Mixer Current Design Status Compared to Preliminary Design Review Configuration	353
214	Mixer Model Work Plan Schedule	355
215	Integrated Core/Low Spool Program Logic Diagram	358
216	Integrated Core/Low Spool Program Work Plan Schedule	359
217	Integrated Core/Low Spool Gearbox Mounting System	361
218	Integrated Core/Low Spool Lubrication System Schematic (Non-Regulated)	362
219	Preliminary Bifurcated Duct Configuration	364
220	Energy Efficient Engine Integrated Core/Low Spool Full Size Mock-up Under Construction	365
221	Energy Efficient Engine Preliminary Plumbing System	366
222	Active Clearance Control System Illustrating External Tubes and Valves	367



1.0 INTRODUCTION

The Energy Efficient Engine Component Development and Integration Program is currently being conducted under parallel contracts with General Electric and Pratt & Whitney Aircraft. The Pratt & Whitney Aircraft effort is funded under NASA Contract NAS3-20646. The program is under the overall direction of Mr. C.C. Ciepluch, who is assisted by Mr. J.W. Schaefer, NASA Project Manager for the Pratt & Whitney Aircraft effort.

The objective of the program is to develop, evaluate, and demonstrate the technology for achieving lower installed fuel consumption and lower operating costs in future commercial turbofan engines. NASA has set minimum goals of a 12-percent reduction in thrust specific fuel consumption (TSFC), 5-percent reduction in direct operating cost (DOC), and 50-percent reduction in performance degradation for the Energy Efficient Engine (flight propulsion system) relative to the JT9D-7A reference engine. In addition, environmental goals on emissions (meet the proposed EPA 1981 regulation) and noise (meet FAR 36-1978 standards) have been established.

The Pratt & Whitney Aircraft program effort is based on an engine concept defined under the NASA-sponsored Energy Efficient Engine Preliminary Design and Integration Studies Program, Contract NAS3-20628. This program was completed under an earlier low-energy consumption contract effort, and is discussed in detail in NASA Report CR-135396. The Pratt & Whitney Aircraft engine is a twin-spool, direct drive, mixed-flow exhaust configuration, utilizing an integrated engine-nacelle structure. A short, stiff, high rotor and a single-stage high-pressure turbine are among the major features in providing for both performance retention and major reductions in maintenance and direct operating costs. Improved clearance control in the high-pressure compressor and turbines, advanced single crystal materials in turbine blades and vanes, and shroudless fan blades are among the major features providing performance improvement.

To meet the program objectives, four technical tasks were established by the Pratt & Whitney Aircraft Project Team and defined in the Program Work Plan.

Task 1, Propulsion System Analysis, Design and Integration - provides for the preliminary design of the Energy Efficient Engine flight propulsion system and for evaluation of the propulsion system/aircraft integration with the assistance of Boeing, Douglas, and Lockheed.

Task 2, Component Analysis, Design and Development - consists of designing, fabricating, and testing the high risk components as well as supporting technology tests in critical areas. The task includes the designing of all components, plus a technology program to obtain design data on hollow fan blade test specimens; two builds of the high-pressure compressor; a full annular combustor and supporting programs to define diffuser parameters and combustor geometry for low emissions; a cooled high-pressure turbine rig and supporting technology programs in aerodynamics, leakage control, and blade fabrication; aerodynamic rigs supporting the design of a low-pressure turbine; and scale model mixer testing.



PRATT & WHITNEY AIRCRAFT GROUP
COMMERCIAL PRODUCTS DIVISION

Task 3, Core Design, Fabrication and Test - provides the design, fabrication, and test of two builds of the core engine. The core consists of the high-pressure compressor, combustor, and high-pressure turbine. The test programs are structured to obtain aerodynamic and thermodynamic performance of the components and core. These test programs also evaluate the mechanical behavior of the structural design.

Task 4, Integrated Core/Low Spool Design, Fabrication and Test - is an option that was exercised by NASA on 5 November 1979. Task 4 consists of design, fabrication, and test of the fan, low-pressure compressor, low-pressure turbine, and mixer, all of which will be installed in a boiler plate nacelle and integrated with the core engine from Task 3. The boiler plate nacelle will be acoustically treated and its lines will duplicate the internal flow lines of a representative flight nacelle. The integrated core/low spool will be tested to obtain aerodynamic and thermodynamic performance, component matching characteristics, and data on acoustic and emission characteristics. These tests will also evaluate mechanical behavior of the integrated core/low spool.

The program logic diagram in Figure 1* indicates the task schedules and the relationships between these tasks and their elements over the duration of the program.

Most of the work planned and approved from contract award through the end of the current reporting period (30 September 1980) has been completed. Exceptions are indicated in the appropriate technical progress sections of this report.

* For all program logic diagrams and work plan schedules presented in this report, the shaded region represents the current reporting period; "*M" denotes a major milestone; and "*D" denotes a key decision point.



PRATT & WHITNEY AIRCRAFT GROUP
COMMERCIAL PRODUCTS DIVISION

ORIGINAL PAGE IS
OF POOR QUALITY

ACTIVITIES/MILESTONES
TASK 1 - PROPULSION SYSTEM ANALYSIS,
DESIGN, AND INTEGRATION
PROPULSION SYSTEM PRELIMINARY DESIGN
CONTROL PRELIMINARY DESIGN
CYCLE AND PERFORMANCE ANALYSIS COMPUTER DECK
PROPULSION SYSTEM AIRCRAFT INTEGRATION
EVALUATION
FPS ANALYSIS, DESIGN AND INTEGRATION,
DESIGN UPDATES
PROGRAM RISK ASSESSMENT
TASK 2 - COMPONENT ANALYSIS, DESIGN,
AND DEVELOPMENT
FAN
COMPONENT DESIGN
FAN SUPPORTING TECHNOLOGY PROGRAM
MILLION BLADE
LOW-PRESSURE COMPRESSOR
COMPONENT DESIGN
HIGH-PRESSURE COMPRESSOR
COMPONENT DESIGN
COMPONENT FABRICATION
HIGH-PRESSURE COMPRESSOR RIG DESIGN
FABRICATION (2 BUILDS)
ASSEMBLY (2 BUILDS)
TEST (2 BUILDS)
ANALYSIS (2 BUILDS)
COMBUSTOR
COMPONENT DESIGN
COMPONENT FABRICATION
COMBUSTOR RIG DESIGN
FABRICATION
ASSEMBLY
TEST
ANALYSIS
COMBUSTOR SUPPORTING TECHNOLOGY PROGRAMS
DIFFUSER/COMBUSTOR MODEL TEST
COMBUSTOR SECTOR RIG
HIGH PRESSURE TURBINE
COMPONENT DESIGN
COMPONENT FABRICATION
HIGH-PRESSURE TURBINE RIG DESIGN
FABRICATION
ASSEMBLY
TEST
ANALYSIS

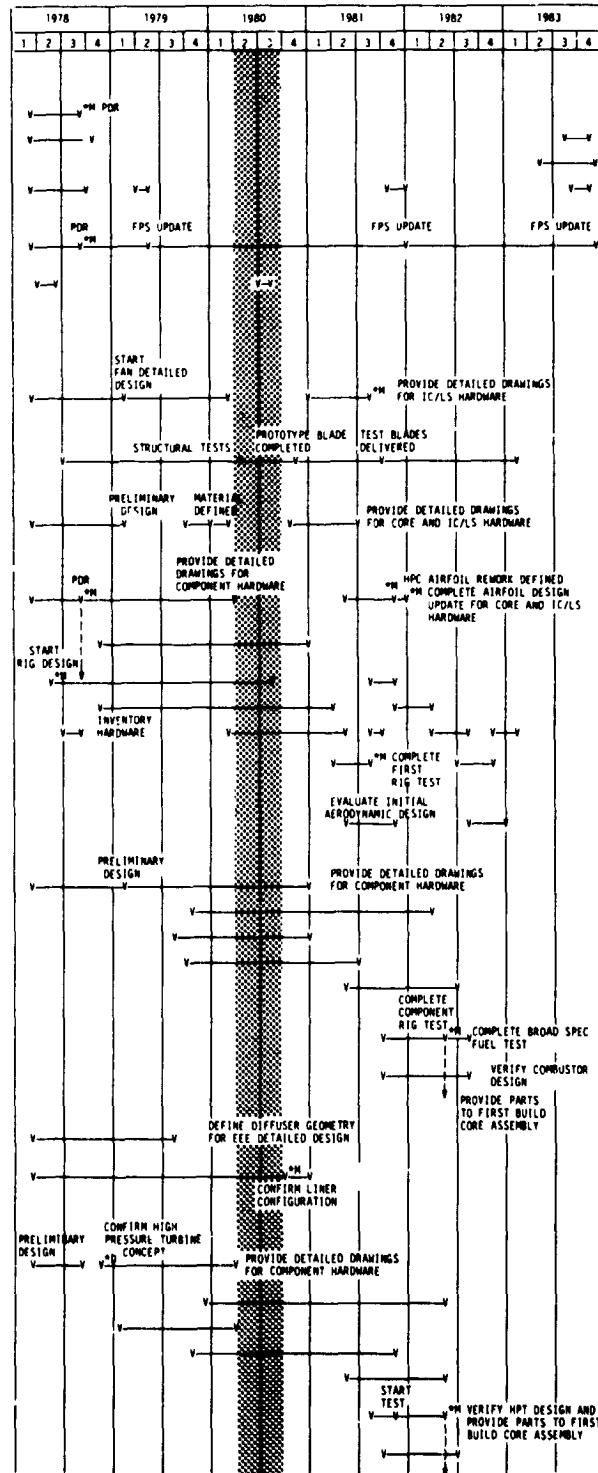


Figure 1 Overall Program Logic Diagram

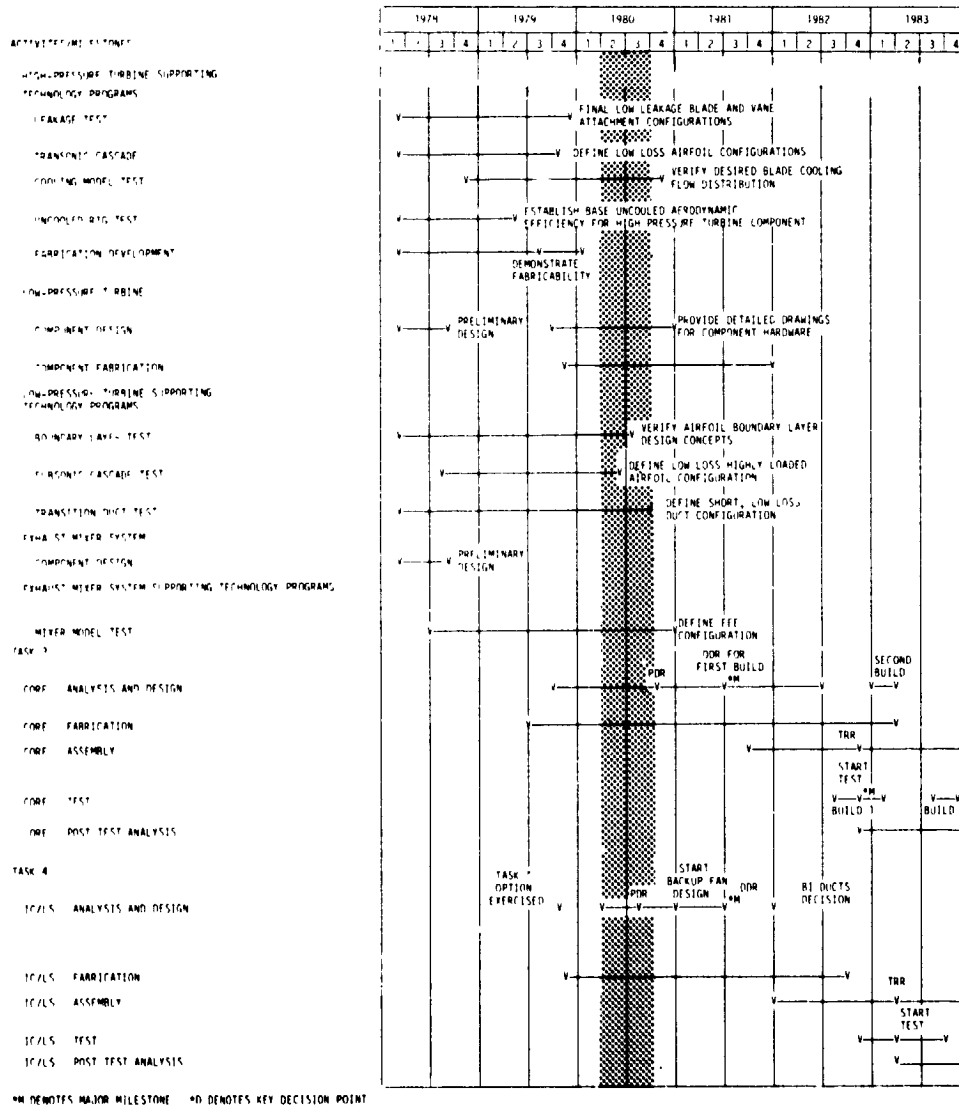
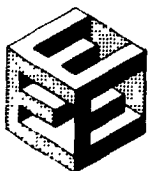


Figure 1 Overall Program Logic Diagram (Cont'd)



PRATT & WHITNEY AIRCRAFT GROUP
COMMERCIAL PRODUCTS DIVISION

Major changes related to the propulsion system design since contract award include a change in the high-pressure compressor hub/tip ratio to improve its aerodynamic performance and a re-sizing of the engine to obtain the maximum technology benefit for smaller thrust engines expected to be required in the 1980's.

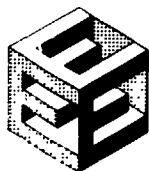
Several program changes were effected during the current reporting period. Some of these resulted from a program review aimed at alleviating a forecast cost overrun. All were made with NASA approval. The significant outcome of this program review was a recommendation to NASA that the Task 3 core effort be deleted and that a second test of the integrated core/low spool be added to Task 4. NASA issued Pratt & Whitney Aircraft a request for proposal after this recommendation, and Pratt & Whitney Aircraft responded with its proposal in August 1980 to modify the contract accordingly. This proposal was still pending negotiation at the end of the current reporting period.

The February 1980 work plan was approved during this reporting period. This work plan was subsequently modified to reflect the NASA redirection of technical effort consistent with the August 1980 proposal. There were three modifications to the February 1980 work plan (1) all core test work was deferred, (2) the analysis and design of the alternate (shrouded) fan was started early to provide timely availability of test hardware for the first test of the integrated core/low spool, and (3) a tangential on-board injection rig test was added to the high-pressure turbine rig program.

Additional program changes included the elimination of the Automated Casting Foundry as the high-pressure turbine blade vendor and deferral of the Task 1 risk assessment update until the fourth quarter of 1981.

Each of the program logic diagrams and work plan schedules presented in this report are in accordance with the February 1980 work plan.

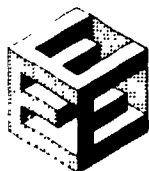
The definition of the propulsion system and its components is periodically updated as program technical objectives are completed. The present propulsion system (see Figure 2) is a five-bearing design with two main support frames and two main bearing compartments. The fan features a hollow, titanium shroudless design to provide efficiency improvement without an offsetting weight increase. The low-pressure compressor utilizes controlled endwall loss and reduced airfoil loss concepts to raise compressor efficiency levels. The high-pressure compressor similarly employs these low loss concepts. The high-pressure compressor operates at higher rotor speeds relative to the JT9D-7A high rotor for reduced weight and cost. It also incorporates an active clearance control system for improved efficiency. A two-stage combustor is utilized for low emissions. The high-pressure turbine features a single-stage design to provide a significant reduction in initial cost and engine maintenance cost. Single crystal alloy airfoils are used to reduce cooling and leakage flows. The high-pressure turbine also incorporates active clearance



PRATT & WHITNEY AIRCRAFT GROUP
COMMERCIAL PRODUCTS DIVISION

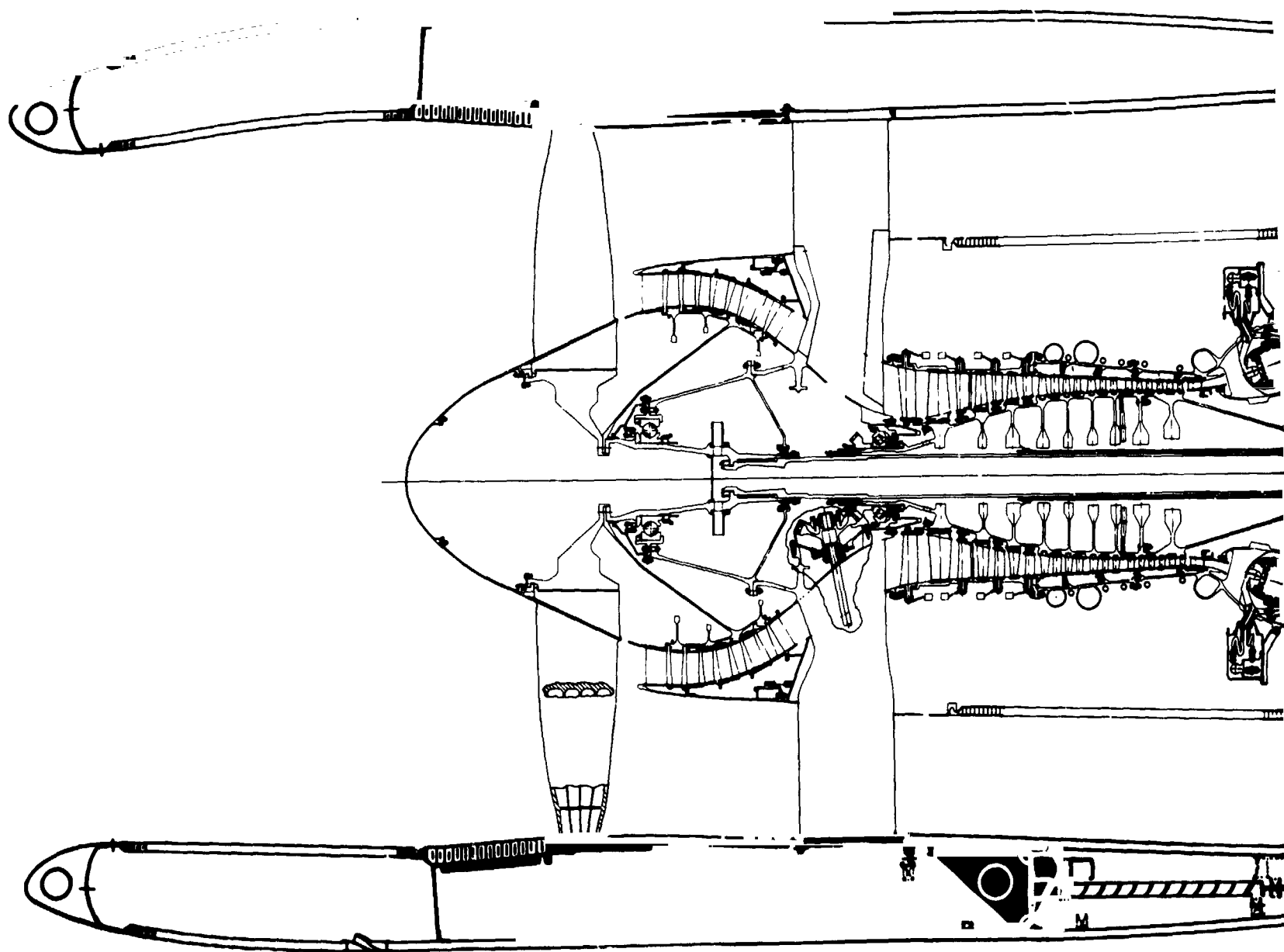
control to improve component efficiency. The low-pressure turbine counter-rotates relative to the high-pressure turbine and incorporates active clearance control to increase component efficiency. The exhaust mixer is a scalloped design for reduced pressure loss, increased efficiency, and light weight. A full authority digital electronic control is used to promote efficient engine operation and reduce the effects of deterioration. The key nacelle features are an integrated engine-nacelle structure which improves engine performance retention by reducing engine deflections caused by thrust and cowl loads. The nacelle is constructed of composite and honeycomb materials for reduced weight and incorporates improved internal and external contouring and advanced sealing techniques for reduced losses.

The remainder of this report presents background information and technical progress for each of the sub-tasks of Tasks 1, 2, 3, and 4. The technical progress sections are appropriately divided to reflect (1) previously completed work that has an impact on the technical progress for the current reporting period, and (2) work accomplished during the current reporting period.



PRATT & WHITNEY AIRCRAFT GROUP
COMMERCIAL PRODUCTS DIVISION

ORIGINAL PAGE IS
OF POOR QUALITY



FOLDOUT FRAME

ORIGINAL DESIGN
OF POOR QUALITY

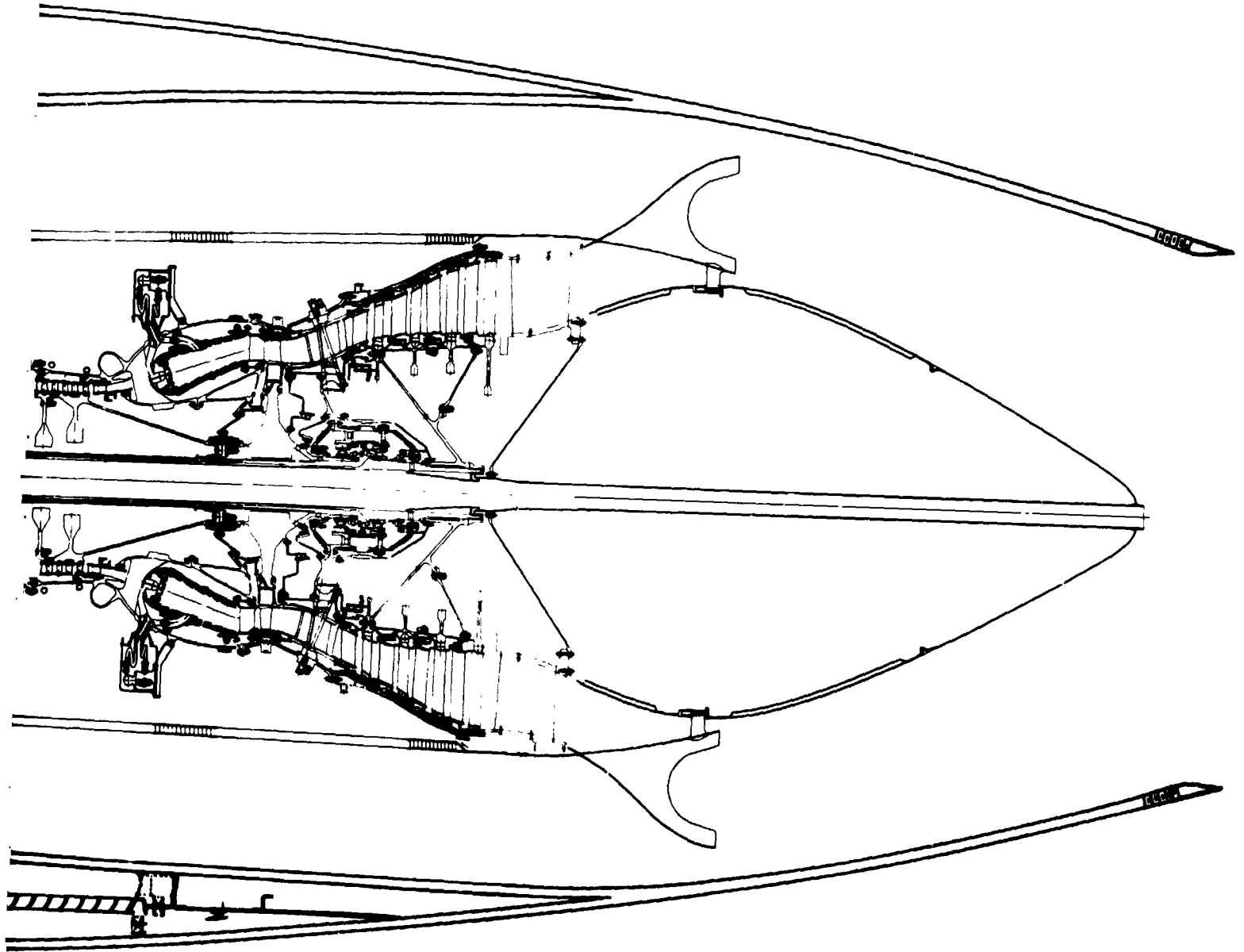
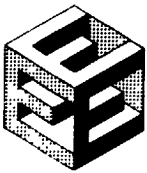


Figure 2 Energy Efficient Engine Flight Propulsion System Cross-Section



PRATT & WHITNEY AIRCRAFT GROUP
COMMERCIAL PRODUCTS DIVISION

2.0 HIGHLIGHTS OF WORK ACCOMPLISHED

- o Detailed analysis and design of the alternate fan was completed and the design was released for detailing.
- o All laminated titanium diamond-shaped specimens were received from TRW. Assembly of these specimens and hot isostatic pressing was also completed. The first attempt to hot isostatically press full size laminated titanium fan blades was unsuccessful because of container leakage.
- o High-pressure compressor drum rotor welds were completed on 6th, 7th, 12th, and 13th stage disks.
- o The results of the tests performed on the combustor sector rig indicate that successfully reduced emission levels were achieved and desired approach power main zone stability was maintained. Altitude relight capability was also demonstrated. In addition, the advanced segmented liner sector rig was assembled in preparation for airflow testing.
- o The combustor component rig interim design review was completed.
- o The full 9-knife edge seal was incorporated into the high-pressure turbine component rig design as a result of an action item from the NASA high-pressure turbine detailed design review.
- o Low-pressure rotor critical speed requirements were met for all modes of concern, except for a tailplug mode. The turbine exhaust case will be stiffened to rectify this concern.
- o The design of the Phase II mixer model test configuration was completed and the technology design review approved. Design fabrication of the mixer test models was initiated at Fluidyne, and Phase II mixer model testing was subsequently initiated.
- o The design of the integrated core/low spool was started. An update of its performance indicates that thrust specific fuel consumption at altitude conditions is estimated to be 10.3 percent below that of the JT9D-7A reference engine.
- o A requirement was established for the damping of the number 5 bearing, based on a forced response analysis with the latest designs of the low-pressure turbine and exhaust case. An oil film damper was subsequently incorporated at the location of the number 5 bearing.
- o A proposal was issued to NASA in August redefining the technical content of the program in order to provide relief from a forecast cost overrun. This proposal called for modifications to portions of Task 2, the entire deletion of Task 3, and the addition of a second test of the Task 4 integrated core/low spool.



3.0 TECHNICAL DISCUSSION

The following sections describe the scope of the total technical effort at the major task level. Work planned for the current reporting period is identified at the sub-task level, and progress and results relative to this planned work are discussed in detail.

3.1 TASK 1 FLIGHT PROPULSION SYSTEM DESIGN

3.1.1 Overall Objective

Produce and maintain the flight propulsion system definition over the period of performance for the contracted work.

3.1.2 Task Overview

The definition of the flight propulsion system (1) forms the basis for assessing the capabilities of the flight propulsion system and integrated core/low spool (measured against program goals) and (2) establishes the design of the experimental hardware for Tasks 2, 3, and 4.

The overall Task 1 effort is accomplished in six sub-tasks: (1) propulsion system preliminary design, (2) control preliminary definition, (3) propulsion system analysis and design update, (4) propulsion system/aircraft integration evaluation, (5) program risk assessment, and (6) cycle and performance analysis computer deck. The logic diagram for Task 1 is shown in Figure 3, and the work plan schedule, in Figure 4.

The two major milestones of the Task 1 work plan schedule are (1) the flight propulsion system preliminary design review and (2) the propulsion system/aircraft integration evaluation. The first milestone is important because detailed design of the components cannot start until the preliminary design of the flight propulsion system is approved. Results of the propulsion system/aircraft integration initial evaluations provide the first major indications of the flight propulsion system capabilities measured against design goals.

All of the work planned and approved from contract award through the end of the current reporting period (30 September 1980) has been completed. This included (1) completion of the flight propulsion system preliminary design and first design update (plus the companion effort associated with the propulsion system/aircraft integration evaluation*), (2) completion of the control preliminary definition, and (3) completion of the initial risk assessment. The flight propulsion system preliminary design and first design update demonstrated that the flight propulsion system can potentially meet NASA program objectives. The control preliminary definition established a full authority, digital electronic system as the primary concept for the flight propulsion system. The initial risk assessment identified the fan, high-pressure compressor, turbine, core, and integrated core/low spool as having the critical program paths that pace the program as scheduled.



PRATT & WHITNEY AIRCRAFT GROUP
COMMERCIAL PRODUCTS DIVISION

Figure 4 identifies those tasks completed during the previous reporting periods and indicates that work on sub-Task 3 was continued during the current reporting period. It also indicates that the risk assessment update (sub-task 5) was to have been completed during the current reporting period. This assessment has been deferred by NASA direction until the fourth quarter of 1981. Sub-task 3 work is described in detail in the following section.

* Documented in NASA reports CR-159487 and CR-159488, respectively.

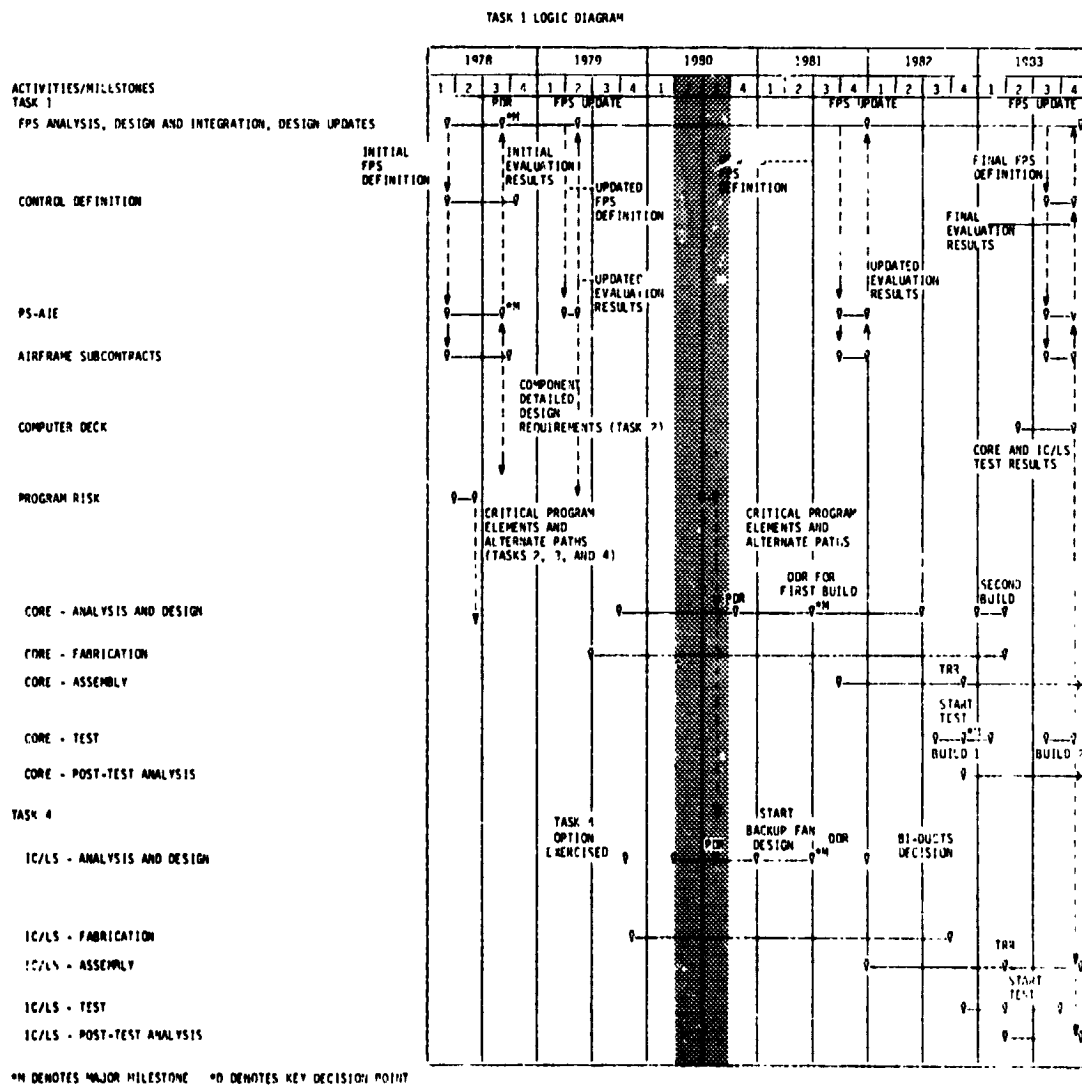
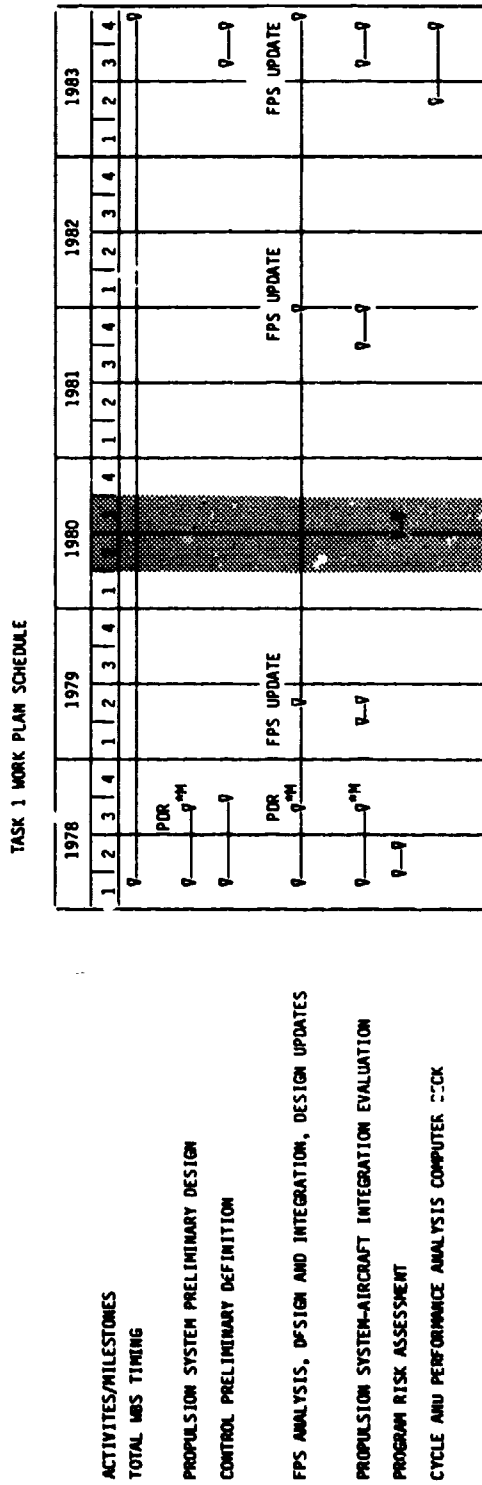


Figure 3 Task 1 Logic Diagram



PRATT & WHITNEY AIRCRAFT GROUP
COMMERCIAL PRODUCTS DIVISION



ORIGINAL COPY
OF POOR COPY

Figure 4 Task 1 Work Plan Schedule



PRATT & WHITNEY AIRCRAFT GROUP
COMMERCIAL PRODUCTS DIVISION

3.1.3 Propulsion System Analysis and Design Update

3.1.3.1 Objective

Continually review the predicted performance levels for the flight propulsion system and integrated core/low spool designs as test data are obtained from Tasks 2 and 3.

3.1.3.2 Scope of Total Work Planned

The propulsion system is updated at the completion of (1) the revised fan and combustor preliminary designs; (2) the detailed design reviews for the components, core, and integrated core/low spool; and (3) the program. The final update includes cycle reoptimization for the flight propulsion system based on the overall program results. At the completion of the component, core, and integrated core/low spool design efforts, and at the end of the program, a propulsion system preliminary design review will be conducted at NASA-LERC to cover the updated and revised analysis and design efforts.

3.1.3.3 Technical Progress

3.1.3.3.1 Summary of Work Previously Completed

The definitions of the propulsion system and its components have been periodically updated as program technical objectives have been met. The evolutionary status of the system performance for the flight propulsion system design, compared to the NASA goals and the JT9D-7A reference engine, is shown in Table 1. Results from the propulsion system/aircraft integration evaluations, where these were conducted, are also included in this table. Table 2 lists the current flight propulsion system performance parameters at significant engine operating conditions.

As part of the evolutionary design process, the propulsion system was resized to obtain the maximum technology benefit for smaller thrust engines expected to be required in the late 1980's. The inlet hub/tip ratio of the high-pressure compressor was also changed to improve aerodynamic performance. These changes are summarized in Table 3.



PRATT & WHITNEY AIRCRAFT GROUP
COMMERCIAL PRODUCTS DIVISION

ORIGINAL PAGE 19
OF POOR QUALITY

TABLE 1
SUMMARY OF FLIGHT PROPULSION SYSTEM DESIGN EVALUATION

	NASA GOAL	PRELIMINARY DESIGN	PSAIE REP'T	FIRST FPS DESIGN UPDATE	STATUS - MAY, 1979	STATUS - OCT., 1979	STATUS - MARCH 1980
TSFC Reduction*	12.0	14.9	14.9	14.9	14.9	14.7	15.1
DOC Reduction*							
Domestic Mission (Avg.)	5.0	7.7	7.6	7.2	7.1	6.5	6.7
International Mission (Avg.)	5.0	9.9	9.8	9.4	9.3	8.7	8.9
Noise							**
	FAR 36 FAR 36-2 (1978) to -4						
Emission							
Carbon Monoxide	3.0	2.0	2.0	1.7	1.7	1.7	**
Unburned Hydrocarbons	0.4	0.3	0.2	0.2	0.2	0.2	**
Oxides of Nitrogen	3.0	4.3	4.3	4.6	4.6	4.6	**
Reduction in Engine Weight*	-	8.6	7.6	2.5	1.3	-3.9	**
Reduction in Engine Cost*	-	5.9	4.7	1.0	1.4	-1.6	**
Reduction in Main- tenance Cost*	-	6.2	4.6	4.2	4.7	2.4	**

*Relative to scaled JT9D-7A base engine

**Not updated



PRATT & WHITNEY AIRCRAFT GROUP
COMMERCIAL PRODUCTS DIVISION

TABLE 2

CURRENT FLIGHT PROPULSION SYSTEM PERFORMANCE PARAMETERS

	<u>Engine Operating Condition</u>			
	<u>Aero. Des. Point</u>	<u>Maximum Cruise</u>	<u>Maximum Climb</u>	<u>Takeoff</u>
Altitude (ft)	35000	35000	35000	0
Mach Number	0.8	0.8	0.8	0
Ambient Temperature (F)	-66	-66	-48	84
Net Thrust (Uninstalled) (lb)	9355	8935	9965	37090
Thrust Specific Fuel Consumption (lb/hr/lb)				
(Uninstalled)	0.5490	0.5480	0.5690	0.3245
(Installed)	0.575	0.575	0.594	0.328
Overall Pressure Ratio	38.55	37.25	40.55	30.80
Bypass Ratio	6.51	6.62	6.33	6.91
Fan Pressure Ratio (Duct Section)	1.74	1.71	1.78	1.58
High-Pressure Turbine Rotor Inlet Temperature (F)	2230	2195	2395	2485

TABLE 3

1979 PROPULSION SYSTEM DESIGN CHANGES

	<u>Original</u>	<u>Revised</u>
Sea Level Static Takeoff Thrust (Uninstalled, lb)	41,100	36,200
Overall Pressure Ratio	38.6	No Change
Bypass Ratio	6.51	No Change
Fan Pressure Ratio	1.74	No Change



PRATT & WHITNEY AIRCRAFT GROUP
COMMERCIAL PRODUCTS DIVISION

TABLE 3 (Cont'd)

	<u>Original</u>	<u>Revised</u>
Turbine Rotor Inlet Temperature (F) (84 F Day Takeoff Condition)	2,500	No Change
Exhaust System Configuration	Mixed Flow	No Change
High-Pressure Compressor Inlet Hub/Tip Ratio	0.63	0.56

The preliminary design of the exhaust mixer for the flight propulsion system was updated, using the mixer model test results obtained in the Phase I supporting technology program. The updated configuration has been used for model definition in Phase II. This configuration features 18 lobes, a 75-percent penetration level, and a length/diameter ratio of 0.606. Study results indicated that an 18-lobe configuration with an increased penetration level contributes to improved mixer equivalent performance (change in thrust specific fuel consumption caused by thrust coefficient, C_v , weight, and drag).

Vibration dampers on the mixer have been eliminated. Pratt & Whitney Aircraft demonstrated engine experience has shown that there are no inherent vibration problems in the mixer. Damping of potential panel vibration has been accounted for through the use of ribbed side panels, which, if necessary, can be welded or riveted to the lobes. A "belly band," directly attached to the outer lobes, will provide damping of buckling or gross lobe vibrations, if required. Additional studies indicated that the temperatures in the tailpipe region permit the use of graphite polyimide honeycomb in place of aluminum-brazed titanium. This substitution results in a 80-lb weight reduction.

The active clearance control system is one of the many design features that contribute toward the achievement of tight running clearances and, therefore, increased performance benefits. A schematic representation of the current active clearance control system is shown in Figure 5. This system incorporates a combination of external fan air impingement on the compressor case during cruise operation and a dual manifold feed system, which supplies the internally cooled turbine case with different temperature air between takeoff and cruise.

Air bleed scheduling requirements have been established, taking into account both steady state and transient engine operation. Gapping allowances have been made for normal manufacturing tolerances, normal imbalance and normal maneuver, and cowl loads. These allowances have been minimized by active clearance control at each flight condition. The resultant gapping requirements for the high-pressure compressor and high-pressure turbine are shown in Table 4.



PRATT & WHITNEY AIRCRAFT GROUP
COMMERCIAL PRODUCTS DIVISION

TABLE 4

GAPPING ALLOWANCE ANALYSIS
(Without Active Clearance Control)

<u>Requirement</u>	<u>Gap Requirement (in.)</u>	
	<u>HPC</u>	<u>HPT</u>
Grind Tolerances and Eccentricities	0.004	0.005
Rotor Whirl, Ovalization, Surge, and Gusts	0.002	0.001
Normal Maneuvers	<u>0.004</u>	<u>0.007</u>
TOTAL	0.010	0.013

The air scheduling system for the high-pressure compressor and the high-pressure turbine is such that the pinch point occurs at the flight conditions shown in in Table 5. The resultant clearances at cruise conditions (status clearances), including those for the low-pressure turbine, are compared with goal clearances in Table 6. The active clearance control bleed scheduling for the low-pressure turbine has been made similar to that of the high-pressure turbine except that the flow rate and mix schedule will be adjusted to minimize low-pressure turbine tip clearances.

TABLE 5

PINCH POINT IDENTIFICATION

<u>High-Pressure Compressor</u>	<u>Pinch Point</u>
Rotor 6	SLTO
7	DECEL
8	SLTO
9	ACCEL TO TAKEOFF
10	BEGIN CRUISE
11	BEGIN CRUISE
12	ACCEL
13	ACCEL
14	DECEL
15	DECEL
<u>High-Pressure Turbine</u> <u>(15th HPC Stage Cooling Air)</u>	
Rotor	ACCEL



PRATT & WHITNEY AIRCRAFT GROUP
COMMERCIAL PRODUCTS DIVISION

TABLE 6
RESULTANT CLEARANCES AT CRUISE CONDITIONS
COMPARED WITH GOAL VALUES

	<u>HPC</u>	<u>HPT</u>	<u>LPT</u>
Average Cruise Tip Clearance	0.012	0.014	*
Goal Cruise Tip Clearance	0.013	0.019	0.019

*To be determined.

The current secondary airflow system incorporates provisions necessary to achieve the required design and low-pressure rotor thrust balance. The secondary flow map is shown in Figure 6.

The items affected by the changes to the secondary flow system include the (1) rear intershaft labyrinth seal and (2) mid-high-pressure compressor bleed requirements.

A carbon seal is used in place of the intershaft labyrinth seal in the rear bearing compartment. This modification substantially minimizes oil leakage, which in turn reduces the demand for discharge bleed air from the compressor intermediate case.

Bleed requirements midway in the high-pressure compressor have been reduced by (1) modifying the inner diameter sealing arrangement in front of the low-pressure turbine, (2) refining the inner cavity cooling requirements of the low-pressure turbine, and (3) re-assessing the requirements for active clearance control in the low-pressure turbine. These refinements reduced secondary air bleed by 0.65 percent.



PRATT & WHITNEY AIRCRAFT GROUP
COMMERCIAL PRODUCTS DIVISION

ORIGINAL PAGE IS
OF POOR QUALITY

ACTIVE CLEARANCE CONTROL SYSTEM SCHEMATIC ILLUSTRATING
EXTERNAL TUBES AND VALVES

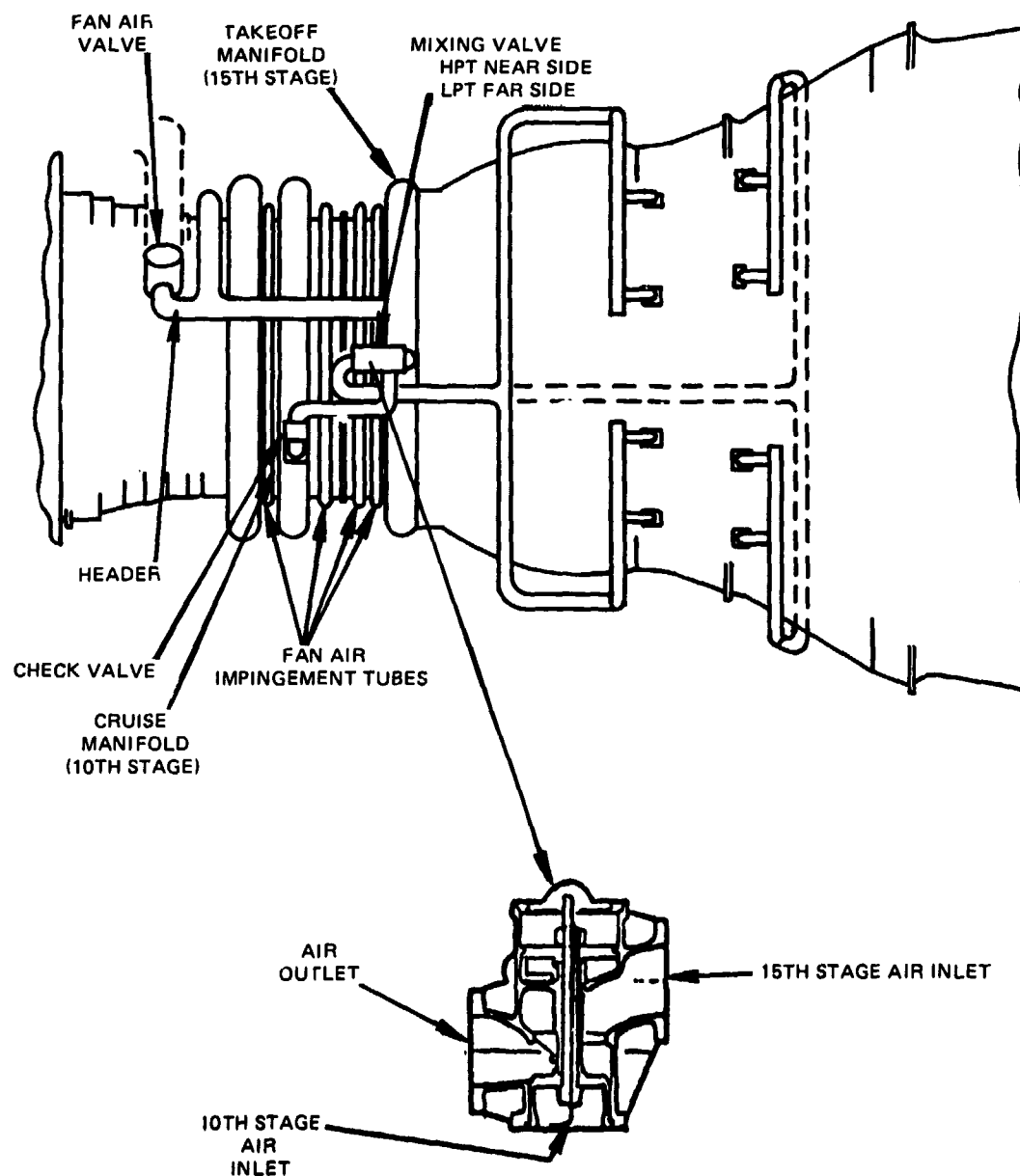


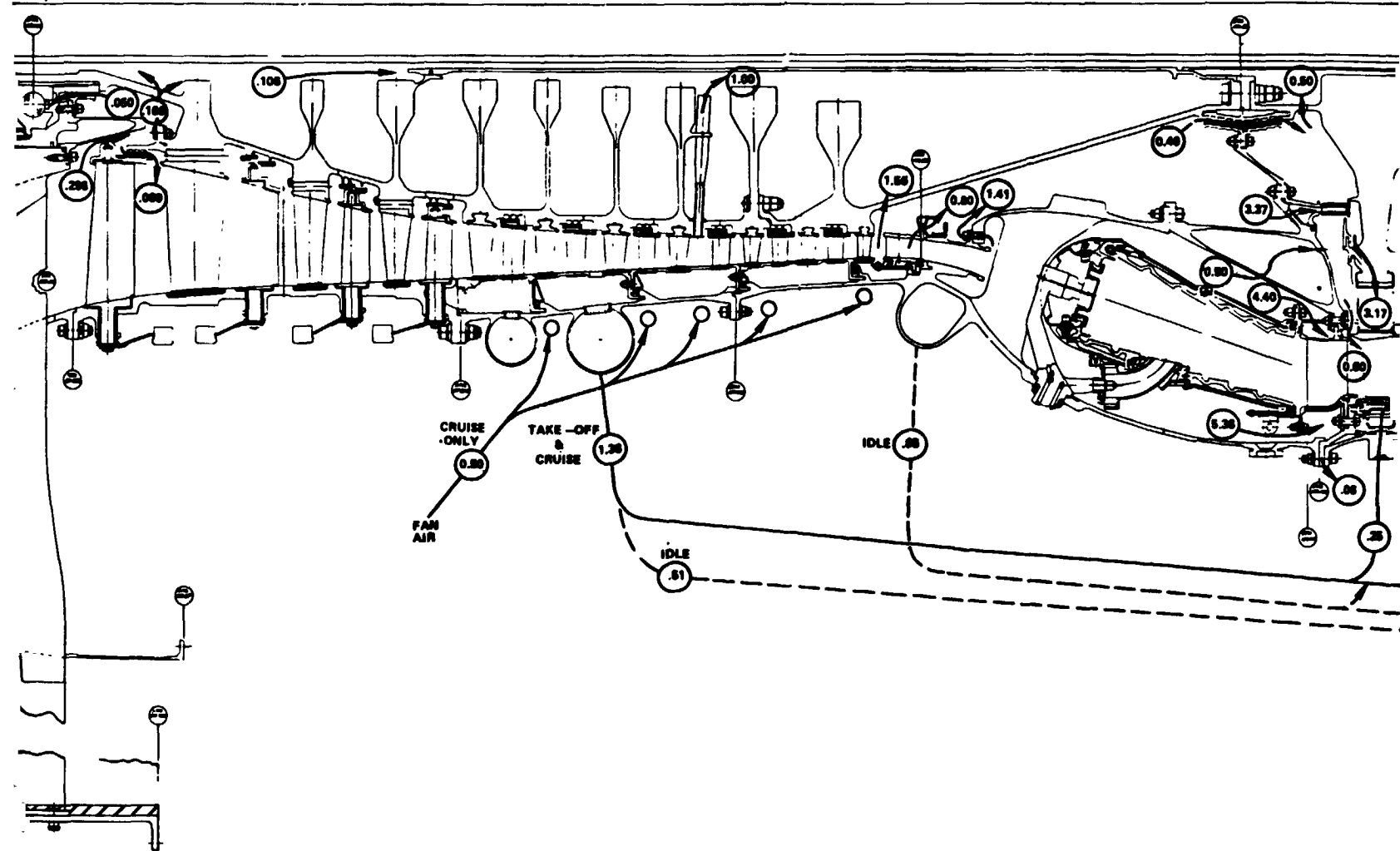
Figure 5 Energy Efficient Engine Current Active Clearance Control System



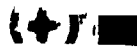
This technical drawing illustrates a mechanical assembly, possibly a pump or engine component, shown in a cross-sectional view. The drawing includes various parts and dimensions, with labels such as .110, .002, .200, and .100. The assembly features a curved housing, a central shaft, and a series of vanes or blades. The drawing is oriented horizontally, with the top of the assembly on the left and the bottom on the right. The drawing is a black and white line drawing, typical of technical specifications.

FOLEGT FRAME

ORIGINAL COPY
OF POOR QUALITY



2 FOLDOUT FRAME



3

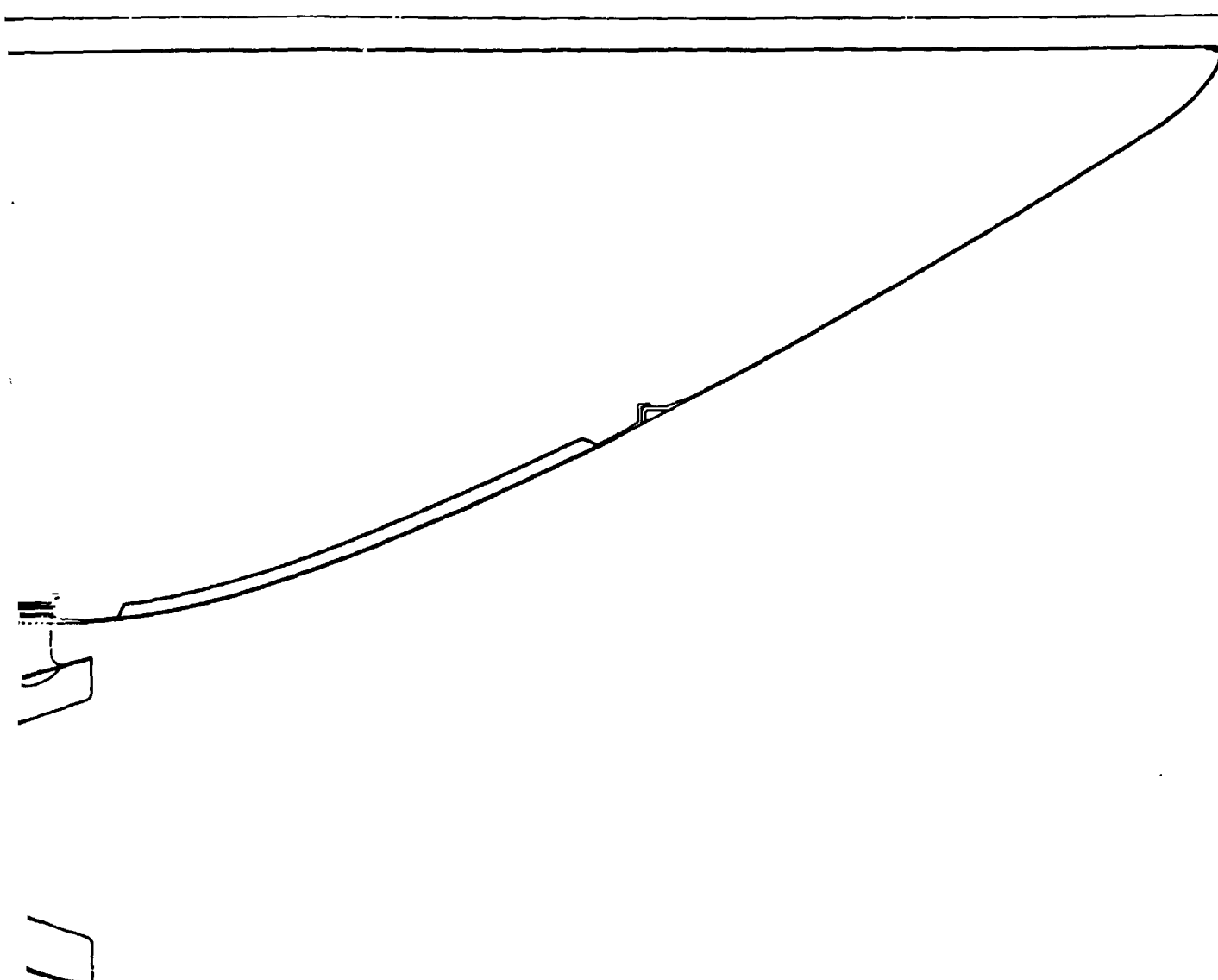
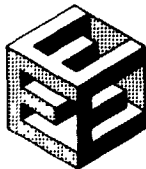


Figure 6 Energy Efficient Engine Secondary Flow Map



PRATT & WHITNEY AIRCRAFT GROUP
COMMERCIAL PRODUCTS DIVISION

3.1.3.3.2 Current Technical Progress

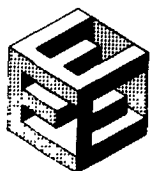
Current Flight Propulsion System Design

Current Materials. The material selection was updated for both the flight propulsion system and the integrated core/low spool. These materials are listed in Table 7, which also provides an explanation of any differences in materials between the flight propulsion system and the integrated core/low spool. A material equivalency listing for reference is presented in Table 8.

Performance Parameters and Detailed Drawings. There were no updates during this reporting period to previously established drawings (showing cooling or secondary flows, active clearance control system, piping, and mount configurations) or performance parameters (including sea level static takeoff, maximum climb, and maximum cruise conditions).

TABLE 7
ENERGY EFFICIENT ENGINE MATERIAL COMPARISON

	<u>FPS</u>	<u>IC/LS</u>	<u>Rationale for IC/LS Difference</u>
<u>Fan</u>			
Blade	PWA1217	PWA1217	
Disk	PWA1215	*AMS4928	Schedule
Stubshaft	AMS4928	AMS4928	
Containment Case	AMS4150/Kevlar	AMS5613	Cost Saving
Sound Treatment	AL Honeycomb	AL Honeycomb	
<u>LPC</u>			
Blades	AMS4928	AMS4928	
Disks	AMS4928	AMS4928	
Hub	AMS4928	AMS4928	
Vanes	*AMS4121	*AMS4121	
Cases	AMS4150	*AMS4135	Schedule
<u>Intermediate Case</u>			
Structural Struts	AMS4911	AMS4911	
Inner Case	PWA1262	AMS4928	Cost Saving
Non Structural Struts	AMS4911	AMS4115	Cost Saving
Outer Case	*AMS4150	*AMS4135	Schedule



PRATT & WHITNEY AIRCRAFT GROUP
COMMERCIAL PRODUCTS DIVISION

TABLE 7 (Cont'd)

	<u>FPS</u>	<u>IC/LS</u>	<u>Rationale for IC/LS Difference</u>
<u>HPC</u>			
Blades			
R6 and R7 R8 - R15	PWA1202 PWA1010	*AMS4928 PWA1010	Schedule
Disks			
R6 and R7 R8 - R11 R12 and R13 R14 and R15	AMS4928 *PWA1224 *PWA1225 MERL80	AMS4928 *PWA1224 *PWA1226 PWA1099	Availability and Cost FPS Material Not Available
Non-Vortex Tubes	AMS4911	AMS4911	
Center Tube	AMS5613	AMS5613	
Vanes			
IGV S6 - S8 S9 - S12 S13 and S14 EGV	AMS4132 AMS5613 AMS5508 AMS5596 PWA649	AMS5613 AMS5613 AMS5616 AMS5662 AMS5663	Aluminum Difficult to Inst. Cost Saving and Schedule Cost Saving and Schedule Cost Saving and Schedule
Front Case	AMS4928	AMS4928	
Rear Case	PWA1214	PWA1214	
IGV ID Shroud	AMS4132	AMS5613	For Compatibility with Vane
<u>Diffuser/Burner</u>			
Diffuser			
Inner Prediff. Wall Strut Assembly	*AMS5662 PWA649 (HIP)	*AMS5662 PWA649	Schedule



PRATT & WHITNEY AIRCRAFT GROUP
COMMERCIAL PRODUCTS DIVISION

TABLE 7 (Cont'd)

	<u>FPS</u>	<u>IC/LS</u>	<u>Rationale for IC/LS Difference</u>
Burner			
Bulkhead	*AMS5754	*AMS5754	
OD Liner Segments	PWA1455	PWA1455	
OD Bird Cage	*AMS5754	*AMS5754	
ID Liner Segments	PWA1455	PWA1455	
ID Bird Cage	*AMS5754	*AMS5754	
<u>HPT</u>			
Rotor			
Blade	MERL200	PWA1480	FPS Material Not Available
Disk/Hub	MERL80	PWA1099	FPS Material Not Available
Sideplate - FRT & RR	MERL80	PWA1099	FPS Material Not Available
Vortex Plate	MERL80	PWA1099	FPS Material Not Available
HPC Discharge Seal	*PWA1075	*PWA1075	
Static			
Vane S1	*MERL200	PWA1480	FPS Material Not Available
OAS	PWA655/Ceramic	PWA655/Ceramic	
OAS Suprts. - FRT & RR	PWA1007	PWA1007	
TOBI System	PWA649/AMS5596	*AMS5662/ AMS5596	Cost Saving and Schedule
Outer Case	*AMS5662	*AMS5662	
<u>Turbine, Intermediate Case</u>			
Hot Strut			
Aero Fairings	*MERL200	*PWA647	FPS Material Not Available
No. 4&5 Brg. Supprt.	PWA649	*AMS5662	Cost Saving and Schedule
Structural Struts	PWA649	*AMS5662	Cost Saving and Schedule
<u>LPT</u>			
Rotor			
Blades R2	*PWA1447	*PWA1447	
R3 and R4	PWA655	PWA655	
R5	MERL101	PWA655	FPS Material Not Available



PRATT & WHITNEY AIRCRAFT GROUP
COMMERCIAL PRODUCTS DIVISION

TABLE 7 (Cont'd)

	<u>FPS</u>	<u>IC/LS</u>	<u>Rationale for IC/LS Difference</u>
Disks	MERL80	PWA1099	FPS Material Not Available
Spacer/Seals	*MERL80	*PWA1099	FPS Material Not Available
Hubs	MERL80	PWA1099	FPS Material Not Available
Static			
Vanes S2 S3 - S5	*MERL200 PWA655	*PWA1480 PWA655	FPS Material Not Available
Shrouds & Seals	AMS5536	AMS5536	
Case	AMS5662	AMS5662	
Exhaust Case			
ID/OD Case	MERL101	AMS5666	FPS Material Not Available
Struts	MERL101	AMS5599	FPS Material Not Available
LPT Shaft	PWA733	PWA733	
<u>MIXER AND EXHAUST</u>			
Mixer			
Mixer Lobes	PWA1231	AMS5599	Cost Saving
Mixer Support	MERL101	AMS5666	FPS Material Not Available
Tailplug	AMS5599/AMS4910	AMS5599	Cost Saving
Center Vent Static	AMS5504	AMS5504	

*Revised from December 1979



TABLE 8
MATERIAL EQUIVALENCY

PWA 647	MAR-M509
PWA 649	Inconel 718
PWA 655	Inconel 713C
PWA 733	17-22-A; Templex (Low Alloy Steel)
PWA 1007	Waspaloy
PWA 1010	Inconel 718
PWA 1075	A286
PWA 1099	Modified IN-100 Alloy (Formerly MERL 76)
PWA 1202	Titanium (8AL-1MO-1V)
PWA 1214	Titanium (6AL-2SN-4ZR-2MO) High Creep Strength
PWA 1215	Titanium (6AL-4V) Forged Below Beta Transus
PWA 1224	Titanium (6AL-2SN-4ZR-2MO) Forged Below Beta Transus
PWA 1225	Titanium (6AL-2SN-4ZR-2MO) Forged Above Beta Transus
PWA 1226	Titanium (6AL-2SN-4ZR-2MO) Forged, Beta Annealed, Precipitation Heat Treated
PWA 1231	Titanium (6AL-2SN-4ZR-2MO) Cross Rolled, Beta Annealed, Precipitation Heat Treated
PWA 1262	Titanium (6AL-4V) Cast
PWA 1422	MAR-M 200 + HF
PWA 1447	MAR-M-247

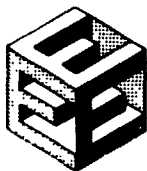


TABLE 8 (Cont'd)

PWA 1455	Modified B-1900
PWA 1480	Single Crystal NI Alloy
MERL 80	Modified IN-100 Alloy
MERL 101	Titanium Aluminide Alloy
MERL 200	Single Crystal NI Alloy

System-Related Activities

All of the work planned for system-related activities for this reporting period was completed. Table 9 presents a summary of the work accomplished, including updates to the design of the flight propulsion system, component design support, economic and fuel burn analyses support, and NASA requests. Results and conclusions are summarized in the following paragraphs.

TABLE 9

SUMMARY OF ANALYSIS AND DESIGN UPDATING EFFORT
FOR THE CURRENT REPORTING PERIOD

<u>EFFORT</u>	<u>FPS DESIGN REFINEMENT</u>	<u>REQUIREMENT COMPONENT DESIGN SUPPORT</u>	<u>BENEFIT EVALUATION</u>	<u>NASA REQUEST</u>
FPS Status Cruise TSFC Breakdown	X	X	X	
Status DOC Update			X	X
Fan Map Update Effect	X	X	X	
Active Clearance Control Philosophy Update	X	X		
Windmilling Performance		X		
Noise Reviews	X	X	X	X
IC/LS Performance Update			X	X
IC/LS Nacelle Design Parameters		X		
IC/LS Acoustic Treatment Options		X	X	



PRATT & WHITNEY AIRCRAFT GROUP
COMMERCIAL PRODUCTS DIVISION

Flight Propulsion System Cruise Thrust Specific Fuel Consumption Breakdown Update. The breakdown of thrust specific fuel consumption improvement of the flight propulsion system relative to that of the JT9D-7A reference engine was redefined, based on the March 1980 update at maximum cruise. Table 10 compares the results with the previous breakdown of May 1979. Performance-related flight propulsion system design changes since the May 1979 update are (1) an improved design point location on the fan rotor map, (2) refined fan duct exit guide vane losses, (3) numerous secondary airflow system revisions, (4) blade tip-to-case clearance improvements in the high-pressure compressor and high-pressure turbine, and (5) a drag increase resulting from an update to the preliminary designs of the exhaust mixer and nacelle.

TABLE 10

COMPARISON OF FLIGHT PROPULSION SYSTEM THRUST SPECIFIC FUEL CONSUMPTION

(JT9D-7A Reference Engine; Maximum Cruise: 35,000 ft;
0.8 Mach no; Standard Day)

	TSFC Change (Percent)	
	MAY 1979 STATUS	MARCH 1980 STATUS
Low-Pressure Spool	-5.8	-6.0
High-Pressure Spool	-3.5	-3.7
Cycle	-3.2	-3.2
Mixing/Installation	-2.4	-2.2
TOTAL	-14.9	-15.1

Flight Propulsion System Direct Operating Cost Update. The effect of the March 1980 maximum cruise thrust specific fuel consumption estimate on the average direct operating cost for the study airplanes and missions was assessed. (Weight and costs were not updated at that time, so their effects on direct operating cost are unchanged from those of the October 1979 update.) The results of this assessment showed an improvement in direct operating cost advantage for the flight propulsion system relative to the JT9D-7A reference engine. These results are summarized in Table 11.



TABLE 11

FLIGHT PROPULSION SYSTEM AVERAGE DIRECT OPERATING COST UPDATE

(JT9D-7A Reference Engine)

<u>Flight Propulsion System Change</u>	<u>Direct Operating Cost Change (Percent)</u>
-0.4% Δ TSFC (Max. Cruise)	-0.2
- - - Δ Weight (Not Updated)	-
- - - Δ Cost (Not Updated)	-
- - - Δ Maintenance Cost (Not Updated)	-
TOTAL	-0.2
10/79 Status	-7.4
3/80 Status	-7.6

Fan Map Update. At the completion of the detailed aerodynamic design of the fan, updates were made to the fan rotor and duct exit guide vane performance maps, and the maps were incorporated into the engine performance simulation. Their impacts on flight propulsion system performance were then determined. Performance changes relative to the previous fan representation were small at the maximum cruise and maximum climb flight conditions and only slightly larger at takeoff (see Table 12). The major cause of these changes is a reduction in fan duct efficiency. Figure 7 shows the resulting difference in part power cruise thrust specific fuel consumption. A 0.1-percent performance penalty occurred at the minimum thrust specific fuel consumption condition. This resulted from a lower peak efficiency relative to that of the previous fan.

The inner stator (S1) and low-pressure compressor representations were not revised in the propulsion system simulation because the designs of these components are not yet complete. The effects of the revisions to the duct section map on low-pressure compressor operating lines, however, were small.



CLIMB FUEL CONSUMPTION
OF POOR QUALITY

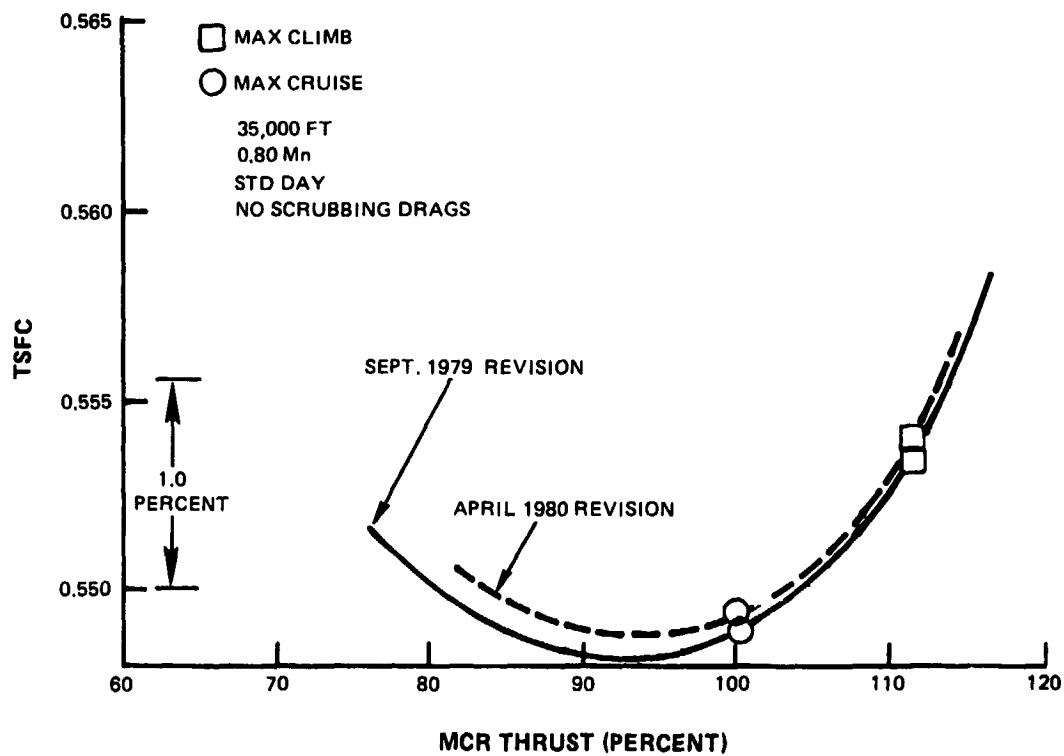


Figure 7 Updated Fan Impact on Flight Propulsion System Cruise Thrust Specific Fuel Consumption - Lower peak fan efficiency has caused a 0.1-percent penalty at part power cruise.

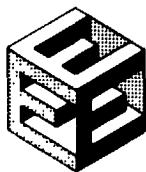
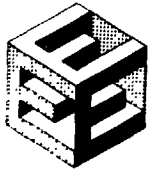


TABLE 12

EFFECTS OF FAN DESIGN MAPS ON FLIGHT PROPULSION
SYSTEM UNINSTALLED PERFORMANCE

	<u>Map Representation</u>	
	<u>September</u> <u>1979</u>	<u>April</u> <u>1980</u>
<u>Maximum Cruise</u> <u>(35,000 ft., 0.8 Mn, Standard)</u>		
Δ Combustor Exit Temperature (F)	Base	0
Δ Thrust (Percent)		+0.17
Δ TSFC (Percent)		+0.05
Δ Fan Duct Efficiency (Δ Percent)		-0.20
Δ Overall Pressure Ratio (Percent)		0
<u>Maximum Climb</u> <u>(35,000 ft., 0.8 Mn, Standard +18 F)</u>		
Δ Combustor Exit Temperature (F)	Base	+15
Δ Thrust (Percent)		+0.20
Δ Thrust Specific Fuel Consumption (Percent)		+0.16
Δ Fan Duct Efficiency (Δ Percent)		-0.10
Δ Fan Duct Pressure Ratio (Percent)		+0.06
Δ Fan Duct Corrected Airflow (Δ Percent)		+0.10
Δ Fan Corrected Rotor Speed (Δ Percent)		-1.00
Δ Overall Pressure Ratio (Percent)		-0.49
<u>Takeoff</u> <u>(0 ft., 0 Mn, Standard +25 F)</u>		
Δ Combustor Exit Temperature (F)	Base	+1
Δ Thrust (Percent)		+0.33
Δ Thrust Specific Fuel Consumption (Percent)		+0.98
Δ Fan Duct Efficiency (Δ Percent)		-1.15
Δ Fan Duct Pressure Ratio (Percent)		+0.13
Δ Fan Duct Corrected Airflow (Δ Percent)		-0.10
Δ Fan Duct Corrected Rotor Speed (Δ Percent)		+1.00
Δ Overall Pressure Ratio (Percent)		+1.00

Active Clearance Control Philosophy Update. Analyses were conducted to establish a refined tip clearance control philosophy for the high-pressure spool components. The results of these analyses were then used to update flight propulsion system performance at the takeoff and climb flight conditions consistent with the March 1980 maximum cruise update. The detailed design of these components during the March 1980 time frame indicated that takeoff and cruise aerodynamic design point tip clearances are similar.



PRATT & WHITNEY AIRCRAFT GROUP
COMMERCIAL PRODUCTS DIVISION

Further investigation of the designs showed that tip clearance at the climb condition was essentially equal to the cruise and design point clearances. Tip clearances are summarized in Table 13.

The high-pressure compressor uses air from the fan duct for clearance control. The fan duct bleed is closed at takeoff, and opens for high-pressure compressor case cooling at cruise and climb conditions.

The high-pressure turbine uses air bleed from the 10th stage of the high-pressure compressor at cruise and climb conditions. For clearance control at takeoff conditions, analysis results indicated that the high-pressure turbine required a 30- to 70-percent air bleed split from the 10th and 15th stages of the high-pressure compressor to maintain the proper tip clearance.

Windmilling Performance. Flight propulsion system windmilling performance was defined in order to provide conditions for combustor sector rig simulated altitude relight testing. These data were derived using the design table performance simulation for consistency within the combustor program. Windmilling performance points were generated in a Mach number range of 0.4 to 0.85 and at altitudes of 20,000 feet and 35,000 feet. A summary of combustor windmilling conditions is presented in Table 14.

Noise Reviews. Several areas of flight propulsion system noise were reviewed. These included a noise comparison with the JT9D-7A reference engine, airplane design data for noise measuring station calculations, and a general updating of estimated noise.

The estimated noise levels of the JT9D-7A reference engine were compared with those of the flight propulsion system installed in the Pratt and Whitney Aircraft international airplane. The results of this comparison (summarized in Table 15) indicates that the noise level of the JT9D-7A reference engine is approximately 2 EPNdB greater than that of the flight propulsion system. A rating philosophy difference between the engines, however, gave the JT9D-7A-powered airplane a relative altitude advantage of over 300 feet at the takeoff noise measuring station. When the rating of the two engines was equalized, the takeoff noise of the flight propulsion system was estimated at 4.3 EPNdB lower than that of the JT9D-7A reference engine.

NASA was supplied with data from the airplanes of both Pratt & Whitney Aircraft and the airframe manufacturers in order to provide additional insight into the impact of engine thrust size or rating philosophy on takeoff altitude over the noise station. Collected data are presented in Table 16. A comparison of the presented data shows that the engines for the airframe manufacturer airplanes are takeoff-sized and that the engines for the Pratt & Whitney Aircraft airplanes are cruise-sized.



PRATT & WHITNEY AIRCRAFT GROUP
COMMERCIAL PRODUCTS DIVISION

TABLE 13

SUMMARY OF UPDATED FLIGHT PROPULSION SYSTEM
HIGH-PRESSURE SPOOL COMPONENT TIP CLEARANCE

	AERO DESIGN POINT (35,000 FT., 0.8 Mn, Std.)		TAKEOFF (0 FT., 0 Mn, Std., +25 F)		MAXIMUM CLIMB (35,000 FT., 0.8 Mn, Std., +18 F)	
	10/79	3/80	10/79	3/80	10/79	3/80
Bleed Source:						
HPC	Fan HPC Stage 10	Fan HPC Stage 10	None HPC Stage 10	None HPC Stage 15	Fan HPC Stage 10	Fan HPC Stage 10
HPT						
Tip Clearance (Avg.):						
HPC (in.)	0.013	0.012	0.019	0.014	0.019	0.014
HPT (in.)	0.019	0.014	0.027	0.013	0.027	0.013

*30/70 percent airflow mixture



PRATT & WHITNEY AIRCRAFT GROUP
COMMERCIAL PRODUCTS DIVISION

TABLE 14

**FLIGHT PROPULSION SYSTEM COMBUSTOR CONDITIONS DURING
WINDMILLING
(FUEL FLOW = 0 LB./HR.)**

<u>ALTITUDE</u> <u>FT.</u>	<u>MACH NO.</u>	<u>AMB. TEMP.</u> <u>(F)</u>	<u>COMB. INLET</u> <u>TEMP</u> <u>(F)</u>	<u>COMB. INLET</u> <u>PRESS.</u> <u>lb/sq. in.</u>	<u>COMB. INLET</u> <u>AIRFLOW</u> <u>lb/sec</u>
35,000	0.40	-66	-46	3.54	0.62
35,000	0.45	-66	-43	3.59	0.77
35,000	0.51	-66	-38	3.67	1.01
35,000	0.57	-66	-33	3.76	1.19
35,000	0.63	-66	-25	3.91	1.44
35,000	0.69	-66	-14	4.09	1.65
35,000	0.75	-66	-3	4.33	1.89
35,000	0.85	-66	25	4.88	2.44
20,000	0.40	-12	11	6.92	1.14
20,000	0.45	-12	15	7.02	1.44
20,000	0.51	-12	20	7.16	1.81
20,000	0.57	-12	27	7.35	2.20
20,000	0.63	-12	38	7.74	2.76
20,000	0.69	-12	52	8.23	3.31
20,000	0.75	-12	66	8.80	3.83
20,000	0.81	-12	85	9.57	4.54
20,000	0.85	-12	102	10.48	5.32

TABLE 15

**COMPARISON OF FLIGHT PROPULSION SYSTEM AND
JT9D-7A (REFERENCE ENGINE) NOISE
EPNdB
PRATT AND WHITNEY AIRCRAFT INTERNATIONAL AIRPLANE**

<u>Noise Condition</u>	<u>JT9D-7A Reference Engine</u>	<u>Flight Propulsion System</u>
Approach	105.6	103.9
Takeoff	104.8	102.9
Sideline	97.8	95.5



PRATT & WHITNEY AIRCRAFT GROUP
COMMERCIAL PRODUCTS DIVISION

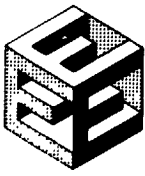
TABLE 16

AIRPLANE DESIGN SUMMARY

ENERGY EFFICIENT ENGINE AND JT9D-7A ENGINE INSTALLATIONS

	<u>DOMESTIC</u>		<u>INTERNATIONAL</u>	
	<u>EEE</u>	<u>JT9D-7A</u>	<u>EEE</u>	<u>JT9D-7A</u>
<u>Pratt & Whitney Aircraft</u>				
Field Length (ft)	8,000	7,000	10,000	8,500
Initial Cruise Alt. (ft)	35,000	35,000	33,000	33,000
<u>Boeing</u>				
Field Length (ft)	6,000	6,000	-	-
Initial Cruise Alt. (ft)	40,000	38,000	-	-
<u>Lockheed</u>				
Field Length (ft)	6,975	6,970	9,460	9,400
Initial Cruise Alt. (ft)	37,000	35,000	34,000	33,000
<u>Douglas</u>				
Field Length (ft)	8,000	8,000	11,000	11,000
Initial Cruise Alt. (ft)	34,400	34,100	33,300	32,700

At the close of this reporting period, a flight propulsion system noise reassessment was started. The purpose of this reassessment was to evaluate the status engine configuration and performance and a revised noise prediction procedure. Engine and airframe data required for this analysis were defined. The airframe used was the Pratt & Whitney Aircraft international quadjet, which has not changed since previous noise estimates. The engine performance data used were consistent in definition with the March 1980 flight propulsion system update, and the dimensions for the engine and nacelle components were based on the flight propulsion system definition of 31 July 1980. Figure 8 shows the resulting flowpath definition and the locations currently available for acoustic treatment. Acoustic analysis now being conducted is including the noise impact of pylon and lower bifurcation wall treatment.



ORIGINAL PAGE IS
OF POOR QUALITY

FLIGHT PROPULSION SYSTEM
7-31-80 DEFINITION (BASE SIZE)

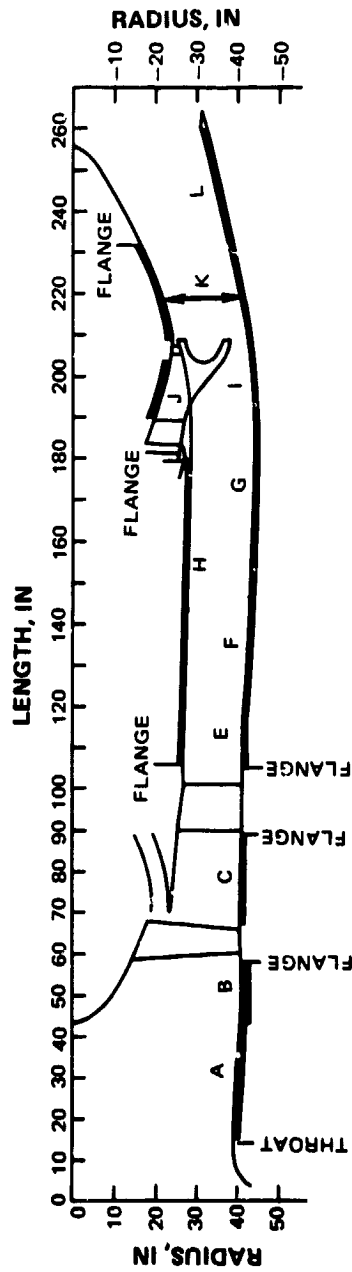
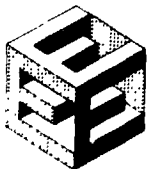


Figure 8 Flight Propulsion System



Integrated Core/Low Spool Performance Update

The integrated core/low spool performance evaluation was updated to account for design changes since September 1978. Major changes affecting performance are (1) secondary system airflow increases and fan map improvements associated with the October 1979 flight propulsion system update; (2) high-pressure compressor and high-pressure turbine tip clearance improvements, secondary system airflow reductions, and a nacelle drag increase associated with the March 1980 flight propulsion system update; and (3) elimination of the scaled fan rig from the program. The results of the integrated core/low spool performance evaluation are presented in Table 17.

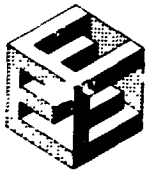
TABLE 17

INTEGRATED CORE/LOW SPOOL PERFORMANCE EVALUATION RESULTS

- o Expected (50% probability of achievement) integrated core/low spool thrust specific fuel consumption at the maximum cruise flight condition is -10.3% relative to the JT9D-7A reference, 0.4 percent worse than the September 1978 estimate.
- o Expected thrust specific fuel consumption results are the same for the integrated core/low spool with the alternate shrouded fan.
- o Compression system sea level operating line shifts relative to the flight propulsion system level are not significant.
- o The integrated core/low spool design table exhaust nozzle area is still optimum.
- o Sea level static takeoff thrust at rated temperature is increased by 1.75%.

A "fixed hardware" approach was used in evaluating the performance of the integrated core/low spool. Turbine geometries were held constant at the component aerodynamic design levels. Mixing plane areas were also held constant at the integrated core/low spool design table levels, and combustor exit temperature (CET) ratings were fixed at the integrated core/low spool design table levels. Jet nozzle area was varied for possible reoptimization. Expected levels of component, turbine cooling air, and secondary system airflow performance were reassessed consistent with the October 1979 and March 1980 flight propulsion system updates and the current program definition. Reassessed component performance results are presented in Table 18.

Factors contributing toward the currently expected integrated core/low spool maximum cruise thrust specific fuel consumption are shown in Table 19. The



PRATT & WHITNEY AIRCRAFT GROUP
COMMERCIAL PRODUCTS DIVISION

itemized component and system changes occurring since September 1978 resulted in a net thrust specific fuel consumption penalty of 0.4 percent. The new status level represents a 10.3-percent advantage for the integrated core/low spool relative to the JT9D-7A reference engine. The results of additional analysis indicated that these performance results are valid for either the shroudless or shrouded fan. Elimination of the shroudless fan scaled rig test from the program reduced the expected outer fan efficiency during the integrated core/low spool testing from 85.7 to 84.5 percent. The efficiency of the alternate fan is also expected to be 84.5 percent in the integrated core/low spool because, although it is inherently lower in fully developed efficiency because of shroud-induced aerodynamic losses, its technology is currently more mature.

A breakdown of the major elements contributing to the thrust specific fuel consumption improvement of the integrated core/low spool relative to that of the JT9D-7A reference engine was defined, based on the May 1980 update at maximum cruise. These elements and their contributions are presented in Table 20.

Figure 9 shows variations of integrated core/low spool thrust specific fuel consumption and thrust with changes in exhaust nozzle area. Takeoff and cruise thrusts are near maximum levels, and cruise thrust specific fuel consumption is essentially optimum with the integrated core/low spool design table area. Therefore, no nozzle area revision is required at this time.



PRATT & WHITNEY AIRCRAFT GROUP
COMMERCIAL PRODUCTS DIVISION

CONFIDENTIAL
OF PROPRIETARY

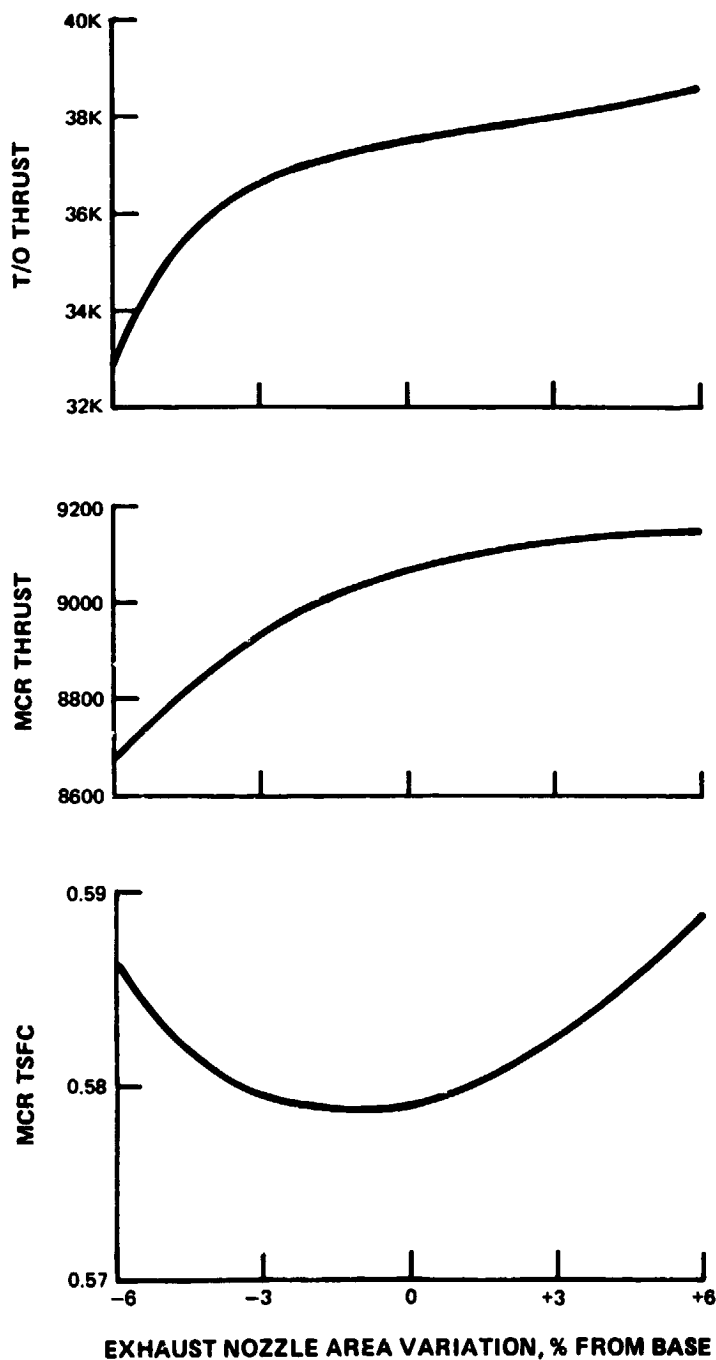


Figure 9 Effect of Exhaust Nozzle Area Variation on Integrated Core/Low Spool Performance (Base area is design table value)



PRATT & WHITNEY AIRCRAFT GROUP
COMMERCIAL PRODUCTS DIVISION

TABLE 18

EXPECTED INTEGRATED CORE/LOW SPOOL COMPONENTS (MAY 1980)
AT RESPECTIVE AERODYNAMIC DESIGN POINTS (35,000 FT., 0.8 MN)
(50% PROBABILITY OF ACHIEVEMENT)

η FNOD	84.5
η FNID	87.5
η LPC	87.4
η HPC	86.5
Δ P/P BURN	5.5%
η HPT	87.3
Δ P/P TRANS	1.5%
η LPT	90.1
Δ P/P TEGV	0.9%
Δ P/P DUCT	0.74%
Δ P/P DUCT MIXER	0.29%
Δ P/P PRI MIXER	0.57%
Δ P/P TAILPIPE	0.43%
TCA % WAE	17.3%
DRAG	385 lb



PRATT & WHITNEY AIRCRAFT GROUP
COMMERCIAL PRODUCTS DIVISION

TABLE 19

INTEGRATED CORE/LOW SPOOL
THRUST SPECIFIC FUEL CONSUMPTION UPDATE SUMMARY - MAY 1980

Maximum Cruise (35K Ft., 0.8 Mn, Standard), JT9D-7A Reference Engine

<u>Component/System Change</u>	<u>TSFC Change (Percent)</u>
10/79 Secondary Flow System (+1.35% Core Flow)	+0.50
10/79 Fan Rotor Map/Exit Guide Vane Loss	-0.30
3/80 Secondary Flow System (-0.5% Core Flow)	-0.25
3/80 Nacelle Drag (+24 Lb.)	+0.25
3/80 +0.1% Δ HPC Efficiency (0.013 - 0.012 in. Average Tip Clearance)	-0.05
3/80 +0.6% Δ HPT Efficiency (0.019 - 0.014 in. Tip Clearance)	-0.35
3/80 -1.2% Δ Fan O.D. Efficiency (Elimination of Scaled Fan Rig)	+0.60
3/80 -0.3% Δ Fan I.D. Efficiency (Elimination of Scaled Fan Rig)	+0.02
Total	+0.42
9/78 Status	-10.7
5/80 Status	-10.3

TABLE 20

INTEGRATED CORE/LOW SPOOL THRUST SPECIFIC FUEL CONSUMPTION IMPROVEMENT
MAY 1980 STATUS

Maximum Cruise (35K Ft., 0.8 Mn, Standard), JT9D-7A Reference Engine

	<u>TSFC Change (Percent)</u>
Low Pressure Spool	-2.8
High Pressure Spool	-1.7
Cycle	-3.9
Mixing/Installation	-1.9
TOTAL	-10.3



Expected integrated core/low spool compression system sea level operating line shifts relative to the flight propulsion system base operating lines are summarized in Table 21. The design match does not affect the fan operating line. Resulting operating line variations slightly improve takeoff surge margins for both compressors. The conclusion based on this analysis is that design turbine vane areas are acceptable for the test program.

TABLE 21

INTEGRATED CORE/LOW SPOOL COMPRESSION SYSTEM OPERATING LINE VARIATION
FIXED TURBINE, EXHAUST MIXER/NOZZLE DESIGN GEOMETRY
SEA LEVEL STATIC, TAKEOFF

<u>Component</u>	<u>Operating Line Change (Percent)*</u>
Fan	0.0
Low-Pressure Compressor	-0.5
High-Pressure Compressor	-1.6

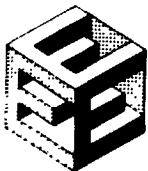
* Relative to flight propulsion system operating line

Component and system changes made since September 1978 combine to improve expected sea level static takeoff thrust at rated combustor exit temperature by 1.75 percent. Integrated core/low spool takeoff thrust is currently estimated to be 37,440 pounds.

Integrated Core/Low Spool Nacelle Design Parameters

Definition of the nacelle performance design parameters for the integrated core/low spool was initiated. The maximum inlet airflow condition and tentative inlet acoustical treatment requirements have been identified. A performance review is now underway to determine the requirements for the maximum fan duct airflow and the exhaust nozzle area variation for the bifurcated duct configuration.

A review of the nacelle inlet requirements was completed. The results of this review indicated that the preliminary design parameters established early in the program for the flight propulsion system should be maintained. The inlet will be designed for growth capability. It will accommodate 8 percent greater airflow than the base level at the maximum flow flight conditions of 36,089 ft, 0.701 Mach number, standard +18 F, and maximum climb. An inlet length was established to allow an acoustical treatment length-to-fan diameter ratio of 0.56. This acoustical design parameter, however, is currently being re-evaluated as part of the noise reassessment.



The performance study to define the design parameters for the bifurcated fan duct was started. The selected configuration uses bifurcated duct hardware from an existing engine, which is adapted to the Energy Efficient Engine fan case with a 30-inch extension. The tailpipe for the core retains the tailplug design being developed for the mixed exhaust system. Based on this system configuration and approximate nominal fan duct nozzle areas, pressure losses were estimated. These are summarized in Table 22. To complete the inputs required for the performance study, flow coefficient estimates were made for the assumed exhaust nozzle configuration, which is convergent with a sharp-cornered throat. These estimates are plotted as functions of nozzle pressure ratio in Figure 10.

TABLE 22

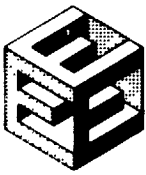
ESTIMATED TOTAL PRESSURE LOSS FOR INTEGRATED CORE/
LOW SPOOL BIFURCATED FAN DUCT SYSTEM
(TAKEOFF: 0 FT., 0 MACH NO., STD)

	<u>Total Pressure Loss - %</u>	<u>Entrance Mach No.</u>	<u>Est. Entrance Area - in.²</u>
Fan Duct			
30 In. Extension	0.17	0.48	2910
Existing Bi-Ducts	1.26	0.35	3750
Nozzles	<u>0.17</u>	<u>0.35</u>	<u>3750</u>
Total	1.60		
Core Tailpipe	0.78	0.31	1065

A preliminary baseline performance estimate was established for the integrated core/low spool with the bifurcated fan duct configuration. Design limits--including compression system stability, maximum airflow through the fan ducts, and possible exhaust nozzle area variation requirements--are now being defined.

Integrated Core/Low Spool Acoustic Treatment Options

Two options for acoustic treatment were evaluated in terms of their impacts on integrated core/low spool test results: (1) bare wall hardware testing with treatment effects analytically derived and (2) use of simple treatment shapes (cones and cylinders) rather than designed contours. Concerns were that if acoustic treatment is eliminated entirely, the accuracy of the noise estimate is reduced, and the use of simple acoustic shapes can adversely affect thrust specific fuel consumption. The results of this assessment indicated: (1) analytically derived, treated noise estimates would be +1.0 to +3.5 EPNdB less accurate than directly measured noise, depending on flight condition and noise source, and (2) the use of simple acoustic shapes will increase thrust specific fuel consumption by approximately 0.2 percent.



The inaccuracies involved in estimating treated noise from hardwall results are summarized in Table 23. These results were derived using an estimated ± 25 percent accuracy for the attenuation predictions.

Simple shapes for acoustic treatment were defined, and the resulting effects on thrust specific fuel consumption were estimated. Assessment results are shown in Table 24. The definition of the acoustic shapes was based on the minimum number of cones and cylinders required to closely approximate the designed flowpath. Resulting losses were estimated based on Mach number and wall static pressure gradient effects.

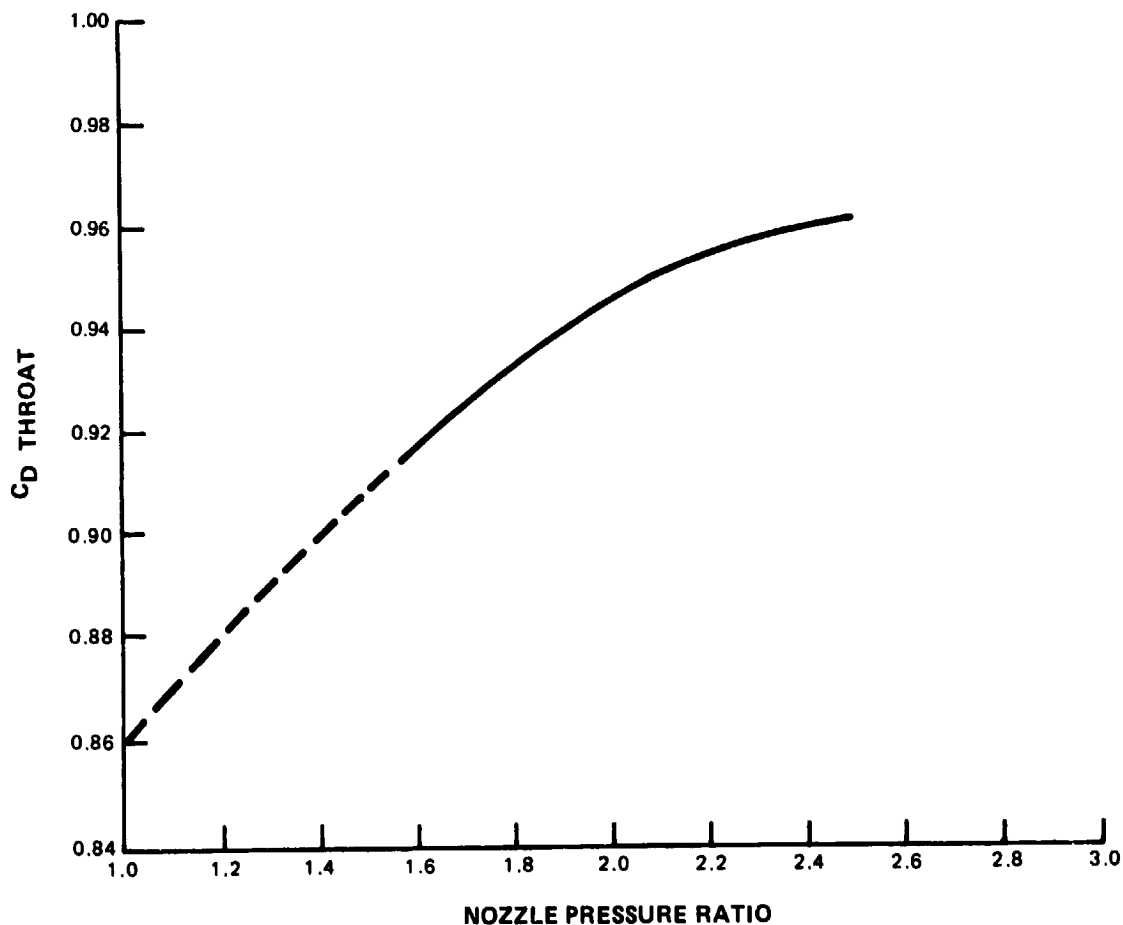
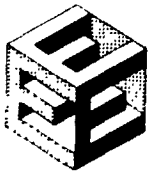


Figure 10 Separate Flow Exhaust Nozzle



PRATT & WHITNEY AIRCRAFT GROUP
COMMERCIAL PRODUCTS DIVISION

TABLE 23

ESTIMATED NOISE TREATMENT ATTENUATION ACCURACY

Noise Source	+ EPNdB	
	Approach	Takeoff
Fan Inlet	1.5	2.0
Fan Aft	3.5	3.0
Turbine	1.0	1.0

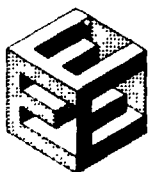
TABLE 24

ESTIMATED PERFORMANCE IMPACT OF SIMPLE ACOUSTIC PANEL SHAPES

Section	Assumed Panel Shape	% TSFC Penalty	Remarks
Inlet	Cone	0.00	Throat to "A" flange is already a cone.
Fan Case	Average Cylinder		"A" flange to blade leading edge.
		0.11	
Fan Duct	Cone		Blade leading edge to fan duct strut.
	Cone	0.04	Inner wall is already a cone.
Tailpipe/Plug	Cone		Outer wall
	Contoured	0.00	Shape set by mixer requirement.
	Total Penalty	0.15%	

3.1.4 Program Risk Assessment

NASA approval was received to reschedule the program risk assessment update to late 1981, for planning purposes.



3.2 TASK 2 COMPONENT TECHNOLOGY

3.2.1 Overall Objective

The overall objectives for Task 2 are to: (1) establish preliminary component configurations, (2) conduct supporting technology programs to evaluate Energy Efficient Engine concepts, (3) produce component detailed designs, and (4) evaluate the Energy Efficient Engine high-pressure compressor, combustor, and high-pressure turbine in full-scale component rigs.

3.2.2 Task Overview

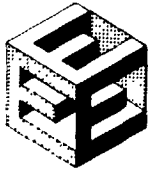
The Task 2 effort focuses on the design, fabrication, and testing of the major components to be used in the core and integrated core/low spool experimental verification programs of Tasks 3 and 4. In addition, the results of Task 2 testing are fed into the flight propulsion system analysis and design updates of Task 1. Specific performance goals for these components are shown in the subsequent component effort sections of this report.

The preliminary component designs are based largely on results from the Energy Efficient Engine Preliminary Design and Integration study (NAS3-20628) combined with results of other government and Pratt & Whitney Aircraft related programs. There are areas where additional evaluation of Energy Efficient Engine concepts is necessary before committing to the Energy Efficient Engine detailed design. In these areas, supporting technology programs provide that evaluation in a timely manner. The detailed component designs are accomplished as an extension of the preliminary component designs, reflecting supporting technology program results, as applicable, and Task 1 input.

Preliminary component designs are "flight" designs and support the propulsion system preliminary design effort of Task 1. Systems (lubrication, breather, thrust balance, and active clearance control) are worked jointly between Tasks 1 and 2 during the preliminary design phase. A detailed design of the exhaust mixer is not accomplished under Task 2. Instead, a test mixer detailed design is provided as part of Task 4.

Program fabrication schedules are stringent, and certain constructions require early starts. In general, raw material is ordered as early as rough shapes can be defined, thus ensuring material availability at the time detailed drawings are completed. As hardware definition becomes known during the detailed design phase, those parts requiring early fabrication are identified and permission to proceed is requested from NASA.

The program logic diagram is shown in Figure 11, and the work plan, in Figure 12. The logic diagram shows the relationship of the supporting technology programs to the component effort. Specific logic diagrams for each component are shown in subsequent sections.



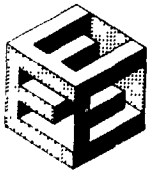
PRATT & WHITNEY AIRCRAFT GROUP
COMMERCIAL PRODUCTS DIVISION

Critical Milestones

- (1) High-Pressure Compressor:
 - (a) Complete first high-pressure compressor rig test.
 - (b) Complete high-pressure compressor airfoil design update.
 - (c) Define the high-pressure compressor airfoil rework for the core.
- (2) Diffuser/Combustor:
 - (a) Confirm the combustor liner configuration.
 - (b) Complete the annular combustor rig test.
- (3) High-Pressure Turbine:
 - o Complete high-pressure turbine rig testing.

Most of the work planned and approved from contract award through the end of the current reporting period (30 September 1980) has been completed. Exceptions are indicated in the appropriate technical progress sections of this report. Figure 12 identifies tasks that were completed during the previous reporting period. It also identifies tasks which were initiated, continued, or completed during the current reporting period. The component discussions that follow describe this work in more detail.

Major program changes affecting Task 2 include (1) elimination of the scaled fan supporting technology program, (2) transfer of the alternate fan analysis and design effort from Task 4 to Task 2, (3) transfer of the primary (shroudless) blade fabrication effort from Task 4 to the TRW subcontract effort is Task 2, and (4) addition of a tangential on-board injection rig test to the high-pressure turbine rig test program.



TASK 2 - COMPONENT ANALYSIS, DESIGN, AND DEVELOPMENT LOGIC DIAGRAM

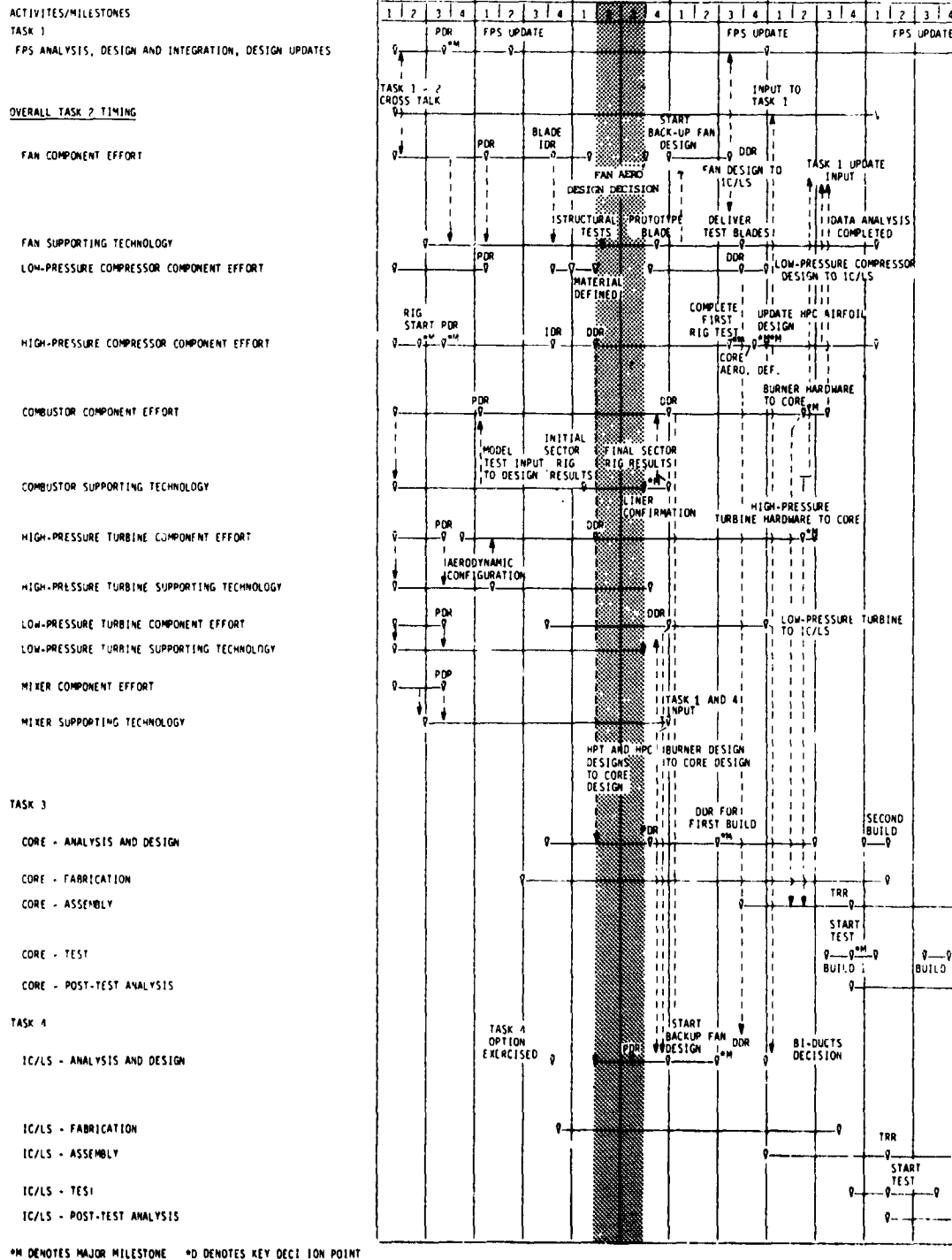
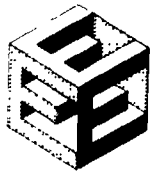


Figure 11 Task 2 Logic Diagram



PRATT & WHITNEY AIRCRAFT GROUP
COMMERCIAL PRODUCTS DIVISION

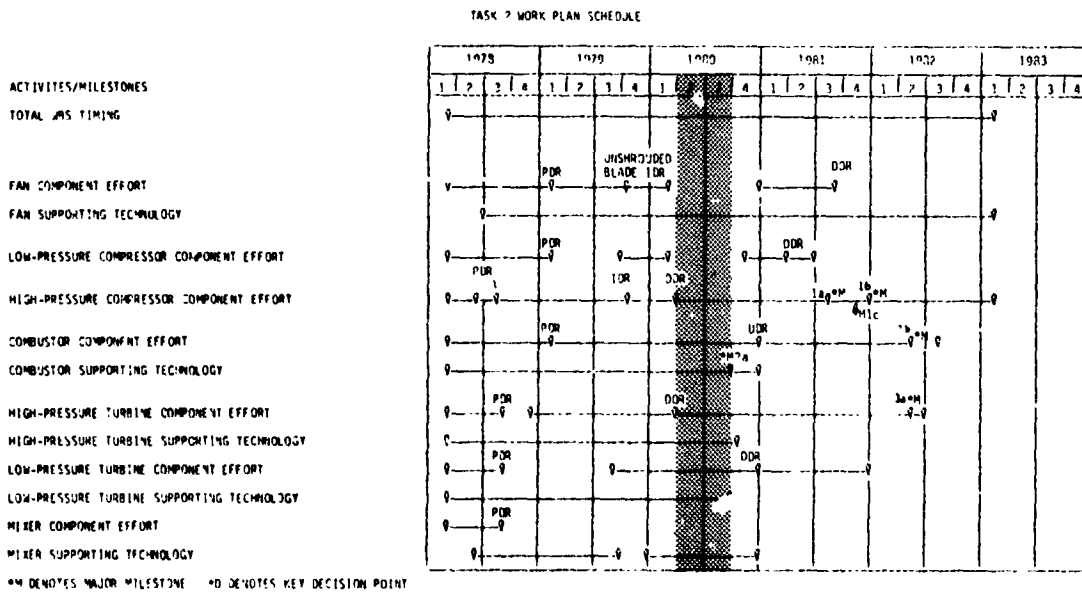


Figure 12 Task 2 Work Plan Schedule



3.2.3 Fan

3.2.3.1 Overall Objective

The overall objective of the fan effort is to design and develop, through supporting technology, a single stage fan utilizing shroudless, hollow titanium blades which produces a pressure ratio of 1.74/1.56 (outer diameter/inner diameter). The duct adiabatic efficiency goal for the flight propulsion system is 87.3 percent, and the expected efficiency of the experimental fan component for the integrated core/low spool phase is 84.5 percent. The aspect ratio of the blade is 2.5. Additional design parameters are shown in Table 25.

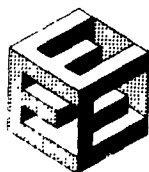
3.2.3.2 Component Program Overview

The overall task effort consists of (1) a preliminary analysis and design phase, which determines the feasibility of the blade design; (2) a shroudless blade detailed design, which completes the blade design and produces drawings for fabrication. (This initial detailed design effort is a two-part program: the blade design is completed in 1979; the remaining fan component hardware design is completed in 1980); (3) an alternate (shrouded) fan component analysis and design task that will provide a more conventional design serving as an alternative to the primary (shroudless) design, if required; and (4) a shroudless blade supporting technology program, which verifies the structural integrity of the blade design. Blades are produced under a subcontract effort by TRW. Figure 13 shows the relationship between program activities and contract Tasks 1, 3, and 4. Critical program milestones of the component effort are noted in the work plan schedule (Figure 14).

TABLE 25

FAN DESIGN PARAMETERS

<u>Specific Parameter Requirements</u>	<u>Aerodynamic Design Point</u>
$W_a \sqrt{\theta T_2} / \sigma T_2$ (lbm/sec)	1372.8
$W_a \sqrt{\theta T_2} / \sigma T_2 / A$ (lbm/sec/sq ft)	43.0
$N / \sqrt{\theta T_2}$ (RPM)	4215.0
$U_{TIP} / \sqrt{\theta T_2}$ (ft/sec)	1496.0
Bypass Ratio (W_a duct/ W_a engine)	6.51
Duct Pressure Ratio	1.74
Duct Adiabatic Efficiency Goal (percent)	87.3
Surge Margin SLTO Goal (percent)	7.5
Aspect Ratio (nominal)	2.5
Hub/Tip Radius ratio	0.34
Taper Ratio	1.46
Number of Fan Blades	24
Design Life (hours)	20,000



PRATT & WHITNEY AIRCRAFT GROUP
COMMERCIAL PRODUCTS DIVISION

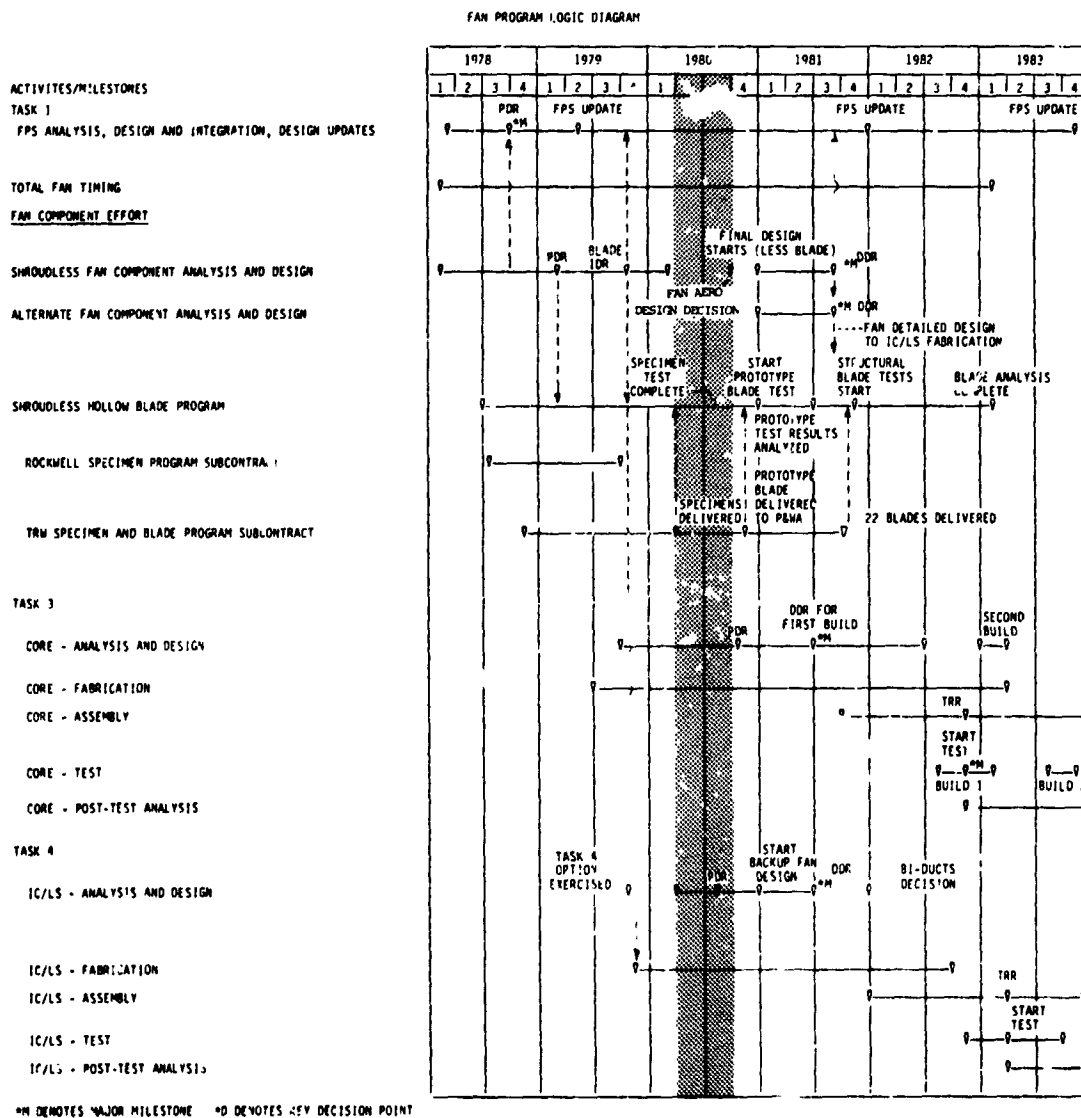


Figure 13 Fan Program Logic Diagram



FAN COMPONENT EFFORT - WORK PLAN SCHEDULE

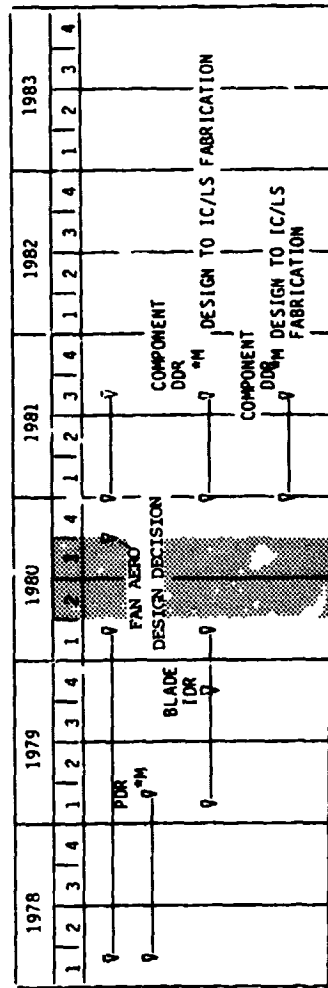


Figure 14 Fan Program Work Plan Schedule



3.2.3.3 Component Effort

3.2.3.3.1 Objective

Design a single stage, hollow, shroudless fan blade that meets or exceeds the stated goals.

3.2.3.3.2 Scope of Total Work Planned

The fan component effort consists of a preliminary analysis and design phase and a detailed analysis and design phase. There is no component rig program. The fan blades for integrated core/low spool testing are fabricated as part of the TRW subcontract effort in Task 2. The remaining component hardware is fabricated as part of the program effort in Task 4.

The preliminary design phase provided a layout drawing and a substantiating design data package (presented to NASA at the preliminary design review in February 1979). This preliminary design of the shroudless fan consisted of a twelve-month effort. During this time, the feasibility of the flight propulsion system fan was also established. The studied designs provided the configuration definition to the supporting technology programs.

The shroudless fan detailed design effort comprises two elements: (1) the detailed design of the blade, completed in 1979, to provide the hollow blade technology program with a blade design which is fabricated under TRW subcontract; and (2) the detailed design of the hub, shaft, nose cone, and fan case in 1981 in time for the Task 4 fabrication phase. An aft part-span shroud fan blade component is designed for possible use as an alternate in the integrated core/low spool phase, should the shroudless blade technology program encounter an unexpected delay. Minimizing cost, this design is based on an existing similar design, and is finished concurrently with the shroudless fan effort in 1981. The results of these detailed design efforts were presented to NASA at an interim design review in September 1979, which will be followed by a detailed design review, presently scheduled for July 1981. Figure 14 indicates that preliminary design of the fan component has been completed and detailed design of the shroudless blade is complete.

3.2.3.3 Technical Progress

3.2.3.3.3.1 Summary of Work Previously Completed

The flight propulsion system fan component is illustrated in Figure 15 and incorporates the following major features: (1) 24 shroudless hollow titanium blades, (2) a cantilevered rotor to eliminate the need for inlet case struts, (3) blade tip clearance control through use of tip trenches and an abradable rub strip, (4) noise reduction through the use of acoustically matched case treatment, (5) Kevlar for blade containment, and (6) an integral fan exit/intermediate case assembly comprising 29 fan exit guide vanes, 10 of which provide structural support for the fan case, thereby eliminating the need for a separate set of struts.



PRATT & WHITNEY AIRCRAFT GROUP
COMMERCIAL PRODUCTS DIVISION

Detailed design of the shroudless hollow titanium fan blade was completed during the previous reporting period, and an interim design review was held at NASA-LERC in October 1979. The final design concept for the blade remains unchanged from that developed in the component preliminary design effort and is shown in Figure 16. The configuration is a 2.5 aspect ratio, two-thirds hollow design with integral platforms. The hollow section comprises three radial ribs and one cross rib. This construction provides adequate stiffness to meet bird strike, flutter, and vibration requirements. An aerodynamic refinement incorporated into the blade during detailed design was improved multiple circular arc airfoil sections to minimize shock losses and maximize efficiency. Table 26 summarizes the shroudless fan blade general parameters, Table 27, significant stage aerodynamic parameters, and Table 28, significant geometric parameters. Current fan performance parameters at significant engine operating conditions are presented in Table 29

TABLE 26

SHROUDLESS FAN BLADE GENERAL PARAMETERS

Hub/Tip Ratio	0.34 (LE) 0.393 (Avg.)
Aspect Ratio $\frac{\text{Avg. Span}}{\text{Root Chord}}$	2.70*
Span - Avg. (in.)	24.572
Root Radius - Avg. (in.)	15.918
Root Chord (in.)	9.093
Taper Ratio $\frac{\text{Tip Chord}}{\text{Root Chord}}$	1.46
t/b at Root	0.0954
t/b at Tip	0.0252
α chord @ Root (degree)	85.82
α chord @ Tip (degree)	21.88
Root angle (degree)	24.28*
Tip Angle (degree)	4.14*
Number of Blades	24



TABLE 26 (Cont'd)

Material	AMS 4928
Airfoil Root Fillet Radius (in.)	0.35
Redline Rotor Speed (rpm)	4267
LoF Rotor Speed (rpm)	3988
U_{tip} at Redline speed (ft/sec)	1515
U_{tip} at ADP (ft/sec)	1385
U_{tip} Corrected at ADP (ft/sec)	1496
Torsional Stall Flutter Parameter (bw_t) (ft/sec)	1895

* A local chord reduction near the airfoil root increases the aspect ratio. A more standard linear chord distribution would yield an aspect ratio of 2.5.

TABLE 27

AERODYNAMIC PARAMETERS; STAGE AVERAGE CONDITIONS

$\Delta T / \theta_{T2} \sim ^\circ F$

Full Span Average	99.7
Fan Duct Portion Only	102.7

Reaction Ratio (Mass Average Including Duct Exit Guide Vanes) 0.845

Velocity (Medial Vectored Average), ft/sec 628

Blockage $\sim \%$

Fan Leading Edge	0.25
Fan Trailing Edge	0.45
Exit Guide Vane Leading Edge	0.63
Exit Guide Vane Trailing Edge	1.62

Swirl \sim ft/sec

Fan Leading Edge	0
Fan Trailing Edge (Full Span Average)	545.4
Exit Guide Vane Leading Edge (Duct Average)	503.5
Exit Guide Vane Trailing Edge	0

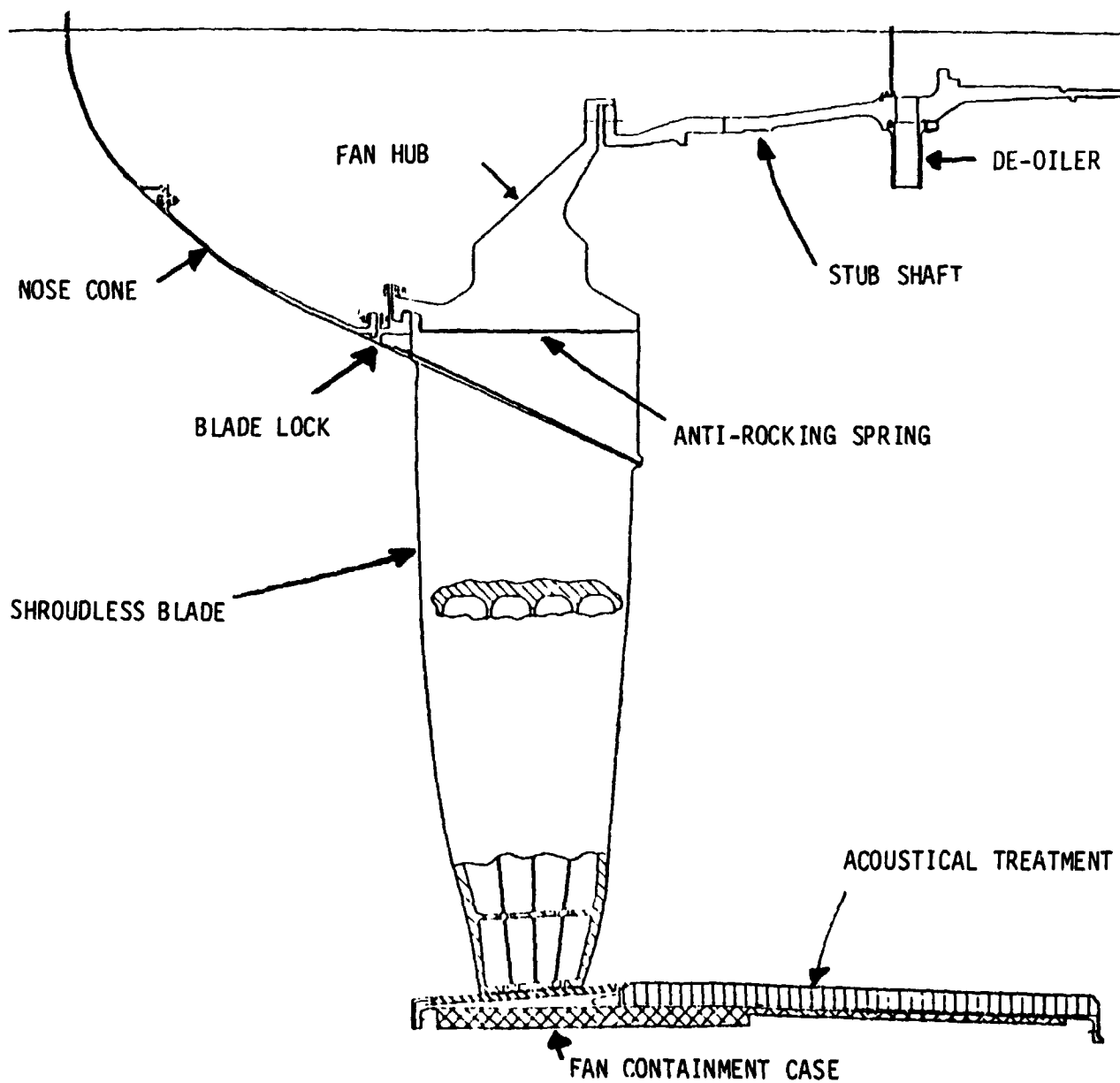


Figure 15 Fan Component



HOLLOW FAN BLADE
25 A/R 24 BLADES

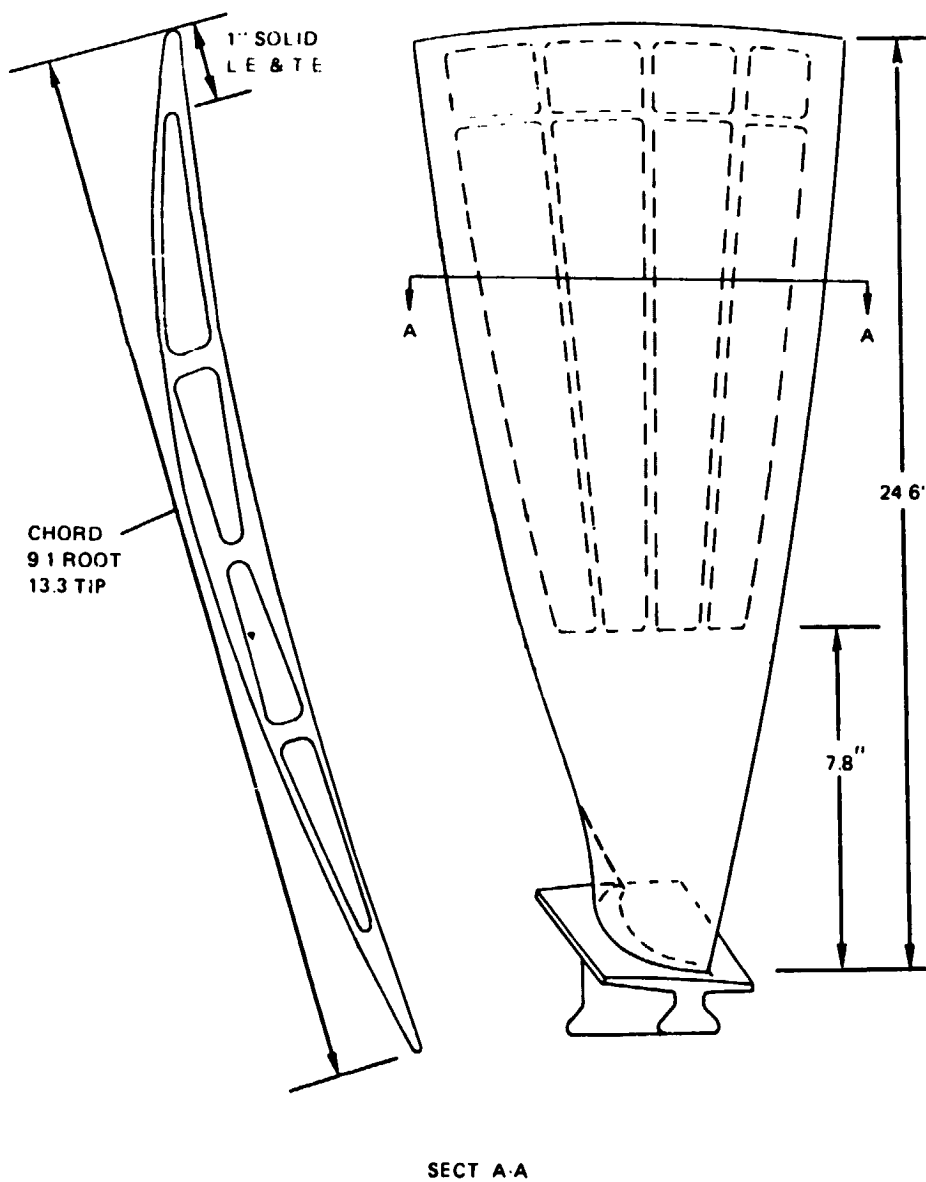


Figure 16 General Blade Description



TABLE 28

GEOMETRIC PARAMETERS

		BLADE SPANWISE LOCATION		
		Root	Mean	Tip
Solidity		2.19	1.59	1.25
Radius	Inches	15.9	28.2	40.5
Camber	Degrees	56.0	15.9	0.6
Stagger	Degrees from Axial	3.7	42.4	68.1

TABLE 29

CURRENT FAN PERFORMANCE PARAMETERS

		Engine Operating Condition			
		Aero. Des. Point	Maximum Cruise	Maximum Climb	Takeoff
Pressure Ratio					
(Duct Section)		1.74	1.71	1.78	1.58
(Core Section)		1.56	1.54	1.60	1.44
Bypass Ratio		6.51	6.62	6.33	6.91
Efficiency (Percent)					
(Duct Section) - Adiabatic		87.3	87.7	86.5	88.9
- Polytropic		88.1	88.5	87.4	89.5
(Core Section) - Adiabatic		90.2	90.5	90.0	91.4
- Polytropic		90.7	91.0	90.5	91.7
Corrected Airflow (lb/sec)					
(Total)		1375	1355	1395	1215
(Duct Section)		1190	1180	1205	1065
(Core Section)		183.0	178.0	190.5	153.5
Inlet Specific Airflow (lb/sec/ft ²)		43.0	42.5	43.7	38.1
Corrected Tip Speed (ft/sec)		1495	1470	1540	1340
Rotor Speed (rpm)		3900	3835	4105	3865
Exit Temperature (F)					
(Duct Section)		72	69	101	169
(Core Section)		51	49	79	149



Structural analysis of the final blade aerodynamic design resulted in small stagger angle changes relative to the preliminary blade design to provide increased torsional frequency margin on 4E resonance at redline speed. Blade resonance and flutter characteristics are such that stability has been achieved in the first three modes of operation. These characteristics are described in Figures 17 and 18.

Steady stresses at the airfoil root caused by centrifugal and untwist loads are considered acceptable for a glass bead peened surface to provide adequate low cycle fatigue life. Stresses in the hollow-solid transition region (internal) are also acceptable and provide adequate low cycle fatigue life for a stress relieved surface. These stresses are summarized in Figure 19 and in Table 30. All stresses were calculated assuming a maximum blade metal temperature of 150 F.

TABLE 30

AIRFOIL AND ATTACHMENT STRESS SUMMARY

<u>Location</u>	<u>Concentrated⁽¹⁾ Stress (ksi)</u>
Root Leading Edge Concave Surface	76.5
Root 40% Chord Concave Surface	101.8
Root 85% Chord Convex Surface	94.8
Internal Surface at Solid to Hollow Transition Region 70% Chord, Concave Side	64.8
Root Dovetail Fillet	89.0 ⁽²⁾

(1) Includes gas bending and tilt stress components @ LCF speed (3988 rpm)

(2) Neck P/A = 17.0 ksi



ORIGINAL DESIGN
OF POOR QUALITY

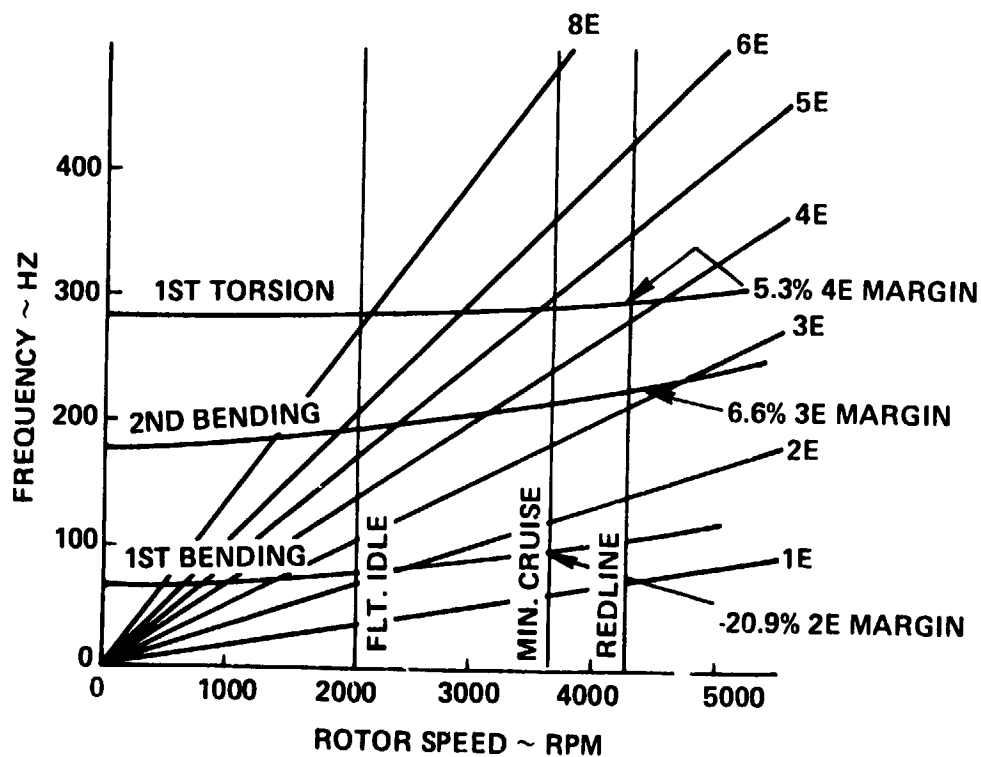


Figure 17 Blade Frequency Characteristics - NASTRAN analysis for the coupled blade and disk was used to tailor the blade geometry first mode so that the 2E resonant frequency occurs a low rpm.



ORIGINAL
OF FOUR

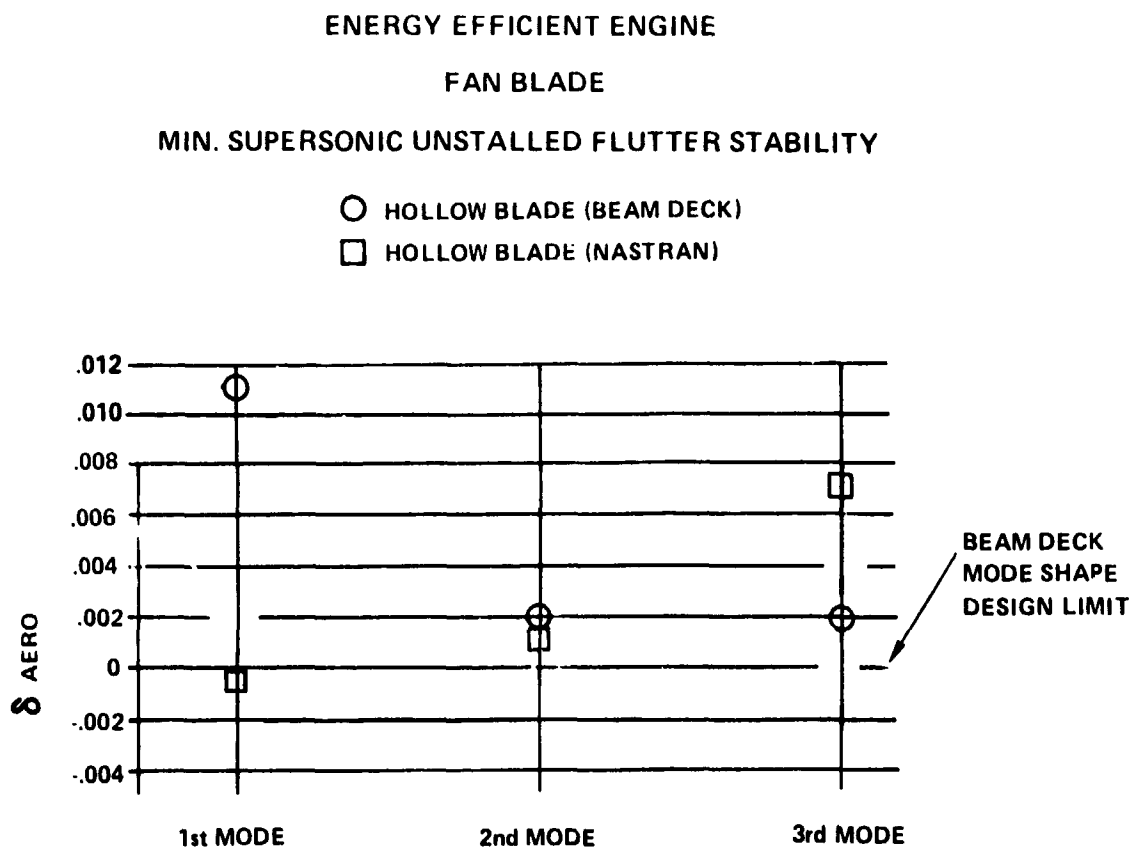
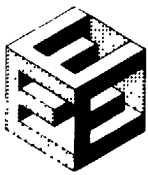


Figure 18

Blade Flutter Characteristics - The hollow blade is predicted to be more stable than the solid blade when using the NASTRAN mode shape.



OF FODDER

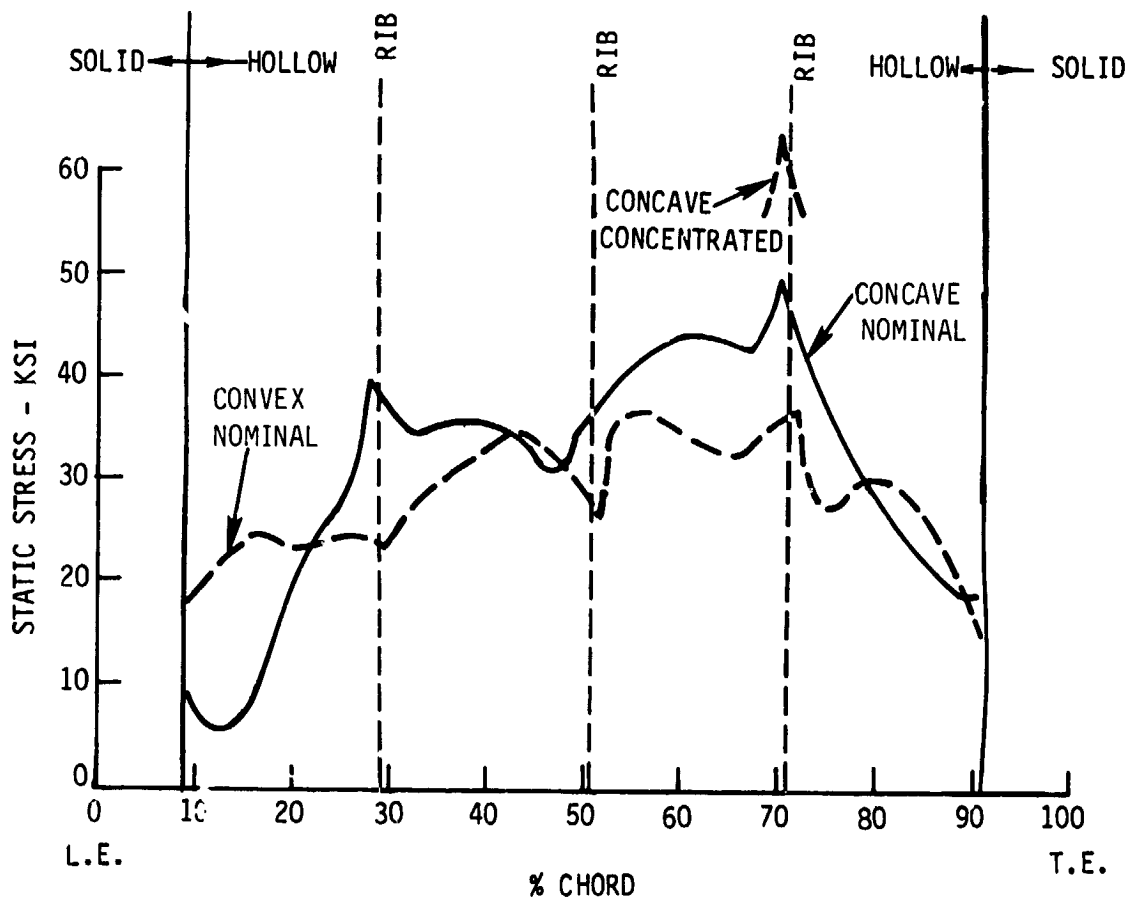


Figure 19 Blade Internal Surface Stresses at Solid-to-Hollow Transition Region



The large size and low aspect ratio of this blade diminish the possibility of gross bending or torsion failures due to bird ingestion. The local leading edge bird ingestion capability was assessed by using a solid blade analysis modified to account for local inertia and shear area changes resulting from the airfoil hollowness. The results of this analysis, shown in figure 20, indicate that although the hollow blade design has less ingestion capability than the comparable solid blade design, it falls below the solid blade limit and is therefore deemed to have acceptable bird strike characteristics.

In addition to the modified solid blade analysis, the local leading edge capabilities were compared to an existing shrouded blade design with NASTRAN analysis. The results of this effort indicated that the stress rise caused by the hollowness was offset by a benefit because of the absence of a shroud hard point.

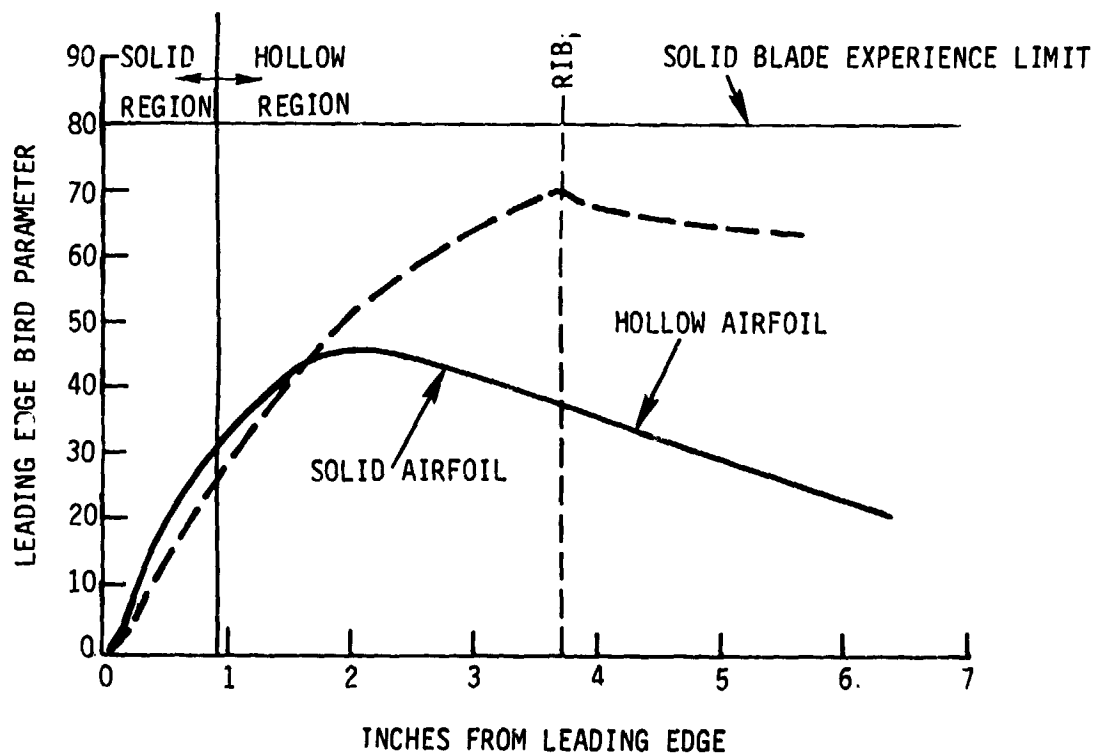
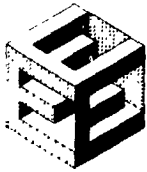


Figure 20 Fan Blade Leading Edge Bird Ingestion Parameter



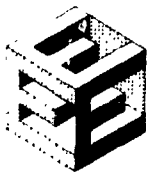
3.2.3.3.2 Current Technical Progress

The analysis and design of the alternate (shrouded) fan component was completed. This effort included aerodynamic, structural, and mechanical design of the fan blade, fan containment case, fan disk, stubshaft, nose cone, and the associated attachment hardware. The shrouded fan rotor was designed to be interchangeable with the primary shroudless fan hardware. Specifically, a common nose cone, blade lock, and stubshaft is used for both designs. The fan containment case design, however, is unique to each configuration because of aerodynamic flowpath differences. A cross-section of the shrouded fan design is shown in Figure 21. Detailing of final blueprints is now in progress.

Aerodynamic Design

The shrouded alternate fan was designed so that it could be easily interchangeable with the shroudless primary fan. The alternate fan, however, is different from the primary fan in a number of ways. The inner flowpath is the same for both configurations, but the outer flowpath of the alternate fan was recontoured in the vicinity of the blade tip in order to restore the area ratio and reduce tip loading. The radial pressure ratio distribution of the primary fan was modified in the alternate configuration. This made up for the additional aerodynamic loss caused by the part span shroud and permitted the use of a common low-pressure compressor inlet stator and fan duct exit guide vane. The alternate fan incorporates design contoured airfoil sections in the outer half of the span and conventional multiple circular arc airfoil sections inboard. The alternate fan blade is thinner than that of the primary fan, so the design contoured airfoil sections avoid excessive acceleration upstream of the shock. A complete description of the fan blade general parameters, overall performance, and airfoil geometry are presented in Tables 31 through 34.

The flowpaths of the alternate and primary fan configurations are compared in Figure 22, and the aerodynamic design parameters are compared in Table 35. Figures 23 through 35 and Table 36 compare the blade design of the alternate fan to that of the primary fan, and Table 37 compares the performance of both configurations. Table 38 shows an additional prediction based on experience with large single part span shroud fan blades.



PRATT & WHITNEY AIRCRAFT GROUP
COMMERCIAL PRODUCTS DIVISION

ORIGINAL PART
OF POOR QUALITY

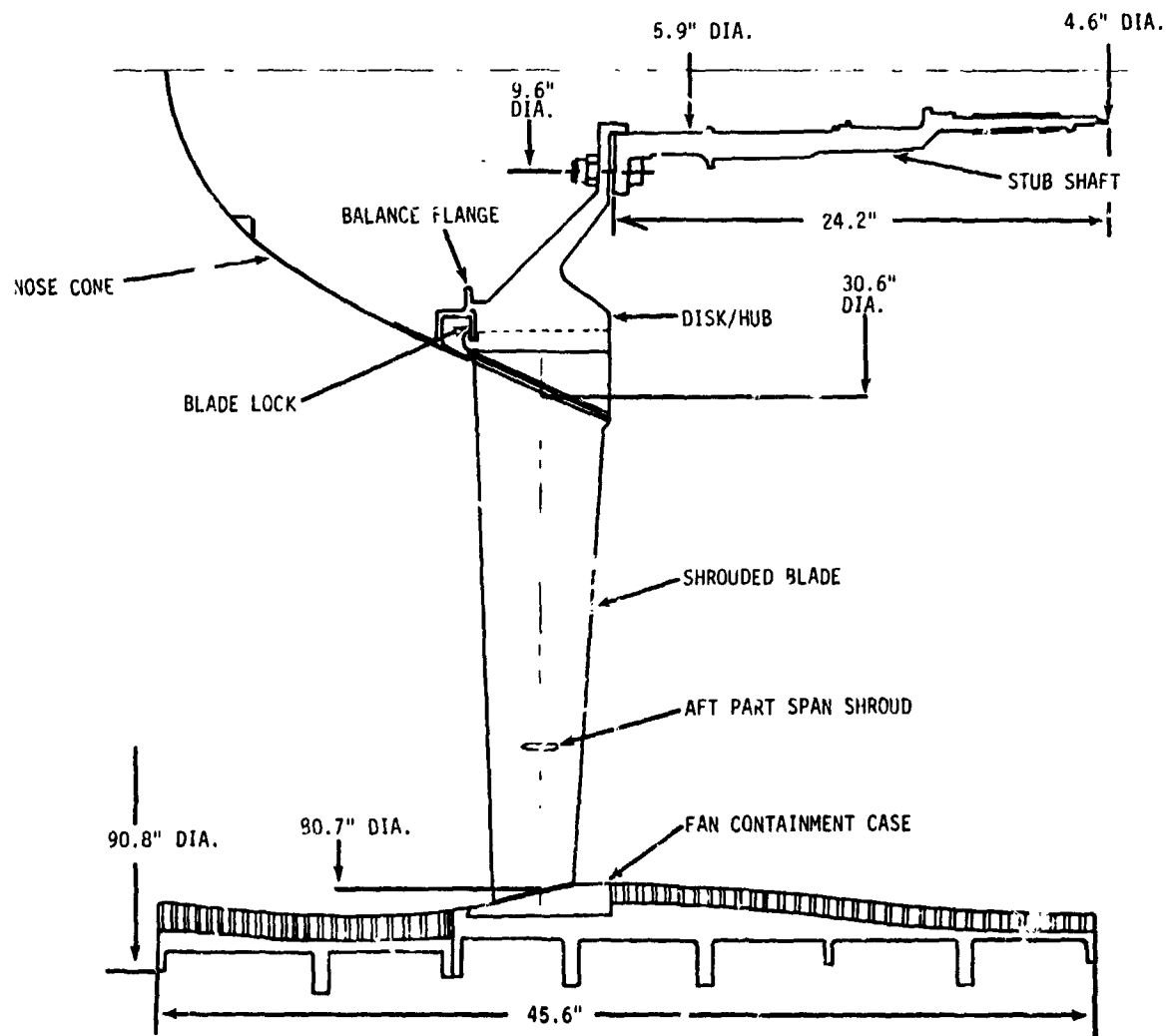


Figure 21 Shrouded Fan Component



TABLE 31

SHROUDED FAN BLADE
GENERAL PARAMETERS

Hub/Tip Ratio	0.34
Aspect Ratio $\left(\frac{\text{Avg Span}}{\text{Root Chord}} \right)$	4.0
Span - Avg. (in.)	24.981 in.
Root Radius - Avg. (in.)	15.28
Root Chord (in.)	6.218
Tip Chord (in.)	9.062
Tip Ratio $\left(\frac{\text{Tip Chord}}{\text{Root Chord}} \right)$	1.457
t/b @ Root (conical)	.095
c/b @ Tip (conical)	.022
α chord @ Root (degrees)	88.25
α chord @ Tip (degrees)	25.52
Root Camber (degrees)	59.5
Tip Camber (degrees)	1.3
Number of Blades	36
Blade Weight (lb)	10.767
Material	Titanium (6Al-4V)
Airfoil Root Fillet Radius (in.)	
Redline Rotor Speed (rpm)	
LCF Rotor Speed (rpm)	3879
Utip at Redline Speed (ft/sec)	1498
Utip at ADP (ft/sec)	1387
Utip Corrected at ADP (ft/sec)	1498



PRATT & WHITNEY AIRCRAFT GROUP
COMMERCIAL PRODUCTS DIVISION

TABLE 32

FAN OVERALL PERFORMANCE

Pressure Ratio	1.74
Efficiency (%) (Adiabatic/Polytropic)	86.3/87.3
Weight Flow (lb/sec) (Corrected)	1373.0
Specific Wt. Flow (lb/sec/ft ²)	43.0

TABLE 33

STAGE AVERAGE CONDITIONS

Reaction	($\Delta P_{\text{rotor}} / \Delta P_{\text{stage}}$)	
	Fan OD - DEGV	0.824
	Fan ID - Stator 1	0.672
Loading (D-Factor)		
	Rotor	0.533
	DEGV	0.394
	Stator 1	0.355
Temperature Rise (ΔF)		
	Fan OD	90
	Fan ID	69
Velocity		
	Rotor CM in/ $\sqrt{\theta} t_2$ (ft/sec)	716
	CM out/ $\sqrt{\theta} t_2$ (ft/sec)	564
	Stator CM in/ $\sqrt{\theta} t_2$ (ft/sec)	
	(OD/ID)	600/633
	CM out/ $\sqrt{\theta} t_2$ (ft/sec)	
	(OD/ID)	636/617
Aspect Ratio		3.8
Blockage	Rotor In	1%
	Rotor Out/Stator In	3%/2.5%
Solidity (Rotor/Stator @ Mid-Span)		1.40/1.63 (OD)
		1.40/1.49 (ID)
Swirl Conditions (ft/sec)		
	Cu/ $\sqrt{\theta} t_2$ Rotor in	0
	out	563
	Stator in	513 (OD) 624 (ID)
	out	2 (OD) 290 (ID)



TABLE 34

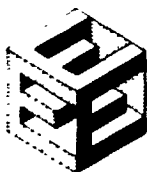
AIRFOIL GEOMETRY

		<u>Root</u>	<u>DEGV</u>
Radius (Inches)	Root	15.28	25.92
	Mean	27.77	33.54
	Tip	40.26	40.26
Solidity	Root	2.59	2.10
	Mean	1.54	1.62
	Tip	1.29	1.36
Camber (B ₂ -B ₁ Conical) (degrees)	Root	59.5	50.1
	Mean	20.0	45.7
	Tip	1.3	54.2
Stagger (degrees) (90 - ch)	Root	1.75	13.60
	Mean	43.48	12.71
	Tip	64.48	15.31

TABLE 35

AERODYNAMIC DESIGN PARAMETERS
FAN COMPARISON CHART

	<u>Alternate Fan</u>	<u>Primary Fan</u>
$W\sqrt{\theta} T_2 / \sigma T_2$	1372.8	1372.8
$N_1 / \sqrt{\theta} T_2$	4215	4215
$U_T \sqrt{\theta} T_2$	1499	1496
W/A	43.0	43.0
Hub/Tip Ratio	0.34	0.34
Aspect Ratio	4.0	2.5
Taper Ratio	1.45	1.46
Number Blades	36	24
Bypass Ratio	6.51	6.51
Duct PR	1.740	1.740
η Duct Goal	86.3	87.3
Surge Margin Goal (Percent)	15	15



PRATT & WHITNEY AIRCRAFT GROUP
COMMERCIAL PRODUCTS DIVISION

ORIGINAL PAGE 13
OF POOR QUALITY

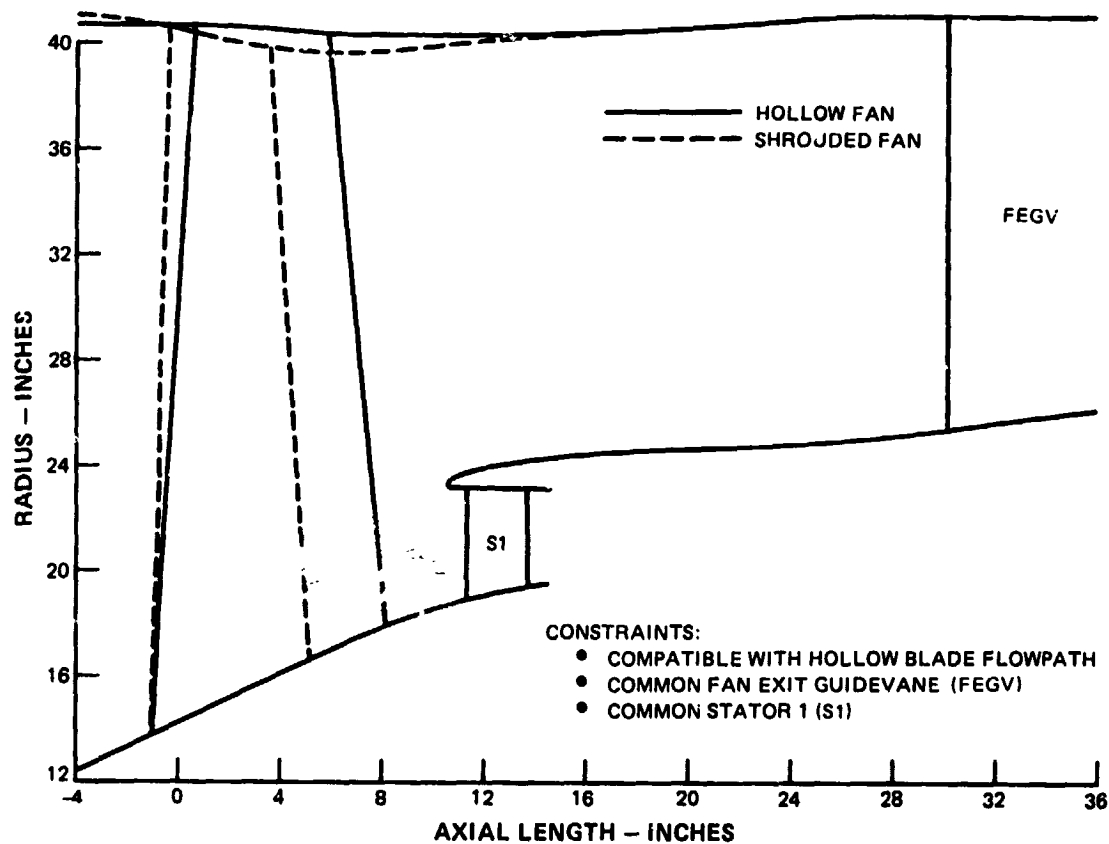


Figure 22 Fan Flowpath



ORIGINAL PAPER
OF POOR QUALITY

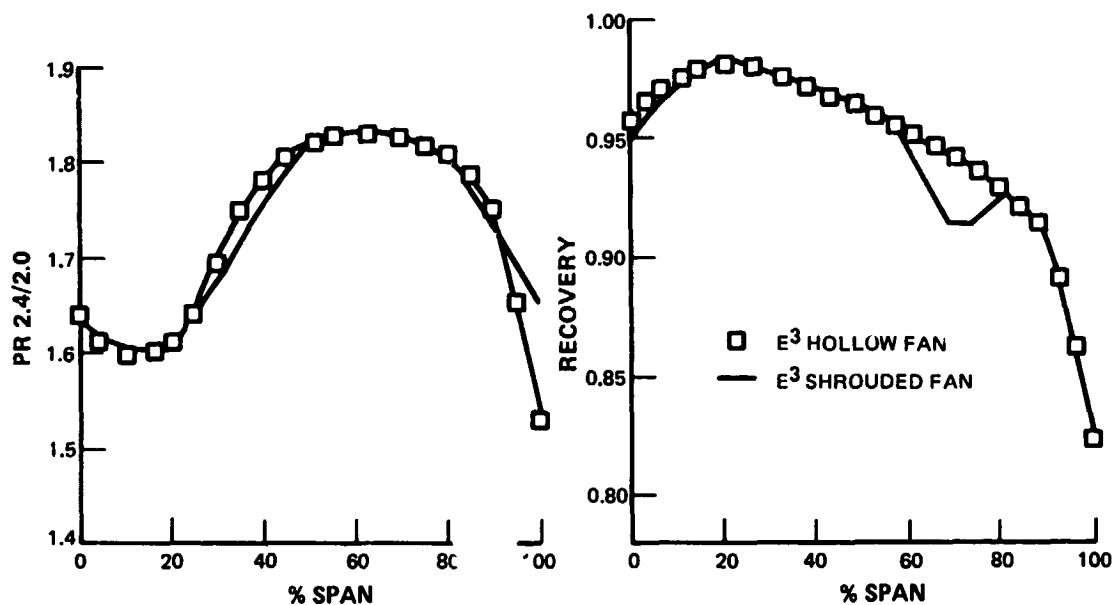


Figure 23 Aerodynamic Design Parameters: Fan Pressure Ratio and Recovery

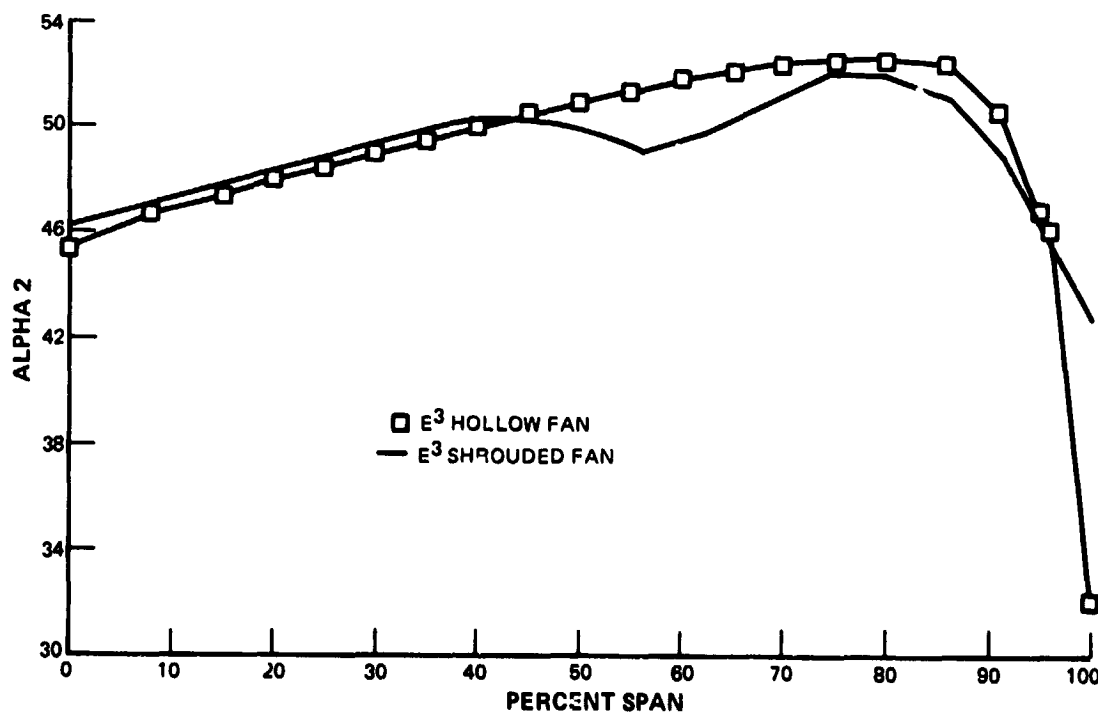


Figure 24 Aerodynamic Design Parameters: Fan Exit Guide Vane Inlet Air Angles

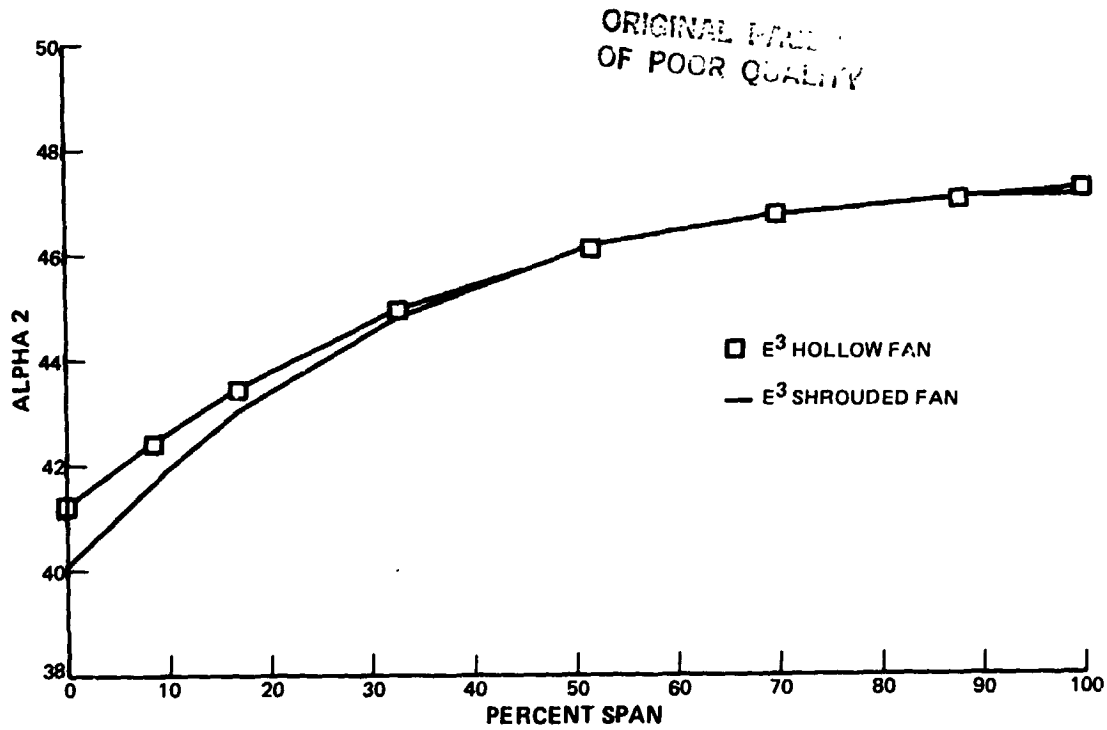


Figure 25 Aerodynamic Design Parameters: Stator 1 Inlet Air Angles

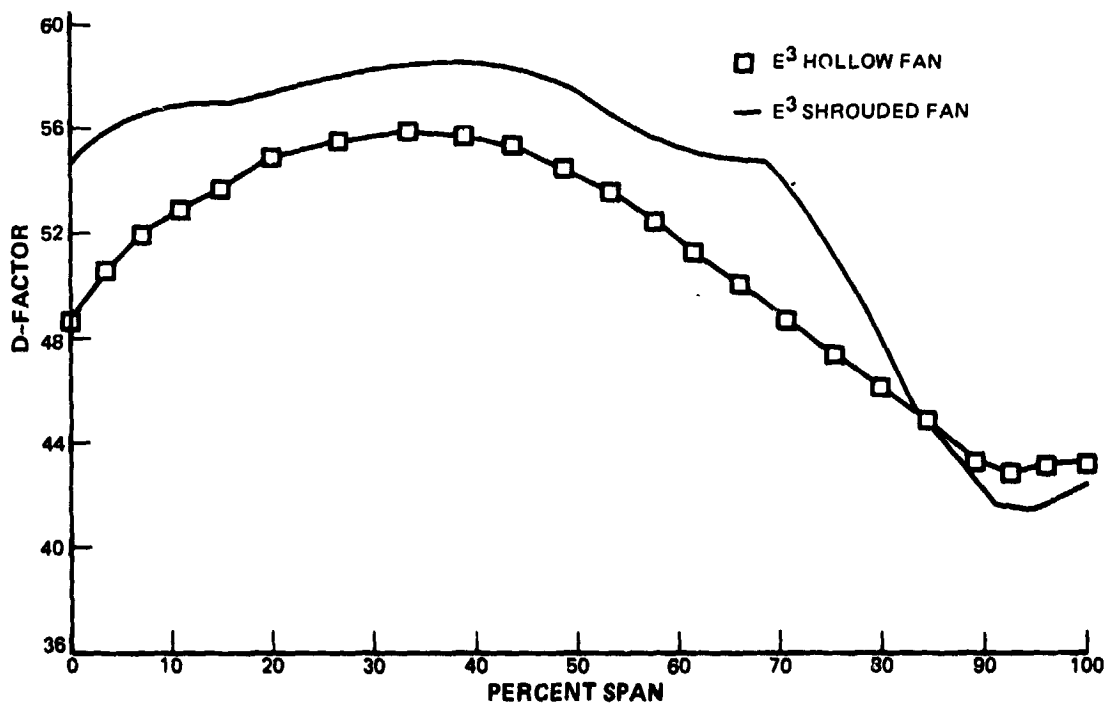
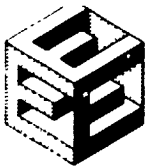


Figure 26 Aerodynamic Design Parameters: Fan Design Loading



ORIGINAL DRAWING
OF POOR QUALITY

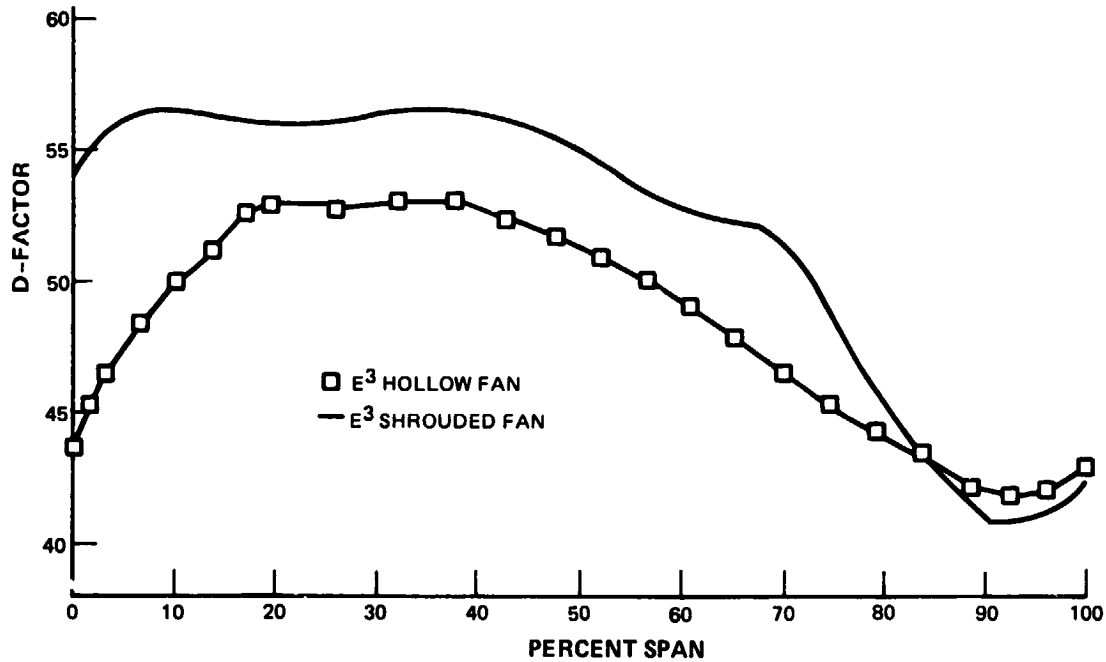


Figure 27 Aerodynamic Design Parameters: Sea Level Takeoff Loadings

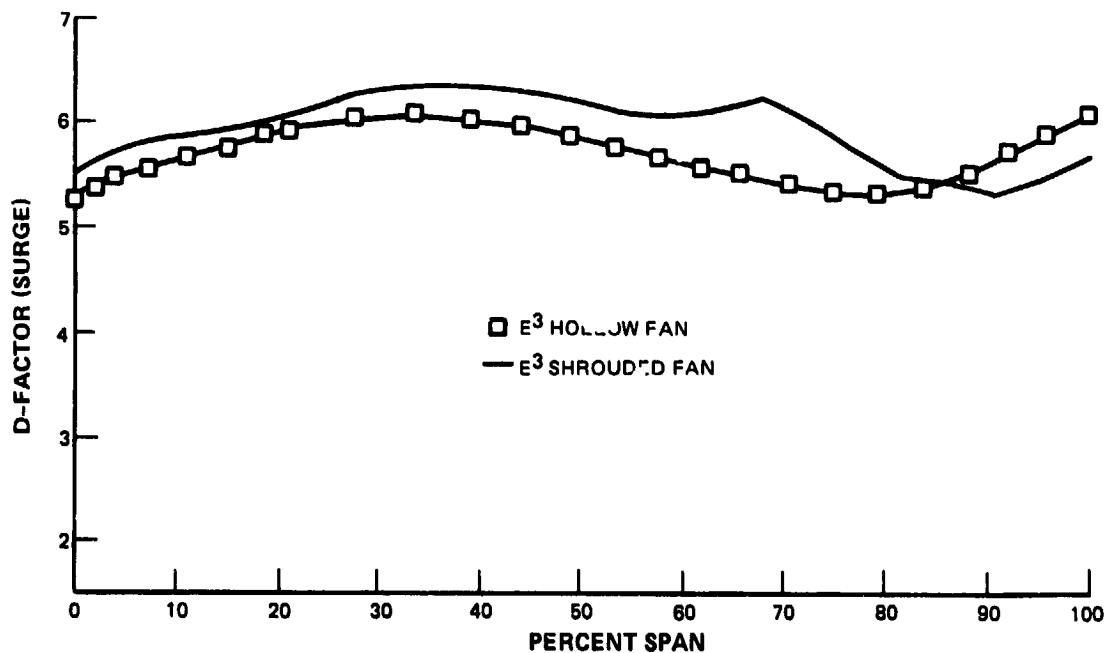
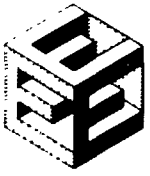


Figure 28 Aerodynamic Design Parameters: Surge D-Factors



PRATT & WHITNEY AIRCRAFT GROUP
COMMERCIAL PRODUCTS DIVISION

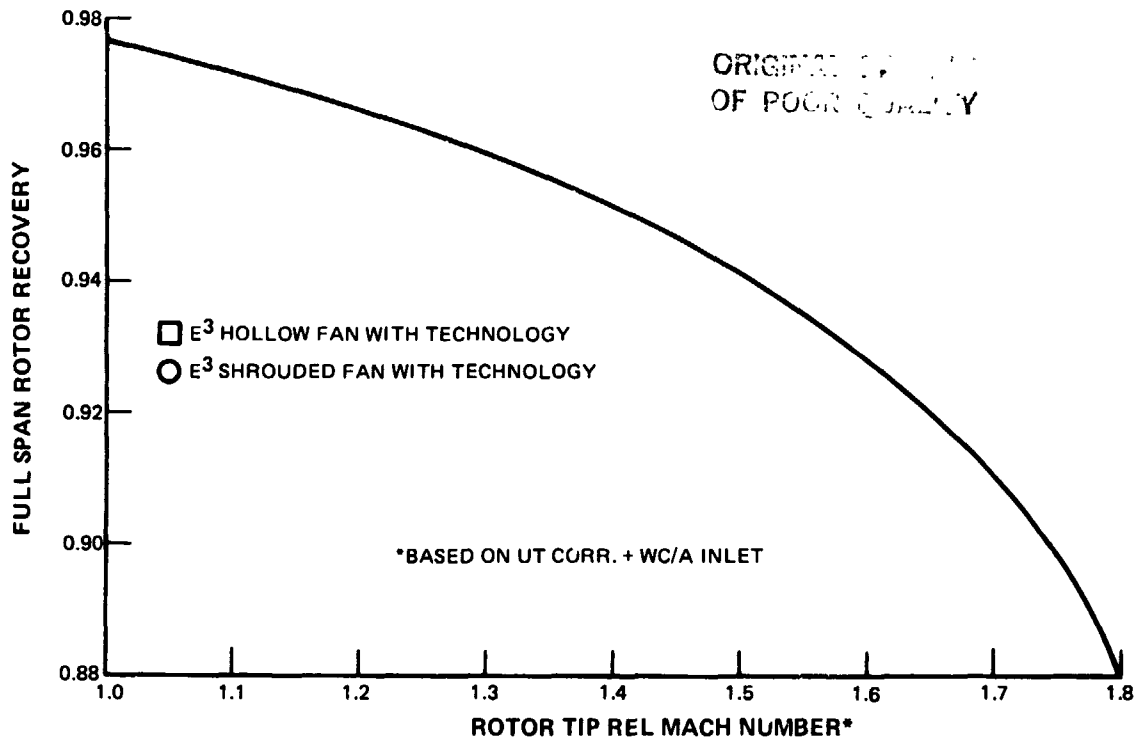


Figure 29 Aerodynamic Design Parameters: Rotor Recovery Versus Tip Mach Number

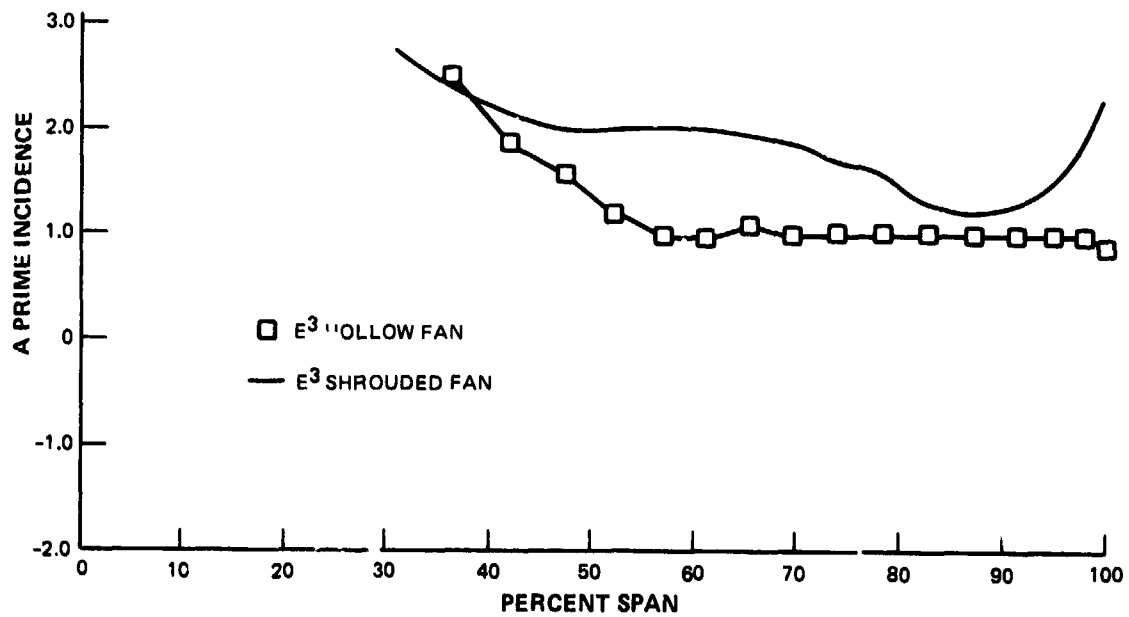


Figure 30 Blade Design Details: A Prime Incidence Versus Span



PRATT & WHITNEY AIRCRAFT GROUP
COMMERCIAL PRODUCTS DIVISION

ORIGINAL FILE
OF POOR QUALITY

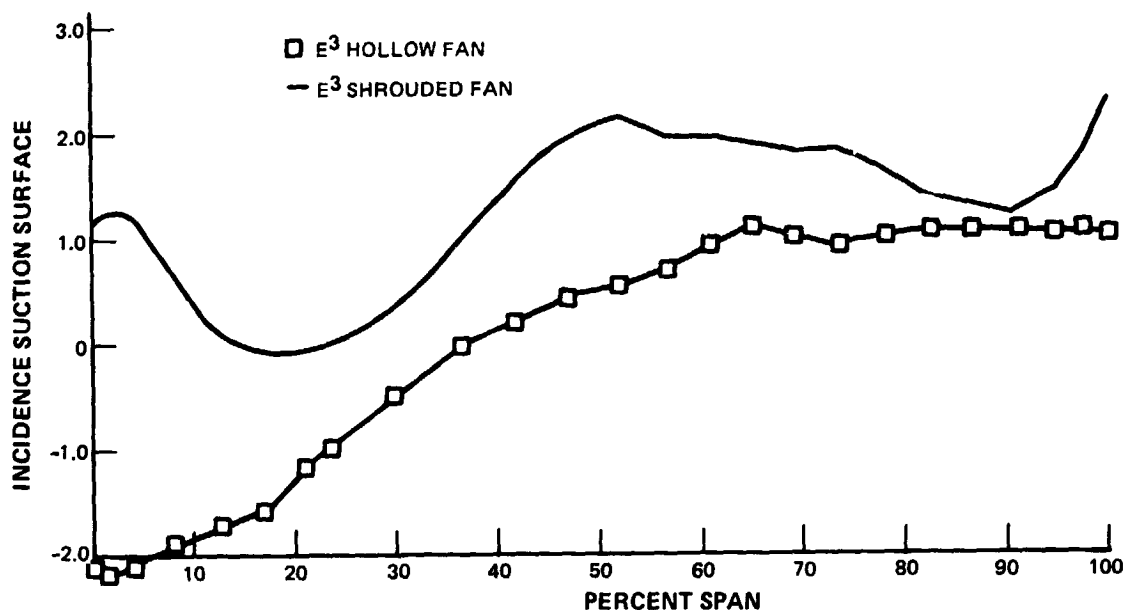


Figure 31 Blade Design Details: Suction Surface Incidence Versus Span

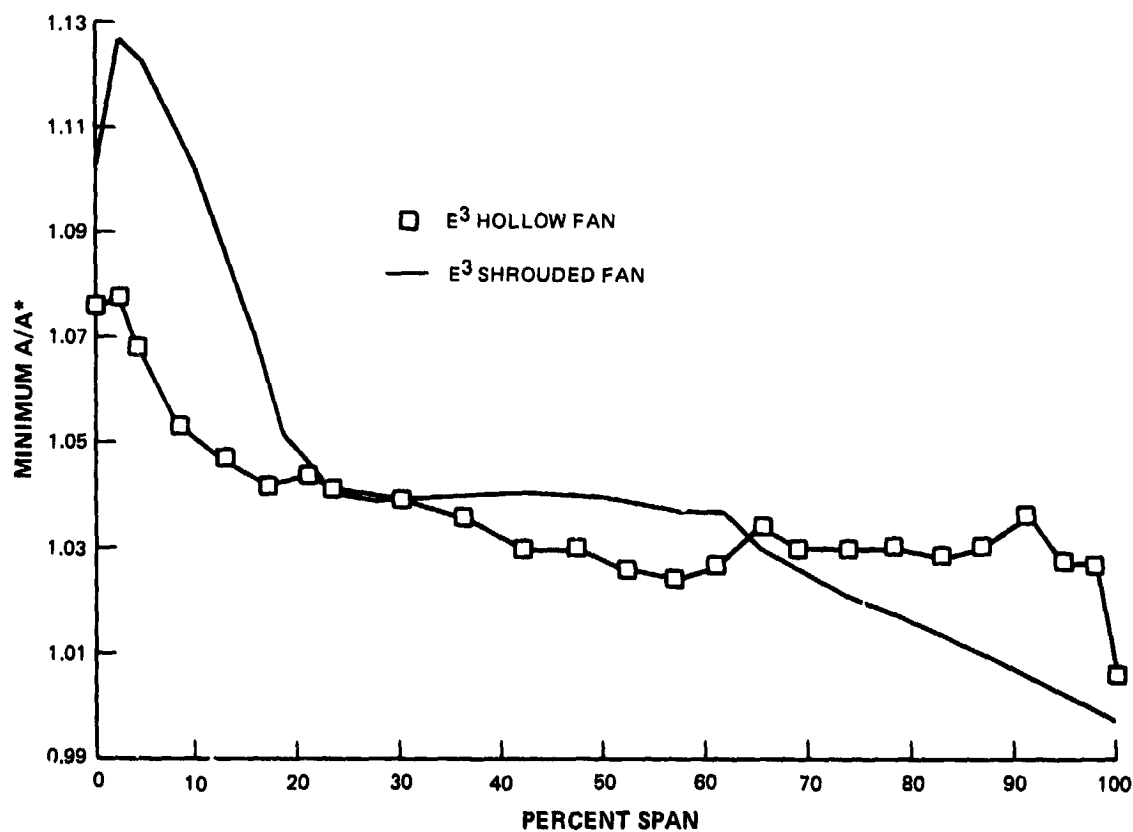
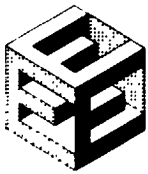


Figure 32 Blade Design Details: Choke Margin Versus Span



ORIGINAL OF POOR QUALITY

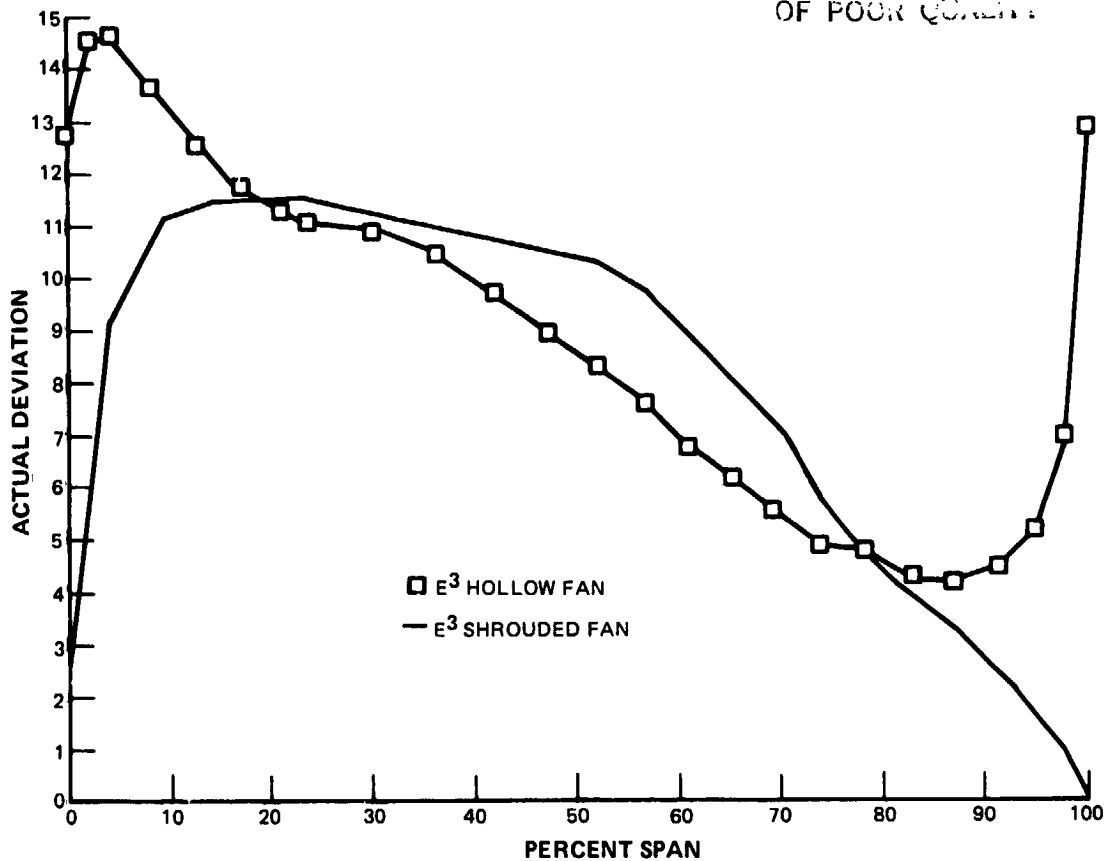


Figure 33 Blade Design Details: Actual Deviation Versus Span

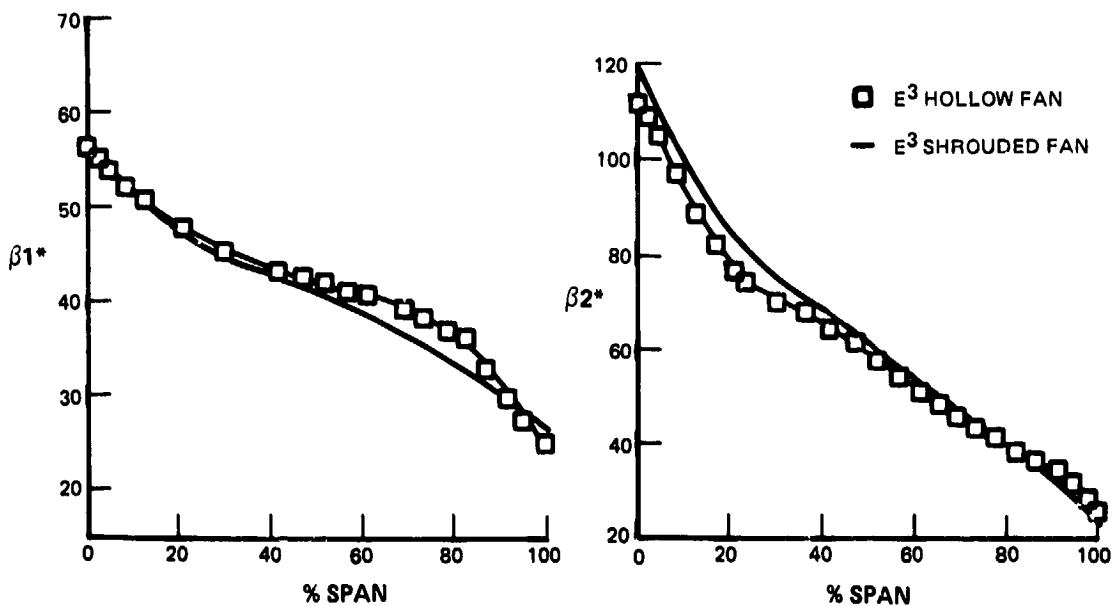
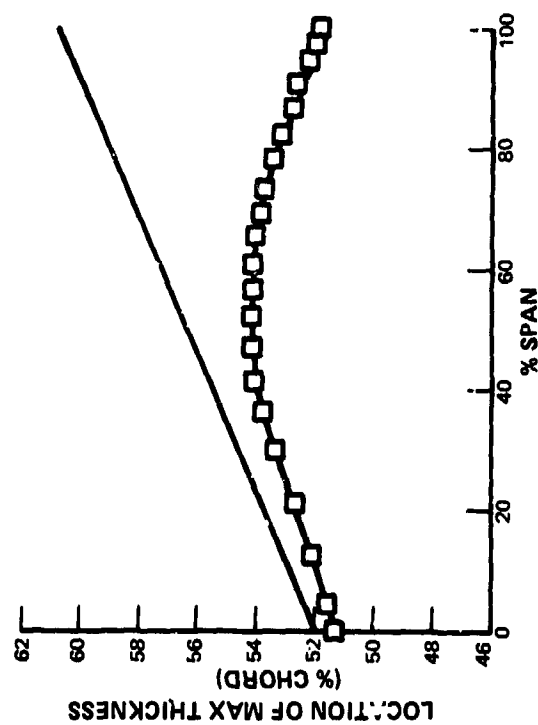
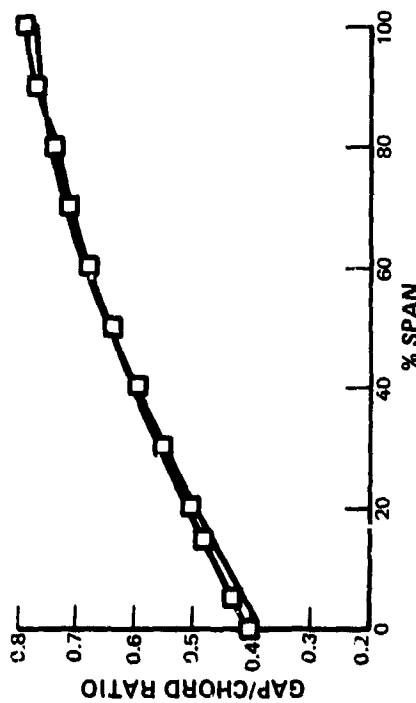
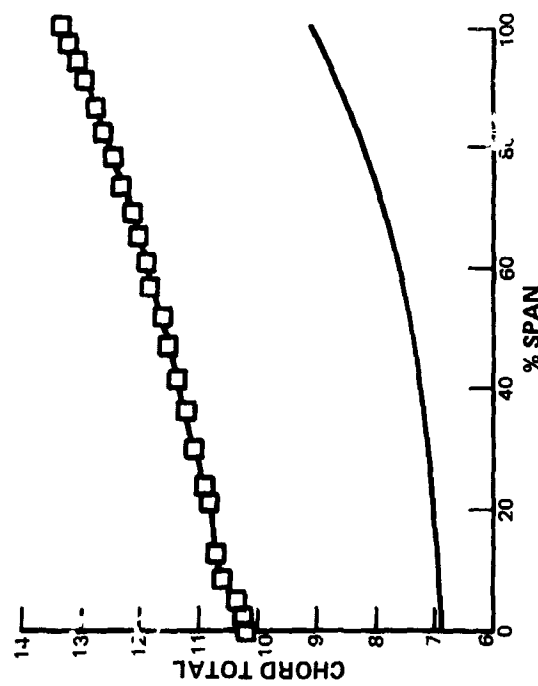
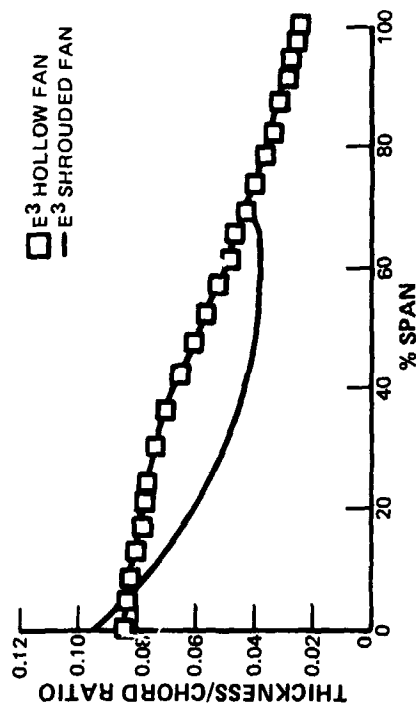


Figure 34 Blade Design Details Metal Angle Versus Span



ORIGINAL FIGURE
OF POOR QUALITY

Figure 35 Blade Design Details Geometry Comparisons



PRATT & WHITNEY AIRCRAFT GROUP
COMMERCIAL PRODUCTS DIVISION

TABLE 36

BLADE DESIGN DETAILS: SHROUD DESCRIPTION

	<u>Alternate Fan</u>	<u>Recent Experience</u>
Shroud Thickness/Span Ratio	1.3%	1.1 - 1.3%
Shroud Spanwise Location	71.5%	68 - 73.5%
Shroud Chordwise Location	Aft	Mid - Aft

TABLE 37

PERFORMANCE PREDICTIONS

DUCT EFFICIENCY - FLIGHT PROPULSION SYSTEM

	<u>Alternate Fan</u>	<u>Primary Fan</u>
Basic Design System	85.2	86.5
Tip Trenching	0.2	0.2
Quasi 3D Design and Design Contoured Airfoil	0.5 - 1.0	0.5 - 1.0
Controlled Diffusion Exit Guide Vane	<u>0.2</u>	<u>0.2</u>
Predicted Efficiency	86.1 - 86.6%	87.4 - 87.9%
Flight Propulsion System Goal	(86.3%)	(87.3%)



TABLE 38

PERFORMANCE PREDICTIONS
EFFICIENCY POTENTIAL BASED ON PREVIOUS EXPERIENCE

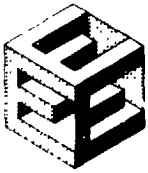
Base Efficiency (Fan Performance Data Plus EEE FEGV Design Prediction)	87.1
Scaled to EEE Tip Speed	-2.7
Scaled to EEE Pressure Ratio	+1.8
Efficiency Potential Without Fan Technology Items	86.2%
Flight Propulsion System Goal	(86.3%)

Fan Blade Mechanical Design

The mechanical design of the alternate fan blade was started. A scaled version of an existing airfoil, serving as a base design, was modified to Energy Efficient Engine vibrational, aerodynamic, and structural requirements. To meet these requirements, the shape and thickness of the scaled airfoil had to be changed considerably.

Bending stresses at the blade root were reduced to zero at low cycle fatigue speed by pre-tilting the airfoil in the direction of the gas load. The final "cold" tilt, which also incorporates the effects of airfoil untwist and uncamber, was established at a position on the airfoil 0.315 inch axially and 0.140 inch tangentially. This balancing of stresses at low cycle fatigue speed resulted in acceptable stresses at the aerodynamic design point. Along with airfoil balancing accomplished by tilt, the blade is balanced about the root by a 0.80-inch stacking line-to-blade root center line offset. This not only accommodates the centrifugal load of the blade and shroud and gas loads, but also the platform and neck pulls, yielding zero moment about the Z plane. Maximum blade pull is 90,000 pounds.

The aft part span shroud, positioned toward the blade trailing edge at the 71.5 percent span location, was designed in accordance with conventional shroud design criteria. Initially, several aerodynamic/structural modifications were required because of the high airfoil bending stresses caused by the shroud. These stresses were reduced to acceptable levels by (1) increasing the airfoil thickness/chord (e/b) ratio in the vicinity of the shroud and (2) revising the shroud geometry. Maximum concentrated stress in the shroud fillet is now 106 ksi at low cycle fatigue speed. A 65-degree shroud angle was incorporated based on recent test results of a similar design blade.



PRATT & WHITNEY AIRCRAFT GROUP
COMMERCIAL PRODUCTS DIVISION

The design of the blade root attachment was selected based on the availability of an existing disk broach tool. Blade attachment stresses, summarized in Figure 36, are well within design limits with this root configuration.

A vibration analysis was conducted on the final aerodynamic design of the blade. Blade resonant and flutter design criteria were met in all areas. Acceptable first, second, and third mode frequency margins were attained (see Figure 37).



PRATT & WHITNEY AIRCRAFT GROUP
COMMERCIAL PRODUCTS DIVISION

ORIGINAL DESIGN
OF POOR QUALITY

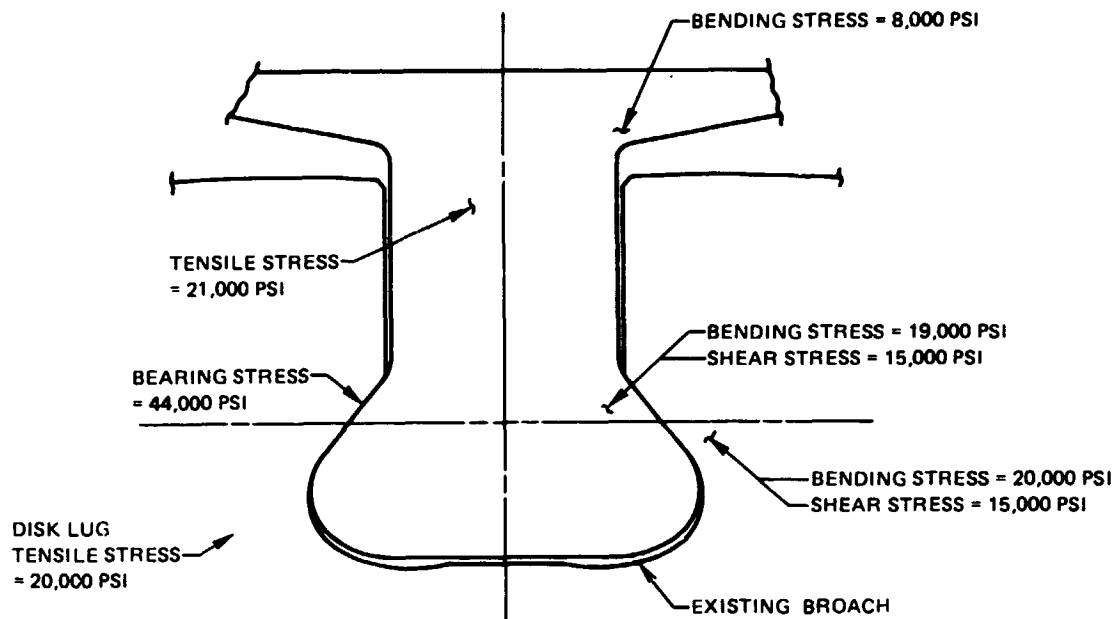


Figure 36 Blade/Disk Attachment Stress Summary

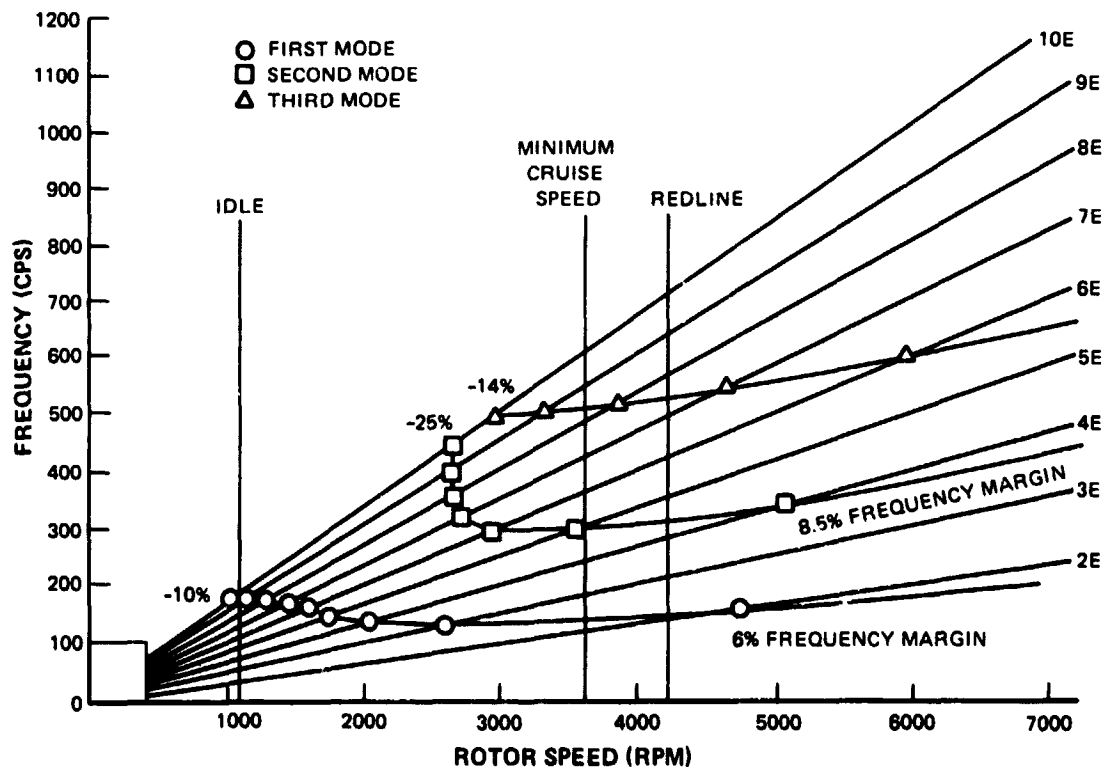


Figure 37 Energy Efficient Engine Shrouded Fan Blade Resonance Diagram



PRATT & WHITNEY AIRCRAFT GROUP
COMMERCIAL PRODUCTS DIVISION

Critical tip mode resonances were calculated and found to be outside the normal engine running ranges. Table 39 summarizes the tip mode margins.

TABLE 39

ALTERNATE FAN BLADE TIP MODE RESONANCE MARGINS

	<u>10E</u>	<u>20E</u>	<u>30E</u>
First Tip Mode	54% @ Redline	-91% @ Min Cruise	-40% @ Min Cruise
Second Tip Mode	236% @ Redline	68.32% @ Redline	12% @ Redline

A cold tip gap of 0.100 inch will allow the blade to run line-on-line with the flowpath at the aerodynamic design point. This gap accounts for steady state thermal and centrifugal loads on the blade, disk, and case, and for gas loads on the airfoil. The effects of case deflection and transients on this tip gap will be considered during a fan and low-pressure compressor gapping study, which is scheduled for completion during the next report period.

Fan Containment Case Design

The fan containment case was designed for the primary fan component, and featured interchangeability with the alternate fan configuration, as required. This case is a two-piece, "non-flight" weight configuration designed for low cost. Its material is AMS 5062 low carbon steel (aluminum is used in the flight propulsion system design) with epoxy composite rub strips and aluminum honeycomb/stainless steel mesh-covered acoustic treatment. A sketch of the case is shown in Figure 38.

The flowpath wall contour was established early in the design phase. The contours of the alternate and primary configurations were compared, and the forward flange of the case was fixed at a point where both flowpaths were common. This allows the use of a common inlet duct for each fan design.

Case thickness was set by containment criteria. The thicknesses required for blade containment were 1.00 inch for the primary fan and 0.850 inch for the alternate fan. The case thickness was therefore established at 1.00 inch. Blade passing resonance was not a factor in the case design. The interaction of the case and rotor vibrational frequencies in the primary shroudless fan indicated that coincidence rings should be incorporated to stiffen the case. These rings are not required in the alternate shrouded fan, however.



PRATT & WHITNEY AIRCRAFT GROUP
COMMERCIAL PRODUCTS DIVISION

ORIGINAL PAGE 10
OF POOR QUALITY

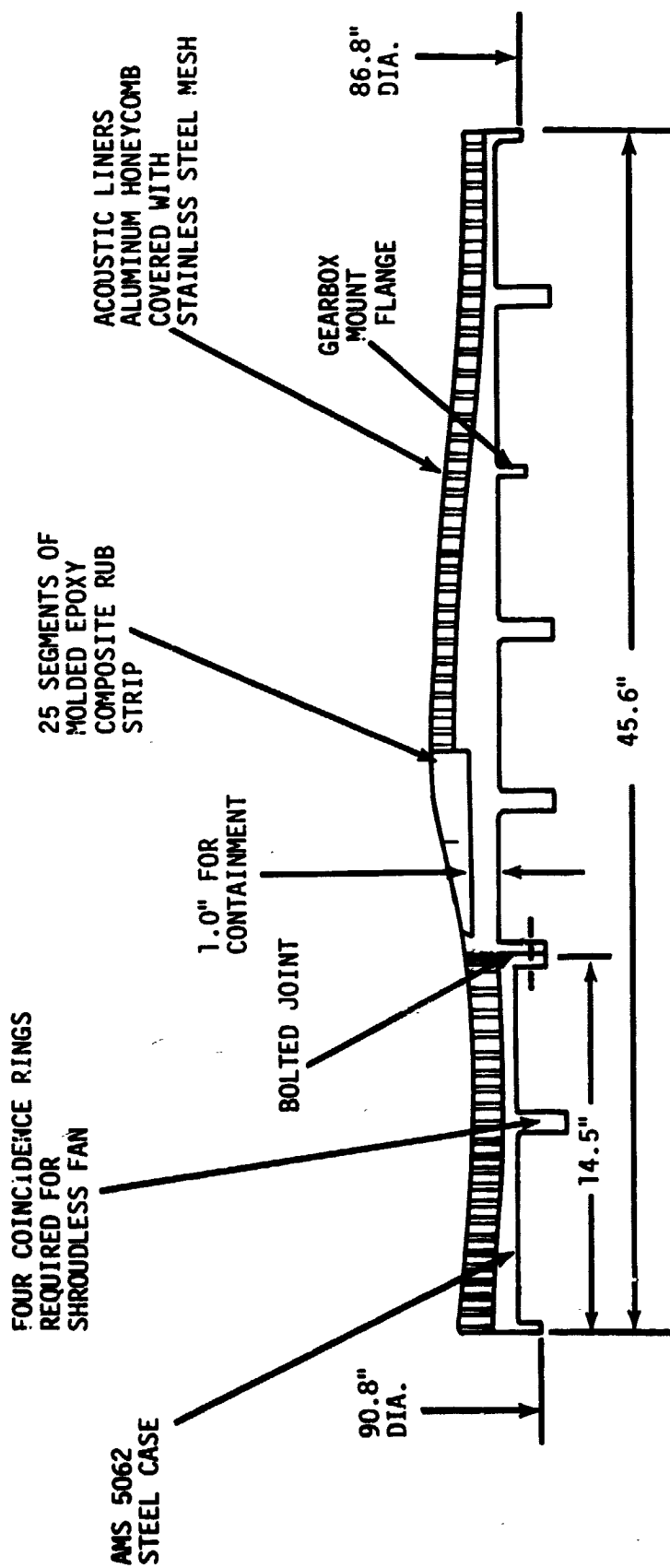
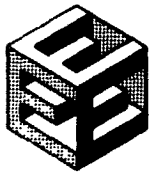


Figure 38 Fan Containment Case - This case can be reoperated for use with the shroudless fan component.



PRATT & WHITNEY AIRCRAFT GROUP
COMMERCIAL PRODUCTS DIVISION

Fan Stubshaft

The stubshaft was sized for use with both the primary and alternate fan components. The size of the stubshaft was established by the design requirements of the heavier rotor for the primary fan configuration. The requirement to withstand a blade loss set the flange thickness and the sizes number, and diameter of the bolts. A sketch of the stubshaft and a stress summary are presented in Figure 39.

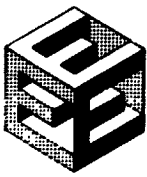
Fan Hub and Nose Cone Design

The fan hub, shown in Figure 40, was designed to flight propulsion system criteria. This hub configuration had to be designed so that the rotor of the alternate fan could be interchangeable with the rotor of the primary fan. To permit interchangeability, the blade centerline is displaced forward to allow the leading edge position of the blade to be common with the shroudless design. This produces a corresponding forward displacement of the hub rim.

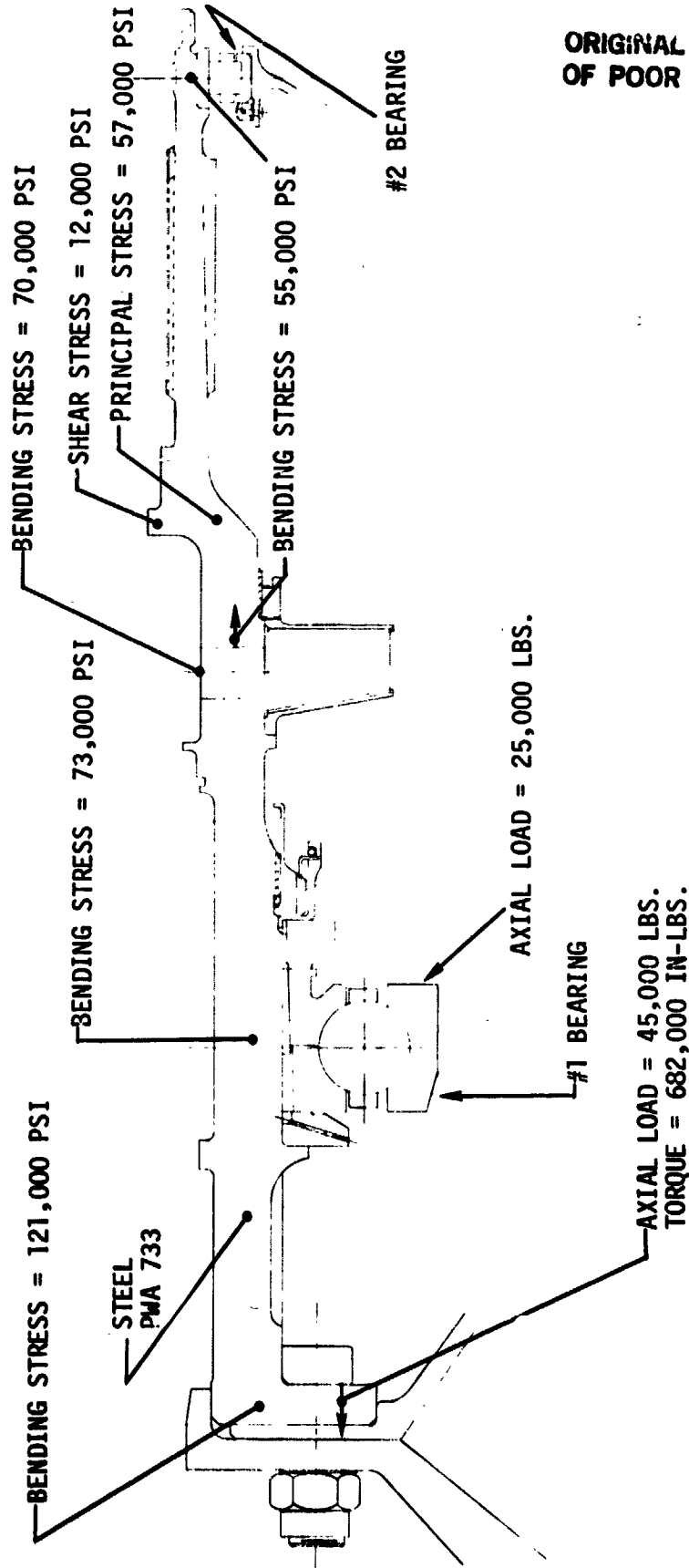
The nose cone assembly, including the blade retention feature, was designed to be interchangeable with either fan design. Aluminum was specified for the integrated core/low spool hardware, and a composite material will be used in the flight propulsion system. All stresses shown in the Figure 41 nose cone assembly description are within design allowables.

Fan Component Materials

A summary of materials incorporated in the shrouded fan component is shown in Figure 42.

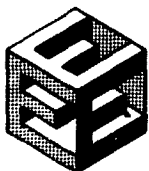


PRATT & WHITNEY AIRCRAFT GROUP
COMMERCIAL PRODUCTS DIVISION



ORIGINAL PAGE 10
OF POOR QUALITY

Figure 39 Fan Stubshaft



PRATT & WHITNEY AIRCRAFT GROUP
COMMERCIAL PRODUCTS DIVISION

ORIGINAL PAGE 10
OF POOR QUALITY

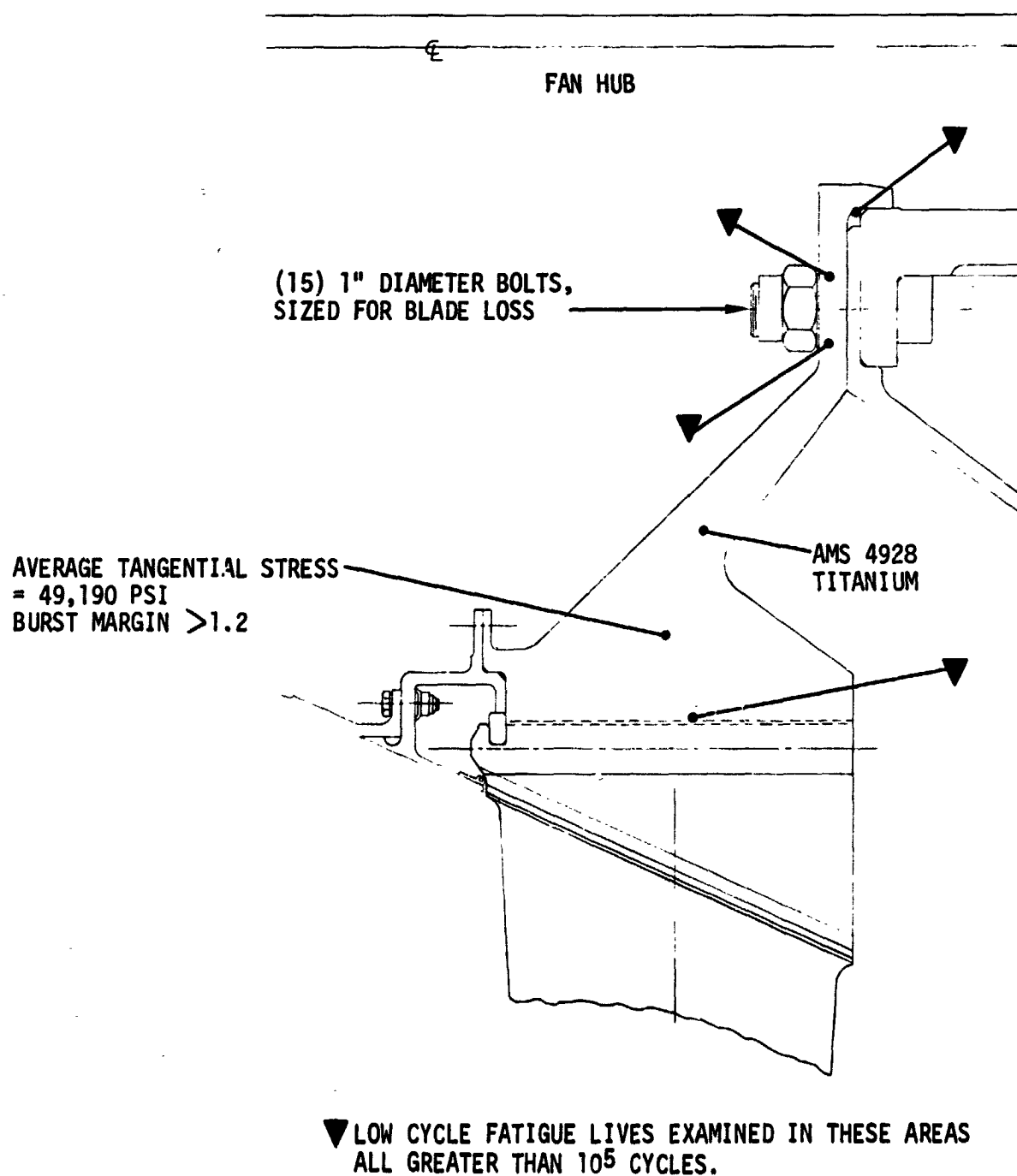


Figure 40 Fan Hub

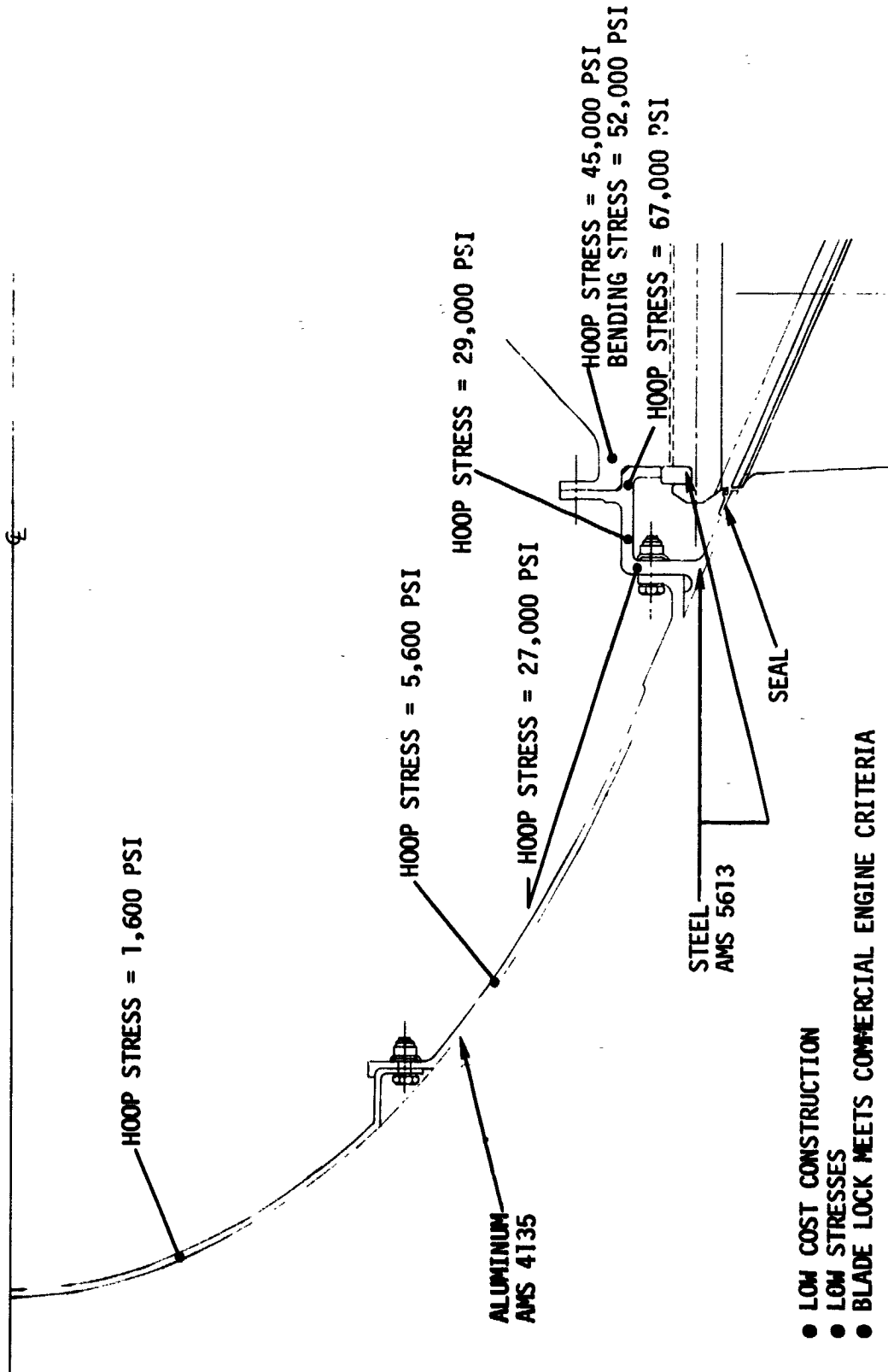


Figure 41 Nose Cone Assembly



PRATT & WHITNEY AIRCRAFT GROUP
COMMERCIAL PRODUCTS DIVISION

ORIGINAL DESIGN
OF POOR QUALITY

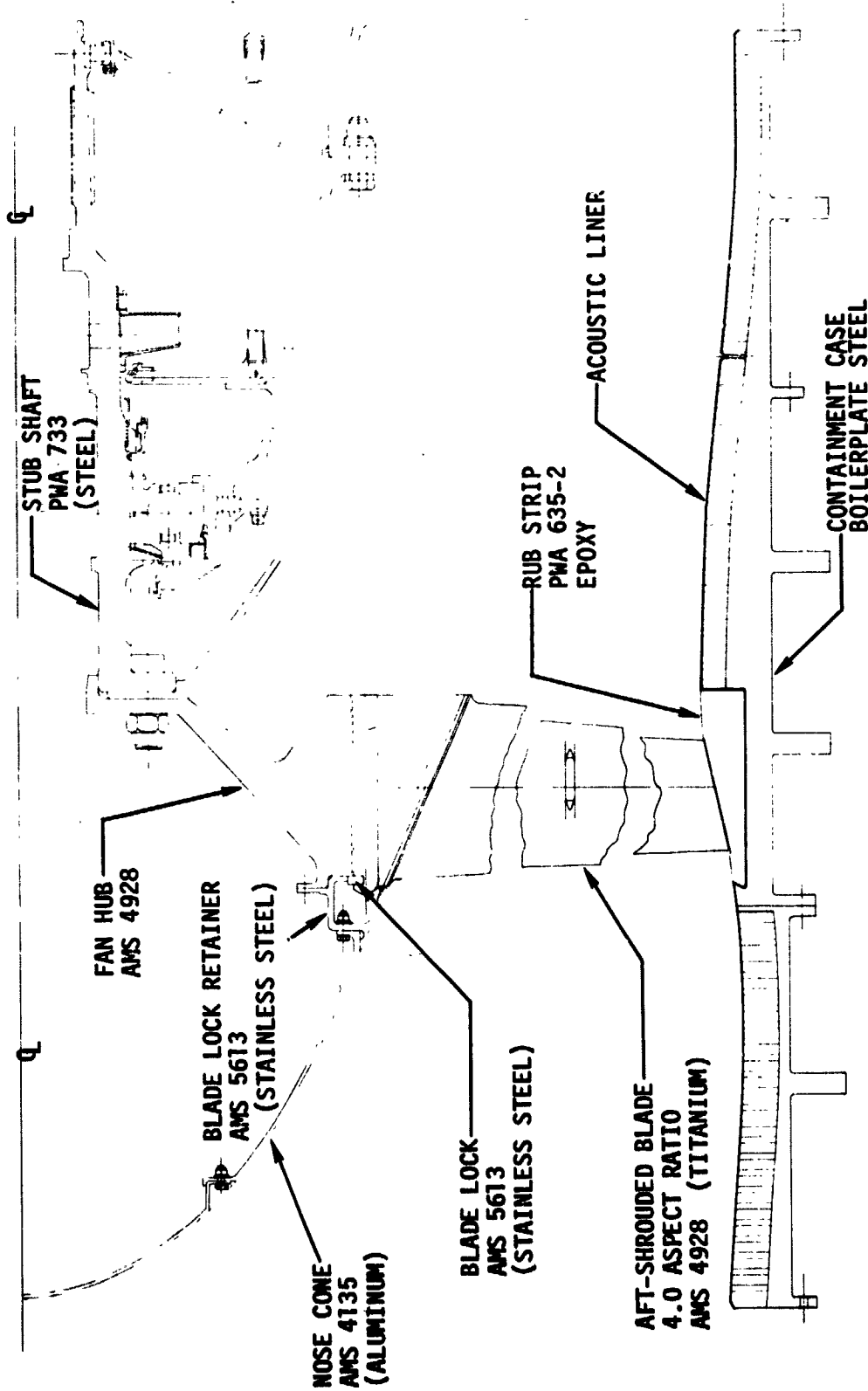


Figure 42 Shrouded Fan Rotor Assembly Materials



3.2.3.4 Supporting Technology

3.2.3.4.1 Scaled Fan Rig Test Program

Pratt & Whitney Aircraft and NASA have mutually agreed to delete the scaled fan supporting technology effort from the overall program because (1) results of rig testing would not be available to affect the final shroudless blade design and (2) re-assessment of the balance between available contract funds and cost of technical work planned for the remainder of the program indicated that the technical effort would have to be reduced.

3.2.3.4.2 Hollow Blade Technology Program

3.2.3.4.2.1 Objective

Evaluate the final construction technique for the hollow fan blade to determine the commercial engine durability of the flight engine fan design employing this technique.

3.2.3.4.2.2 Scope of Total Work Planned

This supporting technology program effort consists of the phases shown in Figure 43. Rockwell International was retained as a subcontractor to provide test specimens fabricated by the superplastic forming-diffusion bonding (SPF/DB) technique. TRW has been retained as a subcontractor to provide full-scale blades for structural testing. Figure 43 identifies those tasks that were initiated and completed in the previous reporting periods, and those that were to have been completed or initiated during the current reporting period.

3.2.3.4.2.3 Technical Progress

3.2.3.4.2.3.1 Summary of Work Previously Completed

Rockwell Efforts

Rockwell, originally scheduled to produce twenty-four specimens to be used in evaluating the superplastic forming/diffusion bonding process, encountered technical difficulties during the fabrication of the original prototype test specimens. Rockwell was unable to solve these problems with the available subcontractor funds; therefore, it was mutually decided to terminate all technical efforts. Rockwell summarized its technical efforts in a final technical report and submitted the report to Pratt & Whitney Aircraft. The Rockwell final report was reproduced in its entirety in the Appendix to the Fourth Semi-Annual Status Report.

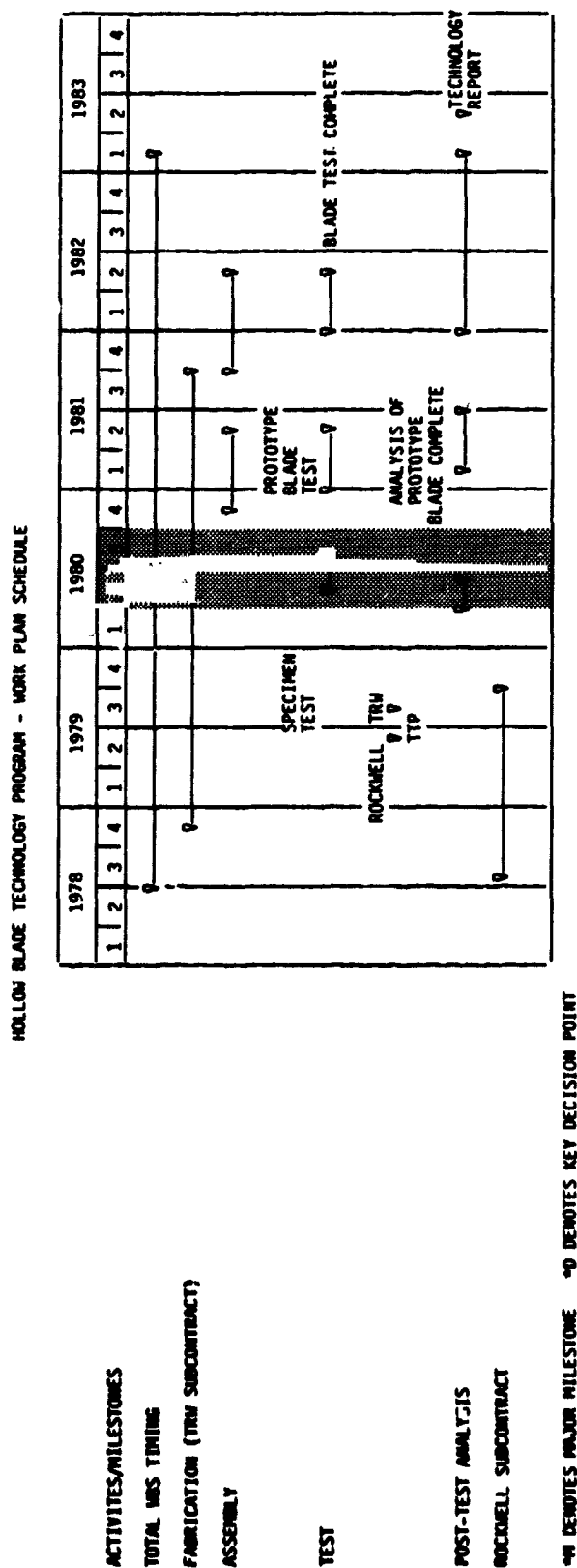
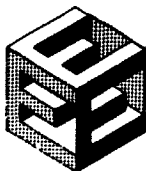
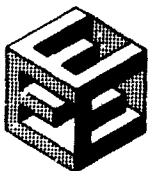


Figure 43 Hollow Blade Technology Program Work Plan Schedule



TRW Efforts

TRW subcontract efforts up to the current reporting period have concentrated on (1) selecting a fabrication method for full size hollow blades and (2) the fabrication of diamond shaped test specimens to be used in verifying the selected fabrication process.

A fully laminated approach (Figure 44) was selected as being more cost-effective in production quantities than conventional forging or isothermal forging. The diamond shaped test specimens (Figure 45) were fabricated using laminated titanium sheets and steel alloy cores to create the hollow sections. By varying fabrication parameters, TRW was able to make a preliminary assessment of the process margins required for fabrication of full-size blades. However, TRW encountered significant difficulties in fabricating diamond specimens suitable for testing. Consequently, the test and post-test analysis efforts were not initiated until the current reporting period. These difficulties included (1) Hot Isostatic Press container leaks, (2) iron core shift, (3) microporosity at the bond interface, and (4) irregular hollow cavity surface finish. Each problem was addressed and corrective action is shown in Table 40.

Full-scale blade fabrication activities have included (1) definition of the geometrical characteristics of the plies and completion of a program to generate the plies with core cutouts, (2) selection of a machining approach as the most cost-effective for producing cores in experimental quantities, (3) completion of the design of the hot isostatic press cans, and (4) significant progress in the fabrication of tooling required to produce the blades.

TABLE 40

SUMMARY OF DIAMOND SPECIMEN FABRICATION DIFFICULTIES

<u>PROBLEM</u>	<u>CORRECTIVE ACTION</u>
Hot Isostatic Press Container Leaks	Increased the width of the container flange which permitted use of a more effective seam weld rather than the fusion butt weld previously used.
Iron Core Shift During Assembly and Hot Isostatic Press Cycle	X-ray inspection was added to the assembly procedure to ensure proper core registry during assembly. Core shift during the Hot Isostatic Press Cycle will require adjustments in the isothermal forging process.
Microporosity at the Bond Interface	Some improvement has been achieved by removing argon from the weld process and by heating the titanium to 900 F while hot vacuum outgassing to eliminate entrapped gases during the container sealing process.
Irregular Hollow Cavity Surface Finish	Substantial improvement in finish was achieved through the use of higher carbon alloy steel cores. However, this alloy caused regions of the titanium to crack while cooling. This is unacceptable and the use of higher carbon steel alloy has been rejected. The impact of these irregularities will therefore be evaluated during the specimen tests.

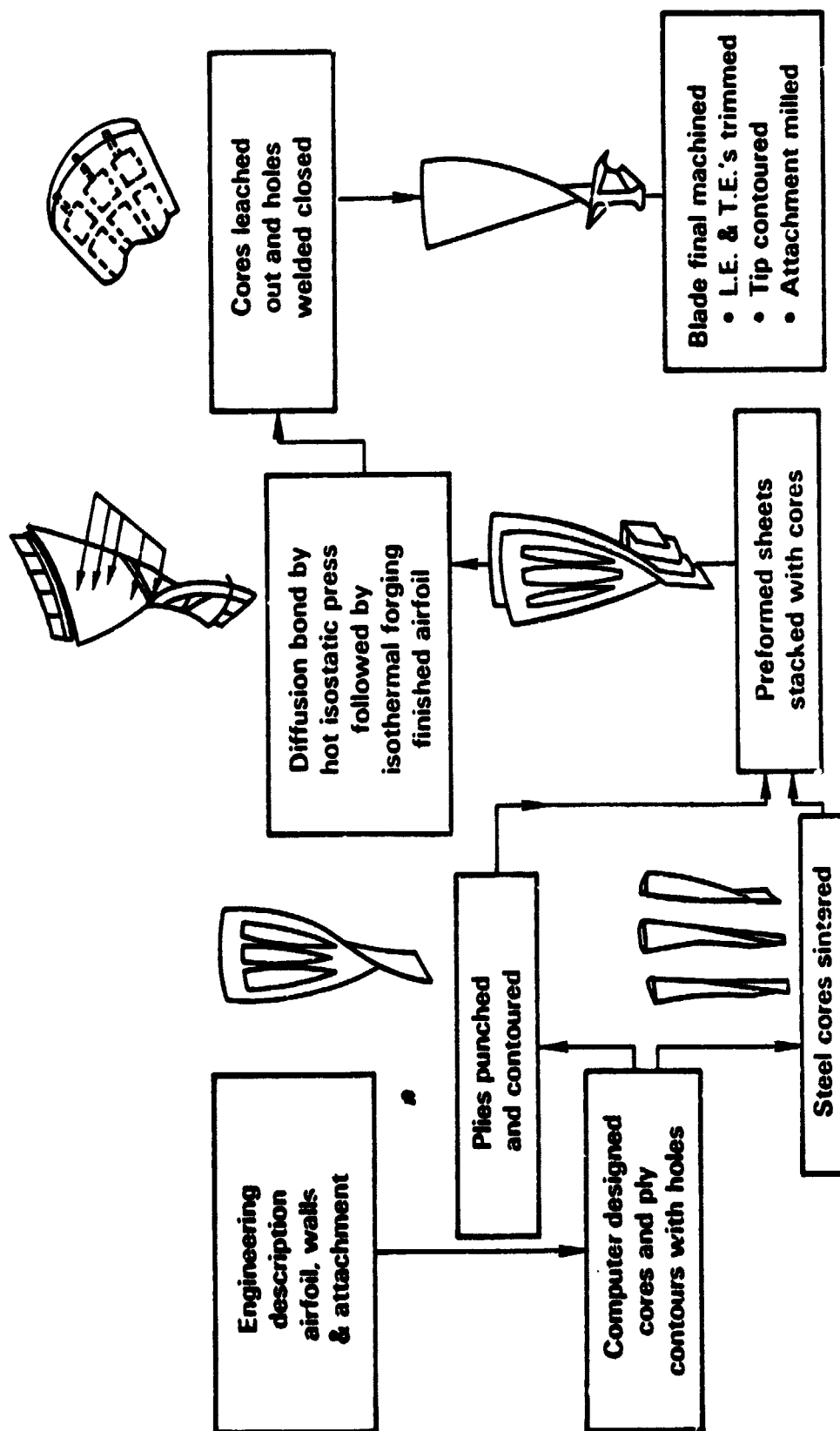
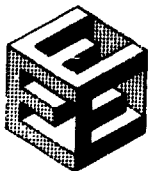


Figure 44 Hollow Blade Production Sequence



PRATT & WHITNEY AIRCRAFT GROUP
COMMERCIAL PRODUCTS DIVISION

ORIGINAL PAGE IS
OF POOR QUALITY

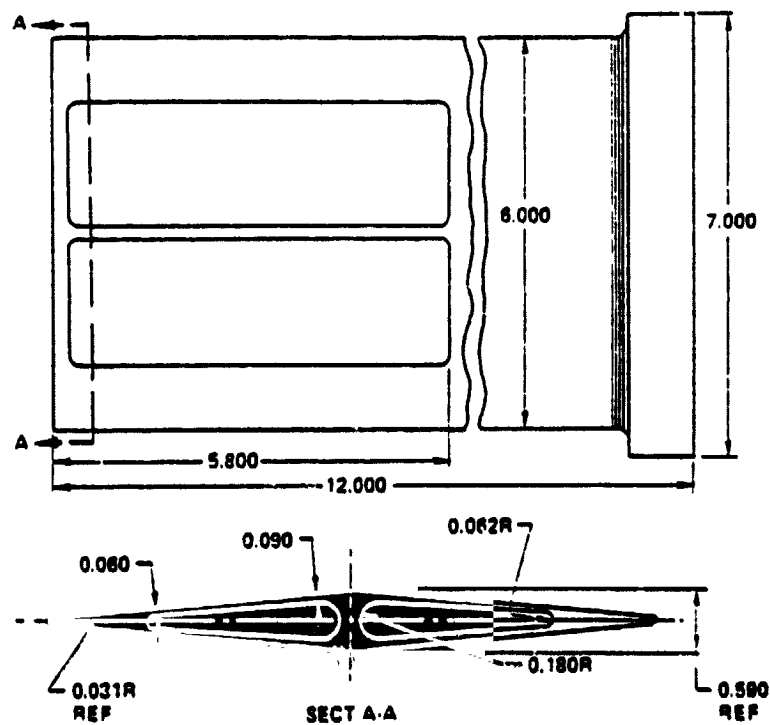
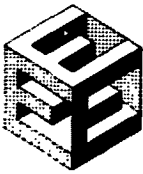


Figure 45 General Description TRW Specimen



3.2.3.4.2.3.2 Current Technical Progress

TRW Program

The TRW test specimen program consists of two phases: (1) critical experiments and specimen fabrication and (2) blade process development. Progress in these two areas is described in the following two subsections. A discussion of the results of a Pratt & Whitney Aircraft analysis of the TRW specimens is also included.

Critical Experiments and Specimen Fabrication

Ten diamond-shaped specimens were hot isostatically pressed as a group in April. Four of these specimens developed leaks in their hot isostatic press containers and were therefore unsuitable for further processing. The six remaining specimens were X-rayed and C-scanned. The results of this analysis indicated that five specimens were well-bonded and one specimen showed evidence of poor bonds. The cores remained in the same position both before and after the pressing cycle. These six specimens were then machined to the proper size. Two 0.125-inch holes were drilled in the tip of each specimen and the cores removed. The interior cavities of the specimens were smoothed by an etching process, and the specimens were shipped to Pratt & Whitney Aircraft in mid-June. The results of the specimen fabrication are summarized in Table 41.

TABLE 41

SUMMARY EVALUATION OF TRW DIAMOND-SHAPED SPECIMENS

<u>Diamond Specimen</u>	<u>Material* Direction</u>	<u>Visual (Decanned)</u>	<u>X-ray</u>	<u>C-scan</u>	<u>Core** Separation (in.)</u>
11	Longitudinal	Good	Good	Good	0.28-0.29
14	Longitudinal	Good	Good	Good	0.23
16	Longitudinal	Good	Good	Good	0.20-0.21
17	Longitudinal	Good	Good	Good	0.22-0.25
18	Longitudinal	Not Bonded	--	--	
20	Transverse	Not Bonded	--	--	
21	Transverse	Good	Good	Good	0.20
22	Transverse	Not Bonded	--	--	
23	Transverse	Not Bonded	--	--	
24	Transverse	Good	Questionable	Questionable	0.19-0.20

. Evidence of poor root consolidation.

* With respect to the material rolling direction.

** Core separation was the same before HIP as it was after.



Blade Process Development

TRW used the results of the critical experiments and specimen fabrication phase to establish an approach for producing the required full-scale blade. There were two approaches considered: (1) cambered assembly and (2) flat assembly.

Cambered Assembly. A cambered assembly procedure was initially considered. In this procedure, the hot isostatic press cans and plies are pre-formed to the desired blade shape prior to lay-up, assembly, and hot isostatic pressing. Canning problems during assembly, however, and the additional cost of ply-forming rendered this approach infeasible.

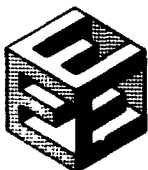
Flat Assembly. In the flat assembly approach, the plies are laid up flat, assembled, hot isostatic pressed, and then cambered and twisted in one operation. This operation appeared feasible, but carried a high degree of risk because of the simultaneous cambering and twisting of the airfoil.

The selected approach (see Table 42) represents a modification of the flat assembly procedure. The hot isostatic press can is formed by welding the outer-most titanium sheets to a root block, into which the laid-up plies are assembled.

TABLE 42

TRW BLADE ASSEMBLY PROCEDURE

- o Weld solid root blocks to titanium sheet cover skins.
- o Lay up flat plies with core-registry maintained by two titanium pins in the root and one titanium pin in the tip.
- o Place assembled package between cover skin. Titanium pins in root area of plies extend into the solid root block.
- o Seam weld, leak check, hot outgas and seal.
- o Hot isostatic press assembled package.
- o Camber, in camber tooling.
- o Twist, in twist tooling.
- o Forge in isothermal forge tooling.
- o Finish machine and leach out cores.



Status of Individual Process Development Efforts

Blade Ply Definition. Ply definition for the blade was completed during this reporting period. Some of the assumptions used in ply generation are as follows: (1) the plies will be 0.030-inch thick; (2) there will be a full ply located along the mean camber line; and (3) there will be full piles on the concave and convex surfaces of the airfoil. A maximum of 10 percent deformation by isothermal forging is planned, and a chemical milling envelope of 0.0025-inch was added. The programs to generate the piles with the core cutouts was completed, debugged, and computer plots were generated.

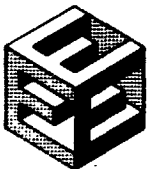
The airfoil comprises 31 plies. The core cavity geometry of the ply was computer-defined, but the radii of the core corners in the ply were manually defined because of the complexity of the core geometry. The computer plots were subsequently modified to include additional stock in the root and tip areas (for the 7 full length piles).

A vendor-run numerical controlled machining operation was selected as the most cost-effective and timely method of producing the 12 sets of plies required for development. Two other methods considered were (1) a tape controlled punch press (Wiedematic) and (2) stamping.

Cores. The length and complexity of the required cores has increased their cost and has made their procurement more difficult. The cores are being produced by numerical control machining. The vendor developed the numerical control tapes, built fixtures, started machining trials in plexiglas to test the tapes, and fabricated 12 sets of cores. The cores were delivered to TRW in August.

Hot Isostatic Press Cans. The hot isostatic press can featured a provision for seam welding and a gutter to divert vapors during welding that may be caused by contamination of the titanium alloy plies. The can material specified was DOAK steel. Cost quotations for can fabrication and associated tooling were solicited from two deep drawing vendors and a hydroform vendor. The cost quotations from the deep drawing vendors were reasonable for can fabrication, but were unreasonable for tooling because the deep draw on the root area required two sets of tooling. The hydroform vendor, considering the cans too long for fabrication, did not provide a cost quotation even when offered an option to fabricate the cans in halves.

TRW decided to use a 0.030-inch titanium skin for can material because of the high costs of the existing can material and because of the unavailability of a hydroform vendor. The titanium cover sheet is approximately 1-inch wider on the sides and end than the maximum dimensions. These will be welded by the tungsten inert gas method. Solid blocks were selected because of the difficulty and cost of forming the sheet around the root. The root blocks are welded to the cover skins before assembly. After assembly, the oversized cover skins are seam-welded together. This design allows for the removal of sufficient material to ensure against any heat-affected zones caused by welding.



PRATT & WHITNEY AIRCRAFT GROUP
COMMERCIAL PRODUCTS DIVISION

Ply-Core Assembly Tooling. The ply-core assembly tooling has been designed and built. The tooling fixture is a flat, wooden block with provisions for two locators at the root end. During assembly, the plies will be secured by a 3/8-inch titanium bar, which will be attached to 2 correspondingly sized holes located 1/4-inch from the root end in a machined area of the airfoil. One hole is located along the blade stacking axis, and the other is located 2 inches from the stacking axis along the root end. Initially, the holes were positioned 3 inches apart; however, when the final design of the ply was established, the holes were placed closer together to maximize the number of double-pinned plies. In addition, a single pin is located at the blade tip along the stacking axis to help in aligning the full length piles.

The root/cover skin-welded assembly is aligned with the airfoil ply assembly by 2 holes drilled approximately 1 inch into the covered skin sheet and root block. These holes also serve as gas exits between the cover skin and root blocks after seam welding.

Camber Tooling. The initial blade lay-up will be uncambered and untwisted. Initially, tooling was designed to subsequently camber and twist the hot isostatically pressed blade in one operation; however, TRW has decided to perform the camber and twist in separate operations because of the inherently lower risk. Camber tooling was designed during this reporting period and an order placed with a tooling vendor. Untwisted versions of airfoil cross-sections were drawn on TRW's computer. These were used by the vendor to produce wooden models, which in turn were used to produce electrical discharge machining electrodes. The camber tooling was completed and delivered to TRW in early September.

The concept of the tool design is relatively simple (see Figure 46). The tip of the blade is held by a fixture. A pin 1-1/2 inches in diameter extends beyond the tip and is located along the stacking axis of the blade. The alignment at the blade root is maintained by the sides of the root block. The blade is placed hot (1600-1700 F) in the die and "squeezed," cambering in the root and airfoil. The excess material in the root is machined after cambering. The camber dies are operated at about 400-600 F, and the cambering is performed in a 1500-ton hydraulic press.

Twist Tooling. TRW completed the design of the twist dies, and these dies were fabricated by a vendor. TRW will use support tooling previously used in a successful Pratt & Whitney Aircraft blade fabrication program. The risk in the current program is considerably lower because of the demonstrated success of this support tooling.



PRATT & WHITNEY AIRCRAFT GROUP
COMMERCIAL PRODUCTS DIVISION

ORIGINAL PAGE 19
OF POOR QUALITY

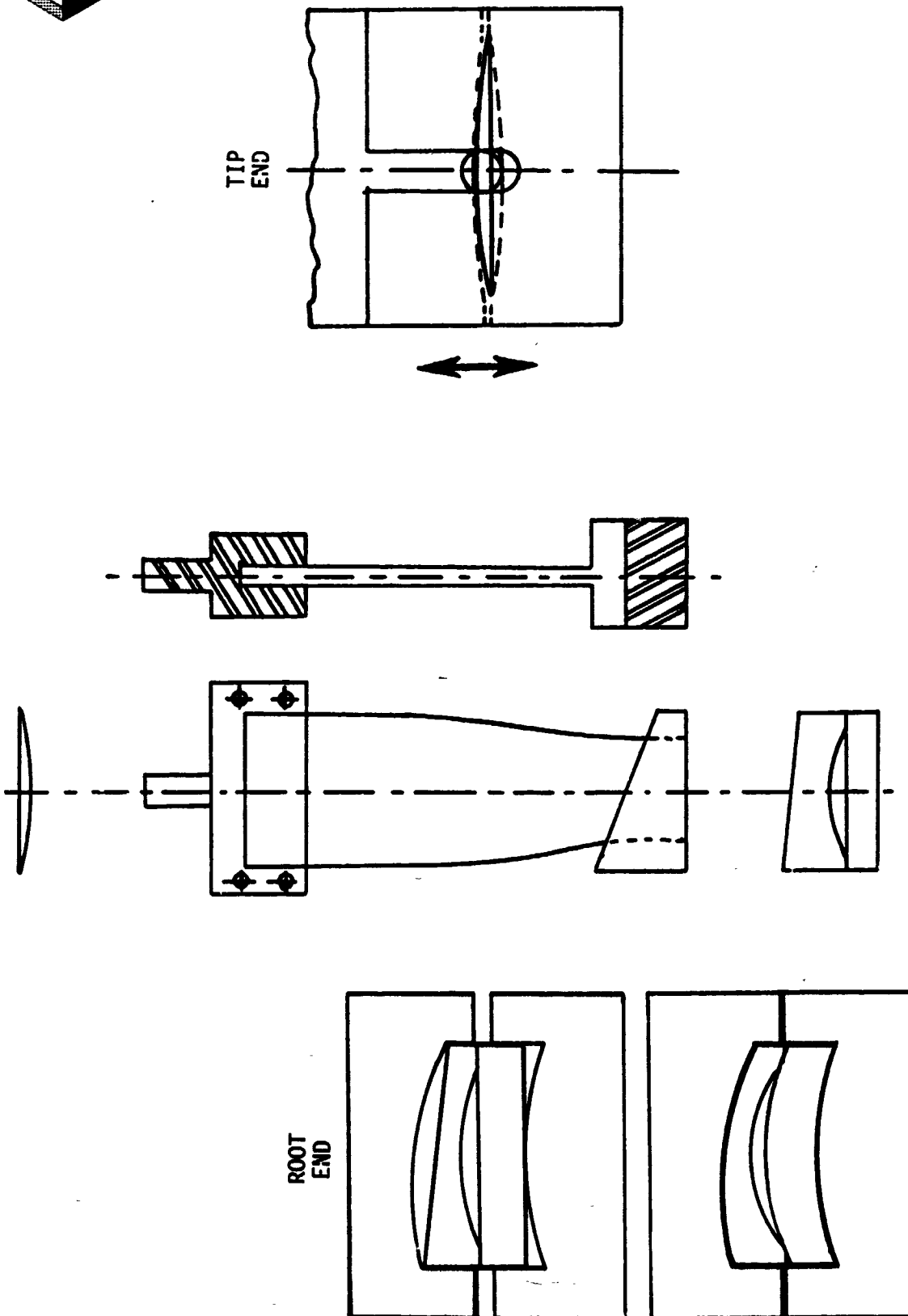
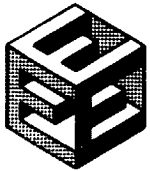


Figure 46 Schematic Illustration of Camber Tooling



The blade is twisted by a two-step approach using a die for each airfoil section: root, center, and tip. First, the airfoil is clamped with the dies at the center of the blade. Second, the dies at the tip are clamped together. The clamping action at the tip allows some twist to be put into the blade. The remaining twist in the center-to-tip section is accomplished by rotating a large bull gear to which the center dies are mounted. This process is repeated for the root-to-blade center section. During twisting, only the center set of dies and either the root or tip dies are used at one time. The twisting is performed at temperatures between 1600 and 1750 F.

Isothermal Forge Tooling. Fabrication of the IN-100 isothermal forging dies was completed. The airfoil electrodes used to electro-discharge machine the airfoil were inspected and found to be acceptable. These electrodes were then released to the tooling vendor for electro-discharge machining of the airfoil surface. The airfoil surface for both the die and punch were electro-discharge machined and the IN-100 castings were returned to TRW for inspection. Following inspection, the dies were released to the tooling vendor. This vendor has also machined root and root gutter electrodes from wooden models supplied by TRW.

Die Nest, Heating Elements, and Insulation. The die nest for holding the IN-100 isothermal forging dies has been built, received by TRW, and inspected (in particular, the cooling plates have been tested for water leaks).

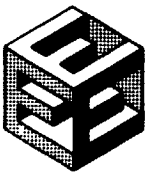
A partial shipment of the heating elements and the IN-100 die set insulation was received. The remaining material is anticipated to arrive during early October 1980.

Blade Fabrication. The fabrication of five blades was started during this reporting period. Table 43 describes the configuration and status of each blade.

TABLE 43

TRW BLADE STATUS

<u>Blade Number</u>	<u>Plys</u>	<u>Cores</u>	<u>Root</u>	<u>Status</u>
1	Hand cut	None	Blocks	HIP'ed, leaked
2	Hand cut	Partial	Blocks	HIP'ed, leaked, re-processing
3	NC machined	Full	None	HIP'ed (no results)
4	NC machined	Full	Blocks	Being Assembled
5	NC machined	Full	Blocks	Being Assembled



PRATT & WHITNEY AIRCRAFT GROUP
COMMERCIAL PRODUCTS DIVISION

Blades 1 and 2 (see Table 43) were assembled and hot isostatically pressed in August. Blade 1 did not have cores, and was therefore assembled using expedient hand-cut titanium plies. Blade 2 was similar to blade 1 except it had small cores, based on the diamond specimen core geometry. Both of these blades developed leaks during the hot isostatic press cycle and did not bond. Leaks were found in small cracks in the heat affected weld zone in the root region of both blades.

Blade 2 was subsequently repaired using an improved weld configuration in the root region. Although not expected to result in good quality bonding, this reprocessing should produce a part suitable for tooling verification trials.

Blade 3 is the first of the blades to be assembled with numerical control machined cores and plies. This blade was fabricated without root blocks in order to simplify first article assembly. It will be processed through the camber, twist, and forge process to evaluate the hollow section.

Blades 4 and 5, except for the addition of root blocks, have the same characteristics as blade 3 and incorporate the improved root area weld configuration. These blades are being assembled and will be shipped to the hot isostatic press vendor in early November 1980.

Evaluation of TRW Hollow Diamond-Shaped Specimens

Random destructive sampling of TRW hollow diamond-shaped sample 25T was conducted. Each bond plane examined was characterized by chain micro-void porosity as shown in Figure 47. Individual voids typically ranged from 0.001 inch to 0.002-inch in diameter. These voids were inspected in the etched condition on a scanning electron microscope at high magnification (they were too small to be inspected in the un-etched condition). The results of this examination indicated that these voids are spherical depressions different from classic surface etch pitting.

Further evidence of the nature and extent of these voids was gained by examining the fracture surface of tensile specimens which failed along bond planes. Tensile specimens were machined from the root simulation areas of specimen 25T. The specimens were machined transverse to the bond planes. Tensile data are shown in Table 44. All but one of the specimens failed through the bond plane in a brittle manner. Visual inspection of failed specimen fracture surfaces indicated varying degrees of discoloration on the surfaces apparently indicative of bond contamination (see Figure 48). Scanning electron microscope Kevex analysis did not identify any chemical differences in the normal versus discolored areas. The nil or low ductility values may have been attributable to this apparent bond contamination. The brittle bond failures enabled the suspect microvoid conditions to be evaluated on a cross-section plane. Scanning electron microscope analysis of these bond planes indicated apparent microvoids (see Figures 49 and 50).



PRATT & WHITNEY AIRCRAFT GROUP
COMMERCIAL PRODUCTS DIVISION

ORIGINAL PAGE IS
OF POOR QUALITY

Figure 47 Chain Micro-voids Along Bond Line at 500x Magnification

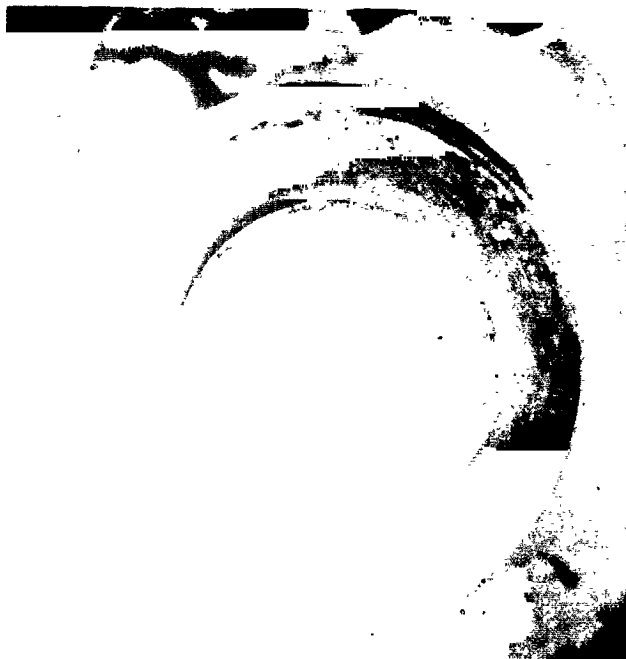


Figure 48 Fracture Surface of Brittle Bond Plane Tensile Specimen Failure
- The dark discoloration area suggests bond contamination.



PRATT & WHITNEY AIRCRAFT GROUP
COMMERCIAL PRODUCTS DIVISION

**ORIGINAL PAGE IS
OF POOR QUALITY**

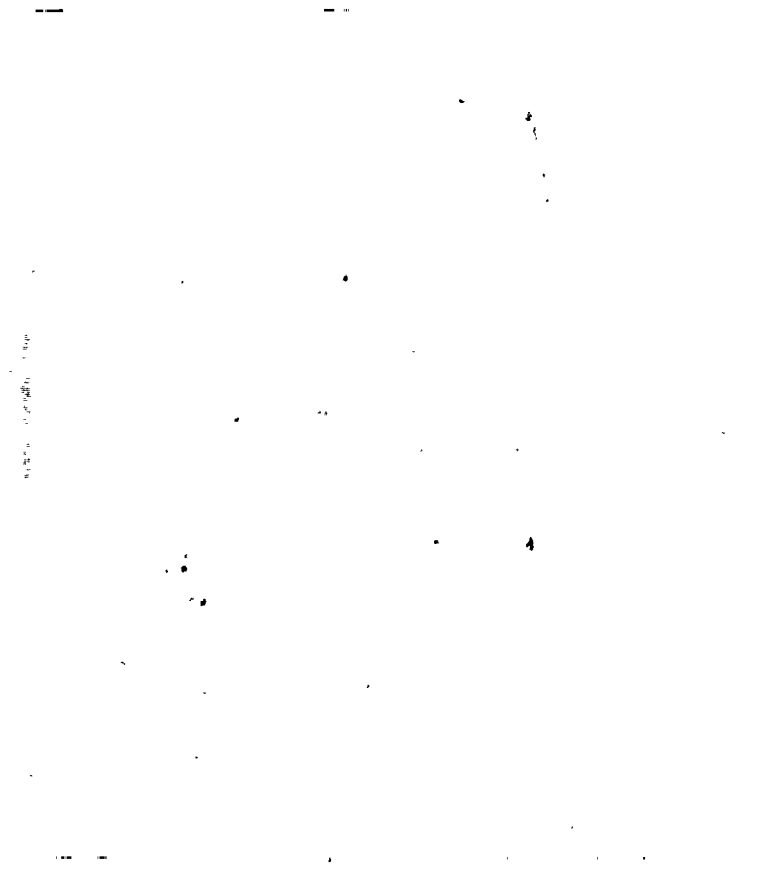
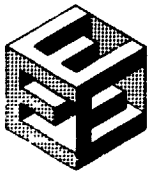


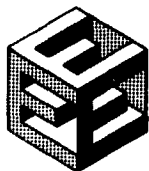
Figure 49 **Scanning Electron Microscope Micrograph of Bond Plane Tensile Failure at 2000x Magnification Showing 4 Apparent Voids on Fracture Surface**



PRATT & WHITNEY AIRCRAFT GROUP
COMMERCIAL PRODUCTS DIVISION

ORIGINAL PAGE IS
OF POOR QUALITY

Figure 50 Stereo Pair Micrograph (500x) of an Apparent Void on Bond Plane
Tensile Failure Fracture Surface



PRATT & WHITNEY AIRCRAFT GROUP
COMMERCIAL PRODUCTS DIVISION

The cause of the microvoid condition was not determined. Gas contamination (shop or process atmosphere) caused by inadequate cleansing, vacuum degassing, or hot isostatic press can sealing could have been responsible. The input material laminates were examined with a scanning electron microscope to determine surface conditions and gain further insight into the apparent causes of the microvoid condition. A micro-pocking condition was observed (see Figure 51) with disparities in size range generally similar to bond microvoids. This condition was considered to be unusual for sheet metal. The effect of this surface condition on future processing is not yet determined.

To improve specimen quality, TRW took steps to improve the specimen fabrication process. These improvements included hot isostatic press package vacuum degassing techniques and hot isostatic press can weldment sealing techniques. TRW then produced a sample incorporating these techniques, and Pratt & Whitney Aircraft evaluated the sample. Eleven destructive microsections were made in various locations around the periphery of the blade and root section. Evaluation of these microsections indicated that the bond planes were again characterized by chain microvoids, which were substantially smaller (0.0002 inch) than in the previous sample (see Figure 52). Several isolated occurrences of beta flec (0.010 to 0.170 inch) were also identified (see Figure 53). The beta flecs were proximate to a bond plane and were mostly centered on the bond line (see Figure 54). This suggests that the problem was caused by the process rather than by the material itself.

TABLE 44

TENSILE DATA

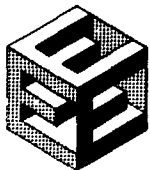
<u>Specimen</u>	<u>Temp.</u> <u>(F)</u>	<u>0.02% YS*</u> <u>(psi)</u>	<u>0.2% YS*</u> <u>(psi)</u>	<u>Ultimate</u> <u>Tensile</u> <u>Strength</u> <u>(psi)</u>	<u>Elong.</u> <u>(%)</u>	<u>Area</u> <u>Reduc-</u> <u>tion (%)</u>	<u>Area</u> <u>(sq. in.)</u>	<u>Load</u> <u>(lb)</u>
1	70	112,190	121,950	123,580	0.9	0.4	0.00615	760
2	70	119,770	125,400	135,850	14.1	43.4	0.00622	845
3	70	120,320	125,200	126,830	0.6	0	0.00615	780
4**	70	105,340	-	106,920	0	0	0.00636	680
5	70	120,830	124,010	131,950	3.4	5.5	0.00629	830
6	70	120,890	125,820	134,050	6.7	8.8	0.00608	815

*YS = Yield Strength

** Specimen 4 fractured at 0.02 percent yield strength

Extensometer located on grips

Elongation measure change in overall length over parallel section

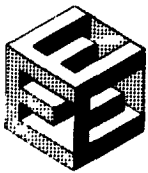


PRATT & WHITNEY AIRCRAFT GROUP
COMMERCIAL PRODUCTS DIVISION

**ORIGINAL PAGE IS
OF POOR QUALITY**

Figure 51 **Scanning Electron Microscope Micrograph (2000x) 0.010-inch Sheet Laminate**

Figure 52 **Chain Micro-voids Along Bond Line at 1000x Magnification - This indicates a smaller void diameter compared with blade samples processed earlier in the program.**



PRATT & WHITNEY AIRCRAFT GROUP
COMMERCIAL PRODUCTS DIVISION

ORIGINAL PAGE IS
OF POOR QUALITY

Figure 53 Linear Beta Fleck Located at Bond Line

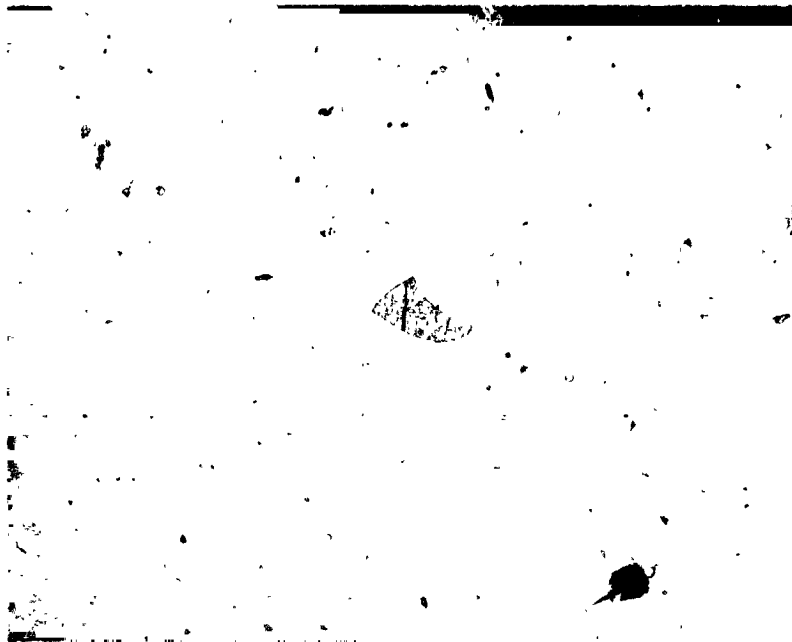
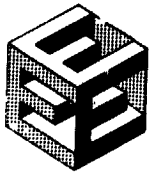


Figure 54 Beta Fleck (200x) Centered on Bond Line - Note delineation of bond line by chain micro-voids.

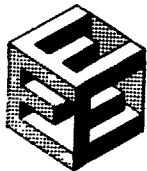
3.2.4 Low-Pressure Compressor

3.2.4.1 Overall Objective

Design a four-stage low-pressure compressor with a design pressure ratio of 1.77 and an adiabatic efficiency of 89.7 percent. The corresponding expected efficiency for the low spool component of the experimental integrated core is 87.4 percent. Additional design goals are an inlet flow of 142.1 lb/sec, a surge margin of 20 percent, and a life of 20,000 missions and 30,000 hours.

3.2.4.2 Scope of Total Work Planned

The program consists of (1) a preliminary analysis and design phase that determines the feasibility of the low-pressure compressor design, and (2) a detailed analysis and design phase that completes the compressor design for use in the integrated core/low spool (Task 4). There is no component rig program or supporting technology program. The design data and the verification of advanced concept are obtained principally from related Pratt & Whitney Aircraft programs such as an in-house supercritical cascade program, the NAVAIR Supercritical Cascade Test (Contract), and the NASA Front Stage Program (Contract No. NAS3-20899). Hardware for the low spool phase of the low-pressure compressor integrated core/low spool phase is fabricated in Task 4. As shown in Figure 55, the preliminary design effort starts at the



beginning of the contract in support of Task 1. The results are presented in a preliminary design review in February 1979. The low-pressure compressor detailed analysis and design begins in October 1979.

Following the acceptance by NASA of the low-pressure compressor detailed design, the low-pressure compressor component is fabricated and tested in the Task 4 integrated core/low spool program. The work plan schedule for the low-pressure compressor component effort is shown in Figure 56 and indicates that the preliminary design has been completed and the detailed design initiated. Critical milestones are noted.

Detailed design activity was initiated earlier than originally planned in order to provide enough design definition in order to permit early procurement of hardware requiring long lead time and to meet the schedule requirements associated with a pending acceleration of the integrated core/low spool test program.

LOW-PRESSURE COMPRESSOR PROGRAM LOGIC DIAGRAM

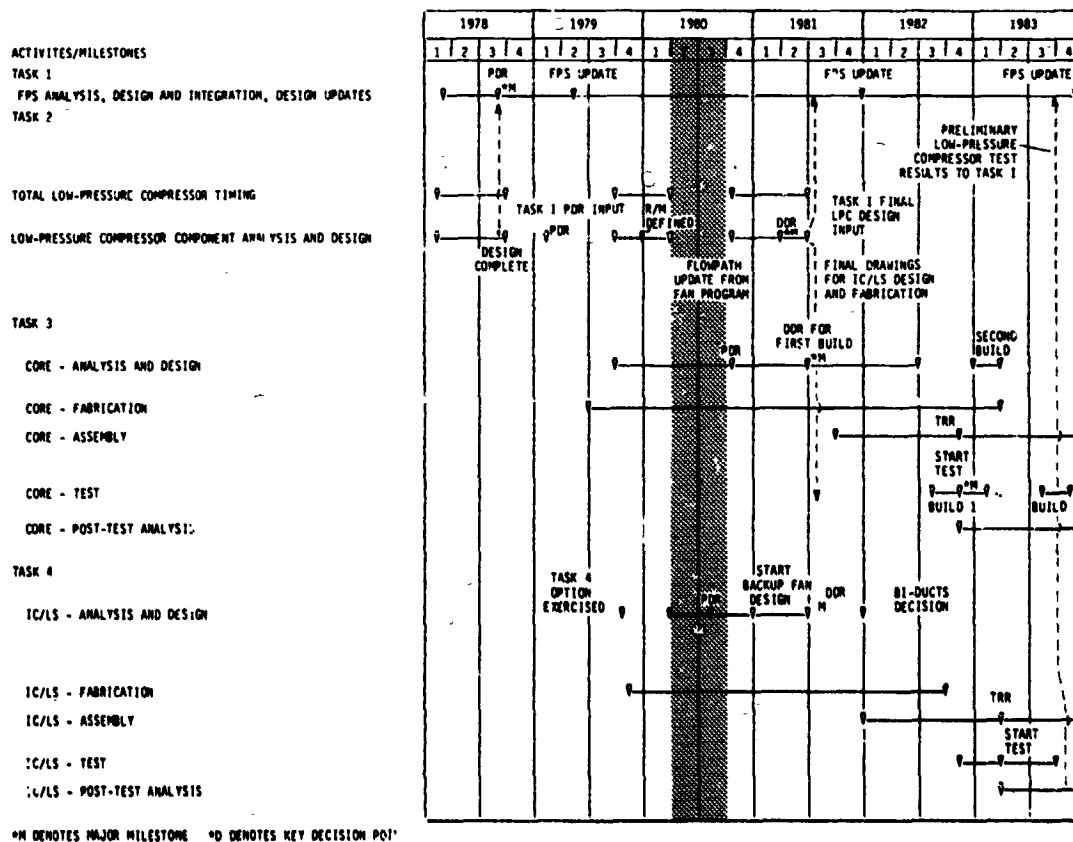
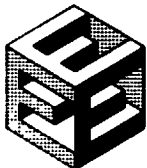


Figure 55 Low-Pressure Compressor Program Logic Diagram



PRATT & WHITNEY AIRCRAFT GROUP
COMMERCIAL PRODUCTS DIVISION

ORIGINAL PAGE IS
OF POOR QUALITY

LOW-PRESSURE COMPRESSOR COMPONENT EFFORT - WORK PLAN SCHEDULE

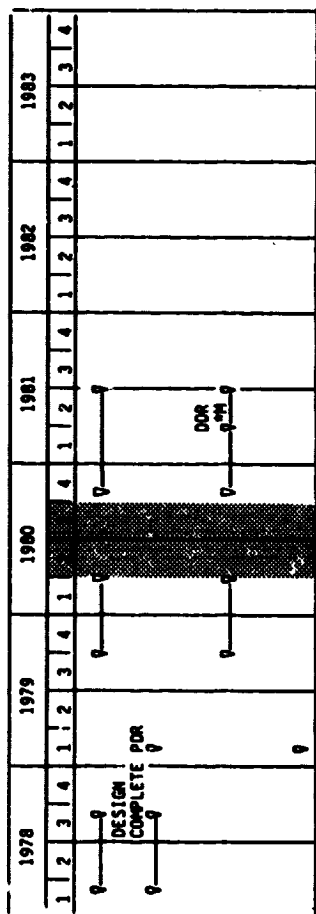


Figure 56 Low-Pressure Compressor Program Component Effort Work Plan Schedule



PRATT & WHITNEY AIRCRAFT GROUP
COMMERCIAL PRODUCTS DIVISION

3.2.4.3 Technical Progress

3.2.4.3.1 Summary of Work Completed

The compressor is composed of 4 stages, 820 airfoils, and features an average blade aspect ratio of 2.3 and an average gap-chord ratio of 0.9. Its hub/tip ratio at the inlet and exit are 0.84 and 0.83, respectively. The component design that evolved from the preliminary design activity is illustrated in Figure 57.

The electron beam welded titanium drum rotor assembly is connected to the low rotor shaft through a single hub bolted to a common fan hub low-pressure compressor hub joint forward of the number 1 bearing. The rotor features canted titanium blades with axial attachments and rotor rim seals for reduced inner cavity volumes.

The compressor stator assembly supporting cases and inlet splitter are fabricated from aluminum for reduced weight. The low-pressure compressor cases feature circumferential, trenched, abradable rub strips over the blade tips to provide the blade tip clearance needed to prevent rubbing under transient engine conditions, while reducing the efficiency penalty associated with tip clearance. The inner stator shrouds also feature abradable rub strips to provide the required clearance control under the rotor knife edge seals. Rub strip material in both inner and outer diameter locations is silicon rubber.

Low power surge protection and reverse thrust stability are provided by a fifth stage annular bleed. Circumferential holes aft of the fifth stator provide required airflow to a fully modulated annular bleed ring, which translates forward via a linkage system to allow bleed air to exit from the compressor and dump into the fan duct forward of the fan exit vanes. The bleed system is sized to provide a maximum of 15 percent of flow extraction from the core flowpath.

The low-pressure compressor design incorporates several aerodynamic features to maximize efficiency. The largest efficiency benefit results from the low axial velocity ratio employed in the flow pattern selection. As a result, it has a somewhat higher aerodynamic tip speed and lower specific weight flow than the JT9D-7A reference engine low-pressure compressor. An additional efficiency improvement is gained through the incorporation of tip trenches over the rotor tips. At typical clearance levels, the trenched rotor has a smaller efficiency loss caused by tip clearance effects.

Controlled diffusion airfoils were selected for use throughout the low-pressure compressor. Back-to-back testing of controlled diffusion airfoils and the more conventional multiple circular arc airfoils has shown that the controlled diffusion airfoil offers an improvement in critical Mach number and an increase in incidence range. Moreover,



analytical predictions indicate that boundary layer separation characteristics were improved in the controlled diffusion airfoils when compared to the 400 series airfoils. Current performance parameters at significant engine operating conditions are listed in Table 45.

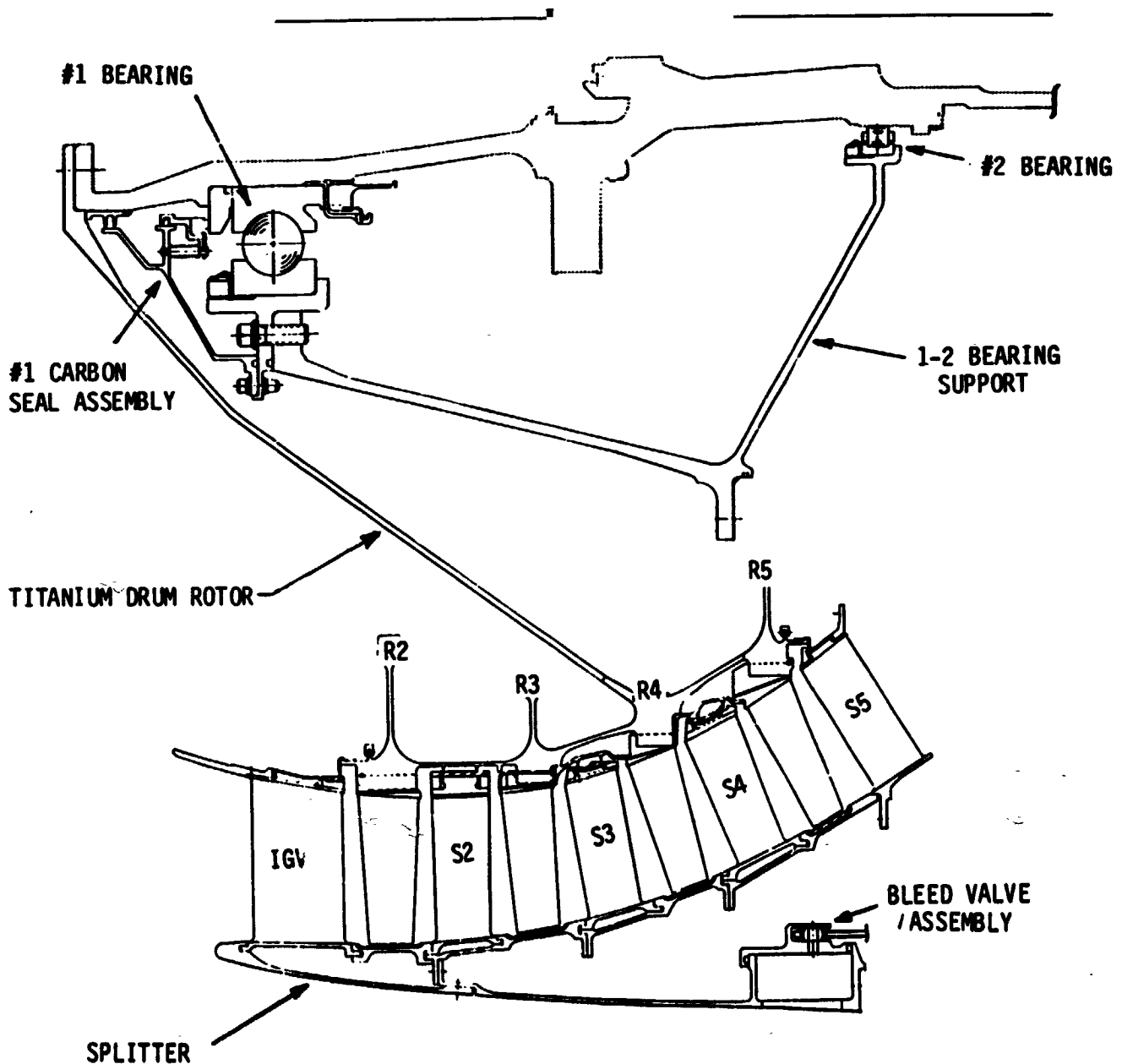


Figure 57 Low-Pressure Compressor Component



PRATT & WHITNEY AIRCRAFT GROUP
COMMERCIAL PRODUCTS DIVISION

TABLE 45

CURRENT LOW-PRESSURE COMPRESSOR PERFORMANCE PARAMETERS

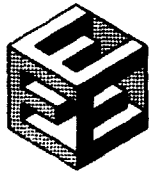
	Engine Operating Condition			
	ADP	Max. Cruise	Max. Climb	Takeoff
Pressure Ratio	1.77	1.74	1.82	1.61
Efficiency (Percent)				
Adiabatic	89.9	90.3	89.5	92.0
Polytropic	90.6	91.0	90.3	92.4
Inlet Corrected Airflow (lb/sec)	125.5	123.5	128.5	112.5
Inlet Specific Airflow (lb/sec/ft ²)	35.6	35.0	36.4	31.9
Inlet Corrected Tip Speed (ft/sec)	797	786	817	723
Exit Temperature (F)	151	146	190	246

3.2.4.3.2 Current Technical Progress

The aerodynamic and mechanical design of the low-pressure compressor component was continued during this reporting period. Aerodynamic design of the blades and stators is nearly complete, and final structural analysis of these airfoils is approximately 75 percent complete. Only minor structural/aerodynamic modifications are expected before this work is completed. The final flowpath and configuration have been selected. The mechanical design of individual parts is now in progress.

Aerodynamic Design

The final aerodynamic design of the low-pressure compressor was initiated, using the aerodynamic guidelines presented in the Fourth Semiannual Status Report. The axial gapping between the blade and vane rows, established during the preliminary analysis and design phase, was found to be inadequate. Therefore, the low-pressure compressor flowpath was redrawn with the correct gapping. This revised gapping, however, resulted in a 2-inch increase in the length of the low-pressure compressor. To correct this problem, the rear stage blade roots were moved closer to the intermediate case (the required spacing between the



PRATT & WHITNEY AIRCRAFT GROUP
COMMERCIAL PRODUCTS DIVISION

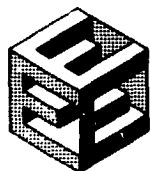
fifth stage rotor and the case was maintained). This reduced the overall length increase to 1 inch, and also reduced the cant angle in the fifth stage rotor from 26 degrees to 17 degrees. Aerodynamic design work then proceeded using this revised flowpath and the previously established airfoil designs.

Aerodynamic loadings were balanced at a performance point with 10 percent surge margin above the 63 percent maximum cruise operating point. The low-pressure compressor aerodynamic design point parameters are presented in Table 46.

TABLE 46

LOW-PRESSURE COMPRESSOR AERODYNAMIC DESIGN POINT SUMMARY

		Stage				
		FAN ID & S1	2	3	4	5
$\Delta T_o / \theta T_2$	$^{\circ}R$	80.7	27.2	30.2	31.2	26.2
Reactions	$\Delta P_{\text{rotor}} / \Delta P_{\text{stage}}$	0.670	0.544	0.563	0.580	0.675
Loading	"D _f " Rotor		0.325	0.368	0.408	0.413
	"D _f " Stator	0.354	0.319	0.373	0.416	0.430
Aspect Ratio Span/b _{root}	Rotor			2.29	2.42	2.29
	Stator	1.51	2.19	2.29	2.46	2.51
% Blockage	Rotor Out/Stator In	4.0	1.9	.7	1.5	2.8
	Stator Out/Rotor In	4.0	2.5	2.4	4.3	6.1
Velocity $C_{\text{mave}} / \sqrt{\theta} T_2$ ft/sec	Rotor In		622	591	556	533
	Rotor Out		568	543	518	484
	Stator In	633	578	556	526	487
	Stator Out	618	579	548	529	494
Swirl $C_{\text{uave}} / \sqrt{\theta} T_2$ ft/sec	Rotor In		290	236	186	118
	Rotor Out		498	472	446	359
	Stator In	624	498	476	453	368
	Stator Out	291	235	184	116	5



PRATT & WHITNEY AIRCRAFT GROUP
COMMERCIAL PRODUCTS DIVISION

The use of controlled diffusion airfoils was maintained throughout the low-pressure compressor because they have more range and exhibit lower loss than conventional series airfoils. The controlled diffusion airfoils were designed at the aerodynamic design point and their performance was evaluated at the following additional points:

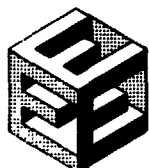
- (1) operating line: 63 percent of maximum cruise.
- (2) 10 percent surge margin at constant speed above the 63 percent maximum cruise point.
- (3) 15 percent surge margin at constant speed above the aerodynamic design point.
- (4) operating line maximum corrected flow.

The controlled diffusion airfoils were designed to maintain low losses at all flight conditions. This approach, however, was proven impossible for some sections of some airfoils. All the airfoils were designed to have sufficient area margin at the maximum flow condition and to be in the low loss range for the operating line condition. Some increase in loss was allowed for the near surge conditions. A comparison design using series airfoils showed that some of the airfoil sections had insufficient low loss range to meet operating line conditions, indicating the gain achievable with controlled diffusion airfoils. A final design geometry summary of the airfoils used in the low-pressure compressor is presented in Tables 47 and 48. Final structural analysis of these airfoils is underway. Completion of this analysis is expected by mid-October 1980.

TABLE 47

FINAL BLADE GEOMETRY SUMMARY

	<u>Stage 2</u>	<u>Stage 3</u>	<u>Stage 4</u>	<u>Stage 5</u>
AF Series	CDA*	CDA	CDA	CDA
No. Foils	82	88	90	74
Material	AMS 4928	AMS 4928	AMS 4928	AMS 4928
Root Radius (in.)	19.52	19.49	18.47	16.60
Mean Radius (in.)	21.46	21.20	20.13	18.42



PRATT & WHITNEY AIRCRAFT GROUP
COMMERCIAL PRODUCTS DIVISION

TABLE 47 (Cont'd)

	<u>Stage 2</u>	<u>Stage 3</u>	<u>Stage 4</u>	<u>Stage 5</u>
Tip Radius (in.)	23.26	22.93	21.80	20.12
Length (in.)	3.74	3.52	3.40	3.46
Hub/Tip Ratio	0.84	0.85	0.85	0.83
Root Chord (in.)	1.55	1.51	1.42	1.60
Mean Chord (in.)	1.65	1.51	1.42	1.59
Tip Chord (in.)	1.77	1.51	1.42	1.60
Aspect Ratio	2.41	2.33	2.39	2.16
t/b_{root}	0.085	0.083	0.085	0.068
t/b_{mean}	0.056	0.064	0.065	0.048
t/b_{tip}	0.030	0.044	0.045	0.036
θ *root deg.	43.4	35.6	43.9	43.2
θ *mean deg.	18.4	20.3	22.2	18.0
θ *tip deg.	27.9	25.8	28.7	26.2
$\alpha_{\text{ch root}}$ deg.	69.02	65.45	65.44	61.60
$\alpha_{\text{ch mean}}$ deg.	58.72	55.68	53.90	52.15
$\alpha_{\text{ch tip}}$ deg.	47.50	43.61	42.40	44.86
Solidity (root)	1.10	1.09	1.10	1.18
Solidity (mean)	1.00	1.00	1.00	1.03
Solidity (tip)	0.92	0.92	0.93	0.94

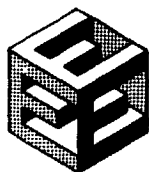


TABLE 48

FINAL VANE GEOMETRY SUMMARY

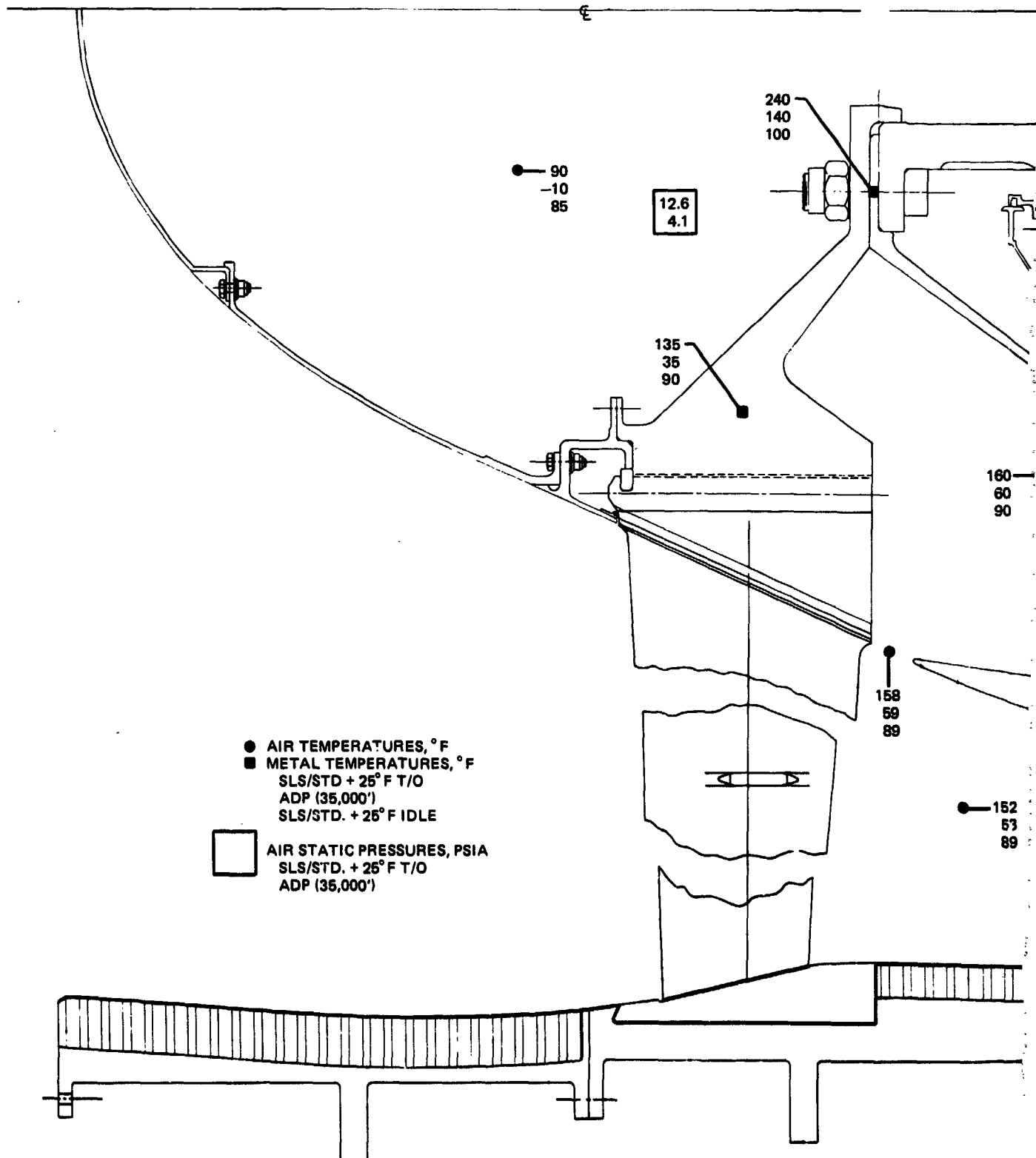
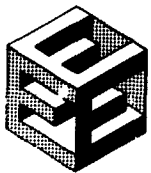
	Stator				
	<u>1</u>	<u>2</u>	<u>3</u>	<u>4</u>	<u>5</u>
AF Series	CDA	CDA	CDA	CDA	
No. Foils	76	102	110	108	90
Material	(Steel)	AMS 4135	AMS 4135	AMS 4135	AMS 4135
Root Radius	19.21	19.59	19.12	17.67	15.43
Mean Radius	21.32	21.41	20.76	19.35	17.32
Tip Radius	23.18	23.17	22.44	21.03	19.03
Length	3.97	3.60	3.40	3.45	
HUB/TIP	0.83	0.85	0.85	0.84	0.81
Root Chord, I.D.			1.65	1.48	1.43
Mean Chord		1.65	1.48	1.43	
Tip Chord, O.D.		1.65	1.48	1.42	
Aspect Ratio		2.18	2.30	2.41	
t/b _{root} , I.D.	0.050	0.070	0.070	0.070	.079
t/b _{mean}	0.061	0.070	0.070	0.070	.077
t/b _{tip} , O.D.	0.070	0.070	0.070	0.070	.073
θ root	39.4	40.8	34.5	47.4	58.6
θ mean	22.7	22.9	27.0	36.3	42.9
θ tip	22.4	36.2	39.5	50.3	56.3
a ch root, I.D.		56.24	58.22	63.92	
a ch mean		62.46	64.43	66.90	
a ch tip, O.D.		55.75	61.55	60.53	
Solidity (root)	1.659	1.363	1.360	1.386	1.426
Solidity (mean)	1.493	1.248	1.252	1.266	1.278
Solidity (tip)	1.341	1.156	1.160	1.171	1.168

A pressure and temperature analysis of the compressor was completed. The data are being used in the design of each part in the component. The analysis results are shown in Figure 58.

Mechanical Design

Rotor. The mechanical design of the low-pressure compressor rotor was initiated during this reporting period. NASA approval was received for using a bolted rotor configuration in place of the drum rotor for the integrated core/low spool. The bolted rotor offers cost benefits in both analysis and fabrication areas. The rotor design also includes the use of existing design rotor fastenings.

Stator and Case Assemblies. Mechanical design of the stator and case assemblies was initiated with the intent of producing a low cost design. The design concept of the flight propulsion system has been



FOLDOUT FRAME

➤ FOLDOUT FRAME

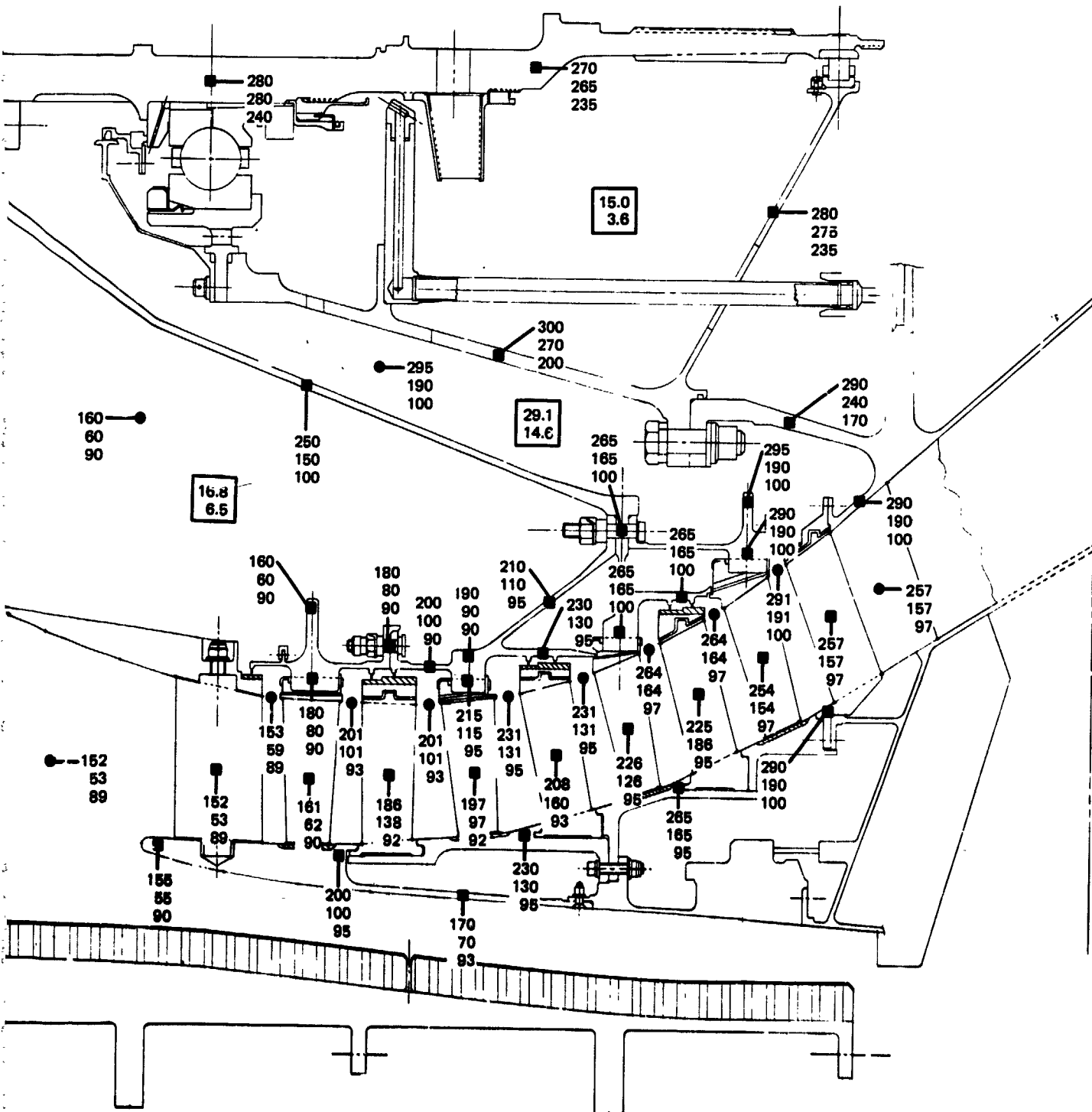
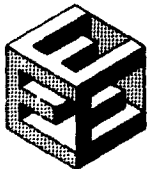


Figure 58 Low-Pressure Compressor Pressure and Temperature Analysis Results



PRATT & WHITNEY AIRCRAFT GROUP
COMMERCIAL PRODUCTS DIVISION

retained. This design, however, will not be optimized to achieve the lightest possible weight for the integrated core/low spool. This will reduce design effort and machining requirements. The current design of the low-pressure compressor component is presented in Figure 59.

Number 1 and 2 Bearing Compartment. The design of the number 1 and 2 bearing compartment was completed during this reporting period (see Figure 60). To reduce cost, this design incorporates as much existing hardware as possible. This hardware includes: (1) number 1 and 2 bearings, (2) bearing housing, (3) bearing support, (4) carbon seal, and (5) fastenings.

The number 1 and 2 bearing compartment houses a ball bearing in the number 1 position and a roller bearing in the number 2 position. Both bearings meet all integrated core/low spool life requirements. The number 1 bearing features a split inner race, and the number 2 bearing is characterized by a double-shouldered outer race. The flight propulsion system requires larger diameter bearings in both positions. The number 2 bearing does not meet flight propulsion system life requirements. A description of the number 1 and 2 bearings is presented in Table 49.

The number 1 bearing housing meets all integrated core/low spool requirements for blade loss loads and oil drainage flow rates. The front flange of this housing is larger than required for the flight propulsion system, and, therefore, could be optimized for reduced weight.

TABLE 49
BEARING DIAMETER

	<u>No. 1 Bearing</u>	<u>No. 2 Bearing</u>
Type	Unflanged Ball Split Inner Race	Unflanged Roller Double Shouldered Outer Race
Size	210 x 350 x 55.9 mm	130 x 180 x 21.9 mm
Material		
Rolling Element	PWA 793	PWA 723
Rings	PWA 793	PWA 723
Cage	AMS 4616	AMS 6414
No. of Rolling Elements	20	26
Rolling Element Size (in.)	1.5625 dia.	0.5512 dia. x 0.5512 long
Internal Radial Clearance (in.)	0.0133-0.0145	0.0036-0.0052
DN Value, max	0.819×10^6	0.507×10^6
Cooling Scheme	Axial Scoop Under Race	Jet



PRATT & WHITNEY AIRCRAFT GROUP
COMMERCIAL PRODUCTS DIVISION

ORIGINAL DESIGN
OF POOR QUALITY

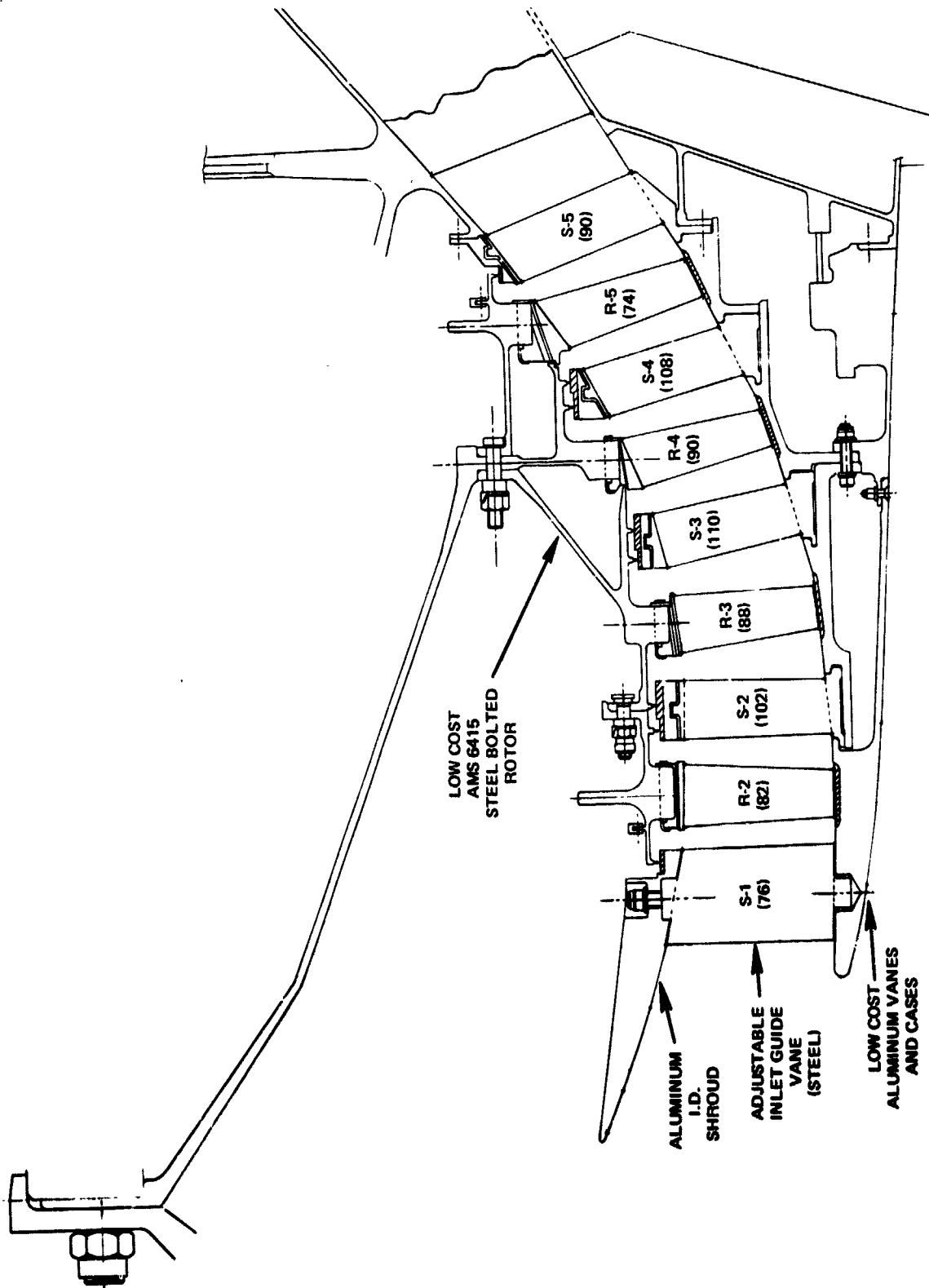
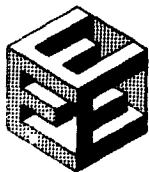


Figure 59 Low Cost Integrated Core/Low Spool Low-Pressure Compressor Component - Aerodynamics remain the same as for the flight propulsion system design.



PRATT & WHITNEY AIRCRAFT GROUP
COMMERCIAL PRODUCTS DIVISION

ORIGINAL PAGE 19
OF POOR QUALITY

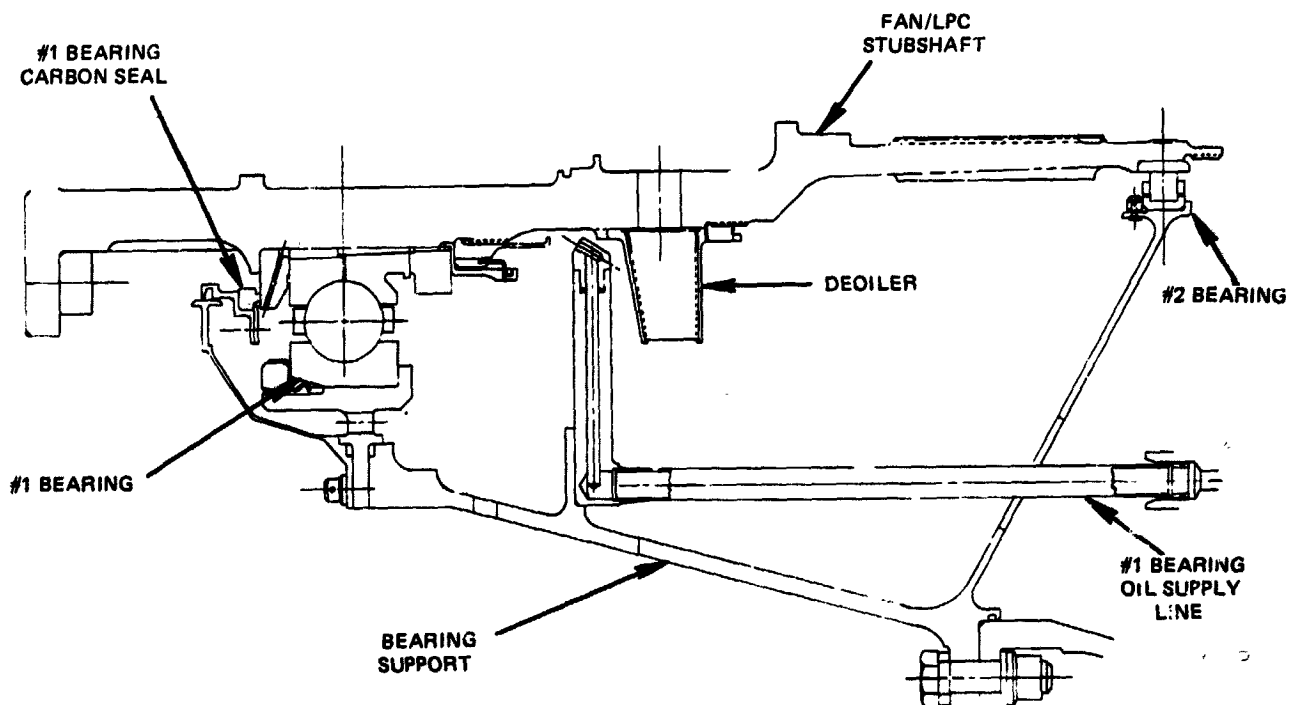


Figure 60 Number 1 and 2 Bearing Compartment

The number 1 and 2 bearing support is designed to meet blade loss load and spring rate requirements. An existing bolt was incorporated at the intermediate case mount flange, which was sized for the fan blade loss requirement. Calculated stresses for the blade loss condition are shown in Figure 61.

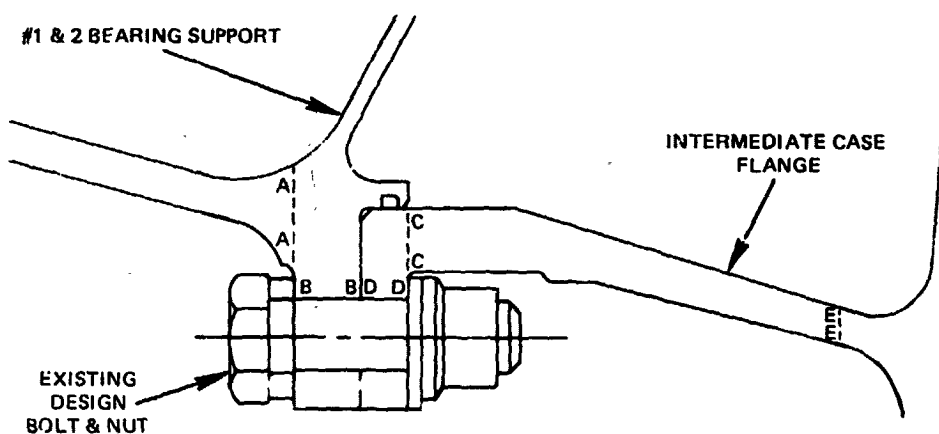
The oil system for the number 1 bearing delivers oil to the number 1 bearing and seal at a rate of 18 lb/min. The oil is routed by way of an axial scoop attached to the bearing nut, and reaches the bearing through slots and grooves in the stubshaft, nuts, and spacers. The oil drains to the intermediate case bottom strut through holes in the bearing housing and bearing support.

The radial vane de-oiler, mounted on the stubshaft, removes the oil vapor from the engine breather air at a flow rate of 0.118 percent W_{ae} . This de-oiler consists of radial vanes brazed into machined grooves in AMS 5062 steel sideplates.



PRA TT & WHITNEY AIRCRAFT GROUP
COMMERCIAL PRODUCTS DIVISION

ORIGINAL PAGE IS
OF POOR QUALITY



BLADE LOSS STRESSES

LOCATION	IC/LS LOADS	FPS LOADS
A-A	60.8K	72.7K
B-B	62.8K	75.1K
C-C	114.1K	136.5K
D-D	108.5K	129.8K
E-E	40.1K	40.1K

Figure 61 Number 1 and 2 Bearing Support Flange



3.2.5 High-Pressure Compressor

3.2.5.1 Overall Objective

Design a ten-stage, high-pressure compressor that produces a pressure ratio of 14, and has an adiabatic efficiency of 88.2 percent and an average blade aspect ratio of 1.5. The corresponding expected efficiency for the experimental integrated core/low spool component is 86.4 percent. Additional design goals are an inlet corrected flow of 77.5 lb/sec, a surge margin of 20 percent, and life of 20,000 missions and 30,000 hours.

3.2.5.2 Scope of Total Work Planned

The program consists of (1) a high-pressure compressor preliminary analysis and design phase, which determines the feasibility of the compressor design; (2) a detailed analysis and design phase, which provides the hardware design for the high-pressure compressor rig program, core test, and integrated core/low spool program; (3) a high-pressure compressor hardware fabrication program, which supplies non-rotating and rotating component hardware to the high-pressure compressor rig program; and (4) a high-pressure compressor component rig program to verify and optimize the compressor design. The design effort does not require a separate supporting technology phase to provide design data and verification for advanced concepts. This information will be obtained principally from other Pratt & Whitney Aircraft programs such as an in-house supercritical cascade program and a NAVAIR supercritical cascade test (Contract).

The preliminary design activity provides layout drawings and substantiating data, which are presented to NASA for approval at a preliminary design review in September 1978. The results of the detailed design activity are presented for NASA approval at a detailed design review in February 1980.

Figure 62 shows the relationship between the elements of this task and contract Tasks 1, 3, and 4. The program shown in the figure begins with the preliminary design activity which provides design input to the high-pressure compressor component rig program and to Task 1 as well as to the detailed design activity that immediately follows. Component and rig hardware is fabricated simultaneously. All component hardware is transferred to the rig program in October 1980 for assembly in the test rig. Upon analysis of the first test data, the high-pressure compressor airfoil designs are updated, as required, to optimize the compressor design. The resultant updated airfoil requirements are transferred to Task 3 for hardware fabrication and to Task 1 for flight propulsion system update. The second rig test incorporates the reworked airfoils and its results are used to evaluate the performance of the optimized compressor design. The critical milestones for the high-pressure compressor effort are shown in the work plan schedule in Figure 63. This figure also indicates that the preliminary design of the component has been completed and that detailed design of both the component and rig were well along at the beginning of this reporting period. Component and rig fabrication efforts prior to this reporting period consisted primarily of early raw material procurement.



ORIGINAL PAGE IS
OF POOR QUALITY

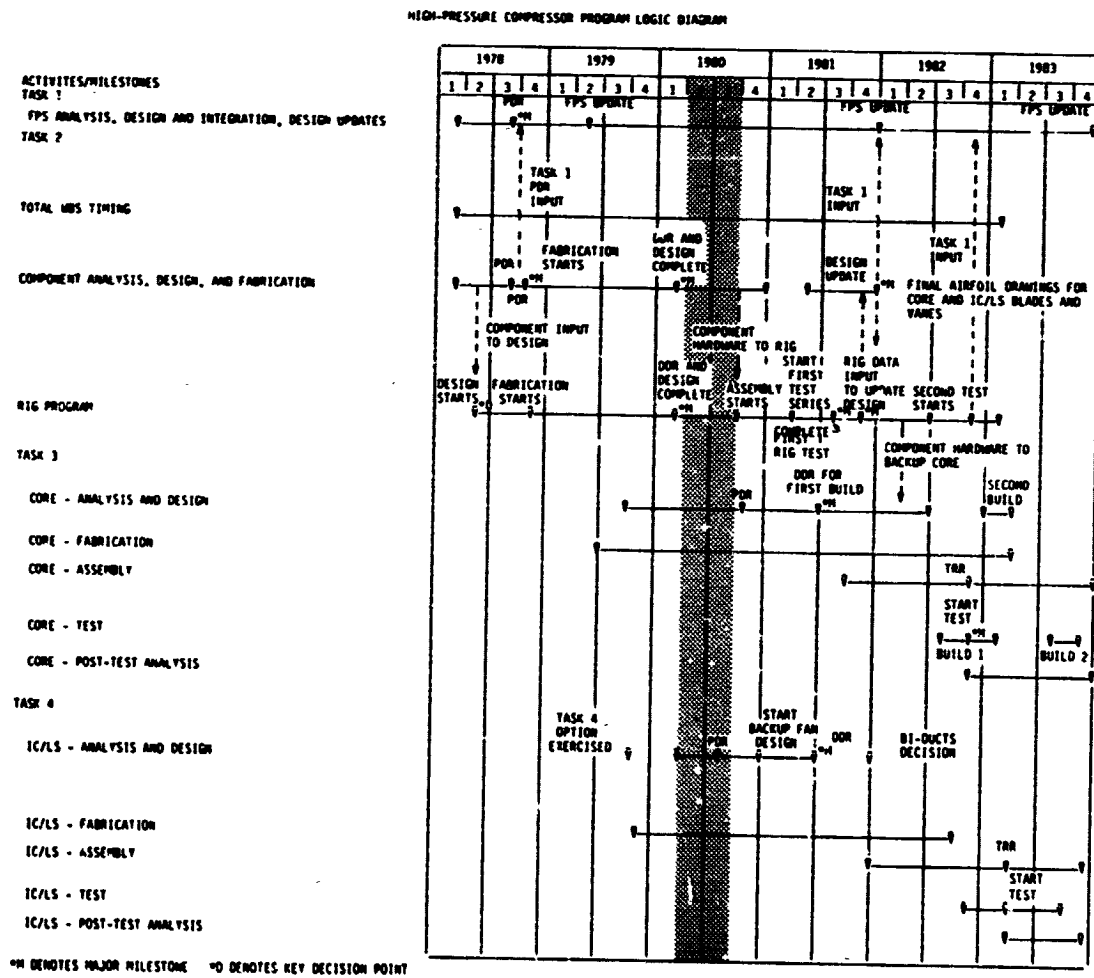


Figure 62 High-Pressure Compressor Program Logic Diagram



PRATT & WHITNEY AIRCRAFT GROUP
COMMERCIAL PRODUCTS DIVISION

ORIGINAL PAGE IS
OF POOR QUALITY

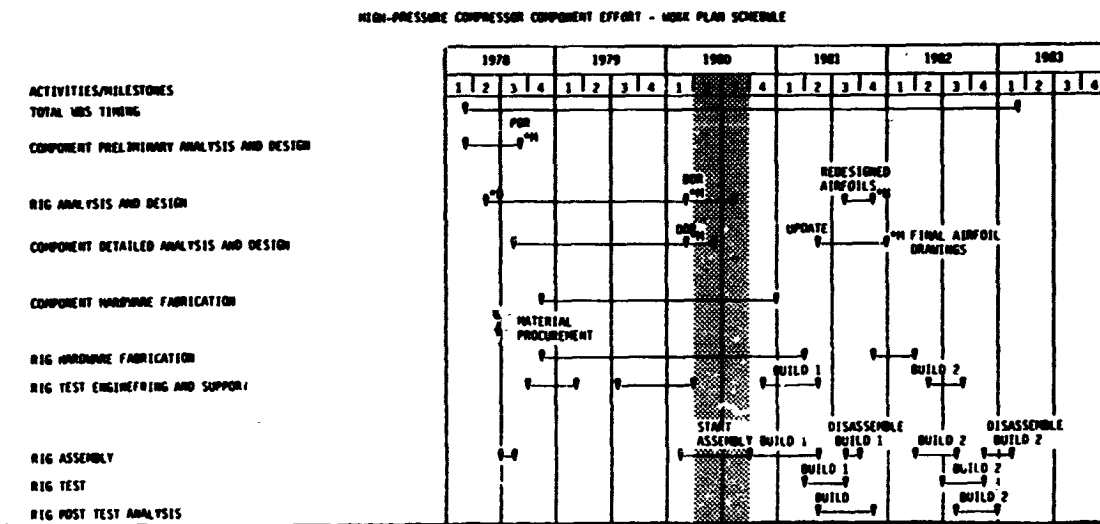


Figure 63 High-Pressure Compressor Component Effort Work Plan Schedule



3.2.5.3 Technical Progress

3.2.5.3.1 Summary of Work Previously Completed

All detailed analysis and design work for the high-pressure compressor component and rig was completed during the previous reporting period, and a design review was held at NASA-LERC in February 1980. A detailed discussion of the results of this effort is presented in the Fourth Semiannual Status Report. A brief summary of these results is presented in the following paragraphs.

The Energy Efficient Engine high-pressure compressor component and its companion rig design are illustrated in Figures 64 and 65, respectively. The compressor has ten stages. The first four stages have variable geometry stators. The front case is split case configuration to accommodate the variable geometry stators. The rear is a single piece. Active clearance control is incorporated in the rear stages.

This high-pressure compressor design also features a drum rotor construction, extensive use of titanium in the static structure, and significantly fewer airfoils. These technology concepts combine to make the compressor assembly lighter, less costly, and easier to maintain.

The drum rotor construction features an electron beam welded titanium front end bolted to the MERL 76 (PWA 1099) powdered metal compaction, nickel alloy, rear section. Axial blade attachments are used in the first three stages, and tangential attachments are used in the fourth through tenth stages. The compressor also employs integral knife edge seals and reduced volume inner cavities for reduced cavity losses. The variable geometry stators employed in the first four stages represent current state-of-the-art design.

The single piece rear case does not have the axial split usually associated with a drum rotor design and therefore results in a lighter, less costly case. These combined features make the case less susceptible to ovalization and more capable of providing improved control of blade tip clearances.

The rear stator and shroud configuration incorporates pairs of vanes brazed into 90-degree shroud assemblies, riveted together in groups of three. These 90-degree groups attach to the case by special hook attachments, located at the ends of each group. The groups are attached to the case at locations selected to provide optimum blade tip clearance. This construction also minimizes steps in the flowpath and allows the most effective use of active clearance control.

The high-pressure compressor rig consists of the following items:

- (1) Inlet section that simulates the low-pressure compressor flowpath, with inlet distortion generation capability,
- (2) High-pressure compressor rotor assembly,



PRATT & WHITNEY AIRCRAFT GROUP
COMMERCIAL PRODUCTS DIVISION

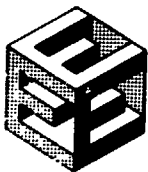
- (3) Component front vane case with associated vane adjustment hardware,
- (4) Unique rig rear compressor case with remotely variable stators in all stages,
- (5) Simulated diffuser and burner section,
- (6) Close-coupled throttling valve, and
- (7) Rig drive system that adapts to the component rotor.

Both internal and external active clearance control systems were evaluated. The selected external active clearance control system eliminates the complex design problems of the internal system. A most important feature of the external system is that it provides a method for which the optimum blade tip clearance might be achieved by case rotor thermal matching.

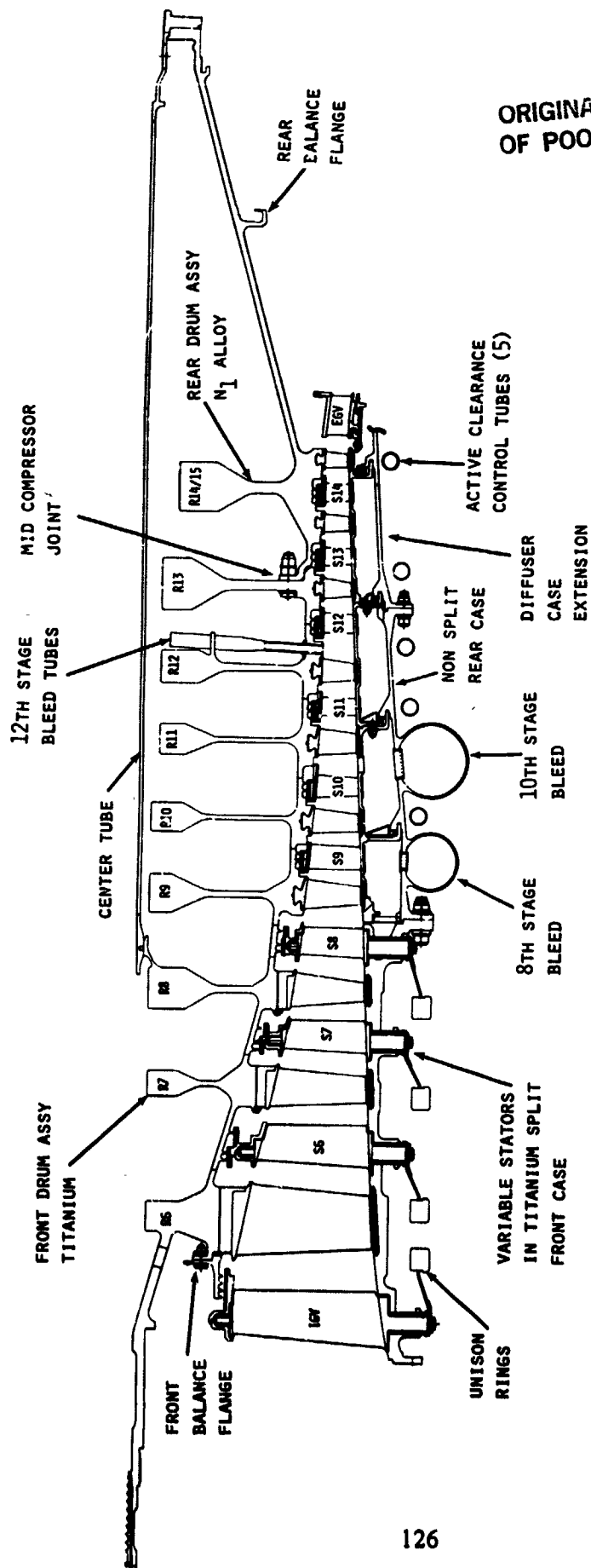
The aerodynamic design of the high-pressure compressor was updated subsequent to the preliminary design review. Aerodynamic revisions included (1) a reduction in inlet hub/tip ratio, (2) reaction changes, (3) endwall camber modifications, (4) gap/chord revisions, and (5) use of controlled diffusion airfoils in all stages with the exception of the first two rotating blade rows. These two blade rows have supersonic and high transonic tip Mach numbers and are bladed with multiple circular arc airfoils. Multiple circular arc design parameters have been optimized in this Mach number range, based on NASA and Pratt & Whitney Aircraft experimental test results.

Table 50 compares the updated design with the previous configuration established at the preliminary design review. The changes to the design parameters shown in Table 50 were presented to NASA at an interim design review in early October 1979. The updated design incorporates the effects of engine downsizing. Current performance parameters at significant engine operation conditions are presented in Table 51.

The mechanical design of the compressor was also updated as the detailed design effort progressed. Table 52 compares the present compressor design status to the goals at the aerodynamic design point.

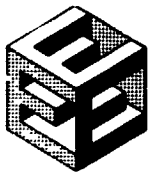


PRATT & WHITNEY AIRCRAFT GROUP
COMMERCIAL PRODUCTS DIVISION



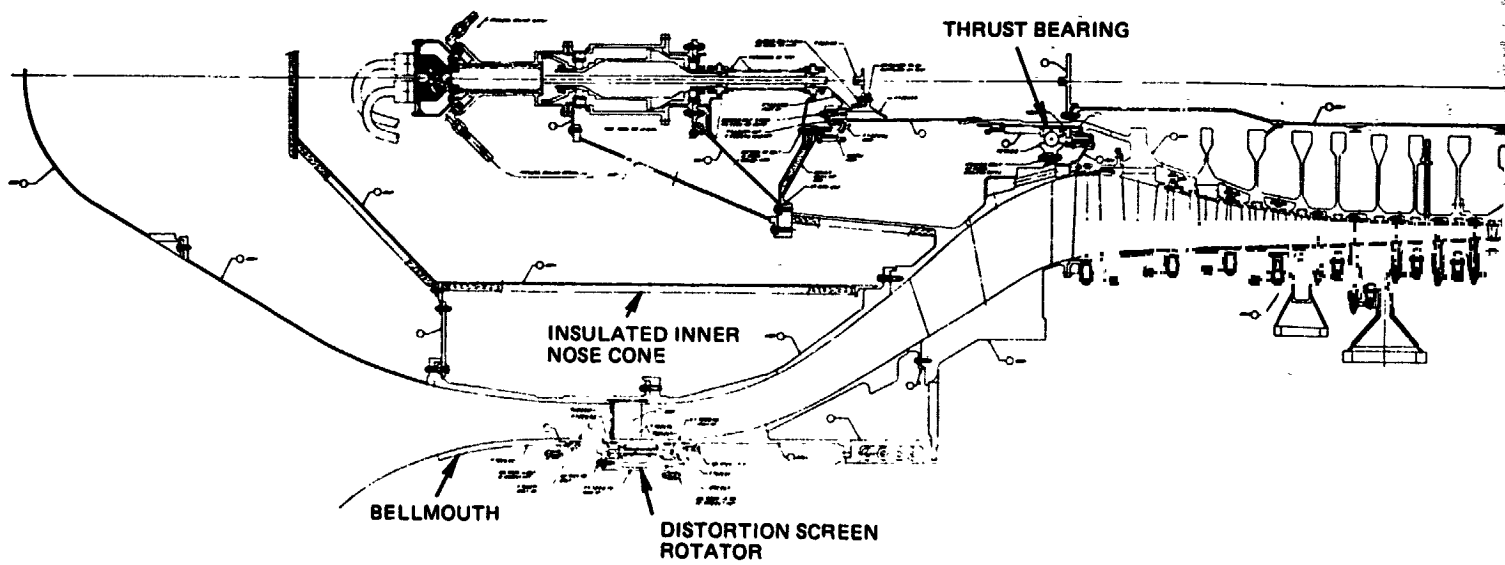
ORIGINAL PAGE IS
OF POOR QUALITY

Figure 64 High-Pressure Compressor Component



PRATT & WHITNEY AIRCRAFT GROUP
COMMERCIAL PRODUCTS DIVISION

ORIGINAL PAGE 13
OF POOR QUALITY



9 FOLDOUT FRAME

ORIGINAL DRAWING
OF POOR QUALITY

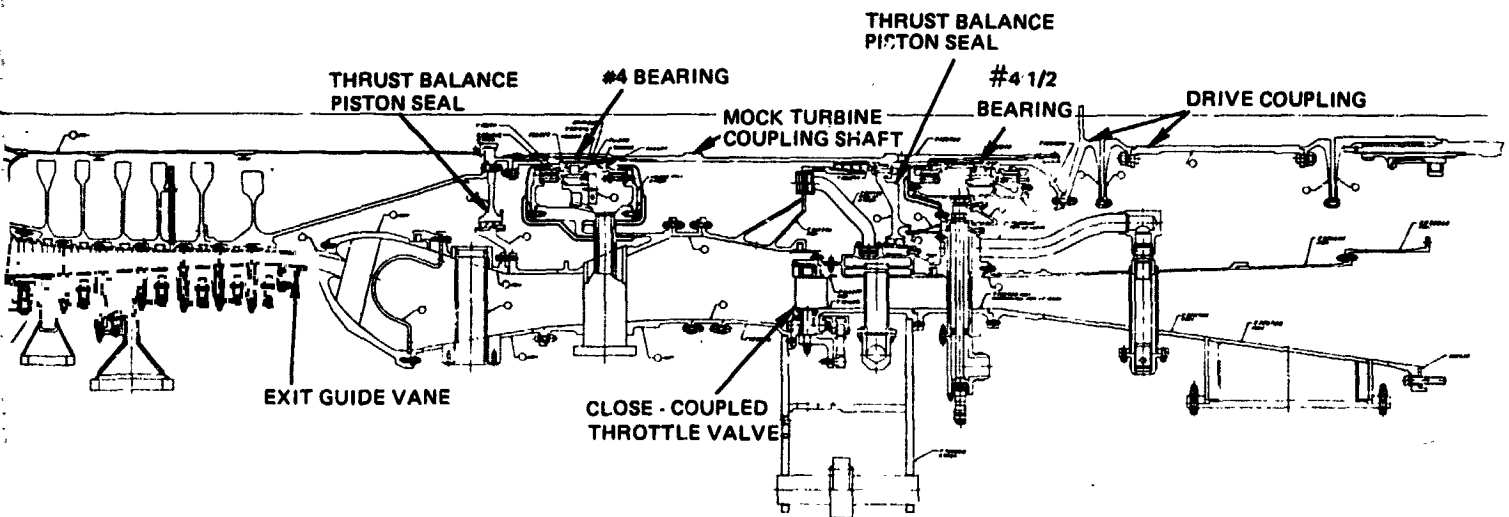


Figure 65 High-Pressure Compressor Rig



PRATT & WHITNEY AIRCRAFT GROUP
COMMERCIAL PRODUCTS DIVISION

TABLE 50

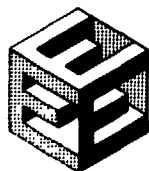
**ENERGY EFFICIENT ENGINE
HIGH-PRESSURE COMPRESSOR DESIGN COMPARISON SUMMARY**

<u>DESIGN PARAMETERS</u>	<u>AERODYNAMIC DESIGN POINT</u>	
	<u>PRELIMINARY DESIGN</u>	<u>UPDATED DESIGN</u>
Number of Stages	10	10
Pressure Ratio	14	14
Adiabatic Efficiency Percent	88.2	88.2
Surge Margin, Percent	25	20
Corrected Flow, lb/sec	88.1	77.5
Corrected Speed, rpm	11,384	12,136
Inlet Corrected Tip speed, ft/sec	1323	1245
Inlet Specific Flow, lb/sec/ft ²	38	38
Inlet Hub/Tip Ratio	0.63	0.56
Exit Hub/Tip Ratio	0.922	0.924
Exit Mach Number (without blockage)	0.28	0.287
Average Aspect Ratio	1.56	1.52
Average Gap Chord Ratio	0.93	0.89
Axial Velocity/Wheel Speed Ratio	0.55	0.56
Number of Variable Stator Rows	4	4
Number of Airfoils (without inlet guide vanes)	1320	1265
Flowpath Type	CMD	CMD

TABLE 51

**CURRENT HIGH-PRESSURE COMPRESSOR
PERFORMANCE PARAMETERS**

	<u>Engine Operating Condition</u>			
	<u>Aero. Des. Point</u>	<u>Maximum Cruise</u>	<u>Maximum Cruise</u>	<u>Takeoff</u>
Pressure Ratio	14.00	13.90	14.00	13.25
Efficiency (percent)				
(Adiabatic)	88.3	88.4	88.3	89.3
(Polytropic)	91.7	91.8	91.7	92.3
Inlet Corrected Airflow (lb/sec)	77.65	77.25	77.50	75.10
Inlet Specific Airflow (lb/sec/ft ²)	38.0	37.8	37.9	36.8



PRATT & WHITNEY AIRCRAFT GROUP
COMMERCIAL PRODUCTS DIVISION

TABLE 51 (Cont'd)

	Engine Operating Condition			
	Aero. Des. Point	Maximum Cruise	Maximum Cruise	Takeoff
Inlet Corrected Tip Speed (ft/sec)	1245	1245	1245	1230
Rotor Speed (rpm)	13180	13095	13580	13970
Exit Temperature (F)	898	882	977	1055

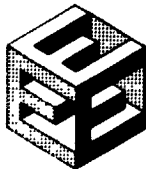
TABLE 52

PRESENT COMPRESSOR DESIGN STATUS COMPARED TO GOALS

<u>Parameter</u>	<u>Goal</u>	<u>Status</u>
Pressure Ratio	14.0	14.0
Flight Propulsion System Adiabatic Efficiency (percent)	88.2	88.3
Integrated Core/Low Spool Adiabatic Efficiency (percent)	86.4	86.5
Average Blade Aspect Ratio	1.50	1.55
Inlet Corrected Flow (lb/sec)	77.5	77.5
Surge Margin (percent)	20	20
Drum Low Cycle Fatigue Life		
Missions	20,000	4000*
Hours	30,000	6000*

* The lives shown represent the predictions for the experimental hardware, given the present state of materials development. These are acceptable for component rig and integrated core/low spool testing. Goal lives can still be achieved with expected advances in materials technology.

The design of the compressor intermediate case was included in the high-pressure compressor preliminary analysis and design effort and was continued into the detailed analysis and design phase. The intermediate case performs many functions in support of other engine parts and components, and



has a very important effect on overall engine cost, weight, and performance. The nine most important functions of the case are listed below.

1. Supports the fan case
2. Provide a portion of the fan flowpath and provisions for clamping of nacelle "D" ducts
3. Carries the nacelle loads (load sharing assumed)
4. Contains the fan exit vanes
5. Supports the low-pressure compressor static structure and bleed actuating mechanism
6. Forms the low- to high-pressure compressor flowpath
7. Supports the fan and high-pressure compressor rotors
8. Provides front mount locations
9. Supports accessory drive shafts and gears

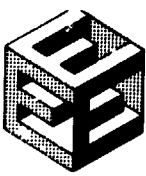
The initial titanium intermediate case design incorporated eleven structural struts. However, structural analysis of the sixth and seventh stage high pressure compressor redesigned airfoils revealed vibration problems with the eleven-strut intermediate case. Based on this analysis, 11E fourth mode and tip mode resonances in the operating range would occur unless the rotor 6 airfoil was significantly modified. To avoid any major impact on the rotor 6 airfoil design, a ten-strut intermediate case was incorporated.

These ten struts are the main structural elements and continue radially inward into the compressor section struts. The remaining nineteen vanes are nonstructural, and are bolted between the fan duct walls. By providing a continuous load path from the fan vanes into the inner case structure, the usual connecting torque box is eliminated. The upper vane forms the leading edge of the pylon, and the remaining vanes are aerodynamically matched to the resulting distribution. Figure 66 shows the intermediate case integrated with the high-pressure compressor component.

The intermediate case has no stress problems. The only structural limitations on the case are those resulting from changes in the fan blade tip clearance and the towershaft clearances. Preliminary analysis indicated that this design met all stiffness requirements.

The ten main structural vanes in the case are of a continuous beam construction. These vanes will be manufactured by diffusion bonding followed by superplastic forming to a finished shape. The parts will have smoother, more accurate aerodynamic shapes. Various standoffs and support collars will also be diffusion bonded in one operation, resulting in considerable savings in cost over conventional techniques.

The high-pressure compressor test rig (see Figure 65), designed to the planned maximum rig test conditions, accurately simulates the speed, temperature, stress level, and secondary flow requirements of the high-pressure compressor component.



PRATT & WHITNEY AIRCRAFT GROUP
COMMERCIAL PRODUCTS DIVISION

OF POOR QUALITY

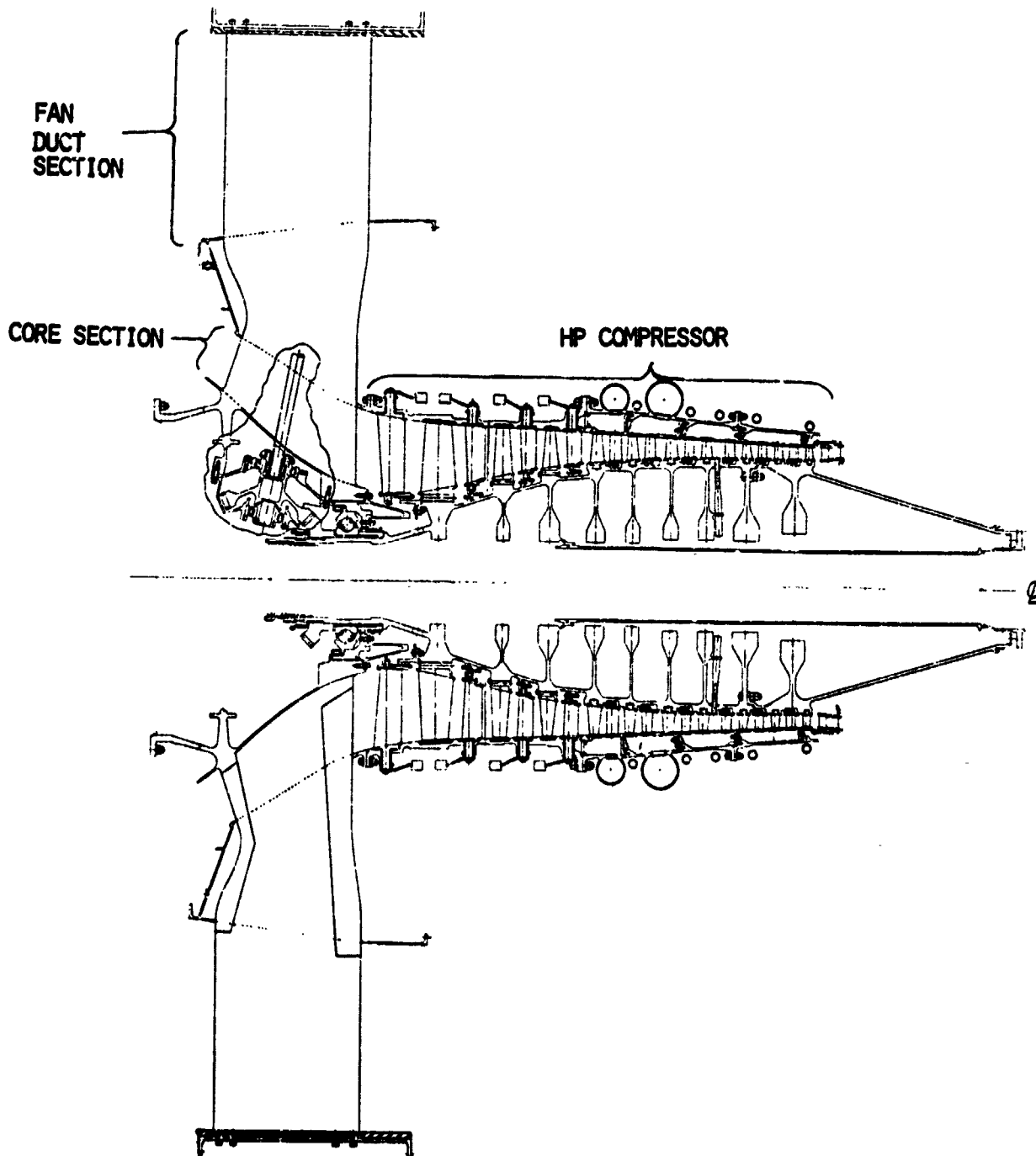


Figure 66 Compressor Intermediate Case Integrated with the High-Pressure Compressor Component



A rotor-frame system analysis identifying critical speeds within the expected operating range of the high-pressure compressor rig was completed.

In the component design, the rear hub was shortened and the bolt circle pulled in radially. This change necessitated a redesign of the rig forward thrust balance piston and the no. 4 bearing hub in order to retain the existing mock-turbine coupling shaft and the tooling to install this shaft. This change resulted in increased rotor length and static exit volume between the exit guide vanes. The close-coupled throttle valve was increased over the original concept, but is still within the range required to properly simulate engine surge/rotating stall boundary characteristics.

3.2.5.3.1 Current Technical Progress

The analysis and design of the high-pressure compressor component was completed during the previous reporting period, but the detailing of the final hardware drawings was continued during the current reporting period. All drawings required to provide component hardware in support of the high-pressure compressor rig were completed. These drawings cover the titanium front drum rotor, nickel alloy rear drum rotor, all ten stages of blades, the front compressor case, the inlet guide vane and the vanes for stages 6 through 8, and the related vane actuation hardware. The drawings of the component hardware not featured in the rig still need to be completed. These include the mid-compressor case and the stators in stages 9 through 14. These drawings should be completed late in the next reporting period in time for the fabrication of the integrated core/low spool.

Intermediate Case

All efforts on the compressor intermediate case were completed during this reporting period. Detailed drawings were prepared for the -15 degree uncamber structural strut, non-structural struts, accessory towershaft system, internal lubrication system areas, towershaft drive gears, and entire assembly. Design revisions that could result from detailed design efforts of the fan, low-pressure compressor, and integrated core/low spool will be conducted as part of the work under the WBS elements corresponding to these items.

High-Pressure Compressor Component Fabrication (in support of the rig program)

Fabrication of all component hardware to be used in the high-pressure compressor rig program was continued during this reporting period. The current status of the hardware is discussed in the following paragraphs.



Titanium Drum Rotor. The machining of all eight rotor disks to their pre-weld configurations was completed. The joining of these rotors by electron beam welding is now in process. Two sub-assemblies have been formed to date: the 6th through 8th stage rotor sub-assembly (see Figure 67) and the 9th through 13th stage rotor sub-assembly (see Figure 68). Joining of these two sub-assemblies, along with the start of final machining of the outer surfaces, is scheduled for mid-October. The rotor will be prepared for blading and instrumentation in early January 1981. Fabrication of the 12th stage bleed tubes and the blade locks is also in progress.

Nickel Alloy (MERL 76) Rear Drum Rotor. Machining of the rotor was continued during this reporting period. All lathe work was completed except for final machining of the knife edge seals, which are machined last to preclude possible handling damage. Flange hole drilling and instrumentation hole drilling is now in process. The rotor is shown in Figure 69. This rotor will be completed, bladed, and instrumented early in the next reporting period. Two spare raw material compactions were also prepared.

High-Pressure Compressor Blades. Two sets (plus spares) of blades were fabricated during this reporting period, and passed first-article aerodynamic inspection. The first set is scheduled for mid-October delivery, and the second set is scheduled to be delivered in January 1981.

Front Compressor Case. The fabrication of the front compressor case was continued. Activities during this reporting period included split flange welding, final inside and outside machining, and vane trunnion hole drilling. Figure 70 shows the case during the vane hole drilling sequence. Instrumentation holes are now being drilled. The completed case will be transferred to the rig assembly effort in early November.

Vanes: Inlet Guide Vane Through Stator 8. Vendor fabrication of the inlet guide vane and stators 6, 7, and 8 was initiated during this reporting period. First-article inspection has been completed, and delivery is expected by mid-October.

Vane Actuation Hardware and Minor Parts. Vane actuation levers and unison rings, vane trunnion bushings, and all fastenings (nuts and bolts) for the compressor assembly are now being fabricated. These parts are expected to be delivered for assembly in the rig by December 1980.

High-Pressure Compressor Rig Analysis and Design

Detailed drawings of all rig hardware were completed during this reporting period with the exception of the diffuser case drawing, which is approximately 95 percent complete. A full-rig assembly drawing, providing a complete parts listing and specific assembly requirements, is also nearing completion.



PRATT & WHITNEY AIRCRAFT GROUP
COMMERCIAL PRODUCTS DIVISION

ORIGINAL PAGE IS
OF POOR QUALITY

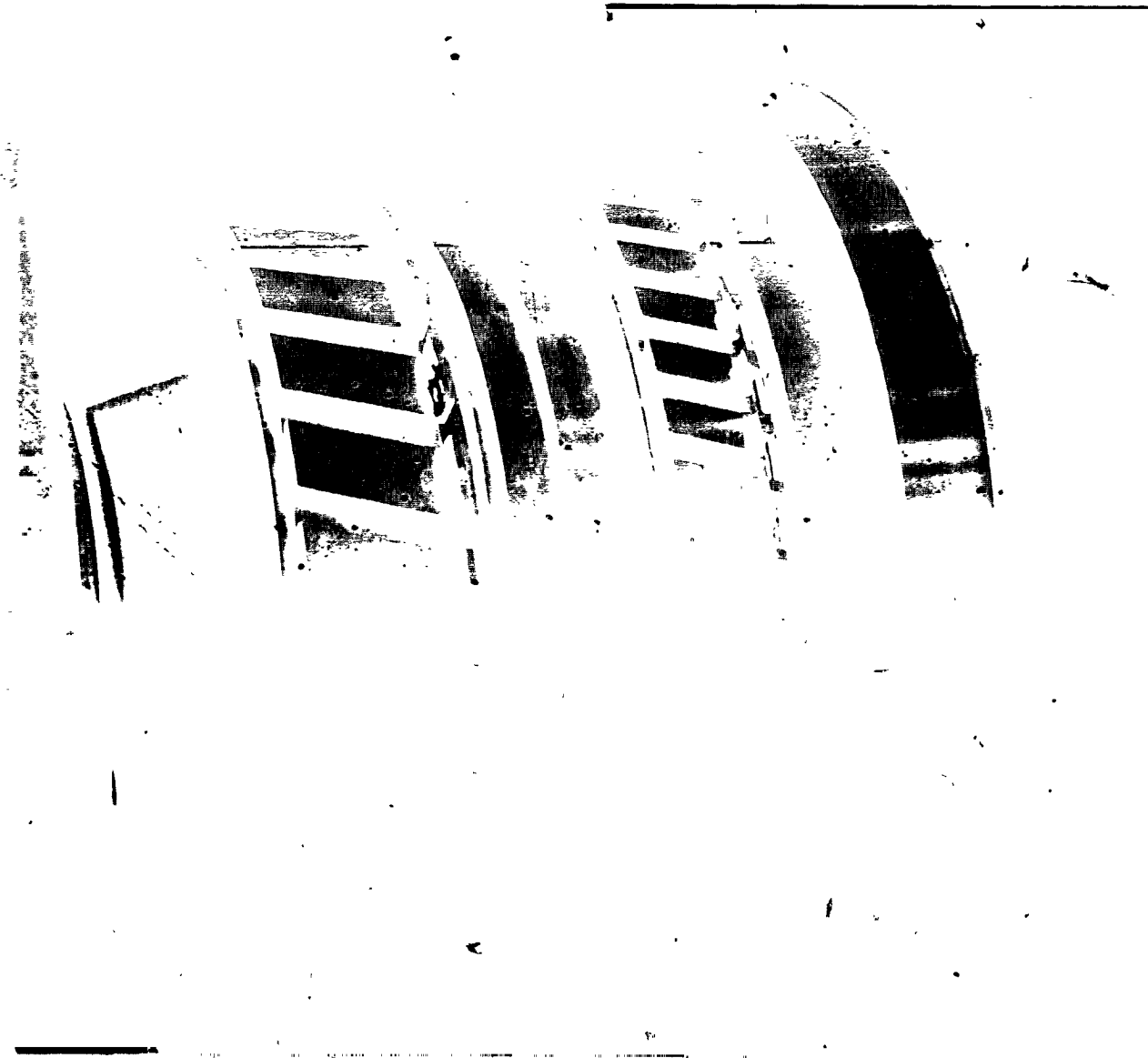


Figure 67 High-Pressure Compressor Drum Rotor Assembly - View showing 6th, 7th, and 8th stage disks after electron beam welding.



PRATT & WHITNEY AIRCRAFT GROUP
COMMERCIAL PRODUCTS DIVISION

**ORIGINAL PAGE IS
OF POOR QUALITY**



Figure 68 High-Pressure Compressor Drum Rotor Assembly - View showing 9th through 13th stage disks after electron beam welding.



PRATT & WHITNEY AIRCRAFT GROUP
COMMERCIAL PRODUCTS DIVISION

ORIGINAL PAGE IS
OF POOR QUALITY



Figure 69 High-Pressure Compressor 14th and 15th Stage Disk



PRATT & WHITNEY AIRCRAFT GROUP
COMMERCIAL PRODUCTS DIVISION

ORIGINAL PAGE 12
OF POOR QUALITY

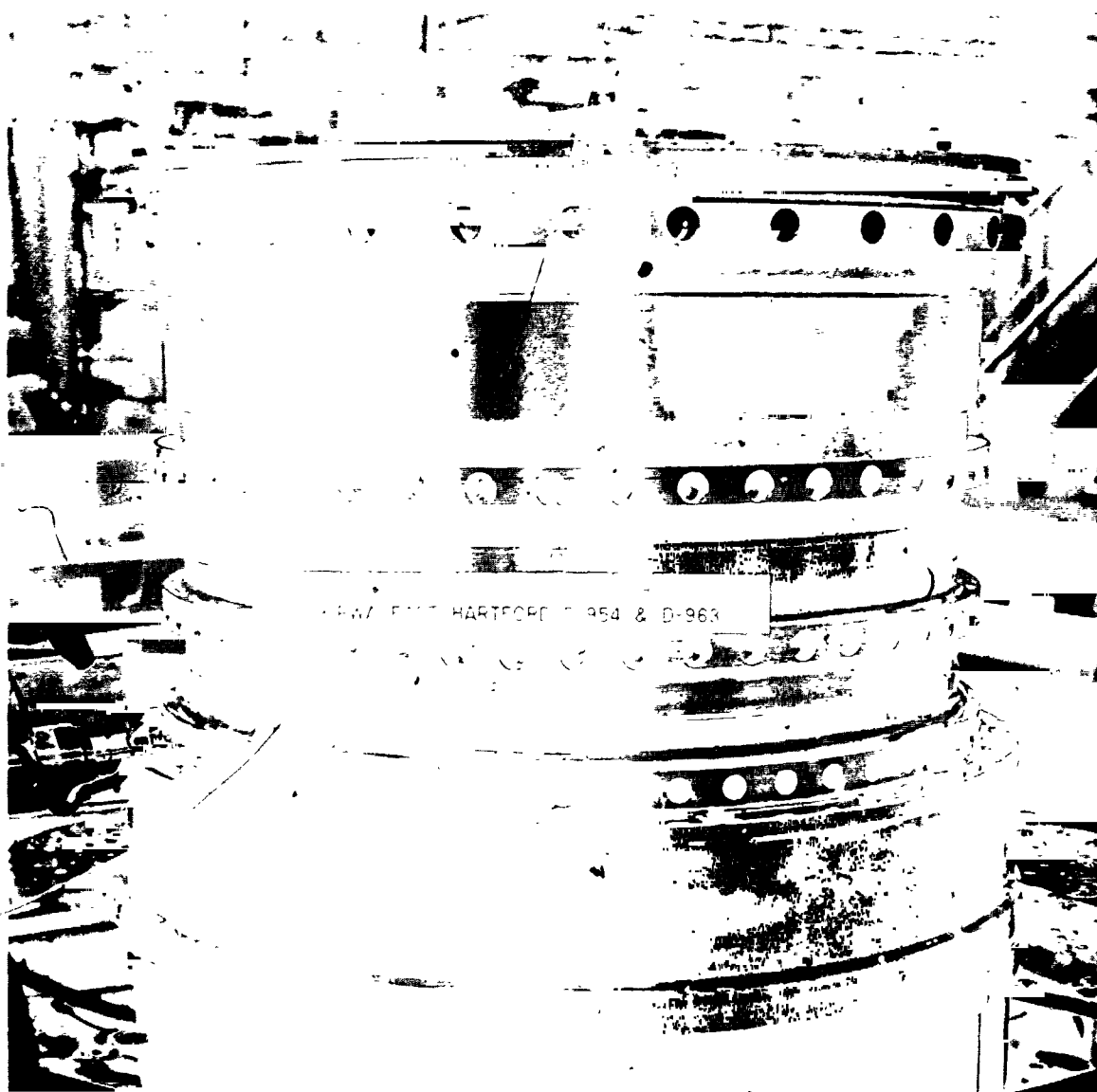
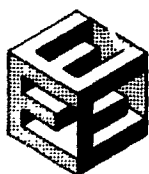


Figure 70 High-Pressure Compressor Rig Split Front Vane Case



PRATT & WHITNEY AIRCRAFT GROUP
COMMERCIAL PRODUCTS DIVISION

The planning and design work on the new tooling required to assemble the component and rig was completed. Thirty-two new tools or adapters were designed, including balance adapters for the front and rear drums, lifting devices for the hubs and cases, various build fixtures, a hydraulic tool to install the vane bushings into the cases, bearing installing and torqueing tools, a special torque wrench for the mid-compressor joint bolts, a rotor transport stand, and 2 vane/arm matching toolings.

The design of the facility adapting hardware and the rig secondary air system hardware was started during the reporting period and is approximately 60 percent complete. This hardware includes flow diagrams, piping arrangements, and electrical control devices for the systems controlling rig bleed air, oil flow, and cooling water flow.

The bleed air system will consist of individual valves and orifice metering sections in each of the nine controlled air systems of the rig. Also, a new front mount is being designed as well as a bellmouth-to-plenum closure adapter.

The rig front mount consists of two vertical struts and one horizontal strut. The vertical struts attach to the horizontal centerline of the intermediate case and to the facility floor through spherical bearings. The horizontal strut attaches to the bottom centerline and the wall. The mount system restrains horizontal and vertical loads in the front case. It permits fore and aft motion of the intermediate case caused by thermal growth, and accommodates rotation about a vertical and horizontal axis perpendicular to the rig centerline.

The results of a recently conducted facility installation study revealed that the rig could be transported to the test stand almost completely assembled. The bellmouth is the only part that would have to be installed at the test stand. This approach offers more advantages over the previously considered method in which the rig had to be disassembled back to the intermediate case before transport. An existing rig transport stand is now being modified for use in the program. This stand will be used in the final stage of assembly to support the instrumentation panels and to move the rig to the test facility.

High-Pressure Compressor Rig Fabrication

Rig hardware fabrication work was continued. All remaining rig hardware details were ordered. Most of the effort is now being directed toward the rear split variable vane case, which is pacing the assembly schedule. The case has been completely welded, including split flanges and both bleed manifolds. The external contours have been finished, and vane trunnion hole drilling is scheduled to begin in early October. The rear vane case is shown in Figure 71.

Fabrication of the rear variable vanes (stages 9 through 14) was also continued. First-piece inspection has been completed, and the "production of each vane row has been approved. All parts are scheduled to be received by the end of October. A partial shipment of the 14th stage vanes has been received. These vanes are being inspected prior to machining for leading edge instrumentation provisions.



PRATT & WHITNEY AIRCRAFT GROUP
COMMERCIAL PRODUCTS DIVISION

ORIGINAL PAGE IS
OF POOR QUALITY

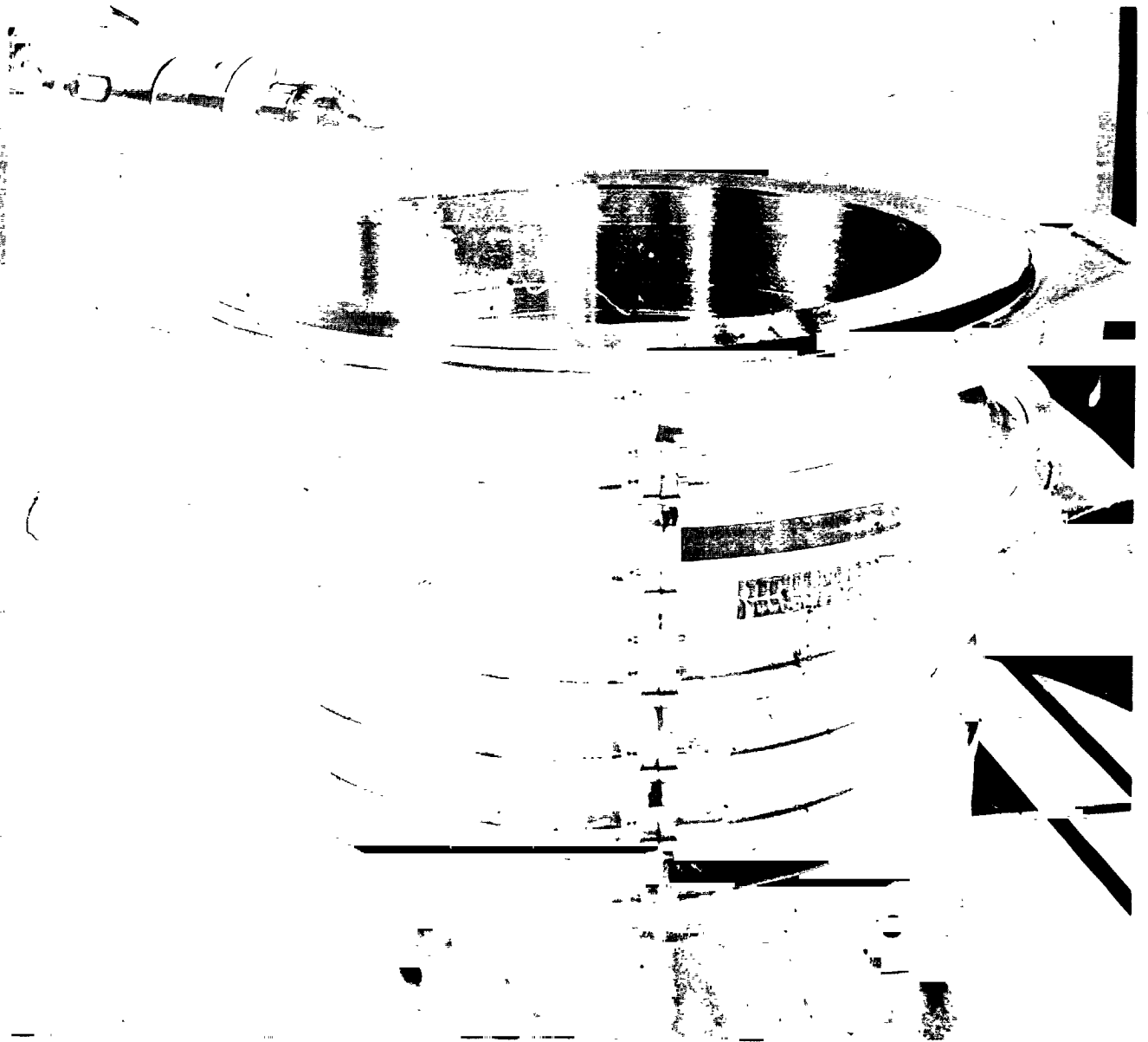
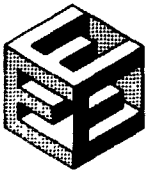


Figure 71 High-Pressure Compressor Rig Split Rear Case During Set-up
Before Final Inner and Outer Surface Machining



PRATT & WHITNEY AIRCRAFT GROUP
COMMERCIAL PRODUCTS DIVISION

The struts of the rig intermediate case were welded into the inner and outer flowpath rings. The case is now being final-machined. The intermediate case inner flowpath, outer flowpath, and strut prior to welding are shown in Figures 72 through 74.

The rear bearing support case has been completely welded and is now being final-machined. The rear bearing support case after welding is shown in Figure 75.

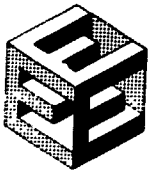
Most of the refurbishment of existing adapting hardware has been completed. This includes weld repair and machining modifications to the aft bearing case and miscellaneous support hardware, plus parts inspection and minor parts replacement on the rig throttle valve case assembly.

The vendor fabrication of the rig diffuser case is on schedule. The vendor is also expected to machine all instrumentation provisions. The instrumentation will be subsequently installed at Pratt & Whitney Aircraft. This fabrication effort is being conducted using preliminary drawings. The final drawings used to complete fabrication will be available in October.

High-Pressure Compressor Rig Assembly

A detailed rig assembly plan was established during this reporting period. The plan was reviewed by the assembly department, and schedule milestones and parts availability deadlines were established. The assembly process will begin on 1 October. The initial stages of this activity will consist primarily of preparing available hardware for the required instrumentation in accordance with the approved instrumentation plan.

The test facility preparation schedule was also set during this reporting period. The necessary adapting hardware will be procured during the fourth quarter of 1980 and during the first quarter of 1981. Hardware installation will start in February 1981 and will be completed in time for the delivery of the rig to the test stand in May 1981.



PRATT & WHITNEY AIRCRAFT GROUP
COMMERCIAL PRODUCTS DIVISION

ORIGINAL PAGE IS
OF POOR QUALITY



Figure 72 High-Pressure Compressor Rig Intermediate Case Inner Case Detail
During Rear Flange Machining Operation

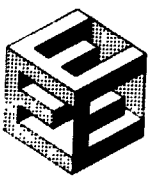
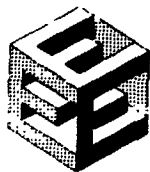


Figure 73 High-Pressure Compressor Rig Intermediate Case Outer Case Detail
After Hole Drilling Operation Before Strut Weldment



PRATT & WHITNEY AIRCRAFT GROUP
COMMERCIAL PRODUCTS DIVISION

ORIGINAL PAGE 13
OF POOR QUALITY



Figure 74 High-Pressure Compressor Intermediate Case Strut



PRATT & WHITNEY AIRCRAFT GROUP
COMMERCIAL PRODUCTS DIVISION

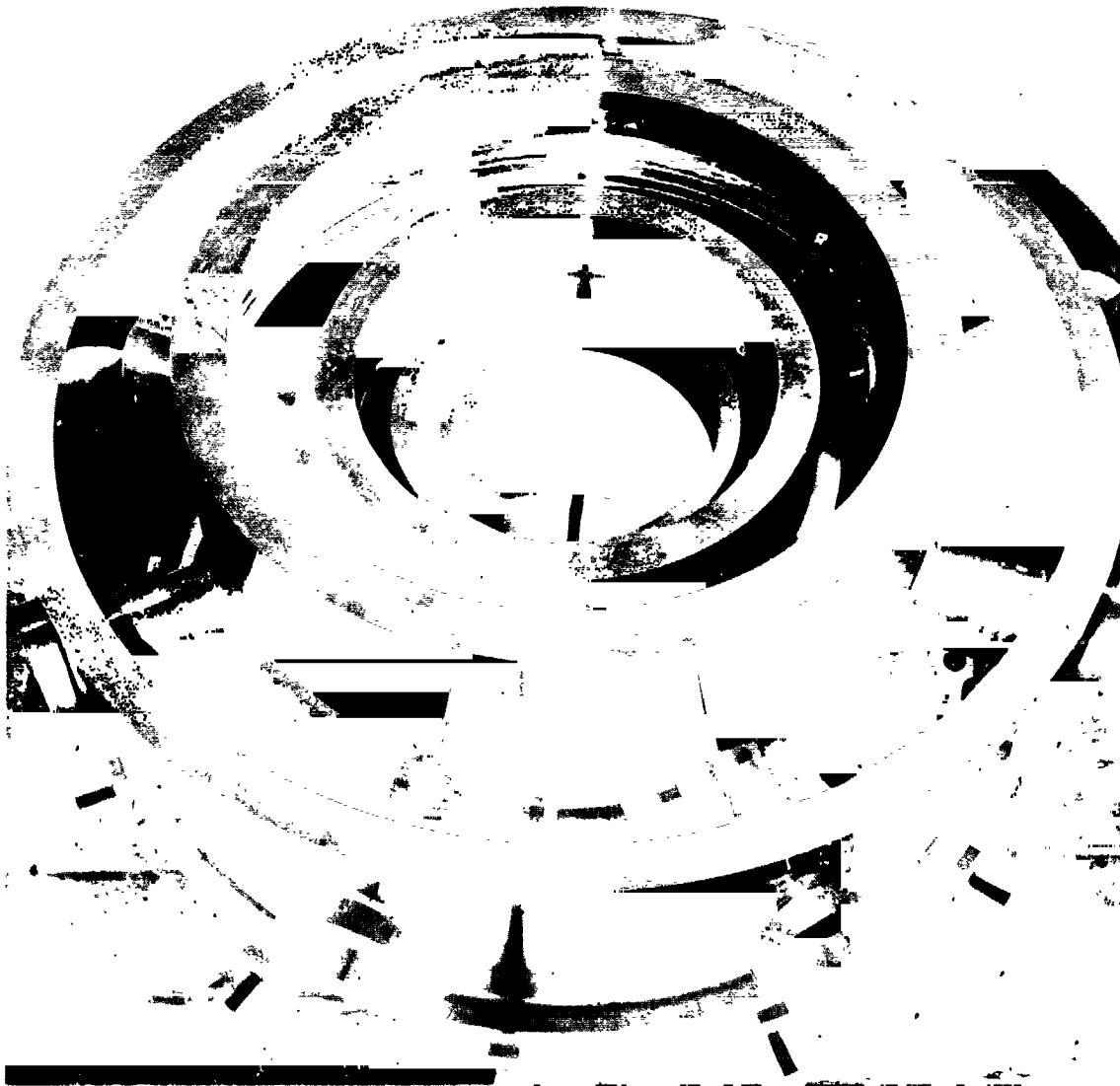


Figure 75 Number 4 Bearing Support Case



PRATT & WHITNEY AIRCRAFT GROUP
COMMERCIAL PRODUCTS DIVISION

3.2.6 Combustor

3.2.6.1 Overall Objective

Design a full-annular two-stage combustor and demonstrate three advanced technology concepts: (1) a curved-wall strutless diffuser, (2) a two-stage combustor having a carburetor tube main zone, and (3) a segmented combustor liner featuring advanced wall cooling. The goals established for the combustor rig are the same as those set for the flight propulsion system component (see Table 53).

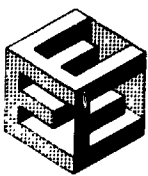
TABLE 53

GOALS ESTABLISHED FOR THE COMBUSTOR COMPONENT RIG

Pattern Factor, Maximum	0.37
Section Pressure Loss	5.5 percent P_{T3}
Hydrocarbon EPAP	0.4
Carbon Monoxide EPAP	3.0
NOx EPAP	3.0
SAE Smoke Number	20
Radial Profile	250 degrees average-peak
Liner Life	8000 hours, 4900 missions

3.2.6.2 Scope of Total Work Planned

The overall task effort consists of a component effort and two supporting technology sub-tasks. The component effort comprises the analysis and design of the combustor component and a combustor rig test program. The two supporting technology programs are (1) the diffuser/combustor model test program and (2) the combustor sector rig program. Figure 76 shows the relationships between these activities and their relationship to Tasks 1, 3, and 4. The work plan schedule for the component effort is shown in Figure 77 and critical milestones are noted.



3.2.6.3 Component Effort

3.2.6.3.1 Objective

Conduct the design, analysis, hardware procurement, and full-annular rig testing activities necessary to develop a full-annular combustor that meets the program goals.

3.2.6.3.2 Scope of the Total Work Planned

The analysis and design effort consists of both a preliminary and a detailed analysis and design phase. The rig program entails the six sub-tasks shown in Figure 77. A preliminary design activity is conducted to establish the feasibility of the combustor as proposed for the flight propulsion system. The studied designs provide configuration definitions to the supporting technology programs. This preliminary activity results in layout drawings and substantiation of design data which are presented to NASA at a preliminary design review in January 1979.

Detailed design activity starts in March 1979. Results available from the supporting technology programs are used to substantiate or improve the configurations established in the preliminary design. Also, more sophisticated design and analytical procedures than those of the preliminary effort are used. The results of this effort are presented to NASA in a Detailed Design Review (DDR) in January 1981. Detailed drawings are scheduled for completion approximately two months later.

Design and fabrication of combustor rig parts progresses concurrently with those of the component parts, permitting the start of full scale rig assembly in the second quarter of 1981. Various modifications to the combustor configuration are tested to develop the final configuration that satisfies program goals. Testing of the various configurations consists mainly of air schedule variations to demonstrate emissions, exit radial temperature profile, performance goals, and durability. In May 1982, the final diffuser/combustor configuration is assembled into the core engine for testing in late-1982.

All of the work planned and approved from contract award through the end of the current reporting period (30 September 1980) has been completed. Figure 77 indicates that component preliminary analysis and design was completed during a previous reporting period. Component detailed analysis and design was initiated during a previous reporting period and continued during the current reporting period. Rig analysis and design was initiated during the previous reporting period, and continued during the current reporting period.

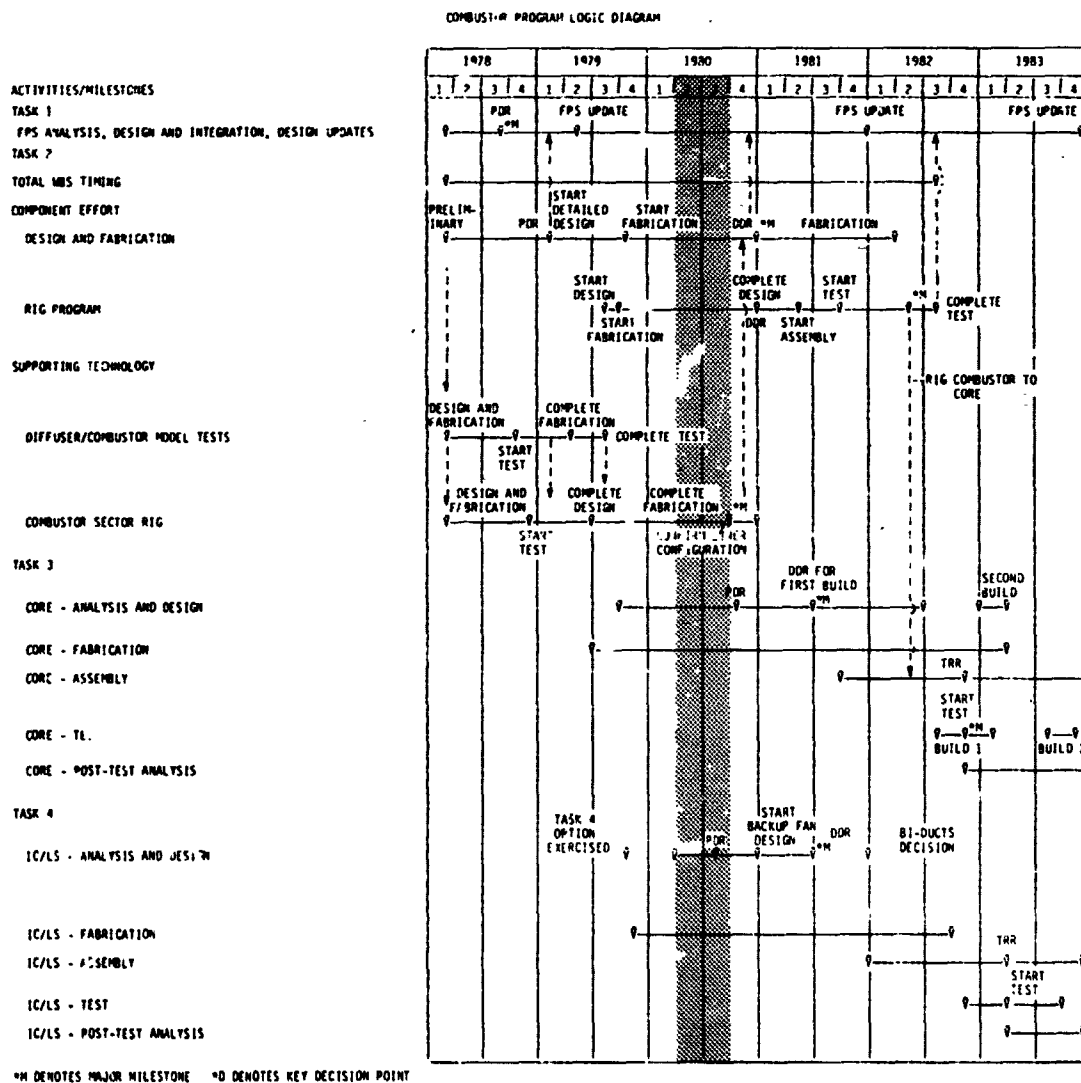


Figure 76 Combustor Program Logic Diagram

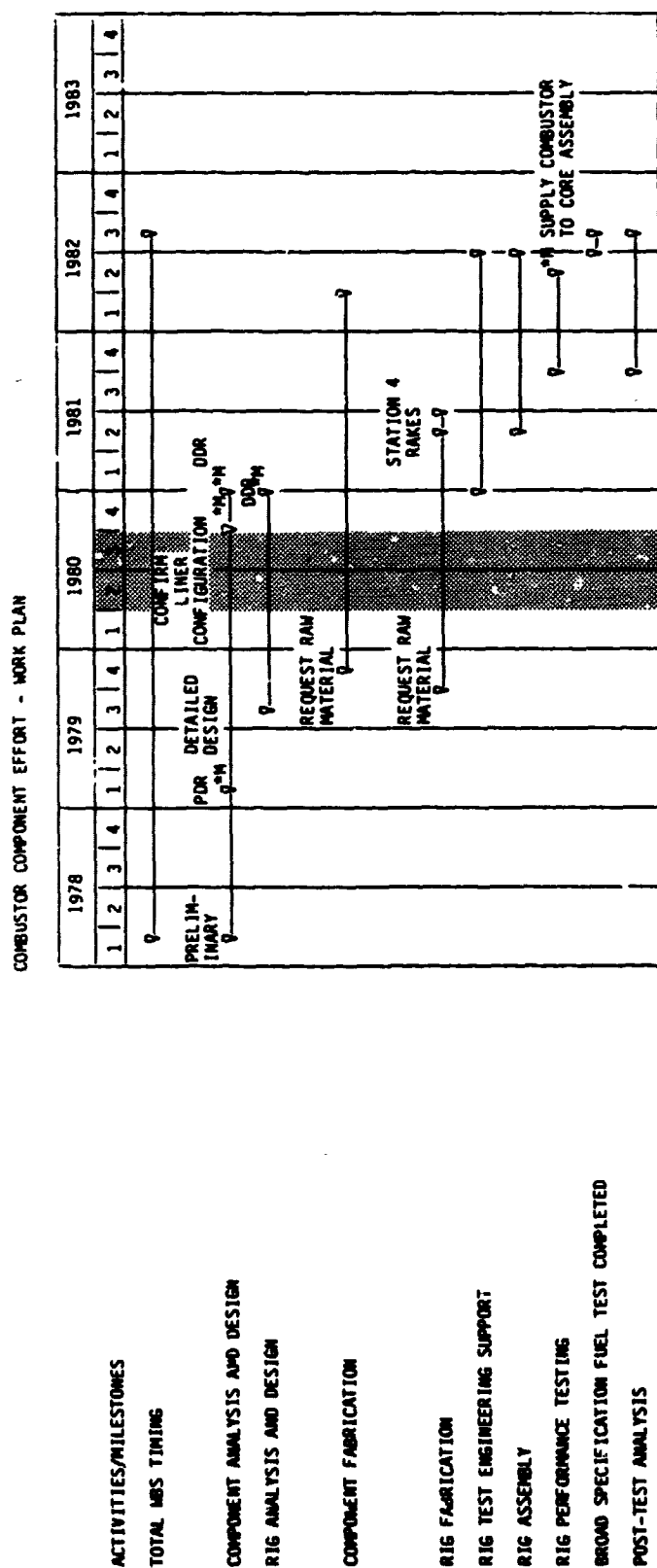


Figure 77 Combustor Component Effort Work Plan Schedule



3.2.6.3.3 Technical Progress

3.2.6.3.3.1 Summary of Work Previously Completed

The combustor component is illustrated in Figure 78, and its companion rig is shown in Figure 79. The basis for the component design was the two-stage Vorbix combustor investigated in the NASA Experimental Clean Combustor Program (ECCP). The design therefore incorporates two distinct burning zones: a pilot zone designed to minimize idle emissions and provide adequate stability and relight characteristics, and a main zone that provides fuel-lean combustion to minimize emissions of smoke and oxides of nitrogen.

The outward-canted, strutless, curved-wall prediffuser aligns compressor exit air with the center line of the combustor to reduce pressure losses associated with flow turning in the combustor hood region. Diffuser case struts are aerodynamic members designed to reduce combustor flow maldistribution and to improve liner durability and pattern factors. The combustor hood is positioned relative to the prediffuser dump plane to minimize the overall prediffuser and shroud pressure losses. The hood features sufficient volume to establish plenum feed characteristics. Pilot zone dome height maintains the same ratio of fuel nozzle spacing to dome height as was used in the Vorbix combustor of the Experimental Clean Combustor Program. A proportionately larger recirculation zone results, which will improve relight and starting characteristics and will enhance the potential for reduction of idle emissions. The rate of pilot zone heat release is reduced (through lower reference velocity and higher pilot zone residence time at idle) to enhance the possibility of meeting the 1981 emissions standards for carbon monoxide and hydrocarbons.

The main zone design retains the features for reducing oxides of nitrogen demonstrated by the Vorbix combustor of the Experimental Clean Combustor Program. The length of the Energy Efficient Engine combustor has been reduced by removing the "throat" section characteristics of the Vorbix combustor. This also reduces the cooling air requirements and increases the possibility of achieving reduced high-power smoke emissions and improved combustor durability. A compact carburetor fuel injection system is used to provide mixing of fuel and air outside the combustor zone. This also leads to reduced smoke emissions. Carburetor tube air transports fuel into the main zone of the combustor. This results in adequate fuel penetration over the entire range of operating conditions. Carburetor tube shroud air (introduced through separate swirlers in the Vorbix design) is introduced through radial in-flow swirlers concentric with the fuel nozzles. The injector concept improves main zone fuel penetration and atomization characteristics over the entire range of combustor operating conditions.

The segmented liner construction uses Counter-Parallel FINWALL^R segments cast from PWA 1455 turbine alloy. The inner and outer liners are divided into circumferential segments in both the pilot zone and main zone. These segments are supported by inner and outer structural frames. Hooks on the back of each



segment engage with circumferential rails on the structural frame to position the segments. Life of a typical liner segment has been estimated at 7200 cycles or 11,700 hours, where life is defined as the number of cycles or hours before a crack appears in the liner segment.

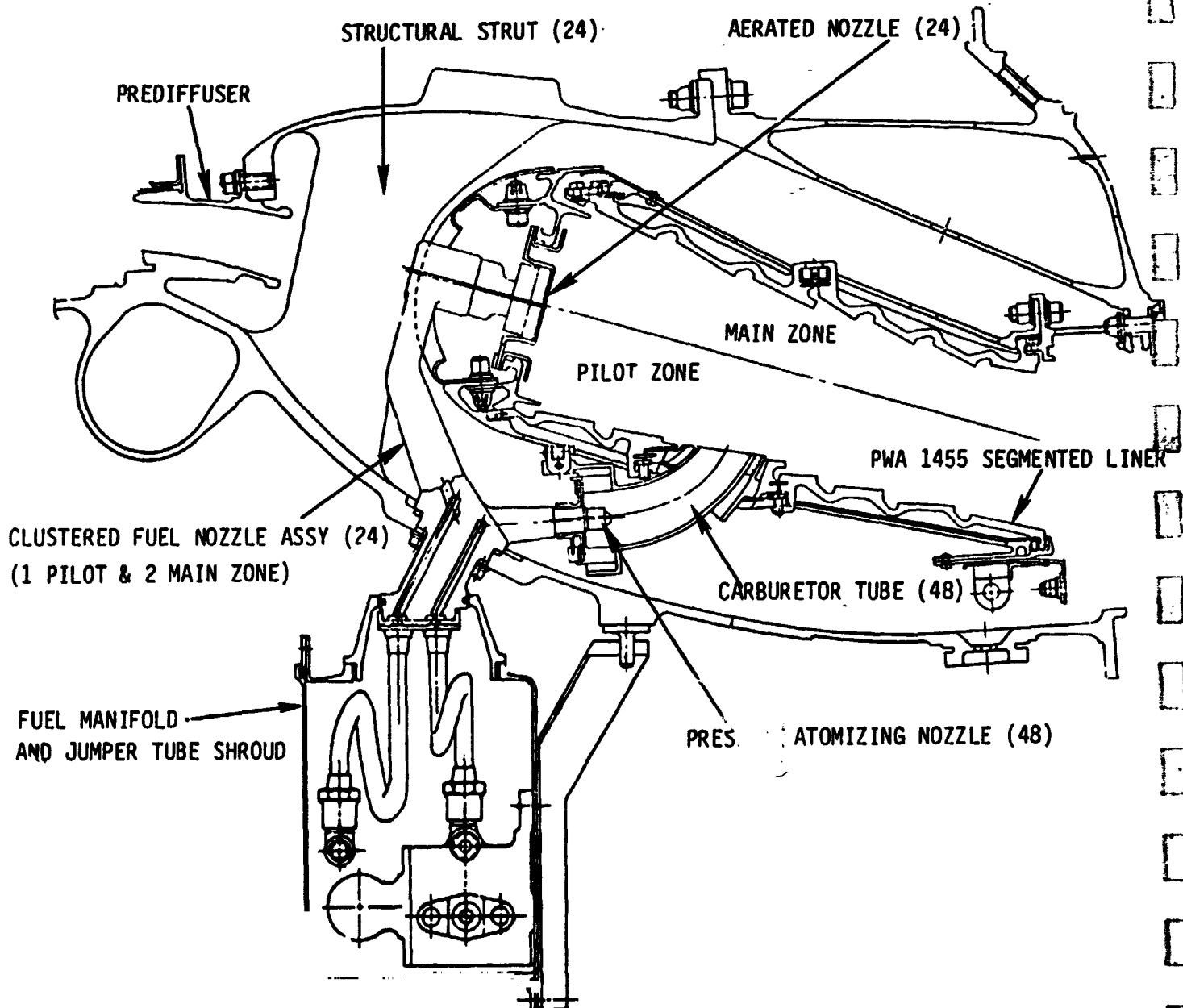


Figure 78 Combustor Component



PRATT & WHITNEY AIRCRAFT GROUP
COMMERCIAL PRODUCTS DIVISION

ORIGINAL DESIGN
OF POOR QUALITY

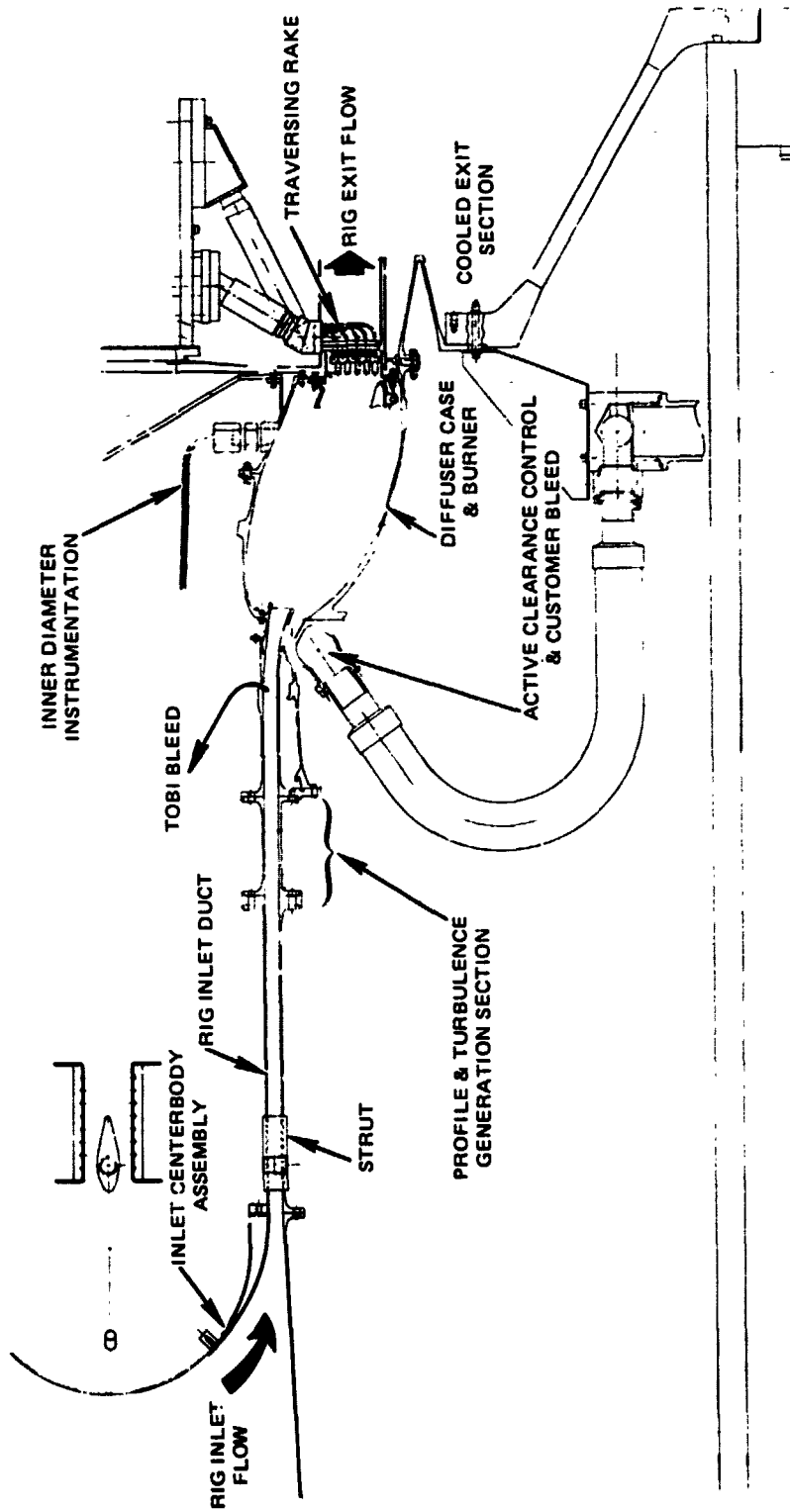
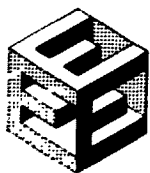


Figure 79 Combustor Component Rig



The design of the compressor exit guide vane assembly was included in the design of the combustor component because of its interaction with the prediffuser duct. The assembly is shown in Figure 80. This configuration features: (1) A vane having integrally attached inner and outer shrouds but circumferentially separated into groups of five vanes to relieve thermal gradient stresses, (2) decoupled inner and outer prediffuser duct walls, (3) sheet metal seal for the gap between the exit guide vane and the inner prediffuser wall, (4) feather seals to control air leakage through the gaps between segments.

The exit guide vane design shown in Figure 80 incorporates a single row airfoil. A back-up design, based on a dual row airfoil approach for air entrance and turning angle, will be fabricated if the expected efficiency of the single row exit guide vane is not demonstrated during testing of the Build 1 high-pressure compressor rig.

Current performance parameters for the combustor component at significant engine operating conditions are shown in Table 54.

TABLE 54
CURRENT COMBUSTOR COMPONENT PERFORMANCE PARAMETERS

	Engine Operating Condition			
	Aero. Des. Point	Maximum Cruise	Maximum Climb	Takeoff
Inlet Corrected Airflow (lb/sec)	6.91	6.92	6.88	6.95
Inlet Pressure (lb/in ² Abs)	203	196	214	453
Inlet Temperature (F)	898	882	977	1055
Section Pressure Loss (Percent)	5.50	5.53	5.46	5.57
Fuel - Air Ratio	0.02415	0.02365	0.02620	0.02670
Exit Temperature (F)	2355	2315	2525	2615
Combustor Efficiency (Percent)	99.95	99.95	99.95	99.95

The component test rig (see Figure 79) will be used to conduct high-pressure, high-temperature tests of the complete combustor to document combustor emissions and to develop performance characteristics (pattern factor, radial, temperature profile, and pressure drop) before installation and testing in the engine core.



PRATT & WHITNEY AIRCRAFT GROUP
COMMERCIAL PRODUCTS DIVISION

ORIGINAL PAGE IS
OF POOR QUALITY

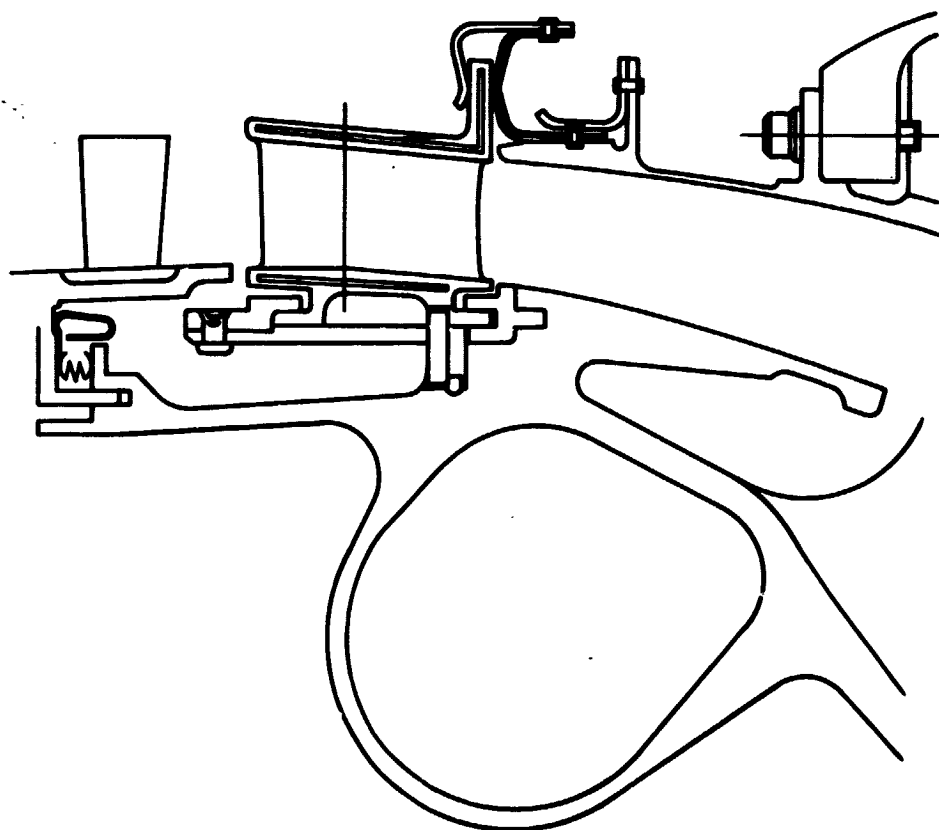
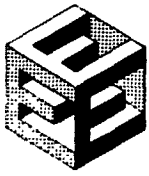


Figure 80 High-Pressure Compressor Exit Guide Vane Assembly



PRATT & WHITNEY AIRCRAFT GROUP
COMMERCIAL PRODUCTS DIVISION

The designs of the prediffuser, diffuser case, combustor section, and fuel injector are tailored to the design specifications of the combustor component. Rig-unique hardware includes (1) an inlet centerbody assembly to provide flow transition between the facility ducting and the rig inlet duct, (2) a profile and turbulence generation section to simulate compressor exit conditions, (3) simulated tangential on-board injection bleed and active clearance control customer bleed ports, and (4) a cooled exit section that mates the diffuser case to the exhaust duct and permits testing with an instrumented traversing rake installed downstream of the combustor.

Detailed design efforts on the rig were completed during this reporting period, and a detailed design review was held at NASA-LERC in September 1980. The results of this design effort are discussed in section 3.2.6.3.3.2.

3.2.6.3.3.2 Current Technical Progress

The following work was performed during the current reporting period:

- (1) The combustor carburetor tube configuration was selected;
- (2) The fuel nozzle support assembly configuration was completed;
- (3) An ignitor configuration was selected, based upon an existing design, and design work on the fuel manifold system was started;
- (4) The design of the component rig was completed;
- (5) Fuel manifold design work was continued; and
- (6) combustor fabrication work was continued.

Each of these items is discussed in the following subsections.

Carburetor Tube Configuration

Final definition of the combustor carburetor tube configuration was completed (see Figure 81). This tube will be cast in Inconel 625 material, a non-cobalt alloy that adequately provides the strength required for such a configuration. The carburetor tube configuration incorporates many of the features developed in the combustor sector rig test program, including (1) radial inflow swirler vane geometry, (2) co-rotational (secondary) swirler vane geometry, and (3) optimized carburetor tube length.

The carburetor tube support was designed to provide positional stability when exposed to maneuver and pressure loads. The front end of the preliminary design configuration was supported, but could move in and out of the burner segment at the rear end. The additional penetration of the carburetor tube into the combustor was acceptable. Although considered very unlikely, the loss of the rear portion of the carburetor tube rear lip could allow the tube to drop significantly since it pivoted at the front end. Additional support lugs were incorporated at the rear end of the carburetor tube to provide a fully supported design.



ORIGINAL PAGE IS
OF POOR QUALITY

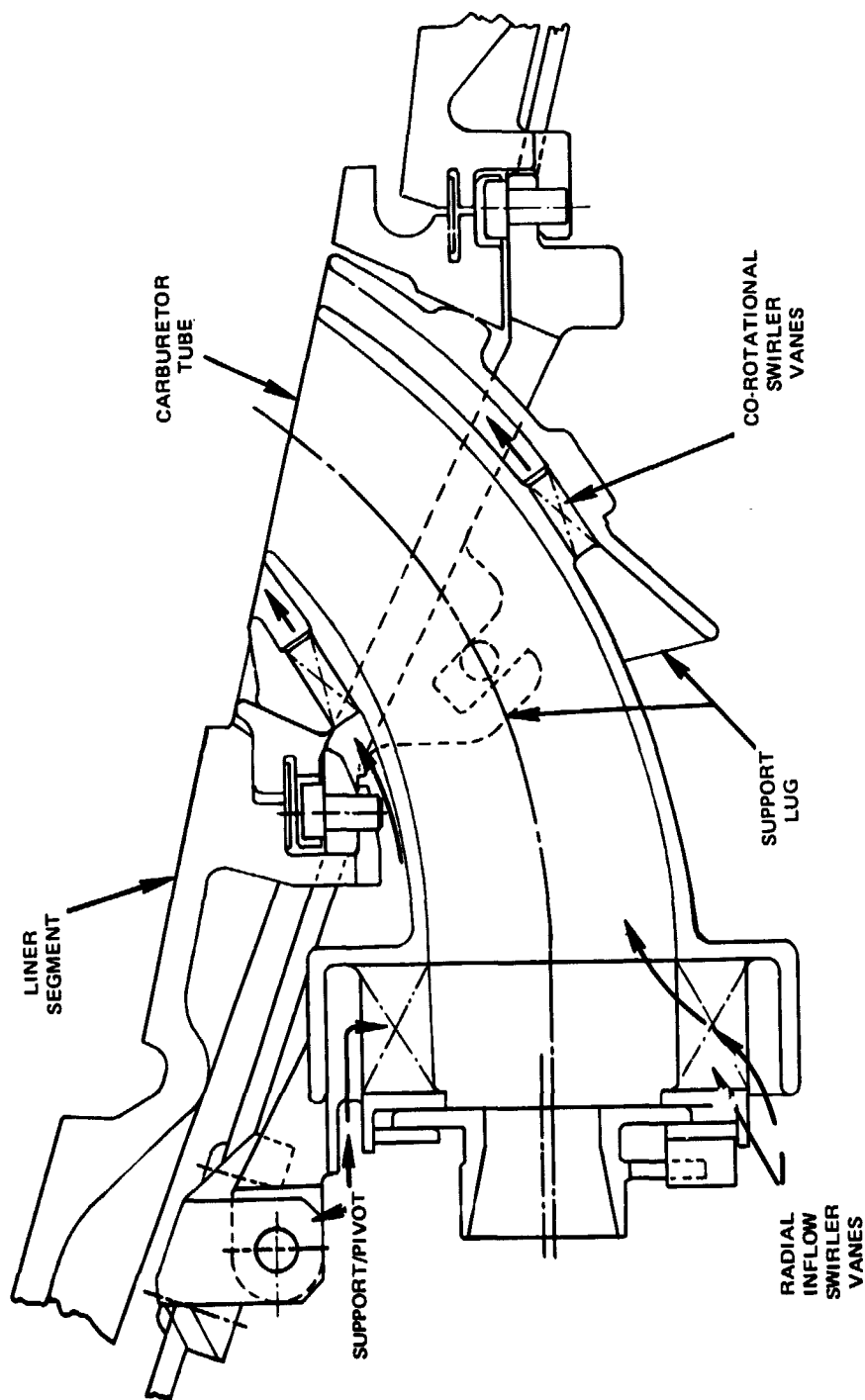
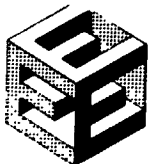


Figure 81 Combustor Carburetor Tube Configuration



Fuel Nozzle Support Assembly

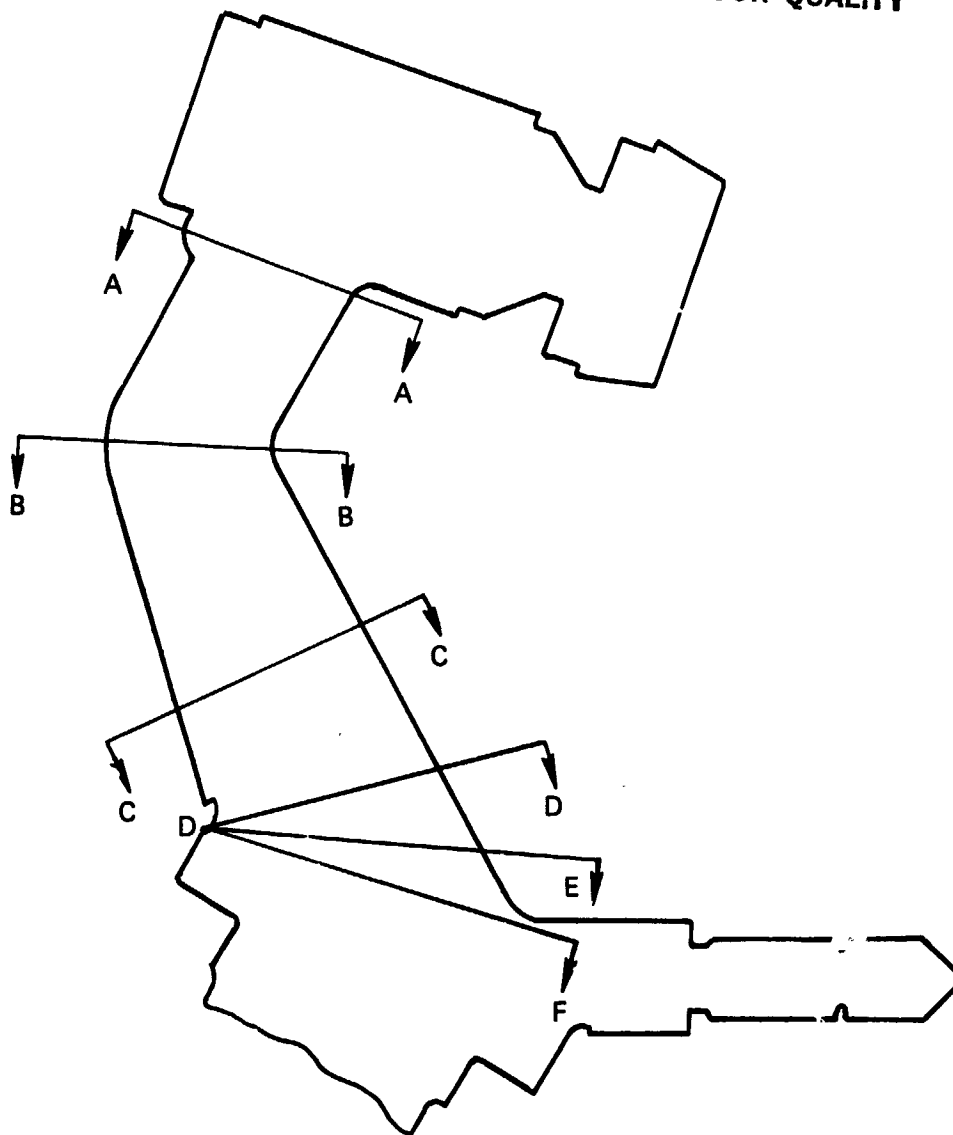
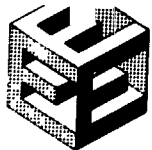
The design of the fuel nozzle support assembly was completed during the current reporting period. Casting was chosen as the fabrication approach because of the complex geometry of this assembly. A conceptual layout was developed in terms of a cast construction.

The material selected for use in the fuel nozzle support assembly is AISI 347 (AMS 5362). This material possesses high temperature capability, good castability, and good ductility. In addition, a structural analysis of the fuel nozzle support assembly indicated that the maximum anticipated stresses for this assembly are well within the capabilities of the material. This material also costs less than Inconel 718 material, and, unlike Inconel 718, does not require precipitation heat treatment after brazing. Each of the candidate materials for the fuel nozzle support assembly is listed in Table 55. The stresses in the support assembly are summarized in Figure 82.

TABLE 55

FUEL NOZZLE SUPPORT CAST MATERIAL REVIEW

Material	Fty 0.2% (F)		Castability	Machinability	Brazability	Resistance to Corrosion	Max Operating Temp. (F)	Ductility @ 700 F	α @ 700 F
	300	700							
AISI 347 (AMS 5362)	20K	25K	Good	Difficult	Good	Excellent	1600	Excellent	9.8
17-4 (AMS 5355)	103K	90K	Good	Good	Good	Good	600	Fair	6.7
Greek Ascoloy (AMS 5354)	36K	57.5K	Fair/Good	Fair	Good	Good	1000	Fair	6.3
Inco 718 (PWA 649)	80K	69K	Very Good	Difficult	Au-Ni Brazed in Solid Con- dition	Good	1800	Good	8.0
ASTM A 296	77.5K	50K	Good	Fair/Good	Good	Good	900	Fair	7.0
ASTM A 439	34K	36K	Good	Good		Good	1500	Poor	8.9
PWA-IM- 4430	33K	27K	Good	Difficult	Good	Good	1300	Excellent	8.7



<u>SECTION</u>	<u>STRESSES (PSI)</u>	
	<u>FORE-AFT</u>	<u>LATERAL</u>
A-A	9300	8400
B-B	13800	13500
C-C	9600	12300
D-D	17700	15900
D-E	12700	13300
D-F	8500	16200

Figure 82 Fuel Nozzle Support Assembly Stress Summary

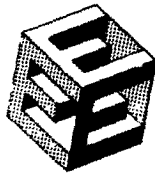


PRATT & WHITNEY AIRCRAFT GROUP
COMMERCIAL PRODUCTS DIVISION

Two vendors were consulted for fabricating fuel nozzles. Detailed nozzle performance requirements were defined based upon sector rig performance data. Table 56 shows fuel scheduling and operational requirements. Each vendor, working within the constraints of the conceptual layout of the nozzle, submitted a proposal for supplying a completely assembled fuel nozzle support (see Figure 83). Both vendors were judged capable of meeting the established performance requirements, but the Ex-Cell-O design was selected because of its lower cost to the program.

TABLE 56
FUEL SCHEDULING AND OPERATING REQUIREMENTS

<u>Condition</u>	<u>Takeoff</u>	<u>Idle</u>	<u>Sea Level Start</u>	<u>Altitude Relight (Atomization Limited)</u>
Burner Inlet Air Temperature (R)	1522	853	541	496
Burner Inlet Air Pressure (psia)	458	64	15.4	4.8
Fuel Flow (pph)	230	42	22.9	18.3
Nozzle Air Passage Effect (flow area, sq. in.)	0.290 min. 0.320 max.	-	-	-
Air ($\Delta P/P$) Across Nozzle	0.040	0.040	0.009	0.022
Spray Droplet SMD (micron)	<50	<50	<100	-
$Wf/\sqrt{\Delta P}f$ (pph/ $\sqrt{\Delta}$ psid)	12.0	-	-	-



PRATT & WHITNEY AIRCRAFT GROUP
COMMERCIAL PRODUCTS DIVISION

ORIGINAL PAGE 10
OF POOR QUALITY

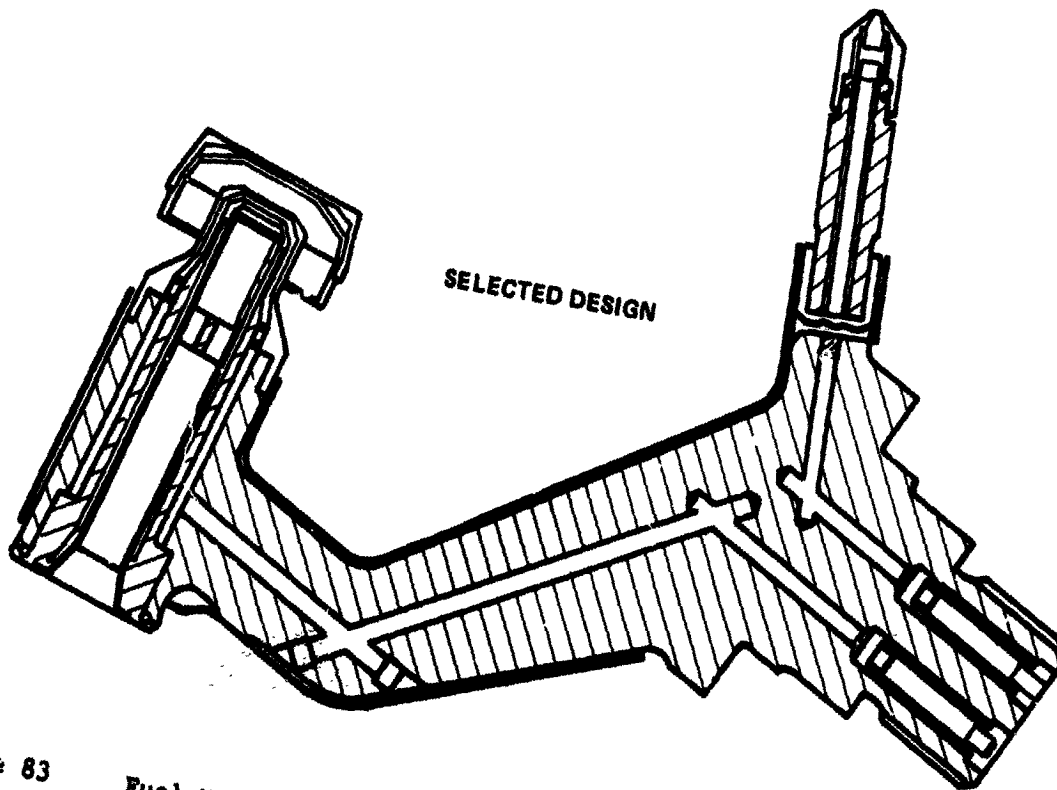
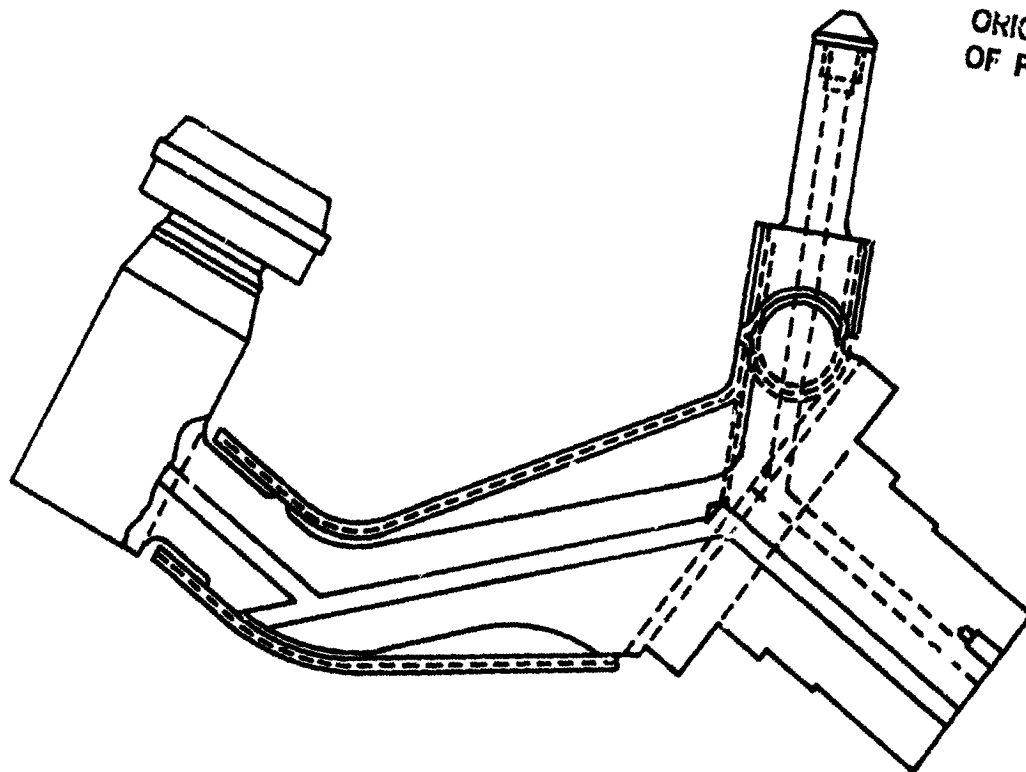
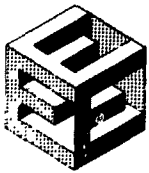


Figure 83 Fuel Nozzle Candidate Designs



Ignitor Configuration

The final ignitor configuration was established. Because the ignitor mounts into the diffuser case and protrudes into the combustor, its final dimensions cannot be established until the designs of the diffuser case and combustor are complete. A dimensional review of existing ignitors indicated that one of these ignitors can be used in the Energy Efficient Engine program. This configuration provides the required reliability and will cost substantially less than a part unique to the program. The only modification it requires is an extension of its mounting thread (see Figure 84).

Combustor Component Rig

Rig Analysis and Design. The design of the combustor component rig was essentially completed during the current reporting period. The only item still requiring work is the fuel system, which is now being designed as part of the component detailed design effort. A review of the combustor component rig design was conducted at NASA-LERC on 18 September 1980, and NASA approved this design on 29 September 1980.

The rig was designed so that it could be easily installed in the Pratt & Whitney Aircraft high-pressure combustion test facility. This facility features modular capsules to expedite installation. As a test series is completed, the capsule is replaced by a previously assembled capsule, and the next series of tests begin.

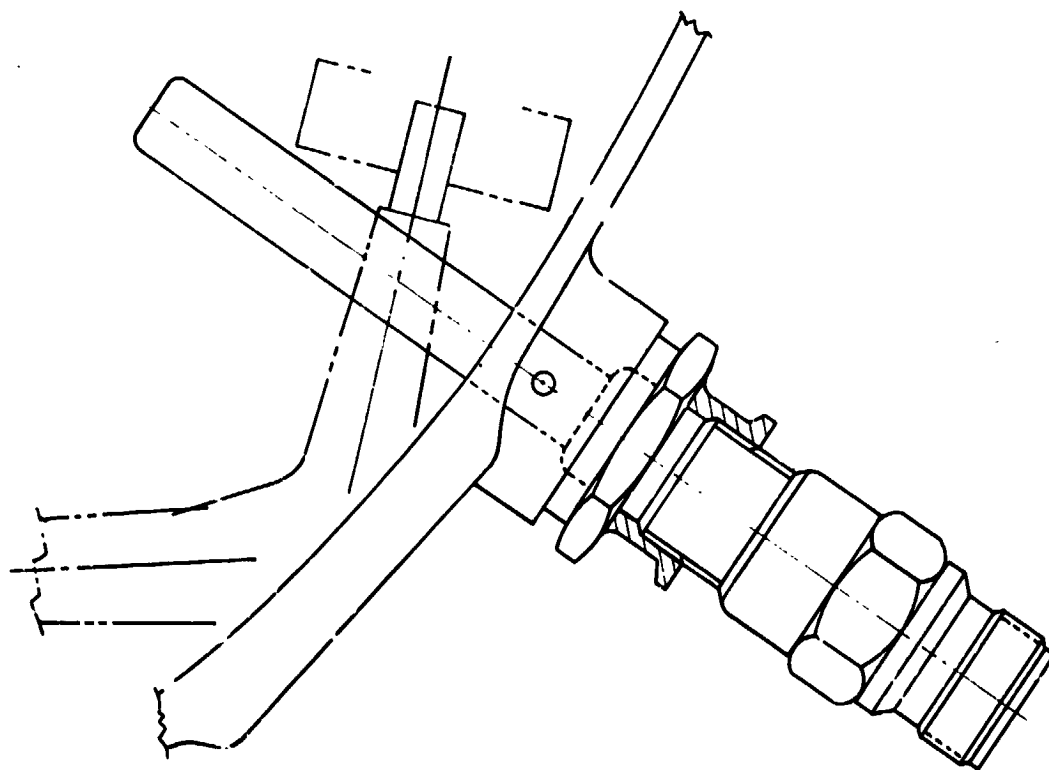
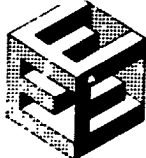
The rig was designed to accommodate combustor inlet temperatures up to 1000 F and combustor exit temperatures averaging at 2500 F with a maximum of 3200 F. A pressure differential was conservatively set at 50 pounds per square inch.

Rig/Facility Mounting. As shown in Figure 85, the rig is mounted within the facility capsule between an inlet bellows and a conical aft support spring. The inlet bellows imposes a 600-lb axial load on the rig.

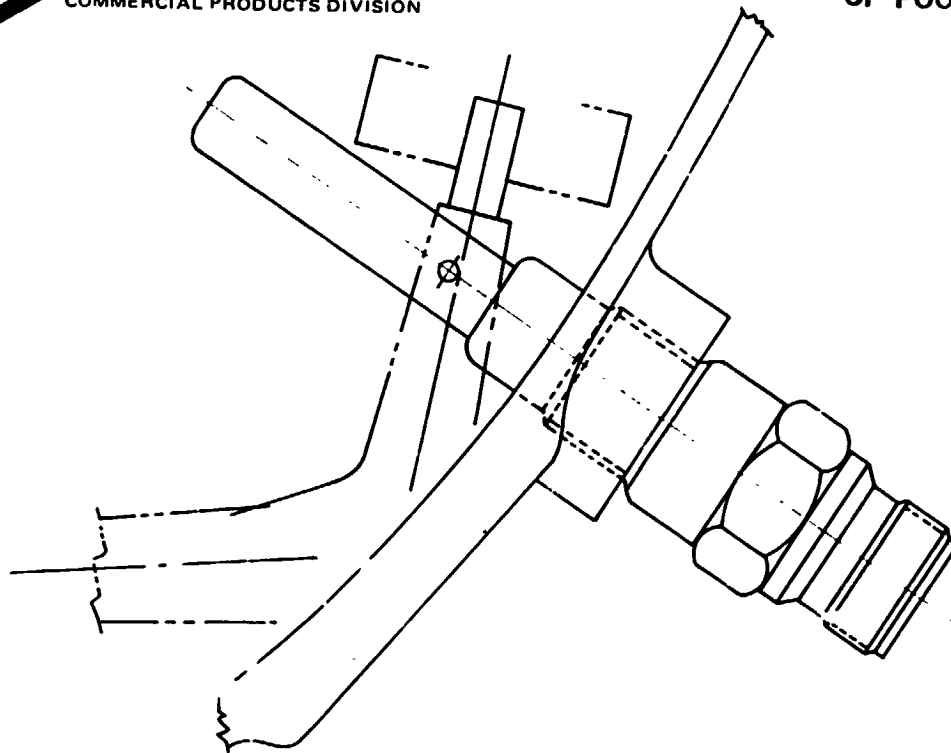
All cases between the facility bellows and the diffuser case are made of AMS 5596 (Inco 718) material and have been checked for elastic buckling. External pressure ΔP used for analysis was 50 psi, which is conservative relative to the expected operating pressure of 6 psi. An axial load of 600 lb and an appropriate moment is applied to each case. This moment results from having the rig mass cantilevered from the rear support. The highest stress, duct, P/789202, is 7400 psi; critical buckling stress is 9000 psi, resulting in an acceptable buckling factor of 0.8.

The most highly stressed flange is on the duct attached to the diffuser case front end with a stress of 71,000 psi relative to a 0.2 percent yield strength for AMS 5596 (Inco 718) at 1000 F of 120,000 psi.

A spring mount is positioned between the diffuser case rear flange and the test facility capsule. This design reduces the stresses introduced into the diffuser case from differential thermal growth. Maximum stress in this spring from 50 psi pressure differential, 600 lb axial load, and a 55,000 inch/lb



MODIFIED FOR USE
IN THE EEE COMBUSTOR



UNMODIFIED EXISTING IGNITOR

Figure 84 Existing Ignitor Modified for Use in Energy Efficient Engine
Combustor



PRATT & WHITNEY AIRCRAFT GROUP
COMMERCIAL PRODUCTS DIVISION

ORIGINAL FACILITY
OF POOR QUALITY

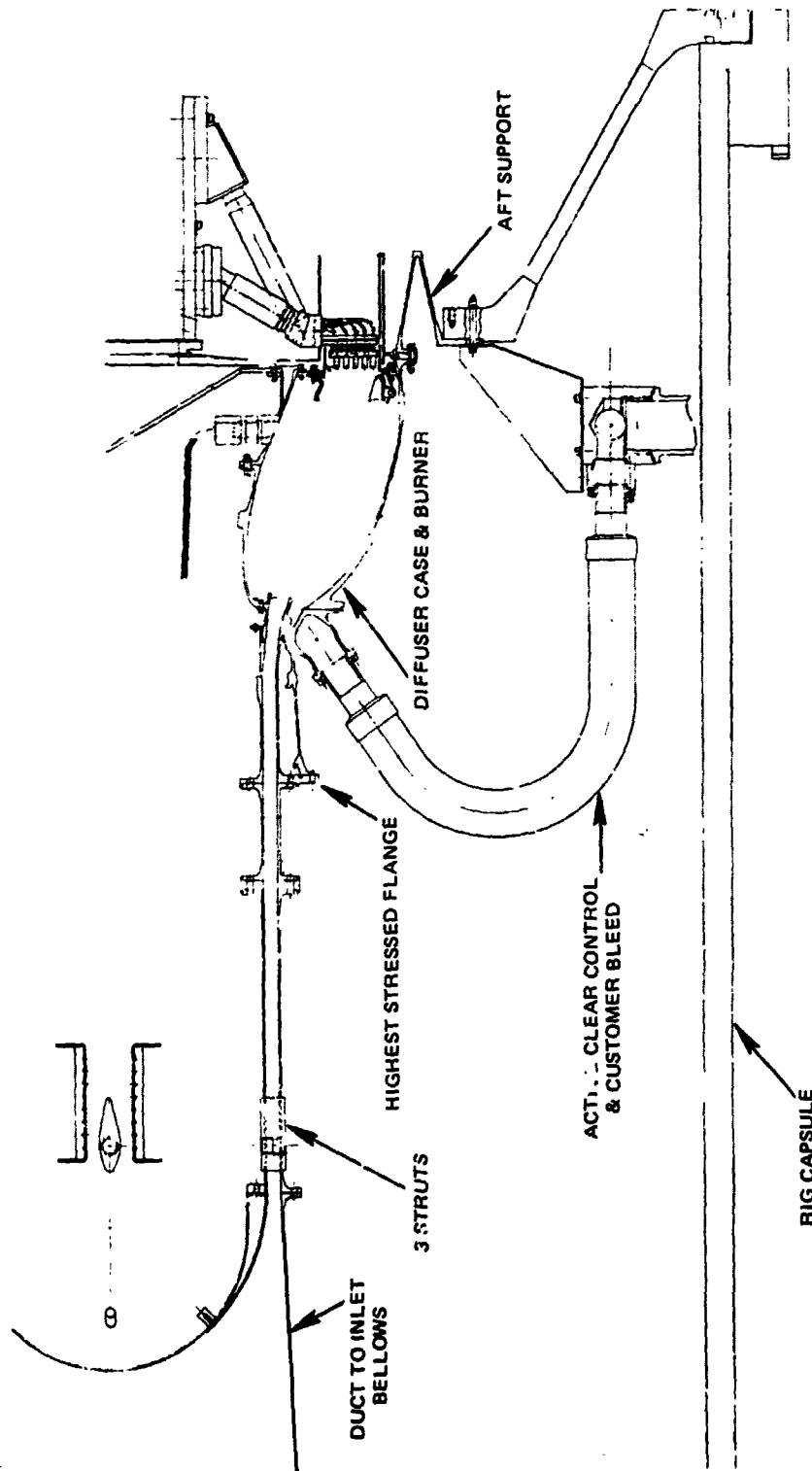
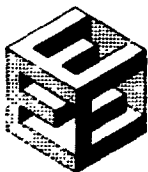


Figure 85 Combustor Rig/Facility Mounting Scheme



moment is 58,200 psi. The material used for this spring is AMS 5596 (Inco 718) with an allowable 0.2 percent yield strength of 120,000 psi at 1000 F.

Provisions have been made for the extraction of air for customer bleed, tangential on-board injection bleed, and active clearance control. Plumbing was designed to connect to bleed ports on the diffuser case bleed annulus for customer bleed and active clearance control air. This air is piped through the capsule wall and vented to ambient air. Because of thermal and tolerance differentials, connection between the rig case and the capsule is made with flexible tubing. Tangential on-board injection bleed air is separately metered from the other bleeds. It is collected in the in-board cavity transmitted through 3 of the 8 hollow struts in the rig inlet case assembly and routed to flexible plumbing. The tangential on-board injection bleed air is then carried through the capsule wall and vented to ambient air.

Rig Instrumentation. Rig instrumentation requirements are shown in Figure J. The station 3.0 and 4.0 probes extend into the gas path and meet all design requirements. The station 3.0 probes will also be used in the integrated core/low spool tests. These probes mount on the diffuser bleed annulus. Because of case structural considerations, the pads could not be positioned in a manner that would allow a probe assembly path normal to the flowpath. The probes are shown in Figure 87.

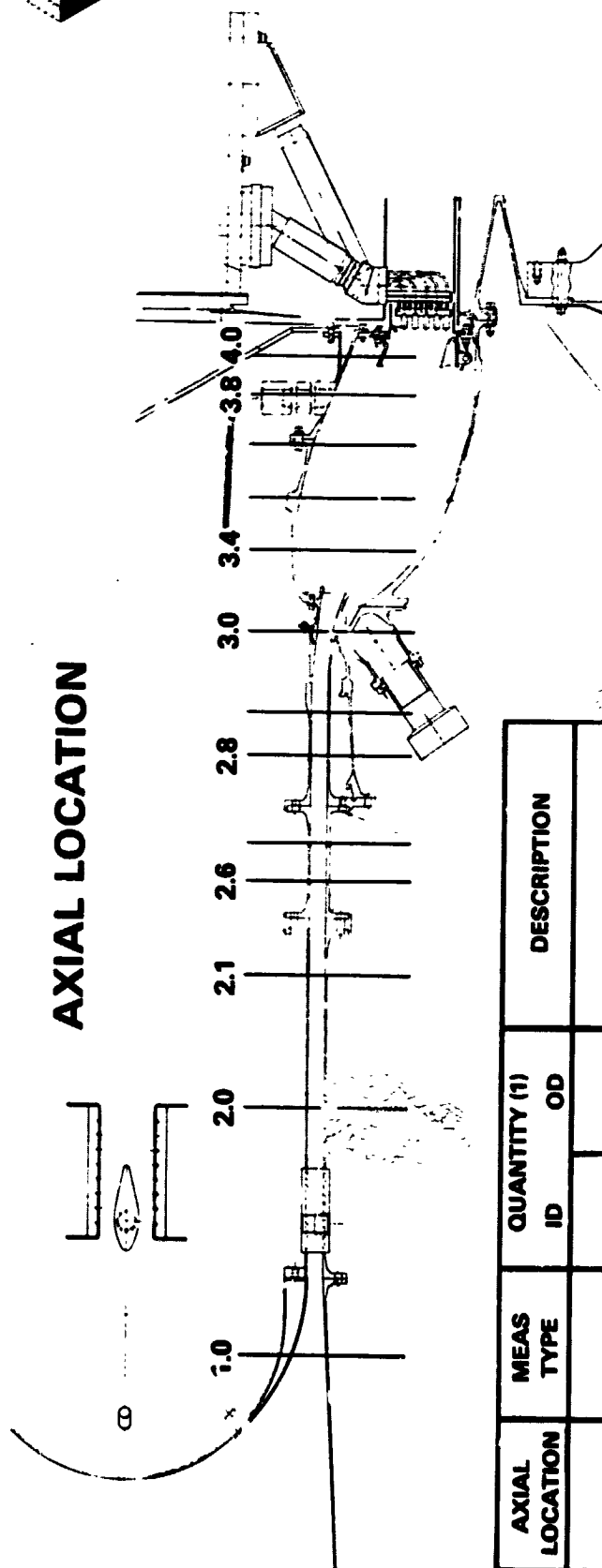
The area between the flowpath and annulus must be adequately sealed because the probes pass through the bleed annulus. To accomplish this, the probe support shaft has been machined into a spring. When the probe is installed and bolted to the outer case, spring compression provides a seal between the flowpath and the annulus. Spring compression results in a maximum stress of 63,400 psi relative to the AMS 5596 material allowable shear stress at 1000 F of 80,000 psi. A right and left hand helix is machined into the spring to eliminate twist. The foregoing stress results from a 0.010 inch preload minus 0.012 inch thermal load and a maximum tolerance deviation of 0.025 inch. The material used is AMS 5596.

The design of the burner emissions rake heads is patterned after those successfully used in previously operated sector rigs. Cooling flow requirements for these rakes are summarized in Table 57 in terms of the following conditions: (1) a ΔP of 100 psi across the head, (2) a maximum burner discharge pressure of 320 psia, (3) cooling air supply maximum inlet pressure 420 psia, and (4) at a temperature of 250 F.

TABLE 57

RAKE COOLING FLOW REQUIREMENTS

Thermocouple sensor support	0.012 lb/sec
Pulsed Thermocouple cooling air	0.07 lb/sec
Gas sample probe	0.03 lb/sec/sensor



ADDITIONAL INSTRUMENTATION

- THERMAL SENSITIVE PAINT
- AIRFLOWS - STAND
- FUEL FLOWS - STAND
- INLET HUMIDITY - STAND

(1) CIRCUMFERENTIAL/RADIAL

AXIAL LOCATION	MEAS TYPE	QUANTITY (1)		DESCRIPTION
		ID	OD	
1.0	T	18/1	10/1	FAC. SUPPLIED
2.0-2.9	PS or T _T	12/1	18/1	INLET DUCT
3.0	PS	20/1	12/5	COMB INLET
3.0	PS	30/1	12/1	COMB INLET
3.4	PS	10/1	12/1	HOOD STATIC
3.4	PT	20/1	8/1	PILOT NOZZLE INLET
3.4-3.9	PS	30/1	20/1	SHPC JD STATICS
3.4-3.9	T	10/1	30/1	LINER TEMP
3.9	UNC	10/1	8/1	SHROUD SNIFFERS
3.4-3.9	S	5/4	10/1	STRAIN MEAS
4.0	E	2/5		EMISSION TRAVERSE
4.0				TEMPERATURE TRAV.

Figure 86 Full Annular Rig Instrumentation



PRATT & WHITNEY AIRCRAFT GROUP
COMMERCIAL PRODUCTS DIVISION

ORIGINAL PAGE IS
OF POOR QUALITY

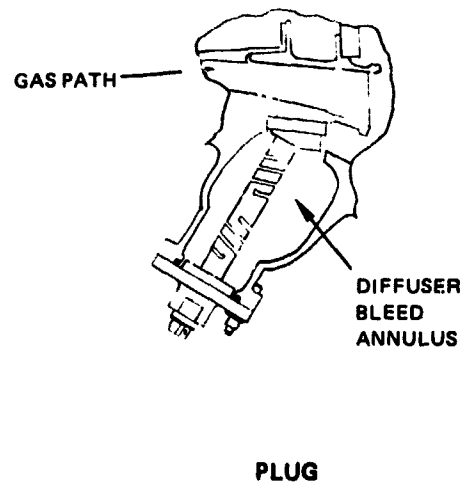
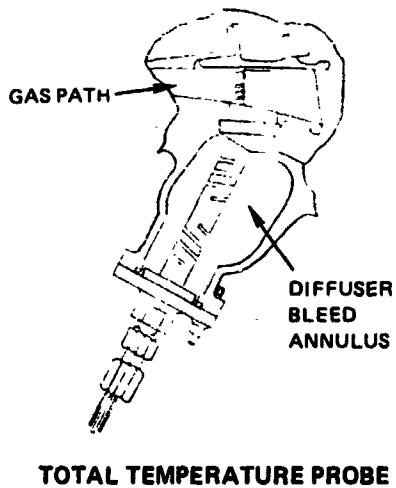
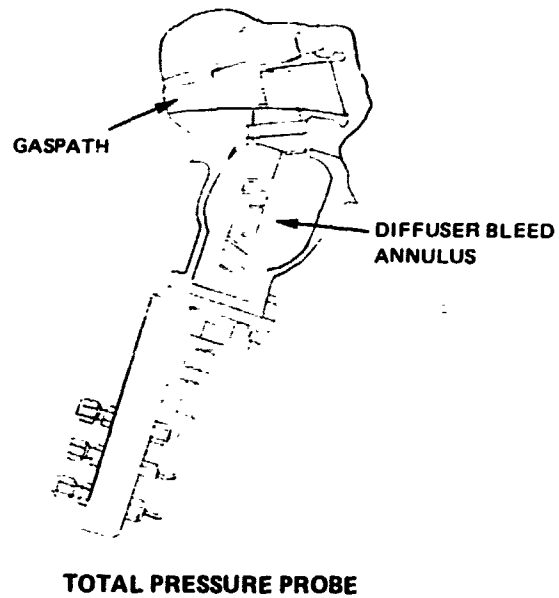


Figure 87 Instrumentation Probes



The station 4.0 instrumentation will be routed out through the facility rake support. Inner flowpath instrumentation will be carried through 5 of the 8 hollow struts in the rig inlet case assembly. All instrumentation will be connected to patch panels mounted on the inner wall of the capsule. This agreement provides for quick disconnecting capability from the test facility to facilitate rapid installation and removal.

Fuel Manifolds

The design of the fuel manifold was initiated during the current reporting period. Fuel manifolding is a straightforward design task wherein the major concerns are to avoid interferences with other lines and to ensure ease of assembly and disassembly. The Energy Efficient Engine design will be totally enveloped by a sealing shroud to preclude the possibility of a fuel leak impinging upon a hot case (see Figure 88).

Pressurizing valves will be included in the fuel manifold scheme. These valves uniformly pressurize the manifold system to prevent head effects at low fuel flow, which might result in fuel dribble and possible maldistribution.

Combustor Fabrication Effort

The objective of the combustor fabrication effort for this reporting period was to identify and procure the raw material requiring a long lead time. Raw material casting orders have been placed.

The diffuser case casting vendor is assembling the first wax pattern. The pattern is assembled by wax-welding 24 segments (see Figure 89) into a complete ring. Bleed and instrumentation bosses are then located by an indexing fixture and are wax-welded in position. Layout inspection of the first wax assembly is scheduled for early October. The investment process will require approximately two weeks. Initial pouring is scheduled for late October.

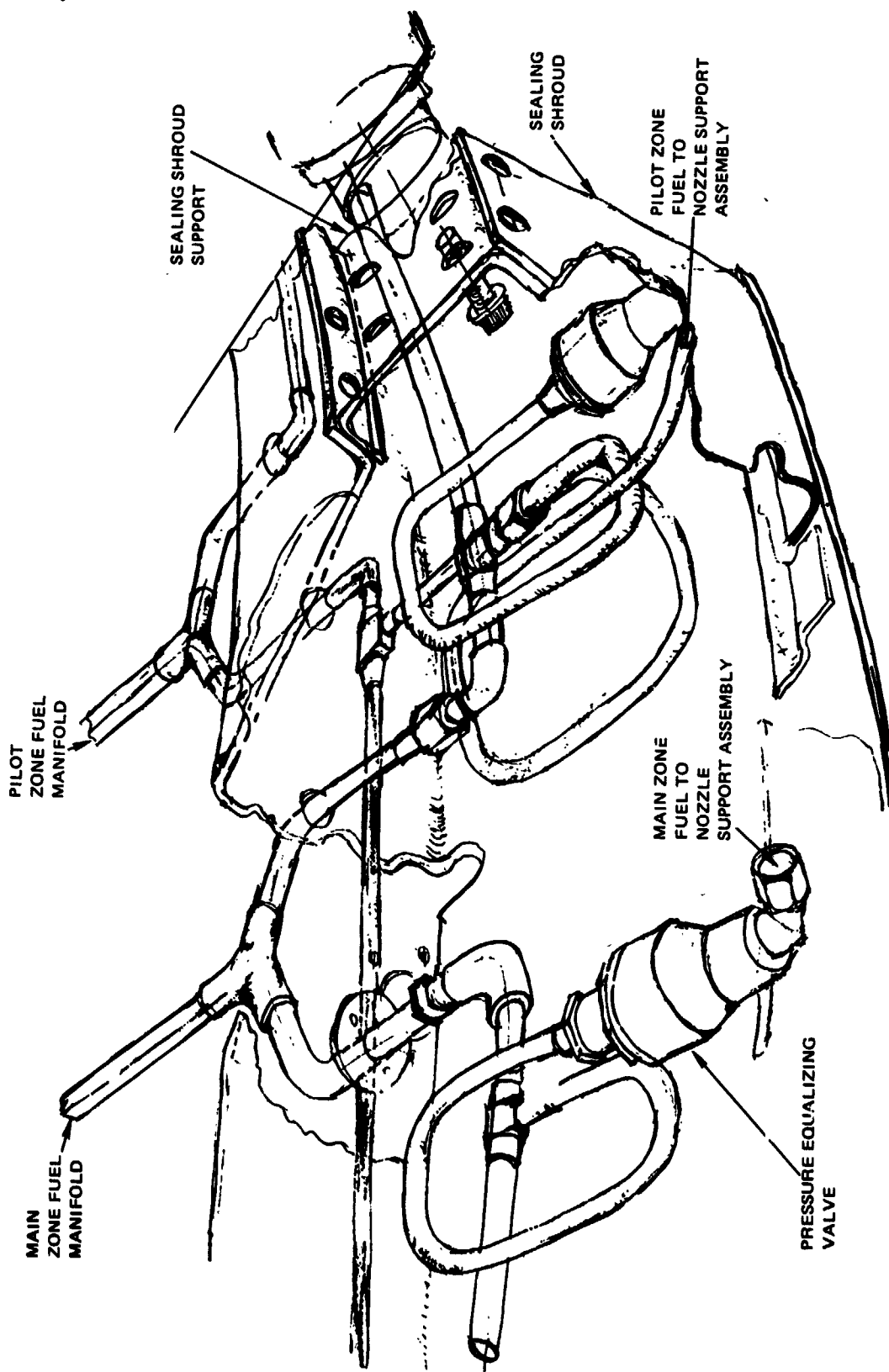
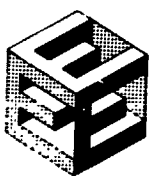


Figure 88 Fuel Supply Manifolds and Shroud

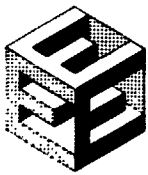


Figure 89 Diffuser Case Wax Pattern

3.2.6.4 Supporting Technology

3.2.6.4.1 Diffuser/Combustor Model Test Program

All work under this supporting technology program has been completed. Program results to date are summarized in section 3.2.6.4.1.3 of the Third Semiannual Status report, dated October 10, 1979. The only work remaining was a retest of the revised thickness diffuser case design. This testing was completed during the current reporting period. Results are described in section 3.2.6.4.1.1.

3.2.6.4.1.1 Current Technical Progress

Structural analysis of the component diffuser case during the detailed analysis and design effort revealed that the baseline strut configuration was not adequate in carrying the case loads. A structurally adequate design with a thickened trailing edge and features that permit easy casting was subsequently designed, fabricated, and evaluated as an addendum to the diffuser/combustor model program.

Performance tests were conducted to evaluate the effect of the revised strut contour on the inner and outer shroud dump losses. Wake rake traverses were conducted on the inlet to the inner shroud. Traverses were performed behind both the baseline and revised struts employing an eleven-element wake rake. A comparison of the baseline and revised strut designs is presented in Figure 90.

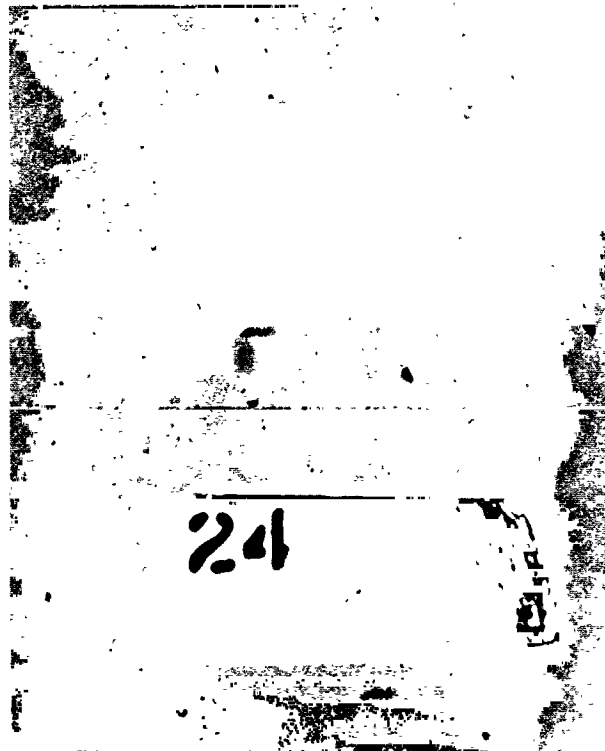


Figure 90 Comparison of the Baseline Strut and the Revised Strut

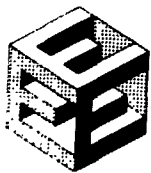
Rig inlet Mach number was varied over a wide range and total pressure losses to the inner and outer shroud were measured. The results of the dump loss measurements are presented in Table 58. The thickening of the trailing edge from 0.120 inch to 0.300 inch as well as the increased taper near the inner and outer diameter case walls (for ease of casting) result in an increase in the dump losses of approximately 0.2-percent P_{T3} .

TABLE 58

COMBUSTOR SECTION TOTAL PRESSURE LOSS SUMMARY
(P_{T3})

	Demonstrated		Program Goals
	Baseline Strut	Revised Strut	
Section	5.2	5.5*	5.3 (cold)
Inner Shroud	2.2	2.40	≤ 3.0
Outer Shroud	2.7	2.95	≤ 3.0

* Combustor hole pattern was designed with pressure distribution data from the baseline strut tests which allowed for higher liner pressure drops. Revision of the hole pattern will enable the goal section losses to be achieved.



Wake rake traverses were conducted behind both the baseline and revised struts at the inlet to the inner shroud annulus (approximately 2.5 in. downstream of the strut trailing edge). The width of the eleven element wake rake encompassed 62 percent of the nominal distance between the struts. Circumferential movement of the rake by one full width therefore ensured more than 100 percent circumferential coverage of the distance between struts. The total pressure characteristics downstream of the struts are presented in Figure 91 at various inner shroud span locations. No wake characteristics are evident in either strut data.

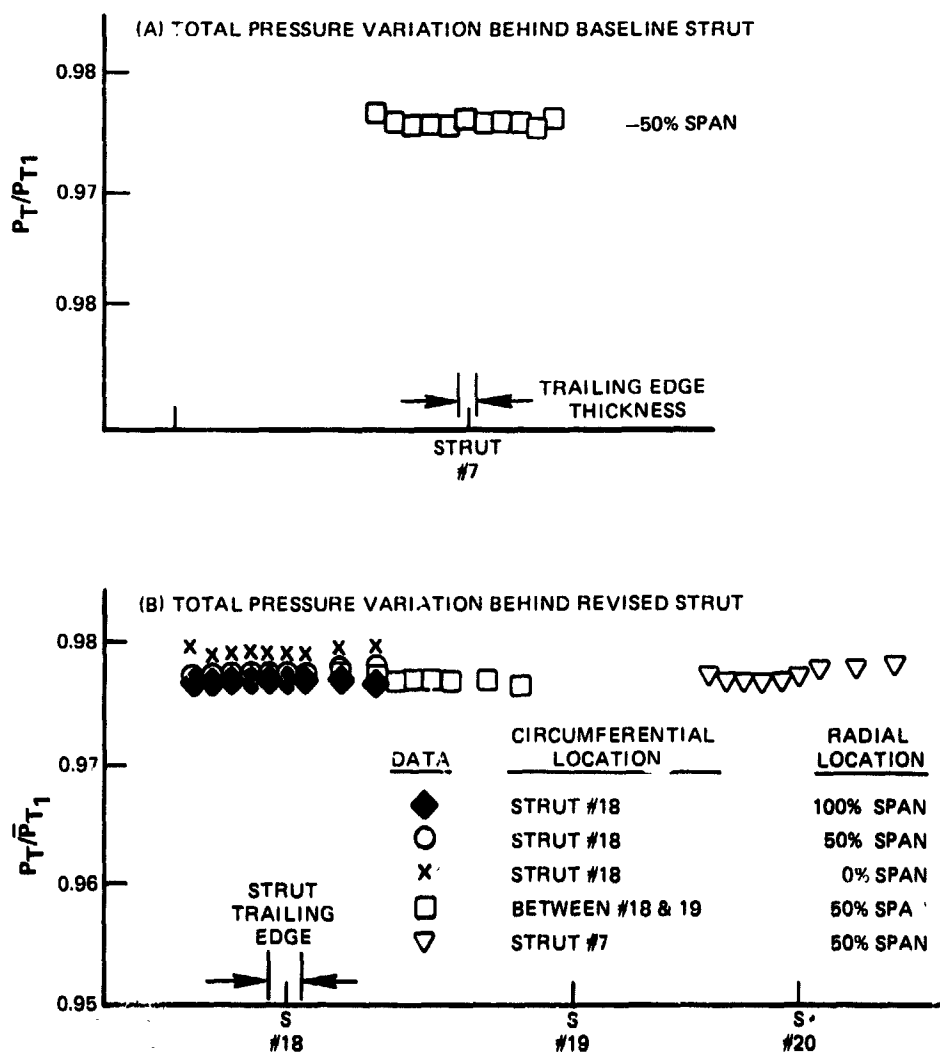
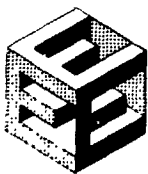


Figure 91 Inner Shroud Wake Rake Traverse Results



3.2.6.4.2 Combustor Sector Rig Test Program

3.2.6.4.2.1 Objective

Evolve and experimentally substantiate the design features of the two stage (aerated nozzle pilot and carburetor tube main zone) combustor. The modifications formulated during the program are aimed at reducing the emissions, pattern factor, and cost and weight as well as improving the durability and maintainability of the combustor section. Specific emissions and performance goals are the same as those of the combustor component.

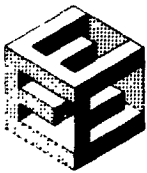
3.2.6.4.2.2 Scope of Total Work Planned

The combustor sector rig test program consists of the five phases shown in Figure 92, which indicates that analysis and design were completed during a previous reporting period and that fabrication, assembly, testing, and post-test analysis were initiated prior to the current reporting period. A modular high-pressure test rig representing a 90-degree sector of the full annular engine diffuser/combustor section is designed, fabricated, and assembled. This rig includes the transition duct (circular to sector cross-section) inlet section, diffuser case, combustor, and instrumentation used to sample pressure, temperature, and exhaust gas. Modular design features are employed to facilitate variation of prediffuser contour, diffuser case strut geometry, prediffuser dump/combustor front-end geometry, and combustor pilot and main zone geometry. The ability to vary the number and type of main zone fuel injectors is also incorporated into the design. A second diffuser case/combustor assembly is also fabricated. The fabrication and assembly efforts for the rig and the second diffuser case/combustor assembly are phased to permit modification of one combustor while the other is being tested. A third combustor liner assembly featuring segmented liners and advanced cooling techniques is also fabricated.

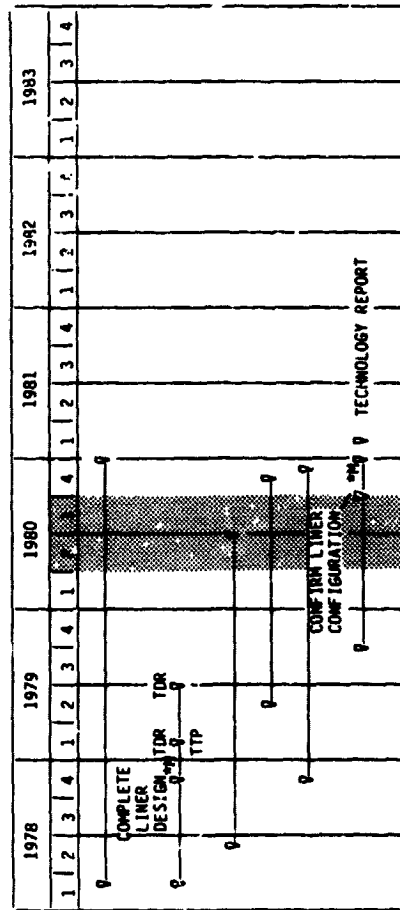
Testing includes pilot zone optimizations, changes in temperature history, variation in number of fuel injectors and fuel spray characteristics, and combustion air variations in the pilot and main zone to regulate exit temperature profiles and emissions. Tests consist of cold flow pressure loss measurements, parametric idle testing with only the pilot zone fuel injectors flowing, definition of lean blow-out characteristics, and pilot/main zone fuel split variations to minimize emissions.

Performance and emissions data are recorded at every test point by utilizing an automatic data recording system. Following definition of an optimum combustor in the high-pressure facility, the sector rig is transferred to the altitude relight facility and tests conducted to determine the altitude relight and stability characteristics of the combustor.

Processed data are analyzed in depth following a test sequence with a particular configuration to evaluate the status of the emissions, performance, and durability characteristics relative to the program goals. Modifications of the rig hardware are then formulated to improve deficient areas.



COMBUSTOR SECTOR RIG TEST PROGRAM - WORK PLAN SCHEDULE



ACTIVITIES/MILESTONES

TOTAL MBS TIME

ANALYSIS AND DESIGN

FABRICATION

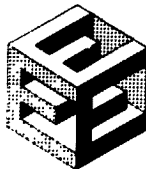
ASSEMBLY

TEST

POST-TEST ANALYSIS

◆◆ DENOTES MAJOR MILESTONE ◆ DENOTES KEY DECISION POINT

Figure 92 Combustor Sector Rig Test Program Work Plan Schedule



3.2.6.4.2.3 Technical Progress

3.2.6.4.2.3.1 Summary of Work Previously Completed

The baseline sector rig assembly with an instrumented vane pack installed in the exit plane is shown in Figure 93. The liners used in early rig testing are of conventional louver construction, employing Hastelloy-X, to expedite configuration changes during the primary test program. The vane pack assembly consists of eight instrumented vanes, four pressure vanes and two "dummy" vanes.

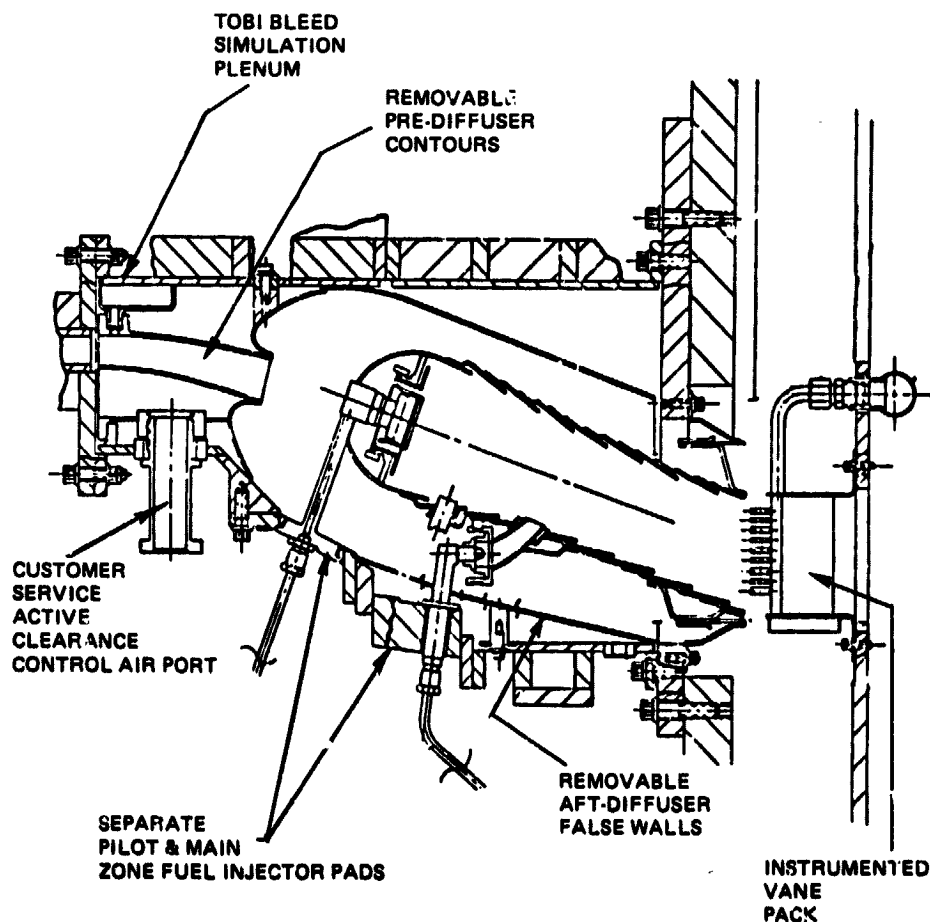
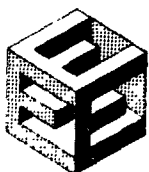


Figure 93 Combustor Sector Rig Cross-Section - The combustor liners for rig application are of conventional louver construction employing Hastelloy-X, thus expediting the configuration changes during the primary test program.



PRATT & WHITNEY AIRCRAFT GROUP
COMMERCIAL PRODUCTS DIVISION

Each instrumented vane features four gas sampling ports and five thermocouple ports. The pressure vanes include five kiel-head pressure sensors and will be used to measure combustor exit total pressure profiles. High-pressure air is used to convectively cool the leading edge of the vane, and is subsequently ducted into the body of the vane for transpiration cooling. The manifolding of the 32 gas sampling lines has been arranged so that either radially averaged or circumferentially averaged exhaust emissions can be obtained. The radial averaging method will be used for the majority of the tests. This will enable evaluation of emissions as they vary circumferentially, that is, in-line with pilot or main zone-nozzles, struts, etc. The circumferential averaging techniques will be employed for selected configurations to evaluate the radial emission profiles.

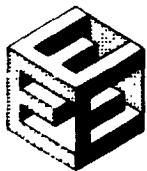
Following the change in segmented liners in the component design, the sector rig combustor design was revised to be compatible with the component design. This revised combustor assembly, featuring the inner and outer liner support frames and the four types of segments, is shown in Figure 94.

The rig structural case (including the strut section), pre-diffuser walls, shroud false walls, and two exit pressure plates were fabricated, and the pilot and main zone fuel injectors were received from vendors. The instrumented exit vane pack and the traversing rake were also fabricated. Fabrication problems with the vane pack and combustor assemblies caused the test date to be postponed to November 1979.

The carburetor tube airflow and fuel spray characterization tests were initiated, and the effect of flow areas and swirl strengths of five carburetor tube geometries were evaluated in an airflow rig. The scaled model geometries included variations in length, rate of convergence, and degree of turning. Fuel spray quality at the discharge plane of the tubes was determined in a spray characterization rig. Through iterative testing in both rigs, the internal geometric characteristics of the carburetor tube were designed to obtain the necessary uniform spray pattern and the most effective fuel atomization. Typical fuel droplet size was measured at 35-40 microns. These features have been incorporated into the high-pressure rig hardware.

The initial conceptual design was compared to the present design that evolved through the test sequence. Results of this comparison are shown in Figure 95. The important areas of change from the initial conceptual design are the floating nozzle guide, nozzle tip immersion depth, and carburetor tube and radial inflow swirler sizing.

Before the start of the current reporting period, six sector rig tests were conducted using the conventional low speed design. The tests consisted of (1) a shakedown test, (2) pilot zone injector comparison test, (3) baseline performance test, and (4) three development tests exhibiting evolutionary changes to the baseline configuration.



PRATT & WHITNEY AIRCRAFT GROUP
COMMERCIAL PRODUCTS DIVISION

ORIGINAL
OF 20

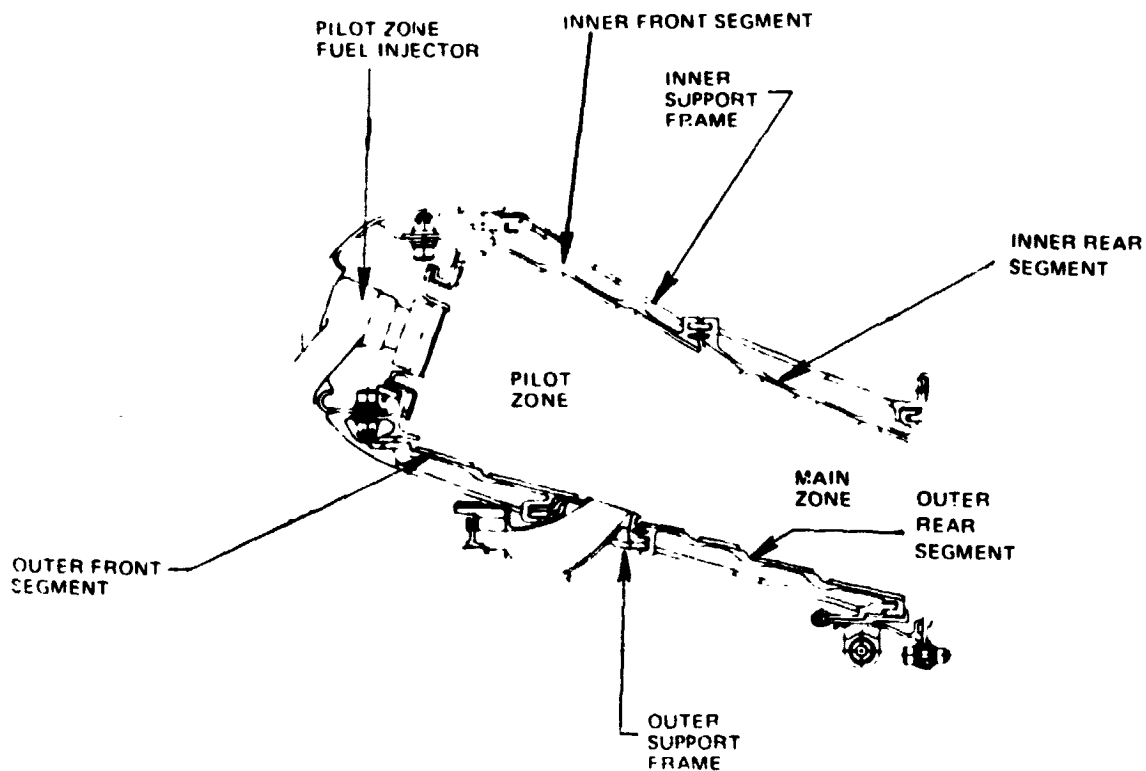


Figure 94 Revised Combustor Assembly with Segmented Liners

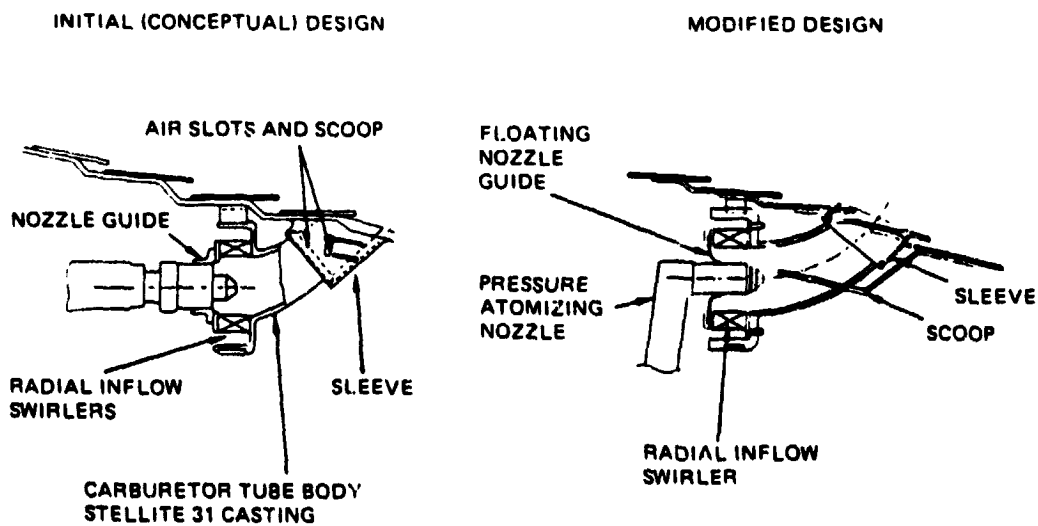


Figure 95 Main Zone Fuel Injector Configurations

C-3



As discussed in the Fourth Semiannual Status Report, the B-type nozzle exhibited a lower swirl strength characteristic than the A-type nozzle. This characteristic resulted in a front-end recirculation zone that caused increased emissions of carbon monoxide and total unburned hydrocarbon emissions. Consequently, the performance tests were conducted using the A-type nozzle.

3.2.6.4.2.3.2 Current Technical Progress

The combustor sector rig effort during this reporting period consisted of (1) fabrication and assembly of the segmented liner evaluation rig, and (2) assembly and testing of the baseline rig.

Segmented Liner Fabrication and Assembly

Finish-machining of all segments, inner and outer liner support frames, and the combustor sideplates was completed during this reporting period. Figure 96 shows the details of the cast liner segments subsequent to the electro-chemical and electro-discharge machining and grind operations. A side view of the overall rig liner assembly is presented in Figure 97.

Based on airflow calibration of the sector rig segments, approximately 31 percent W_{ab} will be required for liner cooling. This value is compatible with the design goal of 32 percent W_{ab} . A detailed breakdown of the segment effective flow areas (AC_d) are presented in Table 59.

TABLE 59

SECTOR RIG SEGMENT AC_d TEST RESULTS

Segment	AC_d (in ²)
Inner Front	0.129
Inner Rear	0.234
Outer Front	0.135
Outer Rear	0.229

Instrumentation and assembly of the rig was completed at the end of the reporting period and the rig was shipped for seal leakage testing.

Sector Rig Tests

Eight sector rig tests were conducted during this reporting period. The tests consisted of six emission/performance evaluations and two altitude relight characterization tests. A brief summary of the test configurations is presented in Table 60.

A typical emissions/performance test comprises cold flow pressure loss measurements, idle, fuel-air ratio excursions, definition of lean blow-out limits, and pilot/main zone fuel split variations at approach, simulated climb



and sea level takeoff operating conditions. Combustor inlet pressure was limited to a maximum of approximately 230 psia by test facility airflow limitations. Altitude relight tests consisted of a series of ignition attempts at combustor conditions representative of compressor windmilling over the Energy Efficient Engine flight envelope. The combustor operating characteristics used to establish the sector rig test conditions are summarized in Table 61.

TABLE 60

SUMMARY OF SECTOR RIG TESTING

<u>Test Type</u>	<u>Purpose/Comments</u>
7 Emission/ Performance	Changes relative to Run 6 configuration <ul style="list-style-type: none">o increased carburetor center tube flow by ~20%o reduced the AC_d of the pilot nozzle inner passage by ~30%o reduced ID louver 6 cooling by ~2% W_{ab}
8 Emission/ Performance	Changes relative to Run 7 configuration <ul style="list-style-type: none">o installed 20° insert type swirlers in carburetor secondary air passageo modified pilot nozzle blockage
9 Emission/ Performance	Changes relative to Run 8 configuration <ul style="list-style-type: none">o reduced ID louvers 5 and 6 by ~35% and ~45% respectivelyo added 0.300 x 0.700 in. dilution slots in ID louver 7
10 Emission/ Performance	Changes relative to Run 9 configuration <ul style="list-style-type: none">o increased carburetor center tube flow by ~10%o reduced carburetor tube length by ~10%o modified OD and ID dilution air schedule
11 Emissions/ Performance	Changes relative to Run 9 configuration <ul style="list-style-type: none">o installed 35° insert type swirlers in carburetor secondary air passageo modified rear dilution schemes to affect radial profile shift.
12 Altitude Relight	Evaluated with Run 10 configuration and Type B pilot nozzles
13 Altitude Relight	Evaluated with Run 10 configuration and Type A pilot nozzles
14 Emission/ Performance	Installed profile generation screen and evaluated the sensitivity to the diffuser inlet pressure profile with Run 11 configuration.



PRATT & WHITNEY AIRCRAFT GROUP
COMMERCIAL PRODUCTS DIVISION

ORIGINAL PAGE 13
OF POOR QUALITY

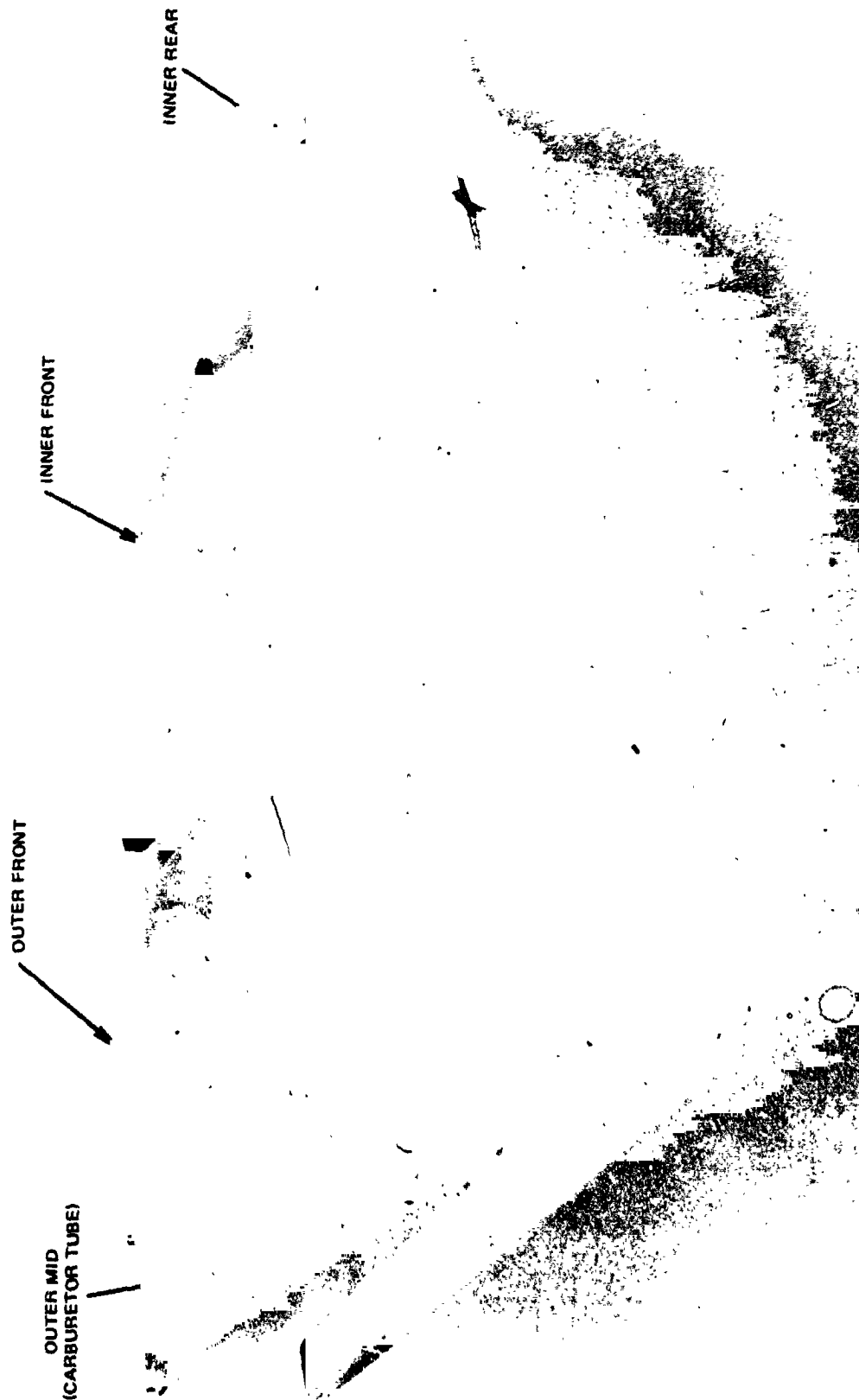


Figure 96 Liner Segment Details - Finish machined segments



PRATT & WHITNEY AIRCRAFT GROUP
COMMERCIAL PRODUCTS DIVISION

ORIGINAL PAGE 13
OF POOR QUALITY



Figure 97 Segment Combustor Rig Assembly



TABLE 61

COMBUSTOR OPERATING CHARACTERISTICS

Condition	P _{t3} (psia)	T _{t3} (F)	(f/a) ₄
Idle	63	391	0.0098
Approach	168	659	0.015
Climb	384 (232)*	934	0.023
Take-off	444 (236)*	991	0.025
Cruise	203	899	0.024

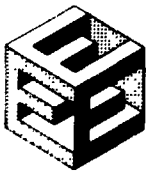
*Values in parenthesis indicate sector rig test conditions when different from actual.

Emission/Performance Tests

The early phase of sector rig testing, as described in the Fourth Semiannual Status Report, consisted of pilot optimization tests to reduce low power emissions of carbon monoxide and total unburned hydrocarbons. Progressive fuel enrichments of the pilot zone in tests 4 and 5 reduced carbon monoxide emissions by 63 percent and total unburned hydrocarbon emissions by 90 percent.

During the current reporting period, efforts were directed toward optimization of fuel staging at the approach operating condition and reduction in high power NO_x emissions. Two approaches for NO_x reduction were evaluated, both directed toward improving main zone fuel injector tube performance. The first (tests 7 and 10) concentrated on increasing the carburetor tube core airflow to improve fuel air preparation and lower overall main equivalence zone (see Figure 98). In the second approach (tests 8 and 14), swirl was introduced in the secondary air passage. These series of tests are discussed in the following two subsections.

Carburetor Tube Characterization Testing. The results of carburetor tube characterization testing, presented in the Fourth Semiannual Status Report, showed that droplet size decreases with increasing core velocity. This means that increased core flow could potentially improve fuel/air preparation as well as reduce main zone stoichiometry. Tests 7 and 10 were conducted to address this possibility. These tests featured increased core flow by using larger radial inflow swirlers and by reducing carburetor tube length. The results of these two tests indicated reductions in the levels of NO_x emissions at climb for each test configuration (see Figure 99(a)).



PRATT & WHITNEY AIRCRAFT GROUP
COMMERCIAL PRODUCTS DIVISION

ORIGINAL FILED
OF POOR QUALITY

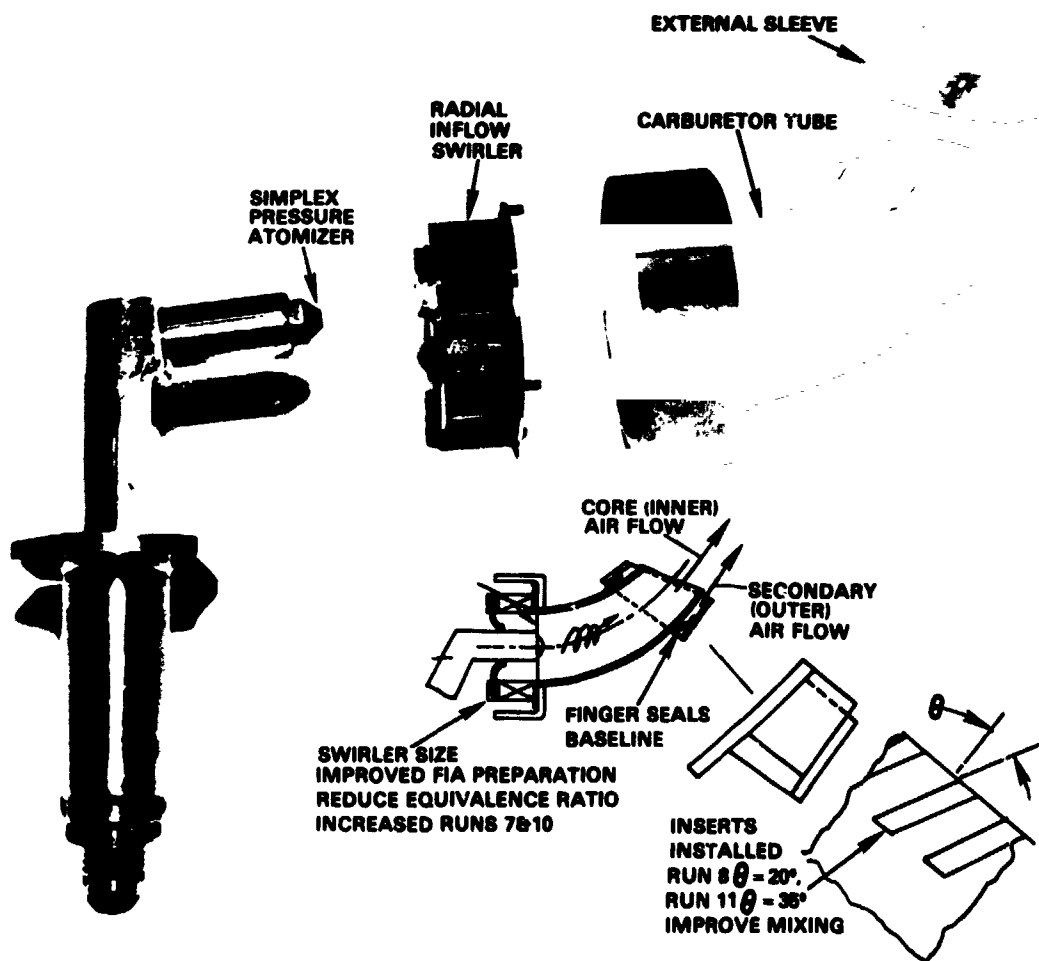


Figure 98 Carburetor Tube Modifications for Reduced NO_x

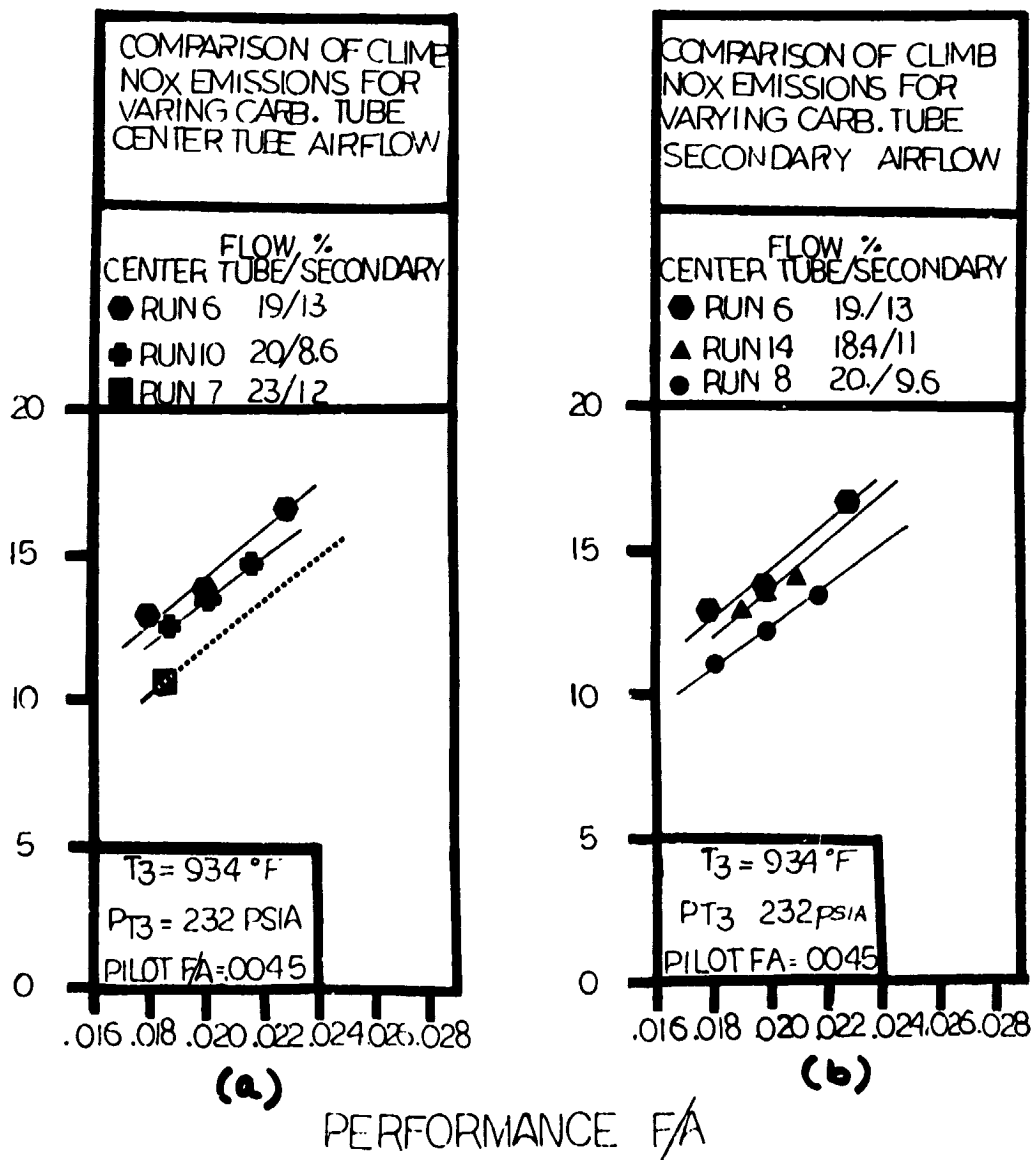
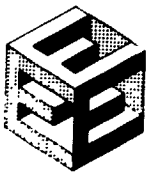
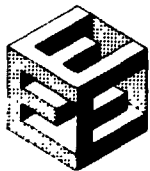


Figure 99 High Power NOx Emissions Characteristics



PRATT & WHITNEY AIRCRAFT GROUP
COMMERCIAL PRODUCTS DIVISION

During the running of tests 7 and 10, combustor section pressure loss varied between the test configurations. This resulted in airflow distributions that caused variations in carburetor tube flows, making it impossible to control one parameter at a time. The NO_x reduction trends, however, were clear.

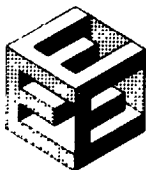
Secondary Swirl. In tests 8 and 14, swirl was introduced in the secondary air passage to provide a triggering action for more rapid mixing between secondary and core airflows. The finger seals shown in Figure 98 were replaced with swirl generation inserts angled in the flow direction (co-rotating with core flow).

A 20-degree swirl angle, evaluated in test 8 (see Figure 99(b)), contributed toward a significant reduction in NO_x emissions. In test 14, the swirl angle was changed to 35 degrees and the number of inserts was reduced. In addition, the passage area was increased to maintain high secondary airflow rates. These modifications, however, failed to offer further reductions in NO_x emissions (see Figure 99(b)). Moreover, these modifications adversely affected emissions of carbon monoxide and total unburned hydrocarbons at the approach operating condition.

An unexpected increase in low power carbon monoxide and total unburned hydrocarbon emissions occurred during test 7. This increase was apparently caused by the airflow split between the inner and outer pilot nozzle swirlers. Test 8 evaluated this sensitivity by incorporating sequential tests with three pilot nozzle designs. Blockage rings installed at the inlet of the inner and outer swirlers were used to vary airflow rates. Significant reductions in idle emissions of carbon monoxide and total unburned hydrocarbons, using each nozzle design, were achieved by reducing center tube airflow rates (see Figure 100).

The results of this investigation were used to select a new pilot nozzle design on the basis of inner/outer passage flow area and swirl strength. New pilot nozzles were configured to these specifications and evaluated during test 10. Comparison of carbon monoxide and total unburned hydrocarbon emissions at idle operating conditions are presented in Figure 101. When stoichiometric differences between configurations are accounted for, the results closely match those of the configuration used in establishing the new design criteria.

Efficient staging of the main zone in a two-stage combustor design at approach conditions is an important concern. At approach, a fueled main zone is desirable in terms of overall operation and durability. Efficient staging of the main zone was first achieved with the test 7 configuration with a pilot-to-main zone fuel split of approximately 15/85 percent. Parametric variations of pilot and main fuel flows at the approach condition conducted with the test 11 configuration are presented in Figure 102. As shown, increasing pilot fuel flow at constant main zone conditions results in reduced levels of carbon monoxide emissions. Since the pilot is essentially 100



PRATT & WHITNEY AIRCRAFT GROUP
COMMERCIAL PRODUCTS DIVISION

ORIGINAL PAGE 12
OF POOR QUALITY

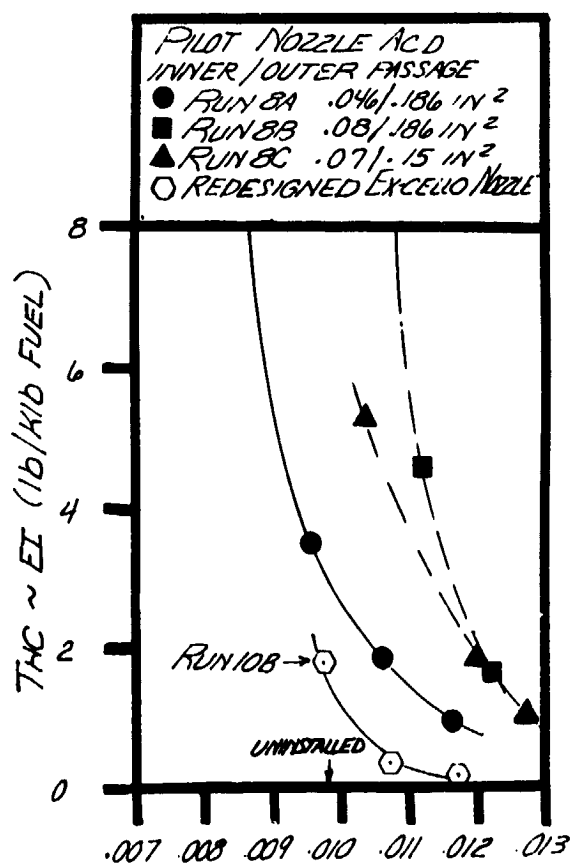
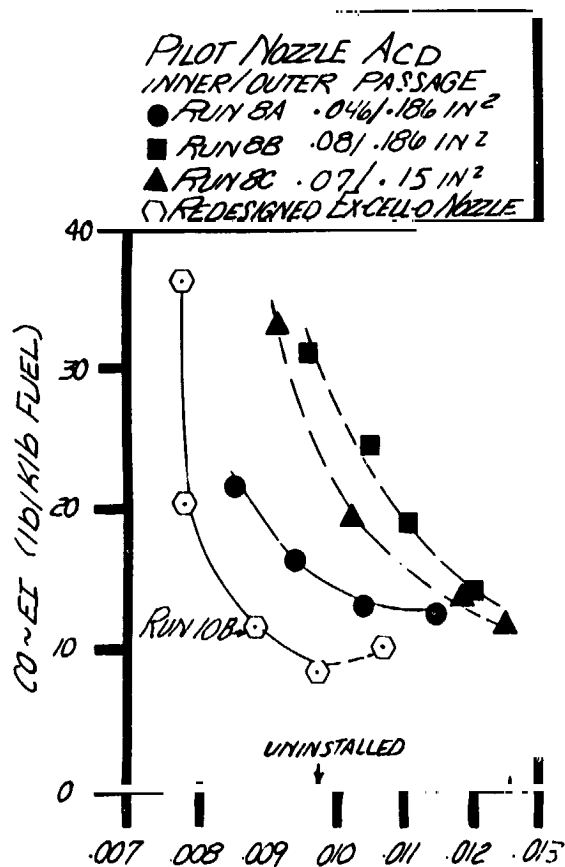


Figure 100 Comparison of Idle Emissions for Various Pilot Inner/Outer Swirler Blockage



PRATT & WHITNEY AIRCRAFT GROUP
COMMERCIAL PRODUCTS DIVISION

ORIGINAL PAGE 18
OF POOR QUALITY

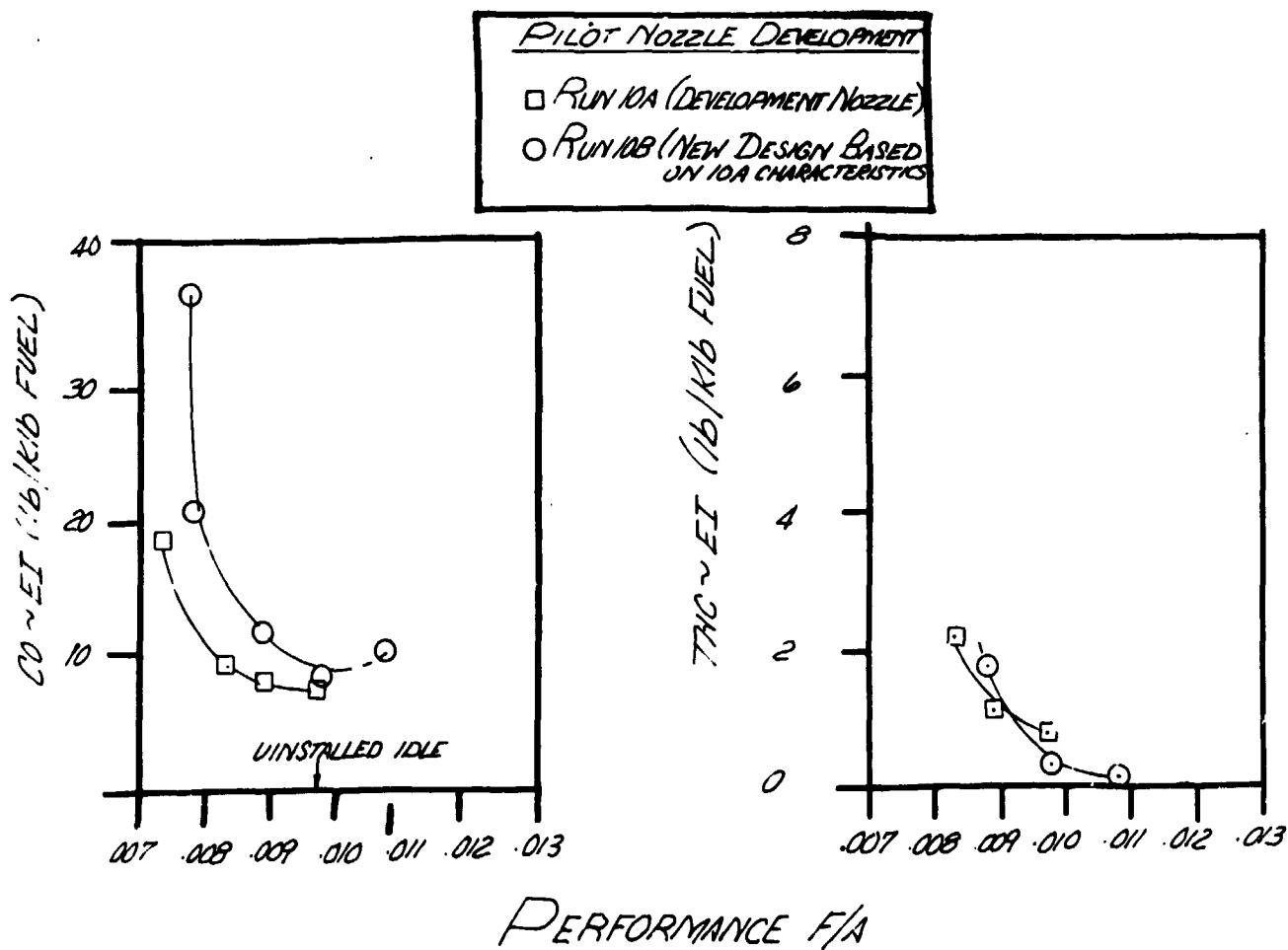
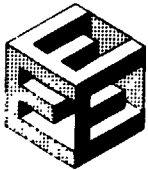


Figure 101 Comparison of Idle Emissions for the Redesigned Pilot Nozzle



ORIGINAL PAGE 13
OF POOR QUALITY

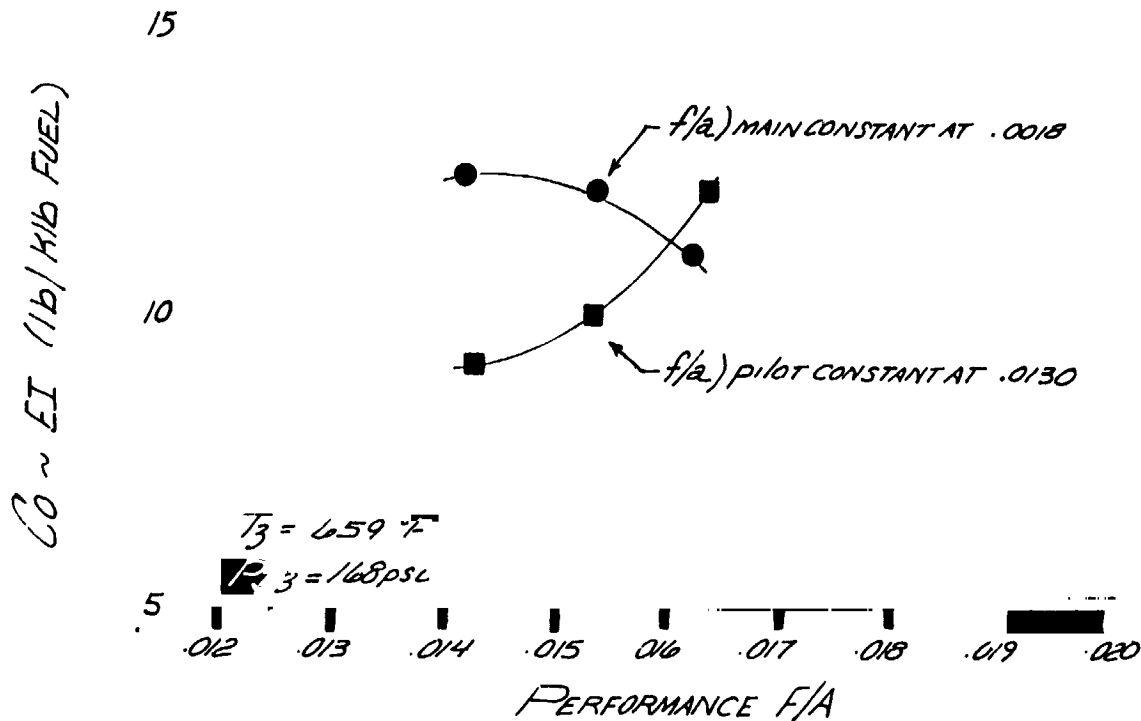


Figure 102 Variations of Carbon Monoxide Emissions With Performance F/A at Approach Condition

percent efficient at these conditions, the decrease in carbon monoxide emissions results from a reduced main zone emission contribution and is proportional to the percentage of main zone fuel. With the pilot conditions fixed, carbon monoxide levels are again influenced by the main zone. These levels also become greater with increases in fuel flow. That the percent increase in the levels of carbon monoxide emissions is less than the percent increase in main zone fuel flow indicates that the main zone combustion efficiency has increased as a result of the higher equivalence ratio.

The prediffuser inlet radial total pressure profile peak was shifted from 40 percent to 65 percent span to assess the impact of inlet flow changes on combustor performance. All performance parameters remained essentially unchanged, exhibiting negligible dependence on the inlet total pressure profile.



PRATT & WHITNEY AIRCRAFT GROUP
COMMERCIAL PRODUCTS DIVISION

The performance characteristics of the most promising configuration (test 10) are summarized in Table 62. The emissions parameters include margins for variability and development. The NO_x parameter is estimated based on a pilot zone fuel/air ratio of 0.003 at climb and sea level takeoff conditions. All emissions data for climb and takeoff conditions were scaled for inlet pressure effects (see Table 62).

TABLE 62

SECTOR RIG CANDIDATE COMBUSTOR PERFORMANCE SUMMARY

Pressure Drop (% P _{t3})		EPAP's	
Section	: 5 37	CO	: 2.07
Outer Liner	: 2.34	THC	: 0.26
Inner Liner	: 3.05	NO _x	: 4.65
		Smoke No.	: 5
		Pattern Factor	: 0.18
		Radial Profile	: 70 deg. F peak-to- average at 50% span

All program performance and emission goals (except NO_x emissions) and the altitude relight requirements were achieved with this configuration. The pilot and main zone fuel injector characteristics were incorporated into the component detailed design effort. Revised combustor air flow distribution, characteristic reference velocities, and liner areas are shown in Figure 103.

Altitude Relight

The altitude relight and sea level start characteristics of the Energy Efficient Engine combustor were evaluated with the test 10 configuration and two candidate pilot nozzle designs. Testing was conducted at combustor inlet conditions representative of compressor windmilling over the Energy Efficient Engine flight envelope. Fuel flow was varied at each condition to determine the minimum level of fuel flow required for ignition. The altitude relight results for the best nozzle design are presented in Figure 104. As shown over the range of conditions representative of the flight envelope, ignition was achieved up to an altitude of 35,000 feet with fuel flows as low as 48 lb/hr, both of which exceeded the required envelope.

At sea level conditions (see Figure 105), ignition was achieved at fuel flows of 192 lb/hr, exceeding Energy Efficient Engine requirements. Although both nozzle designs exhibited similar altitude relight capabilities, sea level start requirements could only be satisfied with one design.



PRATT & WHITNEY AIRCRAFT GROUP
COMMERCIAL PRODUCTS DIVISION

ORIGINAL PAGE IS
OF POOR QUALITY

COMBUSTOR AIRFLOW DISTRIBUTION (BASED ON SECTOR RIG TEST RESULTS)

- ALL FLOWS ARE IN PERCENTAGE OF COMBUSTOR AIRFLOW (W_{A4})
- REFERENCE VELOCITIES BASED ON SECTOR RIG SIMULATED SLTO CONDITIONS

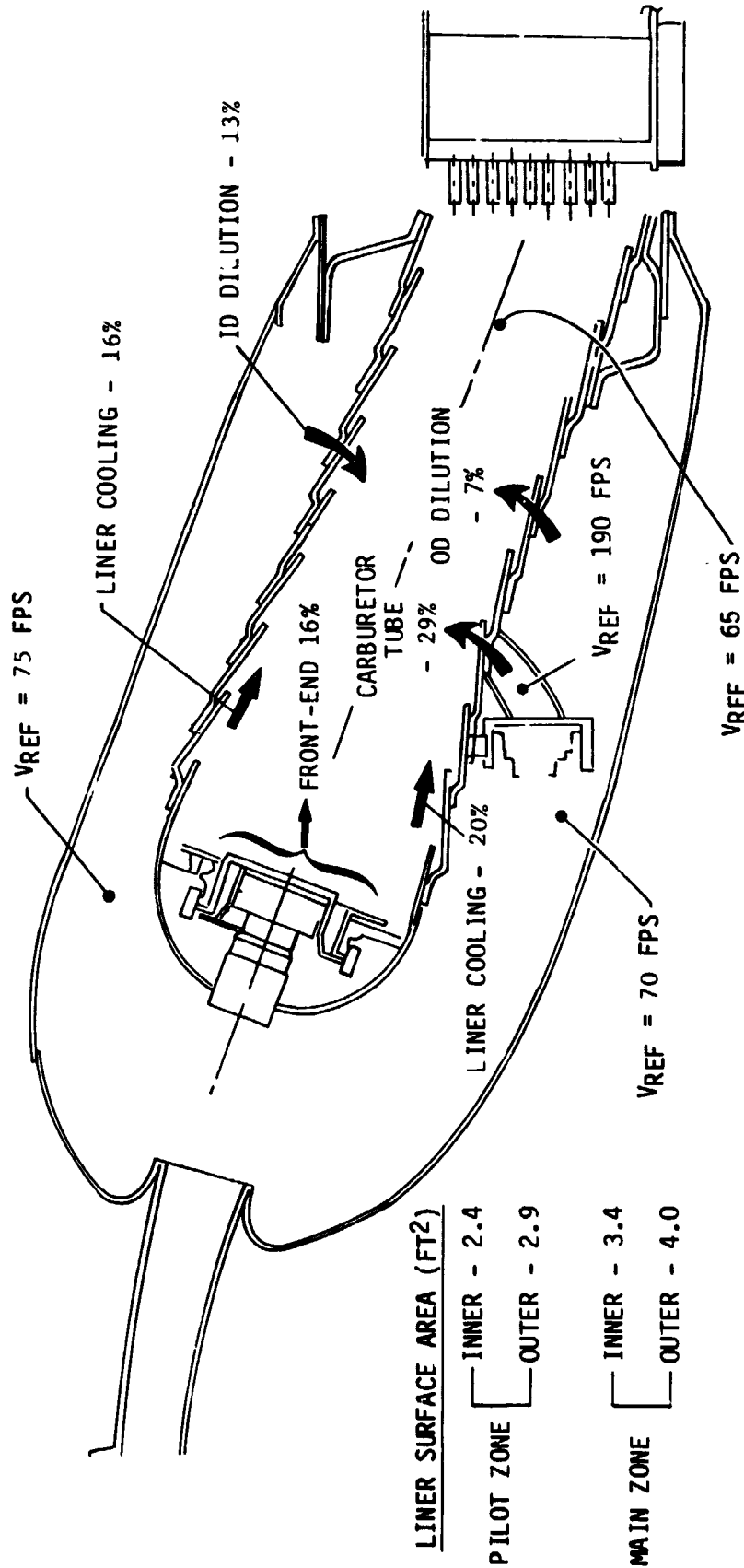
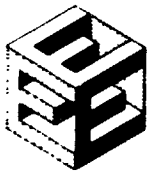


Figure 103 Combustor Air Flow Distribution (Based on sector rig test results)



PRATT & WHITNEY AIRCRAFT GROUP
COMMERCIAL PRODUCTS DIVISION

ORIGINAL PAGE IS
OF POOR QUALITY

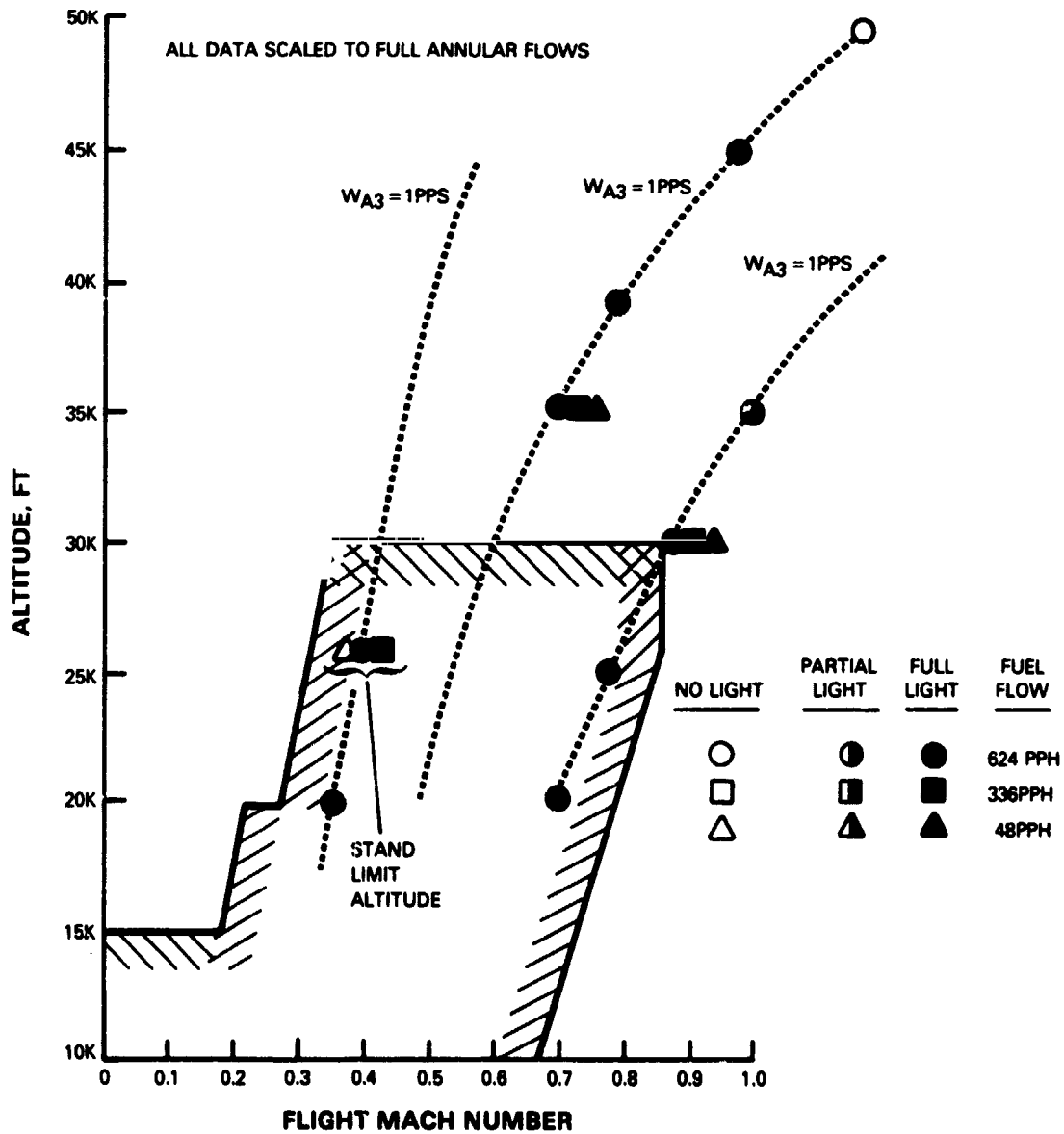


Figure 104 Altitude Relight Test Results



PRATT & WHITNEY AIRCRAFT GROUP
COMMERCIAL PRODUCTS DIVISION

ORIGINAL TEST OF
OF POOR QUALITY

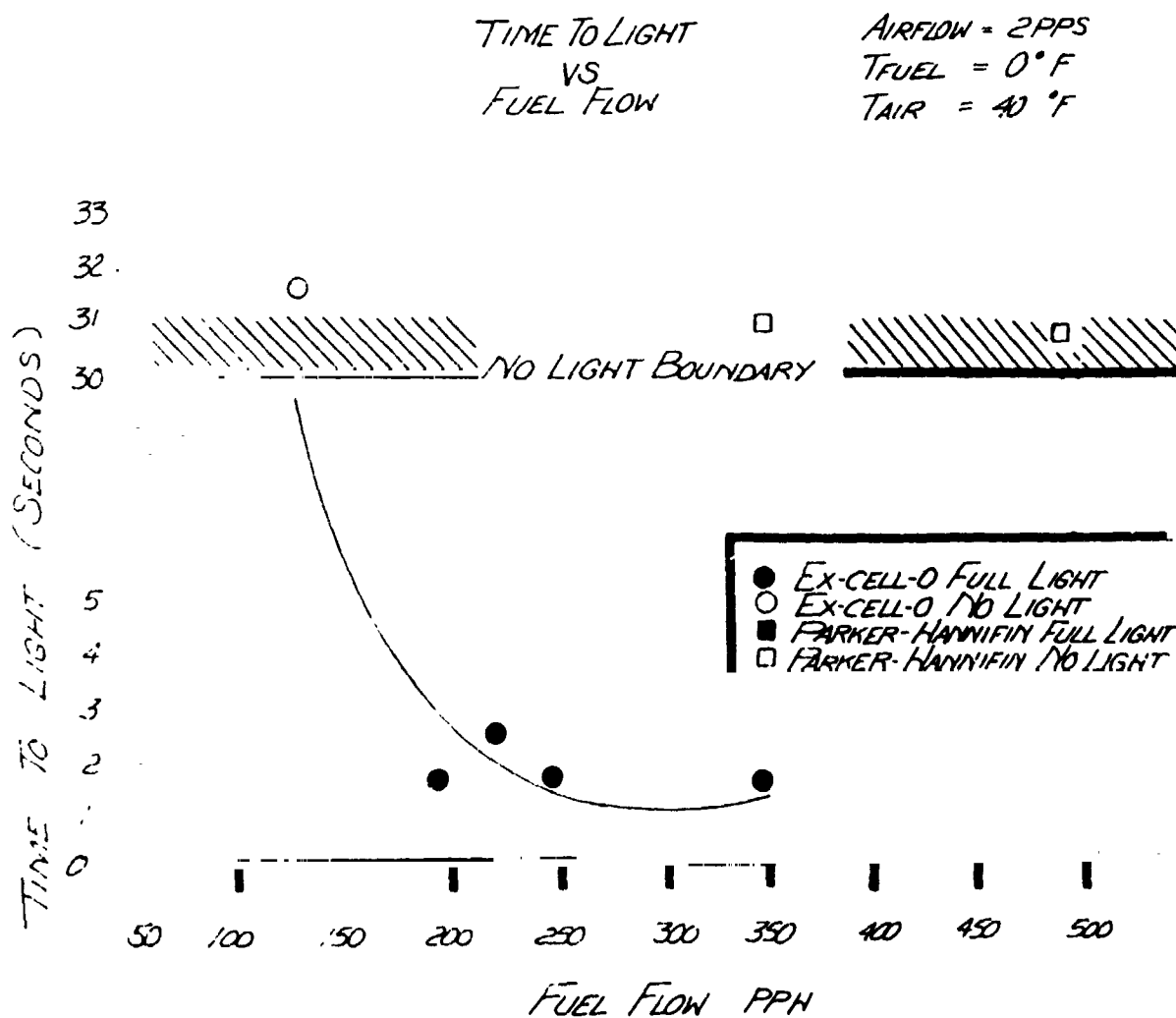


Figure 105 Sea Level Start Program



PRATT & WHITNEY AIRCRAFT GROUP
COMMERCIAL PRODUCTS DIVISION

3.2.7 High-Pressure Turbine

3.2.7.1 Overall Objective

Develop the technology to design a highly efficient single-stage high-pressure turbine. Fabricate and test a full-scale high-pressure turbine rig to substantiate the technology advancements selected for this component. The performance goal for this turbine is 88.2 percent cooled efficiency. Design goals are a combined cooling and leakage flow of 11.2 percent Wae and life of 10,000 hours on the blade and vanes and 20,000 hours on the disk. In addition, blade and vane coating goal life is 6,000 hours.

3.2.7.2 Component Program Overview

The overall task effort consists of a component effort and five supporting technology subtasks. The component effort is composed of the analysis and design of the high-pressure turbine component and a high-pressure turbine rig test program. The five supporting technology programs are (1) the leakage test program, (2) the supersonic cascade test program, (3) the cooling model test program, (4) the uncooled rig test program, and (5) the material fabrication program. Figure 106 shows the relationships between these activities and their relationship to contract Tasks 1, 3, and 4. The work plan schedule for the component effort is shown in Figure 107 and critical milestones are noted.

3.2.7.3 Component Effort

3.2.7.3.1 Objective

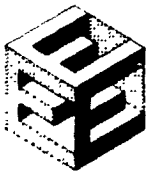
Conduct the design, analysis, hardware procurement and rig testing necessary to develop a full-scale high-pressure turbine that meets the established goals.

3.2.7.3.2 Scope of Total Work Planned

The analysis and design effort consists of a preliminary analysis and design phase and a detailed analysis and design phase. The rig program comprises the six sub-tasks shown in Figure 107.

A six-month preliminary design activity is conducted to establish the feasibility of the high-pressure turbine as proposed for the Flight Propulsion System, Task 1. The studied designs provide configuration definitions for the supporting technology programs. This preliminary activity results in layout drawings and substantiating design data, which are presented to NASA at a preliminary design review in September 1978.

Approximately two months after the preliminary design review, the detailed design work on the high-pressure turbine starts. Results available from the supporting technology programs are used to substantiate or improve the configurations established in the preliminary design. Significant supporting technology input is provided by results of the uncooled high-pressure turbine rig testing. The performance results from this rig allow selection of



PRATT & WHITNEY AIRCRAFT GROUP
COMMERCIAL PRODUCTS DIVISION

ORIGINAL
OF POOR QUALITY

HIGH-PRESSURE TURBINE PROGRAM LOGIC DIAGRAM

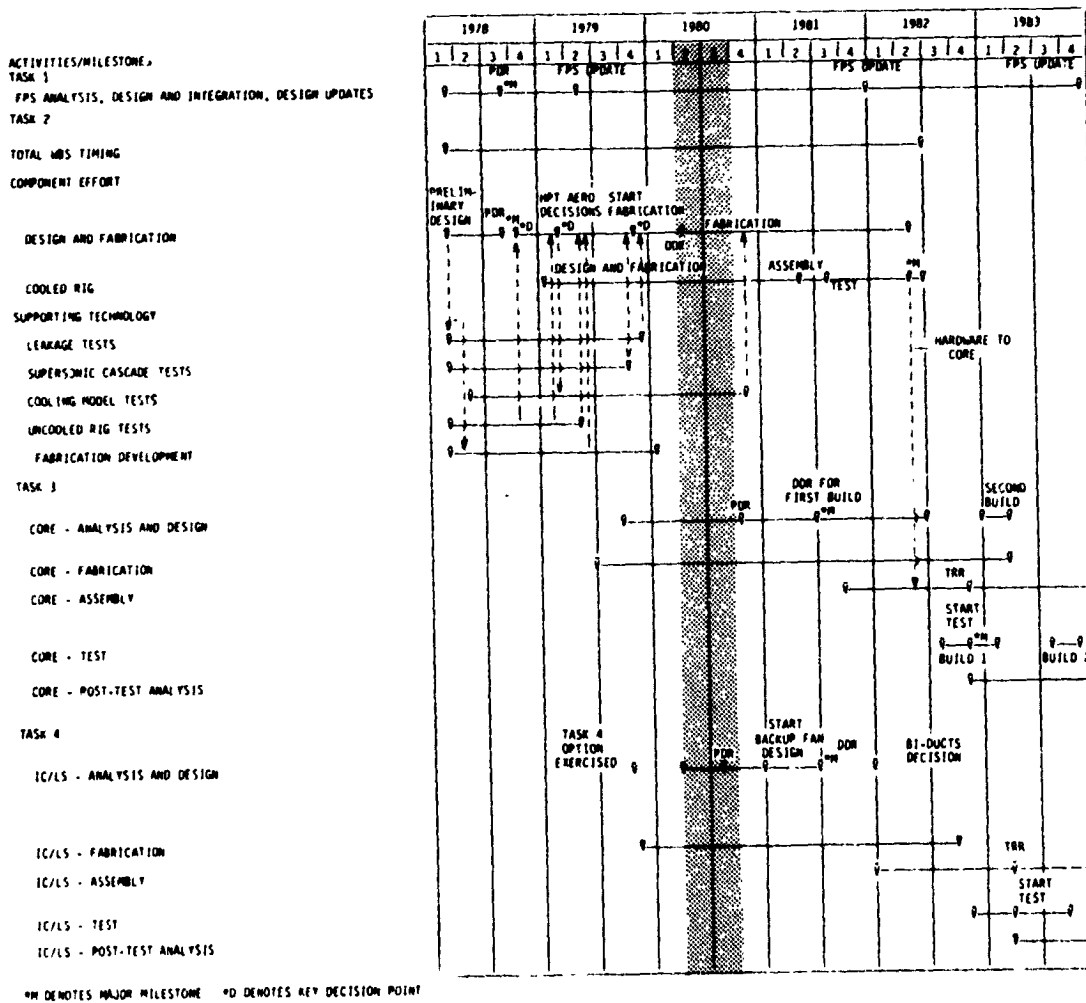


Figure 106 High-Pressure Turbine Program Logic Diagram



PRATT & WHITNEY AIRCRAFT GROUP
COMMERCIAL PRODUCTS DIVISION

ORIGINAL PAGE IS
OF POOR QUALITY

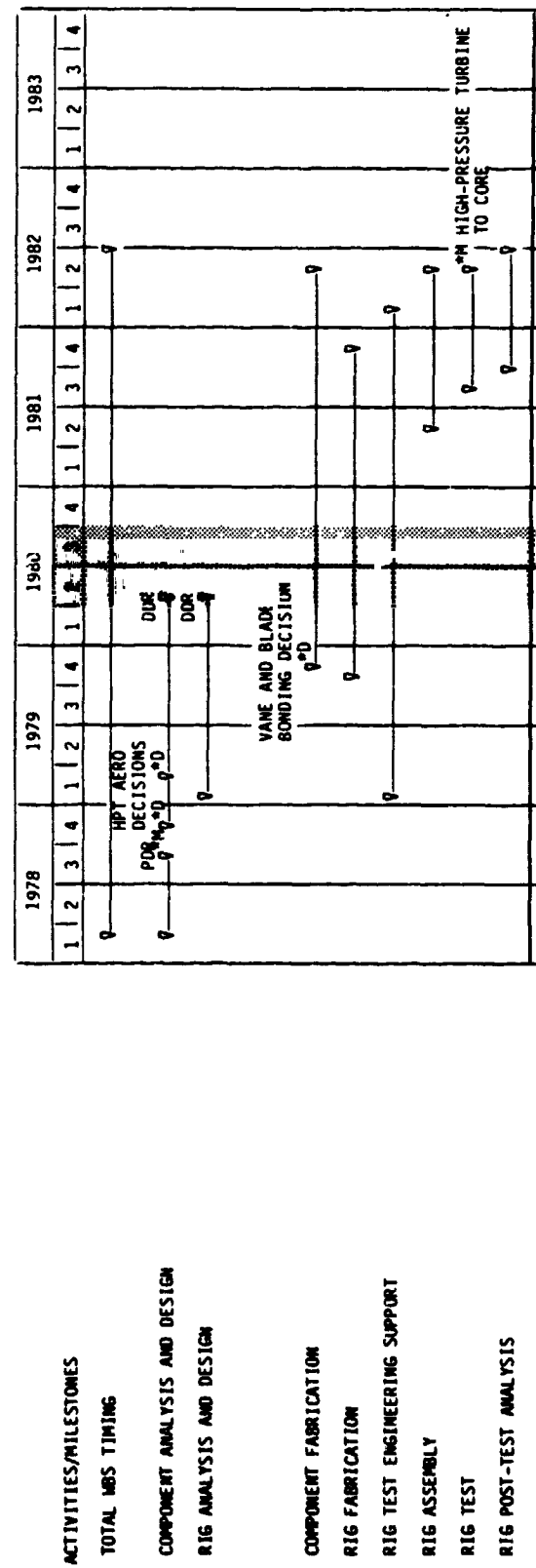
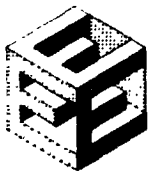


Figure 107 High-Pressure Turbine Component Effort Work Plan Schedule



PRATT & WHITNEY AIRCRAFT GROUP
COMMERCIAL PRODUCTS DIVISION

optimized single-stage aerodynamics. The results of the detailed design effort are completed layout drawings and substantiated design data that form the basis for a detailed design review to be conducted for NASA in May 1980. Detailed drawings are scheduled for completion approximately two months later. The design and analysis of parts peculiar to the test rig are conducted concurrently with the detailed design of the component. Fabrication of rig test parts begins in late 1979 as the designs of the rig parts are completed. Fabrication of the component hardware is not initiated until late in 1979, after the feasibility of the vane/blade casting process has been established.

The two-phase test program consists of an annular cascade test to determine the aerodynamic performance of the vanes and a full-stage test to assess design and off-design performance of the vanes and blades. The test phase of the program lasts approximately six months, starting in the third quarter of 1981. Testing must be completed by May 1982 to ensure that parts for the core engine are supplied in a timely manner.

During the current reporting period, NASA approval was received to conduct a test program to assess tangential on-board injection of high-pressure turbine cooling air in order to improve injection nozzle performance. This work is part of the component rig test effort, and testing is scheduled to start in December 1980 for a duration of 3 months.

3.2.7.3.3 Technical Progress

3.2.7.3.3.1 Summary of Work Previously Completed

The high-pressure turbine component design that evolved from preliminary design efforts and detailed design efforts is illustrated in Figure 108. Major features are noted. Its companion "warm" test rig is illustrated in Figure 109. The present component design represents a number of changes relative to the original preliminary design. The major changes are summarized as follows.

- (1) The high-pressure compressor discharge seal was changed from the rough abrasive wide channel seal to a nine-knife-edge configuration because of the more promising performance benefits of the knife edge configuration.
- (2) The internal cooling configuration of the blade was modified to improve life and to provide the required cooling flow..
- (3) The blade root attachment was changed from a 4- to a 5-tooth design to reduce fillet stresses.
- (4) The aerodynamic design was revised to accommodate (a) integrated core/low spool requirements for torque, airflow, speed, and cooling air leakage rather than designing directly to flight propulsion system requirements, and (b) the 12-percent down-sizing of the engine.



PRATT & WHITNEY AIRCRAFT GROUP
COMMERCIAL PRODUCTS DIVISION

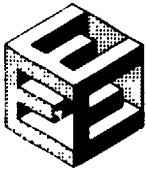
- (5) Selected a 43-percent reaction turbine with radial (non-tilted) vanes using airfoils of the type tested in build 2 of the uncooled rig because of their demonstrated potential for higher turbine efficiency.
- (6) Changed from a 4-piece feather seal configuration in the vane outer platform to a 2-piece configuration to reduce leakage.
- (7) To accommodate thrust balance changes, added a low-pressure turbine front seal, added a seal at the rear of the high-pressure turbine disk, decreased the diameter of the high-pressure compressor discharge seal, and canted the hot strut 15 degrees rearward.
- (8) Changed to a boltless disk sideplate design because of unacceptable stresses (bolt and bolthole) in the bolted design.
- (9) Added a vortex plate to the disk near the TOBI nozzle exit to increase blade cooling air supply pressure.
- (10) Changed the ceramic outer air seal design from a constrained concept to an unconstrained concept.
- (11) Selected carbon seals for the No. 4 bearing seal, No. 5 bearing seal, and intershaft seal.

The major aerodynamic parameters of the high-pressure turbine remained unchanged and are shown in Table 63. Current performance parameters at significant engine operating conditions are listed in Table 64.

TABLE 63

HIGH-PRESSURE TURBINE AERODYNAMIC DESIGN SUMMARY

No. of Stages	1
Expansion Ratio	4.0
Mean Velocity Ratio/NASA Load Coefficient	0.56/1.59
An ² - Maximum	49 x 10 ⁹ in. ² -rpm ²
Rim Speed - Maximum	1730 ft/sec
ΔH, BTU/lb - SLTO	208
Mean Blade Loading (Y)	0.92
Mean Blade Turning	118 deg.
Mean Reaction Level	0.43
Number of Blades	54
Number of Vanes	24



PRATT & WHITNEY AIRCRAFT GROUP
COMMERCIAL PRODUCTS DIVISION

ORIGINAL PAGE IS
OF POOR QUALITY

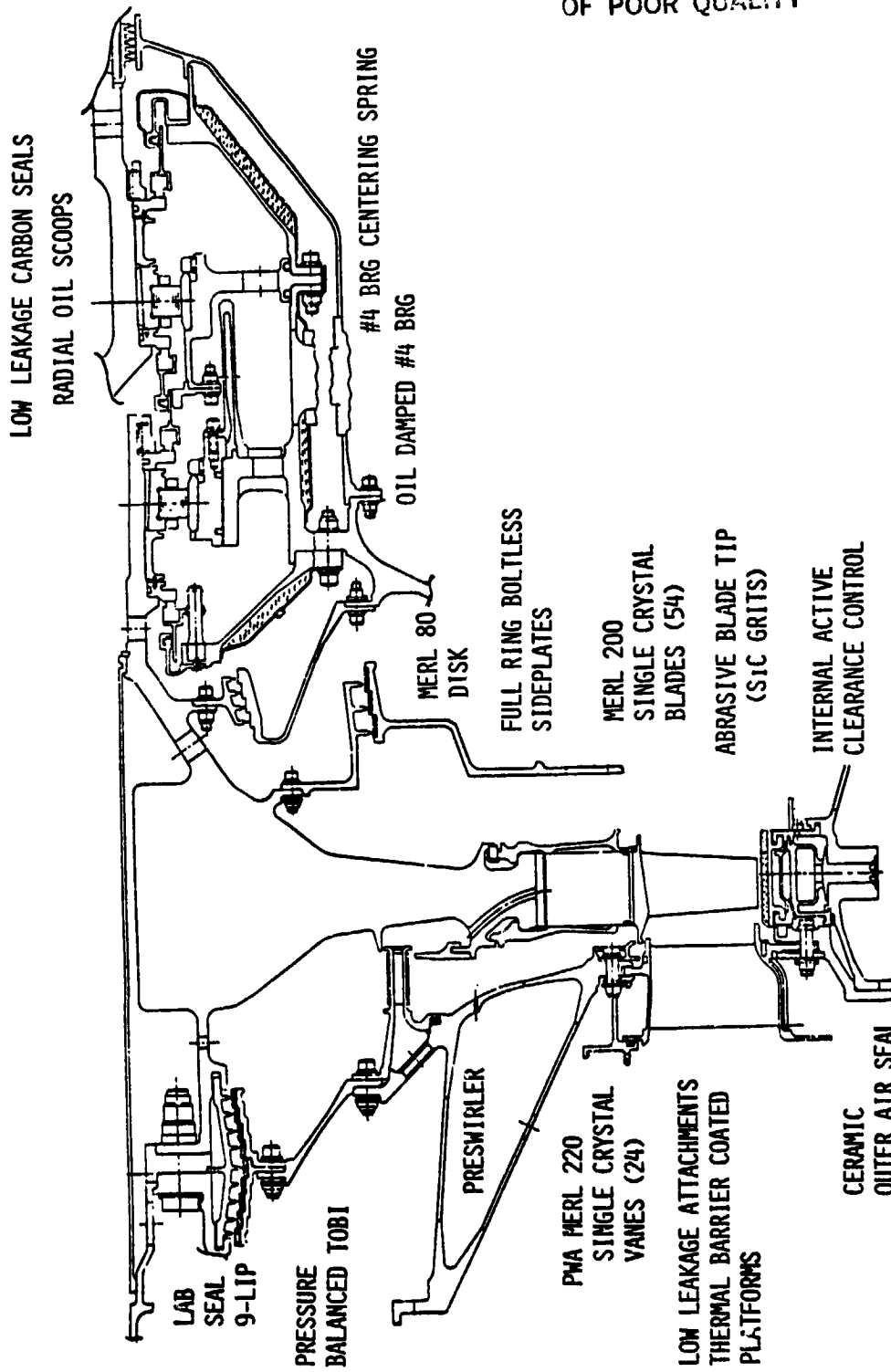
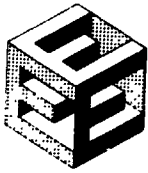


Figure 108 High-Pressure Turbine Component



PRATT & WHITNEY AIRCRAFT GROUP
COMMERCIAL PRODUCTS DIVISION

ORIGINAL PAGE 12
OF POOR QUALITY

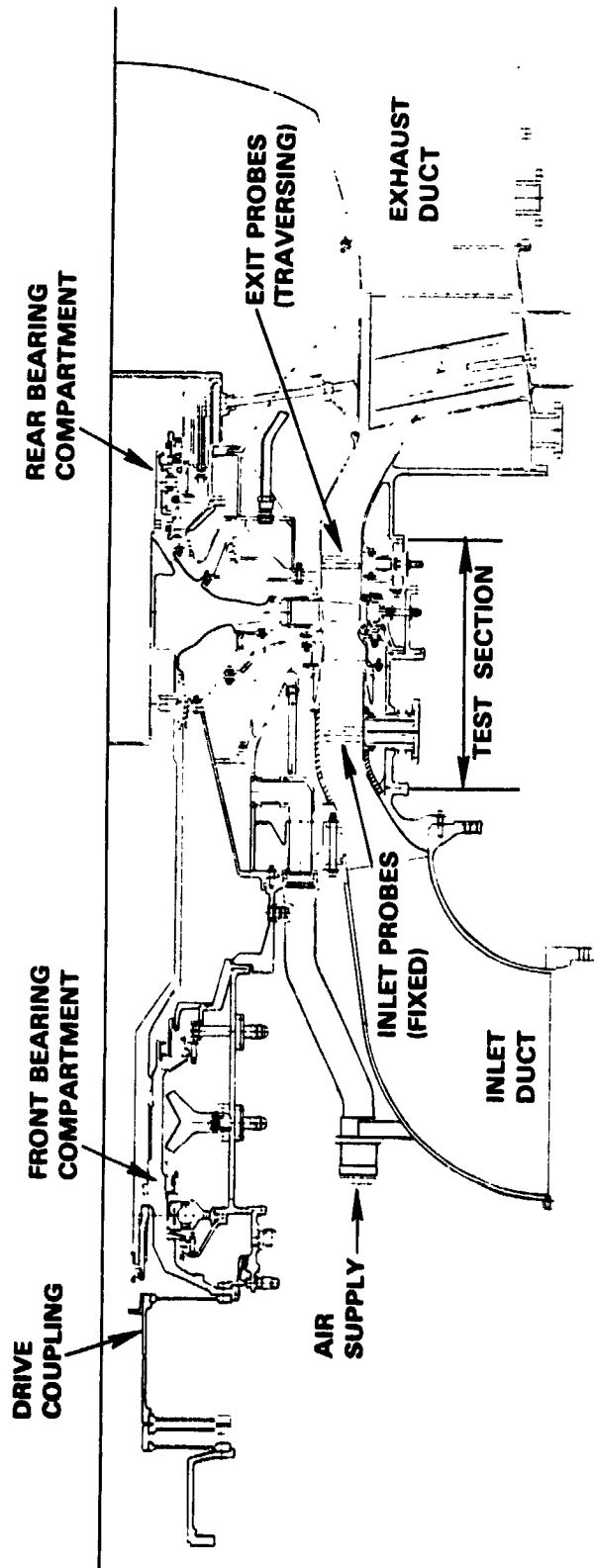


Figure 109 High-Pressure Turbine "Warm" Test Rig

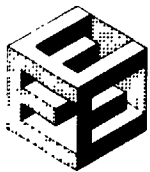


TABLE 64

HIGH-PRESSURE TURBINE CURRENT PERFORMANCE
PARAMETERS AT SIGNIFICANT ENGINE OPERATING CONDITIONS

	<u>Aero. Des. Point</u>	<u>Maximum Cruise</u>	<u>Maximum Climb</u>	<u>Takeoff</u>
Inlet Flow Parameter ($\text{lb}_m \sqrt{\text{OR}}$)($\text{in.}^2/\text{sec}$)(lb_f)	16.70	16.70	16.70	16.70
Rotor Inlet Temperature (F)	2230	2195	2395	2485
Pressure Ratio	4.02	4.02	4.00	4.02
Adiabatic Efficiency (percent)	88.7	88.7	88.7	88.8
Enthalpy Change (BTU/lb)	192.9	190.3	204.2	211.9
Transition Section Pressure Loss (percent)	1.50	1.50	1.49	1.50
Total Cooling Airflow (%) Core Airflow)	14.09	14.09	14.09	14.09

The work on the hot strut case, including the transition duct and fairing, has been divided between the high- and low-pressure turbine component efforts. Layout design work has been assigned to the high-pressure turbine, and drafting work and detailed design review preparation has been assigned to the low-pressure turbine.

A modification to the structural strut and the hot strut fairing surrounding it was completed. This modification was performed because of the structural requirement to cant the strut by 15 degrees in order to accommodate the 25,000 lb rearward pressure load on the hot strut case. In addition, a first stage blade vibratory analysis indicated the need to reduce the number of struts. The differences from the design established for the preliminary design review are: (1) increased annulus area ratio; (2) increased duct length; (3) working struts (fairings), 5 degrees of turning; (4) tilted fairings to fit around the tilted structural struts; (5) number of struts decreased from 14 to 11, to avoid a 14E resonance on the first turbine blade; and (6) increased axial fairing length at the tip. These changes are summarized in Table 65 and illustrated in Figure 110.

The aerodynamic details for four sections from inner to outer diameter for the revised strut are shown in Table 66. With these changes the duct performance is expected to meet the design goal pressure loss, $\Delta \text{Pt}/\text{Pt}$ of 1.5 percent.



PRATT & WHITNEY AIRCRAFT GROUP
COMMERCIAL PRODUCTS DIVISION

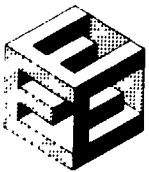
Material selection for fabricating the parts for the hot strut fairing was limited by the high temperatures in the strut environment. Cast alloys, such as the high-cobalt MAR M 509, were the best candidates. The mechanical configuration most practical in terms of fabrication was an 11-segment design. This configuration features fairings with integral inner and outer platforms similar to conventional turbine vane castings. Thick section feather seals are used to seal the circumferential gaps between platforms.

The high-pressure turbine component rig (shown in Figure 109) uses as many existing rig parts as possible to adapt to the Energy Efficient Engine design, thereby minimizing cost. The task of designing new rig parts was thereby reduced to 6 main areas: (1) a front thrust bearing and seal compartment, (2) a drive shaft and coupling stub shaft, (3) an inlet flow adapting duct, (4) an exit flow adapting duct, (5) an active clearance control case, and (6) instrumentation probes and a traversing ring.

The secondary flow system provides rig flows that duplicate all integrated core/low spool design cooling air and leakage flows and pressures associated with the high-pressure turbine flowpath. Flow rates will be determined by at least one of the following methods: (1) direct measurement through calibrated venturi tubes, (2) addition or subtraction of measured flow rates, and (3) static pressure probe measurements coupled with cold flow data of all key hardware. Separate flow controls will be provided for cooling air to the primary and secondary tangential on-board injection.

TABLE 65
TRANSITION DUCT
GEOMETRY COMPARISON

<u>Duct</u>	<u>Prelim. Des. Rev.</u>	<u>Modification</u>
Length (in.)	8.2 (7.7 SCALED)	7.8
L/H	3.0	3.0
Ann. Area Ratio	1.50	1.57
Eff. Area Ratio	1.26	1.42
<u>Strut</u>	<u>Non-working</u>	<u>Working</u>
No. of Foils	14	11
Type	65C/A	400
a *2 - a ₂ FREE VORTEX	0 Degree	5 Degrees



PRATT & WHITNEY AIRCRAFT GROUP
COMMERCIAL PRODUCTS DIVISION

TABLE 66

MODIFIED HOT STRUT

<u>SECTION</u>	<u>L.E. Root</u>	<u>T.E. Root</u>	<u>L.E. Tip</u>	<u>T.E. Tip</u>
Airfoil Type (series)	400	400	400	400
Axial Chord (in.)	4.32	4.43	4.53	4.64
Actual Chord (in.)	8.03	6.81	6.14	5.88
Max. Thickness (in.)	1.0	1.0	1.0	2.0

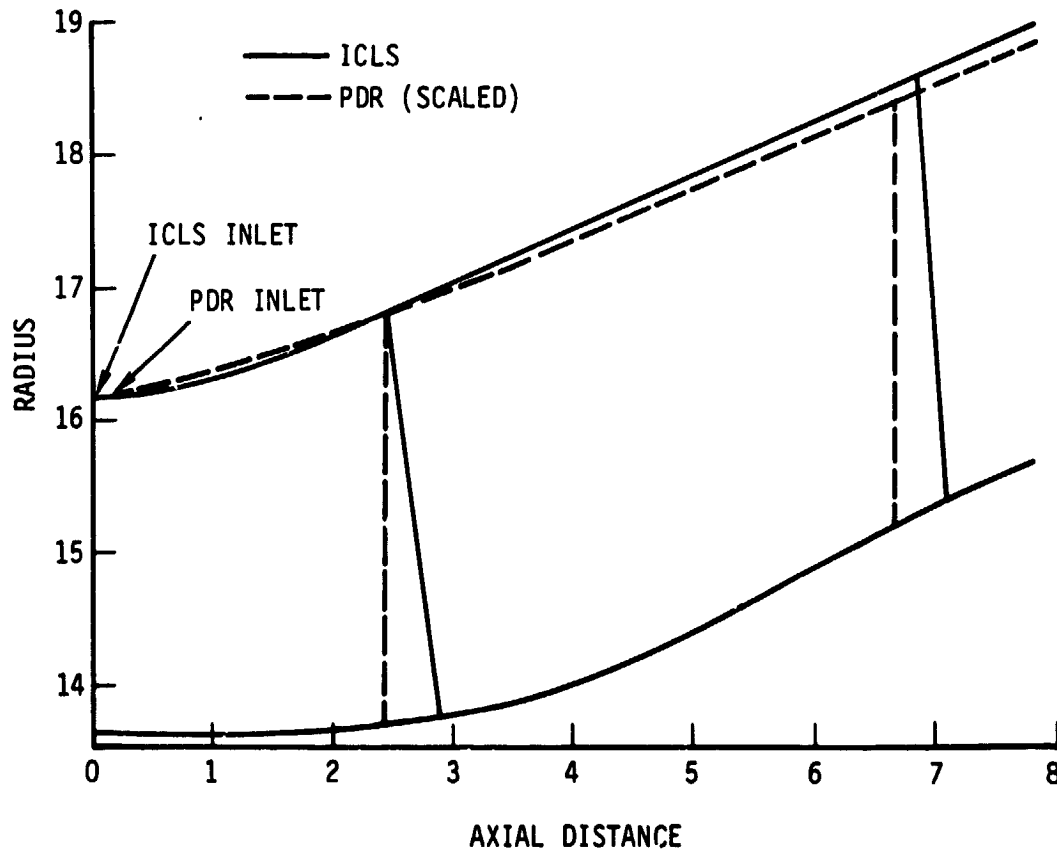
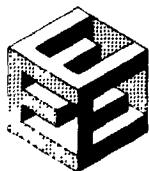


Figure 110 High-Pressure Turbine Transition Duct



PRATT & WHITNEY AIRCRAFT GROUP
COMMERCIAL PRODUCTS DIVISION

3.2.7.3.3.2 Current Technical Progress

All of the analysis and design efforts associated with the high-pressure turbine component and rig were completed during the current reporting period, and a detailed design review was held at NASA-LERC on May 21 and 22, 1980. NASA approved this design on 11 June 1980. Additional work during this reporting period included the layout design and thermal/structural analysis on the hot strut case assembly.

The performance of the high-pressure turbine is compared to the goal performance estimates in Table 67. The performance is unchanged from that reported in the Fourth Semiannual Status Report. The goal efficiency levels are exceeded for both the flight propulsion system and the integrated core/low spool because the actual design tip clearance is less than the previously established value.

TABLE 67

HIGH-PRESSURE TURBINE PERFORMANCE VS. GOALS

	Goal		Current Status	
	FPS	IC/LS TEST	FPS	IC/LS
Efficiency (percent)	88.2	86.7	88.7	87.3

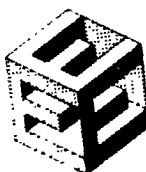
HIGH-PRESSURE TURBINE AERODYNAMIC DESIGN

High-Pressure Turbine Flowpath

The flowpath selected for the high-pressure turbine component is shown in Figure 111. This flowpath features an S-wall first stage vane, and a highly tapered blade with a conical inner diameter. Blade taper is selected to accommodate stress requirements. The design gas triangles (shown in Table 68) are similar to those used in build 2 of the uncooled rotating rig (i.e., 43 percent stage reaction level).

Airfoil Design

The final vane mean section airfoil contour and loading diagrams are shown in Figure 112, and a stacked view of the vane is shown in Figure 113. The final design blade mean section contour and loading diagram are shown in Figure 114, and a stacked view of the blade is shown in Figure 115.



PRATT & WHITNEY AIRCRAFT GROUP
COMMERCIAL PRODUCTS DIVISION

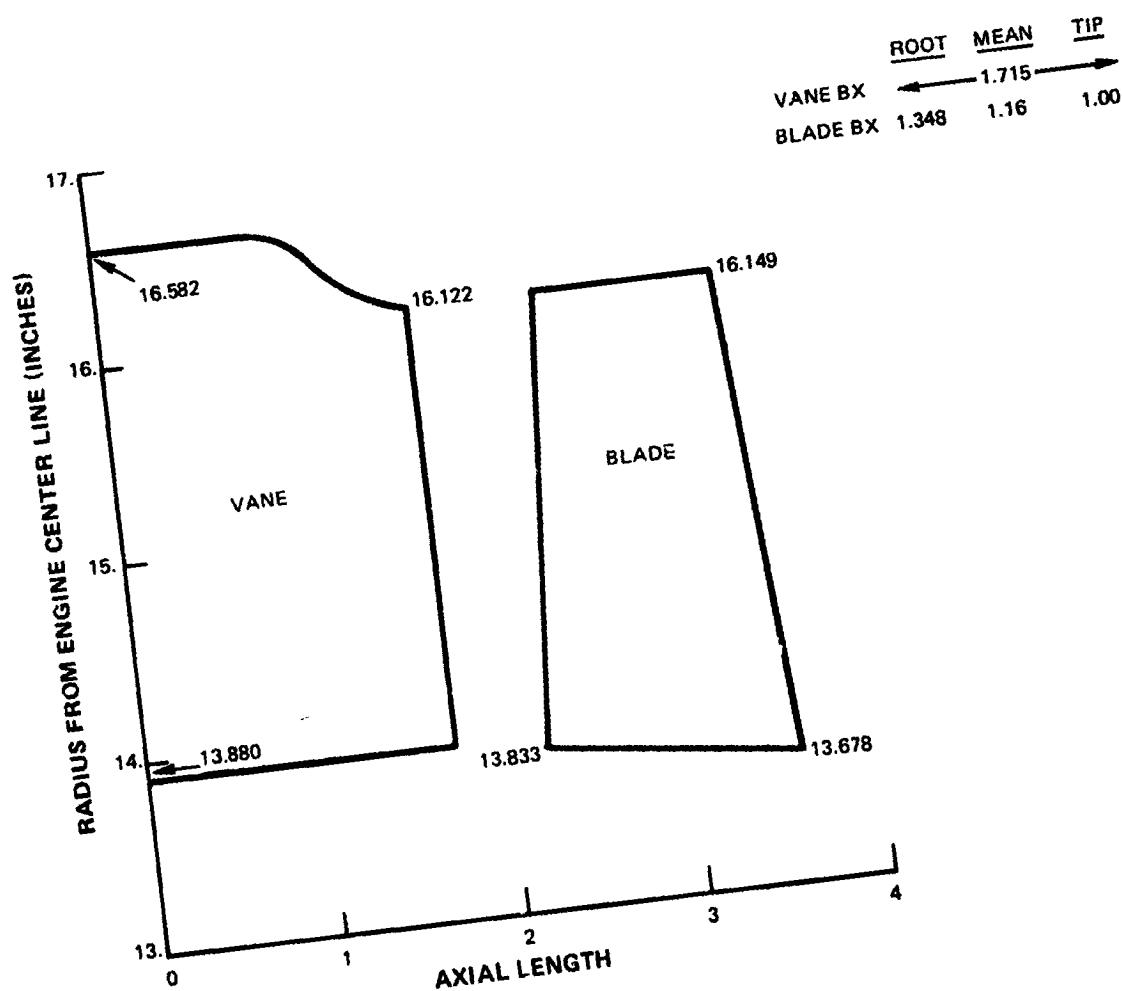


Figure 111 High-Pressure Turbine Component Flowpath



PRATT & WHITNEY AIRCRAFT GROUP
COMMERCIAL PRODUCTS DIVISION

TABLE 68
GAS TRIANGLES

<u>VANE</u>	<u>ROOT</u>	<u>MEAN</u>	<u>TIP</u>
α In	90°	90°	90°
α Out	11.6°	10.3°	9.1°
M In	0.09	0.08	0.07
M Out	1.0	0.92	0.85
θ Gas	78.4°	79.7°	80.4°
<u>BLADE</u>			
β In	33.5°	42.7°	63.6°
β Out	15.9°	16.9°	17.7°
Mr In	0.36	0.25	0.14
Mr Out	1.22	1.24	1.28
θ Gas	130.6°	120.4°	98.7°
α Out	38.0°	43.8°	48.4°
M Out	0.54	0.52	0.52

To account for engine effects not encountered in the rig environment (i.e., combustor exit temperature profiles, cooling and leakage air), the leading edge angle of the blade was altered from that tested in the uncooled rigs. The root and tip sections are undercambered 5 degrees and 10 degrees, respectively, and the mean section is overcambered 8 degrees.

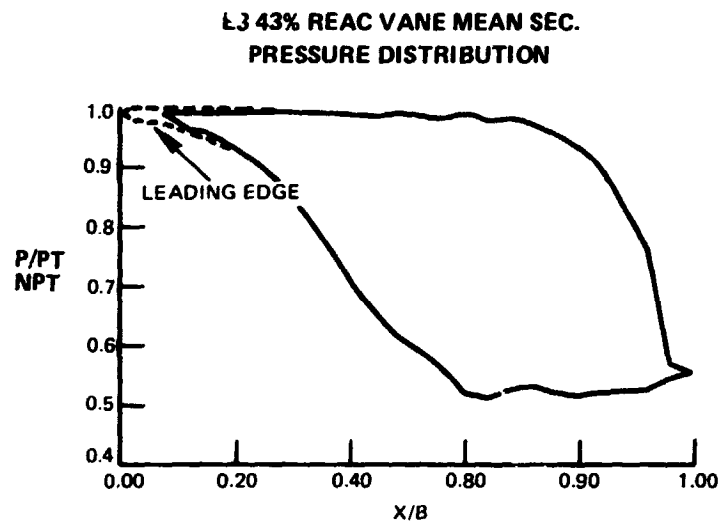
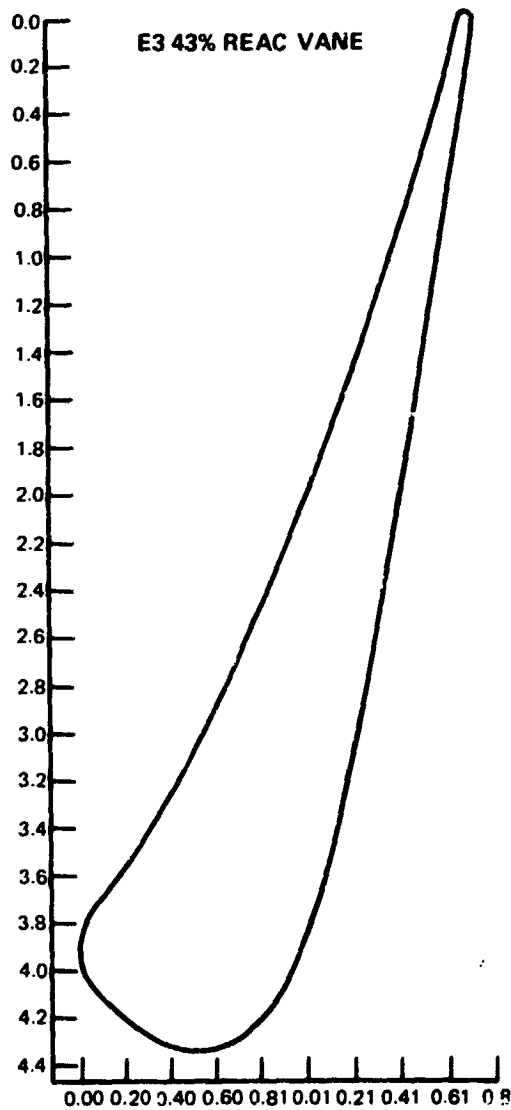
High- and Low-Pressure Turbine Matching

The aerodynamic design of the high-pressure turbine component deviates from integrated core/low spool cycle data as shown in Table 69. The component design assumed a higher efficiency (87.9 percent versus 86.7 percent for the integrated core/low spool table), resulting in a decrease in the expansion ratio for the high-pressure turbine (3.99 versus 4.08). In addition, the high-pressure turbine exit corrected flow is lower than the pure integrated core/low spool data (66.562 versus 68.165).



PRATT & WHITNEY AIRCRAFT GROUP
COMMERCIAL PRODUCTS DIVISION

ORIGINAL PAGE IS
OF POOR QUALITY



RADIUS	15.001"
# FOILS	24
AXIAL CHORD	1.715
L.E. DIAMETER	0.525
T.E. DIAMETER	0.064
UNCOVERED TURNING	9.0
EXIT WEDGE ANGLE	4.0

Figure 112 Final Vane Mean Section Airfoil Contour and Loading Diagrams



PRATT & WHITNEY AIRCRAFT GROUP
COMMERCIAL PRODUCTS DIVISION

ORIGINAL PAGE IS
OF POOR QUALITY

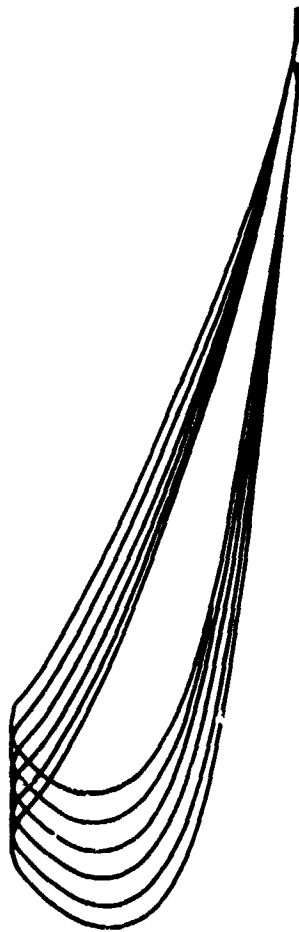


Figure 113 High-Pressure Turbine Vane - Stacked view



PRATT & WHITNEY AIRCRAFT GROUP
COMMERCIAL PRODUCTS DIVISION

ORIGINAL PRICE IS
OF POOR QUALITY

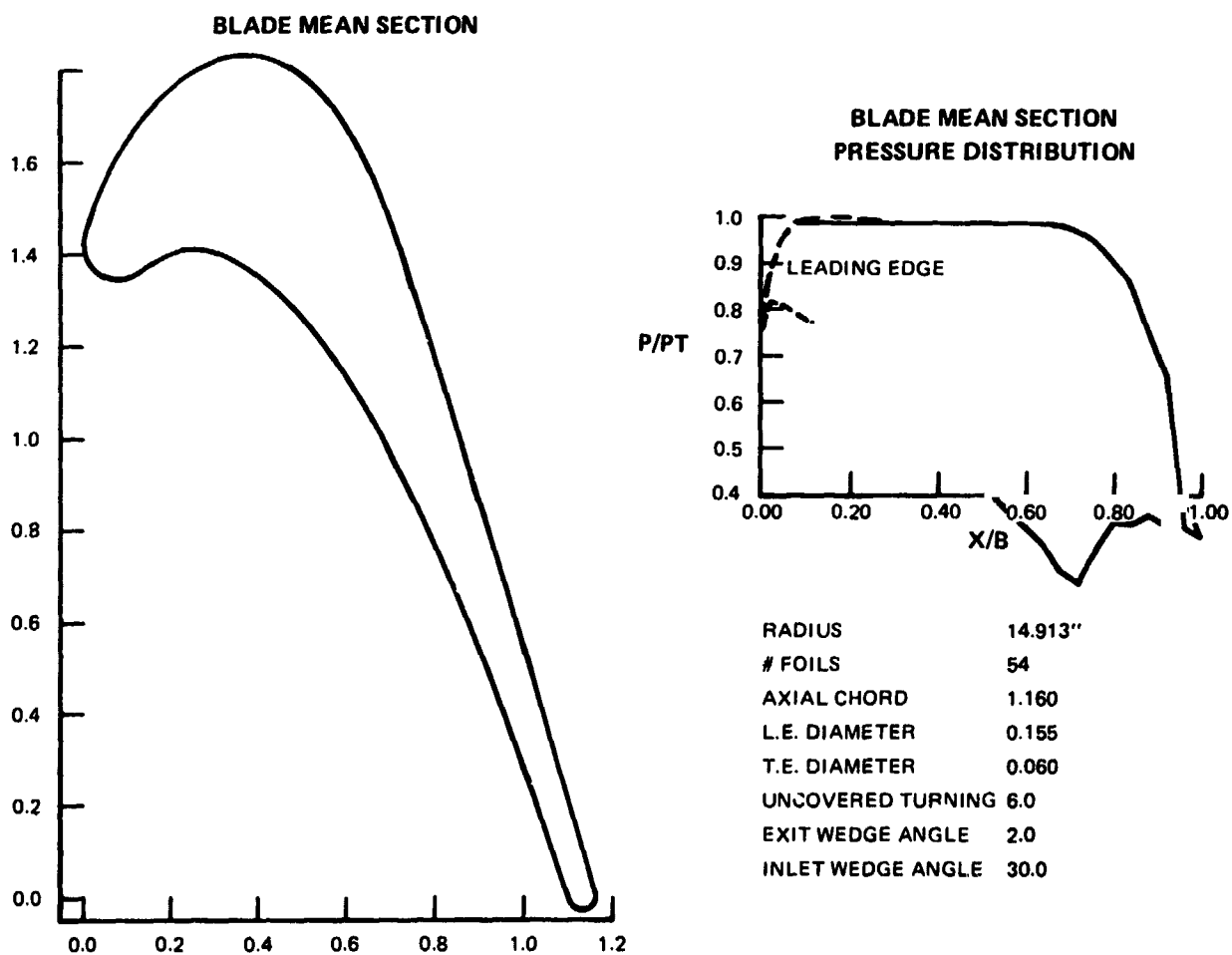


Figure 114 Final Design Blade Mean Section Contour and Loading Diagram



PRATT & WHITNEY AIRCRAFT GROUP
COMMERCIAL PRODUCTS DIVISION

ORIGINAL FILED IN
OF POOR QUALITY

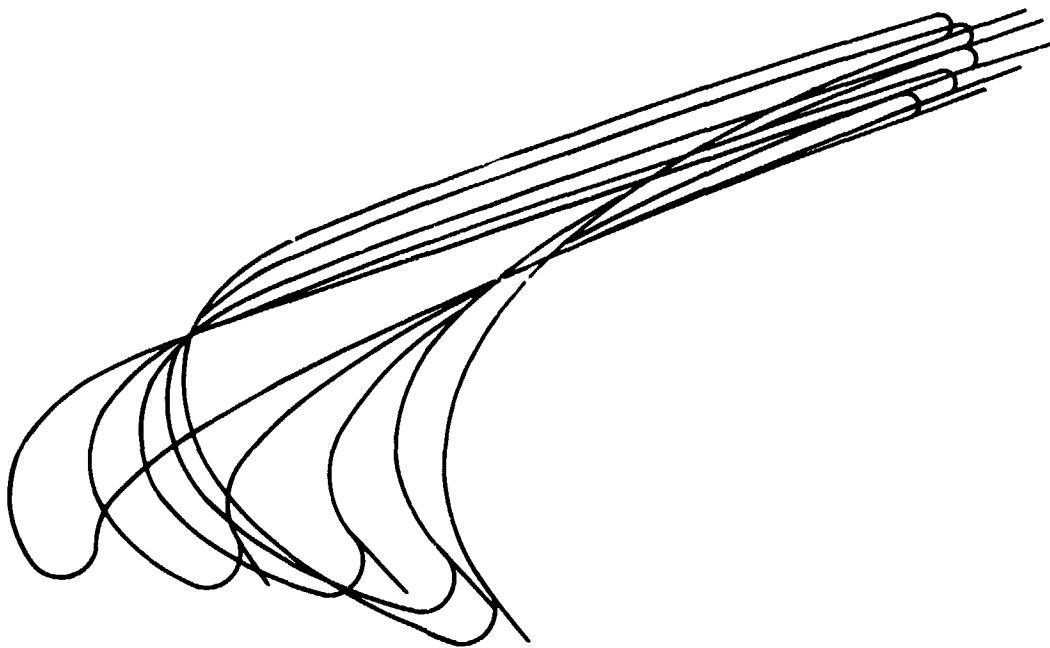


Figure 115 High-Pressure Turbine Blade - Stacked view



TABLE 69

HIGH- AND LOW-PRESSURE TURBINE MATCHING

	<u>INITIAL HPT DESIGN</u>	<u>ICLS DESIGN TABLE</u>	<u>LPT DESIGN</u>
η HPT	87.9%	86.7%	
N (RPM)	13178.	13178.	
ΔH (btu/sec)	13383.	13383.	
FPin	16.983	16.983	
PR hpt	3.99	4.08	
FP out	66.562	68.165	68.165

The low-pressure turbine, however, is being designed to the integrated core/low spool design table. It assumes that the corrected flow out of the high-pressure turbine is 68.165.

Since the low-pressure turbine sets the match, the high turbine will in actuality operate, off-design, at the 68.165 corrected flow. Table 70 summarizes the aerodynamic impact of the high turbine operating this way. Column 2 of Table 70 shows the resulting penalty in high-pressure turbine efficiency, and the increase in Mach number and swirl entering the low-pressure turbine. As indicated by the pronounced decrease in airfoil convergence, the aerodynamic environment of the first stage of the low-pressure turbine has been compromised.

To alleviate these undesirable effects, the high-pressure turbine blade has been restaggered open 0.25 degrees. As shown in column 3 of Table 70, the high-pressure turbine efficiency debit is cut in half, and nominal low-pressure turbine aerodynamics are re-established.

High-Pressure Turbine Efficiency Status

The anticipated efficiency of the high-pressure turbine component is presented in Table 71. The efficiency estimates shown in the table are based on the demonstrated performance of the second build of the uncooled rig, with increments for cooling effects derived from other supporting technology programs.



PRATT & WHITNEY AIRCRAFT GROUP
COMMERCIAL PRODUCTS DIVISION

TABLE 70

LOW-PRESSURE TURBINE SETS HIGH-PRESSURE TURBINE MATCH

	HPT AS DESIGNED (INITIAL ICLS)	HPT RUN AT LPT F.P.	RESTAGGERED HPT RUN at LPT F.P. (FINAL ICLS)
FPhpt In	16.983	16.983	17.023
FPhpt Out	66.562	68.165	68.165
Pr hpt	3.98	4.093	4.084
REACTION hpt	43.0%	43.8%	42.4%
$\Delta \eta$ hpt	Base	0 -0.3%	0 -0.15%
Mn hpt Out	0.523	0.554	0.539
α hpt Out	43.8°	43.0°	44.0°
CONVERG LPT			
Vl root	1.4	1.35	1.4
Bl root	1.3	1.25	1.3

- CONCLUSION

Restagger +.25 degrees to get back $\Delta \eta$ HPT, bearing load (i.e., reaction), and LPT aerodynamics

TABLE 71

HIGH-PRESSURE TURBINE STATUS EFFICIENCY

	<u>FPS</u>	<u>IC/LS</u>
Status cooling flow (percent Wae)	14.09	14.55
Status cooling loss (percent)	-3.7	-3.8
Trailing edge discharge effect on base pressure (percent)	+1.1	+1.1
Off-design effects (percent)	0	-0.1
Status efficiency at 0.0185 clr (percent)	88.3	88.1
Goal efficiency (percent)	88.2	87.9

Other Efficiency Contributions:

Uncooled Rig (build 2) - 91.1 percent
Coating - -0.2 percent



DURABILITY ANALYSIS

Vane and blade cooling schemes and durability features are presented in the following subsections.

Vane Cooling

The final cooling design of the vane is shown in Figure 116. The vane is film-cooled by shower head cooling holes at the leading edge, 2 sets of two rows of cooling holes on the pressure side, and 3 rows of cooling holes on the suction side. Impingement cooling of the core is accomplished by 3 sheet metal impingement tubes (see Figure 116). The trailing edge area is convectively cooled by an array of pedestals or braces between vane walls. Cooling air passes around these pedestals and is discharged through trailing edge slots. The total amount of cooling flow is 6.41 percent W_{ae} .

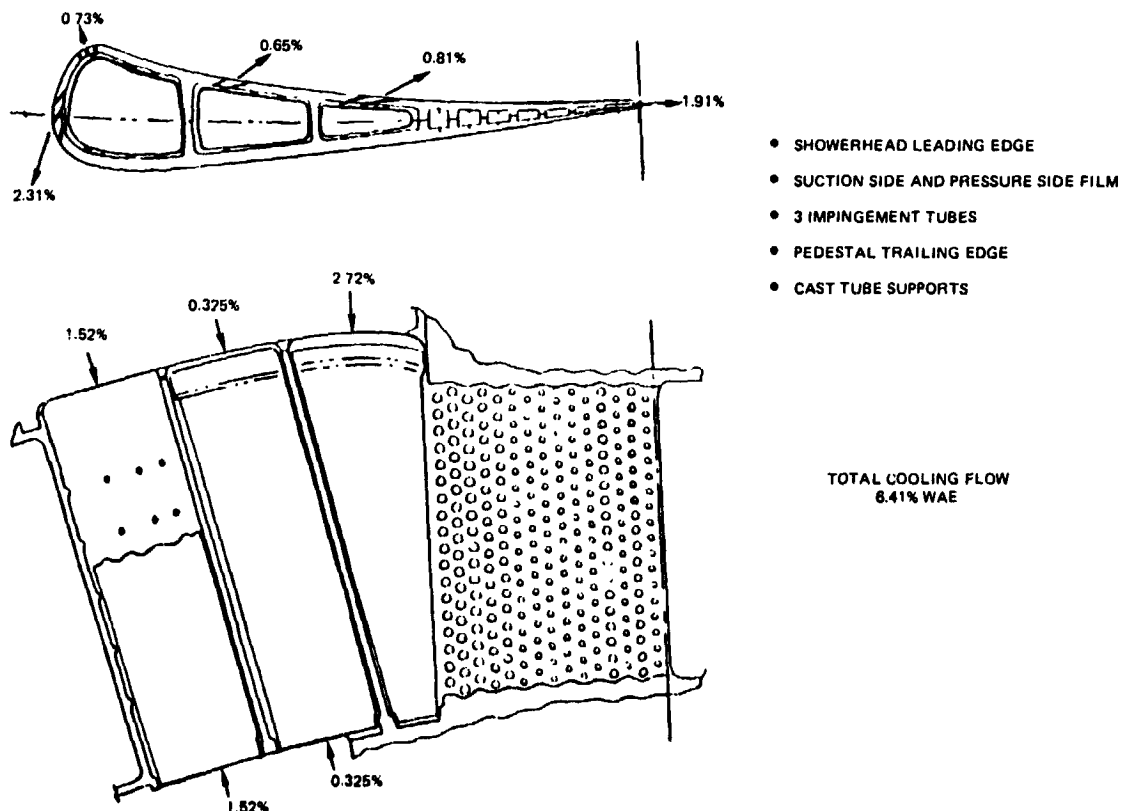


Figure 116 Vane Final Cooling Design



PRATT & WHITNEY AIRCRAFT GROUP
COMMERCIAL PRODUCTS DIVISION

Vane materials and coatings for the flight propulsion system and integrated core/low spool were selected (see Table 72). The combustor exit temperature profile used in the design of the vane (Figure 117) assumes a pattern factor of 0.42. The hottest area of the vane (2239 F) on is the suction side wall adjacent to the 3rd cavity (see Figure 118).

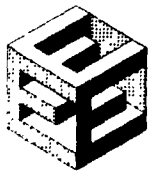
TABLE 72
VANE MATERIALS AND COATINGS

	<u>FPS</u>	<u>IC/LS</u>
Base Alloy	Merl 200 (adv. single crystal)	PWA 1480 (single crystal)
External Coating	Merl 700 (adv. overlay)	PWA 270 (NiCoCrAly)
Internal Coating	PWA 275 (aluminide)	None
Platform Coating	Merl 760 (adv. thermal barrier coating)	Merl 750 (Thermal barrier coating)

The vane inner and outer diameter platform cooling hole arrangement and cooling flow distribution is shown on Figures 119 and 120. An impingement cooling scheme is featured for that portion of the platform adjacent to the vane pressure side. Cooling holes are incorporated on the side rails and aft rail. Thermal barrier coating is applied to the gas path side of both platforms, thereby holding estimated metal surface temperatures to approximately 2100 F.

Vane Durability

The results of an evaluation of vane transient operation strains indicated that the leading edge area of the vane experienced the greatest total strain range (0.7 percent). Strain ranges for other areas of the vane are shown in Figure 121.



PRATT & WHITNEY AIRCRAFT GROUP
COMMERCIAL PRODUCTS DIVISION

ORIGINAL PAGE IS
OF POOR QUALITY

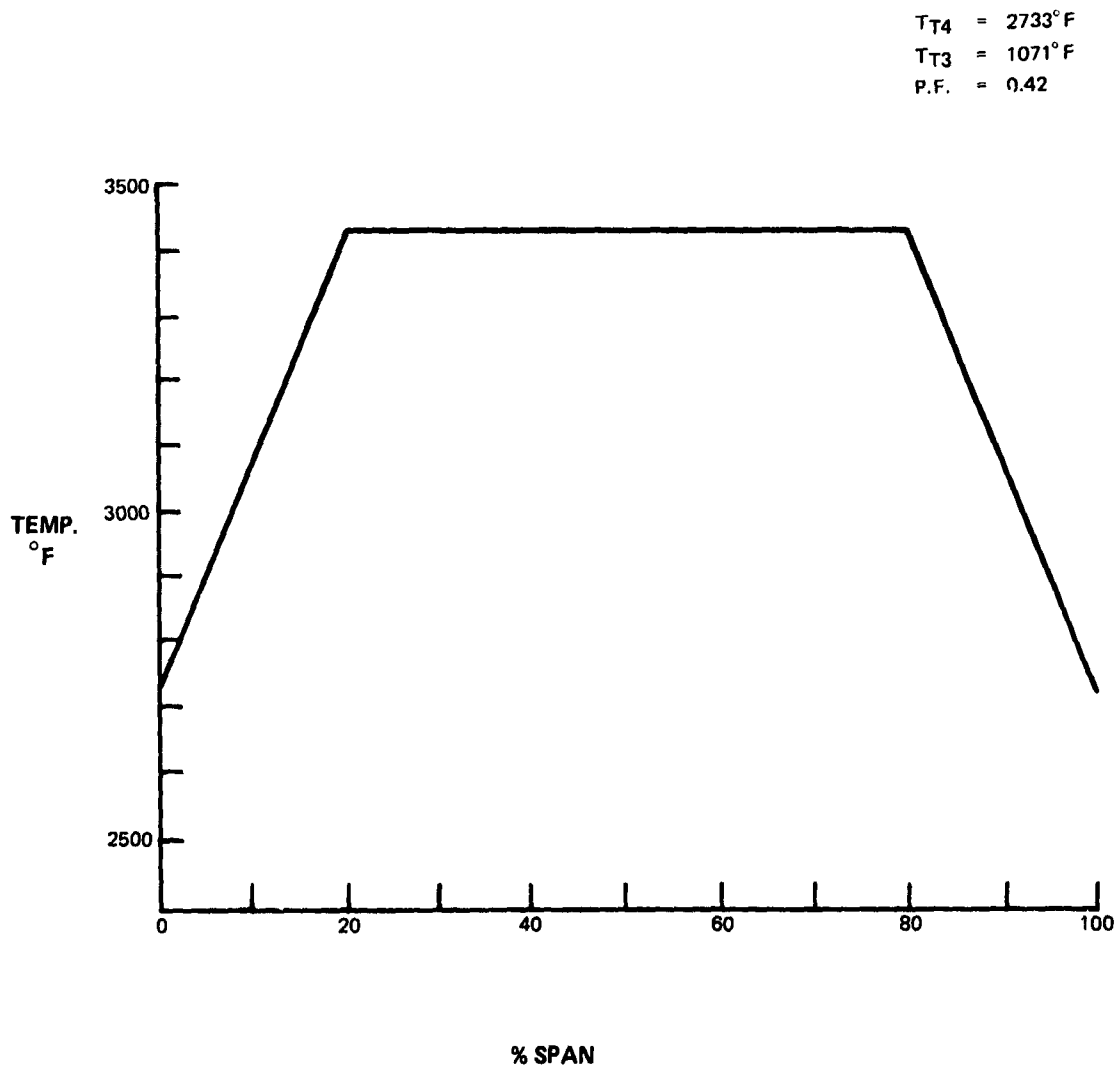


Figure 117 Combustor Exit Temperature Profile Used in Vane Design



Figure 118 Vane Metal Temperature Distribution



PRATT & WHITNEY AIRCRAFT GROUP
COMMERCIAL PRODUCTS DIVISION

ORIGINAL PAGE 12
OF POOR QUALITY

VANE O.D. PLATFORM COOLING FLOW 0.49%

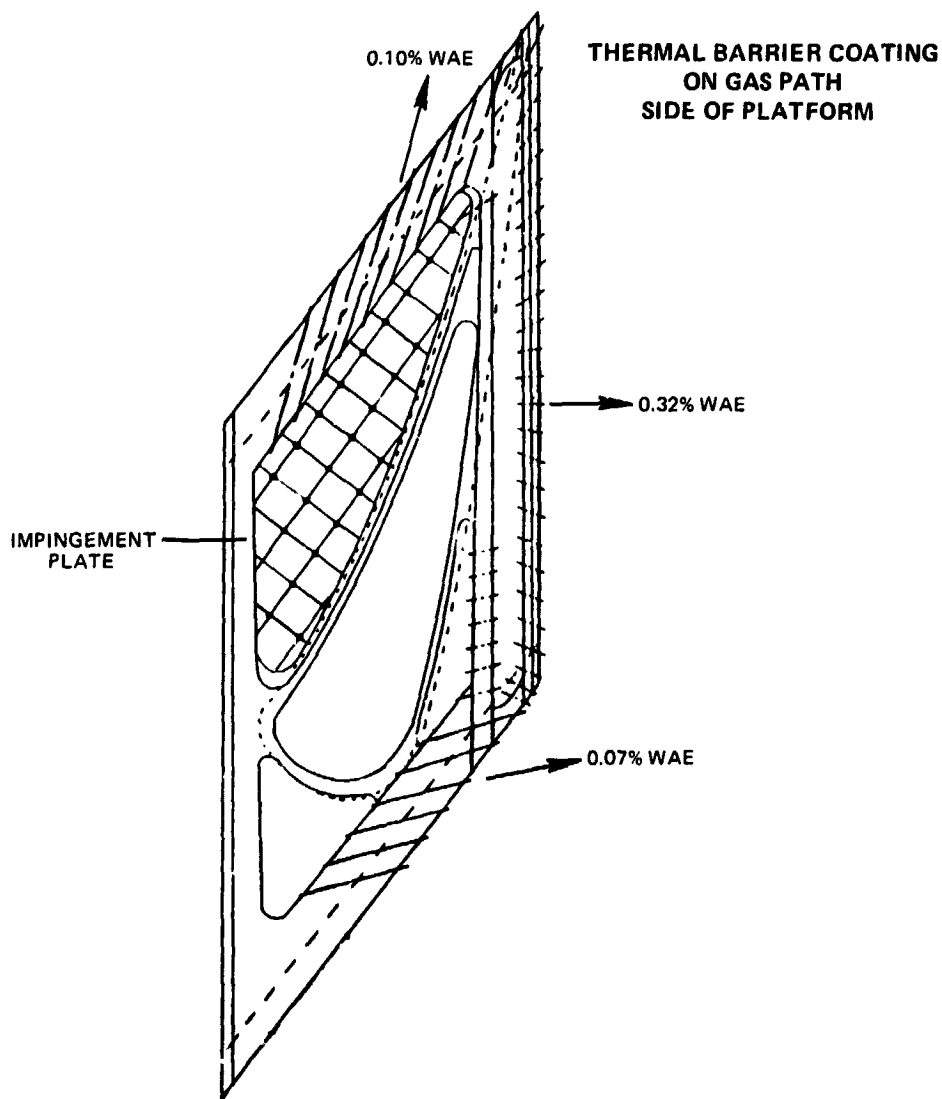


Figure 119 Vane Outer Diameter Platform Cooling Hole Arrangement



PRATT & WHITNEY AIRCRAFT GROUP
COMMERCIAL PRODUCTS DIVISION

ORIGINAL 111 7 83
OF POOR QUALITY

VANE I.D. PLATFORM COOLING FLOW 0.32%

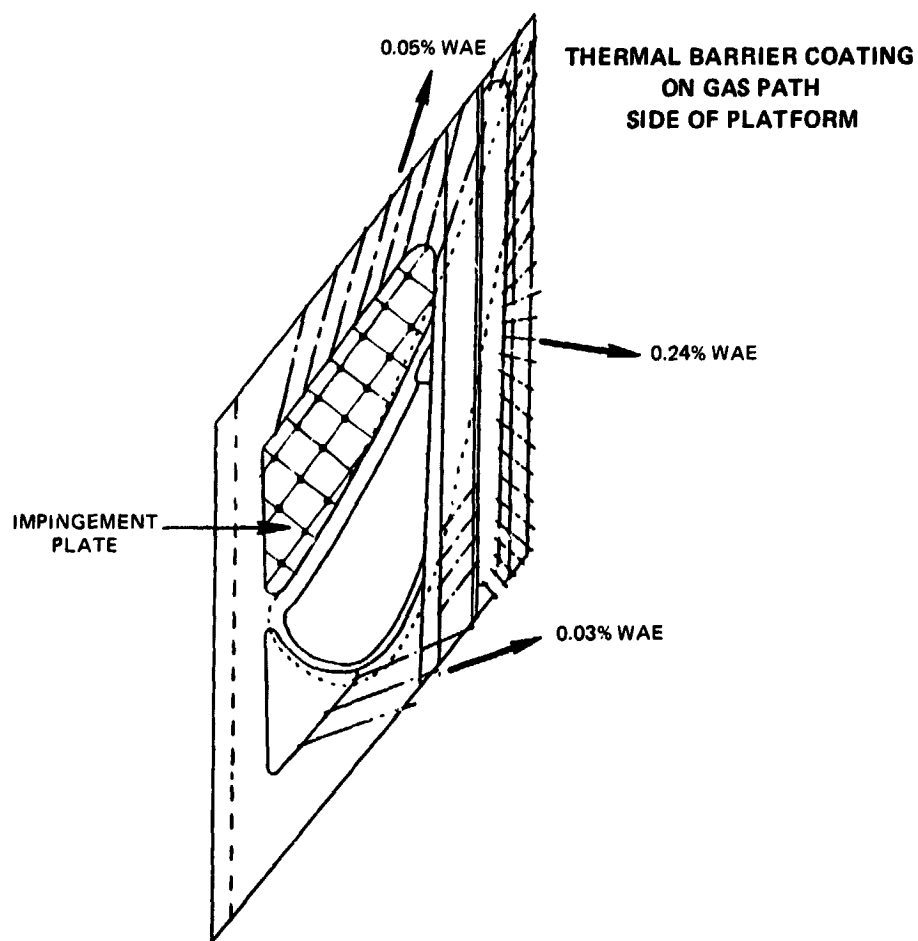


Figure 120 Vane Outer Diameter Platform Cooling Hole Arrangement



ORIGINAL PAGE IS
OF POOR QUALITY

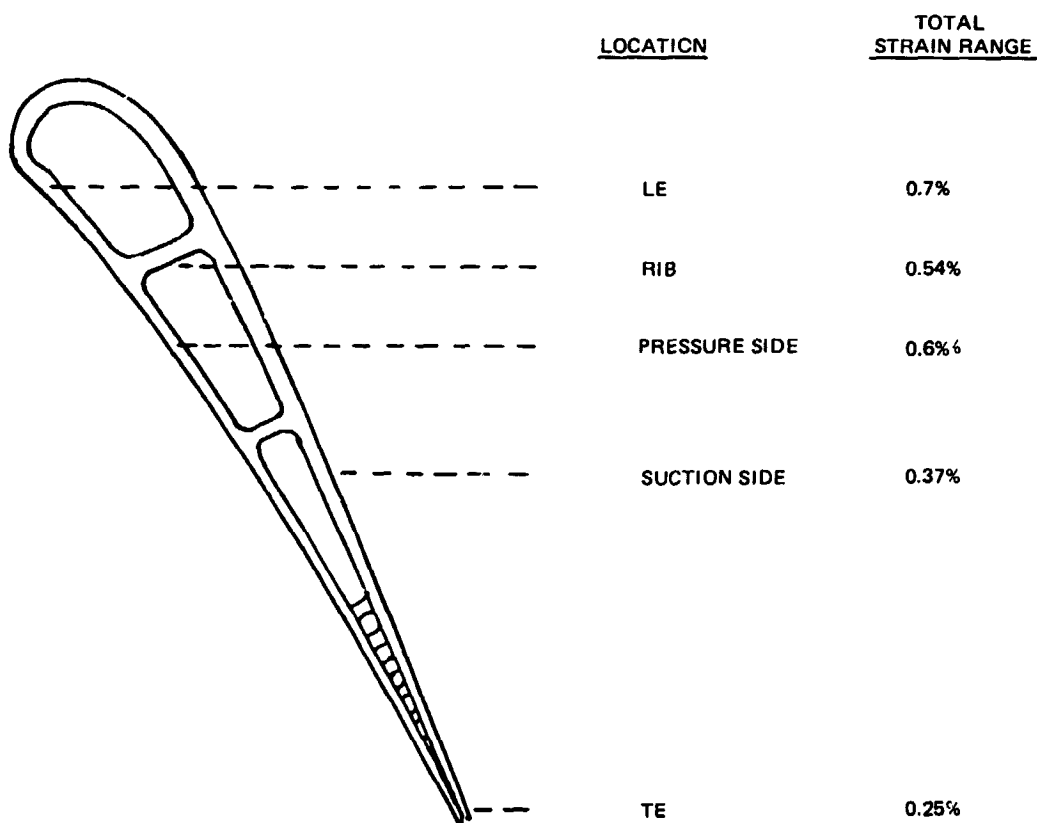


Figure 121 Vane Strain Ranges



PRATT & WHITNEY AIRCRAFT GROUP
COMMERCIAL PRODUCTS DIVISION

The calculated vane life for the flight propulsion system and the integrated core/low spool is compared to life requirements in Table 73. Oxidation and cracking lives exceed goal values by 1000 hours or 300 cycles.

TABLE 73
CALCULATED VANE LIFE

	<u>REQUIRED</u>	<u>CALCULATED</u>
FPS:		
Oxidation	6,000 hrs*	7,000 hr*
Cracking	10,000 hrs (2,200 flt. missions)	11,000 hr (2,500 flt. missions)
IC/LS:		
Oxidation	50 hrs (hot time)	100 hrs (hot time)

NOTE: *10,000 hrs achieved with one recoating

Blade Cooling

The final blade cooling design is shown on Figure 122 and is unchanged from that described in the 4th semiannual report. Multi-pass internal cooling passages supply cooling air controlled by 3 holes in the root metering plate. The front (leading edge) passage feeds the leading edge shower head cooling holes, tip pressure side film holes, and the trailing edge ejection hole. The mid-passage air convectively cools the mid-chord area. This air makes 2 span-wise excursions and then enters the trailing edge passage where it passes through an array of pedestals before exiting.

After air turns at the blade root, an aft passage feed prevents flow separation from rib walls. Trip strips in all passages enhance heat transfer. The results of the two-dimensional water flow model supporting technology programs were used in the final design of the blade cooling arrangement to prevent separation and to reduce pressure loss at the root and tip turn areas.

The blade materials and coatings selected for the final flight propulsion system and integrated core/low spool designs are listed in Table 74. The flight propulsion system design includes a bonded tip section of MERL 711 or Titaloy. The bonded tip is being held optional for the integrated core/low spool, pending the successful achievement of related development programs. The temperature profile used in the design is shown on Figure 123. Peak of the profile occurs at the 65 percent span location.



PRATT & WHITNEY AIRCRAFT GROUP
COMMERCIAL PRODUCTS DIVISION

ORIGINAL DESIGN
OF POOR QUALITY

BLADE COOLING FLOWS (TOTAL 2.75%)

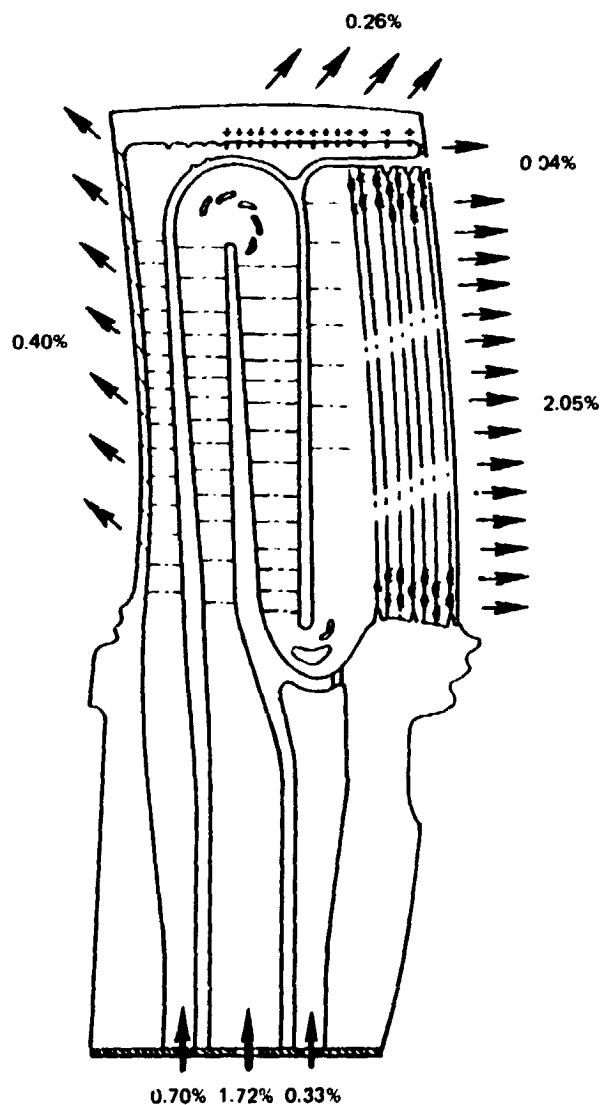


Figure 122 High-Pressure Turbine Blade Cooling Design



PRATT & WHITNEY AIRCRAFT GROUP
COMMERCIAL PRODUCTS DIVISION

ORIGINAL 1-14
ON 1-14-77

TABLE 74

BLADE MATERIALS AND COATING

	<u>FPS</u>	<u>IC/LS</u>
Base Alloy	Merl 200 (adv. single crystal)	PWA 1480 (single crystal)
External Coating	Merl 700 (adv. overlay)	PWA 270 (NiCoCrAlY)
Internal Coating	PWA 275 (Aluminide)	None

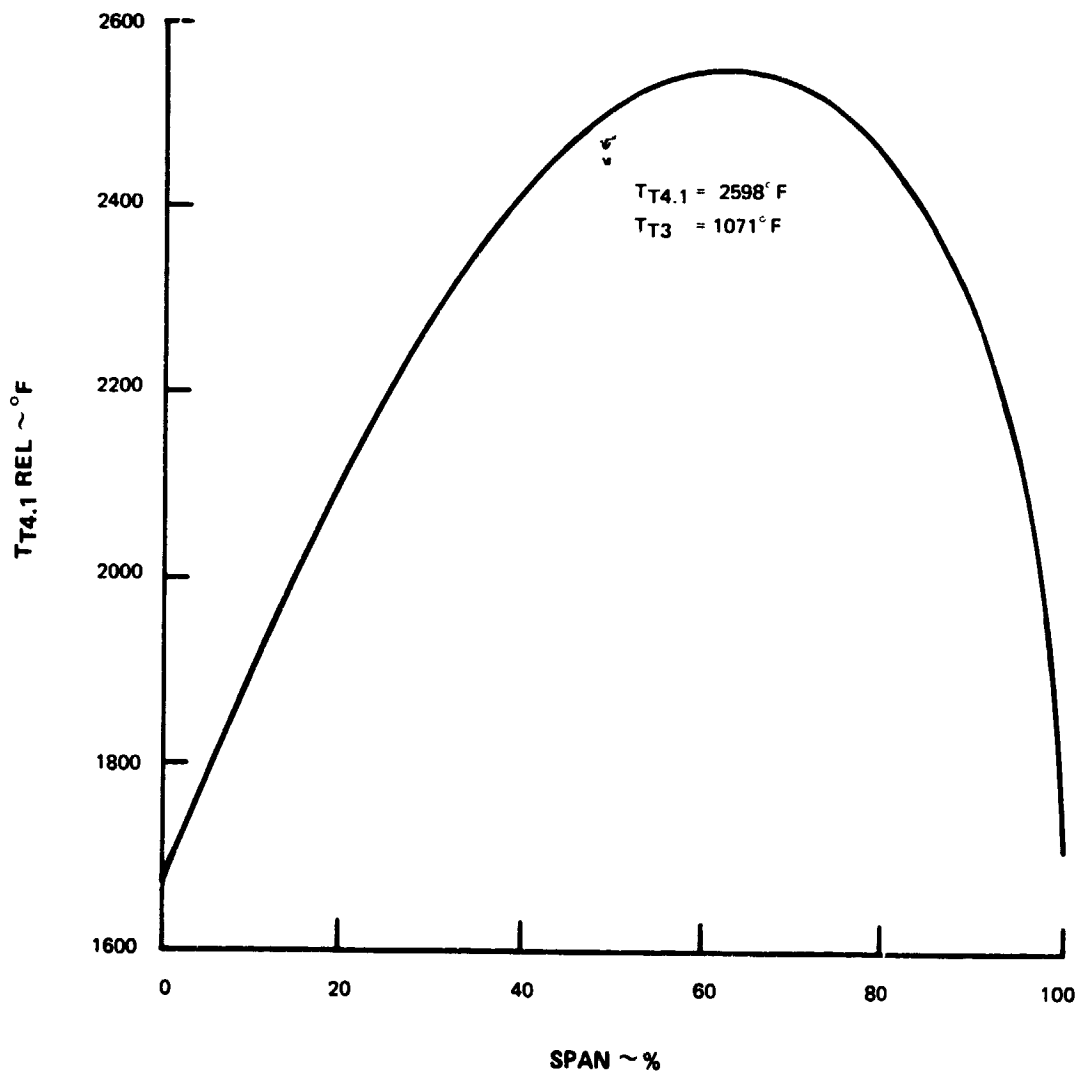


Figure 123 Blade Temperature Profile



PRATT & WHITNEY AIRCRAFT GROUP
COMMERCIAL PRODUCTS DIVISION

ORIGINAL PAGE 13
OF POOR QUALITY

Detailed thermal analysis results are represented by the isotherm for the blade mid-span section in Figure 124. The hottest temperature (slightly greater than 2000 F) occurs on the suction wall surface outboard of the first rib. The coolest temperature (1550 F) on the blade also occurs at the midpoint of the first rib.

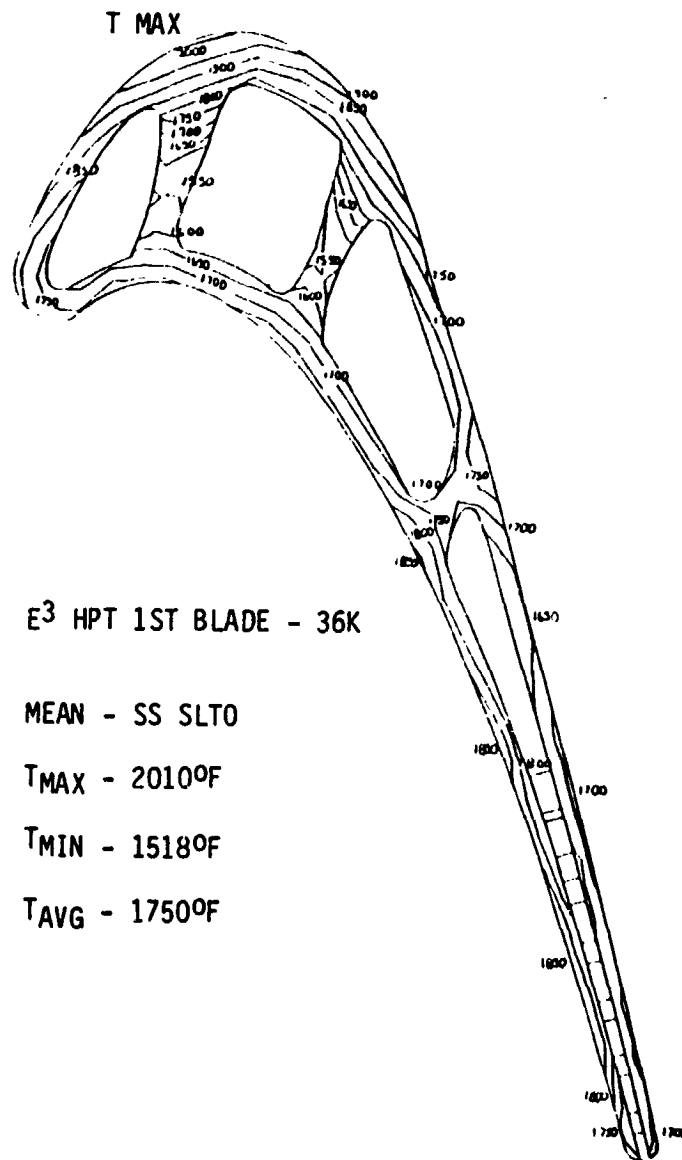


Figure 124 Blade Mid-Span Section Isotherm



PRATT & WHITNEY AIRCRAFT GROUP
COMMERCIAL PRODUCTS DIVISION

Blade Durability

The calculated life of the blades of both the flight propulsion system and the integrated core/low spool is well above the required values (see Table 75). Transient analysis of the blade indicates that the first rib experiences the greatest strain range of all parts of the blade. Figure 125 shows the total strain ranges at various locations in the blade.

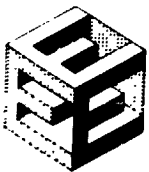
TABLE 75
CALCULATED BLADE LIFE

	<u>REQUIRED</u>	<u>CALCULATED</u>
FPS:		
Oxidation	6,000 hrs	16,000 hrs
Cracking*	10,000 hrs (2,200 flt. missions)	16,000 hrs (3,500 flt. missions)
IC/LS:		
Oxidation	50 hrs (hot time)	400 hrs (hot time)
Creep	50 hrs (hot time)	80 hrs (hot time)

NOTE: *Cracking due to interacting creep and LCF

SECONDARY AIRFLOW

The secondary flow map for the high-pressure turbine is shown in Figure 126, and various rotor secondary flow features are summarized in Figures 127 through 130. The blade supply tangential on-board injection system is a high-efficiency cascade design. Because it is pressure balanced, no inner or outer seals are required. In addition, only a small air flow (0.1 percent Wae) is required around the flow guides at the tangential on-board injection discharge. Because the system is balanced to gas path inner diameter pressure, cooling airflow is insensitive to rim "seal" clearances. The tangential on-board injection system is supplied by high-pressure compressor discharge inner diameter bleed air.



PRATT & WHITNEY AIRCRAFT GROUP
COMMERCIAL PRODUCTS DIVISION

ORIGINAL PART 12
OF POOR QUALITY

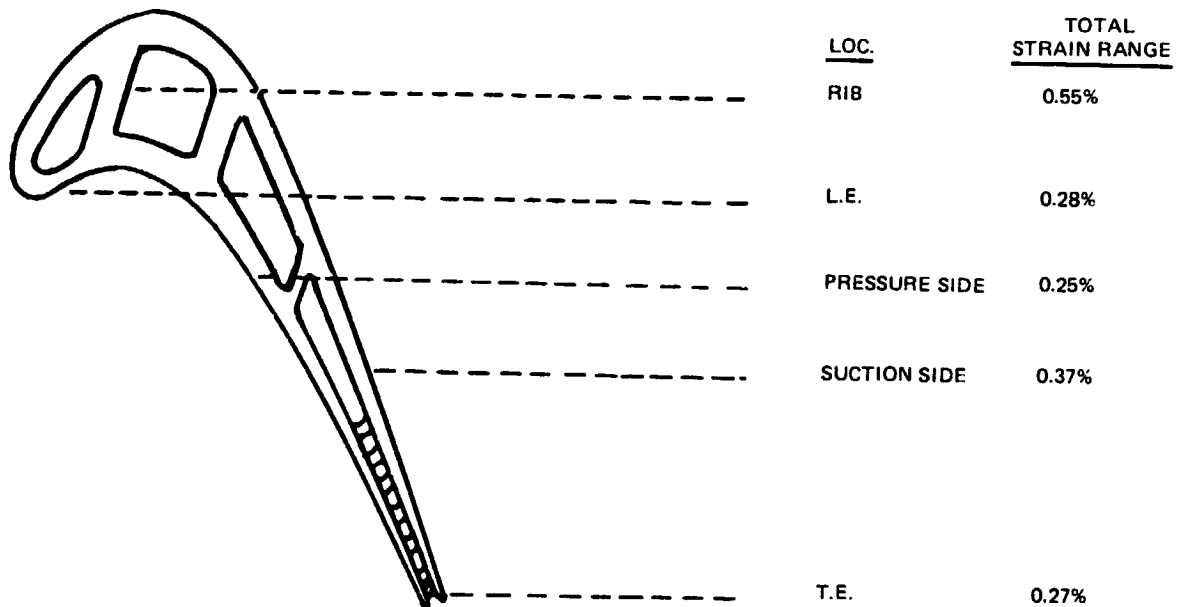


Figure 125 Blade Strain Ranges



PRATT & WHITNEY AIRCRAFT GROUP
COMMERCIAL PRODUCTS DIVISION

ORIGINATOR
OF POOR QUALITY

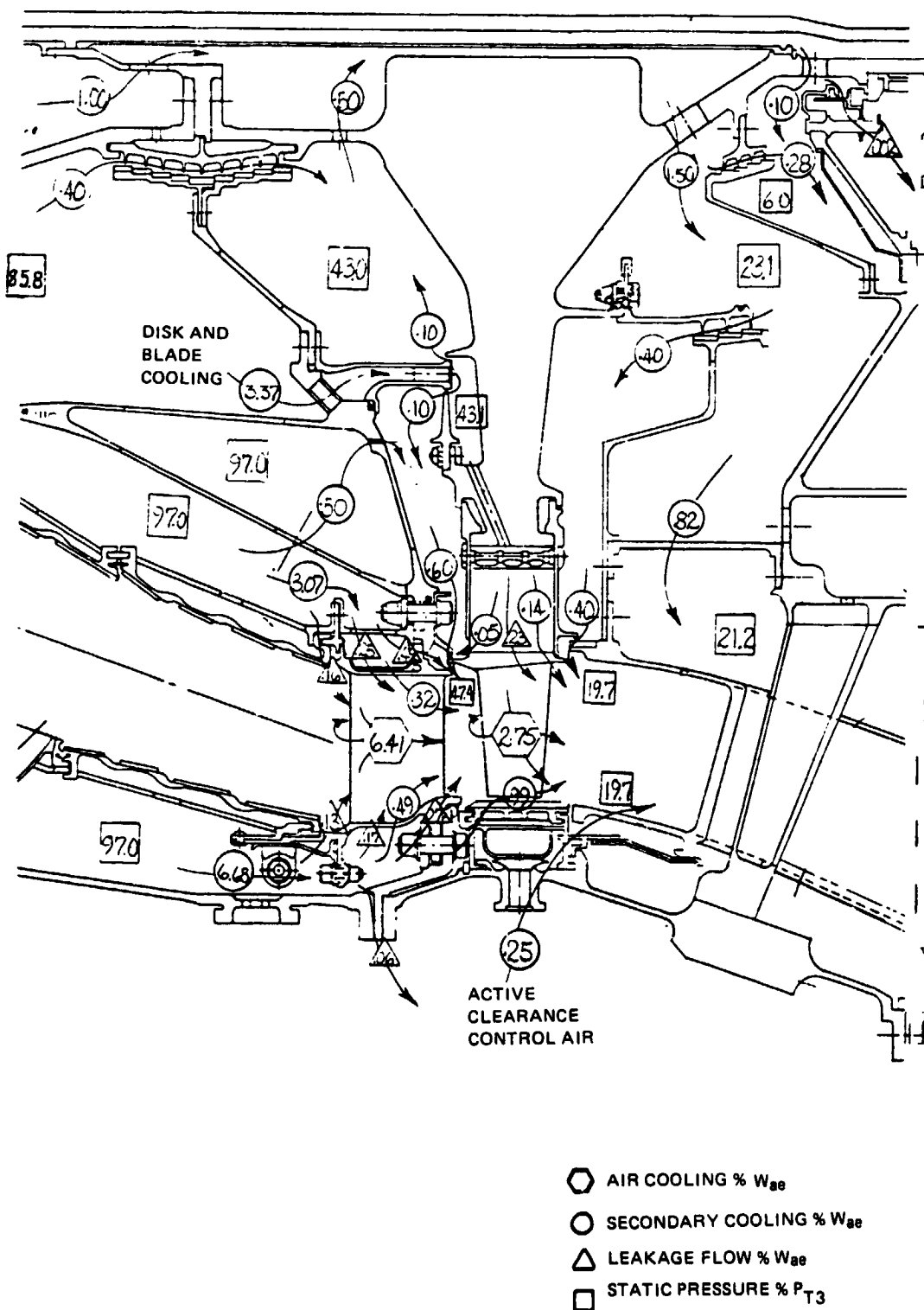


Figure 126 High-Pressure Turbine Secondary Flow Map



PRATT & WHITNEY AIRCRAFT GROUP
COMMERCIAL PRODUCTS DIVISION

ORIGINAL PAGE IS
OF POOR QUALITY

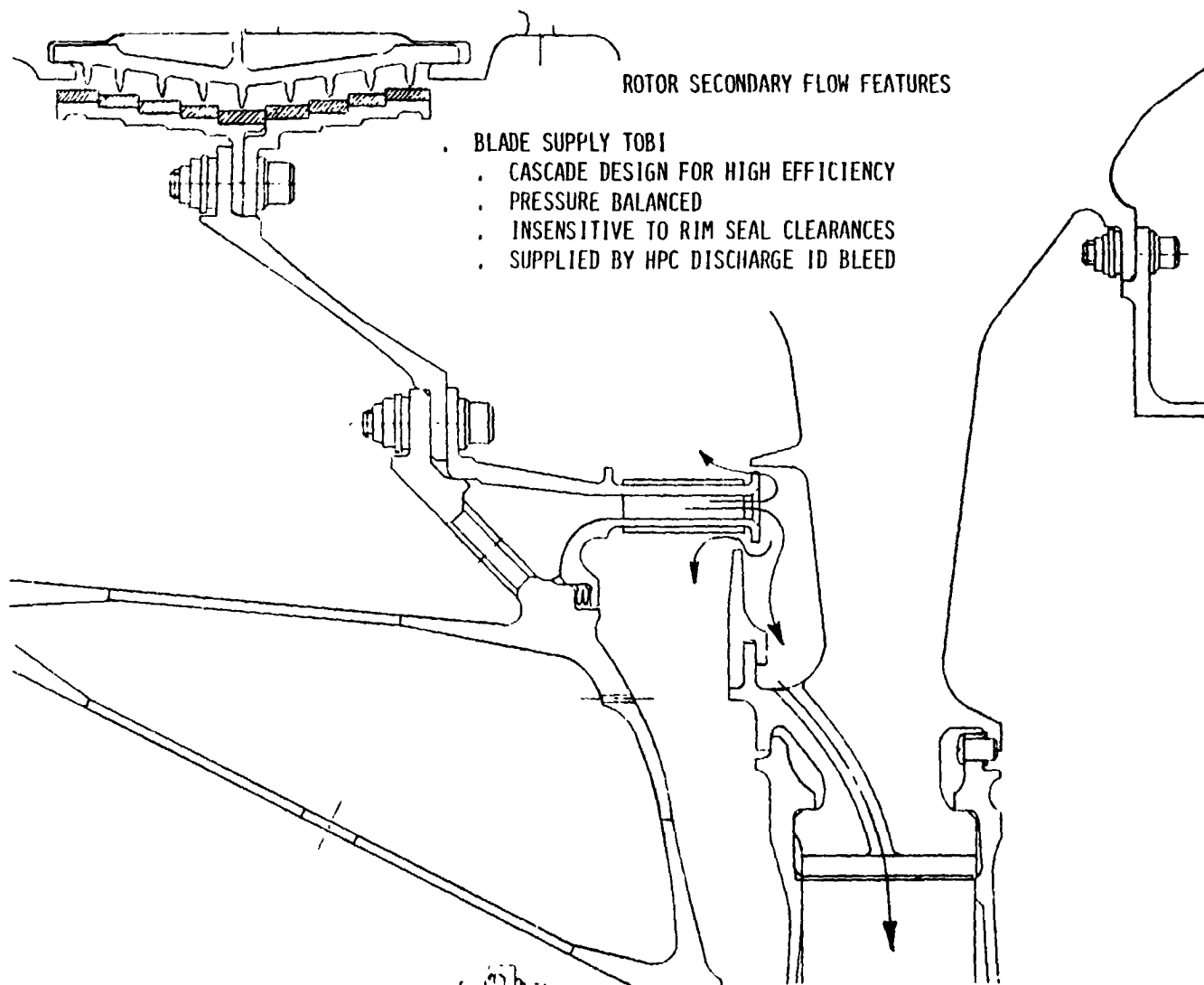
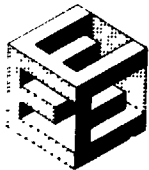


Figure 127 Rotor Secondary Flow Features



PRATT & WHITNEY AIRCRAFT GROUP
COMMERCIAL PRODUCTS DIVISION

ORIGINAL BY ~~PRATT & WHITNEY~~
OF POOR QUALITY

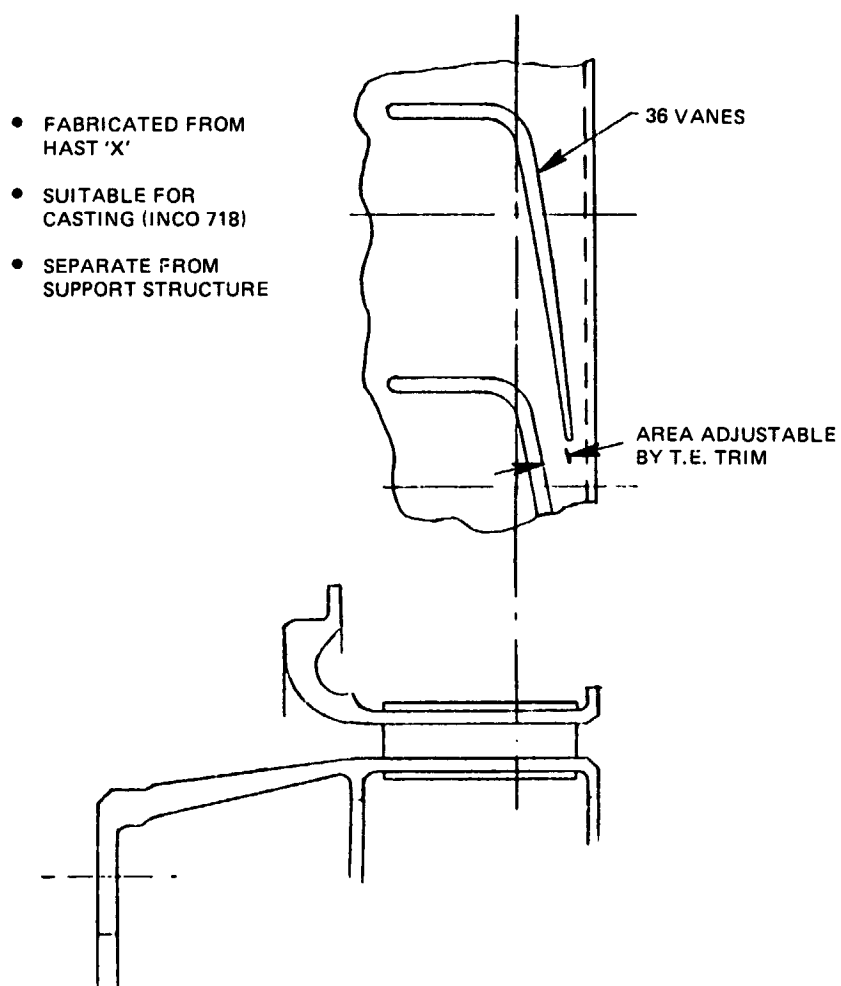


Figure 128 Nozzle Configuration for the Tangential On-Board Injection System

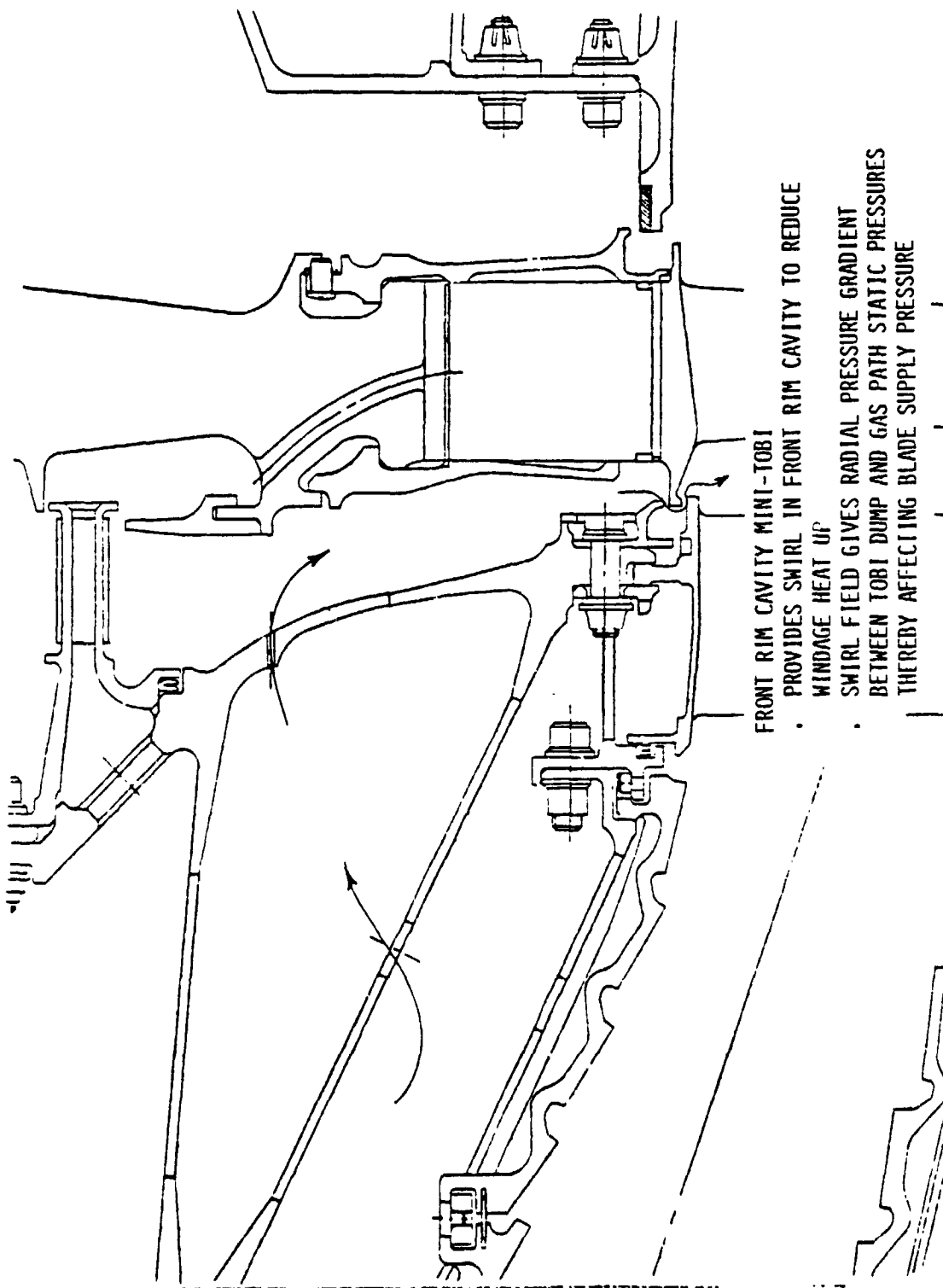


Figure 129 Front Rim Cavity "Mini" Tangential On-Board Injection System



PRATT & WHITNEY AIRCRAFT GROUP
COMMERCIAL PRODUCTS DIVISION

SEE
OF PAGE 100

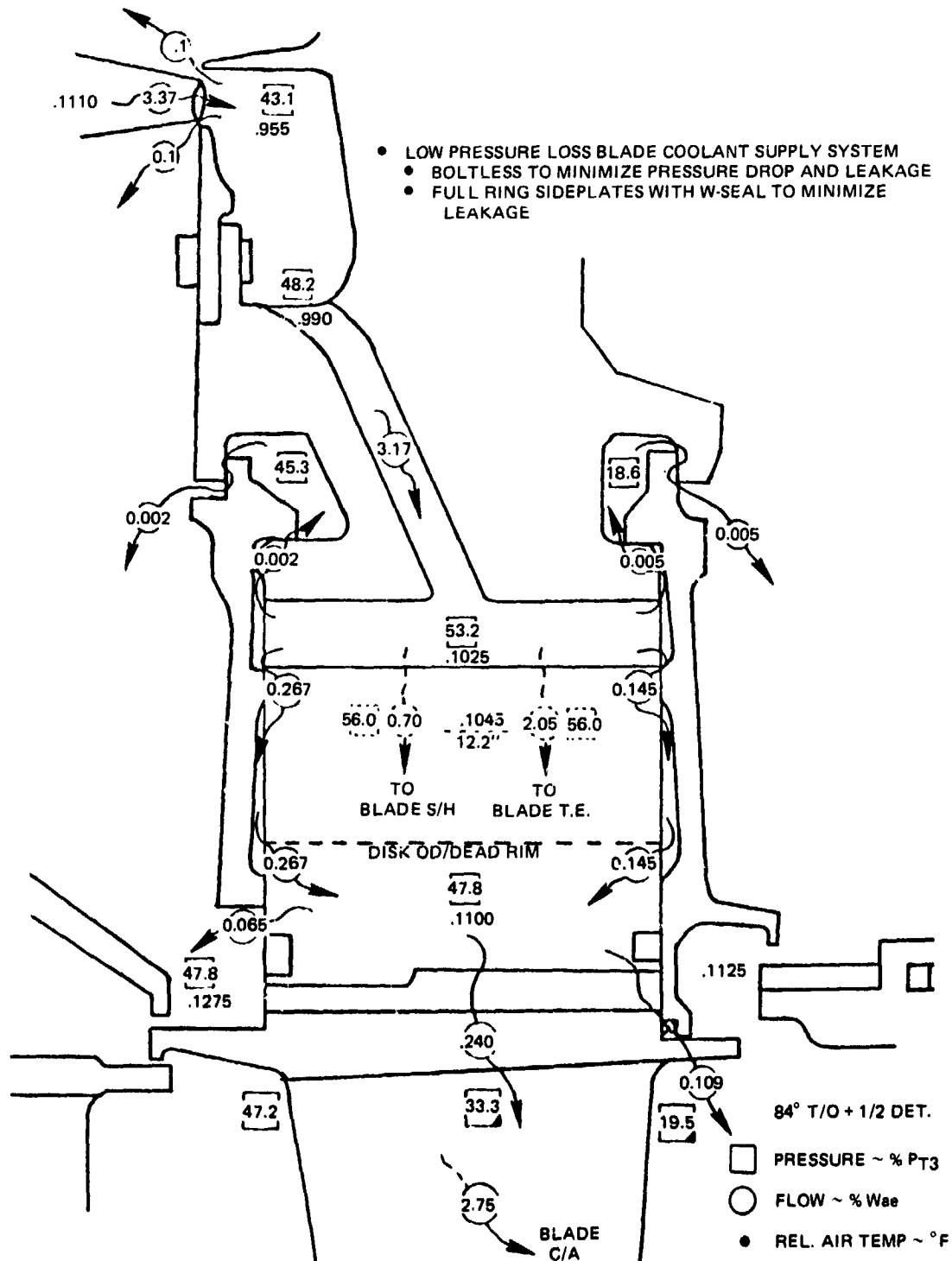


Figure 130 Blade Coolant Supply System



PRATT & WHITNEY AIRCRAFT GROUP
COMMERCIAL PRODUCTS DIVISION

The "mini" tangential on-board injection system preswirls air in the front rim cavity and thereby reduces windage heat-up (see Figure 129). The swirl field also provides a radial pressure gradient between the blade supply tangential on-board injection system and the gas path static pressure, effectively linking the blade supply pressure to the gas path leading edge inner diameter pressure. This keeps the ratio fixed independently of seal leakage, attachment leakage, and blade flow area.

Figure 130 shows details of the blade cooling air flow supply, the blade pressure drop, and leakage. The full-ring sideplate design minimizes leakage. Additionally, the rear plate outer diameter is sealed by a W-seal. The goal blade cooling flow is 2.75 percent Wae at a blade supply pressure of 53.2 percent P_{T3} . The tangential on-board injection dump pressure of 43.1 percent P_{T3} is increased to 48.2 percent P_{T3} by the free vortex pressure recovery, and to 53.2 percent P_{T3} by solid body rotation in the disk feed passages. A tangential on-board injection rig test program is being run to ensure adequate blade supply pressure.

Other rotor secondary flow features include leading and trailing edge rim flow guides to prevent hot gas ingestion. A 9-knife, stepped labyrinth, abradable land, high-pressure compressor discharge seal minimizes leakage, and is predicted to result in an airflow of approximately 0.7 percent Wae at a 0.0125-inch radial clearance. A seal at the rear of the high-pressure turbine is used to provide thrust balance. The high-pressure rotor net thrust is presently calculated at approximately 5,000 lb. A buffer seal is also used at the rear of the high-pressure turbine disk to separate cool low-pressure compressor discharge air from high-pressure turbine bore cooling air for the rear bearing compartment.

The outer air seal consists of ceramic layers sprayed on a metal shoe, which is impingement-cooled with secondary cooling air from the burner. Still at a relatively high pressure, this cooling air is then fed to the inter-segment gaps to cool the exposed intermediate layer and to prevent gas path ingestion. W-seals and feather seals are used extensively to minimize secondary flow leakage.

The flows of the flight propulsion system and the integrated core/low spool are summarized in Table 76. The total flows, 14.09 percent and 14.56 percent Wae, respectively, differ only because the flight propulsion system is assumed to have a higher level of feather seal technology in the vane and outer air seal.

HIGH-PRESSURE TURBINE MECHANICAL DESIGN

Vane

The vane is mechanically retained by clamping at the outer diameter attachment and engagement in a slot at the inner diameter attachment (see Figure 131). The inner diameter attachment rail fits the inner support slot with minimum clearance to restrict vane twist, yet allow thermal growth. Vane reaction loads in the circumferential direction are taken out at the outer diameter



PRATT & WHITNEY AIRCRAFT GROUP
COMMERCIAL PRODUCTS DIVISION

TABLE 76
HIGH-PRESSURE TURBINE FLOW SUMMARY

	% WAE AT ADP	
	FPS	IC/LS
Disk		
Front rim cavity	0.60	0.60
Rear rim cavity	0.40	0.40
Sub Total	1.00	1.00
Blade		
Foil cooling flow	2.75	2.75
Sideplate cooling	0.19	0.19
Leakage	0.23	0.23
Sub Total	3.17	3.17
Vane		
Foil cooling flow	6.41	6.41
Platform cooling	0.81	0.81
Leakage	1.40	1.83
Sub Total	8.62	9.05
Case		
Outer air seal cooling	0.99	1.03
Active clearance control	0.25	0.25
Flange leakage	0.06	0.06
Sub Total	1.30	1.34
TOTAL	14.09	14.56

attachment rather than the inner diameter. This avoids excessive torque loads at the inner support structure and improper loading of the diffuser case struts. Pressure loads in the axial direction are divided between the inner case and outer case.

Feather seals, used to seal gaps between vanes, were incorporated based on the results of the leakage supporting technology program. The feather seal slots are ground to provide an optimum sealing surface for the feather seals (see Figure 131).



ORIGINAL PAGE IS
OF POOR QUALITY

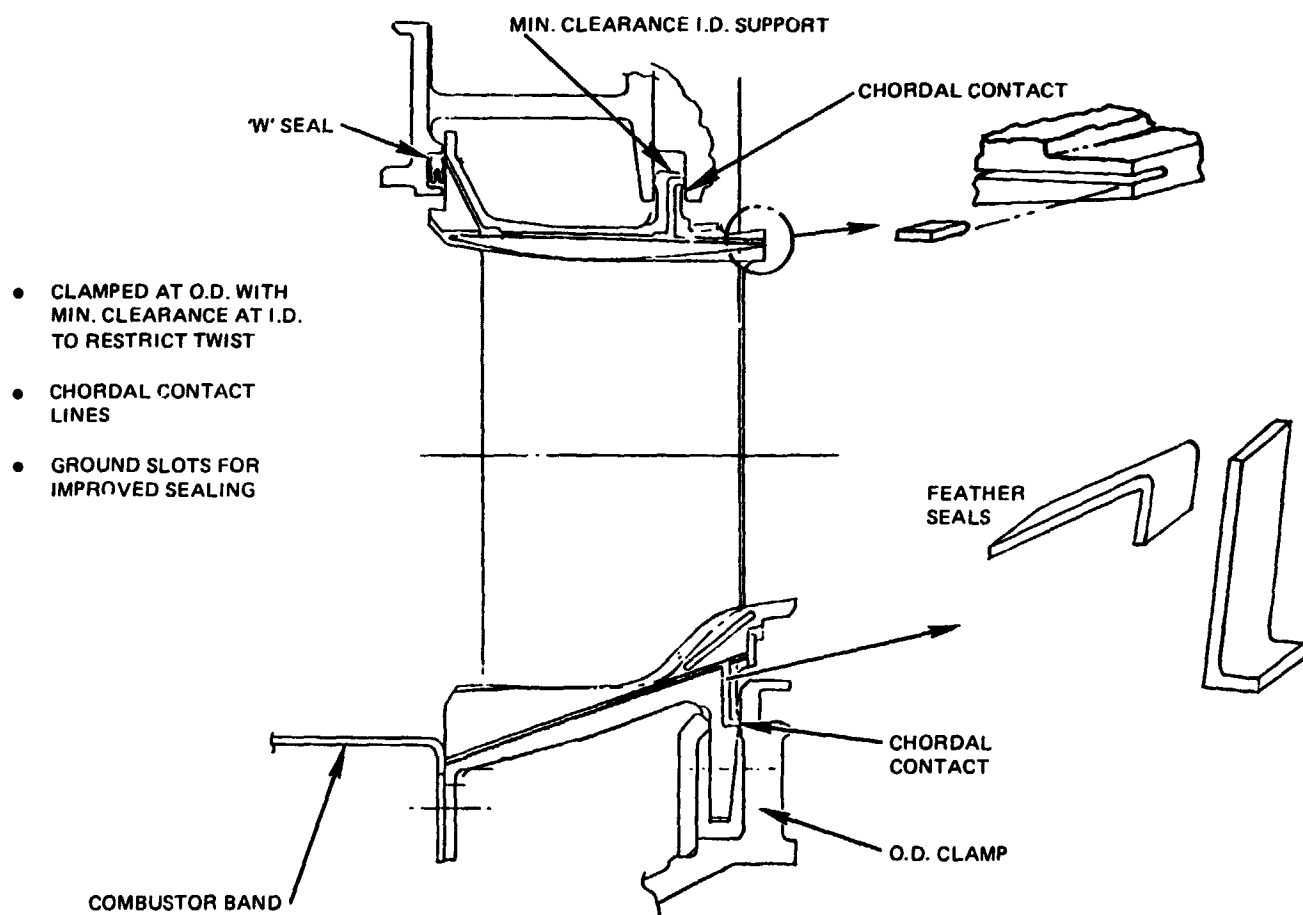


Figure 131 Vane Cooling Air Sealing Arrangement



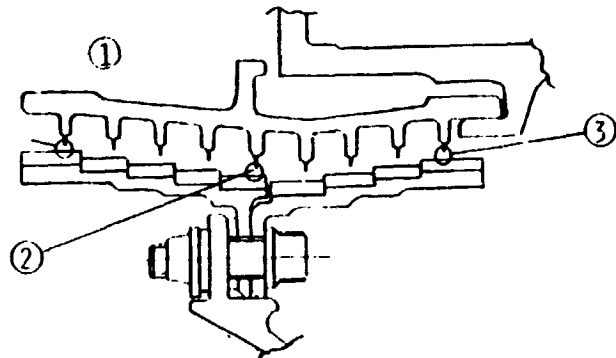
Compressor Discharge Seal

Thermal and structural studies on the high-pressure compressor discharge seal resulted in the clearances listed in Figure 132. Felt metal is used as a rubstrip material.

Rotor

The final design of the disk, blades, sideplates and vortex plate is shown in Figure 133. The complete rotor with attached front and rear seals is illustrated on Figure 134.

- MIN. ASSEMBLY CLEARANCE OF .015
- DESIRED SLTO CLEARANCE OF .0125
- NO RUB AT MANEUVER .0076



• RESULTS

	①	②	③
COLD GAP	.017	.029	.016
PINCH PT	~60 SEC, DECEL	~10-12 SEC, ACCEL	~80 SEC, DECEL
AVE GAP @:			
• ADP	.012	.014	.011
• SLTO	.0125	----->	

Figure 132 High-Pressure Compressor Discharge Seal

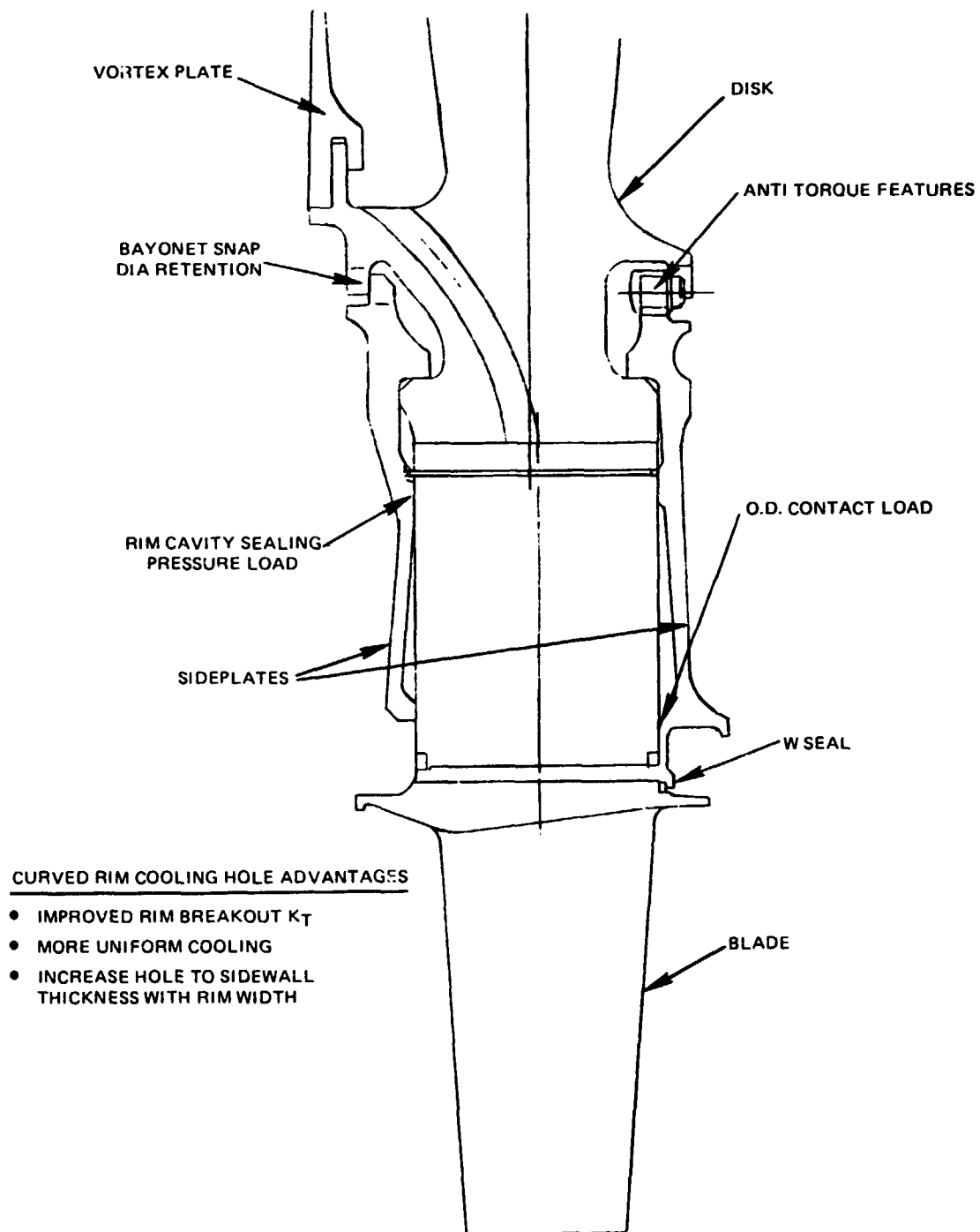


Figure 133 Disk, Blade, Sideplate, and Vortex Plate Final Design

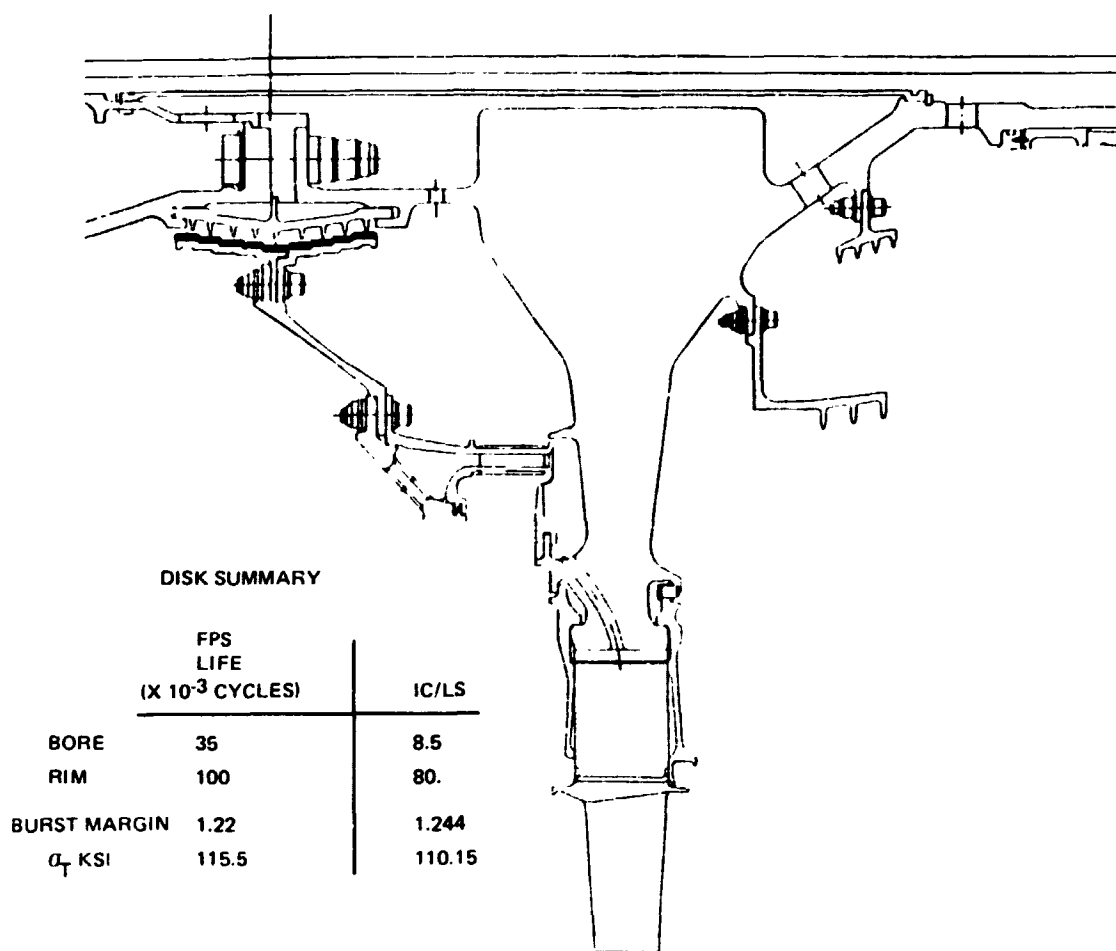


Figure 134 High-Pressure Turbine Rotor

As reported in the Third Semiannual Status Report, the full ring front and rear sideplates attach to the disk by means of a bayonet lock, thereby eliminating the need for bolts. The plates are radially canted so that centrifugal loading keeps them in firm contact with the disk to minimize leakage. Analysis of a bolted design showed unacceptable stresses in the bolts because of thermal excursions and bolt loading required for sealing.

Cooling air is directed to the blade roots through 54 curved, elliptical cross-section holes. The elliptical shape of the cooling hole improves the rim breakout stress concentration factor relative to round holes and the curvature provides increased hole-to-front-sidewall thickness compared to a straight hole.

Both two- and three-dimensional type stress analyses were performed on the rotor in the area of the disk rim and attaching plates. The results of these analyses indicated that stresses were within the allowable limits for both the flight propulsion system disk and plates (MERL 80 material) and the integrated core/low spool parts (MERL 76 material). Resulting rim area and cooling hole cyclic lives for the flight propulsion system and the integrated core/low spool are shown in Figure 135. The minimum life requirement is 12,000 cycles.

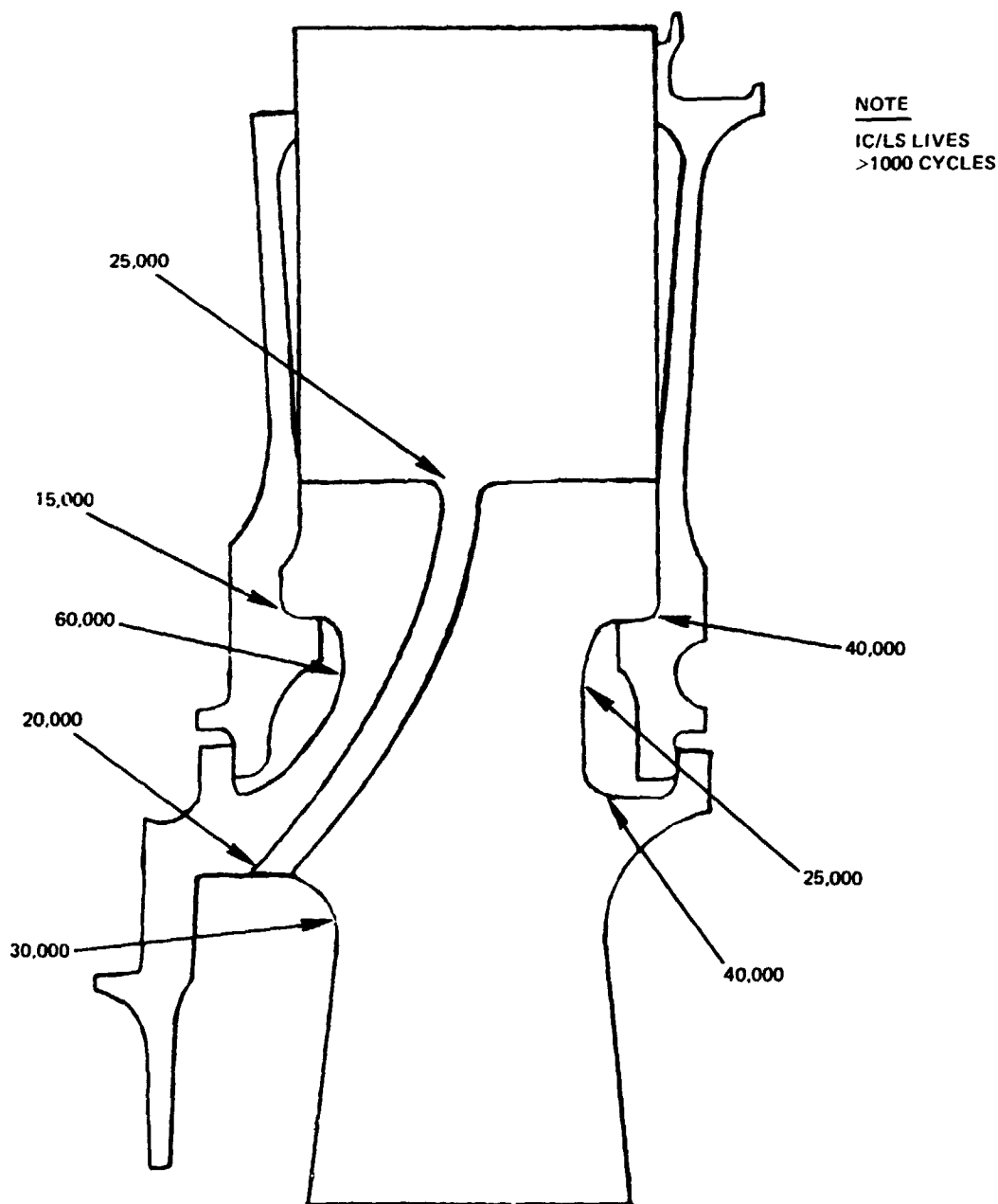


Figure 135 Rim Area and Cooling Hole Cyclic Lives

Results of the blade attachment stress study (see Figure 136) indicate that the integrated core/low spool blade and disk have less than allowable stresses for the required 1000 cycles. The flight propulsion system results indicate comfortable margins for the blade and stresses greater than allowable of up to 12 percent for the disk. Further fine tuning of the attachment design is required to balance the stresses to reduce the blade margin and to bring the disk stresses within allowable limits.



PRATT & WHITNEY AIRCRAFT GROUP
COMMERCIAL PRODUCTS DIVISION

ORIGINAL DESIGN
OF POOR QUALITY

+ = GREATER THAN
ALLOWABLE
- = LESS THAN
ALLOWABLE

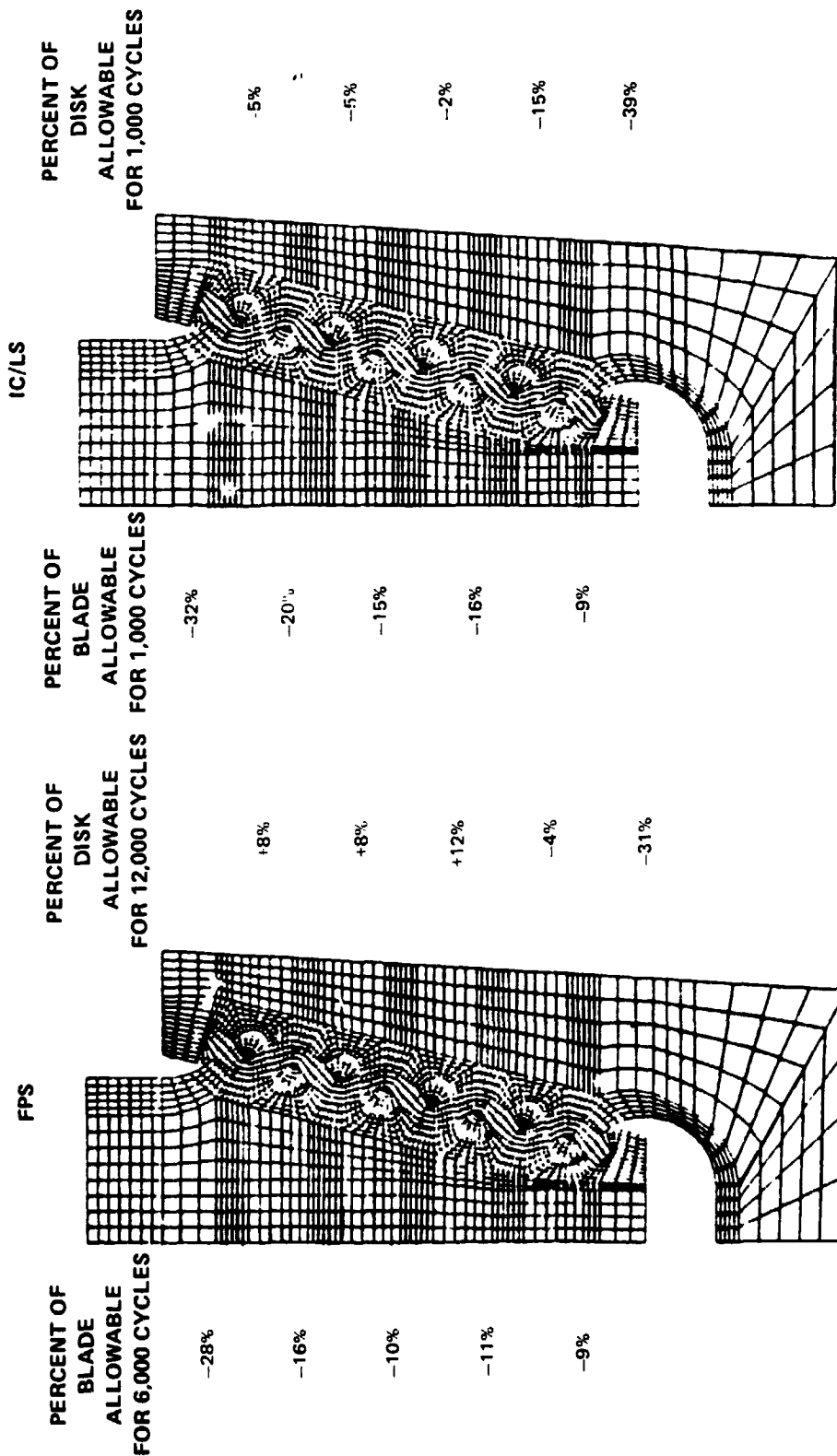


Figure 136 Blade Attachment Stress Study Results



A NASTRAN vibration analysis was completed on the turbine blade. The results obtained from studying 5 resonant modes of airfoil vibration indicated that the trailing edge region from mid-span to tip was the area of greatest vibrational amplitude. The anisotropic properties of elasticity of the single crystal material were considered in the analysis. By aligning the maximum in-plane elastic modulus (see Figure 137) parallel to the trailing edge chord line for the blade tip section, upper mode frequencies could be moved to higher frequencies. This move permitted avoidance of 24E excitation of the 4th or 5th modes in the engine operating range (see Figure 138). The 11E excitation also avoids first or second modes by ample margins. This orientation of elasticity for the single crystal material requires that all blade castings have the primary axis oriented in the radial direction $[001]$ and the secondary axis rotated 25 degrees clockwise from the rearward axial direction $[100]$.

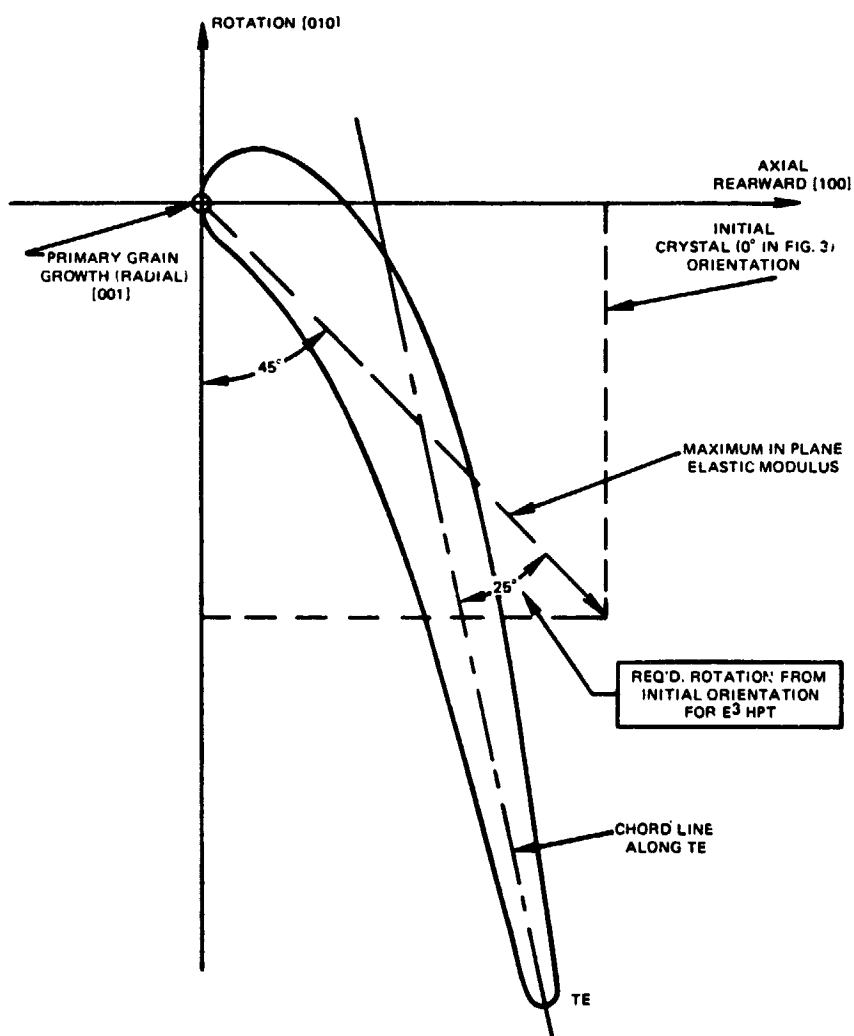


Figure 137 High-Pressure Turbine Required Secondary Axis Crystal Orientation



ORIGINAL PAGE 19
OF POOR QUALITY

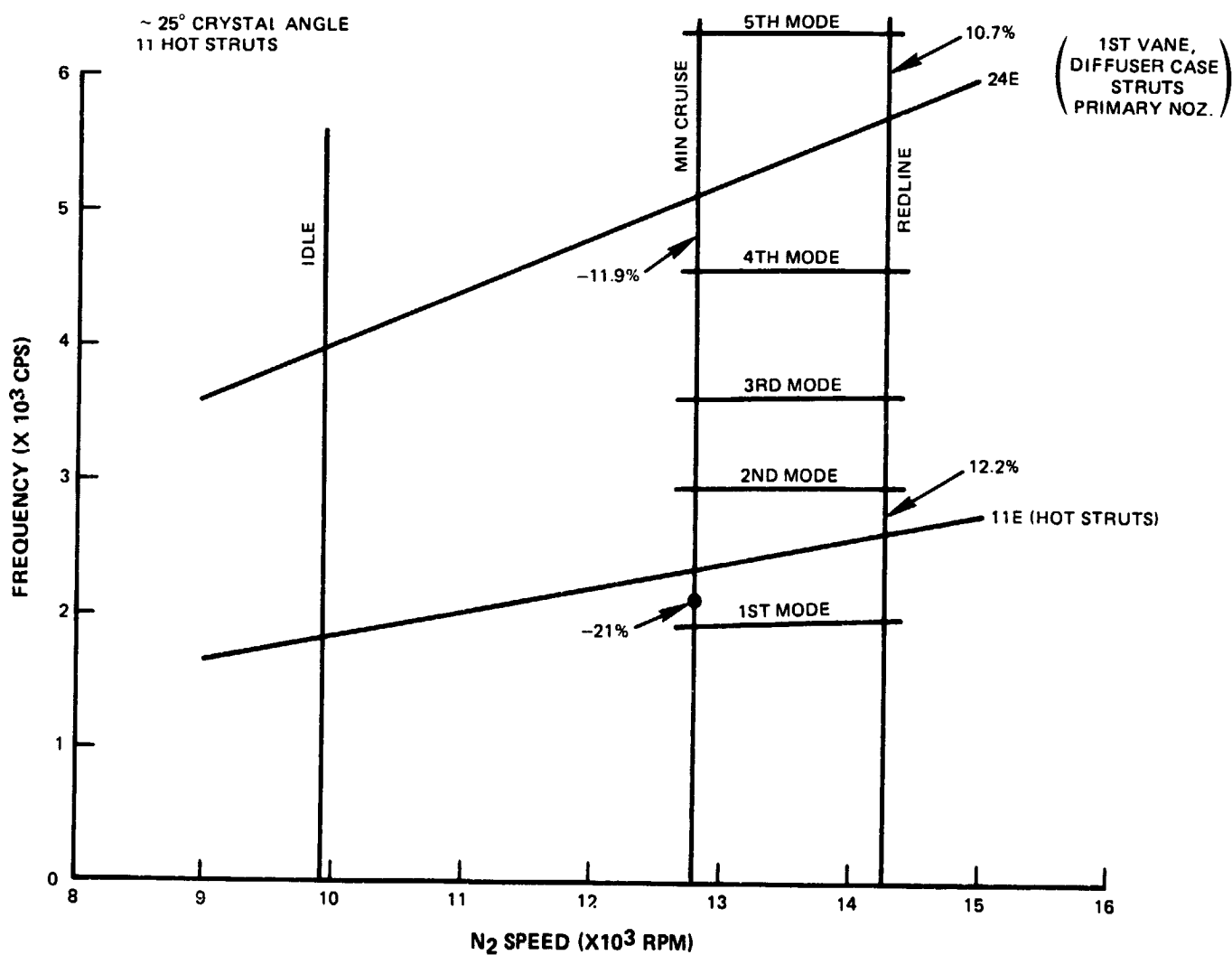


Figure 138 High-Pressure Turbine Blade Resonance Diagram



Vibration analysis was also conducted on the three labyrinth air seals of the rotor assembly. The rotating and stationary parts of the seal were analyzed for resonances and coincidence. Results of these analyses showing the percent margins these seals have to coincident or resonant conditions are presented in Table 77.

TABLE 77

HIGH-PRESSURE TURBINE LABYRINTH SEAL VIBRATION

<u>Seal</u>	<u>Resonance Margin Stator/Rotor</u>	<u>Coincidence Margin Stator to Rotor</u>	<u>Remarks</u>
HPC Discharge	35%/300%	175%	Acceptable
No. 4 Brg. Buffer	37%/>100%	36%	Acceptable
Thrust Balance	46%/20%	69%	Acceptable

Active Clearance Control

The purpose of the high-pressure turbine blade outer air seal active clearance control system is to maintain optimum blade tip gaps. It accomplishes this by impinging controlled temperature air on the outer air seal support rails to move the blade outer air seal shoes radially. This configuration is shown in Figure 139.

The controlled temperature air enters the active clearance control manifold through eight bosses in the high-pressure turbine case, flows through holes in the active clearance control manifold to impinge on the outer air seal support rails, and axially discharges through holes in the rear outer air seal support rail to an annulus between the hot strut outer diameter fairing and the high-pressure turbine case.

During idle, 15th stage air heats the rails, moving the outer air seal shoes away from the blade tip in preparation for takeoff power. A mixture of 10th and 15th stage air is required during takeoff and climb to 20,000 feet to maintain a blade tip gap to within 0.027 inch. At cruise (greater than 20,000 feet), tenth stage air closes the blade tip gap to within 0.0186 inch.

High-pressure compressor discharge air cools the outer air seal shoes. The air is metered through holes in the inlet guide vane support, passes through holes in the front outer air seal support rail to the C/A manifold, then flows through radial holes in a circumferential impingement ring to cool the outer diameter of the outer air seal shoes.

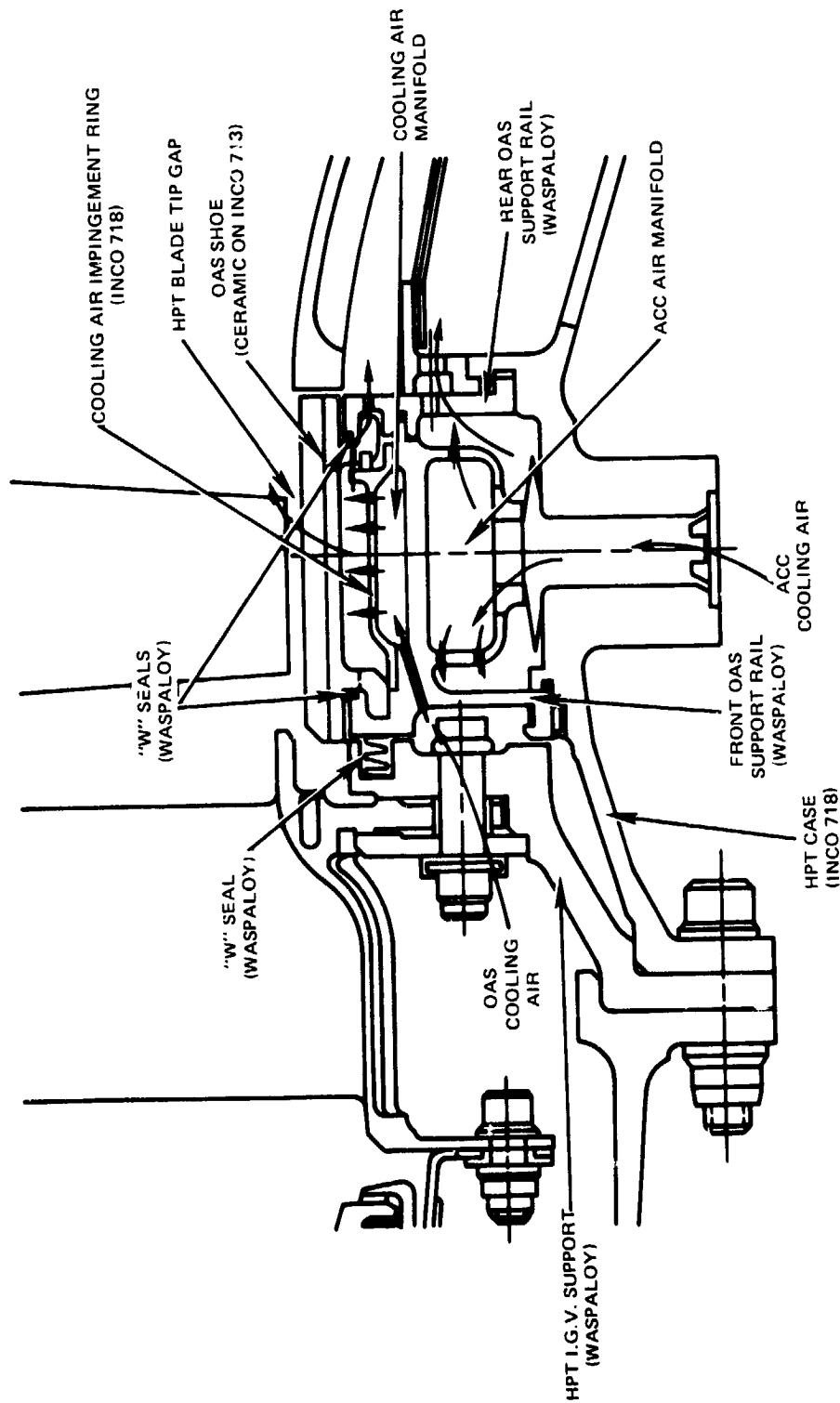
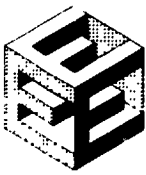
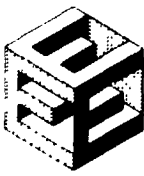


Figure 139 High-Pressure Turbine Active Clearance Control Blade Outer Airseal Features



After the outer air seal shoes are cooled, portions of the air flow to three different areas: (1) the majority of the air flows through holes at one circumferential end of the shoes into the gap between shoes to prevent intrusion of gas path air into the gap and to lower the metal and ceramic temperatures adjacent to the gap; (2) a small amount of the air leaks past the "W" seals located between the outer air seal shoes and the support rails; and (3) some of the air passes through axial holes in the hook area of the rear outer air seal support rail to heat the rail to the same temperature as the front rail. Temperatures of the rear and front rails are kept similar to ensure uniform deflection of both rails.

The blade outer air seal shoes (Figure 140) feature a ceramic coating 0.129 inch thick over a PWA 655 (Cast Inco 713) shoe nominally 0.100 inch thick. Slots in the shoe reduce its spring rate. This prevents the ceramic material from being overstressed as it cools following engine transient conditions.

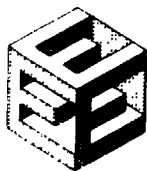
To minimize cooling air leakage, "W" seals are used on the front and rear hook areas of the shoe. Feather-seals are used at the circumferential ship lap joint between shoes. The shoes are held radially inward by the pressure differential across the shoes. The ceramic is an abradable yttrium stabilized zirconia.

Blade Tip Clearance. Blade tip clearance philosophy is such that there are no rubs in normal revenue service when the following items are considered:

- o Thermals and centrifugal gradients;
- o Tolerances, eccentricities, and rotor whirl; and
- o Maneuver and cowl loads.

Table 78 shows the gapping requirements for flight propulsion system.

Figure 141 indicates the resultant blade tip clearances for an accel/decel cycle and for cruise. The pinch point occurs at approximately six seconds into the snap acceleration. The gap throughout the snap acceleration is maintained at a constant 0.0134 inch by varying the mixture of 10th and 15th stage active clearance control air. A schedule for cooling air at various power settings is shown in Table 79. Table 80 shows a tabulation of goal vs. status blade tip clearances. The current status shows that goals have been exceeded resulting in improved turbine efficiency.



PRATT & WHITNEY AIRCRAFT GROUP
COMMERCIAL PRODUCTS DIVISION

ORIGINAL PAGE 18
OF POOR QUALITY

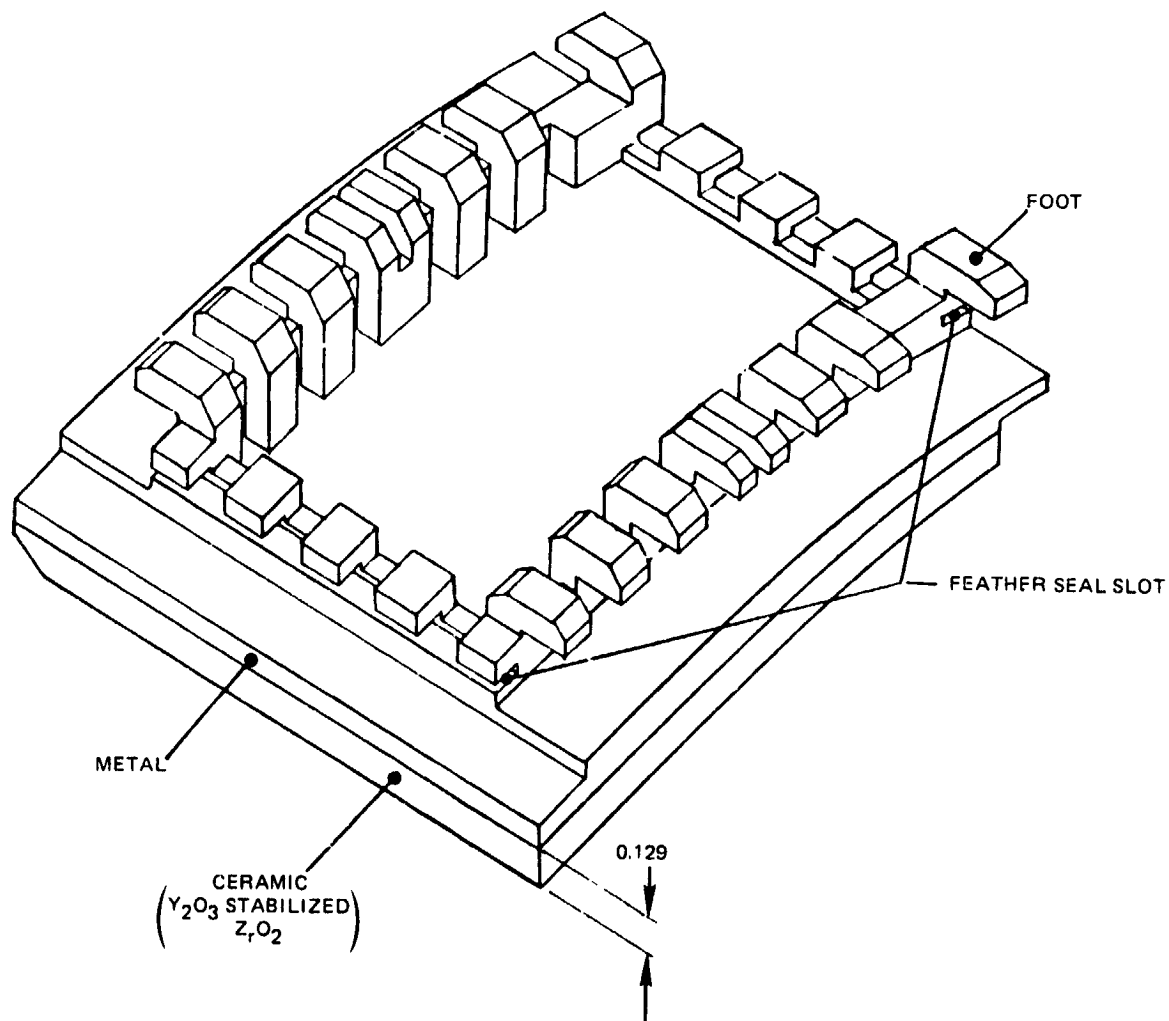


Figure 140 Ceramic Outer Air Seal Shoe



TABLE 78

HIGH-PRESSURE TURBINE GAPPING REQUIREMENTS
(Inches)

	<u>START-IDLE</u>	<u>ACCEL-SLTO</u>	<u>ADP</u>
Tolerances	0.0023	0.0023	0.0023
Eccentricity	0.0034	0.0034	0.0034
Rotor Whirl	0.0010	0.0010	0.0010
Normal Maneuvers		0.0065	0.0010
Cowl Loads		0.0002	0.0002
Bowed Roto · Whirl	0.0180		
TOTAL	0.0247	0.0134	0.0079

TABLE 79

HIGH-PRESSURE TURBINE ACTIVE CLEARANCE CONTROL SYSTEM

<u>Flight Condition</u>	<u>Bleed System</u>
Idle	All 15th
Accel-SLTO	Mixed 10th and 15th
ADP	All 10th

TABLE 80

HIGH-PRESSURE TURBINE BLADE TIP CLEARANCE RESULTS

	<u>Clearance (inch)</u>	
	<u>Goal</u>	<u>Status</u>
Cold		0.06850
Idle		0.04900
SLTO	0.0270	0.0134
ADP	0.0186	0.0126

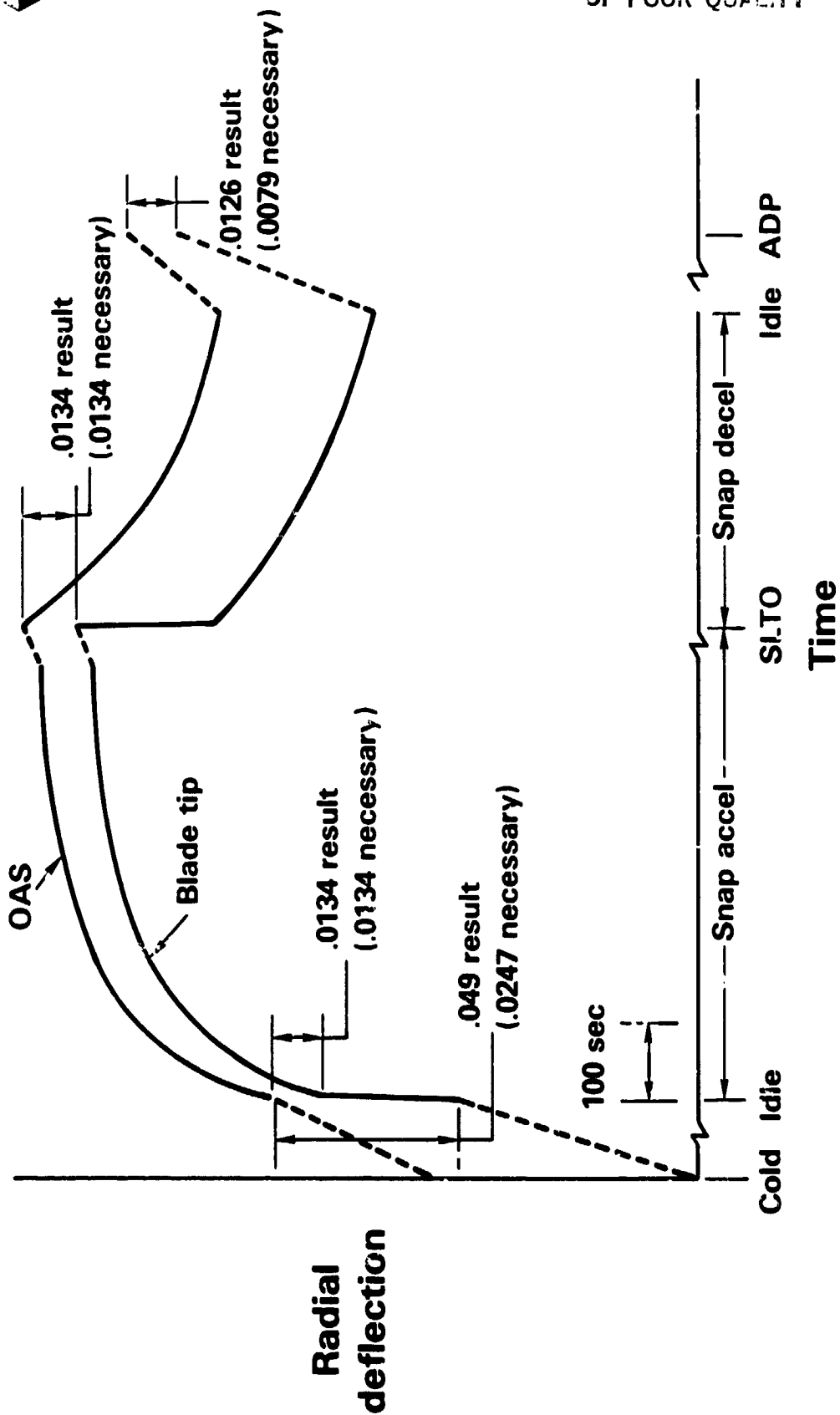
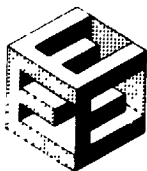


Figure 141 High-Pressure Turbine Blade Tip Clearances



REAR BEARING COMPARTMENT

The design of the number 4 and 5 bearing compartment was completed during the previous reporting period. During forced-response vibration investigations on the low-pressure turbine rotor, a high hot strut case sensitivity to low rotor imbalance was discovered. An oil damped number 5 bearing was therefore incorporated (see discussion in section 3 2.8.3.3.2).

HIGH-PRESSURE TURBINE COMPONENT FABRICATION

Following approval of the detailed design of the high-pressure turbine in June 1980, orders for finished parts were processed as detailed drawings became available. All raw material requiring long lead time procurement and all blade and vane castings have been ordered early to ensure schedule compliance.

Single piece vane casting work progressed through the completion of the wax pattern injection tool and the core injection tool. Sample solid wax injections and sample cores were produced.

Blade casting work progressed through the completion of the wax pattern injection tool and the core injection tool. Rework of the wax pattern tool was required in order to modify the trailing edge area.

The procurement of the two-piece Transient Liquid Phase^R bonded blades was cancelled to reduce the cost of the program.

Hot isostatic press containers for MERL 76 powder were completed for the high-pressure turbine disk, vortex plate, sideplates, and rear thrust balance seal.

Waspaloy forgings for the active clearance control rails, first vane outer support, and fishmouth seal were delivered ahead of schedule.

The fabrication of tooling for electro-chemical machining of the disk curved elliptical hole was continued and is nearing completion.

HOT STRUT CASE

Layout designs and thermal/structural analysis of the hot strut case assembly was completed during the reporting period. The final cross-section configuration of the case is shown in Figure 142. The aerodynamics of the hot strut fairings remain as reported in the Fourth Semiannual Status Report.



ORIGINAL PAGE 13
OF POOR QUALITY

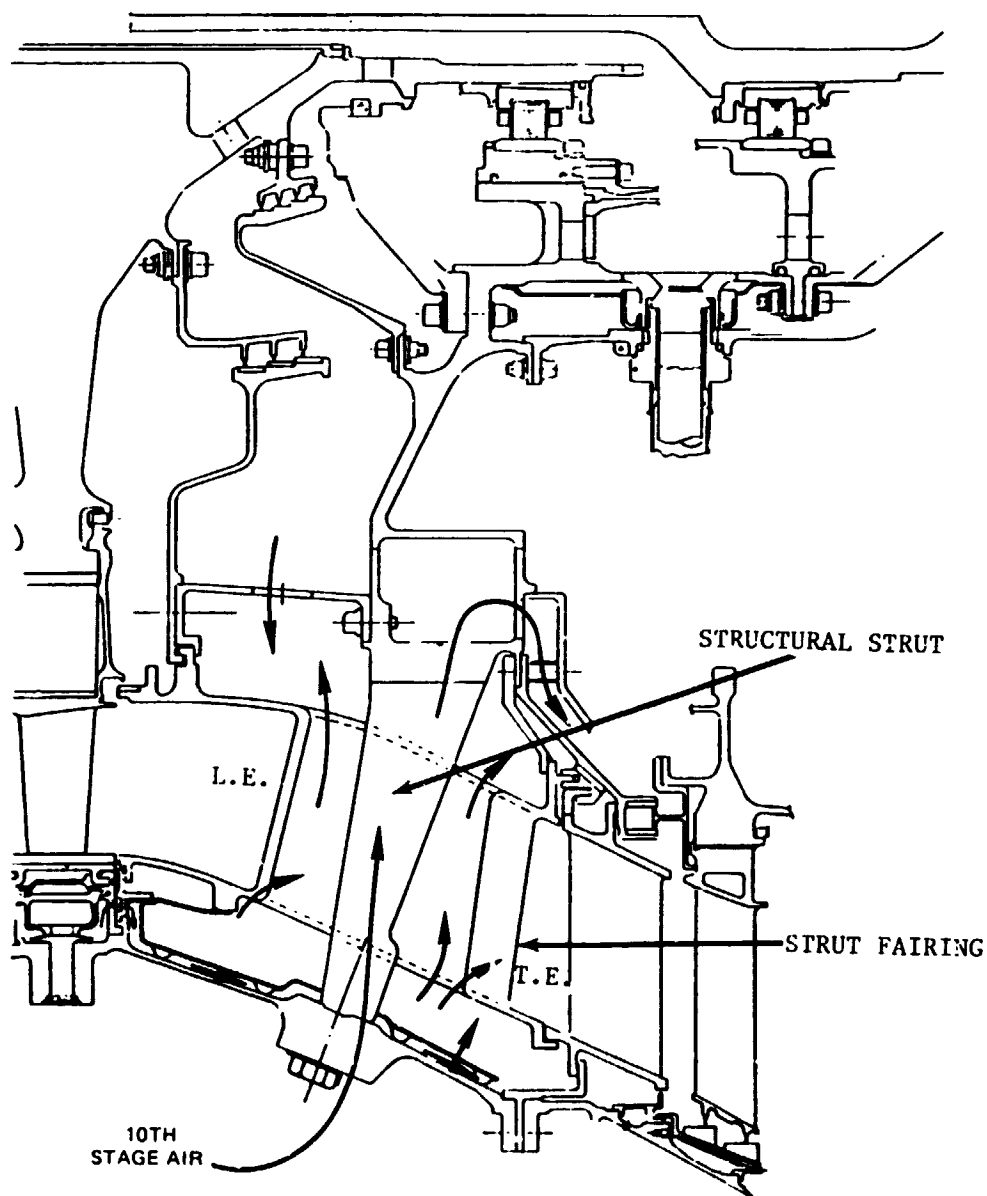


Figure 142 Final Definition of the Hot Strut Case



Hot Strut Case Design

The case structure consists of weld-fabricated forgings of Inco 718. Eleven structural struts connect the inner structure to the outer case. High strength bolts hold the outer ends of the struts to the outer diameter case. Mar-M509 aerodynamic fairings surround the structural struts, shielding them from the hot gas path and turning the gas path flow by 5 degrees. The fairings have integral inner and outer platforms similar to turbine nozzle vanes, which form the inner and outer diameter gas path walls. Platforms gaps are sealed with feather seals.

A simplified NASTRAN model of the hot strut case was constructed to determine structural strut deflections (see Figure 143). Loads included in the analysis for the integrated core/low spool design were (1) case ΔP , (2) axial pressure load (thrust balance load), (3) thermal loads, (4) mount loads, and (5) rotor imbalance. Maneuver loads for the flight propulsion system were also included in this analysis.

Deflection Analysis

A summary of deflections of the hot strut case is presented in Figures 144 and 145. The results of the deflection analysis indicated that the location of minimum clearance to the inner diameter of the fairing occurs at section K-K (see Figure 145). At this location, a minimum gap of 0.000 inch axially or 0.010 inch tangentially exists, assuming worst dimensional stack-up of tolerances (see Figure 146). The strut exterior is coated with aluminum oxide to further guard against excessive heat transfer to the structural strut.

Active clearance control air flow from the high-pressure turbine case is directed over the inner diameter wall of the outer case by means of a sheet metal flow guide to improve thermal response of the outer diameter case during transients. The flow then passes into the cavity outboard of the outer diameter fairing platform, where it leaks into the gas path or passes between the structural strut and fairing to the cavity inboard of the inner diameter fairing platform.

Tenth stage compressor air is fed into the outer diameter of the structural struts and passes through the center of the struts by means of drilled holes (see Figure 147). This air cools the strut and cools the rim area of second stage disk. Next, this air leaks past the thrust balance seal to pressurize the cavity between the low-pressure rotor and hot strut case and then passes into the drum of the low-pressure rotor to cool spacers and disk rims of stages 3 through 5.



PRATT & WHITNEY AIRCRAFT GROUP
COMMERCIAL PRODUCTS DIVISION

ORIGINAL PAGE 17
OF 1004 CUREN

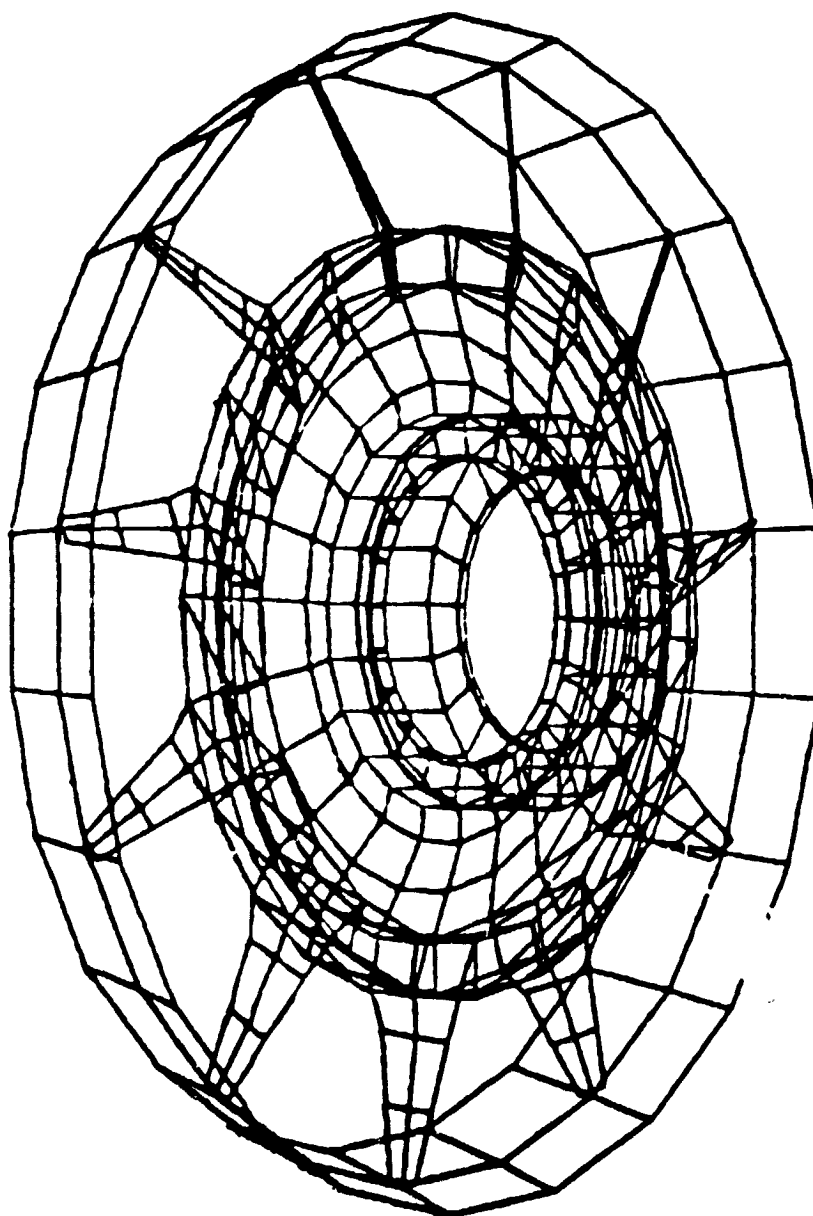


Figure 143 NASTRAN Model of the Hot Strut Case



CIRCUMFERENTIAL DEFLECTION DUE
ALMOST ENTIRELY TO THERMAL FIGHT

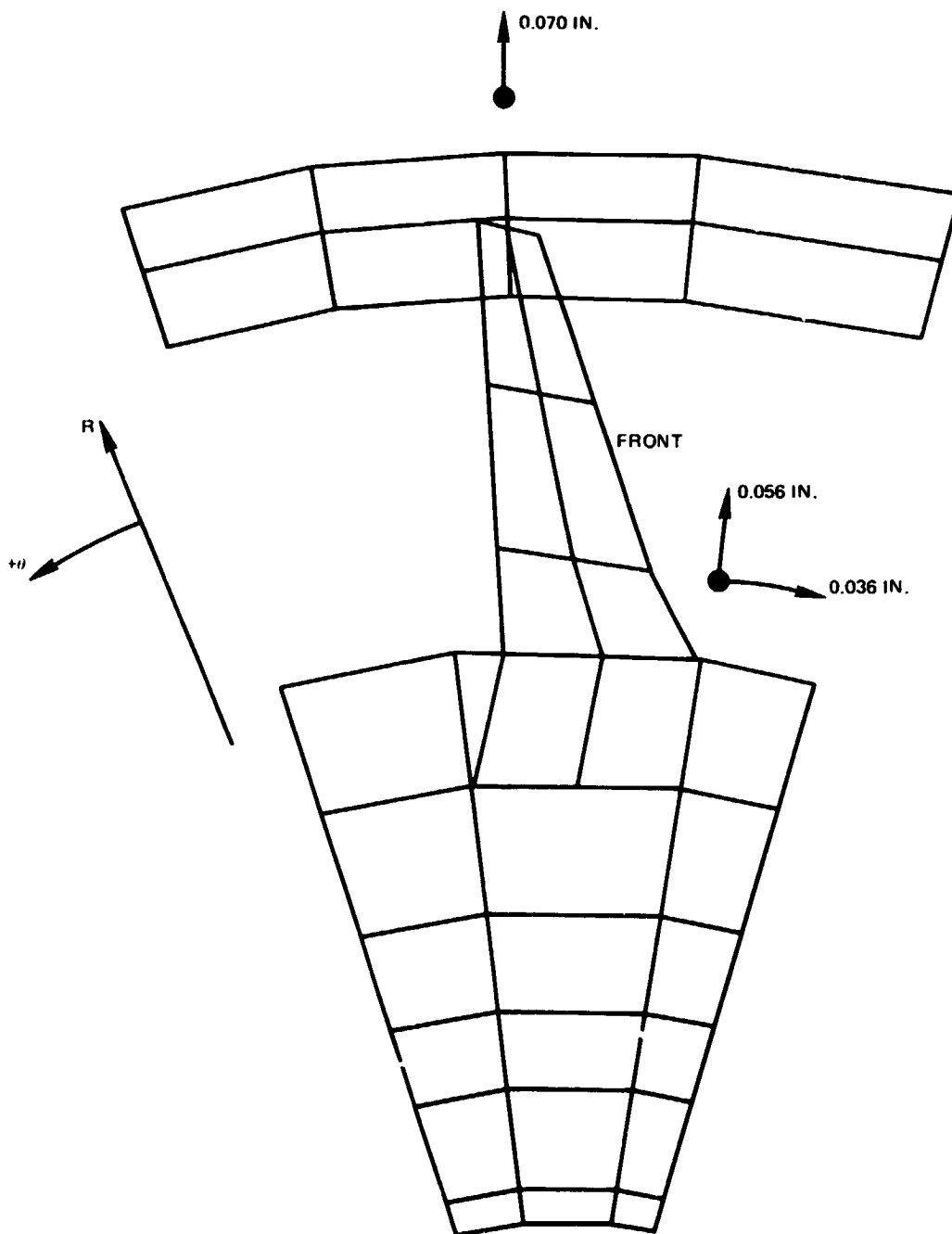
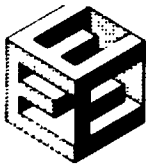


Figure 144 Hot Strut Case Radial and Circumferential Deflection Summary



ORIGINAL PAGE 12
OF POOR QUALITY

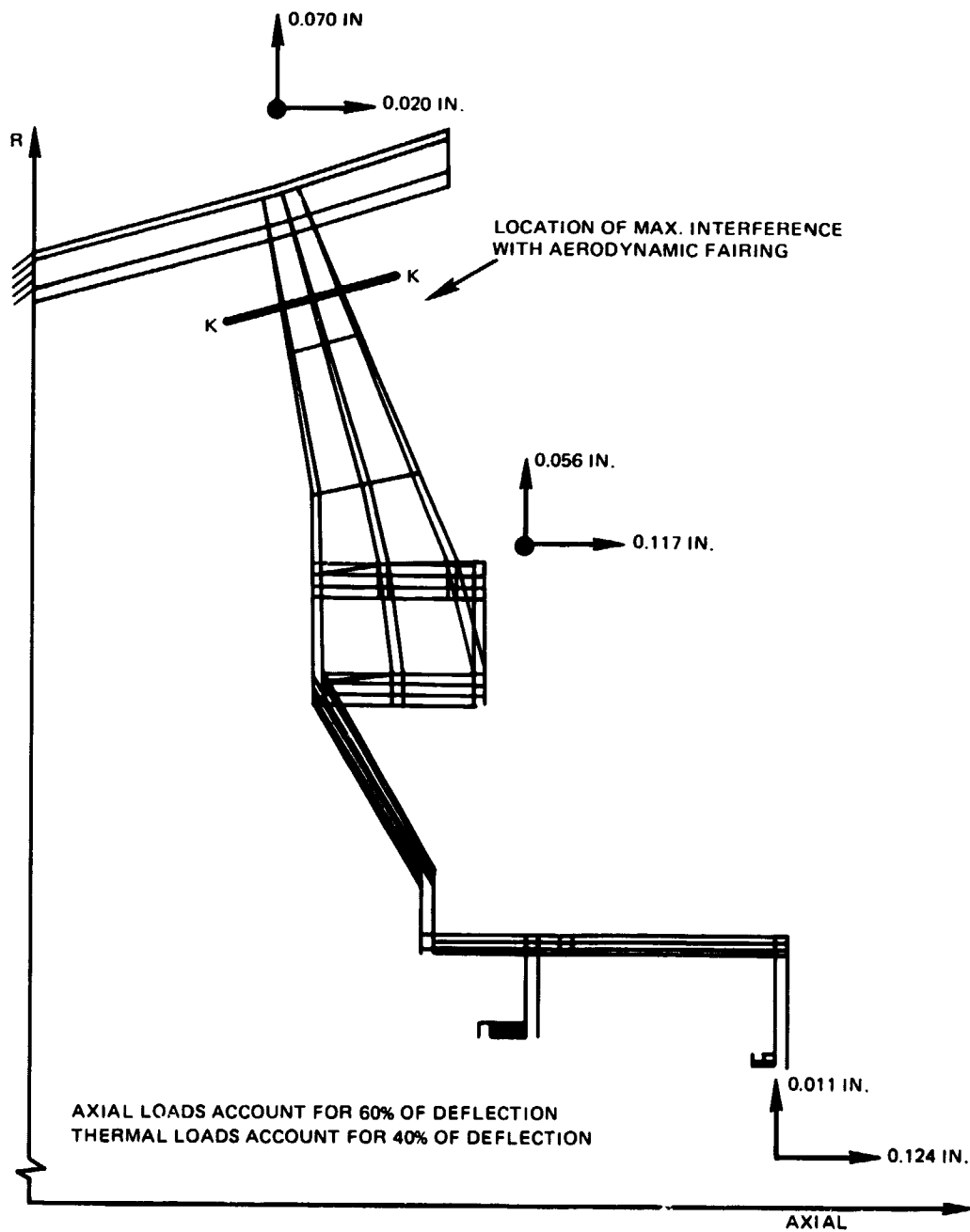


Figure 145 Hot Strut Case Radial and Axial Deflection Summary



PRATT & WHITNEY AIRCRAFT GROUP
COMMERCIAL PRODUCTS DIVISION

ORIGINAL FILED IN
OF POOR QUALITY

STRUCTURAL STRUT – AERODYNAMIC FAIRING CLEARANCES DETERMINED FROM NASTRAN DEFLECTIONS

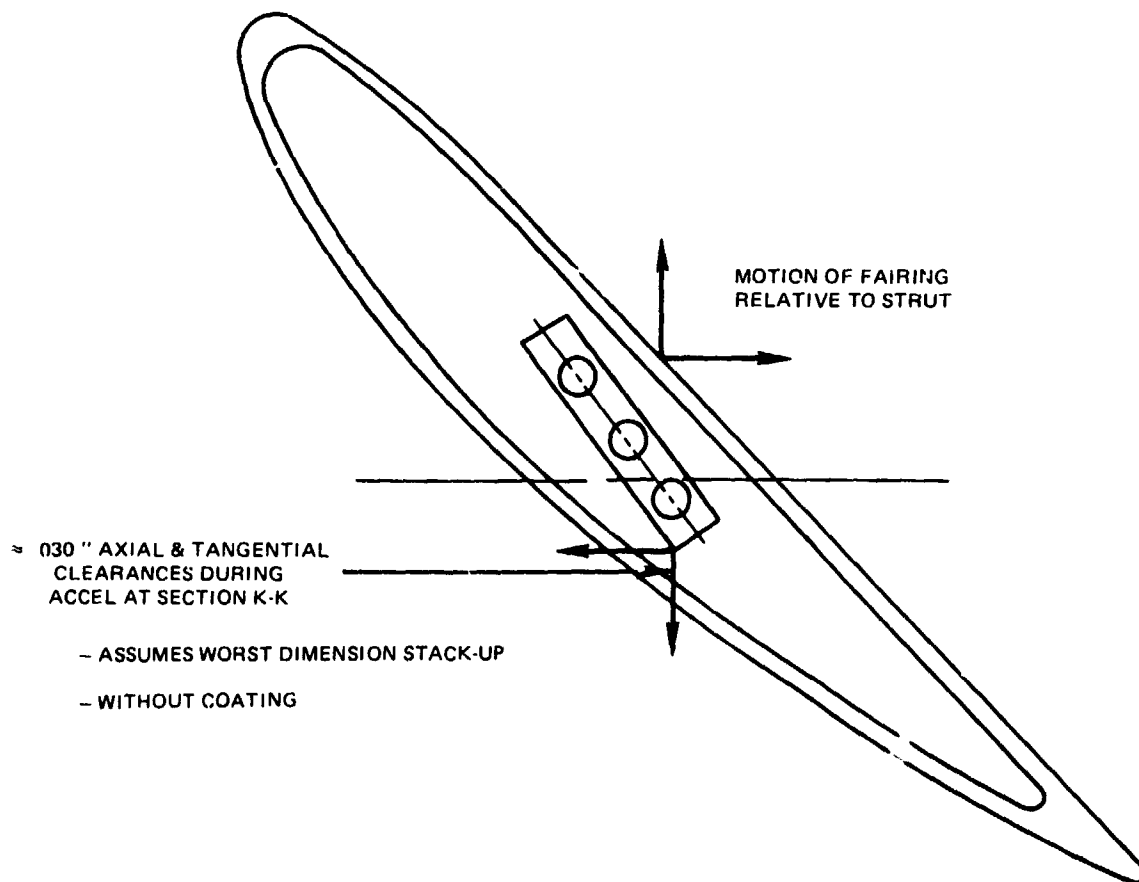


Figure 146 Hot Strut Fairing Clearance Summary



Life Analysis

Cyclic life analysis of the case assembly indicated that minimum life occurs in the structural struts. The calculated flight propulsion system lives for various strut sections are shown in Figure 147 and those for the integrated core/low spool in Figure 148. The life requirement is 20,000 cycles for the flight propulsion system and 1000 cycles for the integrated core/low spool. Figure 147 indicates that life requirements have not yet been met at the inner cooling air holes. Current design efforts are continuing toward a resolution of this problem area.

Retention Bolt Stress Analysis

The outer case-to-strut retention bolt was analyzed in detail because it carries all of the loads from the inner strut to the outer case. The results of a stress analysis conducted on this bolt are listed in Table 81. For the integrated core/low spool, a high-strength MP159 bolt, which is common with the high-pressure turbine disk to high-pressure compressor rear hub rotor retention bolt, was used for schedule and cost reasons. A larger diameter bolt of Inco 718 material was selected for the flight propulsion system. As shown by the summary, calculated stresses are below the yield stresses.

TABLE 81
HOT STRUT BOLT STRESS SUMMARY

	TENSILE STRESS <u>Ksi</u>	MAX. SHEAR STRESS <u>Ksi</u>	MAX. PRIN. STRESS <u>Ksi</u>	σ_{ys} <u>Ksi</u>	σ_{ult} <u>Ksi</u>
IC/LS MP159					
Cold Assembly	175	115	200	240	275
Steady State	145	85	155	200	225
FPS INCO 718					
Cold Assembly	130	85	145	165	200
Steady State	110	70	125	145	185



ORIGINAL PAGE 12
OF POOR QUALITY

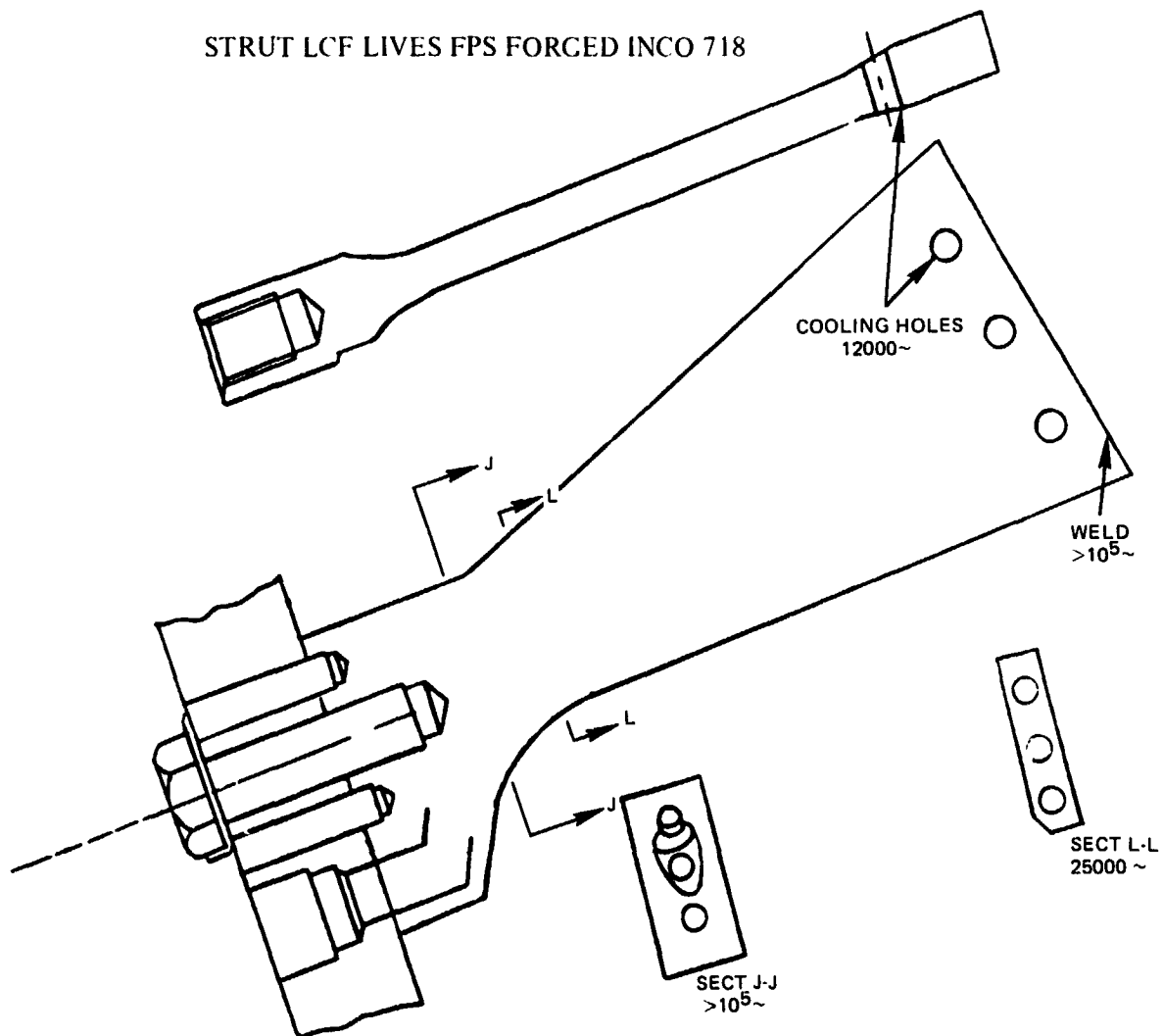


Figure 147 Flight Propulsion System Hot Strut Low Cycle Fatigue Lives

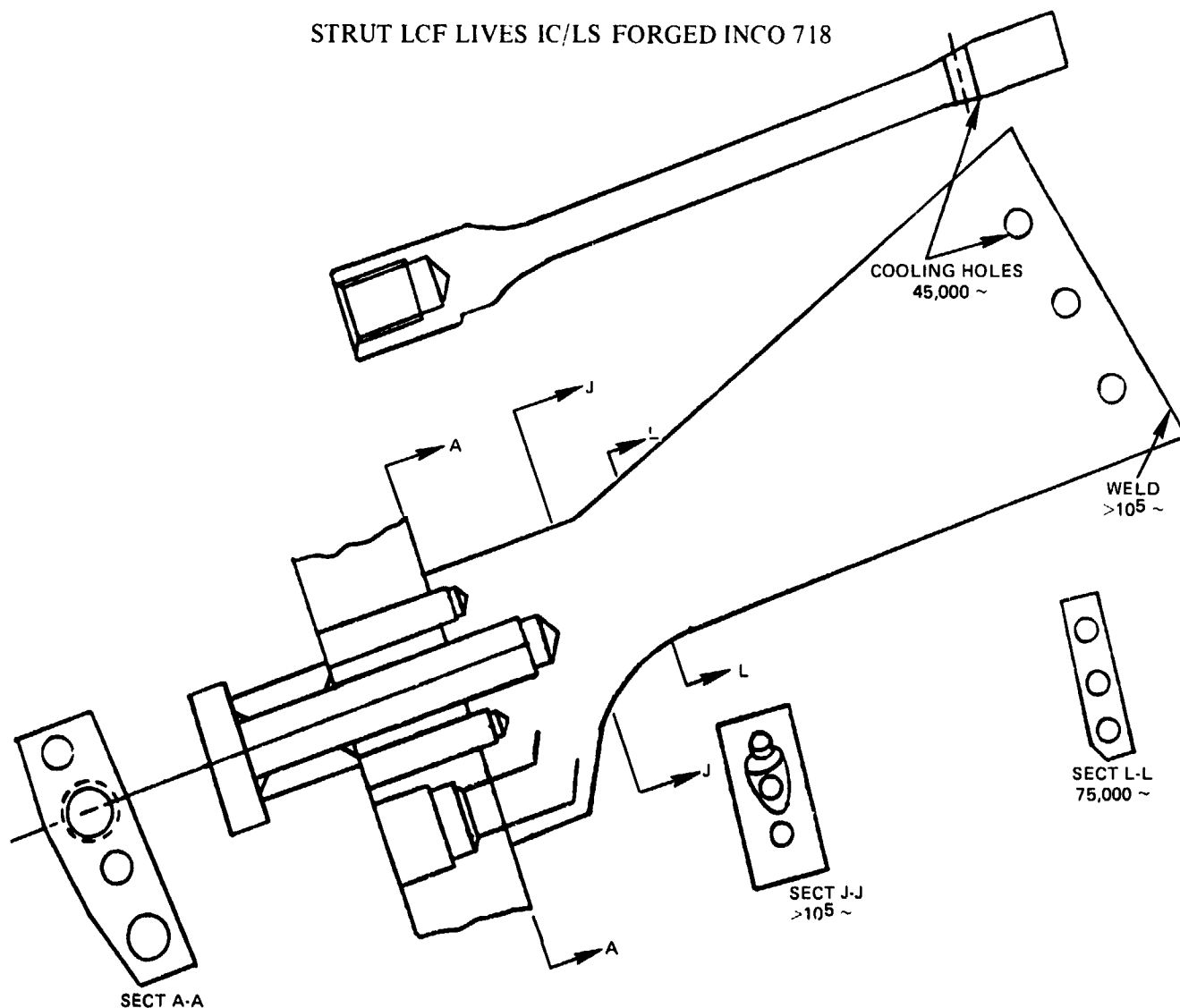
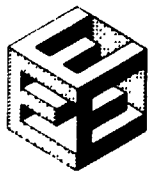


Figure 148 Integtated Core/Low Spool Hot Strut Low Cycle Fatigue Lives



HIGH-PRESSURE TURBINE "WARM" RIG

All layout design work and thermal/structural analysis on the high-pressure turbine "warm" rig was completed during the current reporting period. A detailed design review for the rig was held concurrently with the that for the component at NASA Lewis on May 21 and 22 1980. Approval of the design was granted on 11 June 80.

The "warm" rig is the vehicle in which the components will be first tested and the aerodynamic performance fully measured and developed. This will be accomplished by conducting a cascade loss test followed by a full stage performance test.

Rig Design Features

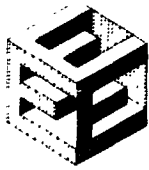
The major features of the rig assembly include rig inlet section, rotor and vane assembly, and rig exhaust section. The rig will feature separate controls for all secondary flows as well as main flow. In addition, a separate system is provided for the active clearance control system, which covers an approximate 300 F temperature range for clearance change. The main flow temperature will be 800 F with the appropriate secondary air temperature ratio to simulate engine conditions. A circumferential traverse instrumentation ring has been provided to acquire a more thorough mapping behind the vanes and blades. A cross-section of the rig is shown in Figure 109.

Materials

Raw material requirements for the initial rig design phase were established by using the preliminary rig cross-section layout as the basic design concept. All rig hardware exposed to main airflow or secondary airfoil has been designed using stainless steel or comparable rust-resistant alloys to prevent rust build-up during testing. In addition, the 800 F inlet temperature dictated certain materials with proper thermal response. One example of this is the inlet outer case, which needed a high thermal expansion plus high strength. PWA 1075 was chosen for this application. Insulation is being used on the inlet flowpath cases to prevent the secondary cooling air from adversely affecting the main flow temperature. External rig hardware will be of less expensive low carbon steel material.

Rig Safety Features

The rig safety system is characterized by three primary modes. The first is an explosive system activated by the occurrence of an overspeed condition. The main stream airflow bypasses the rig and re-enters in the exhaust duct. The second system is a pop-valve, which also allows the airflow to bypass the rig. In addition to speed, the pop-valve can be excited by loss of oil flow, bearing compartment adverse pressure gradients, excessive vibration, and excessive bearing temperature. The third system is an alarm system, which is activated when the limits of various rig parameters are exceeded.



Secondary Flow System and Thrust Balance

The "warm" rig simulates engine cooling air and leakage flows and blade tip clearances while preventing oil weepage from the bearing compartments and excessive thrust bearing loads. Figure 149 presents a schematic representation of the rig secondary flows.

Extensive rig instrumentation will allow measurement of these key flows with calibrated venturis or cold flow calibrated hardware. It will also provide confirmation of leakage and swirl field flows with static and total pressure sensors and cooling air temperatures and windage heat generation with thermocouples. Key thrust balance cavity pressures will be continuously monitored and processed to give on-stand read-out of thrust load.

The high-pressure compressor rear seal air supply will be injected tangentially to simulate the high-pressure compressor discharge bleed swirl in the engine. There will be separate control of the disk front rim cavity "mini" tangential on-board injection flow to change the swirl level and, hence, blade supply pressure. This will also affect thrust load. The temperature of the active clearance control air will also be controlled between 65 F and 400 F. This control will change outer air seal (blade tip) clearances over the range available with the engine active clearance control system. The bearing compartments will be vacuum-pumped to provide a positive pressure gradient across the seals, thus preventing oil weepage. The rotor has been thrust-balanced so that the maximum load is 8,839 lb.

Rig Active Clearance Control System

The active clearance control system is used in the test program to evaluate its effectiveness during rig performance testing. The internal hardware of the active clearance control system for the integrated core/low spool is also used in the rig. The integrated core/low spool outer turbine case could not be used because of the requirement to place the exit probes in a specific axial location incompatible with the case design. A rig-unique case was therefore designed to accommodate the required instrumentation. The material chosen for the rig case, INCO 600, is a relatively low-cost nickel-based alloy that adequately matches the PWA 1007 (Waspaloy) material of the integrated core/low spool in thermal expansion properties. The rig design was analyzed to ensure that the outer air seal, over the turbine blade tip, moves out parallel to the rig centerline in order to maintain essentially chordwise clearance between the blade tip and outer airseal platform during temperature excursions. The active clearance growth summary is shown in Figure 150.

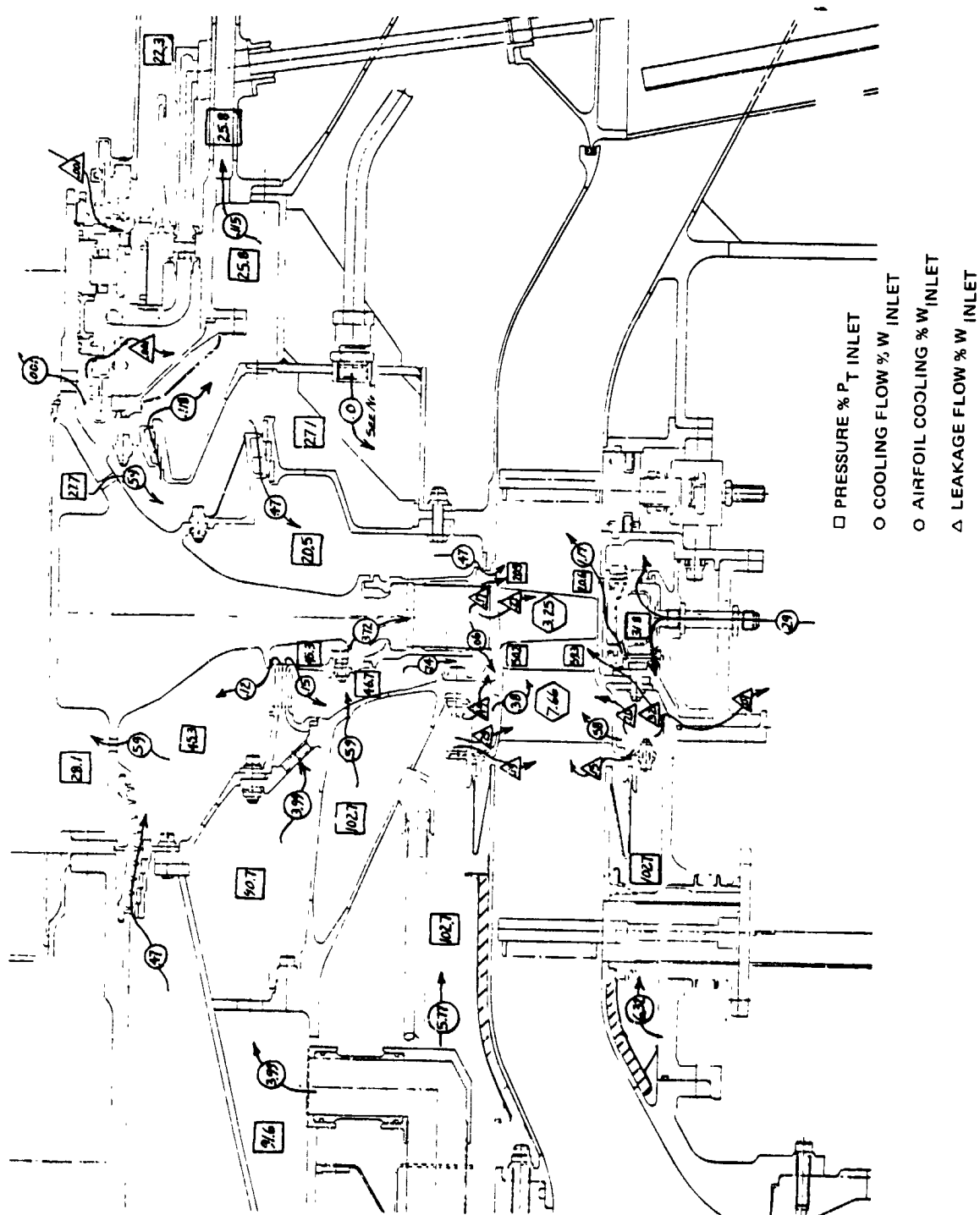
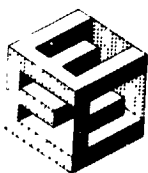
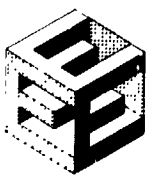
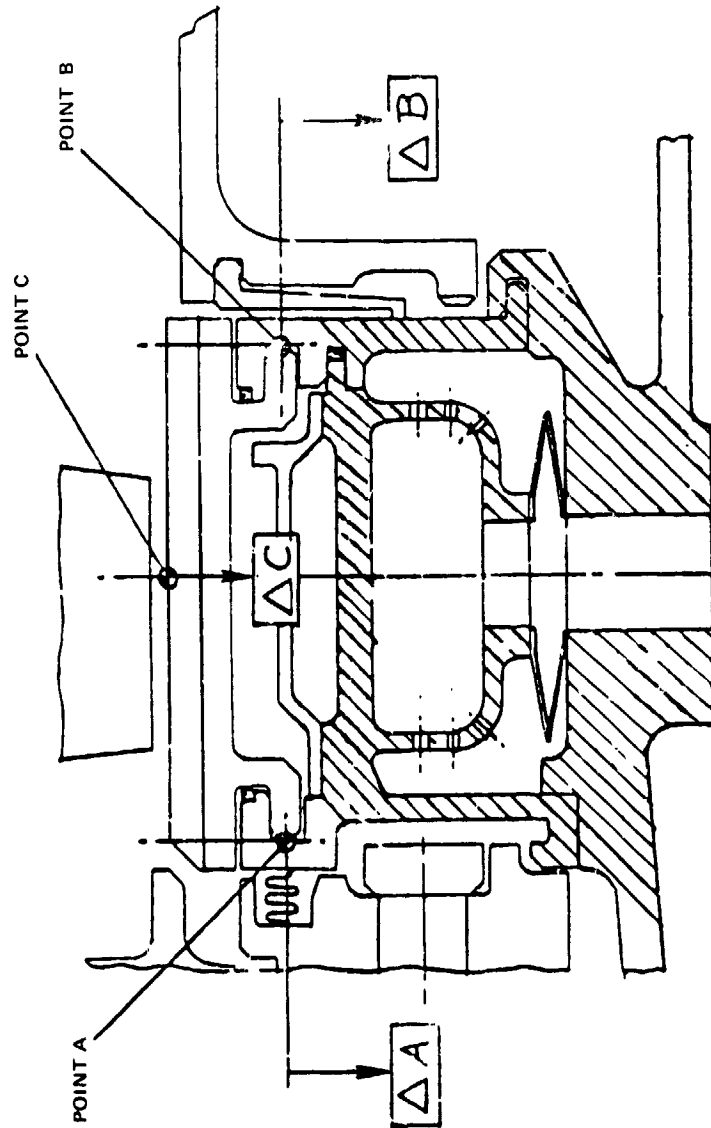


Figure 149 High-Pressure Turbine Rig Secondary Flows



ORIGINAL PAGE 18
OF POOR QUALITY



- CONDITION 1
- GROWTH AT RIG RUNNING TEMPS
- CONDITION 2
- GROWTH WITH +200°F ΔT (CROSS-HATCH AREA)

COND.	Δ GWTH PT A	Δ GWTH PT B	Δ GWTH PT C
1	0.0110	0.0098	0.0086
2	0.0235	0.0242	0.0249
DIFF. PTS 1&2	0.0125	0.0144	0.0163

Figure 150 Active Clearance Control Growth Summary



Rotating Hardware

The rig rotor design was analyzed for critical speeds, and rotor tie bolts were analyzed for blade loss capability. In addition, the rotor air seals were reviewed for resonance and coincidence. The critical speeds and mode shapes determined from the rotor dynamics study are shown in Figure 151. Because the mode shapes indicate a critical condition, a forced response analysis was conducted. The result at bearing loads corresponding to 1 mil of bearing support vibration at the speeds shown were judged to be acceptable (see Table 82).

TABLE 82

HIGH-PRESSURE TURBINE "WARM" RIG
FORCED RESPONSE RESULTS

Rotor Speed (rpm)	Bearing Loads for 1 Mil Bearing Support Vibration (lb)		Remarks
	Front Bearing	Rear Bearing	
4500	75	306	Acceptable
9850	508	851	Acceptable

The calculated stress in the rotor tie bolts resulting from a blade loss situation is 70,000 psi., which is well under the 0.2-percent yield stress level of INCO 718.

Seal dampers were provided for the rotor air seals as a conservative measure to avoid resonance or coincidence problem. The dampers are fitted to the static seal lands.

Bearings and Seals

The bearing compartments were designed using existing parts with minor modifications. Key features of the front and rear bearing compartments are described as follows.

The front bearing compartment has a 220 mm bore and a 320 mm flanged outer diameter. Its maximum DN is 2.1×10^6 , and its maximum load is less than 10,000 lb. Calculated B1 life is greater than 250 hours.

The front compartment seals are the dry face type with an oil-cooled carbon rubbing plate. Stackpole 2090 carbon grade seals are used for improved durability. Air temperature in the compartment is estimated to be 150 F. The seal operating conditions are listed in Table 83.



PRATT & WHITNEY AIRCRAFT GROUP
COMMERCIAL PRODUCTS DIVISION

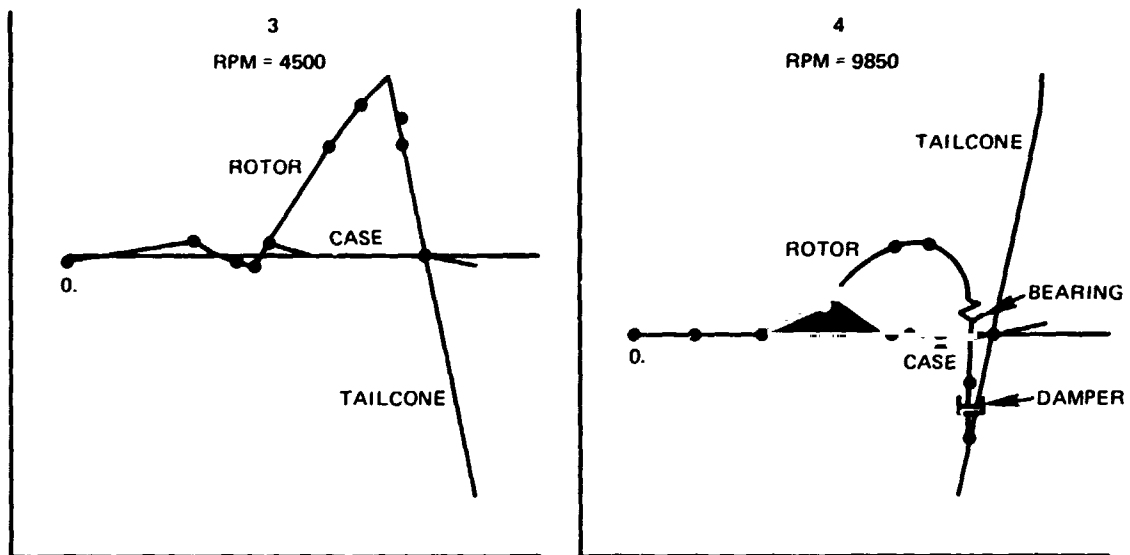


Figure 151 High-Pressure Turbine "Warm" Rig Critical Speeds and Mode Shapes



TABLE 83

FRONT COMPARTMENT OPERATING CONDITIONS

<u>Condition</u>	<u>Seal ΔP (psi)</u>		<u>Rubbing Speed (ft/sec)</u>
	<u>FORWARD</u>	<u>REAR</u>	
ADP	33	32	400
Max. Speed	38	37	440
ΔP Range*	27-51	26-50	

* Range expected to be encountered during rig operation

The design of the rear compartment bearing for the rig is the same of that of the number 4 bearing for the integrated core/low spool. This oil-damped bearing has a 100 mm bore and a 222 mm outer diameter, and is equipped with a soft centering spring. It also features preloading and under race oil cooling. Its maximum radial load is less than 1000 lb, and its calculated B1 life is greater than 1000 hours. The maximum DN is 1.6×10^6 ,

The design of the rear compartment forward seal is the same as that of the number 4 seal for the integrated core/low spool, and the rig rear seal is derived from the integrated core/low spool number 5 rear seal. Both are the dry-face type seal with oil cooled rubbing plates. Stackpole 2080 carbon grade seals are used for improved durability. The temperature of the surrounding air is maintained at 150 F. Operating conditions of the seals are shown in Table 84.

Rig Instrumentation

High-pressure turbine rig instrumentation measures overall stage performance and provides basic aerodynamic data as well as airfoil and endwall aerodynamic loading information. In addition, it monitors rig safety parameters and also assesses the performance of the "mini" tangential on-board injection system and active clearance control system. Both the cascade and the full-stage rigs have essentially the same instrumentation. A rig supervisory system will be employed to automatically control all of the secondary flow systems. All probes and wires are calibrated before installation.

The following subsections describe rig performance instrumentation, rig design instrumentation, and facility/rig adaptation. A summary of "warm" rig instrumentation is presented in Table 85.



PRATT & WHITNEY AIRCRAFT GROUP
COMMERCIAL PRODUCTS DIVISION

TABLE 84

OPERATING CONDITIONS OF THE REAR COMPARTMENT SEALS

<u>Condition</u>	<u>Seal ΔP(psi) Both Seals</u>	<u>Rubbing Speed (ft/sec)</u>
ADP	6	293
Max Speed	6	324

Operating Requirement: 10 psia Compartment Pressures

TABLE 85

INSTRUMENTATION SUMMARY

	<u>T_T</u>	<u>P_T</u>	<u>T_{Air}</u>	<u>T_{metal}</u>	<u>P_S</u>	<u>Miscellaneous</u>
Rig Super- visory Control	2	2	10	-	16	-
Inlet	80	40			24	
Vane Surface & Shrouds					153	
Blade OAS & ACC			22	28	22	4 Laser Prox.
Exit	48	48			24	4 Air Angle
Vane Cooling			15		16	
TOBI			22		22	
Disk Bore Cooling		12	64		64	
Exit Cavities			8		8	



TABLE 85 (Cont'd)

	<u>T_T</u>	<u>P_T</u>	<u>T_{Air}</u>	<u>T_{metal}</u>	<u>P_S</u>	<u>Miscellaneous</u>
Bearing Com- partments			10	24	22	10 Vibration 3 speed
Totals	P _T	100	Laser Proximity		4	
(perf)	T _T	128	Vibration		10	
	P _S	355	Speed		3	
(non perf)	T _{AIR}	142	Air Angle		4	
	T _{metal}	52				

Performance Instrumentation. Performance instrumentation measures inlet and exit flow, blade tip clearance, and torque.

Inlet Instrumentation. Inlet instrumentation consists of 4 total pressure rakes, each with 10 sensors. In addition, there are 6 static pressure taps located on both the inner and outer flowpath. The inlet rakes are properly located circumferentially to prevent any rotor excitation.

Exit Instrumentation. Exit instrumentation consists of 4 total pressure rakes and 4 total temperature rakes each with 12 sensors. In addition, there are six static pressure taps located in both the inner and outer flowpath. The rakes are located on a ring that can be traversed circumferentially approximately 30 degrees. These rakes are positioned 90 degrees apart. Coupled with the pressure and temperature rakes, there are 4 air angle probes located at the exit plane. These probes are wedge shaped and have the ability to traverse radially as well as circumferentially. They are used to measure two static pressures and a total pressure, and are also used to calculate exit air angle.

Blade Tip Clearance Measurement. Four laser probes equally spaced will be used to measure and monitor the blade tip clearance. These probes will be attached to the blade outer air seal shoes, permitted to grow through the outer cases, and sealed by means of piston rings. Temperature variations in the flow to the active clearance control system will provide tip clearance changes. Probe measurements will then be used to determine any changes in performance resulting from variations in tip clearance.



PRATT & WHITNEY AIRCRAFT GROUP
COMMERCIAL PRODUCTS DIVISION

Torque Measurement. A load cell torque measuring system will be used in addition to the standard thermal techniques of determining overall performance. The load cells are activated by lever arms attached to dynonometers.

Design Verification Instrumentation. Design instrumentation verifies design assumptions and measures static temperatures, pressures, and bearing temperatures. Probe strain gages and accelerometers are also used.

Static Pressure. Two turbine vanes will be instrumented on the airfoil surface at three spanwise locations. Seventeen airfoil static pressure taps will be positioned at each location, 10 on the suction surface and 7 on the pressure surface. Endwall static pressure taps will be placed at both the inner and outer flowpath platforms. The number of these used will depend on available platform area. Static pressure taps will also be located throughout the rig in order to determine cooling and leakage flows.

Static Temperature. One vane will be instrumented in the airfoil section to determine the effectiveness of the cooling scheme. In addition, instrumentation will be located on the active clearance control system to verify its operation. All cooling flow systems will be instrumented to monitor and maintain control of coolant flow temperatures.

Bearing Temperatures. Thermocouples will be located in the bearing compartments to ensure proper bearing and seal operating temperatures. This instrumentation will be monitored throughout the test program.

Probe Strain Gages. The fixed inlet rakes will be strain gaged at the root of the rake to detect probe vibratory modes that might exist at test conditions.

Accelerometer. Both horizontal and vertical accelerometers will be located on the front and rear bearing supports. These will be monitored throughout the test program.

Facility/Rig Adaptation. The facility for testing the high-pressure turbine "warm" rig will provide a closed-loop air supply system. Two natural gas burners heat the primary air to approximately 800 F. The secondary air, supplied by the mainstream air upstream of the burner, is delivered to the rig at approximately 150 F, thus maintaining the proper main air temperature and cooling air temperature ratio. Power generated by the turbine is absorbed through two 10,000 hp dynonometers. The rig is connected to the power absorption system through a coupling and gearbox. There are provisions for seven independent secondary cooling air systems. Flow for both the primary and secondary air systems is metered through critical flow venturies. An automated data secondary system will be used to process data, and a rig supervisory system will be employed to control all secondary flows.



3.2.7.4 Supporting Technology

3.2.7.4.1 Leakage Test Program

The objective of this program is to investigate and minimize the coolant air leakage paths related to the blade attachments and vane inner and outer platform regions. The goal high-pressure turbine cooling and leakage flow for the flight propulsion system is 11.2 percent Wae.

The leakage test program comprises four phases. Blade and vane attachment leakage areas are identified during the preliminary design phase of the high-pressure turbine component effort. A plastic model of the high-pressure turbine blade attachment is fabricated and assembled to help visualize and correct assembly and sealing requirements. Metal models are fabricated and assembled to quantitatively define the leakage flow associated with the attachment areas. Static pressure instrumentation is used for these measurements. Evaluated concepts include flange seals, full ring side plates, and feather seals between adjacent vanes.

Testing of each model documents leakage flow parameters over pressure ratio ranges consistent with Energy Efficient Engine applications. Flow, temperature, and static and total pressure measurements are taken at each condition. Each leakage path is systematically sealed off to determine its contribution to engine leakage. High leakage areas are redesigned and retested to verify leakage reduction. Comparisons between experimental data and predicted leakages from the design system are used to complete the design of blade and vane attachments.

All efforts under this supporting technology program are complete. Program results are summarized in the Fourth Semiannual Status Report. A draft of the technology report has been submitted to NASA for review and approval.

3.2.7.4.2 Supersonic Cascade Test Program

The objective of this program is, through a combination of analyses and test activities, to improve the ability to optimize the design of a low-loss airfoil for the high-pressure turbine.

The supersonic cascade test program consists of five phases. To initiate the program, six airfoil configurations are selected and designed. Cascade assemblies are designed and fabricated in preparation for testing. In addition, instrumentation is designed, data reduction methods established, and a test plan defined. The low-loss concepts investigated include controlled coolant discharge, end wall contouring, and optimized distribution of airfoil loading.

Cascade testing simulates flight propulsion system Reynolds numbers and Mach numbers. Test data are compared to analytical predictions, and the high-pressure turbine airfoil design is updated accordingly.



All technical effort for this supporting technology program is complete. Program results were presented in the Third Semiannual Status Report.

3.2.7.4.3 Cooling Model Test Program

3.2.7.4.3.1 Objective

Verify, through water flow visualization tests, that the desired distribution of cooling flow within the high-pressure turbine blade is achieved.

3.2.7.4.3.2 Scope of Total Work Planned

This program consists of the four phases shown in Figure 152. Initially, the program considers a simplified large scale two-dimensional Plexiglas blade model incorporating internal features and flow areas of the Energy Efficient Engine design. Qualitative and quantitative test data analysis determines if the configuration is acceptable. The results are incorporated into the full-scale blade design.

During the detail design for the high-pressure turbine, a second model incorporating internal features plus twist and curvature is designed and tested to verify fully attached internal flow and pressure drop. By using flow visualization models, areas of stalled low velocity or recirculating flow can be identified prior to hardware procurement.

3.2.7.4.3.3 Technical Progress

3.2.7.4.3.3.1 Summary of Work Previously Completed

As indicated in Figure 152, efforts associated with the two-dimensional test phase of this program were completed prior to the current reporting period, as was the analysis and design of the three-dimensional flow visualization model.

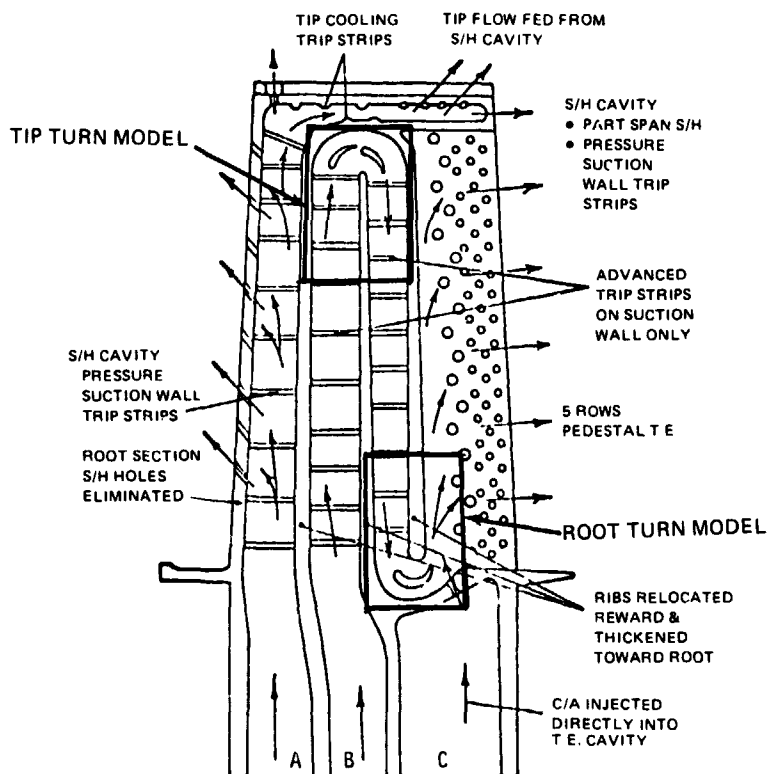
The two-dimensional model is illustrated in Figure 153. Initially, root and tip turn configurations without turning vanes were tested in this model.

Testing results revealed flow separation and recirculation in an acute corner of one of the flow cavities. Turning vanes were added, and the root model showed no improvement. The tip model, however, exhibited significant improvement with only slight flow separation. A corner fillet was installed in the tip model, and testing indicated that this addition also reduced corner recirculation. Taper was added to the turning vanes, but failed to further rectify the turning problem. This model was subsequently modified to provide radial flow discharge, fillets, and additional blade root coolant injection to more nearly simulate the full size blade configuration that was evolving out of the analysis and design effort. Initial testing of this configuration

[illegible]

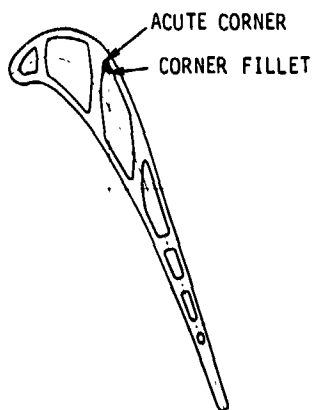
**H DENOTES MAJOR MILESTONE *D DENOTES KEY DECISION POINT

Figure 152 Cooling Model Test Program Work Plan Schedule

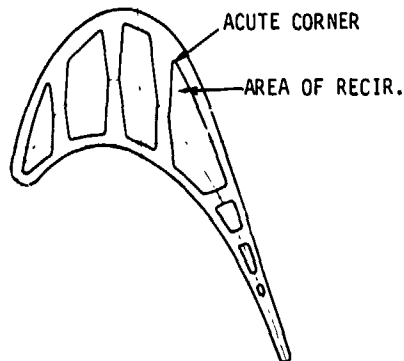


FLOW REDISTRIBUTED TO
MAINTAIN TOTAL C/A FLOW = 2.57% WAE

"OPTIMIZED" CONFIGURATION



1/4 TIP SECTION



ROOT SECTION

Figure 153 Root and Tip Turn Flow Visualization Models



evaluated variations in coolant flow rate through passage "C" of Figure 153 to eliminate the root corner separation and recirculation problems. Slight improvement was observed with high flow injection. The model was again modified to increase pedestal area and to simulate a less convergent turn. Visual inspection revealed that this modification successfully eliminated the separation and recirculation of flow in the acute corner of the root section. The modified two-dimensional model is illustrated in Figure 154.

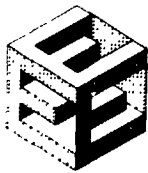
Following completion of the analysis and design of the three-dimensional flow visualization model, a technology design review was held at Nasa-Lewis in March 1980. This model was designed at five times normal size in order to more clearly illustrate the cooling flow patterns of the high-pressure turbine blade. In addition, this model was characterized by the same twist and curvature of the actual airfoil. The correct channel flow blockage was simulated by incorporating trip strips, draft angle on ribs, spanwise area distribution, and pedestal distribution. The 5x plastic model is illustrated in Figure 155.

In addition to completing the analysis and design effort, a test plan was formulated with the objectives of (1) identifying flow distribution problems, (2) eliminating separation zones, (3) verifying any subsequent design changes, and (4) providing information to the high-pressure turbine component detailed design effort.

3.2.7.4.3.3.2 Current Technical Progress

The work plan (see Figure 152) indicates that fabrication of the three-dimensional model was to have been completed during the current reporting period, and testing and post test analysis were supposed to have been initiated. Because of technical problems at the vendor, however, fabrication was not completed until late in the reporting period.

An inspection of the cooling model after fabrication indicated that the model contained some dimensional discrepancies. The model was subsequently returned to the vendor for corrections, further delaying testing. As a result, only testing associated with leakage checks was started at the end of this reporting period. The completed model is shown in Figure 156.



PRATT & WHITNEY AIRCRAFT GROUP
COMMERCIAL PRODUCTS DIVISION

ORIGINAL PAGE IS
OF POOR QUALITY

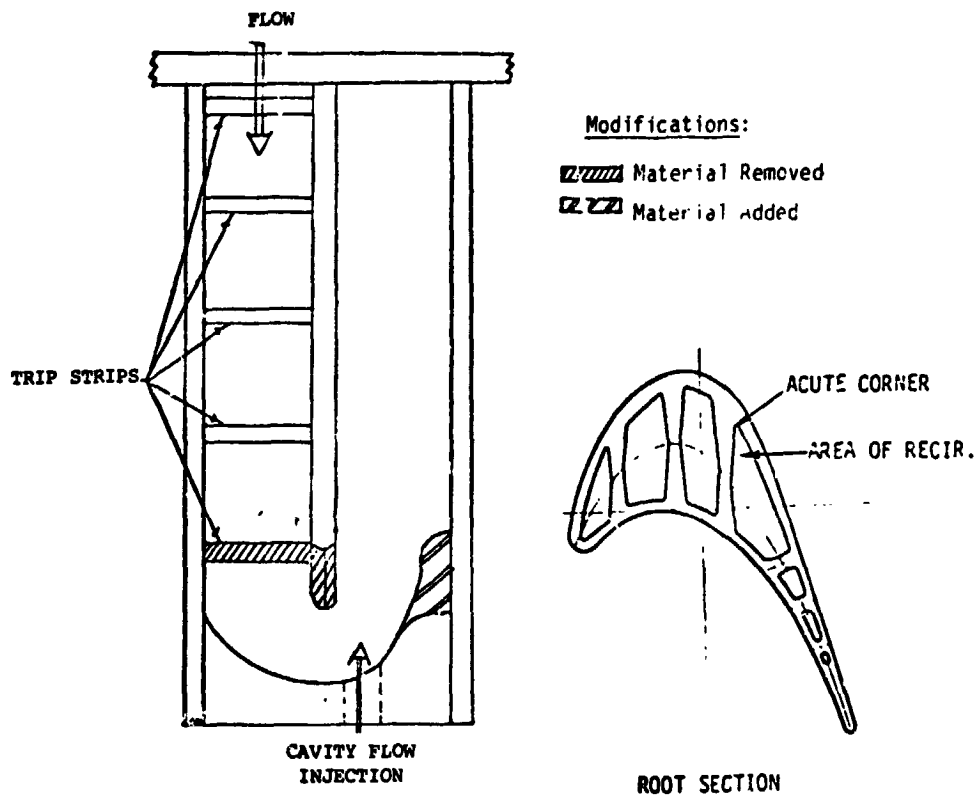


Figure 154 Modified Two-Dimensional Cooling Model

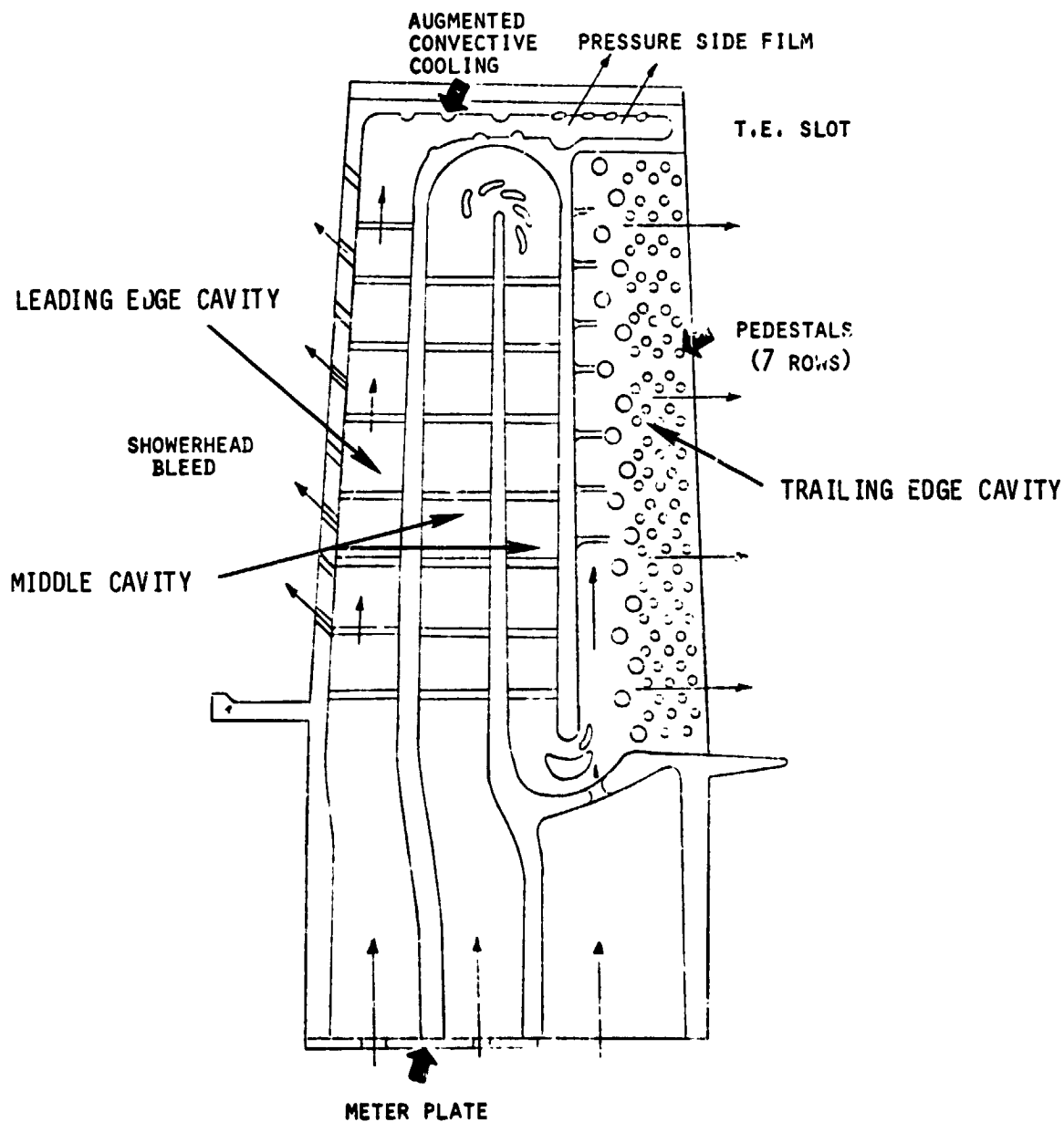


Figure 155 High-Pressure Turbine 5x Blade Plastic Cooling Model - The plastic cooling model was designed at 5 times normal size to improve the view of the internal flow distribution.



PRATT & WHITNEY AIRCRAFT GROUP
COMMERCIAL PRODUCTS DIVISION

ORDERING INSTRUCTIONS
OF POOR QUALITY



Figure 156 High-Pressure Turbine Three-Dimensional Cooling Model



3.2.7.4.4 Uncooled Rig Test Program

The objective of this program is to establish the uncooled aerodynamic efficiency base for the high-pressure turbine component by verifying the benefits of large turbine annulus area and high rim speed, defining the optimum reaction level, and evaluating the endwall loss reduction potential of a canted vane configuration.

A test program is conducted to determine the uncooled efficiency benefits gained by increasing rim speed and annulus area (AN^2), and increasing the turbine reaction level from 35 percent to 43 percent. In addition, the vane is canted 15 degrees in the direction of rotation to determine loss reductions. Vane annular cascade testing is conducted for each of the rotating rig builds, and blade stress studies are conducted on the second build (43-percent reaction level). The major effort comprises design, fabrication, and testing of three vane cascades and two rotating rigs.

All technical work for this supporting technology program has been completed. Program results appear in NASA report CR-165149.

3.2.7.4.5 High-Pressure Turbine Fabrication Development Program

The objective of this program is to apply Pratt & Whitney Aircraft single crystal two-piece airfoil casting and bonding technology to the fabrication of Energy Efficient Engine high-pressure turbine blade and vane shapes.

The program consists of three major phases. In the analysis and design of the airfoil, interactions between airfoil aerodynamics, heat transfer, structural analysis and tool design are considered. Wall thickness, internal passage configuration, trailing edge thickness and shape, type and location of cooling holes, and definition of bond surface are prime concerns.

Molds for airfoil casting and tools for bonding are designed and fabricated. A test plan is defined and airfoils are cast and bonded. Trial specimens undergo creep and tensile tests, microstructural analysis, and nondestructive inspection to verify the quality of the castings and bonds.

All technical work on this supporting technology program has been completed. Program results appear in the Fourth Semiannual Status Report. A draft of the technology report is currently being prepared.



3.2.8 Low-Pressure Turbine

3.2.8.1 Overall Objective

Develop the technology required to design a highly efficient low-pressure turbine, and to incorporate this technology into design and fabrication to demonstrate the potential for achieving the Energy Efficient Engine flight propulsion system low-pressure turbine performance goals of 91.5 percent efficiency, 0.7 percent pressure loss in the transition duct, and 0.9 percent pressure loss in the exit guide vane. Design goals are disk life of 20,000 missions/ 30,000 hours, blade and vane life of 15,000 hours, hot strut life of 9,000 hours/15,000 missions and vane, blade, and transition duct coating life of 9,000 hours.

3.2.8.2 Component Program Overview

The overall task effort consists of a component effort and three supporting technology sub-tasks. The component effort comprises the analysis and design and fabrication of the low-pressure turbine component. The three supporting technology programs are (1) the boundary layer test program, (2) the subsonic cascade test program, and (3) the transition duct test program. The original program effort included a turbine exit guide vane supporting technology test program. This program was cancelled at the first work plan update in March 1979 because it was judged to be of minimal technical risk. Figure 157 shows the relationships between these activities and their relationship to Tasks 1, 3, and 4. The work plan is shown in Figure 158.

3.2.8.3 Component Effort

3.2.8.3.1 Objective

Conduct the design, analysis, and hardware procurement activities necessary to develop a low-pressure turbine that meets the established goals.

3.2.8.3.2 Scope of Total Work Planned

The analysis and design effort consists of a preliminary analysis and design phase and a detailed analysis and design phase as shown in Figure 158. A six-month preliminary design activity is conducted to establish the aerodynamics of the low-pressure turbine flowpath and to determine the mechanical and structural feasibility of that configuration. This preliminary activity results in layout drawings and substantiating design data, to be presented to NASA at a preliminary design review in September 1978.

Approximately 14 months after the preliminary design review, a detailed design activity starts. Results available from the supporting technology programs are used to substantiate or improve the configurations established in the preliminary design. More sophisticated design and analytical procedures than those of the preliminary effort are used. The results of this effort are



PRATT & WHITNEY AIRCRAFT GROUP
COMMERCIAL PRODUCTS DIVISION

ORIGINAL PAGE IS
OF POOR QUALITY

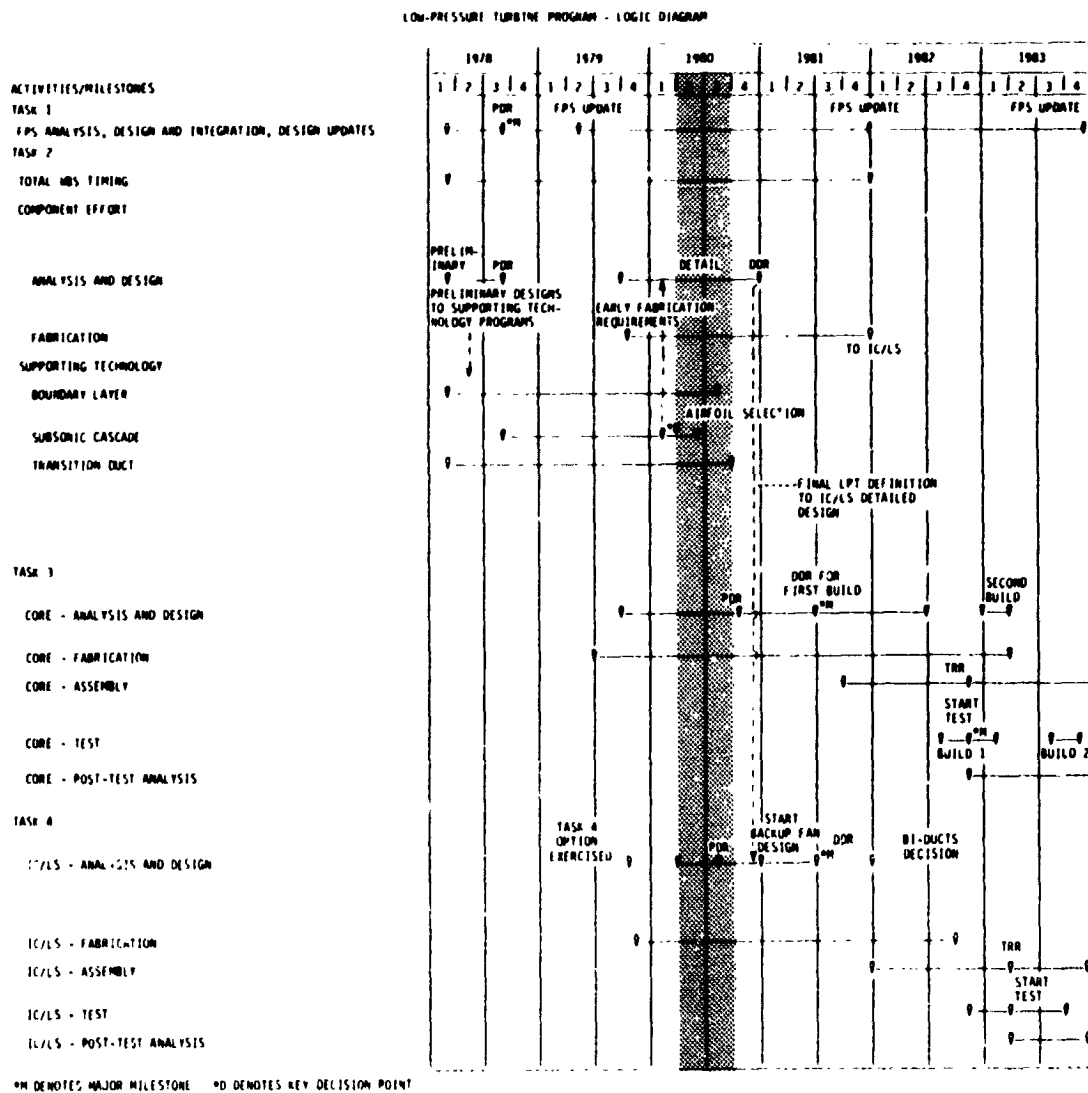


Figure 157 Low-Pressure Turbine Program Logic Diagram



LOW-PRESSURE TURBINE COMPONENT EFFORT - WORK PLAN SCHEDULE

	1978				1979				1980				1981				1982				1983			
	1	2	3	4	1	2	3	4	1	2	3	4	1	2	3	4	1	2	3	4	1	2	3	4
ACTIVITIES/MILESTONES																								
TOTAL WBS TIMING																								
COMPONENT ANALYSIS AND DESIGN																								
COMPONENT FABRICATION																								



PRATT & WHITNEY AIRCRAFT GROUP
COMMERCIAL PRODUCTS DIVISION

presented to NASA at a detailed design review in January 1981. Fabrication of the component parts is scheduled to start in the fourth quarter of 1980 and be completed in the fourth quarter of 1981.

Figure 158 indicates that all of the work associated with the preliminary analysis and design of the low-pressure turbine component was completed during a previous reporting period. The figure also shows that component detailed analysis and design work and fabrication work were continued during the current reporting period.

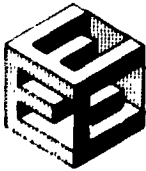
3.2.8.3.3 Technical Progress

3.2.8.3.3.1 Summary of Work Previously Completed

The low-pressure turbine design that evolved prior to the current reporting period is shown in Figure 159. This configuration is an uncooled, counter-rotating (relative to the high rotor) design featuring four stages, 749 blades, and a mean velocity ratio of 0.47. The need for cooling air is eliminated by the advanced materials used in the hot strut, second vane, and second blade. The counter-rotating feature reduces the losses from the inlet guide vane because of reduced turning. The rotor and stator assembly is coupled to the high-pressure turbine by a transition duct (turbine intermediate case). Turbine airflow is exhausted to exit guide vanes, which turn the flow axially into the mixer/nozzle.

The rotor and stator assembly incorporates the following features:

1. Double wall case construction with case-tied outer air seals and internal active clearance control for second and third stages.
2. Single backbone bolted rotor with front and rear hubs.
3. Stepped labyrinth, full ring, third through fifth stage inner air seals and second stage case-tied knife edge inner air seals.
4. Blade leading edge and trailing edge flow guides.
5. Advanced materials for cost effectiveness and benefits in weight and performance. (A complete listing of materials is shown in Table 86.)



PRATT & WHITNEY AIRCRAFT GROUP
COMMERCIAL PRODUCTS DIVISION

ORIGINAL PAGE 19
OF POOR QUALITY

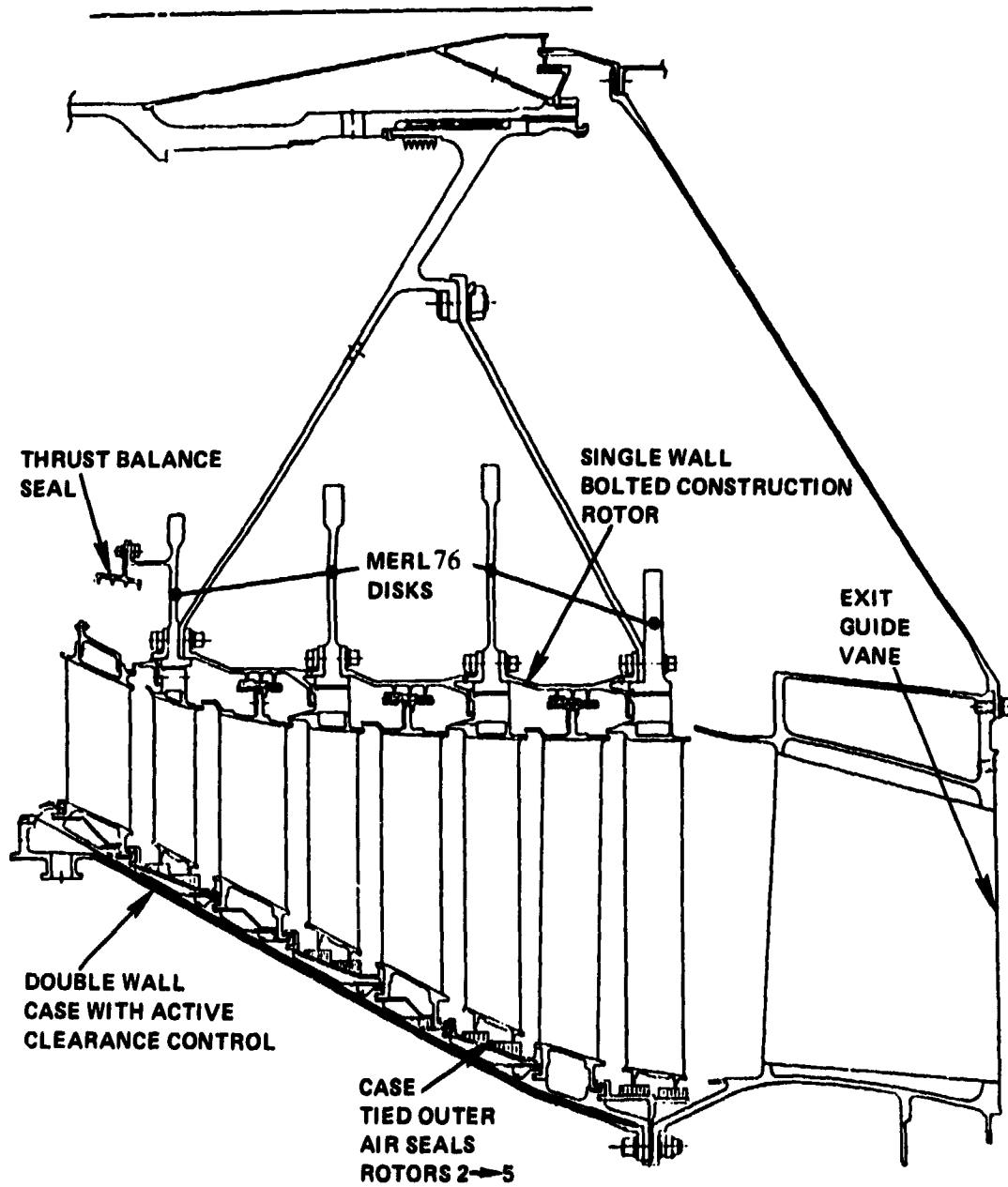


Figure 159 Low-Pressure Turbine Component



TABLE 86

LOW-PRESSURE TURBINE MATERIAL SUMMARY

<u>Part</u>	<u>Material</u>
2nd & 5th Disk/Hub	MERL 80 Disk with
Front Hub and Rear Cone	PWA 1003
3rd & 4th Disk	MERL 80
Rotor Spacers & Front Airseal	PWA 1003
2nd Vane	MERL 200/220, MERL 700 Coating
2nd Blade	PWA 1422/PWA 273 Coating
3rd Vane & 3rd Blade	PWA 655/PWA 73 Coating
4th & 5th Vane, 4th Blade	PWA 655/No Coating
5th Blade	MERL 101/No Coating
Case	Fabricated Wrought INCO 718
2nd & 3rd OAS (Case-Tied)	AMS 5754
4th & 5th OAS (Full Ring)	AMS 5771
Inner Airseal	AMS 5771

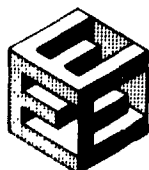
The turbine exhaust case includes a turbine exit guide vane to remove swirl from the low-pressure turbine exit flow. It is an integral ring-strut-ring structure with the 24 struts doubling as airfoils for the low-pressure turbine exit guide vanes. The inner ring supports the tailcone, which also provides the inner mixer support. The outer ring/case provides the mixer outer diameter support, provides the cone engine attachment for the engine/nacelle cowl load sharing, and transfers all loads from the turbine exhaust case forward to the low-pressure turbine outer case.

A summary of the aerodynamic characteristics of the low-pressure turbine resulting from the preliminary analysis and design is shown in Table 87. Current performance parameters at significant engine operating conditions are shown in Table 88.

The projected efficiency of 91.5 percent at the aerodynamic design point includes benefits derived from improved aerodynamics, reduced work factor, and reductions in clearances and leakage.

The hub design was re-evaluated in terms of deflection and weight reduction benefits. Results of this evaluation confirmed the selection of the double hub or "A-frame" configuration from the Preliminary Design Review.

The aft-loaded aerodynamic concept was selected as the most promising approach for the low-pressure turbine airfoils because it exhibited lower pressure loss than the "squared-off" concepts evaluated.



PRATT & WHITNEY AIRCRAFT GROUP
COMMERCIAL PRODUCTS DIVISION

TABLE 87

ENERGY EFFICIENT ENGINE LOW PRESSURE TURBINE
AERODYNAMIC PARAMETERS

Parameter

Number of Stages	4
Expansion Ratio	5.7
Mean Velocity Ratio	0.47/2.26
Cx/u	0.73
VRIM (fps Maximum)	650
$\Delta P/P$ Exit Guide Vane (percent)	0.9
$\Delta P/P$ Turbine Transition Duct (percent)	0.7
Area Ratio (Transition Duct, percent)	1.5
LPT to HPT Diameter Ratio	16%
Inlet Speed Parameter, N/\sqrt{T}	82.1
Inlet Flow Parameter, $W\sqrt{T/P}$	75.0
Blade Tip Clearance, Min./Max.	0.02
Inlet Mach No. (Abs.)	0.39
Exit Mach No. (Abs.)	0.41
Inlet Swirl Angle (degree)	-53
Exit Swirl Angle (degree)	+33
Number of Blades and Vanes	749
Efficiency (percent)	91.5

TABLE 88

LOW-PRESSURE TURBINE CURRENT PERFORMANCE PARAMETERS
AT SIGNIFICANT ENGINE OPERATING CONDITIONS

	<u>Engine Operating Condition</u>			
	<u>Aero. Des.</u>	<u>Maximum</u>	<u>Maximum</u>	
	<u>Point</u>	<u>Cruise</u>	<u>Climb</u>	<u>Takeoff</u>
Inlet Flow Parameter ($lb \sqrt{R} \text{ in.}^2/\text{sec} \sqrt{lb_f}$)	67.05	67.15	66.75	67.15
Inlet Temperature $^{\circ}(F)$	1530	1495	1655	1725
Pressure Ratio	5.63	5.55	5.75	4.97
Adiabatic Efficiency (percent)	91.5	91.3	91.7	90.2
Enthalpy Change - BTU/lb	173.5	169.5	187.5	178.0
Exhaust Case Pressure Loss (percent)	0.90	0.87	0.95	0.68



3.2.8.3.3.2 Current Technical Progress

Work during the current reporting period was directed toward the following areas: (1) component design, (2) airfoil durability analysis, (3) stage vibration analysis, (4) flutter analysis, (5) critical speed analysis, (6) rotor design, and (7) case design.

Component Design

Low-pressure turbine component design studies indicated that airfoil axial gapping had to be increased. The amount of this increase depended on the following factors: (1) thermal growth of shaft, cases, blades and vanes; (2) pressure load deflections of airfoils, case, shaft and hub; (3) vibratory deflections; (4) mechanical tolerances and bearing play; and (5) blade meshing criteria. The resultant flowpath is shown in Figure 160.

The required re-gapping also resulted in revisions to the vane and blade stagger angles (see Table 89).

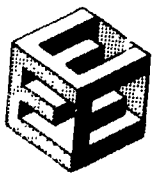
TABLE 89

LOW-PRESSURE TURBINE VANE AND BLADE STAGGER ANGLES

<u>Location</u>	<u>Restagger</u>	<u>Flow Area Change (percent)</u>
2nd Vane (Inlet Guide Vane)	Closed	-0.37
2nd Blade	Opened	+0.12
3rd Vane, new design, all sections	Redesign	
3rd Blade	Closed	-0.38
4th Vane	Closed	-0.98
4th Blade*	Closed	-0.16
5th Vane	Closed	-0.08
5th Blade	Closed	-0.25
Exit Guide Vane	Unchanged	

* Design sections at 20 percent span, mean, 1/4 tip, and tip were changed

Airfoil section contours remain as reported in the Fourth Semiannual Status Report except for the third stage vane and fourth stage blade as noted in Table 89. Velocity triangle data describing the regapped and restaggered flowpath are shown in Table 90. Mean section contours and pressure profiles for all low-pressure turbine airfoils are shown in Figures 161 through 170.



PRATT & WHITNEY AIRCRAFT GROUP
COMMERCIAL PRODUCTS DIVISION

ORIGINAL PAGE IS
OF POOR QUALITY

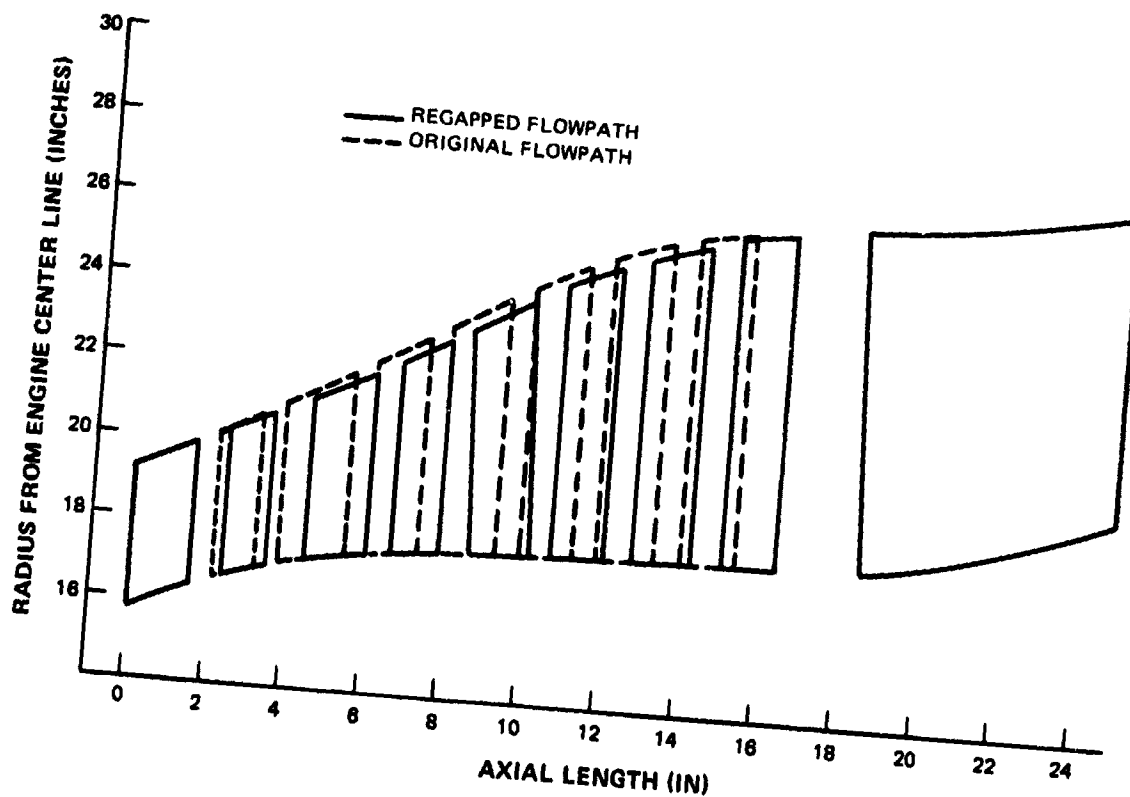


Figure 160 Low-Pressure Turbine Flowpath Comparison



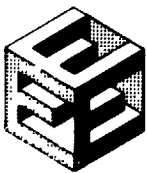
PRATT & WHITNEY AIRCRAFT GROUP
COMMERCIAL PRODUCTS DIVISION

TABLE 90

LOW-PRESSURE TURBINE VELOCITY TRIANGLE DATA IN TERMS OF REVISED
FLOWPATH GAPPING AND REVISED AIRFOIL STAGGERING

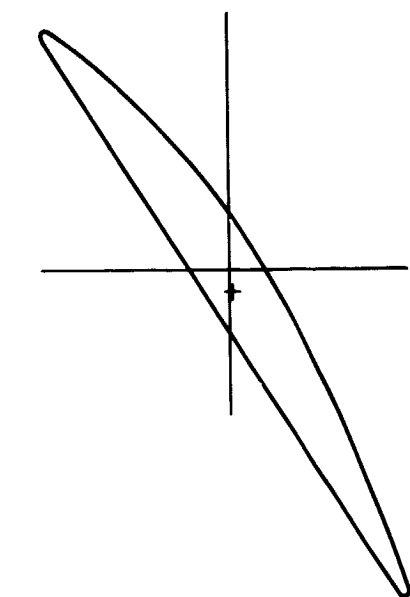
	VANE 2(IGV) MEAN	BLADE 2 MEAN	VANE 3 MEAN	BLADE 3 MEAN
Inlet Ang.	141.300	40.700	47.600	41.700
Inlet Mach no.	000.394	00.394	00.349	00.365
Inlet Mx	000.239	00.246	00.254	00.238
Exit Ang.	024.200	25.900	22.800	22.700
Exit Mach no.	000.658	00.620	00.656	00.665
Exit Mx	000.267	00.266	00.254	00.254
	VANE 4 MEAN	BLADE 4 MEAN	VANE 5 MEAN	BLADE 5 MEAN
Inlet Ang.	42.900	40.900	45.600	44.700
Inlet Mach no.	00.357	00.359	00.348	00.385
Inlet Mx	00.239	00.229	00.248	00.269
Exit Ang.	21.200	22.200	22.600	25.500
Exit Mach no.	00.689	00.689	00.736	00.791
Exit Mx	00.248	00.258	00.283	00.339
		EGV MEAN		
Inlet Ang.		50.100		
Inlet Mach no.		00.441		
Inlet Mx		00.337		
Exit Ang.		90.000		
Exit Mach no.		00.350		
Exit Mx		00.346		

- o All values along streamlines
- o Integrated Core/Low Spool Aerodynamic Design Point



PRATT & WHITNEY AIRCRAFT GROUP
COMMERCIAL PRODUCTS DIVISION

ORIGINAL PAGE IS
OF POOR QUALITY



RADIUS	18.115"
INLET METAL ANGLE	137.5°
EXIT METAL ANGLE	24.4°
AXIAL CHORD	1.565
FOILS	54.
SOLIDITY (bx)	.743
ELLIPSE RATIO	4/1

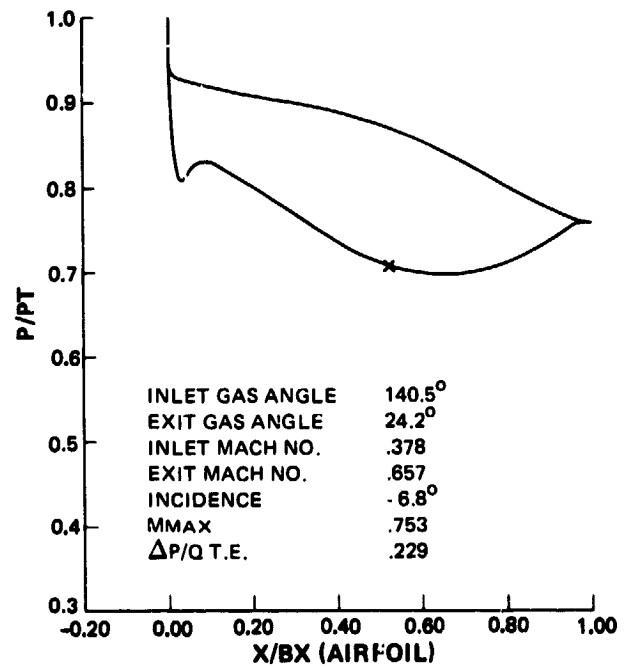
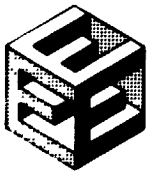
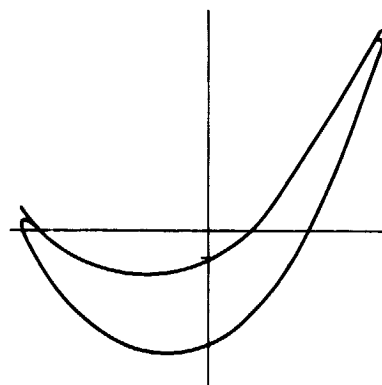


Figure 161 Low-Pressure Turbine Second Vane Mean Section Geometry



PRATT & WHITNEY AIRCRAFT GROUP
COMMERCIAL PRODUCTS DIVISION

ORIGINAL PAGE IS
OF POOR QUALITY



RADIUS	18.803"
INLET METAL ANGLE	36.4°
EXIT METAL ANGLE	25.2°
AXIAL CHORD	1.05"
FOILS	120.
SOLIDITY (bx)	1.07
ELLIPSE RATIO	4/1

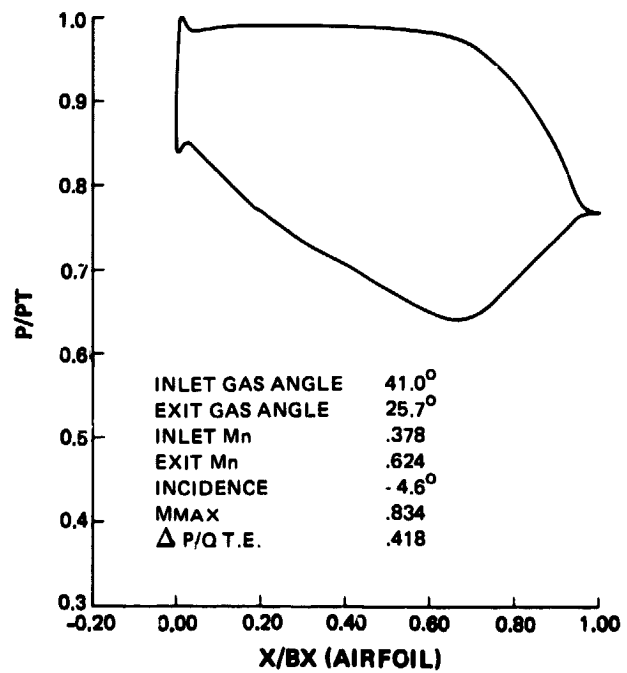


Figure 162 Low-Pressure Turbine Second Blade Mean Section Geometry



PRATT & WHITNEY AIRCRAFT GROUP
COMMERCIAL PRODUCTS DIVISION

ORIGINAL PAGE IS
OF POOR QUALITY

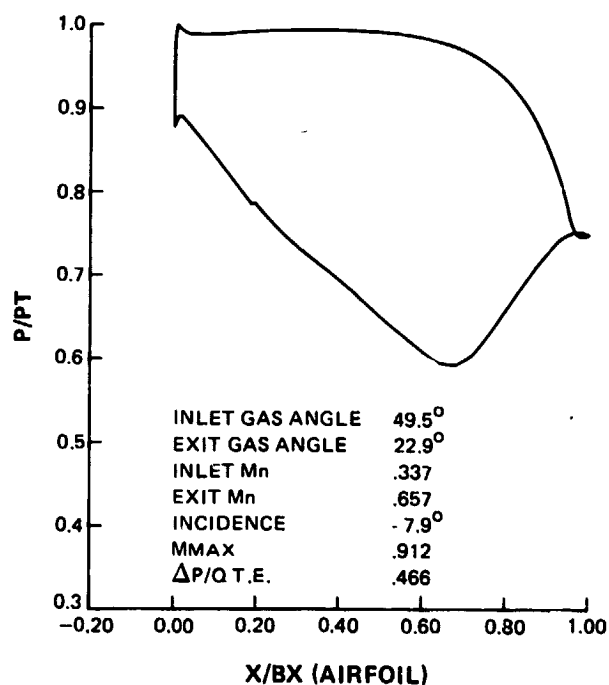
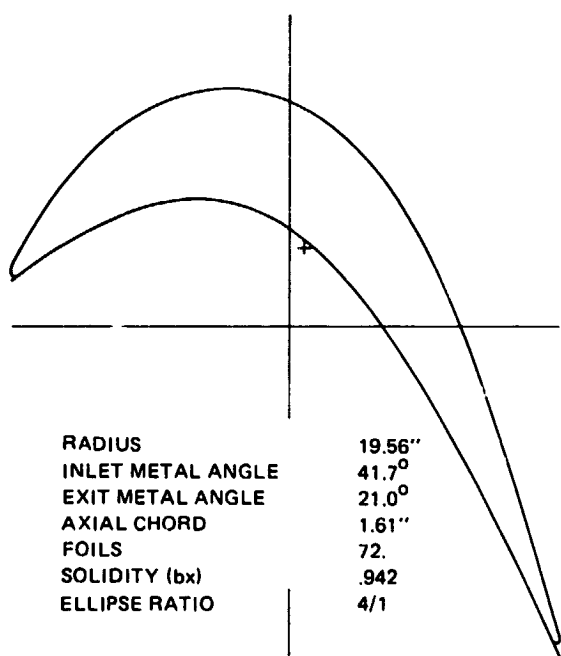
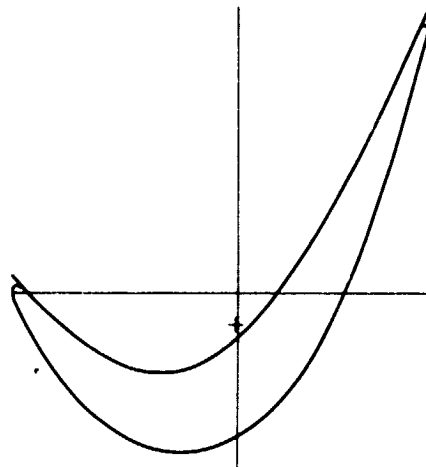


Figure 163 Low-Pressure Turbine Third Vane Mean Section Geometry



PRATT & WHITNEY AIRCRAFT GROUP
COMMERCIAL PRODUCTS DIVISION

ORIGINAL TEST
OF POOR QUALITY



RADIUS	20.154"
INLET METAL ANGLE	35.2°
EXIT METAL ANGLE	20.6°
AXIAL CHORD	1.208"
FOILS	96
SOLIDITY (b2)	.916
ELLIPSE RATIO	3/1

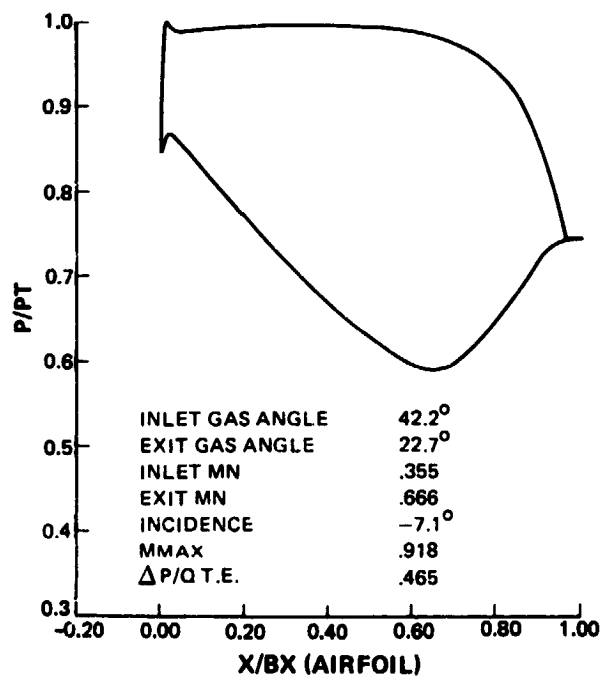
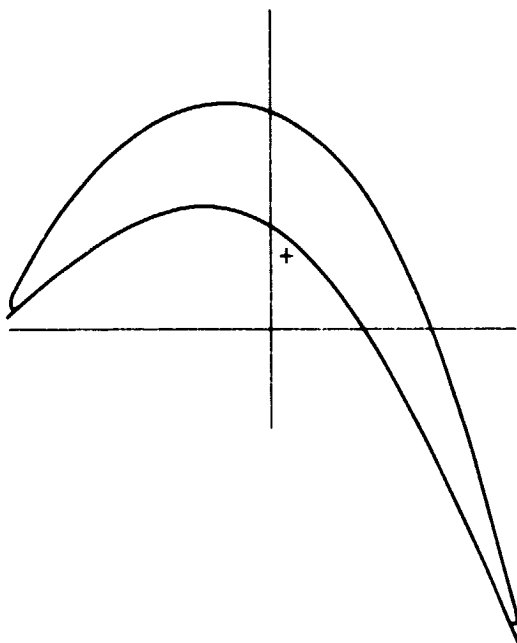


Figure 164 Low-Pressure Turbine Third Blade Mean Section Geometry



PRATT & WHITNEY AIRCRAFT GROUP
COMMERCIAL PRODUCTS DIVISION

ONE OF FOUR QUARTERS



RADIUS	20.748"
INLET METAL ANGLE	38.7°
EXIT METAL ANGLE	18.9°
AXIAL CHORD	1.47"
FOILS	84
SOLIDITY (bx)	.9445
ELLIPSE RATIO	4/1

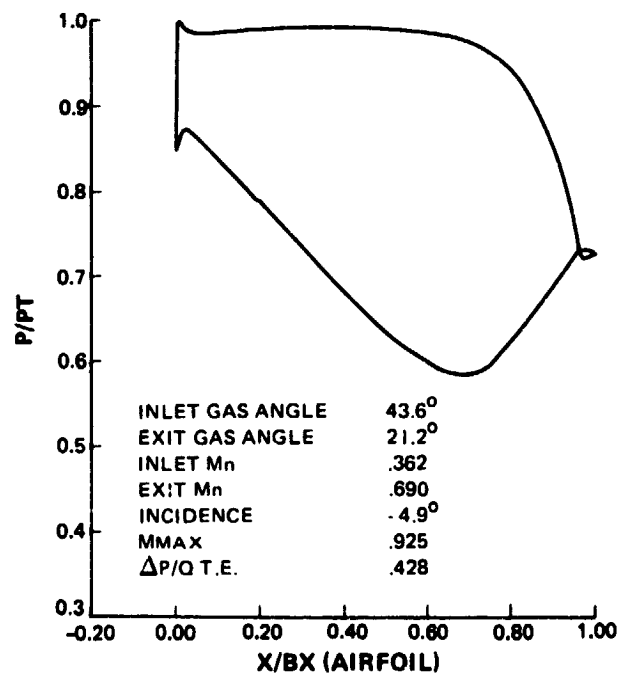
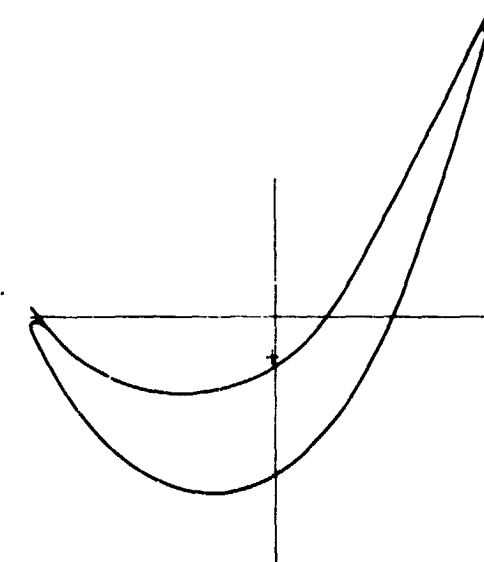


Figure 165 Low-Pressure Turbine Fourth Vane Mean Section Geometry



PRATT & WHITNEY AIRCRAFT GROUP
COMMERCIAL PRODUCTS DIVISION

ORIGINAL PAGE IS
OF POOR QUALITY



RADIUS	21.245"
INLET METAL ANGLE	33.8°
EXIT METAL ANGLE	22.1°
AXIAL CHORD	1.33
FOILS	100.
SOLIDITY (bx)	.9954
ELLIPSE RATIO	4/1

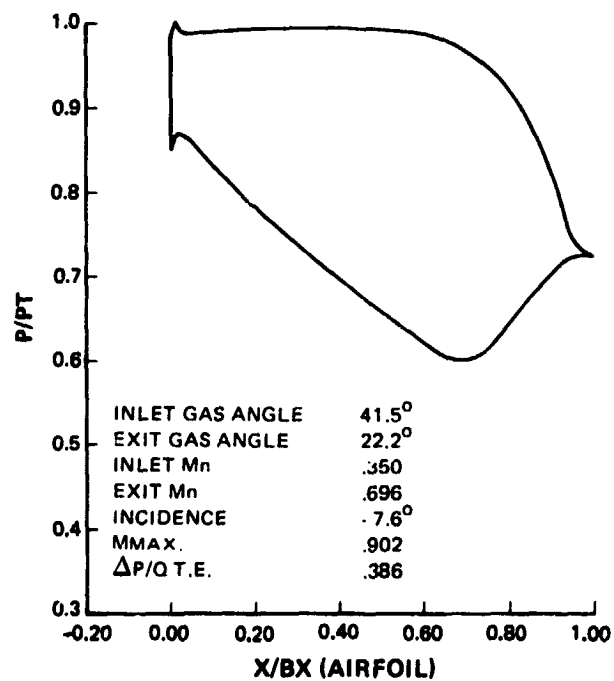


Figure 166 Low-Pressure Turbine Fourth Blade Mean Section Geometry



PRATT & WHITNEY AIRCRAFT GROUP
COMMERCIAL PRODUCTS DIVISION

ORIGINAL PAGE IS
OF POOR QUALITY

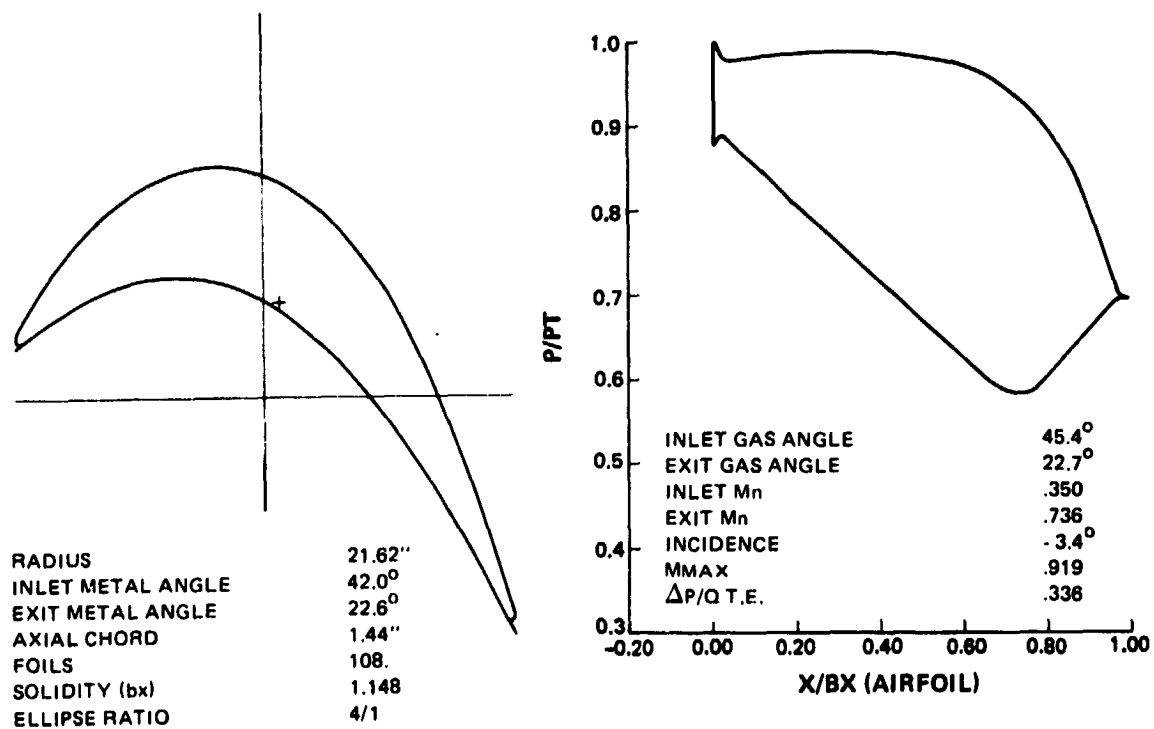
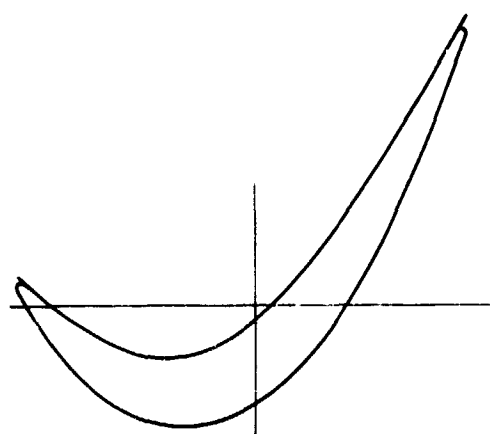


Figure 167 Low-Pressure Turbine Fifth Vane Mean Section Geometry



PRATT & WHITNEY AIRCRAFT GROUP
COMMERCIAL PRODUCTS DIVISION

ORIGINAL QUALITY
OF POOR QUALITY



RADIUS	21.851"
INLET METAL ANGLE	40.2°
EXIT METAL ANGLE	25.5°
AXIAL CHORD	1.31"
FOILS	122
SOLIDITY (bx)	1.161
ELLIPSE RATIO	4/1

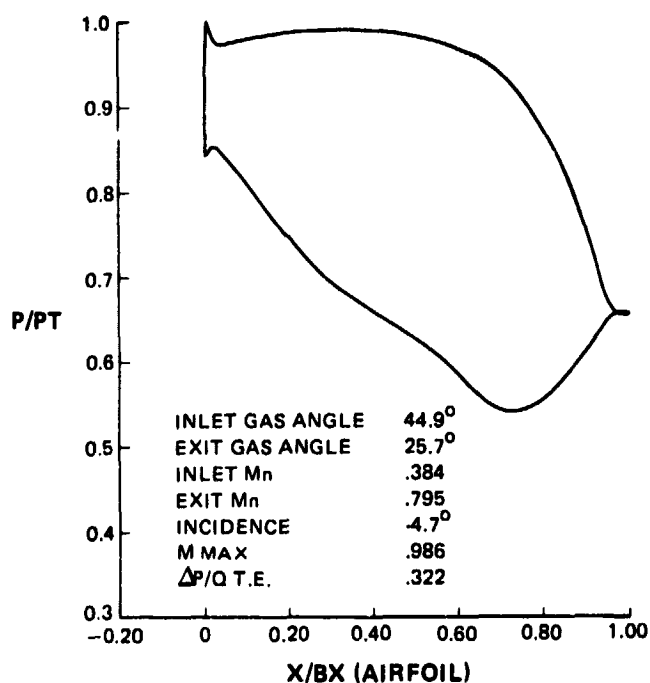


Figure 168 Low-Pressure Turbine Fifth Blade Mean Section Geometry



PRATT & WHITNEY AIRCRAFT GROUP
COMMERCIAL PRODUCTS DIVISION

ORIGINAL FILED IN
OF POOR QUALITY

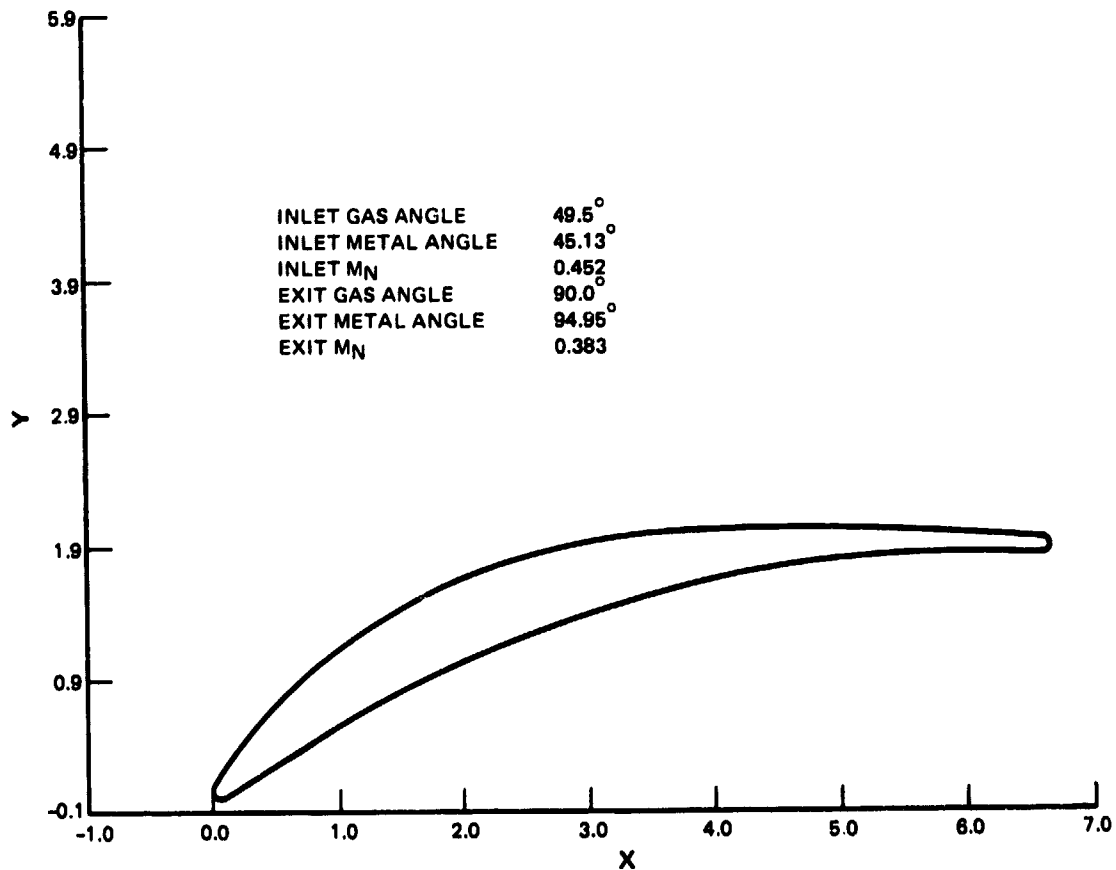
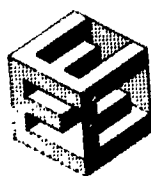


Figure 169 Low-Pressure Turbine Exit Guide Vane Mean Section Geometry



PRATT & WHITNEY AIRCRAFT GROUP
COMMERCIAL PRODUCTS DIVISION

ORIGINAL PAGE IS
OF POOR QUALITY

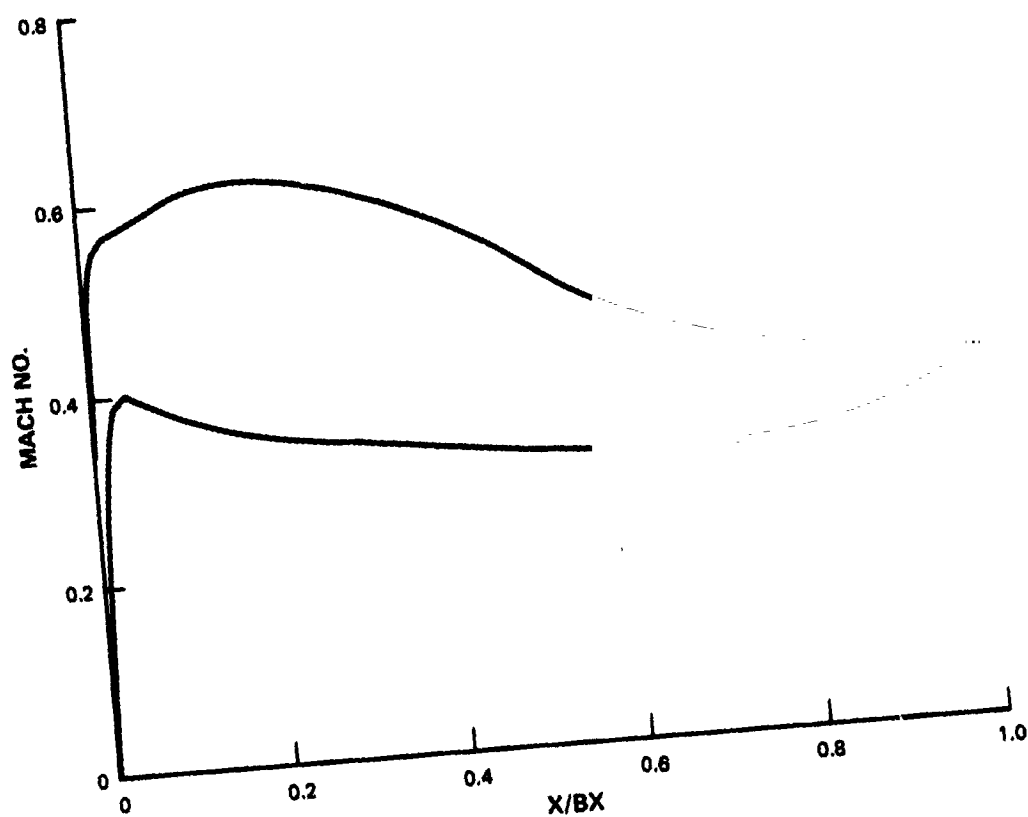
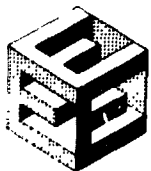


Figure 170

Low-Pressure Turbine Exit Guide Vane Mean Section Compressible
Mach Number Distribution



Airfoil Durability Analysis

An airfoil durability analysis for the integrated core/low spool was completed. The results of this analysis indicated that all blades and vanes met the goal life of 50 hours hot time. Figures 171 through 178 show the calculated vane and blade stresses at design temperature conditions. All blades and vanes displayed adequate stress margin. Material selection and coatings (where needed) are also indicated. Analysis of the lives of the flight propulsion system airfoils was not completed during this reporting period.

Stage Vibration Analysis

Stage vibration analysis of the low-pressure turbine rotors for the integrated core/low spool was completed. The rotors were analyzed for blade resonance, blade- and disk-coupled resonance, and blade flutter.

For the 2nd stage rotor, 11E and 22E resonances were of concern because of the proximity of the 11 upstream hot struts. Figure 179 shows that for the 11E first mode, a frequency margin of 9.8 percent at the maximum rotor speed is predicted. For 22E first mode, a margin of -10.7 percent at the minimum cruise speed is calculated. All critical second mode resonances occur well out of the operating range.

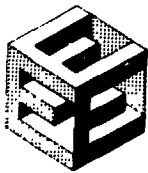
The 3rd stage final design has a -38 percent 22E and a -16 percent 11E first mode frequency margin at the minimum cruise speed, with the 22E resonance occurring away from the idle range. The 3E first mode frequency margin is 14 percent and the 22E 2nd mode frequency is also 14 percent at the maximum rotor speed (see Figure 180).

Critical resonances for stage 4 were limited to the low orders. The final design resulted in margins of 52 percent 2E and 18 percent 3E for the first mode at the maximum rotor speed (see Figure 181). Avoidance of the 11E and 22E resonances was not required.

The 5th stage resulting design has a 9 percent first mode 3E resonance margin at maximum rotor speed. The 30E first and second mode resonance are predicted to occur at 1400 and 1760 revolutions/minute, respectively. These were considered acceptable for the integrated core/low spool (see Figure 182).

Flutter Analysis

Figure 183 presents the results of a flutter analysis on the four low-pressure turbine rotors. The Energy Efficient Engine designs are compared to previous Pratt & Whitney Aircraft designs in terms of aerodynamic damping and tip exit reduced velocity parameters. The results of this analysis indicate that all 4 rotors operate well above the unstable limit and are therefore not expected to encounter flutter problems.



PRATT & WHITNEY AIRCRAFT GROUP
COMMERCIAL PRODUCTS DIVISION

ORIGINAL DESIGN
OF POOR QUALITY

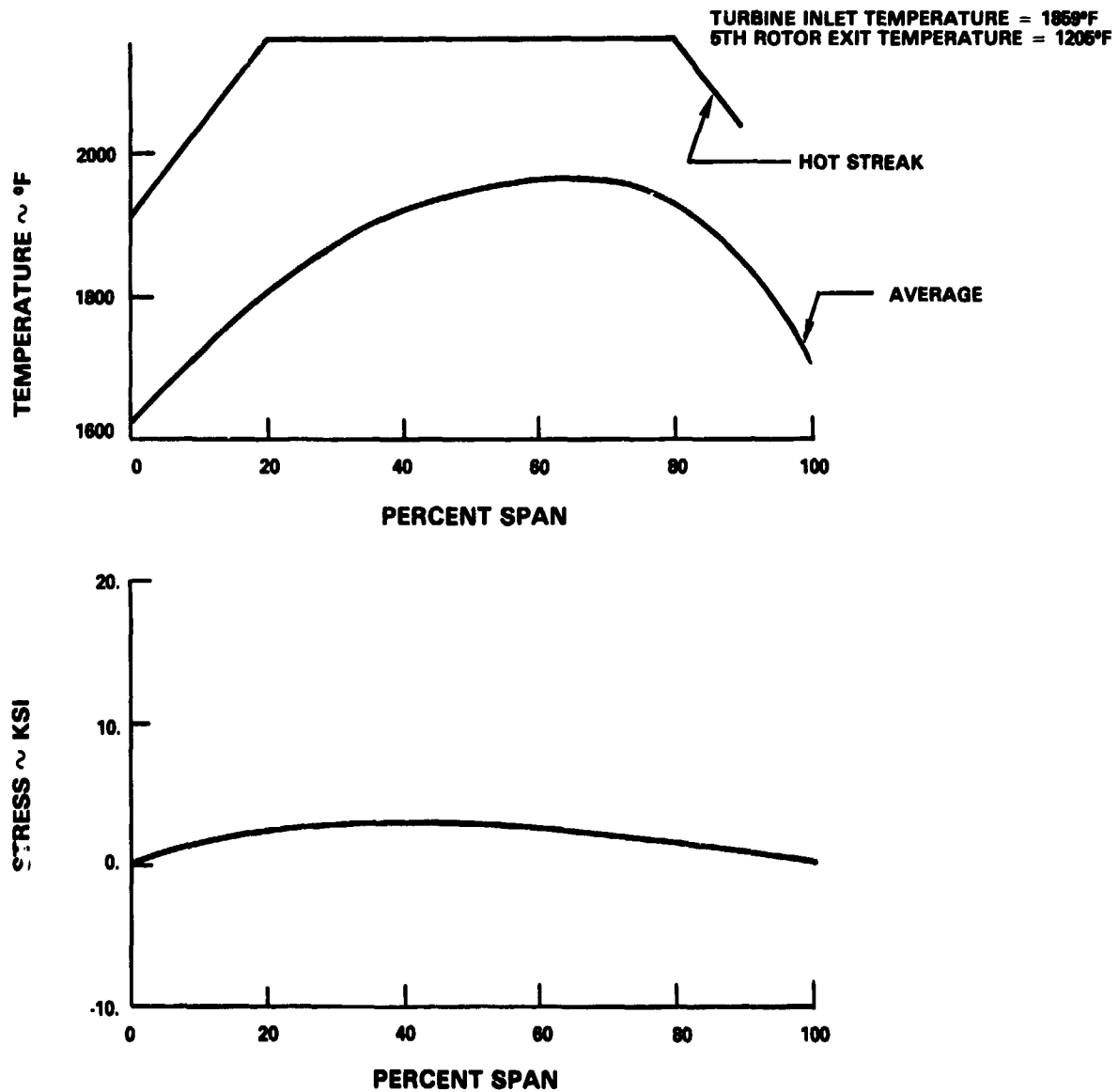
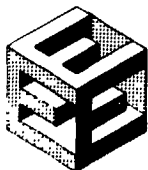


Figure 171 Second Stage Vane Durability Design Conditions and Calculated Stress (Vane material: PWA 1480; Coating: PWA 73)



PRATT & WHITNEY AIRCRAFT GROUP
COMMERCIAL PRODUCTS DIVISION

ORIGINAL PAGE IS
OF POOR QUALITY

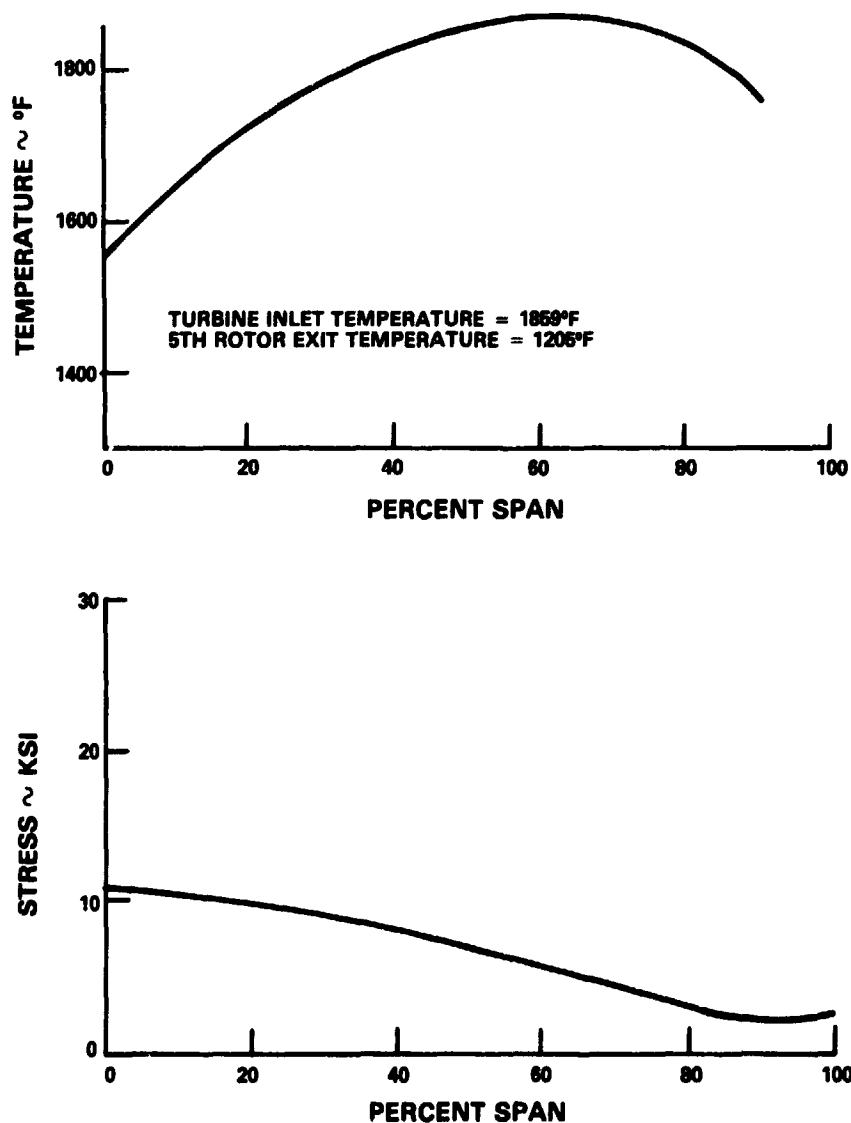
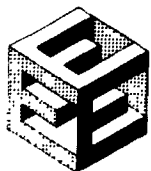


Figure 172 Second Stage Blade Durability Design Conditions and Calculated Stress (Blade material: PWA 1447; Coating: PWA 73)



PRATT & WHITNEY AIRCRAFT GROUP
COMMERCIAL PRODUCTS DIVISION

ORIGINAL PAGE IS
OF POOR QUALITY

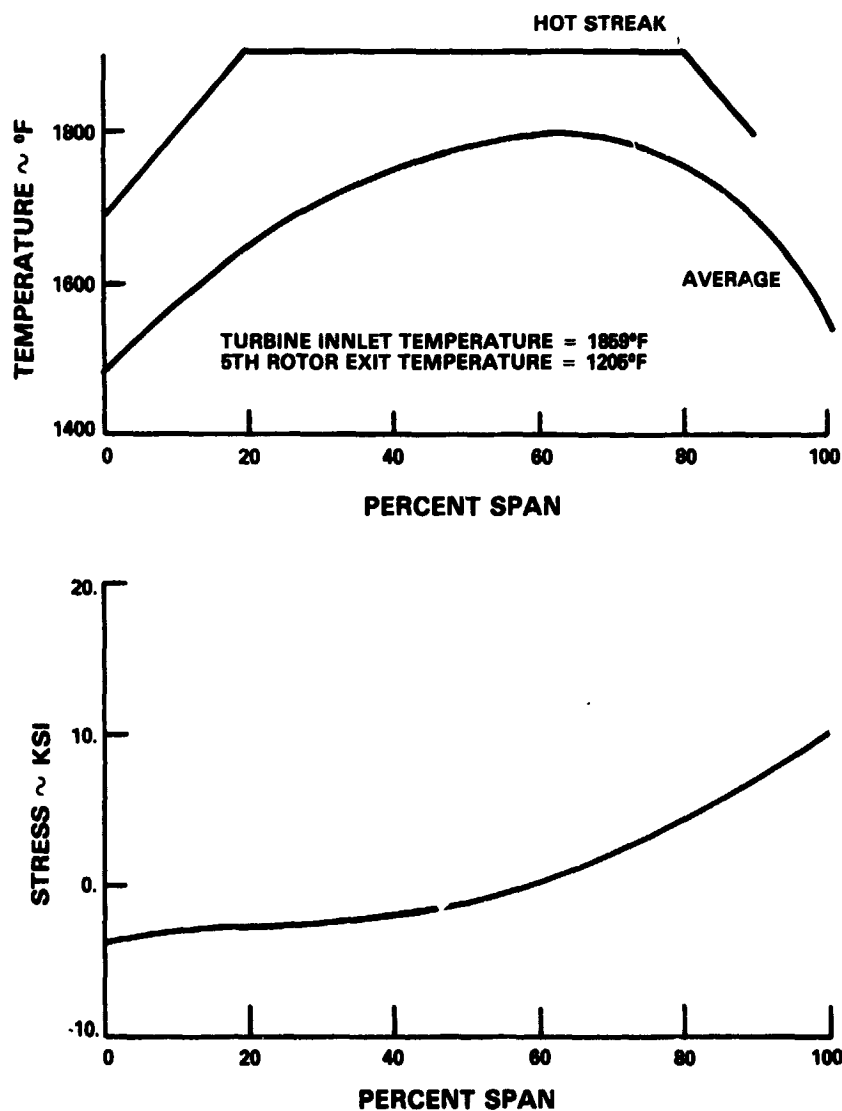
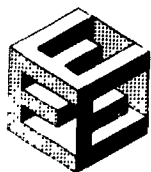


Figure 173 Third Stage Vane Durability Design Conditions and Calculated Stress (Vane material: PWA 1455; No coating)



PRATT & WHITNEY AIRCRAFT GROUP
COMMERCIAL PRODUCTS DIVISION

ORIGINAL PAGE IS
OF POOR QUALITY

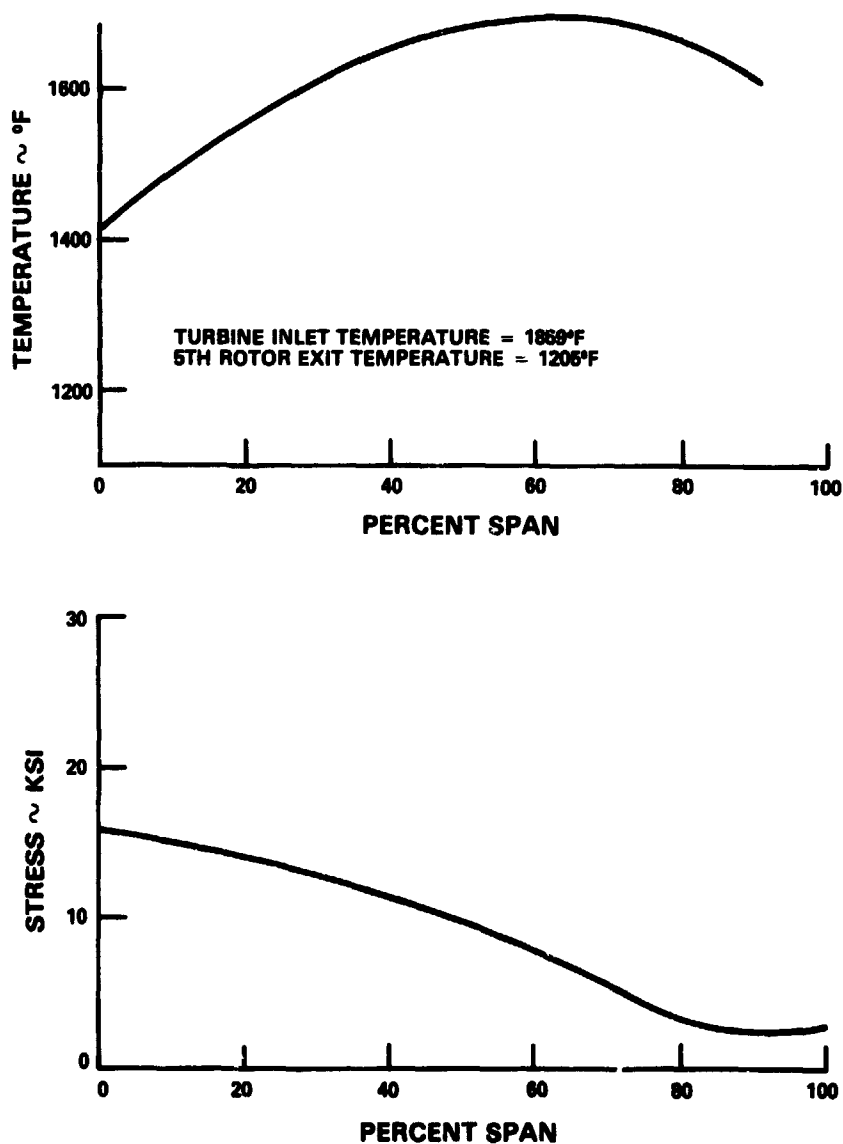
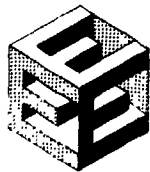


Figure 174 Third Stage Blade Durability Design Conditions and Calculated Stress (Blade material: PWA 655; No coating)



PRATT & WHITNEY AIRCRAFT GROUP
COMMERCIAL PRODUCTS DIVISION

ORIGINAL FIGURE
OF POOR QUALITY

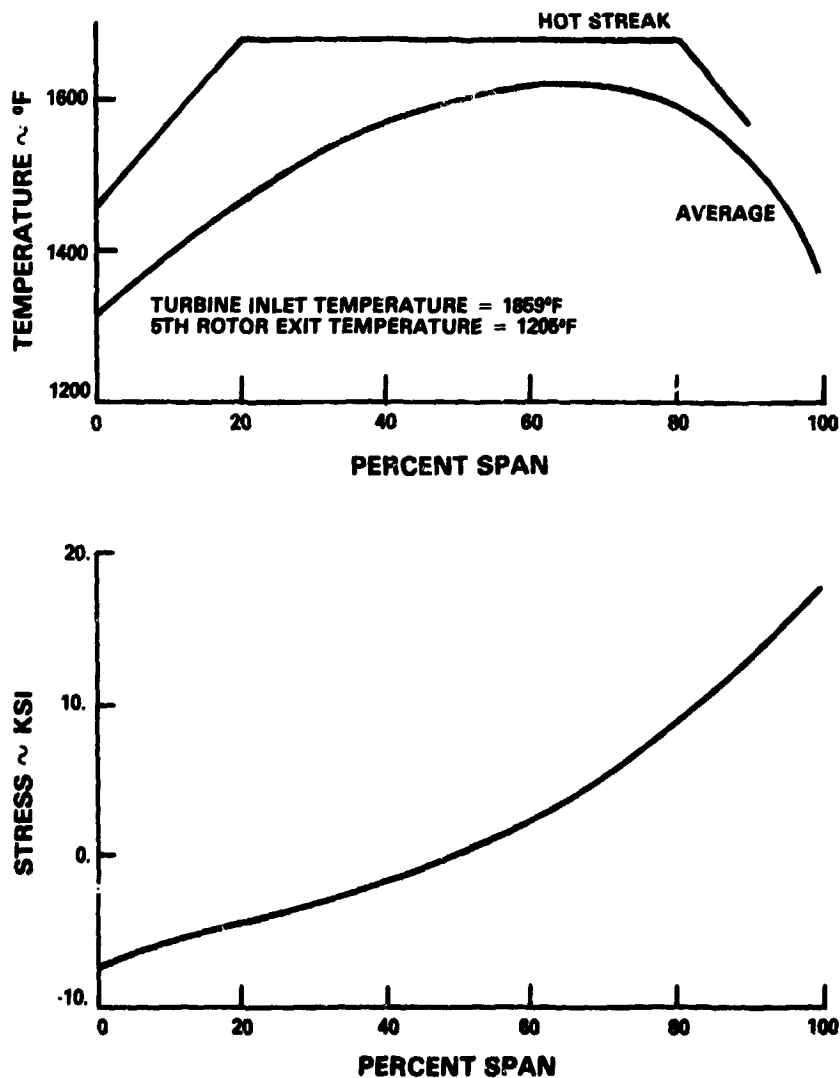


Figure 175 Fourth Stage Vane Durability Design Conditions and Calculated Stress (Vane material: PWA 655; No coating)



PRATT & WHITNEY AIRCRAFT GROUP
COMMERCIAL PRODUCTS DIVISION

ORIGINAL DESIGN
OF POOR QUALITY

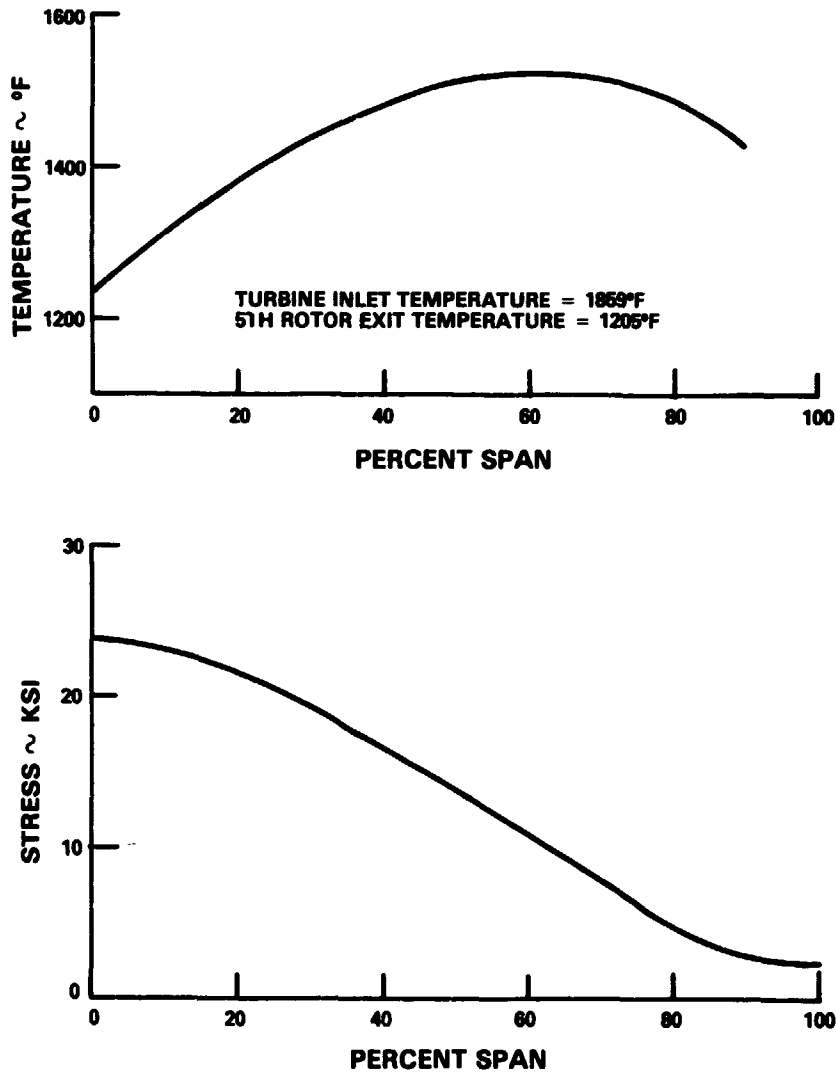


Figure 176 Fourth Stage Blade Durability Design Conditions and Calculated Stress (Blade material: PWA 655; No coating)



PRATT & WHITNEY AIRCRAFT GROUP
COMMERCIAL PRODUCTS DIVISION

ORIGINAL PAGE IS
OF POOR QUALITY

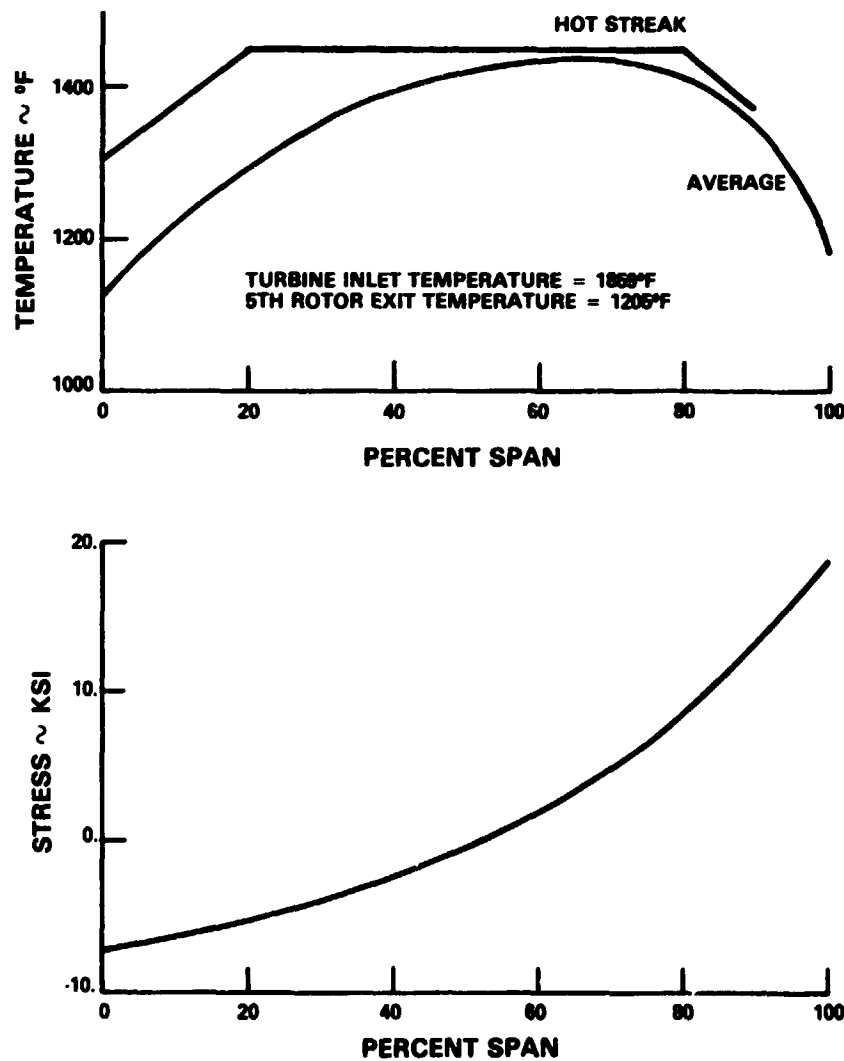


Figure 177 Fifth Stage Vane Durability Design Conditions and Calculated Stress (Vane material: PWA 655; No coating)



PRATT & WHITNEY AIRCRAFT GROUP
COMMERCIAL PRODUCTS DIVISION

ORIGINAL FILED IN
OF POOR QUALITY

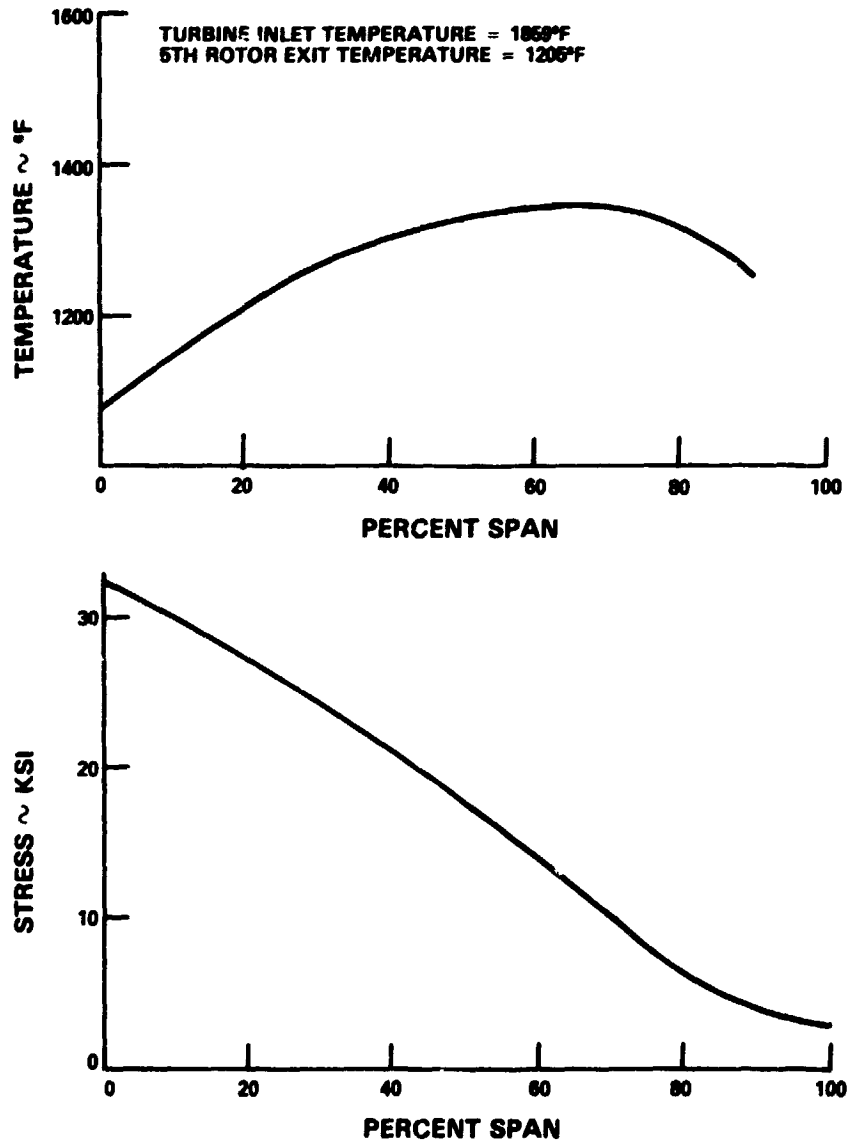
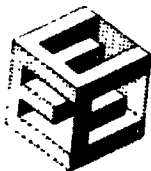


Figure 178 Fifth Stage Blade Durability Design Conditions and Calculated Stress (Blade material: PWA 655; No coating)



PRATT & WHITNEY AIRCRAFT GROUP
COMMERCIAL PRODUCTS DIVISION

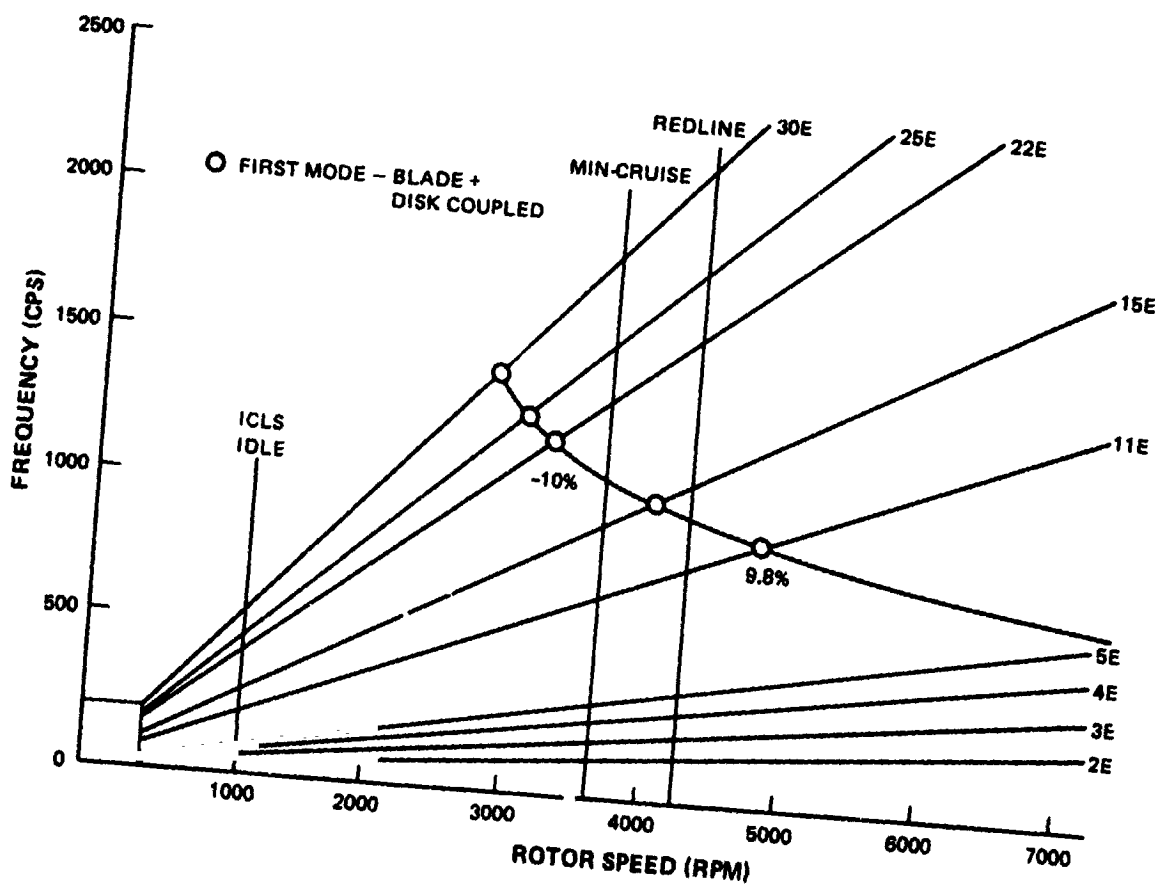


Figure 179 Low-Pressure Turbine Second Stage Rotor Resonance Diagram



PRATT & WHITNEY AIRCRAFT GROUP
COMMERCIAL PRODUCTS DIVISION

OF POOR QUALITY

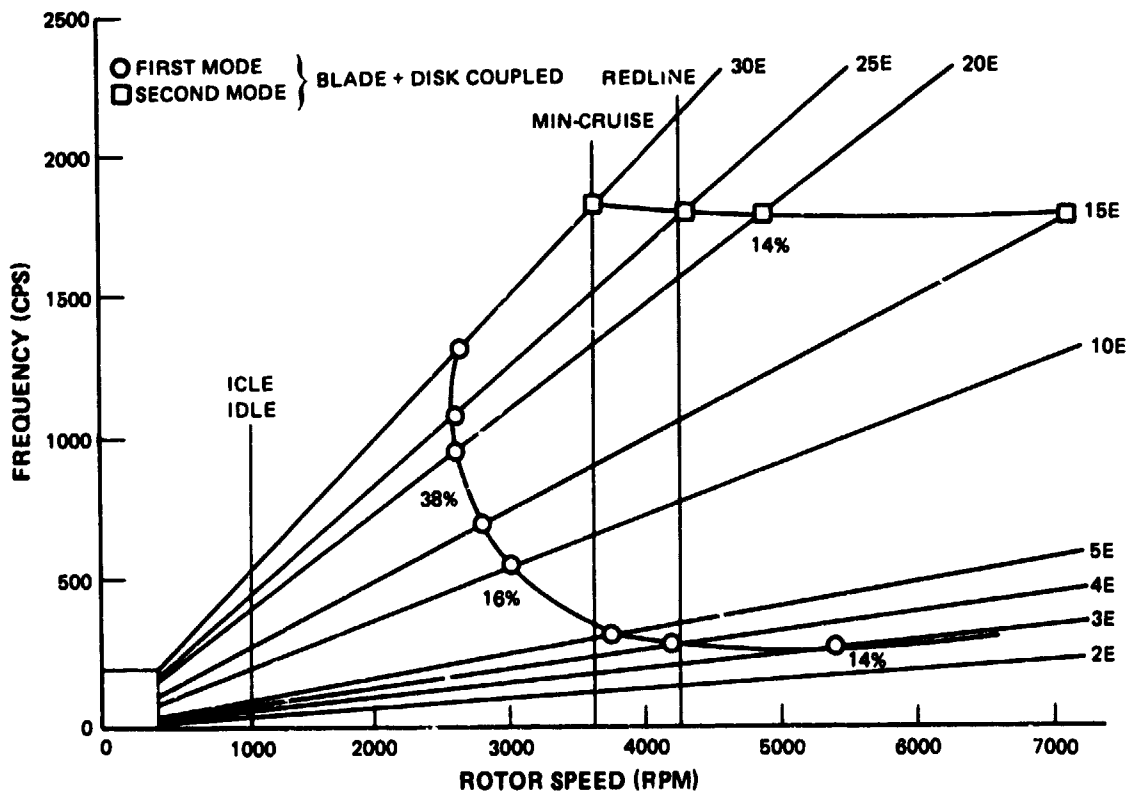
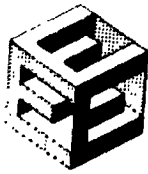


Figure 180 Low-Pressure Turbine Third Stage Rotor Resonance Diagram



PRATT & WHITNEY AIRCRAFT GROUP
COMMERCIAL PRODUCTS DIVISION

ORIGINAL PAGE IS
OF POOR QUALITY

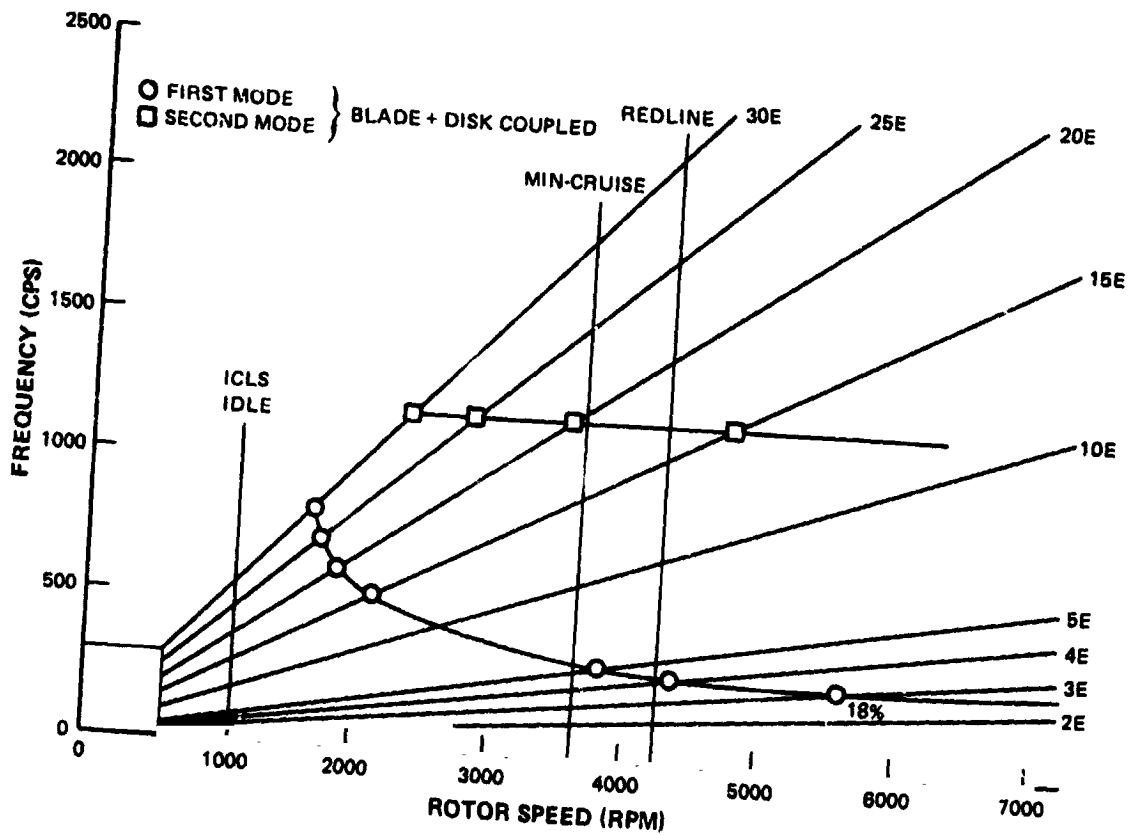
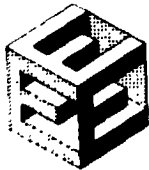


Figure 181 Low-Pressure Turbine Fourth Stage Rotor Resonance Diagram



PRATT & WHITNEY AIRCRAFT GROUP
COMMERCIAL PRODUCTS DIVISION

ORIGINAL PAGE IS
OF POOR QUALITY

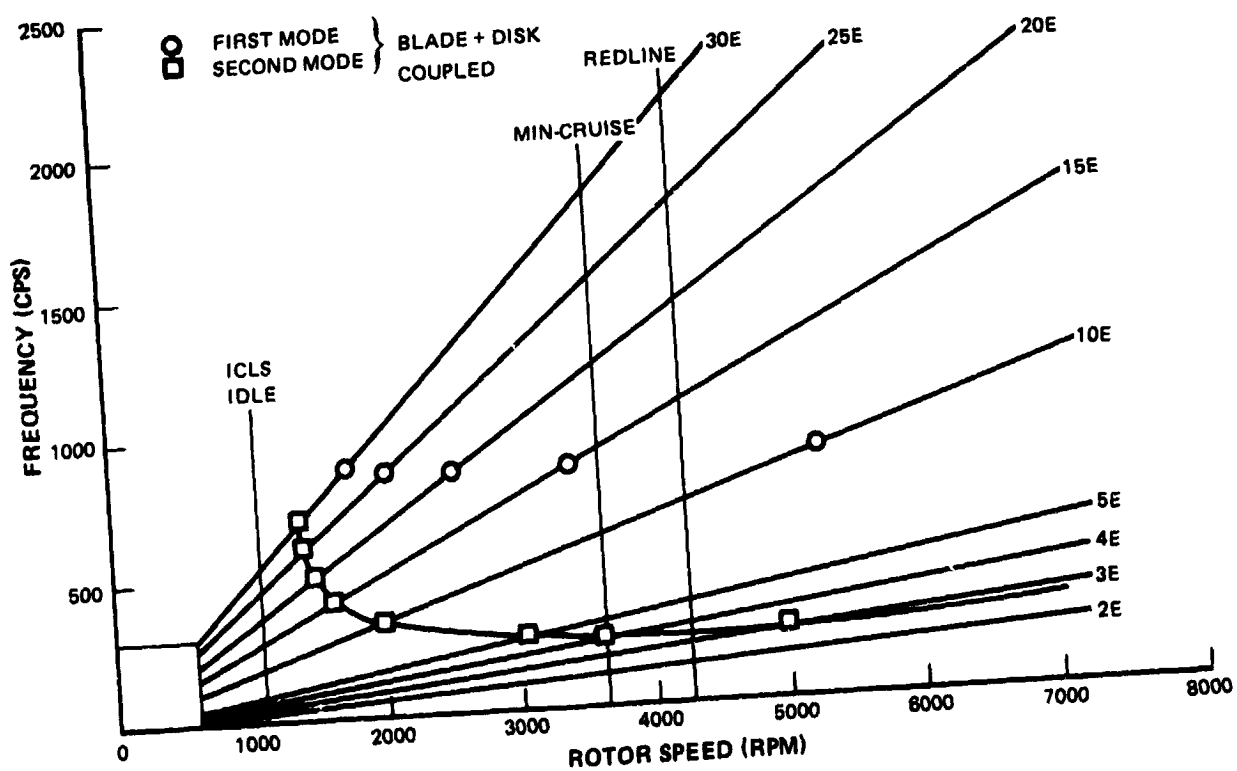


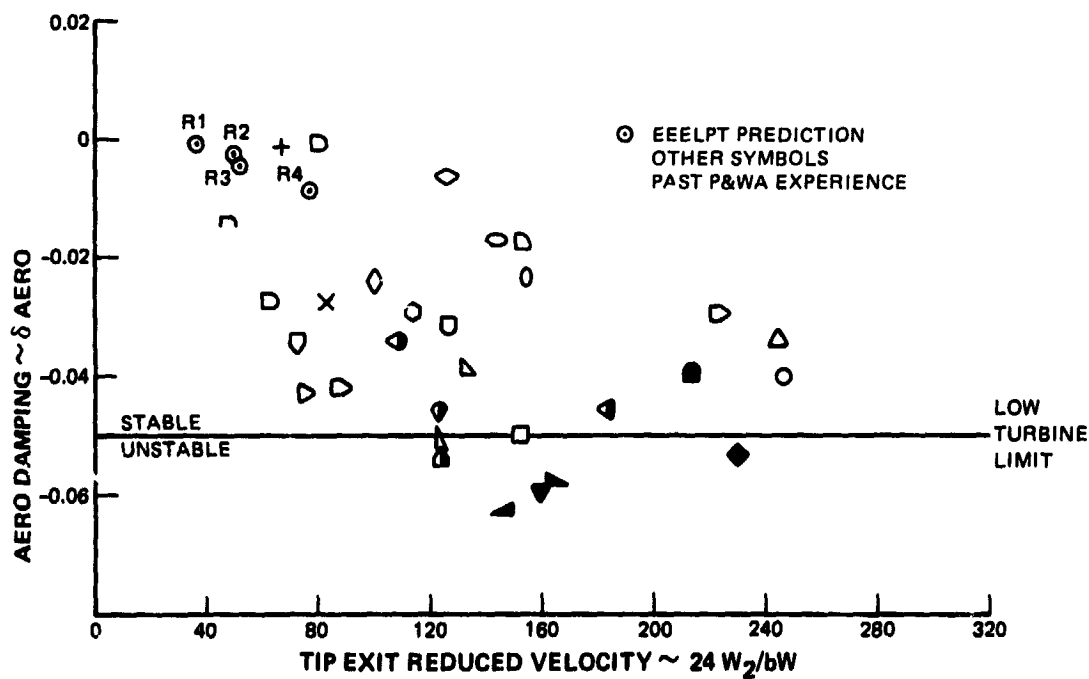
Figure 182 Low-Pressure Turbine Fifth Stage Rotor Resonance Diagram

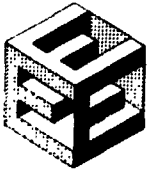


PRATT & WHITNEY AIRCRAFT GROUP
COMMERCIAL PRODUCTS DIVISION

ORIGINAL PAGE IS
OF POOR QUALITY

SHROUDED TURBINE BLADE FLUTTER EXPERIENCE





Critical Speed Analysis

A critical speed analysis was completed on the low-pressure rotor of the integrated core/low spool. The results of this analysis indicated that a low-pressure turbine mode of vibration exists at 3015 revolutions/minute, which is in the operating speed region (see Table 91). At this mode of vibration, the low-pressure rotor possesses 23 percent of the total strain energy of the engine. Previous operating experience indicates that this percentage is too high. Further analysis with selected amounts of imbalance placed at various positions on the rotor showed the outer hot strut case deflection to be sensitive to low-pressure turbine imbalance (1.7 oz.-in. of imbalance was found to produce one mil of deflection).

TABLE 91

INTEGRATED CORE/LOW SPOOL CRITICAL SPEED ANALYSIS UPDATE
(Undamped Number 5 Bearing)

<u>Mode (LRX)</u>	<u>Rotor Critical Speed (RPM)</u>	<u>Comments</u>
Fan Mode	2029 RPM (5.45% S.E.)	Low Strain Energy Within Running Range.
LPT Mode	3015 RPM (23.55% S.E.)	Case Deflection Very Sensitive to LPT Unbalance. Need #5 Damper.
Low Shaft Mode	7373 RPM (78.6% S.E.)	89% Above Max. N., 25% Below N ₂ IDLE.
Tailplug Mode	4752 RPM (22.1% S.E.)	21.7% Above Max. N ₁

(N₁)Idle = 1103 rpm

(N₁)max = 3902 rpm

To desensitize the hot strut case to low-pressure turbine imbalance, an oil damped number 5 bearing was incorporated in the design (see Figure 184). The critical speed analysis with the damped number 5 bearing (see Table 92) indicates a reduction in strain energy percentage and a reduction in the critical speed revolutions/minute. Case deflection was desensitized to 10.25 oz.-in. imbalance per mil deflection.



PRATT & WHITNEY AIRCRAFT GROUP
COMMERCIAL PRODUCTS DIVISION

ORIGINAL PAGE IS
OF POOR QUALITY

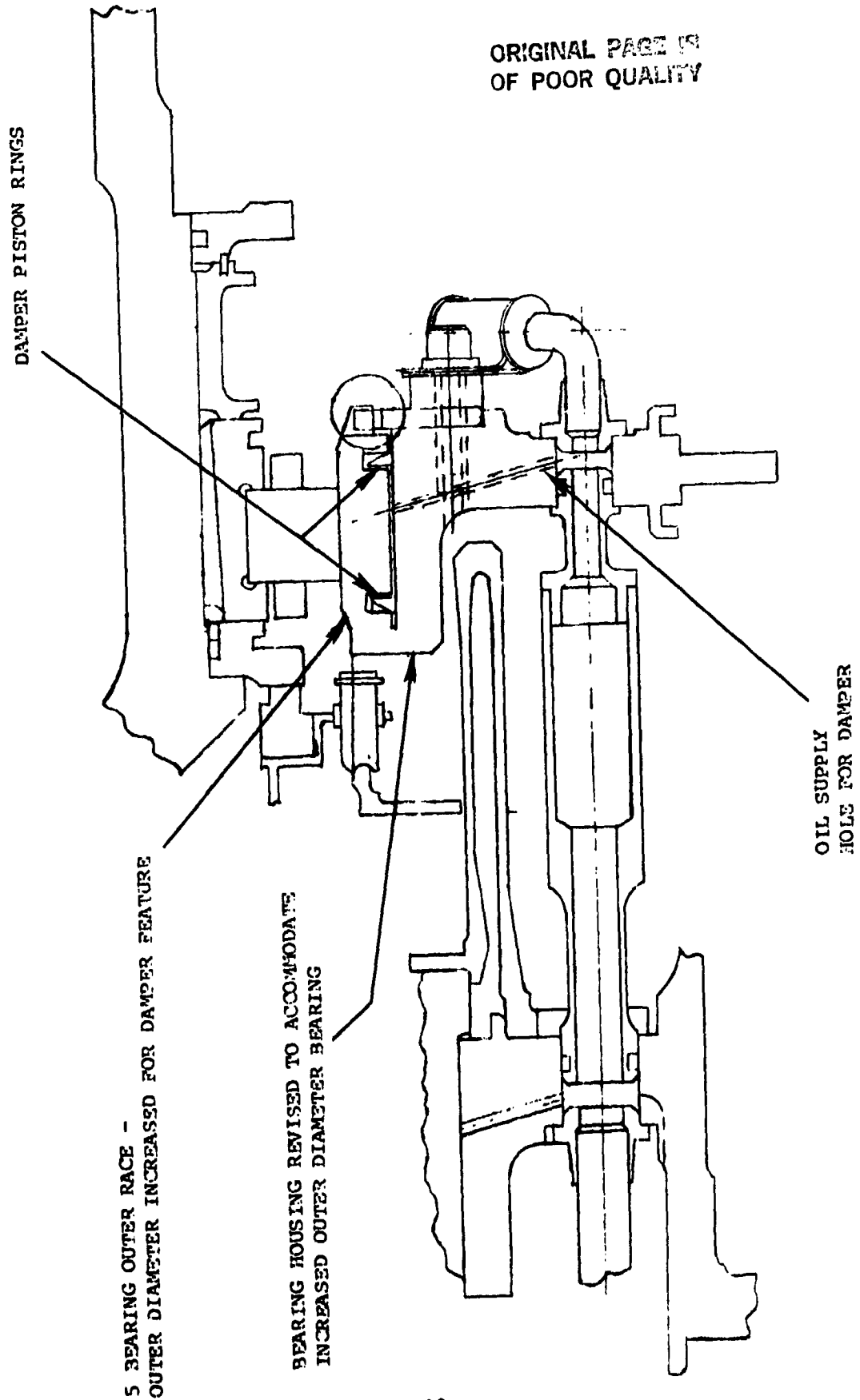
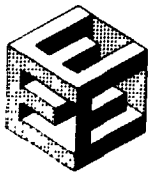


Figure 184 Low-Pressure Turbine Damped Number 5 Bearing Compartment



PRATT & WHITNEY AIRCRAFT GROUP
COMMERCIAL PRODUCTS DIVISION

TABLE 92

INTEGRATED CORE/LOW SPOOL CRITICAL SPEED ANALYSIS UPDATE
(7 Mil Viscous Damper at number 5 bearing)

<u>Mode (LRX)</u>	<u>Rotor Critical Speed (RPM)</u>	<u>Comments</u>
Fan Mode	2031 RPM (5.39% S.E.)	Low Strain Energy Within Running Range.
LPT Mode	2700 RPM (19.25% S.E.)	Case Deflection Less Sensitive to LPT Unbalance with #5 brg. Damper.
Low Shaft Mode	7303 RPM (80.99% S.E.)	87% Above Max. N., 25.9% Below N ₂ IDLE.
Tailplug Mode	4723 RPM (22.49% S.E.)	21% Above Max. N ₁

(N₁)Idle = 1103 rpm

(N₁)max = 3902 rpm

Rotor Design

The design of the rotor (disks, hubs, spacers and shaft) was continued, and is nearing completion. The current rotor construction is shown in Figure 185. The major design changes since the preliminary design review (see Figure 186) are as follows:

1. Rotating inner seals were removed from structural spacers and included as part of nonstructural spacers. Analysis of the preliminary rotor showed that in the event of a heavy rub, secondary damage could result in release of a disk. The current configuration not only ensures rotor integrity, but shields the structural rotor from hot gas path flow (see item 3).
2. Wide channel seals were replaced by stepped 3- or 2-knife edge labyrinth seals riding inside honeycomb seal lands. The axial excursion of the low rotor assembly and the deflection of the inner diameter ends of the vanes under thermal/gas bending loads was estimated to require larger than desired radial gaps (clearances) for wide channel seals to prevent rubbing. Little, if any, advantage over the conventional knife edge on honeycomb combination could be established.



PRATT & WHITNEY AIRCRAFT GROUP
COMMERCIAL PRODUCTS DIVISION

ORIGINAL PAGE 17
OF POOR QUALITY

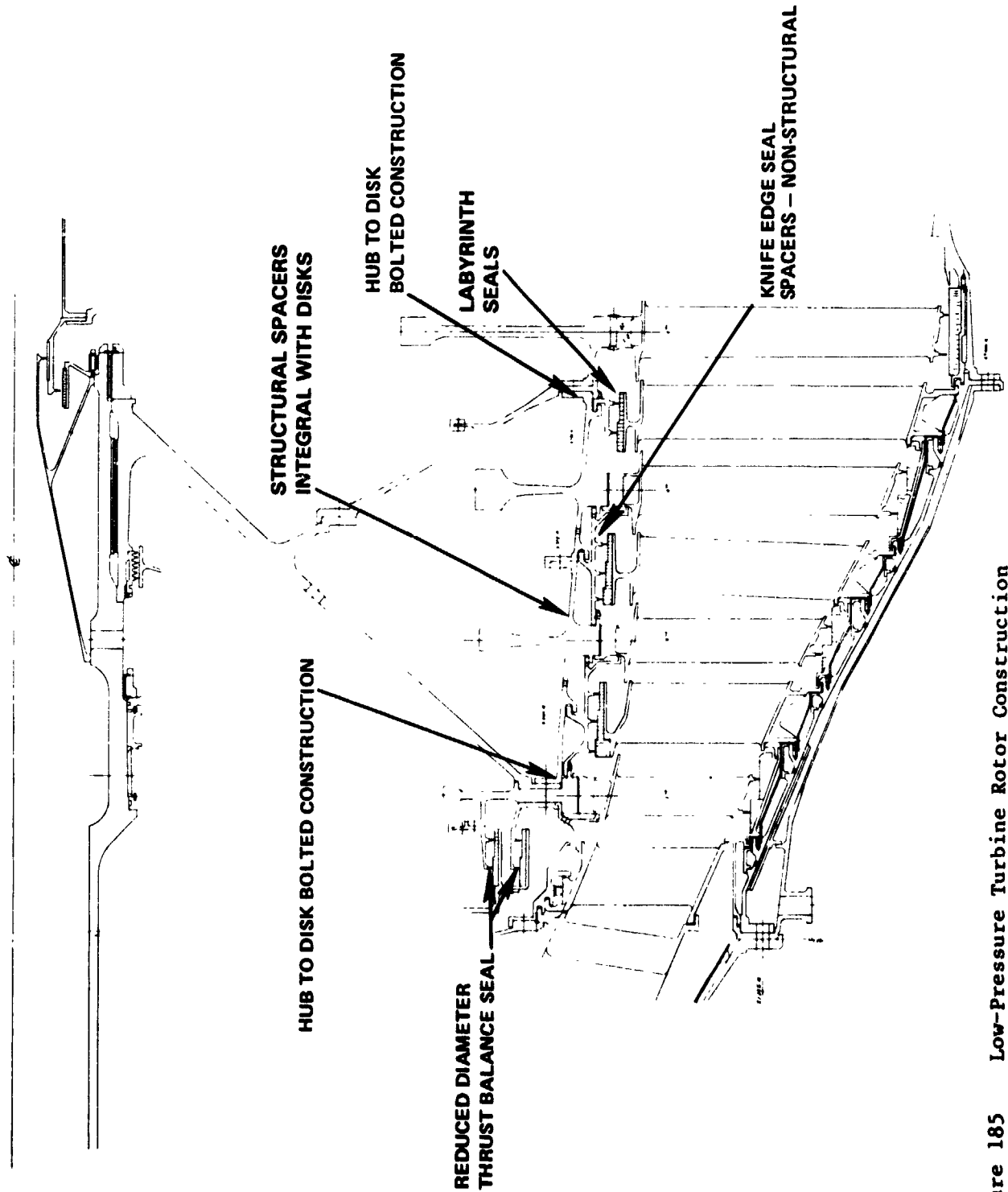
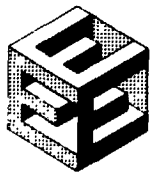


Figure 185 Low-Pressure Turbine Rotor Construction



PRATT & WHITNEY AIRCRAFT GROUP
COMMERCIAL PRODUCTS DIVISION

ORIGINAL FILED IN
OF POOR QUALITY

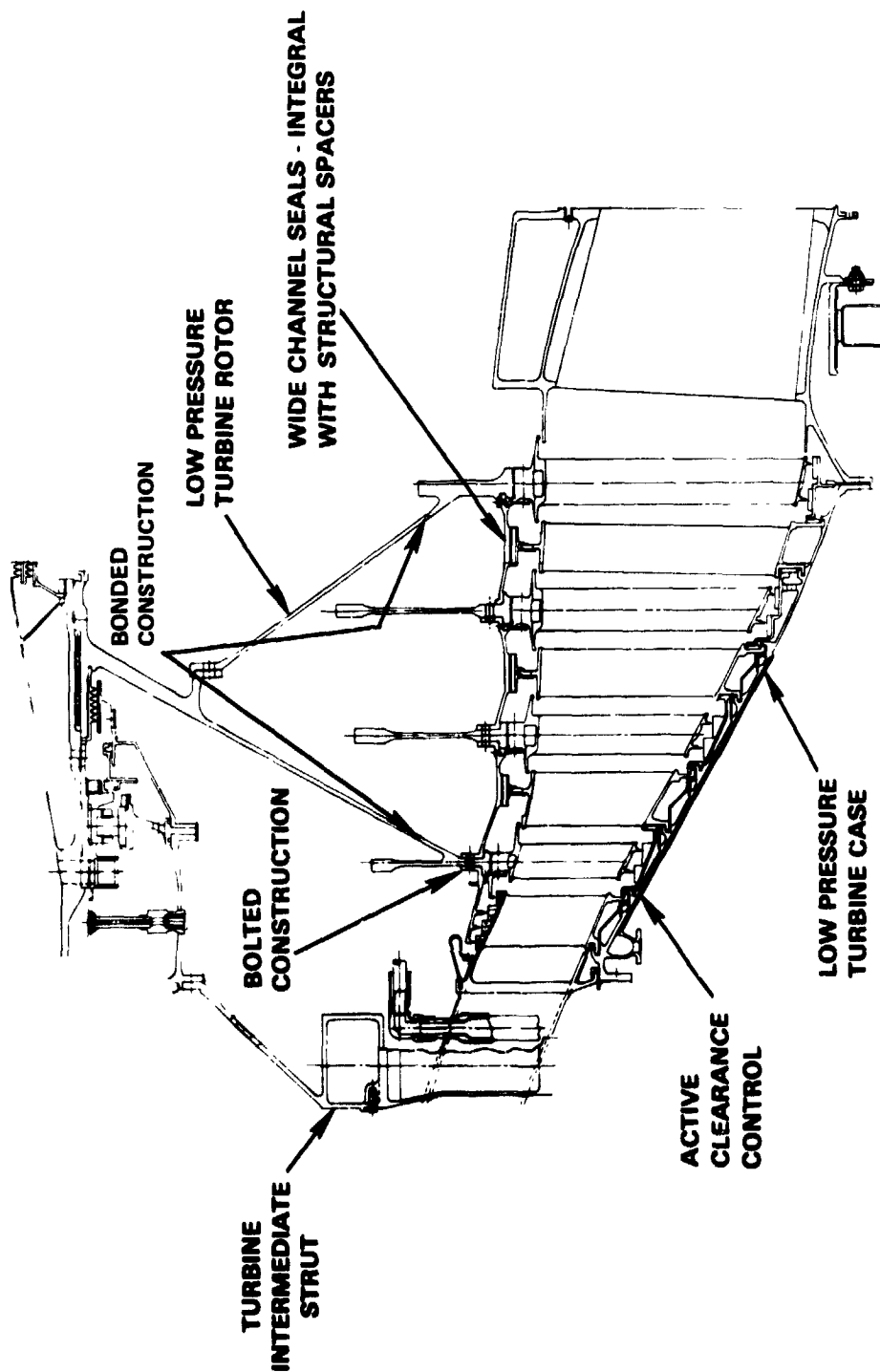
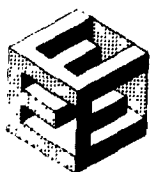


Figure 186 Low-Pressure Turbine Component Major Features (Preliminary Design Review Configuration)



PRATT & WHITNEY AIRCRAFT GROUP
COMMERCIAL PRODUCTS DIVISION

In addition thermal studies showed a clearance advantage to an air seal design which shielded the structural rotor, especially with cooling air flowing between the air seal and structural rotor (see Figure 187).

3. The front hub and rear hub are bolted rather than welded or bonded to the 2nd stage disk and 5th stage disk, respectively.
4. The thrust balance seal on the front of the 2nd stage disk was revised to a reduced diameter in keeping with the required thrust balance load. Two seals of a 2-step labyrinth configuration each were selected based on the pressure drop between gas path and the cavity forward of the 2nd stage disk. Vibration analysis of these seals is in process prior to completing the design.

Case Design

Thermal analysis work on the low-pressure turbine case was conducted to optimize the active clearance control system. The feasibility of using internal active clearance control with case-tied outer air seals was established during the preliminary design effort. For this design, cooling air from the high-pressure compressor discharge (15th stage) was to be used at sea level takeoff and 10th stage air was to be used at cruise. The case configuration (see Figure 188) allowed cooling air to pass between inner and outer case walls to cool the outer air seal hooks of stages 2 and 3 and the front hooks of stage 4. A 0.050-inch gap between case walls was incorporated in order to improve heat transfer characteristics.

Analysis conducted during the current reporting period resulted in the modified configuration shown in Figure 189, which incorporates the following changes:

1. A mixture of cooling flows from the 10th stage and 15th stage bleeds may be used instead of either 10th or 15th stage air. Studies now in process will determine if the same mixture selected for high-pressure turbine active clearance control can be used in the low-pressure turbine.
2. Cooling was extended aft to the 5th stage vane front foot. Cooling is now introduced at 6 axial locations at the rate of 0.1 percent Waa at each location.



PRATT & WHITNEY AIRCRAFT GROUP
COMMERCIAL PRODUCTS DIVISION

ORIGINAL PAGE IS
OF POOR QUALITY

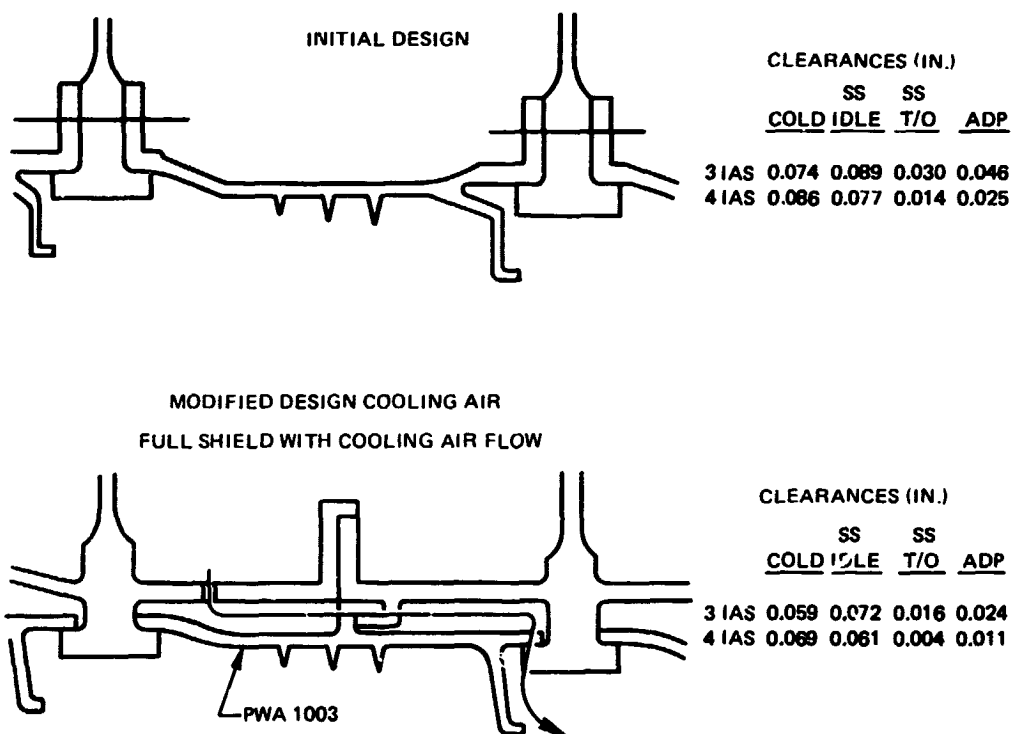
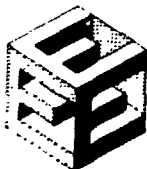
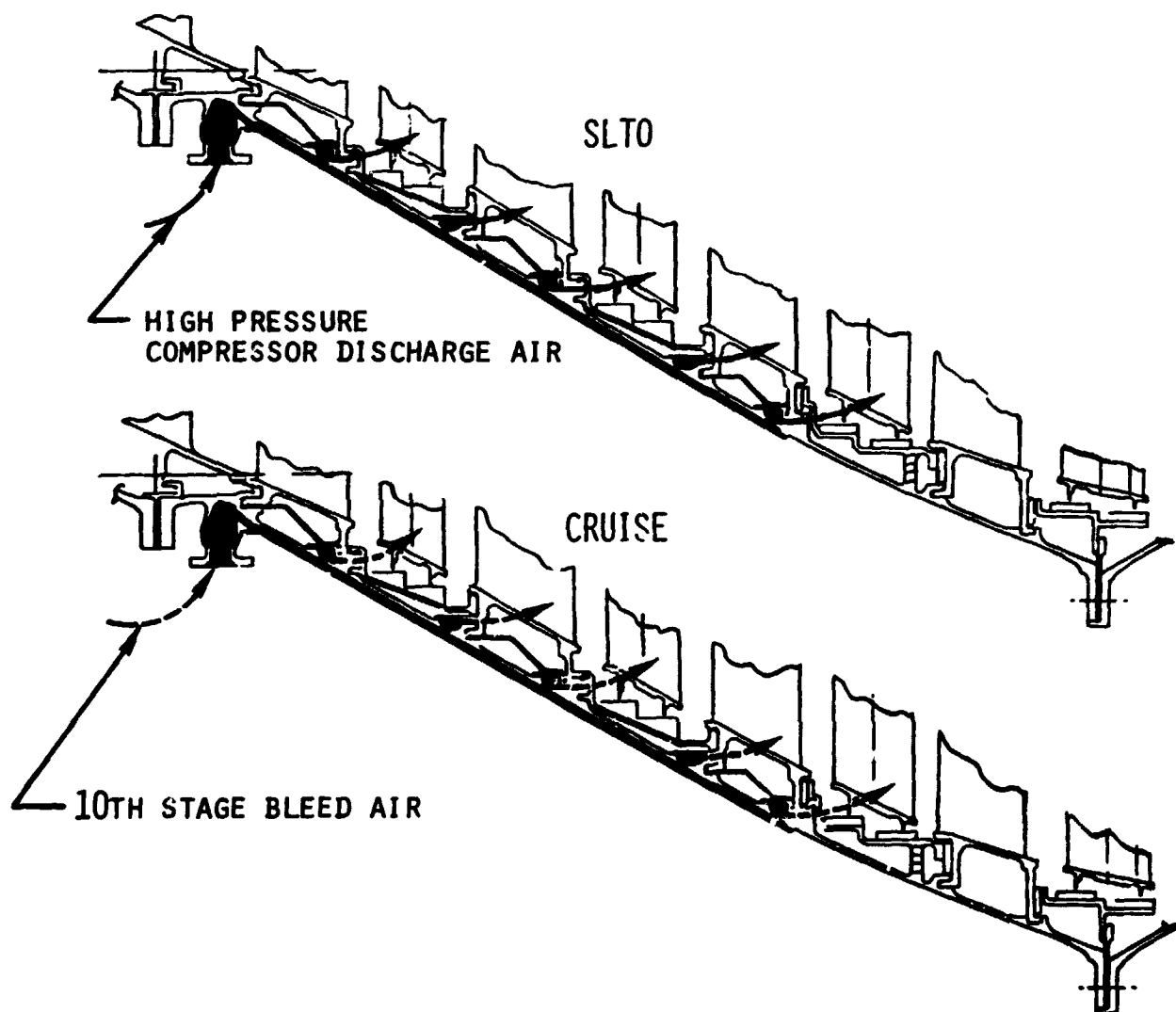


Figure 187 Low-Pressure Turbine Inner Air Seal Design Schemes



PRATT & WHITNEY AIRCRAFT GROUP
COMMERCIAL PRODUCTS DIVISION

ORIGINAL
OF POOR QUALITY



J19596-79
782208

Figure 188 Low-Pressure Turbine Active Clearance Control System
(Preliminary Design Review Configuration)



PRATT & WHITNEY AIRCRAFT GROUP
COMMERCIAL PRODUCTS DIVISION

ORIGINALLY DESIGNED
OF POOR QUALITY

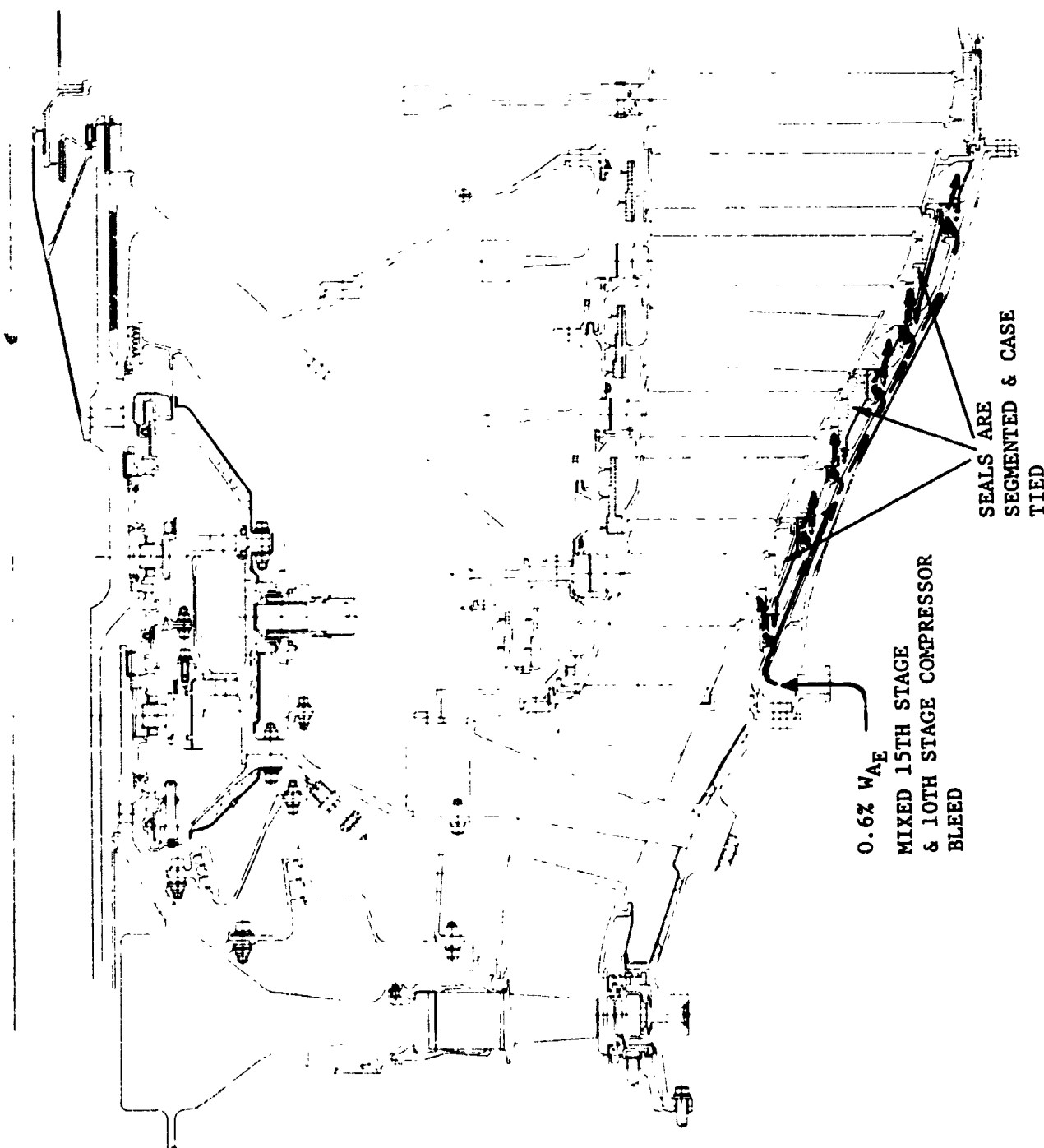


Figure 189 Modified Low-Pressure Turbine Active Clearance Control System



3. Cost studies indicated that maintaining a 0.050-inch gap between inner and outer case walls was too costly. As an alternative approach, a design was devised that provides a 0.065-inch gap for the stage 2 rotor area, where higher temperatures call for more effective cooling and control of the blade tip gap. The controlled gap is provided by machining grooves 0.065 inch deep in the case and brazing segmented plates over the grooves to cooling passages (see Figure 190). Cooling air for aft of the second stage is controlled by directing flow between inner and outer cases and then through holes in the inner case wall to manifold rings. From these locations the flow is directed over vane and outer air seal attachment areas.

Low-Pressure Turbine Component Fabrication

With NASA approval, raw material procurement was started earlier than planned during this reporting period in order to maintain existing schedule requirements for fabricating the low-pressure turbine parts for the first build of the integrated core/low spool. The following items were ordered in advance of approval of the low-pressure turbine design:

- o Disk MERL 76 compactions,
- o Hub and rear cone forgings,
- o Vane and blade castings,
- o Forgings for the low-pressure turbine case and the hot strut case,
- o Hot strut fairing castings, and
- o Long lead time nuts and bolts.



PRATT & WHITNEY AIRCRAFT GROUP
COMMERCIAL PRODUCTS DIVISION

ORIGINAL PAGE IS
OF POOR QUALITY

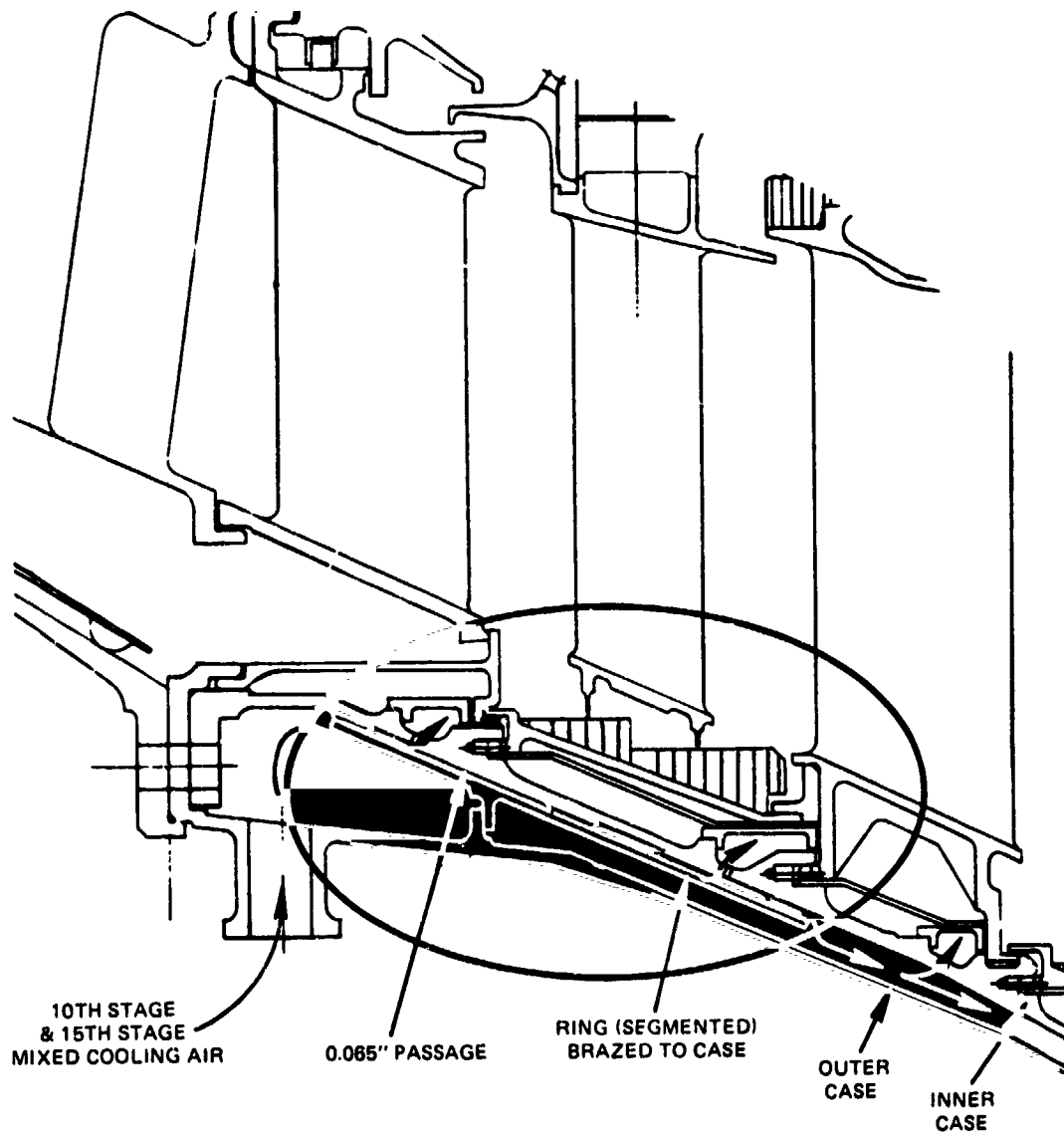


Figure 190 Low-Pressure Turbine Cooling Passages



3.2.8.4 Supporting Technology

3.2.8.4.1 Boundary Layer Test Program

3.2.8.4.1.1 Objective

Verify boundary layer design concepts employed in the Energy Efficient Engine low-pressure turbine component.

3.2.8.4.1.2 Scope of Total Work Planned

The boundary layer test program consists of four phases shown in Figure 191. All test sections for the UTRC suction surface boundary layer wind tunnel are designed, fabricated, and assembled. Unique test hardware and instrumentation is incorporated. Test objectives and procedures, hardware, instrumentation, and analysis and reporting methods are described in the technology test plan. Airfoil configurations selected for analysis include two forward transition type flows typical of the suction surface of the Energy Efficient Engine low-pressure turbine airfoils. Salient non-dimensional parameters including Reynolds number are preserved. Boundary layer development of the four flows is measured in terms of mean velocities and turbulence levels. Measuring instruments, determined by the flow region being investigated, include conventional boundary layer pitot probes, hot wire anemometers, and flush-mounted hot film probes. The turbulence model in the finite difference boundary layer program is verified, and the criteria used in designing a set of low-pressure turbine airfoils are substantiated.

3.2.8.4.1.3 Technical Progress

3.2.8.4.1.3.1 Summary of Work Previously Completed

The suction surface was tested prior to this reporting period. Initial test results indicated that the pressure distribution of the "squared-off" design generated 8 percent lower loss than that of the "aft-loaded" design. Regions of laminar, transitional, and turbulent flow regimes were identified by flush-mounted hot film probes. The transition zone for the "squared-off" distribution was approximately 3 times longer than that of the "aft-loaded" (baseline) profile. All technical work on this task was completed during the current reporting period.

3.2.8.4.1.3.2 Current Technical Progress

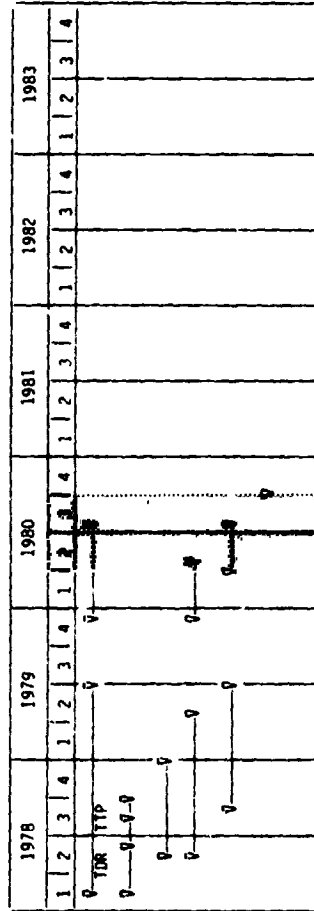
The data obtained in the low-pressure turbine boundary layer supporting technology program were reduced and analyzed. The results of this program are summarized in the following paragraphs.



PRATT & WHITNEY AIRCRAFT GROUP
COMMERCIAL PRODUCTS DIVISION

ORIGINAL...
OF POOR QUALITY

BOUNDARY LAYER TEST PROGRAM - WORK PLAN SCHEDULE



ACTIVITIES/MILESTONES
TOTAL WBS TIMING
ANALYSIS AND DESIGN
FABRICATION
UTRIC EFFORT
POST-TEST ANALYSIS
SUBMIT TECHNOLOGY REPORT

*M DENOTES MAJOR MILESTONE *D DENOTES KEY DECISION POINT

Figure 191 Boundary Layer Test Program Work Plan Schedule



Background

Aft-loaded and squared-off pressure distributions were tested in terms of losses resulting from boundary layer development on the suction surface of low-pressure turbine airfoils. Velocity distributions were simulated on flat plates in a low-speed, high-aspect-ratio wind tunnel specifically designed for boundary layer investigations. Detailed measurements of the boundary layer mean velocity and turbulence intensity profiles were obtained for an inlet turbulence level of 2.4 percent and an exit Reynolds number of 8×10^5 . Flush-mounted hot-film probes were used to identify the boundary layer transition regimes located in the adverse pressure gradient regions for the two velocity distributions.

Results

The results of the boundary layer supporting technology program indicated that the squared-off velocity distribution generated a momentum loss thickness of approximately 8 percent less than the aft-loaded distribution.

The data from this test were used to substantiate the prediction capability of the Pratt & Whitney Aircraft boundary layer deck. This deck was in turn used to conduct an analytical study to assess the magnitude of losses expected for the various stages of the Energy Efficient Engine low-pressure turbine.

The results of this study indicated that lower losses in the low-pressure turbine could be attained by incorporating aft-loaded airfoils in the front stages and squared-off design airfoils in the aft stages. The difference in losses for the two types of airfoils, however, was small (+5 percent of the average loss).

The limited amount of test data, combined with the inherent uncertainty of the turbulence level in the low-pressure turbine, made it difficult to recommend one type of airfoil over another for use in the low-pressure turbine component. The experience gained in testing of the low-pressure turbine subsonic cascade (see section 3.2.8.4.2 of this report), however, suggests that the aft-loaded airfoil design offers more promising performance benefits. Because the boundary layer investigation does not provide contrary results, the aft-loaded design concept will be maintained in the Energy Efficient Engine low-pressure turbine.

Mean Velocity Profile. Twenty mean velocity profiles were measured, ten for each of the two pressure distributions. Nine of these profiles were located in the laminar flow region, four in the transitional flow region, and the remaining seven in the fully turbulent flow region. A comparison of the mean velocity profile data in the transitional and turbulent boundary layer regimes with well-established semi-empirical formulations is as follows.



All turbulent boundary layer data have a universal region where Equation 1 is valid.

Equation 1:

$$U^+ = \frac{1}{k} \ln y^+ + B$$

The fully turbulent boundary layer mean velocity profile data from the two configurations are plotted in Figure 192 using the dimensionless parameters of Equation 1.

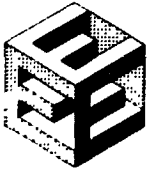
Squared-off Pressure Distribution. Experimental data for the integral parameters from the squared-off design are plotted in Figure 193 along with predicted values. In general, the predictions were in good agreement with the test data.

Detailed mean velocity profile data are compared with predictions in Figure 194. The predictions were in good agreement with laminar and turbulent velocity profiles, but in poor agreement with the transitional boundary layer profile data.

Aft-Loaded Pressure Distribution. A comparison of the experimental test data and the predictions for the aft-loaded test is presented in Figure 195. Predictions and test data were in good agreement for the accelerating part of the flow, but showed flow separation in the diffusing part. The calculations were repeated, and the boundary layer was artificially made transitional at a distance of two boundary layer thicknesses upstream of the expected separation point in order to obtain theoretical predictions. On the basis of the present data, it is difficult to ascertain whether the boundary layer had actually separated at the predicted location. The calculated separation point, however, was slightly upstream of the transition region identified with the hot-film probes. Even if separation had occurred, it did not influence the behavior of intermittency factor in the transitional region.

Figure 196 provides detailed velocity profile data along with predictions. Again, measured and predicted mean velocity profiles were in good agreement for the laminar and turbulent regions.

Profile Loss Assessment. Relative magnitudes of profile losses associated with aft-loaded and squared-off pressure distributions can be evaluated by a direct comparison of the integral parameters obtained from the test data. The distribution of the three integral parameters (boundary layer momentum loss thickness Reynolds number (Re_θ)), shape factor (H), and skin friction (C_f)) is plotted in Figure 197. The test results obtained in terms of these three integral parameters are presented in the following paragraphs.



PRATT & WHITNEY AIRCRAFT GROUP
COMMERCIAL PRODUCTS DIVISION

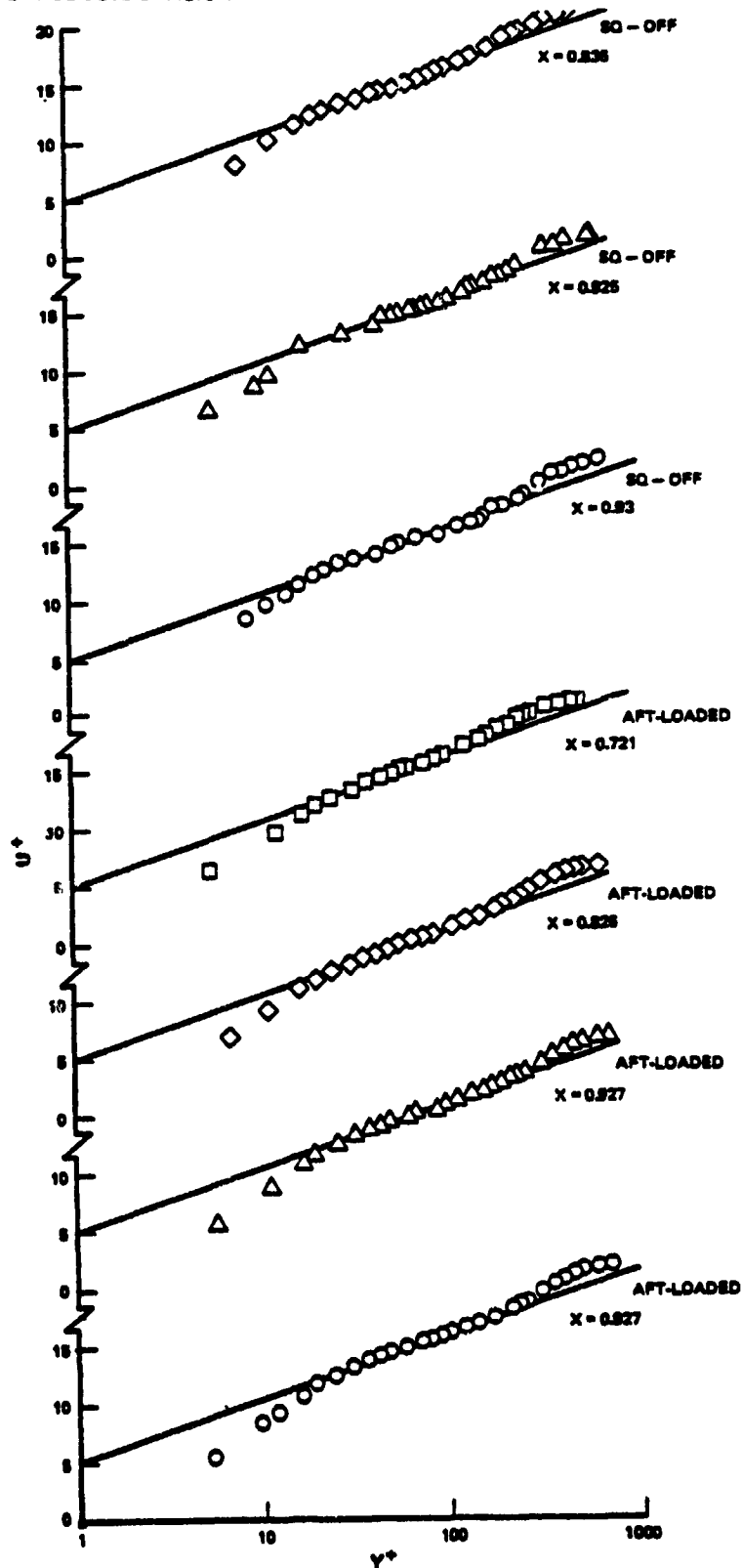


Figure 192 Turbulent Boundary Layer Velocity Profiles Using Dimensionless Parameters



PRATT & WHITNEY AIRCRAFT GROUP
COMMERCIAL PRODUCTS DIVISION

ORIGINAL PAGE IS
OF POOR QUALITY

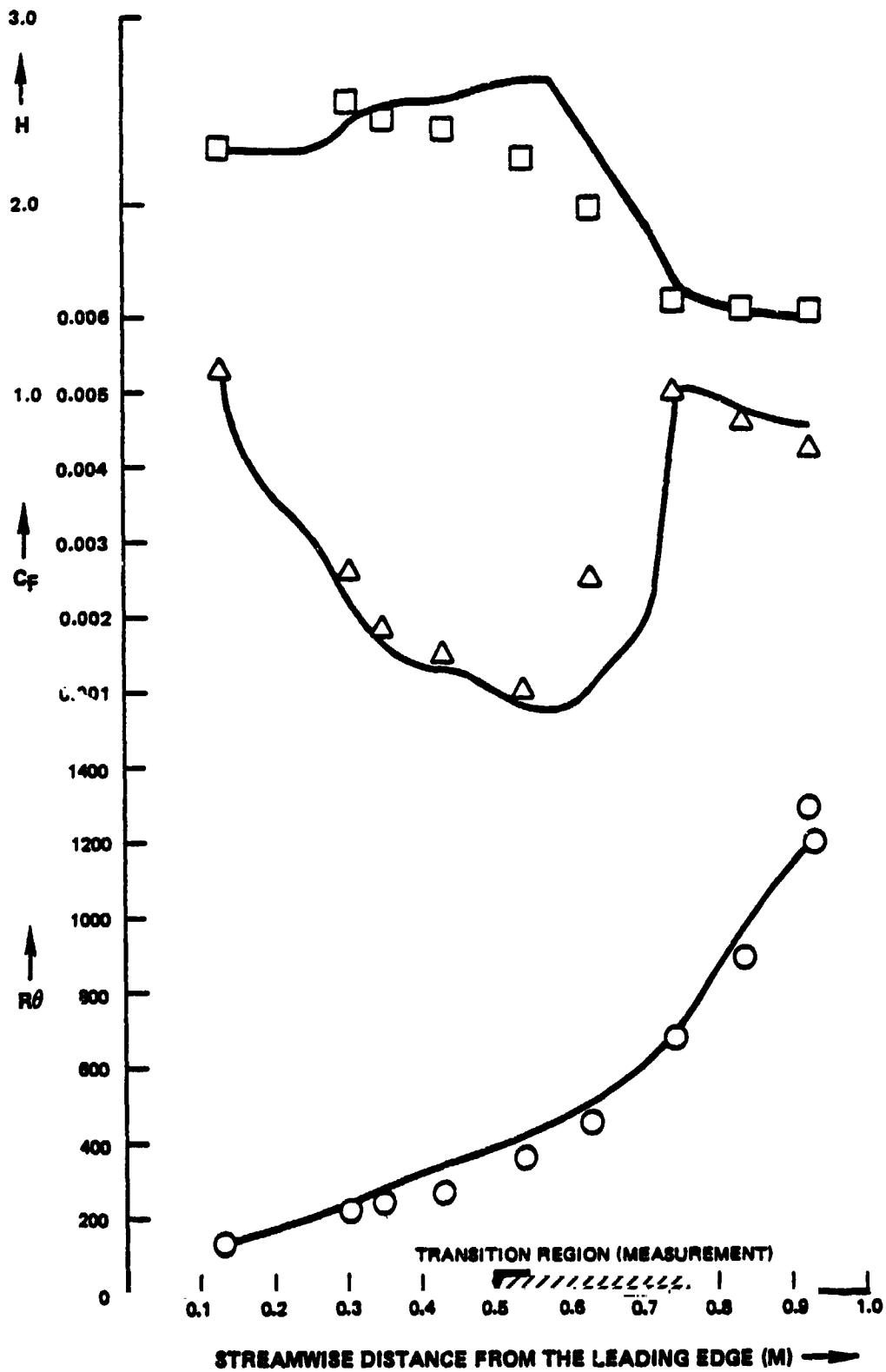


Figure 193

Comparison of Measured Integral Parameters for the "Squared-off" Test Section with Theoretical Predictions



PRATT & WHITNEY AIRCRAFT GROUP
COMMERCIAL PRODUCTS DIVISION

ORIGINAL PAGE 13
OF POOR QUALITY

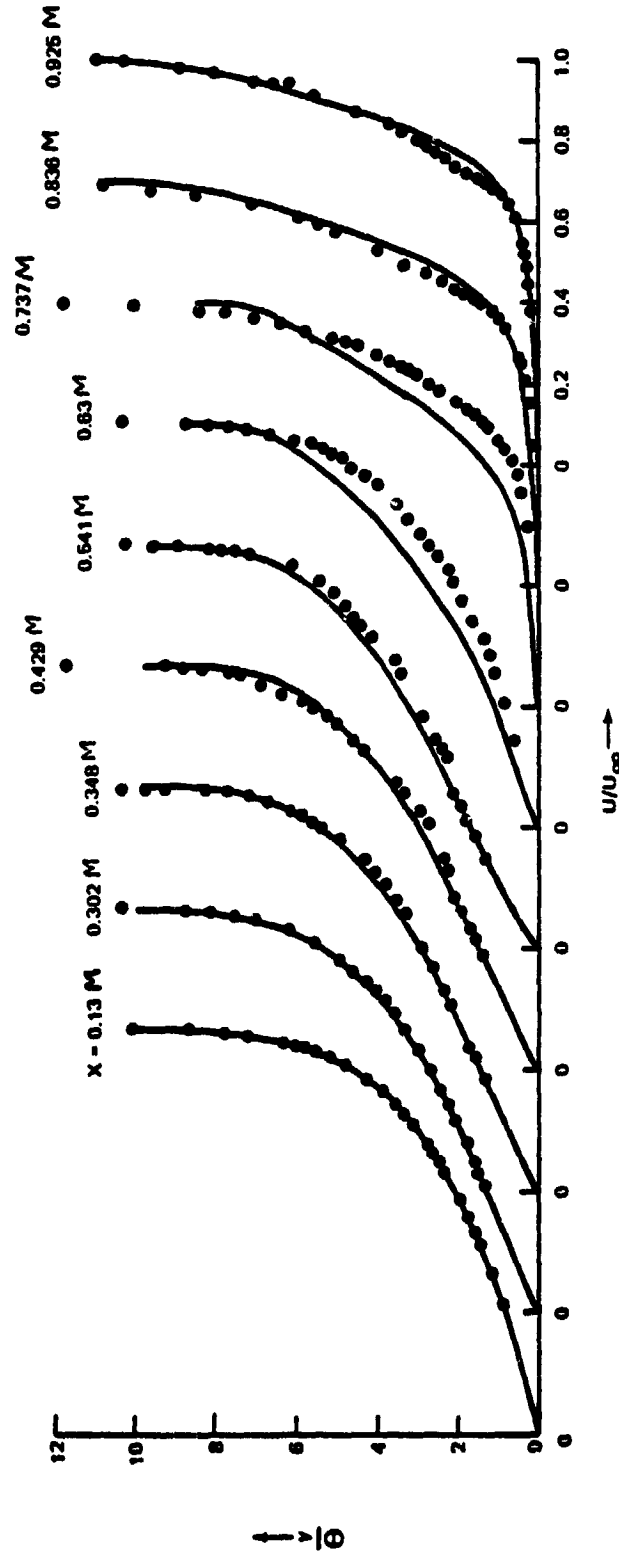
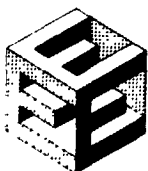


Figure 194 Comparison of the Measured Mean Velocity Profile Data
(Squared-off) with Theoretical Predictions



PRATT & WHITNEY AIRCRAFT GROUP
COMMERCIAL PRODUCTS DIVISION

ORIGINAL PAGE IS
OF POOR QUALITY

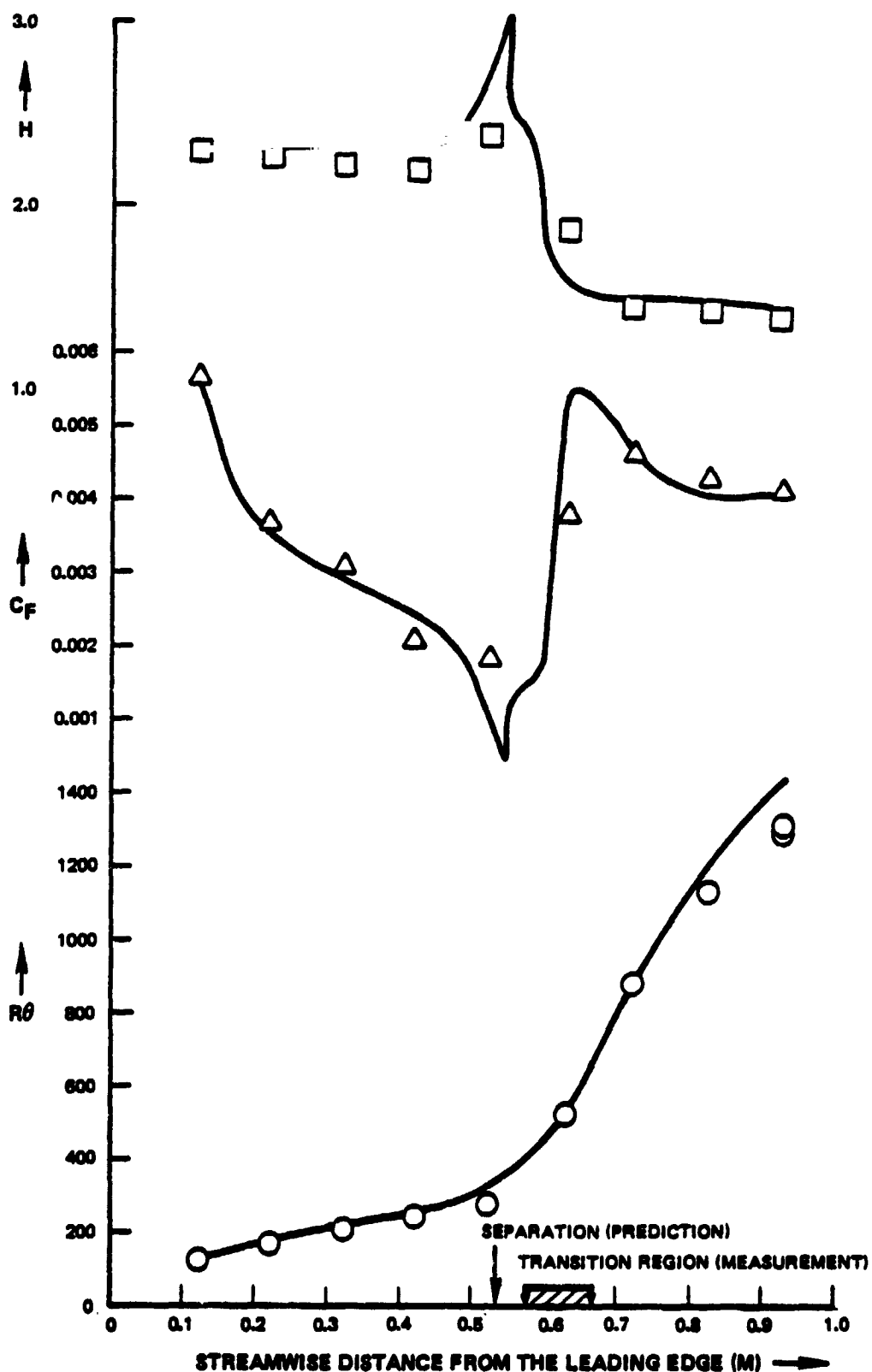


Figure 195 Comparison of Measured Integral Parameters for the Aft-loaded Test with Theoretical Predictions



PRATT & WHITNEY AIRCRAFT GROUP
COMMERCIAL PRODUCTS DIVISION

ORIGINAL FILE COPY
OF POOR QUALITY

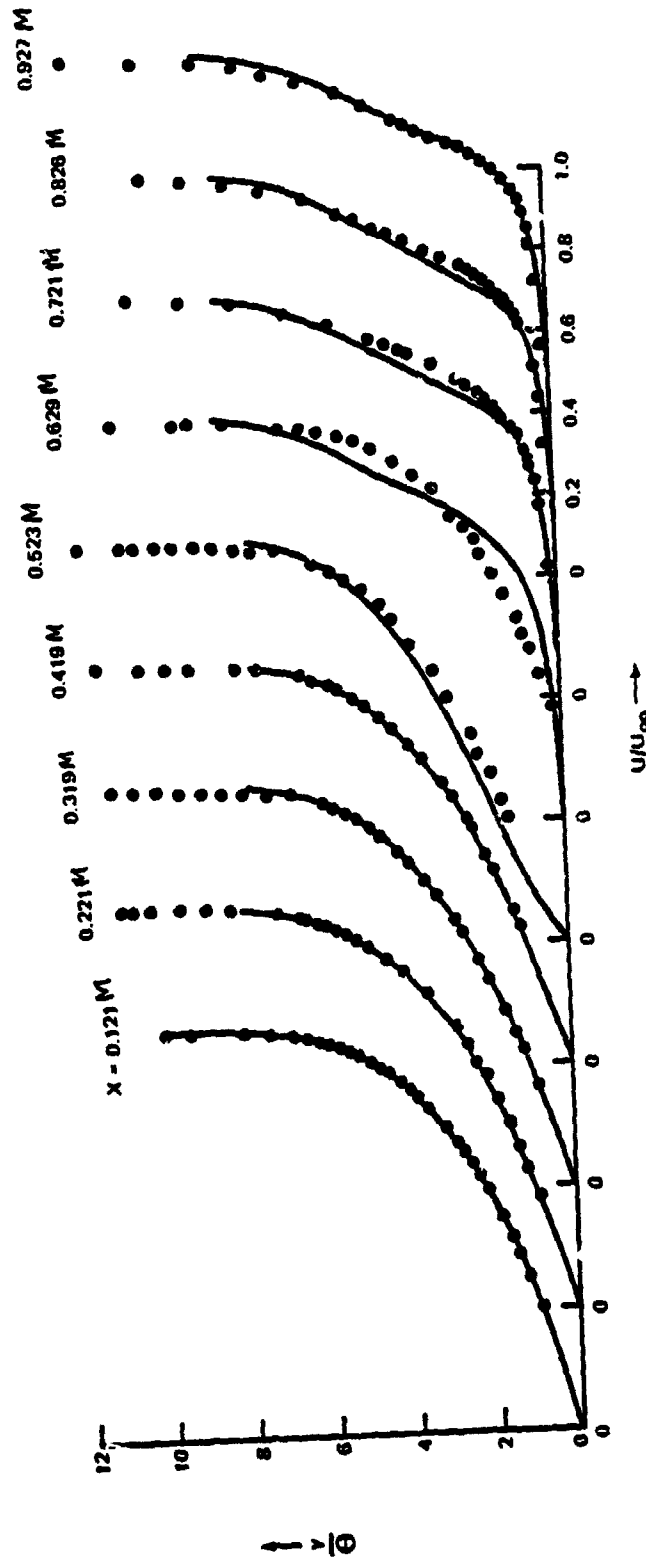
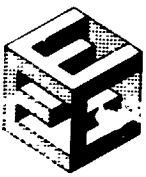


Figure 196 Comparison of the Measured Mean Velocity Profile Data
(Aft-loaded) with Theoretical Predictions



PRATT & WHITNEY AIRCRAFT GROUP
COMMERCIAL PRODUCTS DIVISION

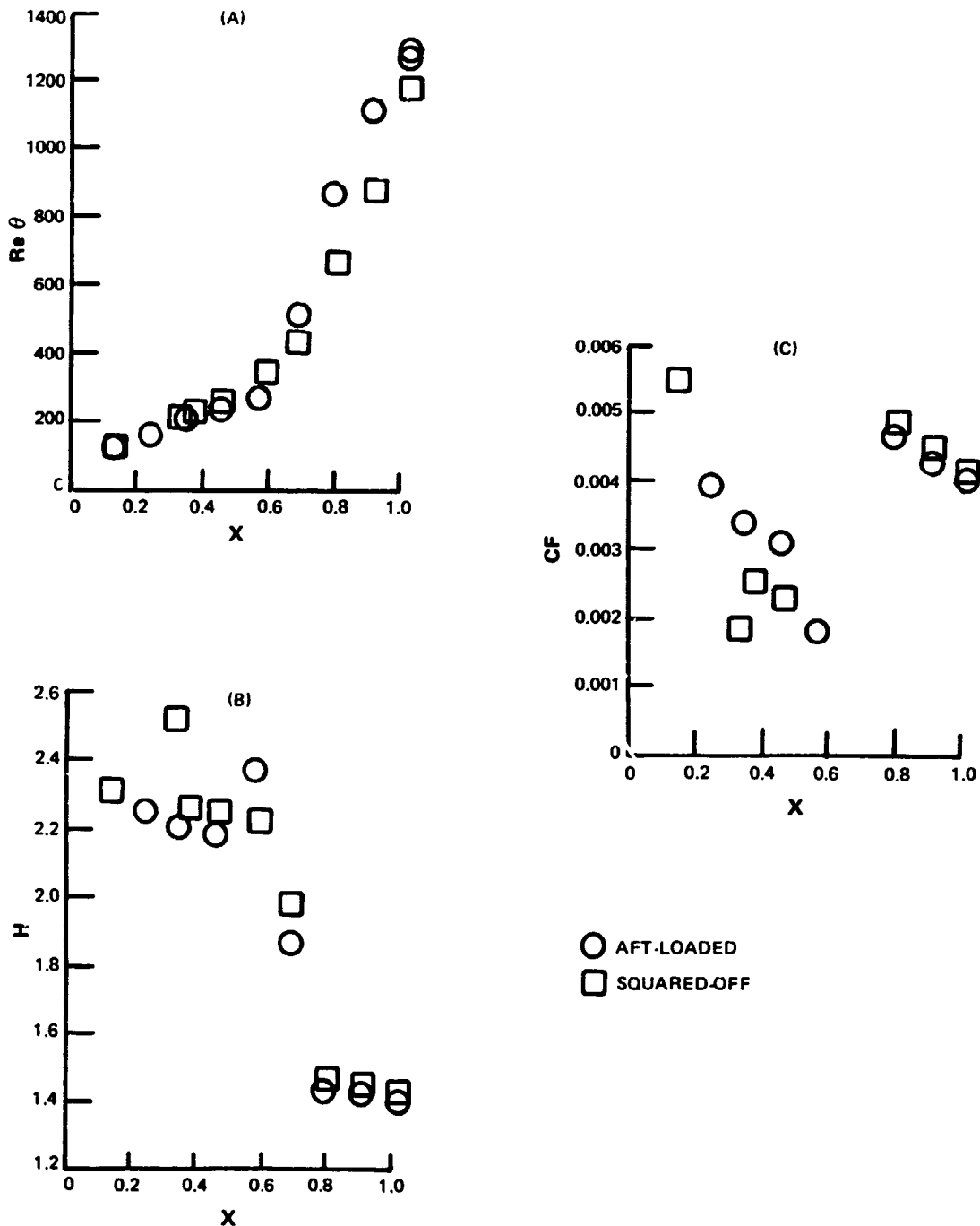


Figure 197 Distribution of Boundary Layer Momentum Loss Thickness Reynolds number (Re_{θ}), Shape Factor (H), and Skin Friction (C_f)



Momentum Loss Thickness. Test results indicated that the momentum loss thickness (δ^*) for the aft-loaded airfoil section was 8 percent larger than for the squared-off section (see Figure 197(a)). This means that a squared-off airfoil of the same design as the aft-loaded airfoil would have an 8-percent lower suction side loss.

Shape Factor. The shape factor ($H = \delta^*/\theta$) associated with the aft-loaded test increased at a location before the transition region, thus indicating a possibility of separation before transition. The distribution of boundary layer shape factor is shown in Figure 197(b). The distributions for each airfoil design are similar in the laminar regime ($H = 2.3$) and the turbulent regime ($H = 1.4$).

Skin Friction. No procedure is available for estimating skin friction (C_f) for the transitional region; therefore, the data for this region have been omitted. The distribution of laminar and turbulent skin friction showed similar behavior. The aft-loaded skin friction rate of decrease with stream distance was high, indicating that laminar separation may have occurred.

Boundary Layer Turbulence Intensity Profiles. Boundary layer turbulence intensity profiles are discussed in the following paragraphs for the following flow regions: turbulent, transitional, and laminar.

Turbulent Region. Turbulent intensity profiles were obtained from the three components of turbulence (u^2 , v^2 , and w^2) measured at the exit plane of the two airfoil designs. Test data were in good agreement with flat plate data (see Figure 198). Relative magnitudes of the streamwise (u^2) and normal (v^2) components are shown for the squared-off configuration in Figure 199. The data indicated that the streamwise component contained approximately 50 percent of the total intensity and the normal component, about 20 percent, which is consistent with the Pratt & Whitney Aircraft prediction system.

Transitional Region. Relative magnitudes of turbulence intensity components for the transitional region of the squared-off design are shown in Figure 200. The program data show that the streamwise and the normal components contain approximately 80 and 10 percent of the total turbulence intensity, respectively. This means that the turbulence in transitional boundary layers is more non-isotropic than in fully turbulent boundary layers.



ORIGINAL PAGE 19
OF POOR QUALITY

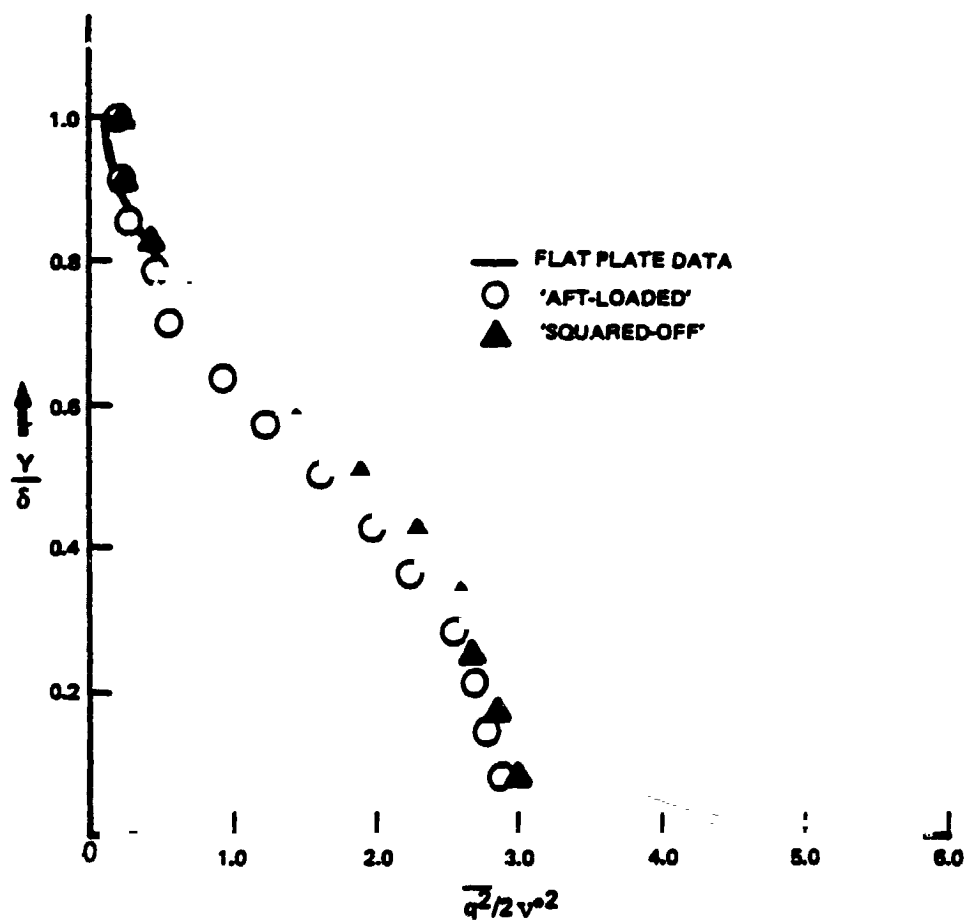


Figure 198 Comparison of Measured Total Turbulence Intensity Profiles with Flat Plate Data



ORIGINAL SOURCE
OF POOR QUALITY

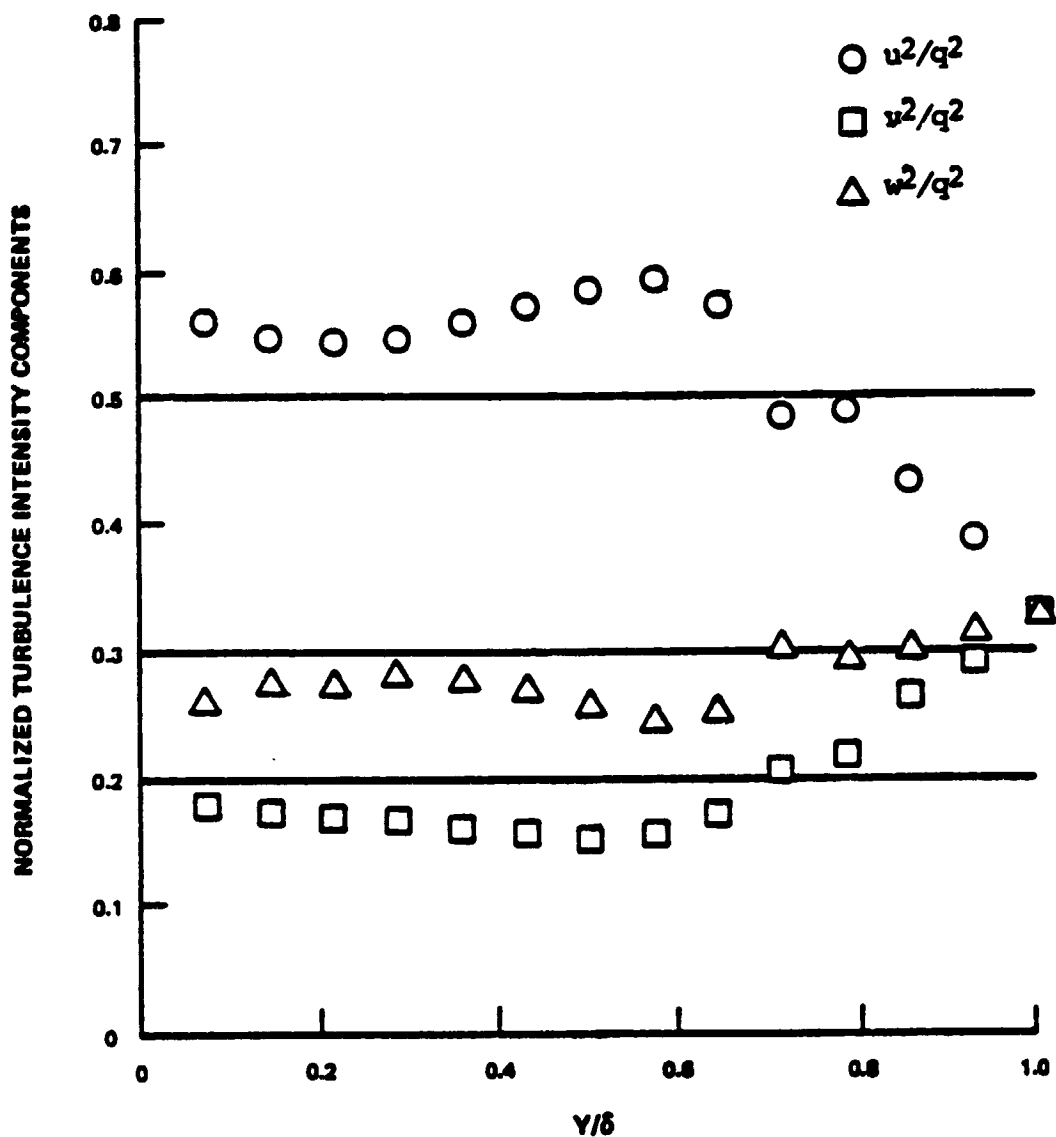


Figure 199 Distribution of Normalized Turbulence Intensity Components in the Fully Turbulent Region of the Squared-off Test Configuration



ORIGINAL PAGE IS
OF POOR QUALITY

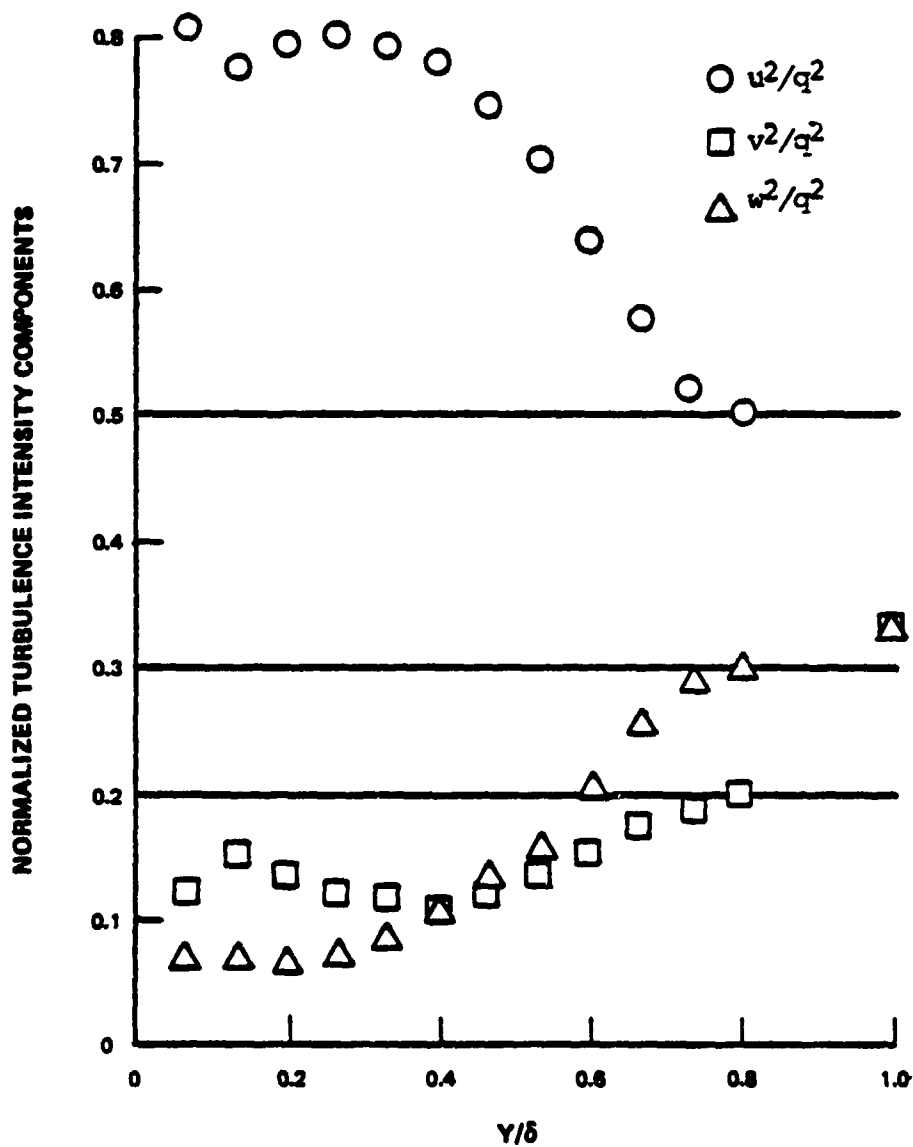


Figure 200

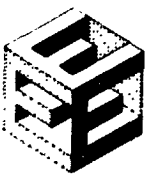
Distribution of Normalized Turbulence Intensity Components in
the Transitional Region of the Squared-off Test Configuration



Laminar Region. Systematic growth of the streamwise component of turbulence intensity was observed in the laminar region of both airfoil designs. Dimensionless turbulent intensity (u^+) data in the laminar boundary region for both airfoil designs were presented as functions of y^+ in Figure 201, which indicates two important features: (1) turbulence intensity profiles in the laminar region had a maximum value of approximately $y^+ = 25$, and (2) maximum turbulence intensity (u^+ at $y^+ = 25$) increased in the downstream direction as the onset of transition was approached.

It is apparent that a knowledge of the magnitude of turbulence in low-pressure turbines is important for estimating losses associated with airfoil boundary layers. Although measurements of turbulence levels in full-scale engine turbines are not available, the levels are believed to be higher than those encountered in the experimental portion of the present program.

The test results for momentum loss thickness were fairly well predicted by the Pratt & Whitney Aircraft boundary layer prediction methods. Therefore, these methods can be used to estimate the profile losses for the Energy Efficient Engine low-pressure turbine airfoils with a fair degree of accuracy if a realistic estimate of turbulence level is assumed for the low-pressure turbine.



PRATT & WHITNEY AIRCRAFT GROUP
COMMERCIAL PRODUCTS DIVISION

ORIGINAL PAGE IS
OF POOR QUALITY

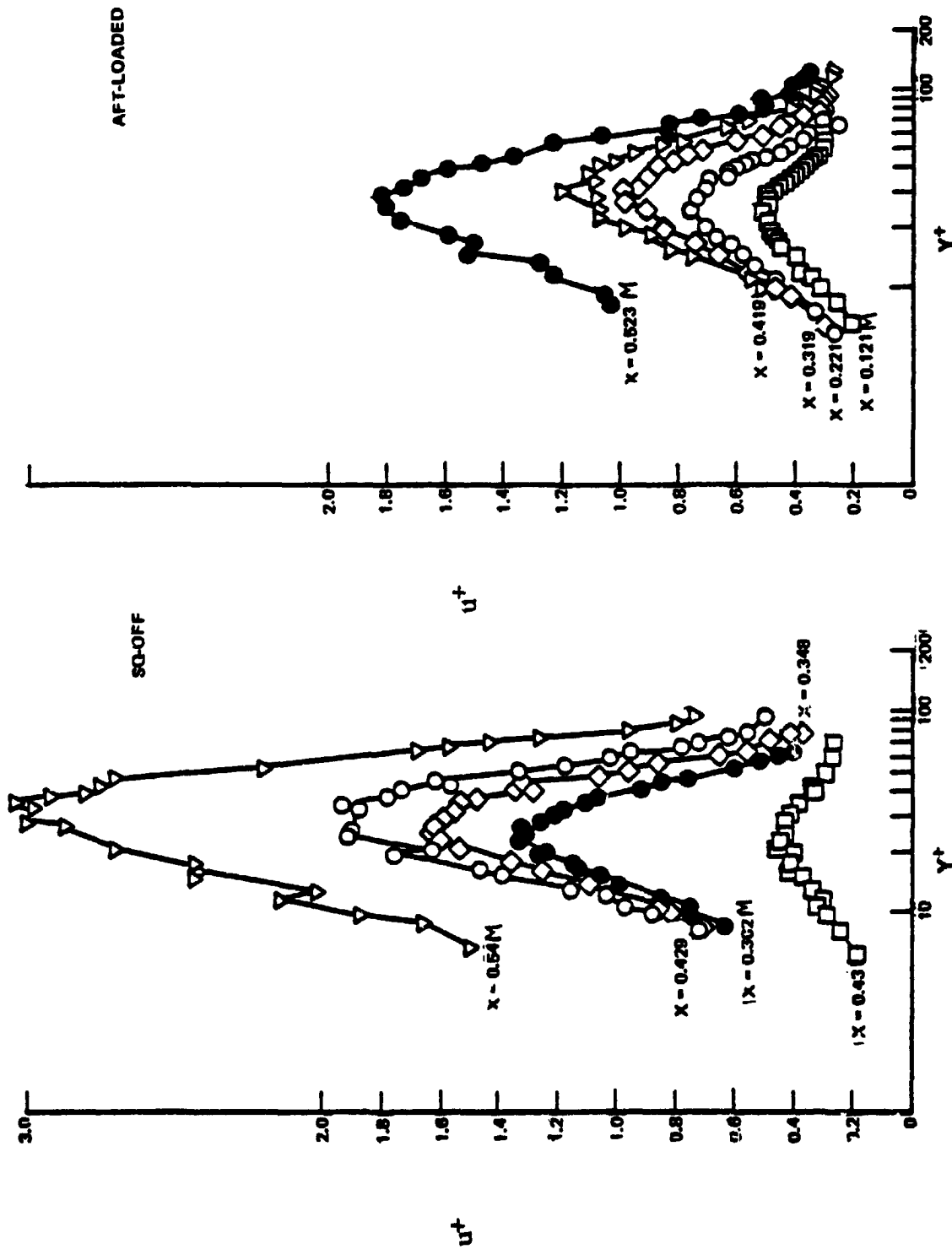


Figure 201 Growth of Turbulence Intensity in the Laminar Region of Each Boundary Layer



3.2.8.4.2 Subsonic Cascade Test Program

3.2.8.4.2.1 Objective

Develop (through analysis and testing) the design of low-loss, highly loaded airfoils for the flight propulsion system low-pressure turbine component design.

3.2.8.4.2.2 Scope of Total Work Planned

This program comprises the four phases shown in Figure 202. Five airfoil packs, representing different chordwise and spanwise load distributions, are designed, fabricated, and assembled for testing. Mach number, Reynolds number, and loading consistent with Energy Efficient Engine specifications are maintained. Other considerations are endwall and profile losses, endwall pressure distribution, and airfoil loading. A traversing probe and a turbulence grid are designed to facilitate testing of the blade mean section. A test plan defines test objectives and procedures, hardware and instrumentation, and analysis and reporting methods.

The airfoil cascades are tested at varying pressure ratios and inlet incidence angles to investigate off-design characteristics. Pressure distributions, loss maps, and flow visualization results are used to verify low-pressure turbine predictions. Figure 202 indicates those activities completed in previous reporting periods. It also indicates that testing and post test analysis were initiated during the previous reporting period and were continued during the current reporting period.

3.2.8.4.2.3 Technical Progress

3.2.8.4.2.3.1 Summary of Work Previously Completed

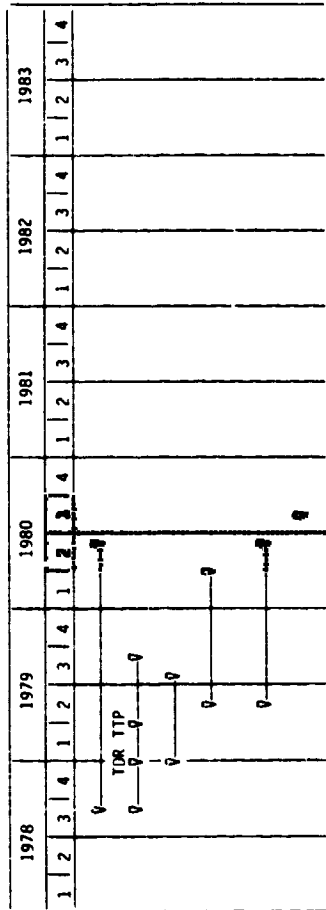
The low camber first vane, fourth blade root front-loaded airfoil, and fourth blade mean "aft-loaded" baseline airfoil (for the root exit Mach number) were tested at two levels of turbulence. Mid-span and endwall loss data indicated that the aft-loaded airfoil exhibited the lowest pressure loss over the range of Mach numbers and inlet air angles evaluated. All technical work on this task was completed during the current reporting period. Most of the results from this program are described in the Fourth Semiannual Status Report. The remaining effort is described in section 3.2.8.4.2.3.2 of this report.

3.2.8.4.2.3.2 Current Technical Progress

The data obtained from the low-pressure turbine subsonic cascade technology program were reduced and analyzed. The results of this program are presented as follows: (1) low camber first vane performance, (2) testing of an alternate aerodynamic loading distribution on the fourth blade root section, and (3) verification of low-pressure turbine design concepts.



SUBSONIC CASCADE TEST PROGRAM - WORK PLAN SCHEDULE



ACTIVITIES/MILESTONES

TOTAL MBS TIMING

ANALYSIS AND DESIGN

FABRICATION

TEST

POST-TEST ANALYSIS

SUBMIT TECHNOLOGY REPORT

*M DENOTES MAJOR MILESTONE *D DENOTES KEY DECISION POINT

Figure 202 Subsonic Cascade Test Program Work Plan Schedule



Low Camber First Vane Performance

Background. The low camber first vane was tested to determine (1) the two-dimensional performance for the vane section as a function of inlet air angle (incidence) at design Mach number conditions and (2) the cascade secondary loss at the design point.

Results. The results obtained by testing the low-pressure turbine low camber first vane indicated that the incidence angle of this vane should be changed from -5 degrees to -8 degrees to improve the negative incidence range.

Specifically, the results were as follows:

- (1) The measured profile loss was 0.52 percent $\Delta P_t/P_t$ at design point conditions agrees with the predicted value (see Figure 203).
- (2) Based on the measured off-design incidence performance at constant exit Mach number, the vane section showed a negative incidence range of 8 degrees and a positive incidence range of 12 degrees as defined by the point where the loss level is 50 percent above the design point loss (see Figure 203).
- (3) The measured gross secondary loss was 0.56 percent $\Delta P_t/P_t$ at design point conditions.
- (4) The exit flow is overturned by 1.3 degrees.

Alternate Loading Distribution

Background. Two airfoil packs were used in evaluating the alternate loading distribution for the fourth blade root section. One pack was characterized by transonic aft-loaded pressure distribution on the airfoil suction surface. The other pack featured a subsonic squared-off pressure distribution. The data obtained for this test were as follows:

- o Airfoil surface static pressure distributions,
- o Exit air angles,
- o Airfoil mid-span losses at the design incidence angle,
- o Five sets of exit Mach numbers for each airfoil and also with airfoils fixed at design exit Mach number, and
- o Five sets of inlet angles.

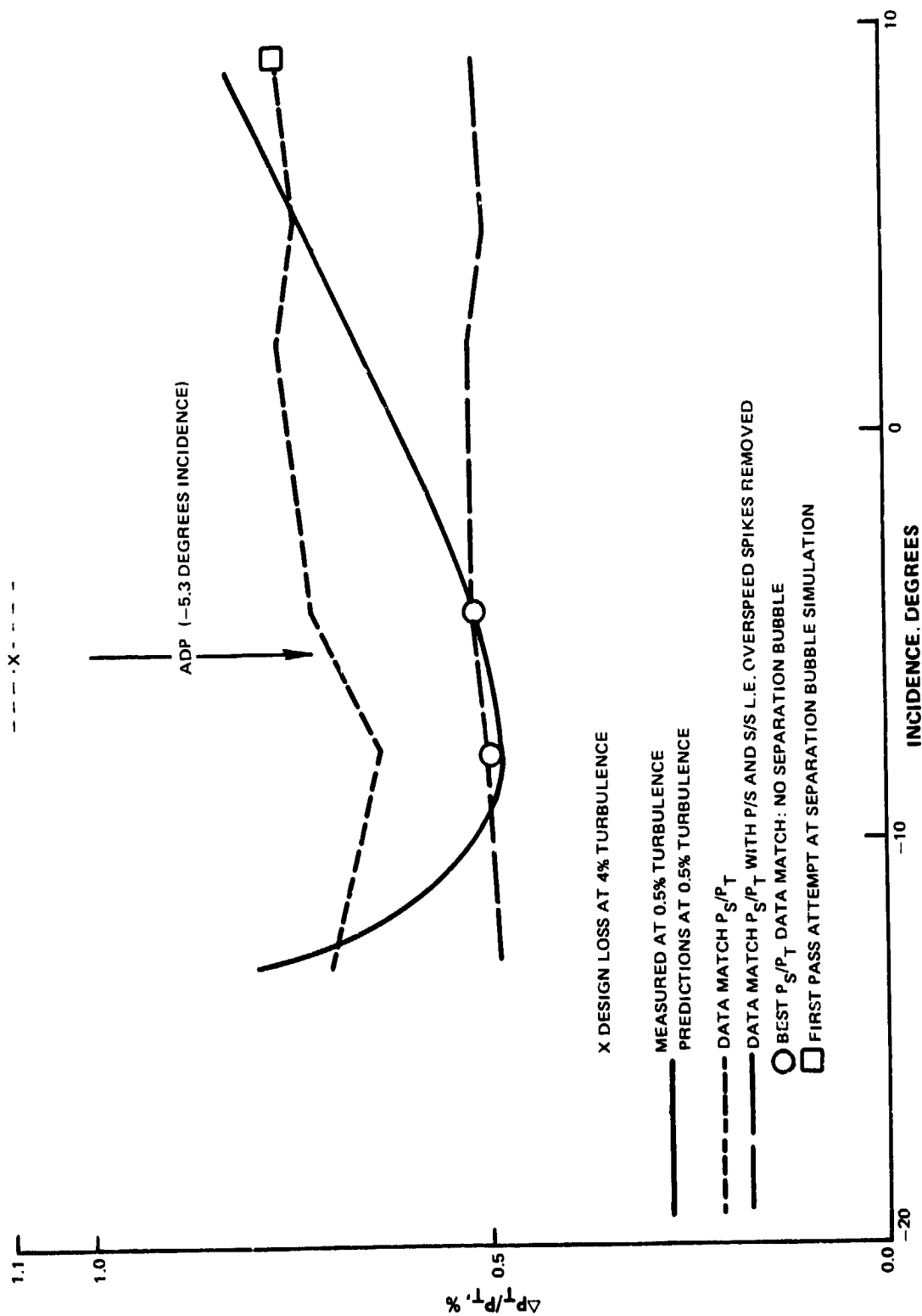
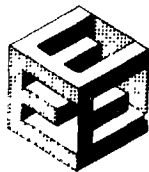


Figure 203 Subsonic Cascade Losses Compared to Incidence



Results. The performance of the aft-loaded transonic airfoil and the squared-off subsonic airfoil was measured at mid-span in terms of incidence angle and Mach number. These measurements (see Figure 204) determined that the performance of the aft-loaded airfoil design was approximately 18 percent better than that of the squared-off design over the entire range of incidence investigated (-15 degrees to +5 degrees). Similar results were obtained with variations in Mach number (0.78 to 0.94) at the design incidence angle (see Figure 205).

Secondary loss measurements show that the aft-loaded airfoil design performs approximately 6 percent better than the squared-off airfoil at the design incidence and Mach number.

Verification of Low-Pressure Turbine Design Concepts

Background. Three airfoil packs were used to evaluate the low-pressure turbine design concepts: (1) the base aft-loaded airfoil pack operating at subsonic conditions, (2) a squared-off conventional airfoil pack (heavy airfoil), and (3) a squared-off lightweight airfoil pack (ribbon airfoil). The data obtained for this test were as follows:

- o Airfoil surface static pressure distribution,
- o Exit air angles and airfoil mid-span losses at the design incidence angle,
- o Five sets of exit Mach numbers for each airfoil and also with airfoils fixed at the design exit Mach number,
- o One set of inlet angles obtained with a turbulence grid (this grid was installed at the inlet section to generate a turbulence level of 2.8 percent) at the design Mach number for each of the three airfoil packs.

These data were sufficient to determine the relative performance of the airfoils over a wide range of incidence angles and Mach numbers. Secondary loss and exit air angle data at the design exit Mach number and three sets of inlet gas angles (one design and the other positive and negative incidence) were obtained for each of the three airfoils. Flow visualization was also conducted on the airfoil and endwall surfaces for each of the airfoil packs at the design incidence angle and Mach number. All of the total pressure loss data were obtained at the 40-percent axial chord location downstream of airfoil trailing edge.

Results. Based on the test results obtained, the aft-loaded airfoil pack offered the most promising performance characteristics of the three types of airfoils tested. The ribbon airfoil generated the greatest losses. The installation of the turbulence grid had no apparent effect on the performance characteristics of any of the airfoil packs. The measured performance loss

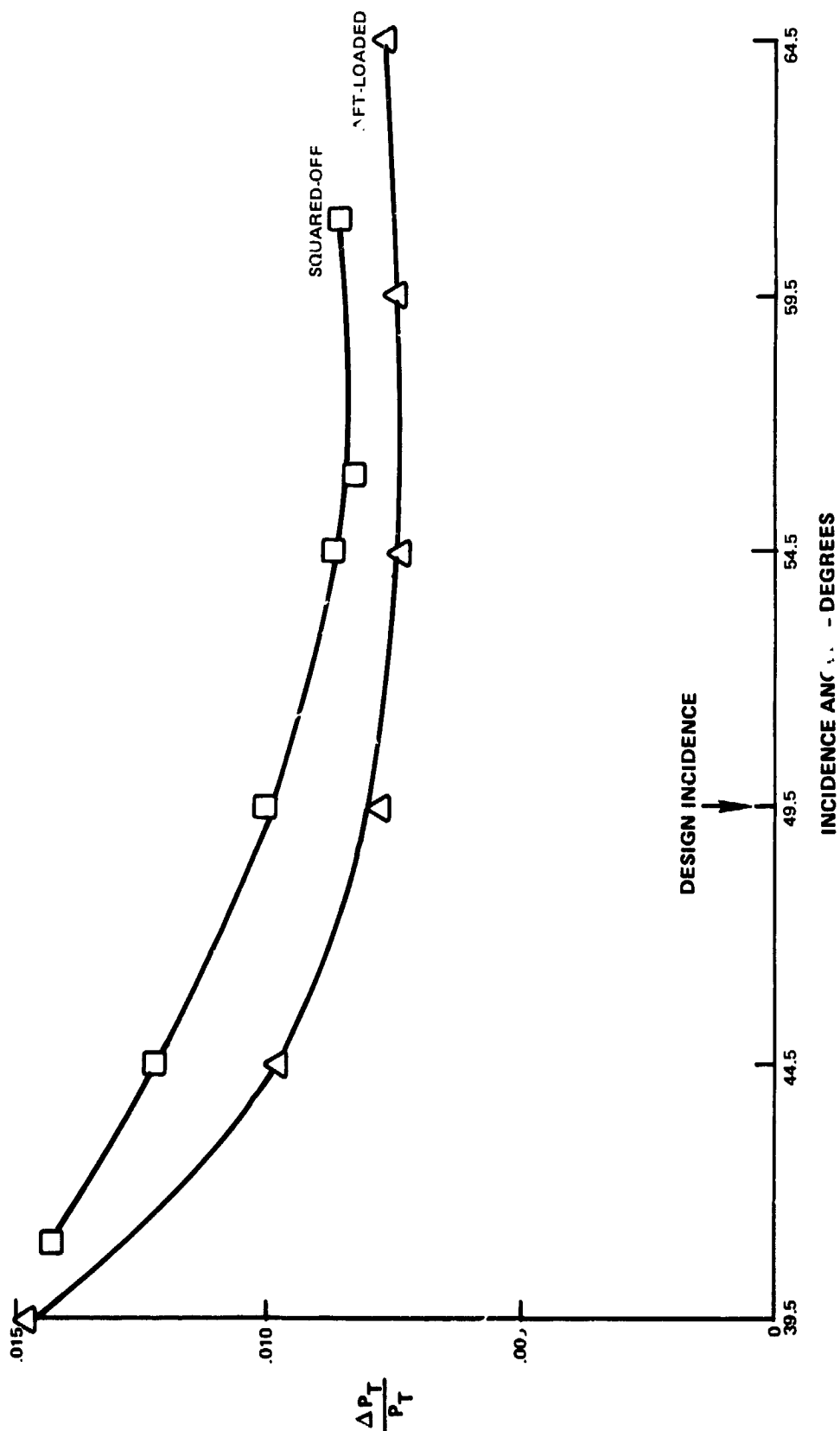
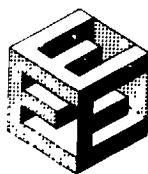
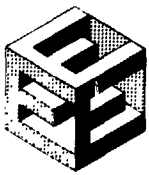


Figure 204 Subsonic Cascade Losses Compared to Incidence



ORIGINAL PAGE IS
OF POOR QUALITY

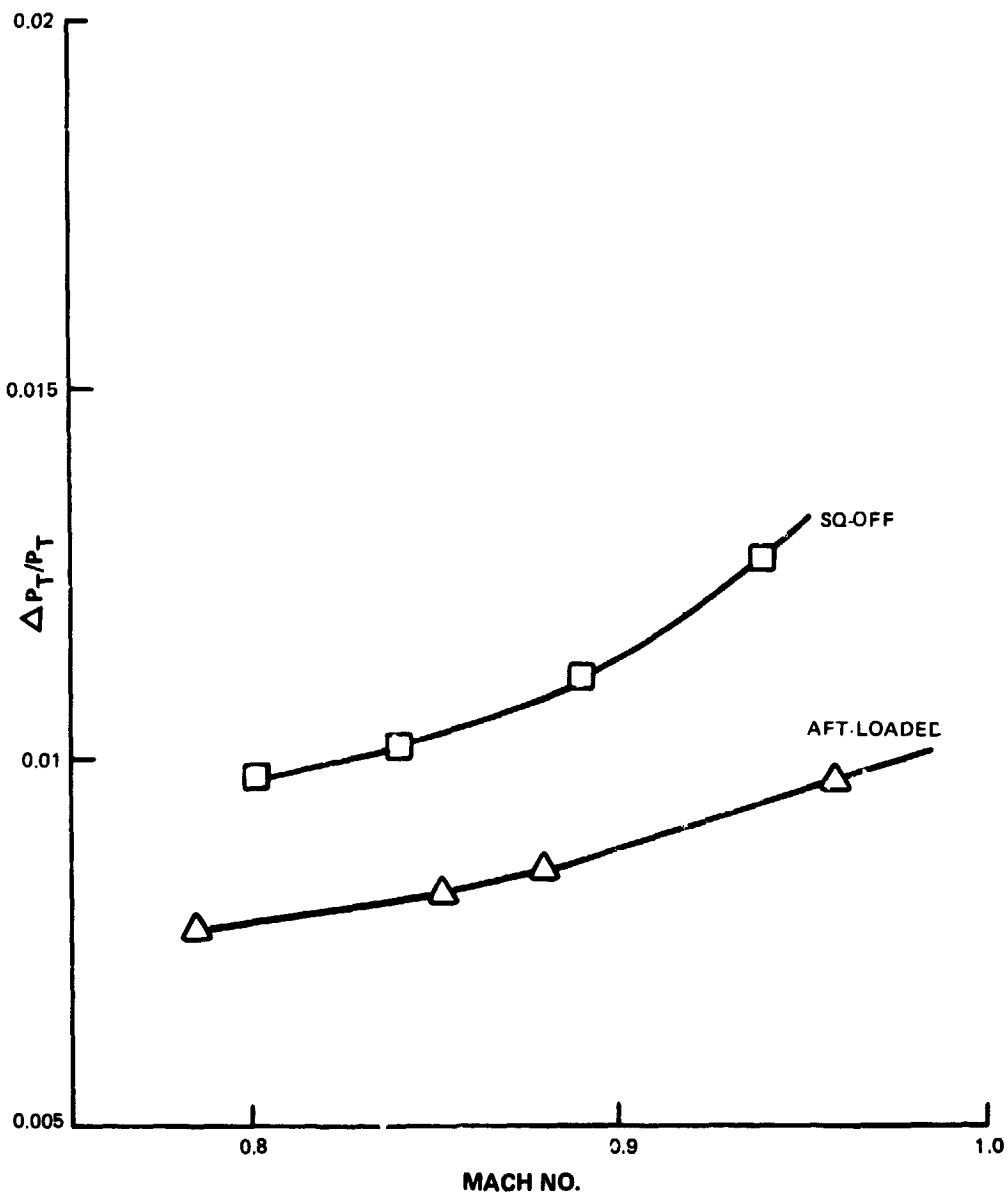


Figure 205 Subsonic Cascade Losses Compared to Mach Number



data taken at mid-span at design incidence and over the entire range of Mach numbers (0.63 to 0.94) indicate that the aft-loaded airfoil performed 27 percent better than the squared-off subsonic "heavy" airfoil and 40 percent better than the squared-off "ribbon" airfoil (see Figures 206 and 207).

The measured mid-span total pressure loss data at design Mach number and over the entire range of inlet gas angles (19.5 degrees to 64.5 degrees) indicate that the aft-loaded airfoil pack demonstrated the lowest loss of the three airfoil packs. The difference in losses in these airfoils are highest at the minimum inlet angle (maximum positive incidence) whereas there were little difference in losses at higher inlet gas angles (negative incidence).

No significant influence of the installation of turbulence screens at inlet to the cascade test section was observed on the airfoil mid-span loss.

Based on the testing and comparisons with available analytical tools, the following recommendations were made for the execution of the design for the Energy Efficient Engine low-pressure turbine component.

- (1) The design inlet incidence angle should be approximately -10 degrees instead of the presently used -5 degrees if the range of airfoil operation is to be improved.
- (2) Aft-loaded airfoils should be incorporated because they generate lower profile and secondary losses than the squared-off airfoils.



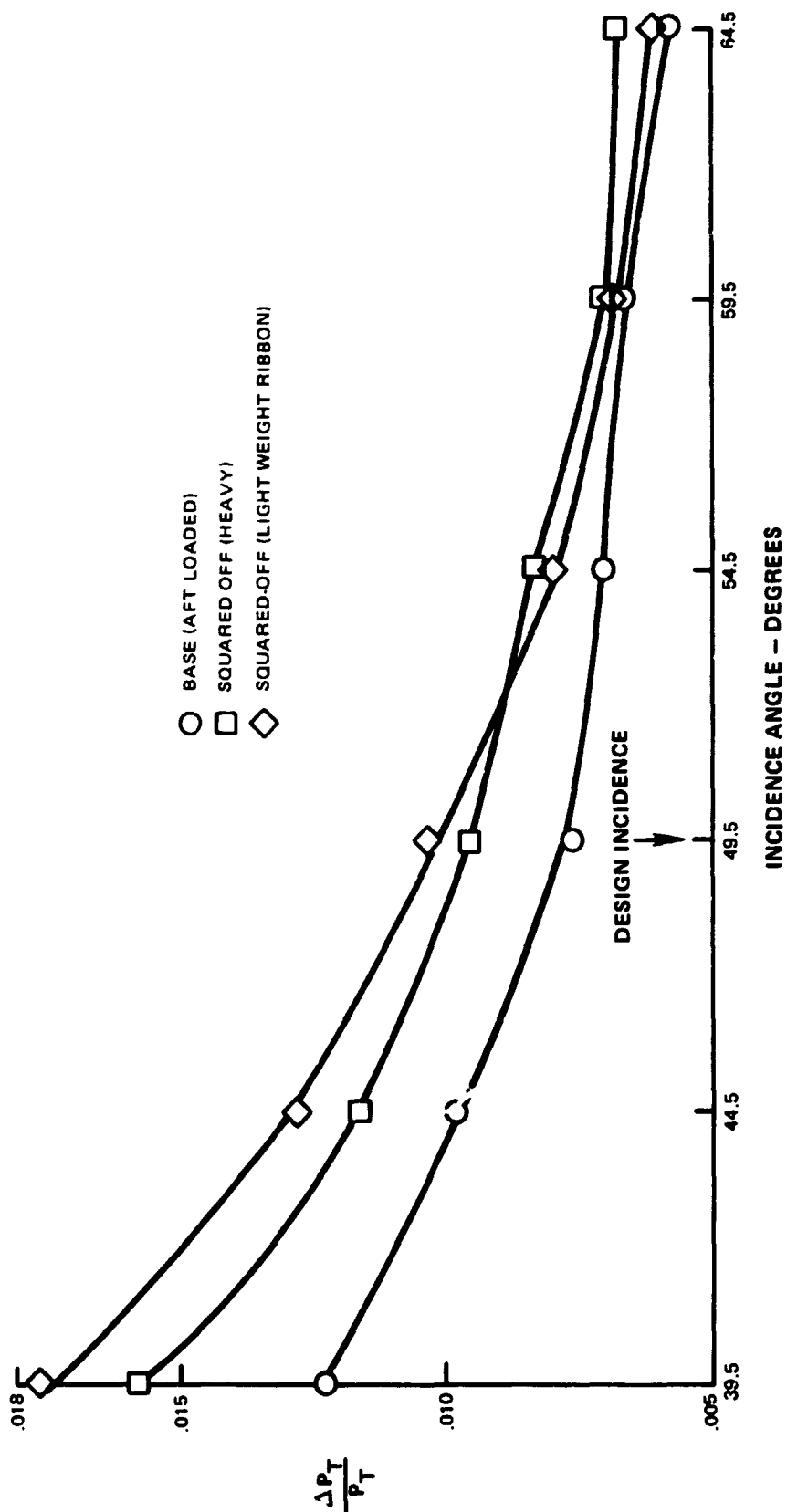


Figure 206 Subsonic Cascade Losses Compared to Incidence



ORIGINAL PAGE IS
OF POOR QUALITY

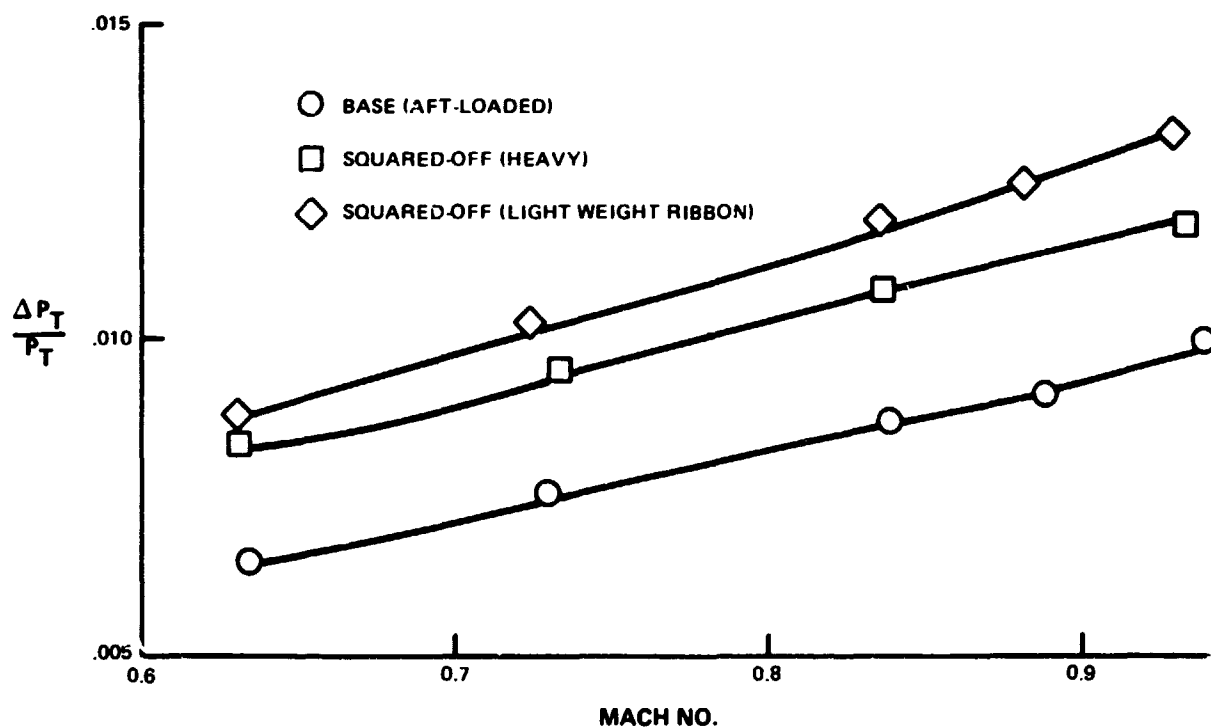


Figure 207 Subsonic Cascade Losses Compared to Mach Number



3.2.8.4.3 Transition Duct Test Program

3.2.8.4.3.1 Objective

Develop and experimentally verify the design of a short, low-loss, advanced technology transition duct for the flight propulsion system low-pressure turbine component design.

3.2.8.4.3.2 Scope of Total Work Planned

The transition duct test program consists of four phases. Figure 208 shows these phases and identifies those tasks and activities that were completed during the previous reporting periods and those scheduled to have been initiated, continued, or completed during the current reporting period.

An inviscid/viscid analytical coupling procedure is used until incipient stability is obtained. This analysis is applied to an initial transition duct design obtained from a minimum structural length considerations. The inner and outer diameter contours, strut fairing shape, and locations are varied to obtain the most desirable design. This first design is incorporated as the base low-pressure turbine transition duct. A second duct is used to address problem areas discovered in the first duct test. The design includes the intermediate case strut and low-pressure turbine inlet vane. The models, hardware, and instrumentation are designed, fabricated, and then assembled into an air flow tunnel facility. Pressure measurements and flow visualization studies are conducted at Energy Efficient Engine conditions. Aerodynamic losses, local separation, and nonuniform flow patterns are analyzed.

3.2.8.4.3.3 Technical Progress

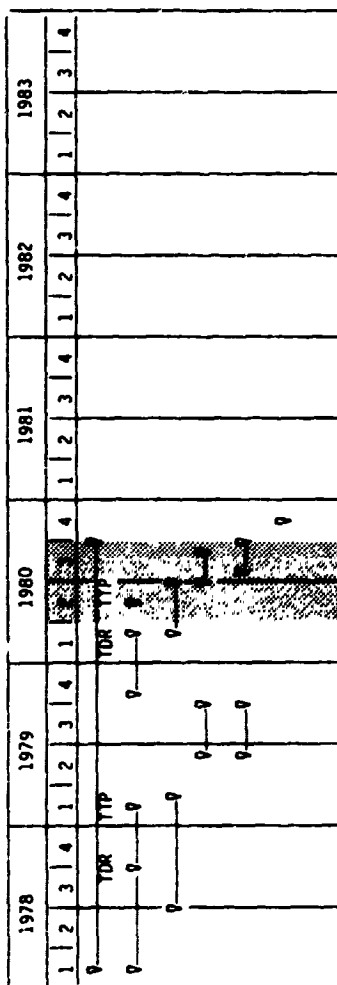
3.2.8.4.3.3.1 Summary of Work Previously Completed

As shown in Figure 208, the test and post test analysis activities associated with the first duct model were completed before the current reporting period. Results of these activities are summarized below.

- o At design flow conditions, the total pressure loss including the low-pressure turbine first vane is 1.5 percent versus a 2.6 percent design value. At off-design swirl conditions up to 5 degrees, pressure loss increased to 2.1 percent.
- o The pressure coefficient along the duct outer diameter wall indicated that the desired diffusion was attained across the strut. Strut airfoil pressure distribution data indicated an unloaded condition with no separation.



TRANSITION DUCT TEST PROGRAM - WORK PLAN SCHEDULE



ACTIVITIES/MILESTONES
TOTAL WBS TIMING
ANALYSIS AND DESIGN
FABRICATION
TEST
POST-TEST ANALYSIS
SUBMIT TECHNOLOGY REPORT

*M DENOTES MAJOR MILESTONE *D DENOTES KEY DECISION POINT

Figure 208 Transition Duct Work Plan Schedule



- o Inlet, strut exit, and first vane exit air angle data bracket design values with some overturning in the root areas. With a five-degree off-design inlet swirl angle, the struts returned the unturned flow to within one degree of the design point swirl.
- o The measured inlet turbulence was 2 percent versus a 4-percent rig design prediction.

3.2.8.4.3.3.2 Current Technical Progress

The start of the analysis and design work for the second build of the transition duct model was previously delayed because of the slippage in defining the component strut configuration. Consequently, analysis and design of the second duct model was not completed until the current reporting period. A technology design review was conducted in May 1980, and the fabrication of the second duct model was subsequently initiated.

Build 2 of the transition duct incorporates changes to the Build 1 design. These changes, highlighted in Figure 209, include: (1) increased area ratio (1.52 from 1.50), (2) reduced number of struts (11 from 14), and (3) forward canting of the struts. In addition, the strut was transformed into a "working" strut by incorporating a flow turning capability of 5 degrees.

The aerodynamics associated with the second build of the strut are shown in Table 70 of the Fourth Semiannual Status Report. The test rig and the hardware required for second build testing are shown in Figure 210. A test plan for this phase of testing was prepared for and submitted to NASA.



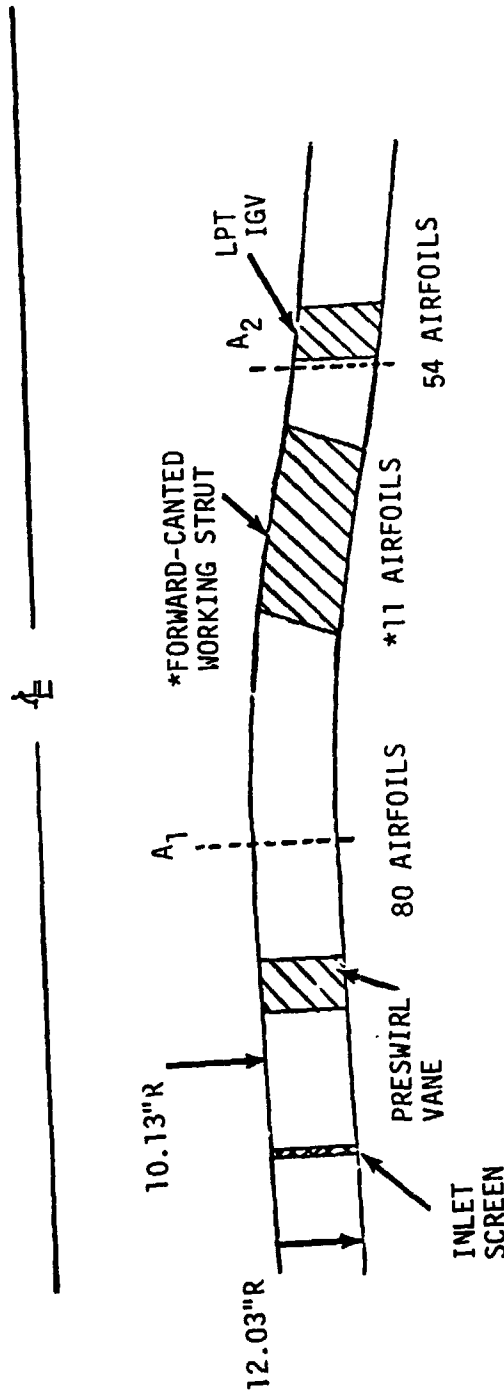
PRATT & WHITNEY AIRCRAFT GROUP
COMMERCIAL PRODUCTS DIVISION

ORIGINAL PAGE 11
OF POOR QUALITY

LOW PRESSURE TURBINE TRANSITION DUCT - SECOND BUILD

SCALED FROM ENGINE

SCALE FACTOR = 0.7434



*ANNULUS AREA RATIO (A_1/A_2) = 1.52
*FLOW AREA RATIO = 1.39

(*) - CHANGE FROM FIRST BUILD

Figure 209 Low-Pressure Turbine Build 2 Transition Duct



PRATT & WHITNEY AIRCRAFT GROUP
COMMERCIAL PRODUCTS DIVISION

ORIGINAL PAGE 19
OF POOR QUALITY

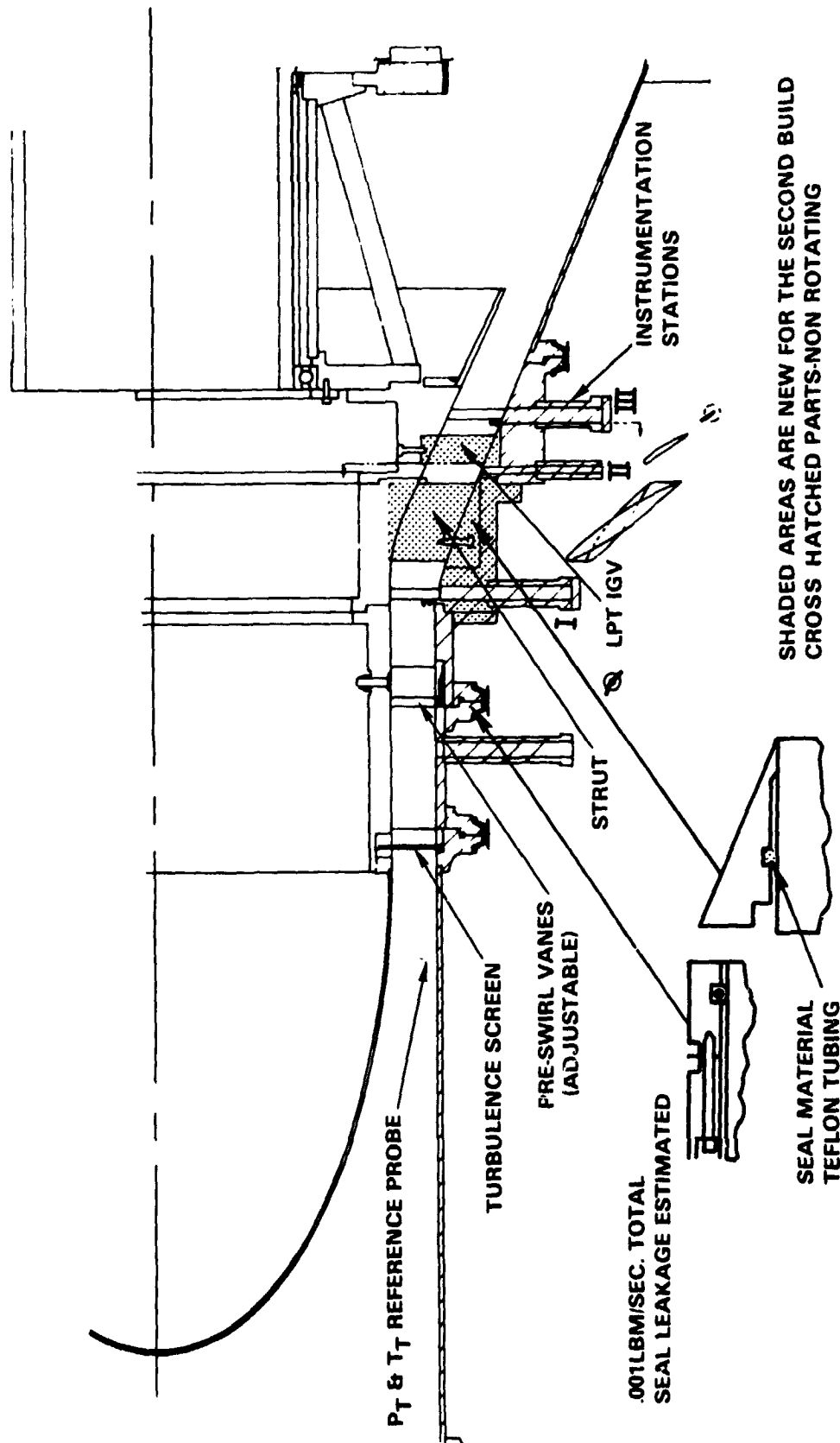


Figure 210 Low-Pressure Turbine Transition Duct Rig Showing Modifications
for Build 2



3.2.9 Exhaust Mixer System

3.2.9.1 Overall Objective

Design and develop exhaust mixer aerodynamics that will achieve the goal mixing efficiency of 85 percent, both for the flight propulsion system component and for the experimental integrated core/low spool.

3.2.9.2 Component Program Overview

The overall task effort consists of a component effort and a mixer model supporting technology sub-task. Figure 211 shows the relationships between these activities and their relationship to Tasks 1, 3, and 4. The work plan schedule for the component effort is shown in Figure 212. There are no program-critical milestones or decision points in this task.

3.2.9.3 Component Effort

3.2.9.3.1 Objective

Provide the aerodynamic definition of the mixer and tailpipe and calculate mixer stresses, deflections, and thermal loadings.

3.2.9.3.2 Scope of Total Work Planned

The initial mixer component analysis and design effort is aimed at defining the mixer/tailpipe flowpath. Mixer deflections, stresses, and thermal loading are then estimated and a preliminary layout is defined. This preliminary layout is incorporated into the overall nacelle design, and the total system is evaluated through interface meetings between Pratt & Whitney Aircraft and airframe subcontractors. The design resulting from this refinement process is fed into the model test program. The final refinements to the mixer design are completed in the Task 4 analysis and design work package. A test facsimile is fabricated and tested in Task 4.

Figure 212 indicates that all of the work associated with the preliminary analysis and design of the mixer component is complete. The supporting technology program effort was continued through the current reporting period and is discussed in section 3.2.9.4.

3.2.9.3.2.1 Summary of Work Previously Completed

Tests on the Phase I mixer model were conducted following the completion of the preliminary design. Test results indicated that mixer performance could be improved by modifying the preliminary design. Consequently, the component design was modified to reflect these changes (see section 3.1.3.3). The major features of the modified mixer design are compared to the original configuration in Figure 213. The modified design is the design anticipated for the flight propulsion system (subject to revision based on the Phase II model



ORIGINAL
OF POOR QUALITY

EXHAUST MIXER SYSTEM PROGRAM - LOGIC DIAGRAM

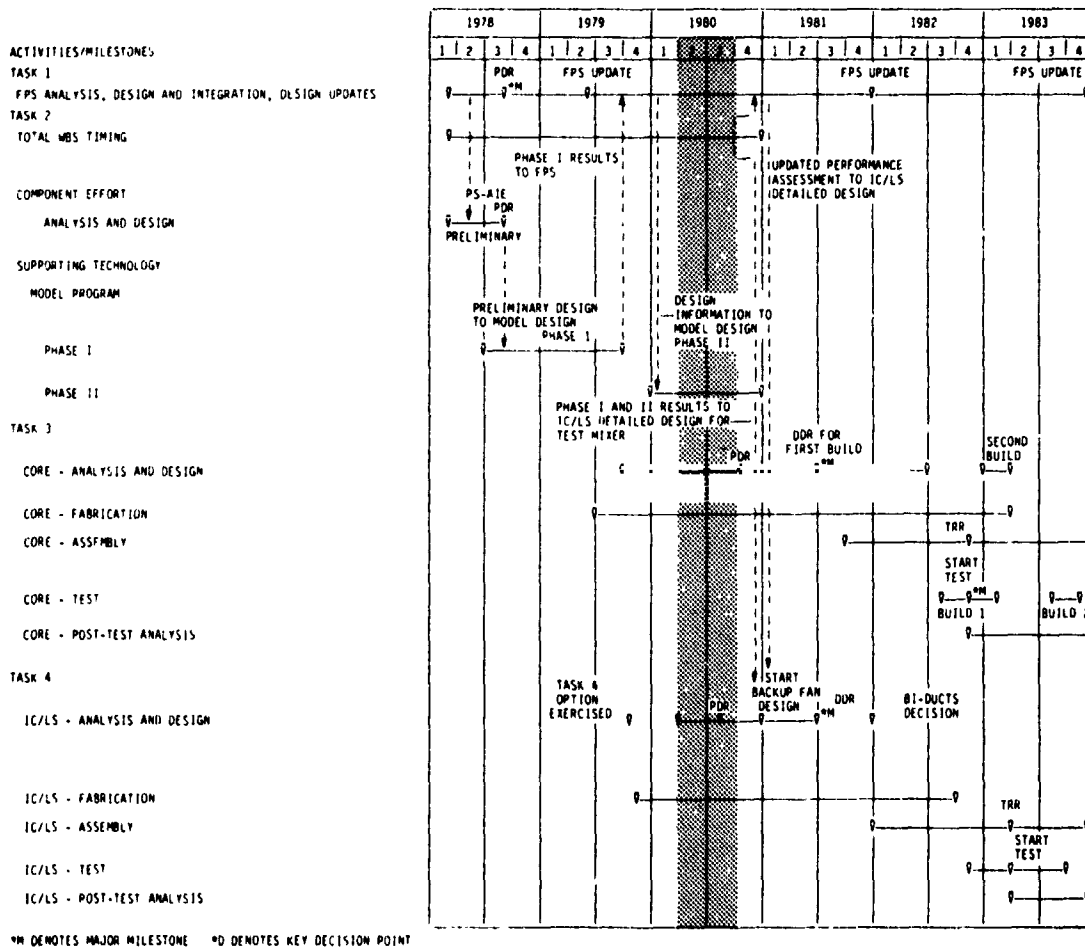


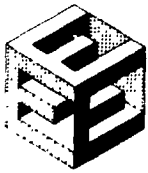
Figure 211 Mixer Component Logic Diagram



MIXER COMPONENT EFFORT - WORK PLAN SCHEDULE

	1978				1979				1980				1981				1982				1983			
	1	2	3	4	1	2	3	4	1	2	3	4	1	2	3	4	1	2	3	4	1	2	3	4
ACTIVITIES/MILESTONES																								
TOTAL MBS TIMING	0	0	0	0	0	0	0	0	0	0	0	0	0	0	0	0	0	0	0	0	0	0	0	0
COMPONENT ANALYSIS AND DESIGN	0	0	0	0	0	0	0	0	0	0	0	0	0	0	0	0	0	0	0	0	0	0	0	0

Figure 212 Mixer Component Work Plan Schedule



tests). The mixer system to be employed in the testing of the integrated core/low spool will have the same flowpath but will include material substitutions.

The modified design features 18 lobes arranged around a central plug and housed within a converging tailpipe. The forward half of the plug is acoustically treated.

Additional design features (see Figure 213) include the rear support ring, inner diameter support struts, breather system center vent tube, and outer fairing. The rear support ring supports the plug, which is made in three pieces for ease of assembly and maintenance. The scalloped mixer is supported at the inner diameter by the support struts and at the forward flange by the rear support ring. The fairing provides transition for the flow from the fan duct to the mixer. The breather center-vent tube exhausts at the rear of the plug.

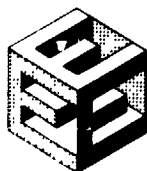
The materials used for the strut and forward plug are titanium-aluminide and Inconel 625, each selected for its high temperature withstanding capacity (1100 F). A beta process titanium alloy was chosen for the mixer, which is located in a temperature region below 1100 F. A low cost conventional titanium alloy was chosen for the region behind the mixer. Each of these materials provide a lightweight structure that can adequately support the static loadings.

The major design changes incorporated since preliminary design definition are (1) a change from 12 to 18 lobes, (2) an increased radial flow penetration of the lobes, (3) increased tailpipe (and plug) length, and (4) removal of outer lobe vibration dampers.

Performance parameters and goals for the modified mixer design are listed in Table 93 at significant engine operations conditions.

TABLE 93
CURRENT EXHAUST/MIXER PERFORMANCE PARAMETERS
AT SIGNIFICANT ENGINE OPERATING CONDITIONS

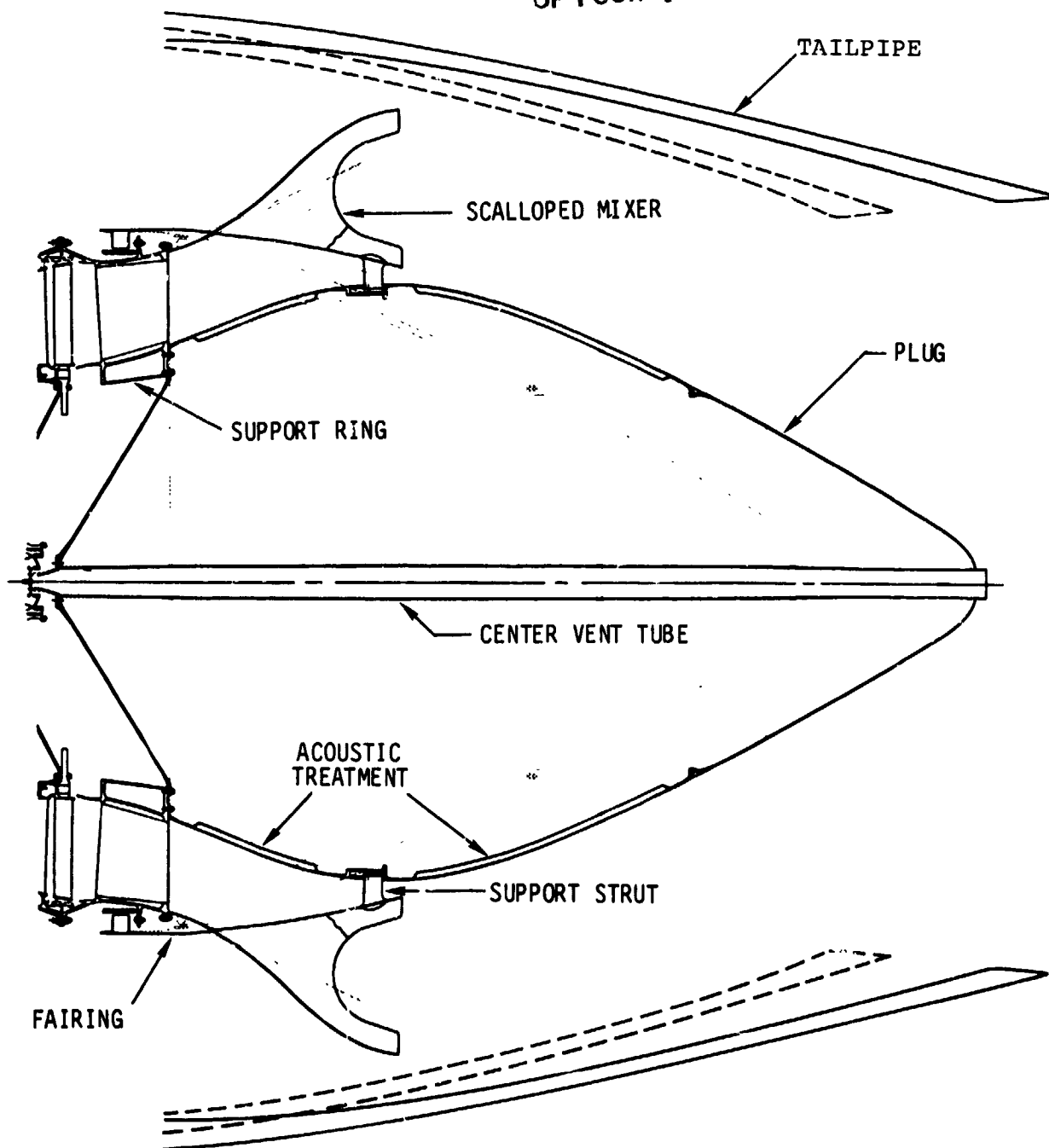
	Engine Operating Condition			
	Aero. Des. Point	Maximum Cruise	Maximum Climb	Takeoff
Mixer Pressure Loss (percent)				
(Core Section)	0.24	0.23	0.25	0.19
(Duct Section)	0.18	0.18	0.18	0.17
Mixer Efficiency (percent)	85.0	85.0	85.0	85.0
Nozzle Pressure Loss (percent)	0.34	0.34	0.34	0.29
Gross Thrust Coefficient	0.9958	0.9959	0.9956	0.9906
Fan Duct Pressure Loss (percent)	0.60	0.61	0.59	0.54



PRATT & WHITNEY AIRCRAFT GROUP
COMMERCIAL PRODUCTS DIVISION

--- PDR DESIGN
— CURRENT DESIGN STATUS

ORIGINAL PAGE 18
OF POOR QUALITY



FOLDOUT FRAME

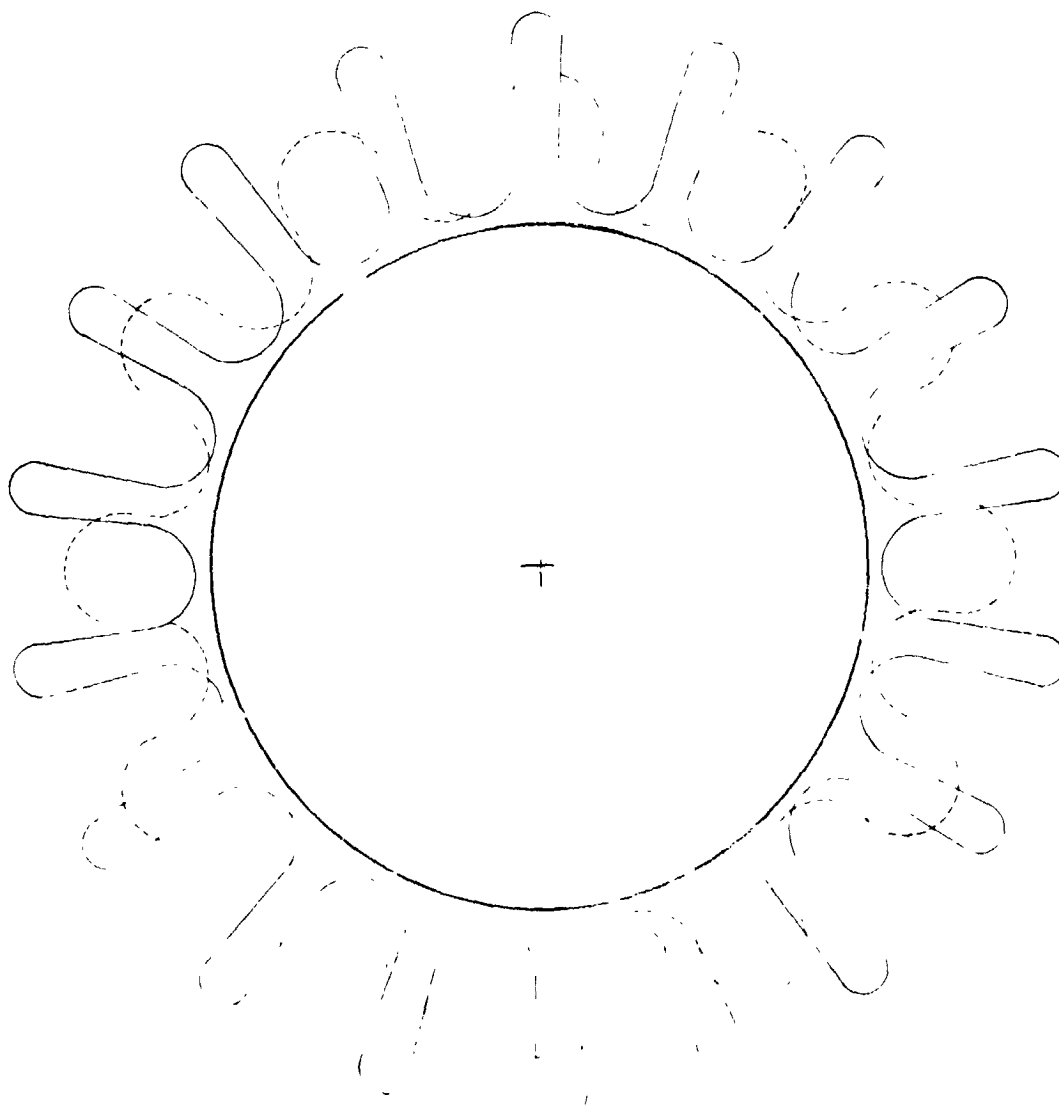
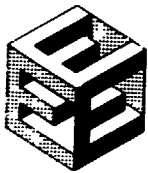


Figure 213 Mixer Current Design Status Compared to Preliminary Design Review Configuration - The modified design features increased penetration for improved performance.



3.2.9.4 Supporting Technology

3.2.9.4.1 Mixer Model Test Program

3.2.9.4.1.1 Objective

Parametrically optimize the advanced mixer to meet the flight propulsion system and integrated core/low spool mixer component requirements.

3.2.9.4.1.2 Scope of Total Work Planned

This program consists of an extended period of scale model testing, starting with the exhaust system basically defined in Task 1. The first model program (Phase I) evaluates pertinent major variables, with the results used for updating the full scale flight propulsion system design in late-1979. A second model program (Phase II) is conducted to refine the design, prior to defining the configuration for the integrated core/low spool tests. Each phase includes model design, fabrication, testing, and post-test analysis. During model analysis and design configurations are selected for testing. Following NASA Project Manager approval of the configurations, detailed design and fabrication is initiated. The proposed test hardware is fabricated to Pratt & Whitney Aircraft specifications by Fluidyne Engineering Corporation. The tests are conducted in the Fluidyne Channel 11 static thrust facility. Nozzle thrust and flow coefficients are measured for each test point. Analysis of test data occurs during and after the test period and identifies the most promising configurations. The conclusions from these analyses are then used as final inputs to the flight engine exhaust mixer design definition.

The mixer model test program consists of the two phases shown in Figure 214, which indicates that all Phase I activities were completed during the previous reporting period and that Phase II activities were continued during the current reporting period.

3.2.9.4.1.3 Technical Progress

3.2.9.4.1.3.1 Summary of Work Previously Completed

The results of Phase I testing are summarized in section 3.2.9.4.1.3 of the Third Semiannual Status report. A more detailed assessment of those results is discussed in section 3.2.9.4.1.3.2 of the Fourth Semiannual Status Report.

Analysis and design of the Phase II mixer model has been completed, and four mixed flow exhaust configurations were selected for testing in 1980. Each of these configurations feature 18 lobes, 75 percent penetration, and a 0.6 tailpipe length/diameter ratio. Two of the mixers will be scalloped, one will be equipped with hoods. A steeper, shorter plug will also be tested. The gap between the plug and the mixer will be optimized by testing the series of configurations.



MIXER MODEL TEST PROGRAM - WORK PLAN SCHEDULE

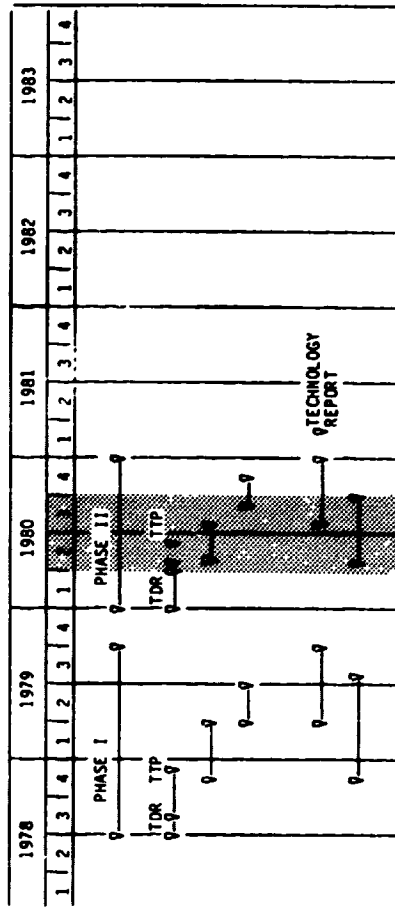


Figure 214 Mixer Model Work Plan Schedule



3.2.9.4.1.3.2 Current Technical Progress

The detailed design and fabrication of the Phase II mixer model test configuration was completed. These configurations were identified and discussed in the Fourth Semiannual Status Report.

The mixer model technology Phase II test plan was submitted to and approved by NASA. The test configuration will be evaluated at 150 points in the Channel 11 static flow facility at Fluidyne Engineering Corporation. Total pressure and temperature surveys will be made at the tailpipe exit plane for all test configurations. In addition, flow visualization techniques will be used to assess all configurations.

The testing sequence was started at Fluidyne Engineering Corporation with the ASME nozzle calibrations. A number of data inconsistencies, however, became apparent during calibration. These were caused by a water leak near the cooling water jacket around the hot flow venturi. Attempts to isolate and seal the leak were unsuccessful, so Fluidyne replaced the venturi/water jacket. The data calibration resulting from tests with the replacement assembly show good repeatability. Testing was resumed at the close of this reporting period.



3.3 TASK 3 - CORE DESIGN, FABRICATION, AND TEST

Analysis and design of the core was initiated during the previous reporting period, but this effort was suspended in February 1980, when an agreement was reached with NASA to initiate a contract modification to eliminate Task 3 from the program in order to gain funding relief from a forecast cost overrun. To replace the Task 3 core program, it was further agreed to expand Task 4 into two builds of the integrated core/low spool. Hence the only work performed under the Task 3 program during this reporting period was that which was directly applicable to Task 4. Most of this activity was related to raw material procurement.

3.4 TASK 4 - INTEGRATED CORE/LOW SPOOL DESIGN, FABRICATION, AND TEST

3.4.1 Objective

Design, fabricate, and test the Energy Efficient Engine integrated core/low spool at sea level takeoff conditions. The following performance will be demonstrated:

TSFC	0.340 lbm/hr-lbf (corrected to standard day)
Emissions	1981 EPA Rule
Noise (EPNdB)	Takeoff 102.9
	Approach 103.9
	Sideline 95.5

3.4.2 Scope of Total Work Planned

A preliminary design of the integrated core/low spool is conducted to define the test nacelle and mixer configuration, gearbox adaptation, lubrication system, active clearance control system, control system, and externals. A data package summarizing the preliminary design of the integrated core/low spool is prepared for NASA review and approval. Following approval, the design effort is continued in order to produce a detailed design, using the detailed designs from Task 2 components. A detailed design review data package is then prepared, and the design is presented to NASA for review and approval.

Fabrication is initiated after approval of the detailed design review. Core hardware for this effort is made available from Task 3 and from Task 2 rig parts.

The lack of flexibility of the program fabrication schedules may require that fabrication begin before the detailed design review. Most of the material requiring long lead time procurement is ordered as soon as deemed necessary.



The integrated core/low spool is tested initially in an indoor sea level test stand to evaluate component performance and the mechanical performance of the low-pressure spool. It is then partially disassembled to inspect the hot section and to remove excessive low-pressure spool instrumentation. Following this, the integrated core/low spool is reassembled and tested at an outdoor sea level test stand to demonstrate levels of thrust specific fuel consumption, noise, and emissions.

The integrated core/low spool program logic diagram is shown in Figure 215, and the work plan schedule is shown in Figure 216.

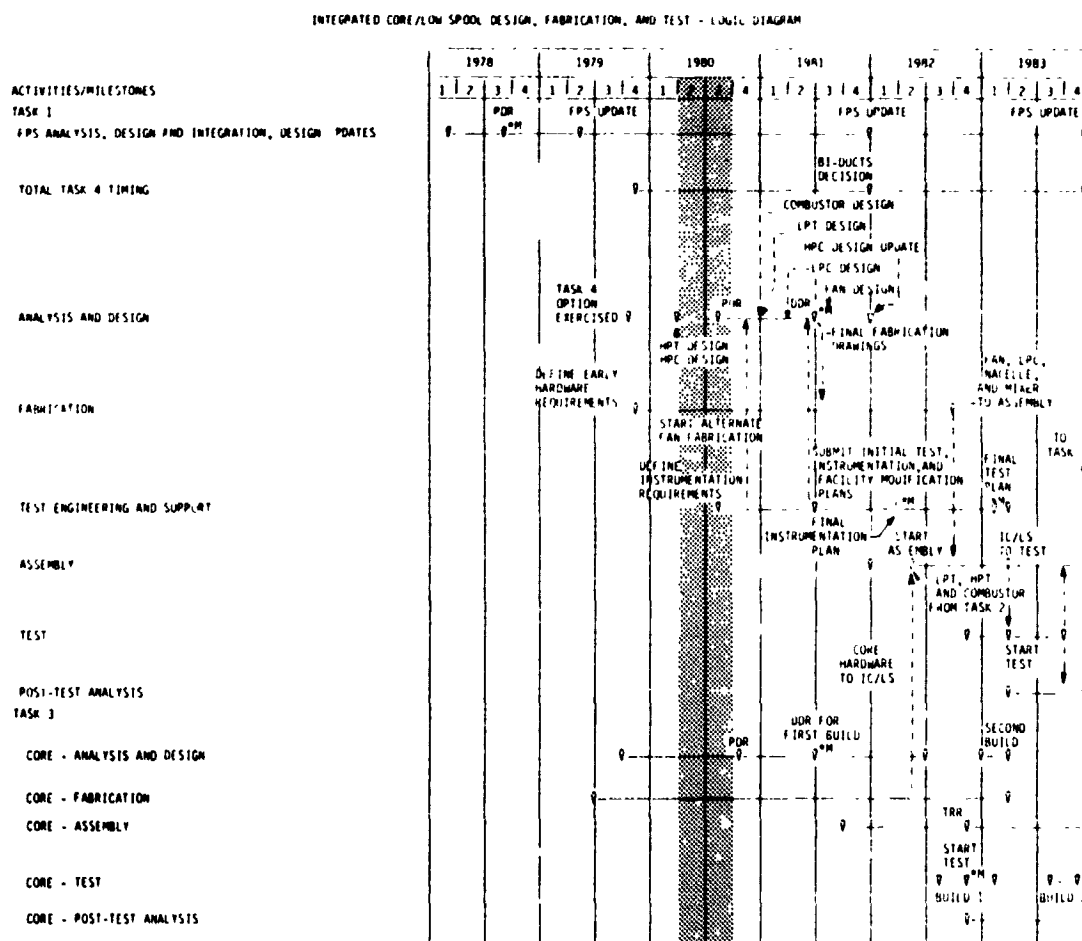


Figure 215 Integrated Core/Low Spool Program Logic Diagram



INTEGRATED CORE/LOW SPOOL DESIGN, FABRICATION, AND TEST - WORK PLAN SCHEDULE

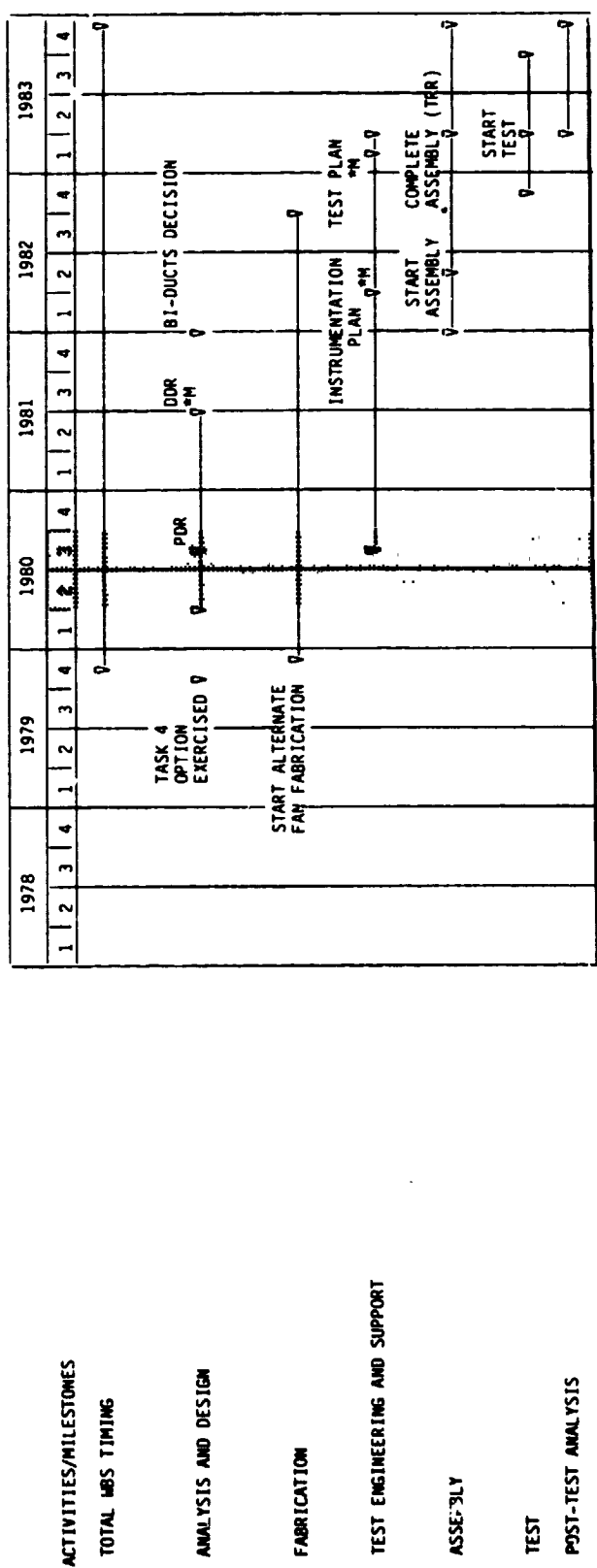


Figure 216 Integrated Core/Low Spool Program Work Plan Schedule



3.4.3 Technical Progress

3.4.3.1 Summary of Work Previously Completed

NASA approval was received for the early procurement of raw material for the alternate and shroudless fan configurations and for the low-pressure compressor. The raw material was subsequently ordered and received, and vendor cost quotations were solicited for forging various fan and low-pressure compressor subsystems.

The integrated core/low spool analysis and design effort was initiated. Mounting of the gearbox was the first item addressed.

3.4.3.2 Current Technical Progress

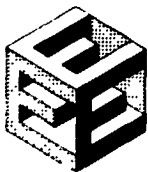
Integrated Core/Low Spool Analysis and Design

At the beginning of the current reporting period, the analysis and design of the integrated core/low spool was directed toward the adaptation of a gearbox and angled drive configuration previously used in another experimental engine program. The top-mounted gearbox approach is shown in Figure 217. The gearbox was selected because of its availability and low cost. The starter, fuel pump, and oil pump will be mounted on this gearbox. It is anticipated that this configuration will run as successfully in the Energy Efficient Engine program as it did in the previous program because its output speed will be similar (see Table 94). A schematic representation of the non-regulated oil system and the expected flows associated with the oil pumps (pressure and scavenge) externally mounted on the gearbox is shown in Figure 218.

TABLE 94

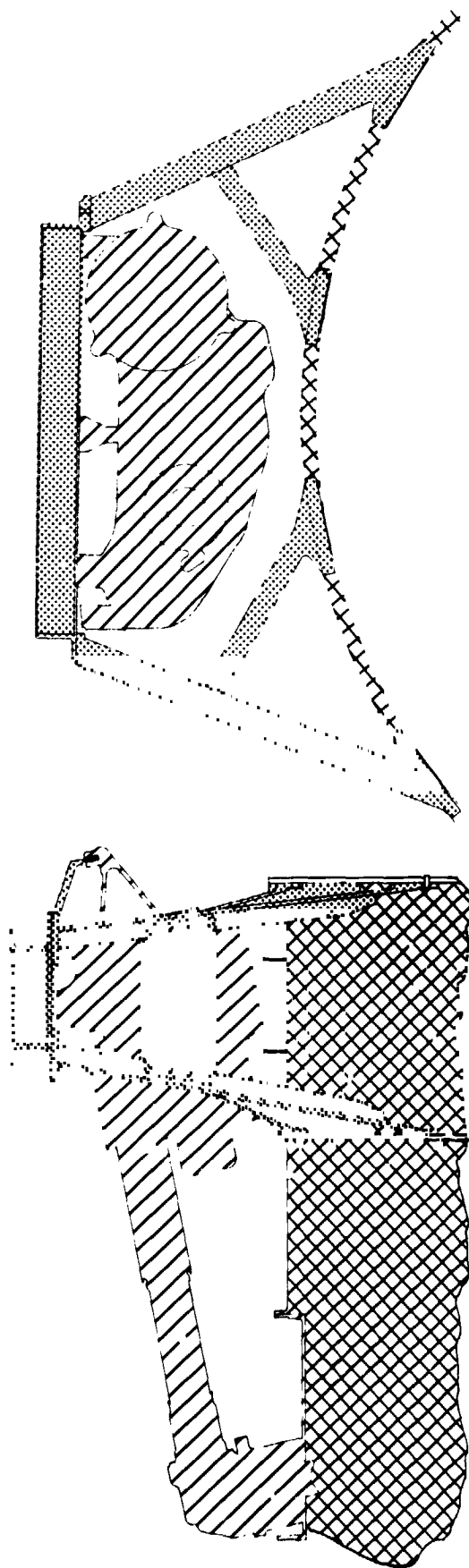
PREVIOUS APPLICATION VS. INTEGRATED CORE/LOW SPOOL
COMPARATIVE SPEEDS
(All Speeds Based on M . RPM Rotor)

	<u>Previous Application</u>	<u>Integrated Core/Low Spool</u>
Starter Pad	7321	7476
Fuel Pump Pad	4368	4459
Hyd. Pump Pad	3582	3656



PRATT & WHITNEY AIRCRAFT GROUP
COMMERCIAL PRODUCTS DIVISION

ORIGINAL PART IN
OF POOR QUALITY





-  Gearbox mounts
-  Gearbox & drive system
-  Engine cases

Figure 217 Integrated Core/Low Spool Gearbox Mounting System

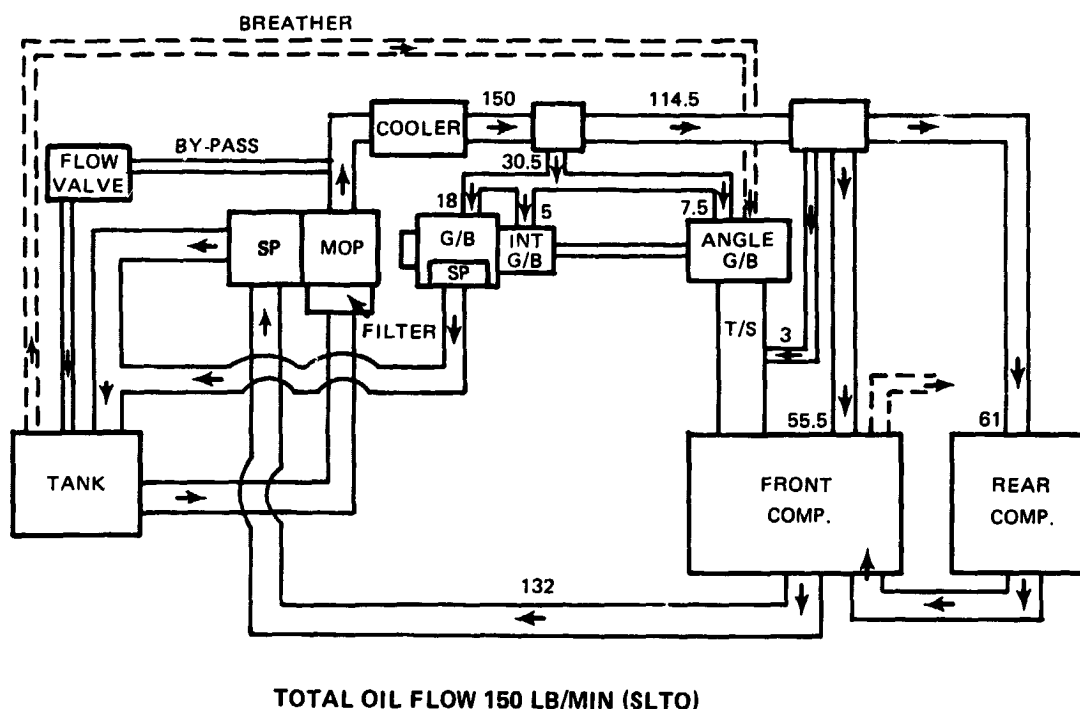


Figure 218 Integrated Core/Low Spool Lubrication System Schematic
(Non-Regulated)

A suitable plan for testing the experimental integrated core/low spool was established based on the pending decision to delete Task 3 from the program. To accommodate the large amount of instrumentation planned for such a test, a bifurcated duct configuration was evolved in order to split the fan air into two equal segments. This air flow split facilitates access to the core and contributes to decreased losses that normally result from crossing the fan stream with instrumentation. This preliminary bifurcated duct configuration is shown in Figure 219. Bifurcated ducts from existing engines will be suitable for this testing when modified and equipped with a 30-inch adapter ring forward of the ducts.

The design of the fuel system for the integrated core/low spool was started. This fuel system features a dual channel full-authority electronic control mounted on the fan case. The control is a modified design from an existing engine. Communication between channels will be maintained by a "cross-talk" link. An existing fuel pump will supply fuel to the metering portion of the fuel system called a flow body, which receives electrical commands from the control.



The flow body contains the torque motor, metering valve and associated pressure regulating devices. Hydraulic pressure from an outside source is supplied to the flow body for torque motor servo pressure. Commands from the control also establish the primary and secondary fuel flow splits in the flow divider or split valve. The pilot zone fuel during shutdown is dumped by a pressurizing and dump valve. A manually operated solenoid performs the same function for the main zone. The main zone fuel downstream of the manifold passes through 24 check valves (1 for each pair of nozzles). These valves are designed to permit the whole main manifold to fill before the fuel starts to flow out of the nozzles.

A full-size wooden mock-up of the integrated core/low spool has been fabricated (see Figure 220) to facilitate the design of the external plumbing. The fuel and lubrication system, along with associated plumbing, is schematically represented in Figure 221. The plumbing for the active clearance control system will also be simulated on the mock-up. The active clearance control system for the integrated core/low spool is shown in Figure 222. High- and low-pressure turbine mixing systems are still in the planning stages.

Instrumentation planning was started during this reporting period. Instrumentation requirements are now being reviewed to determine the lowest cost approach that will still satisfy data requirements. A telemetry unit featuring 31 transmitters has been packaged in the area of the number 3 bearing. The total number of units of instrumentation information from the high-pressure rotor is dependent on the transmitter utilization capabilities (1 strain gage/transmitter or 6 thermocouples/transmitters).

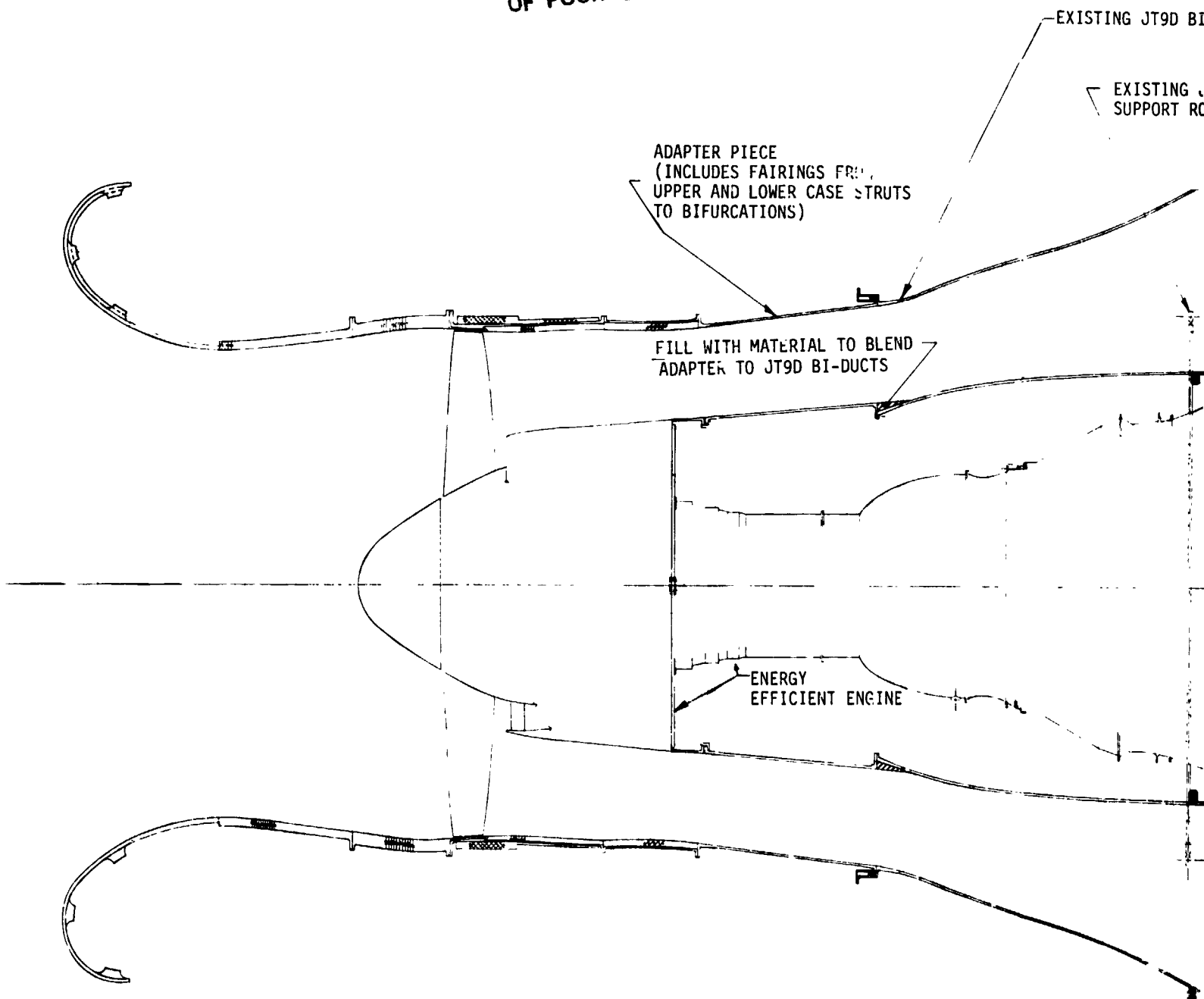
The work planned for the next reporting period is directed toward the nacelle, bifurcated ducts, instrumentation, and fuel and lubrication system.

Integrated Core/Low Spool - Fabrication

The procurement of the raw material for the intermediate case was continued. Some of the required titanium was received and processed. In addition, NASA approval was received for the early procurement of steel. This would be used for an intermediate case material substitution if the diffusion bonding/superplastic forming process for the fabrication titanium case struts is not successfully demonstrated. The early procurement of several components of the accessory drive system and lubrication system was also initiated in order to maintain existing fabrication schedules.



ORIGINAL PAGE IS
OF POOR QUALITY



TOP VIEW WITH BIFURCATED DUCTS

Figure 219 Preliminary Bifurcated Duct Configuration

OF POOR QUALITY

EXISTING JT9D BIFURCATED DUCTS

CONICAL NOZZLE

EXISTING JT9D REAR
SUPPORT RODS

REAR SUPPORT
(FOR GROUND HANDLING AND SHIPPING
ONLY - WILL BE REMOVED DURING TEST
AND REPLACED BY A WEIGHT AND CABLE
SYSTEM)

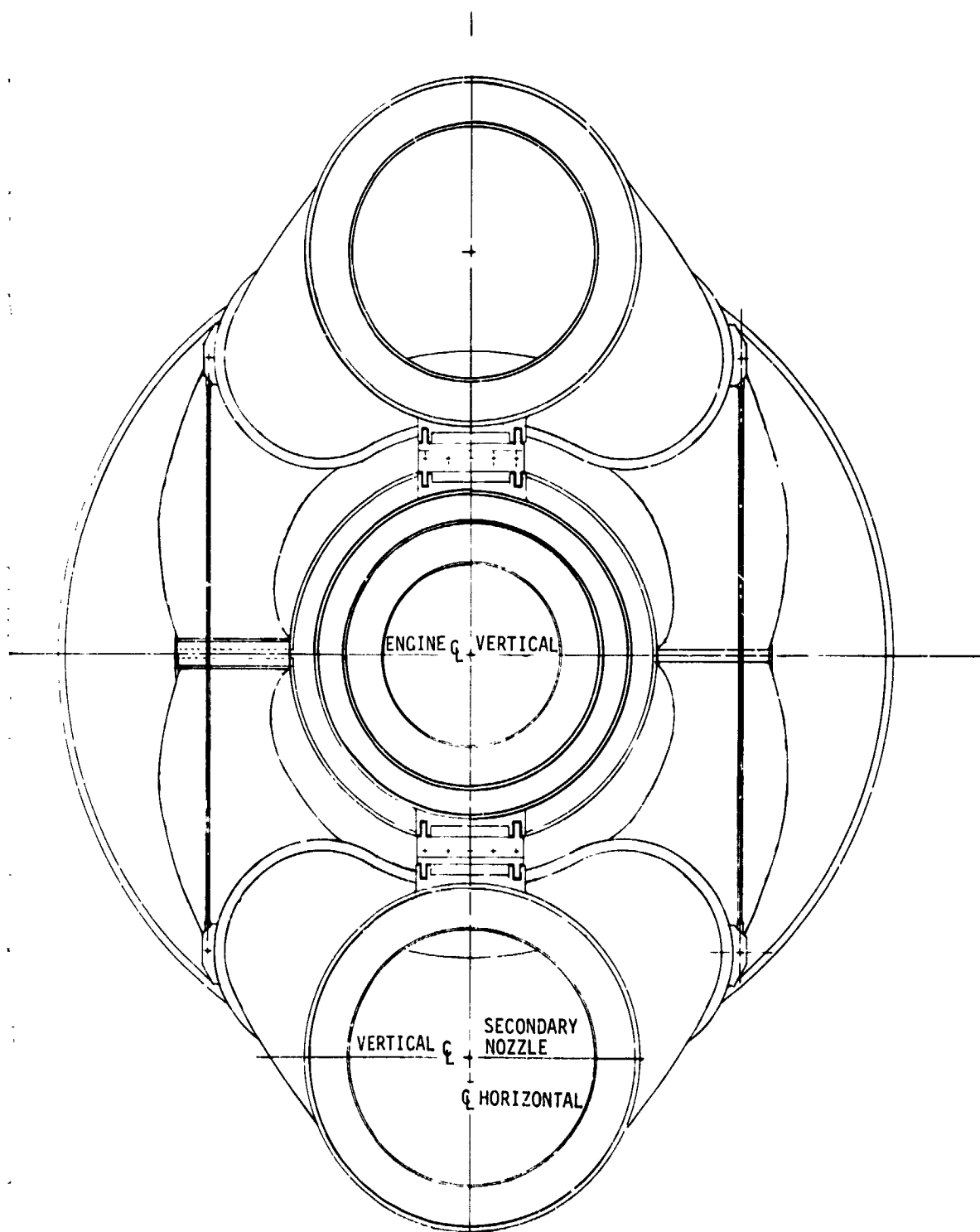
PRIMARY NOZZLE

ENGINE C

VERTICAL C

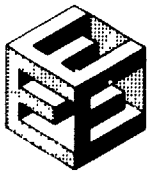
DUCTS

FOLDOUT FRAME



REAR VIEW

3 FOLDOUT FRAME



PRATT & WHITNEY AIRCRAFT GROUP
COMMERCIAL PRODUCTS DIVISION

On 10/10/17



Figure 220 Energy Efficient Engine In Grated Core/Low Speed Full
Size Mock-up Under Construction

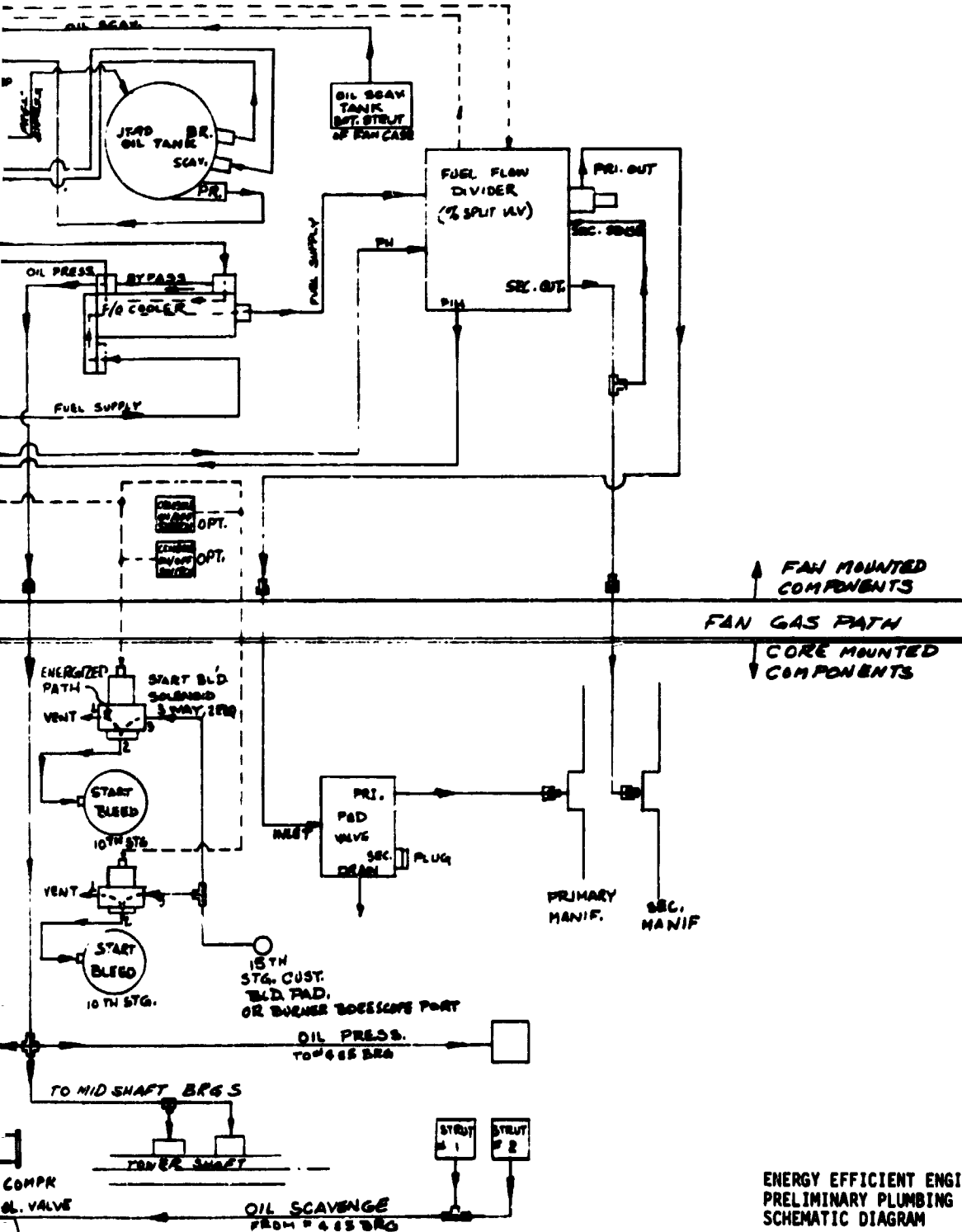


ORIGINAL PAGE IS
OF POOR QUALITY



Figure 221 Energy Efficient Engine Preliminary Plumbing System

C-5



ENERGY EFFICIENT ENGINE
PRELIMINARY PLUMBING
SCHEMATIC DIAGRAM



PRATT & WHITNEY AIRCRAFT GROUP
COMMERCIAL PRODUCTS DIVISION

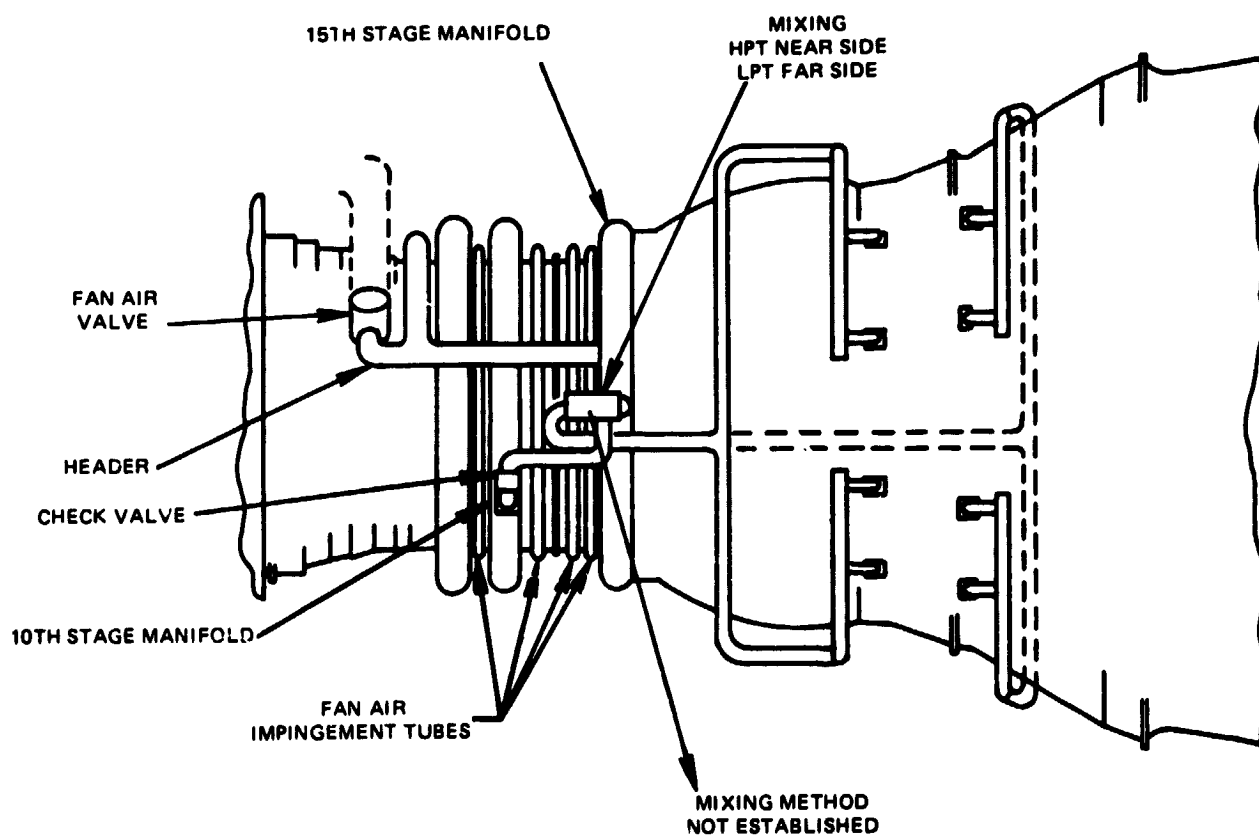


Figure 222 Active Clearance Control System Illustrating External Tubes and Valves